Var gene transcription and clinical disease manifestation in African *P. falciparum* malaria field isolates

Helen Marie Kyriacou

Thesis submitted for the degree of Doctor of Philosophy to
The University of Edinburgh

19th December 2007

Abstract

The *Plasmodium falciparum* erythrocyte membrane protein 1 (PfEMP1) variant surface antigens, encoded by the *var* gene family, play a crucial role in malaria pathogenesis through mediating immunomodulation and host cell adhesion. *Var* genes can be sub-grouped according to genetic or functional features. This thesis examined *var* gene transcription of conserved groups of *var* genes in the context of clinical malaria disease manifestation in African field isolates.

Analysis of *var* gene transcription in 26 *P. falciparum* field isolates from Malian children revealed that field isolates from children with cerebral malaria show significantly higher transcription of group A *var* genes than the field isolates from children with equally high parasite burdens but no symptoms or signs of severe malaria (hyperparasitaemia). These results suggest that group A *var* genes are important determinants of parasite virulence and strengthen the growing body of evidence associating group A *var* expression with severe disease in children.

Analysis of *var* gene transcription in six *P. falciparum* placental malaria field isolates showed that *var2csa* was transcribed in all placental malaria field isolates, but not in 10 childhood isolates examined. This finding, also reported in other recent and subsequent studies, suggests that *var2csa* expression is a critical factor in the onset of clinical malaria disease in pregnant women.

Examination of type 3 *var* gene transcription in laboratory and field isolates established that these *var* genes were commonly transcribed in blood-stage parasites,

and sequence analysis of the transcribed domains confirmed a very high level of conservation across this *var* gene sub-family.

Finally, rosetting is a property of some group A PfEMP1 and is associated with disease severity in African childhood malaria. Certain glycoconjugate compounds can disrupt rosetting, possibly due to the functional similarities of interactions between rosetting PfEMP1 and host rosetting ligands. A non-toxic compound (curdlan sulfate) was found to be effective at disrupting rosettes in all 18 rosetting field isolates examined, showing potential for use in treatment of severe malaria due to rosetting *P. falciparum* isolates.

The findings presented in this thesis expand current knowledge of the role and significance of *var* genes/PfEMP1 in *P. falciparum* malaria disease pathogenesis. The work demonstrates the importance of continued research on *var* genes/PfEMP1 in further understanding this complex parasite, and ultimately in combating this severe disease.

Declaration

The following contributions were made to my thesis:

1. Childhood malaria samples were a gift from the Bandiagara Malaria Project case-control study of severe malaria and were cultured by Ahmed Raza. Data for age, parasitaemia, rosette frequency and platelet-mediated clumping were collected by Dr Alex Rowe. The phylogenetic network (Appendix 2) was created by Dr Graham Stone.

2. Dr Stephen Rogerson collected the placental field isolate samples, and Dr Alex Rowe had previously prepared the RNA and cDNA and assessed the number of genotypes present in each isolate. TM180CSA had been selected by Dr Alex Rowe.

3. *P. falciparum* laboratory isolate gDNA and cDNA for type 3 PCR and RT-PCR had previously been prepared by Dr Alex Rowe and Ahmed Raza where stated. Kilifi field isolate gDNA was a gift from Dr Pete Bull.

4. Eurogentec prepared and purified the peptides for antibody production, immunised the two chickens and collected and pooled the egg yolks.

5. Various *P. falciparum* cultures were provided from other members of the Rowe laboratory: Ahmed Raza, Jean-Philippe Semblat, Ruth Corrigan and Antoine Claessens, as stated.

Subject to the above exceptions, I declare that the material presented in this thesis is my own work and has not been submitted to any other university or for any other degree or qualification.

Helen M. Kyriacou, Edinburgh, December 2007.

Acknowledgements

I am much indebted to Alex Rowe for excellent supervision, and for the experience of work in such a great lab. Thanks to all Rowe lab members past and present, especially Ruth and Antoine for being excellent office and lab mates, and Ahmed, JP, Monica, Anne-Marie and Fran for all their help. I am grateful to the Graham Stone for botanical advice and to Joanne Thompson for all her help throughout my PhD, especially with affinity purification. Thanks to Keith and the Matthews lab, for advice, carrot cake and anything I might have "borrowed". Many thanks to Kevin Marsh for inviting me to come to Kenya, an amazing experience I will always remember. Thanks and "jambo" to everyone in Kilifi, especially Pete Bull for his constant and contagious enthusiasm for *var* gene sequences.

I am much indebted to Kirsten Lyke, Mahamadou Thera, Abdoulaye Kone, Ogobara Doumbo, Christopher Plowe, and the children and families from the Bandiagara vaccine trial site, Mali, for the childhood malaria field isolates, and to Stephen Rogerson and all the participating patients from Queen Elizabeth Central Hospital in Blantyre, Malawi, for the placental field isolate samples. Thanks also to my examiners Lars Hviid and Paul Hunt for such an interesting and thought provoking viva.

I am of course hugely grateful to the Wellcome Trust for funding, and to everyone involved in the 4-year PhD programme, for the opportunities it has given me and for the amazing friends I have made. Special thanks to Oscar, Nicky, Josefin, Katie, Laura, Ellie, especially to Paul, and also to the Ashworth Rocky Horror Panto Show 2006, for keeping me happy and sane.

Finally, thanks to my parents for their continual love and support.

Abbreviations

ANOVA	Analysis of variance
ATS	Amino terminal sequence
BSA	Bovine serum albumin
CIDR	Cysteine-rich interdomain region
CRDS	Curdlan sulfate
CSA	Chondroitin sulfate A
DAPI	4,6-diamidino-2-phenylindole
DBL	Duffy-like binding domain
DIG	Digoxigenin
EDTA	Ethylenediaminetetraacetic acid
ELISA	Enzyme-Linked ImmunoSorbent Assay
EtBr	Ethidium Bromide
GAG	Glycosaminoglycan
HA	Hyaluronic acid
HEPES	4-(2-hydroxyethyl)-piperazine-ethanesulfonic acid
Hr	Hour
HS	Heparan sulfate
IE	Infected erythrocyte
IFA	Immunoflourescence assay
IgG	Immunoglobulin G
IgM	Immunoglobulin M
IgY	Immunoglobulin Y
KDa	Kilo daltons
KLH	Keyhole limpet hemocyanin
LB	Luria-Bertani
Min	Minute
OD	Optical density
O/N	Overnight
P	*Plasmodium*
PAGE	Polyacrylamide gel electrophoresis
PBS	Phosphate-buffered saline
PBST	Phosphate-buffered saline Tween
PCR	Polymerase chain reaction
PfEMP1	*P. falciparum* erythrocyte protein 1
PMC	Platelet-mediated clumping
Pt	Parasitaemia
PVDF	Polyvinylidene difluoride
R+	Rosetting
R-	Non-rosetting
RF	Rosette frequency
RPMI	Roswell Park Memorial Institute
RT	Room temperature
RT-PCR	Reverse transcriptase polymerase chain reaction
SD	Standard deviation
SDS	Sodium dodecyl sulfate
SE	Standard error

TI	Triton-X100 insoluble
TS	Triton-X100 soluble
TM	Transmembrane
Ups	Upstream sequence
UV	Ultra Violet
VSA	Variant surface antigen
WHO	World Health Organisation

Table of contents

Chapter 1

Introduction

1.1 *P. falciparum* malaria general background

1.1.1 Global burden of *P. falciparum* malaria

Plasmodia are members of the apicomplexan parasite family of eukaryotic protozoa. Four *Plasmodia* infect humans, *P. vivax, P. ovale, P. malariae* and *P. falciparum*, the last of which causes the majority of malaria cases worldwide (Fig. 1.1). Of these at least 90% occur in sub-Saharan Africa, where there are an estimated 200 million clinical events and 1-5 million deaths per year, predominantly in children under 5 years of age (Snow *et al.* 1999; Breman 2001; Snow *et al.* 2005). Clinical immunity to malaria disease symptoms in malaria endemic areas is achieved by adulthood, though an asymptomatic infection can persist throughout life.

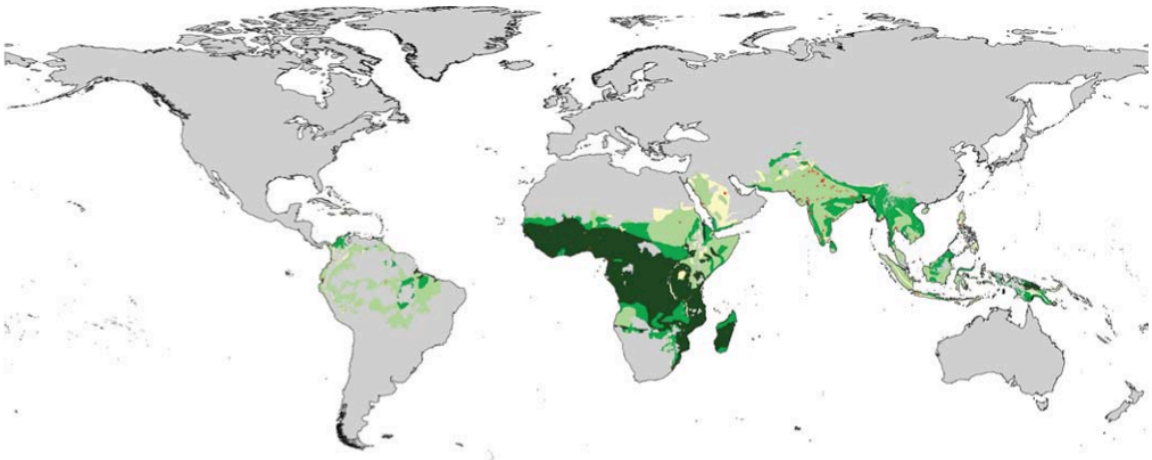

Fig.1.1. Global burden of malaria map. *P. falciparum* endemicity map taken from Snow *et al*. (2005). Childhood infection prevalence: light green, <10%; medium green, 11% to 50%; dark green, >50%; yellow, unclassified; grey areas are outside the limit of transmission.

1.1.2 *P. falciparum* lifecycle

P. falciparum has a compex lifecycle, dependent on transmission via an invertebrate host, the anopheles mosquito. An infection starts during a mosquito bite as sporozoite-stage parasites from the mosquito salivary gland are delivered into the blood. The free sporozoites travel in the blood circulation until they reach the liver to which they adhere using surface adhesive proteins circumsporozoite protein (CSP) and thrombospondin-related adhesive protein (TRAP) (Robson *et al*. 1995; Pradel *et al*. 2004). The sporozoites then glide across the liver sinusoidal cells, passing through Kupffer cells, the macrophages of the liver (Frevert *et al*. 2005). They traverse several hepatocyes, before settling within a particular hepatocyte for differentiation and mitotic replication (Tarun *et al*. 2006). After approximately 6 days, thousands of new parasites, merozoites, have been created. These are released into the circulation as the hepatocyte ruptures (Frevert *et al*. 2005; Tarun *et al*. 2006).

The erythrocytic cycle of asexual development (reviewed in(Bannister *et al*. 2000) now begins. The free merozoites attach to the surface of an erythrocyte, usually to separate erythrocytes, though multiply-infected cells are also seen (Deans *et al*. 2006). The attached merozoite reorientates so that the apical end can form a tight junction with the erythrocyte. An actin-myosin motor complex then pulls the merozoite inside the erythrocyte (Keeley and Soldati 2004).

The merozoite is now contained within the parasitophorous vacuole, which is then released into the erythrocyte cytoplasm through the proteolytic shedding of surface proteins by subtilase and transmembrane rhomboid proteases (Harris *et al*. 2005; O'Donnell *et al*. 2006). Invasion processes are complex with a high level of

redundancy in the pathways and the exact combination of parasite receptors and host ligands used varies considerably between different laboratory and field isolates (Cowman and Crabb 2006; Nery *et al*. 2006; Cortes *et al*. 2007; Deans *et al*. 2007). Merozoite surface protein 1 (MSP-1) and apical membrane protein 1 (AMA-1) appear to be essential (O'Donnell *et al*. 2000; Triglia *et al*. 2000). Antibodies to MSP-1 and AMA-1 interfere with invasion, and both proteins are vaccine candidates (Cavanagh *et al.* 2004; Malkin *et al.* 2005; Malkin *et al.* 2007). Proteins containing Duffy binding-like (DBL) domains, including EBA-175, EBA-140 and EBA-181, are also involved, and are linked to the actin-myosin motor via a TRAP homolog (Baum *et al.* 2006). These bind erythrocyte ligands glycophorin A, glycophorin C and sialic acid on the erythrocyte (Orlandi *et al.* 1992; Duraisingh *et al.* 2003; Maier *et al.* 2003; Cowman and Crabb 2006). The interaction between EBA-175 and glycophorin A is the dominant chymotrypsin-resistant invasion pathway in *P. falciparum* (Duraisingh *et al*. 2003).

The newly internalised parasite adopts a cup-shaped ring-like morphology (Aikawa *et al*. 1967), and is thus known as a ring stage trophozoite, commonly referred to simply as a ring. As the ring stage parasite matures it becomes larger, more rounded and increasingly complex. The endoplasmic reticulum and Golgi increase in size reflecting the high level of protein production. Approximately 16 hours post-invasion, parasite-derived proteins begin to be exported to the erythrocyte surface, often via Maurer's clefts, membranous structures in the erythrocyte cytosol (Atkinson *et al.* 1988; *Hae*ggstrom *et al.* 2004; Knuepfer *et al.* 2005). Many proteins destined for the erythrocyte membrane, including PfEMP1, are deposited in knobs (Baruch *et al.* 1995; Horrocks *et al.* 2005). These are protrusions of the erythrocyte surface, several

thousand of which appear 16-18 hours post invasion, and are structurally maintained by internal parasite-derived proteins such as knob-associated histidine-rich protein (Gruenberg *et al.* 1983; Rug *et al.* 2006). Once on the erythrocyte membrane, the surface proteins perform the dual function of adhesion and sequestration of infected erythrocytes, and antigenic variation for immune evasion. There is also an increase in the rigidity of the erythrocyte containing the mature trophozoite (Suwanarusk *et al.* 2004).

Repetitive cycles of nuclear division and parasite multiplication commence in the trophozoite stage, resulting in the creation of 16-20 new merozoites encased within the parasitophorous vacuole membrane of the parasite, now referred to as a schizont. These nonmotile merozoites are disseminated by an explosive rupture of the schizont, and are released for a new cycle of invasion (Glushakova *et al*. 2005).

The whole erythrocytic cycle takes approximately 48 hours. This stage is responsible for the disease pathology of malaria. Repeated cycles of erythrocyte invasion, intracellular maturation, schizogeny, erythrocyte rupture and merozoite release take their toll, causing anaemia and inflammatory responses. In addition, the adhesive properties of infected erythrocytes including sequestration within the body and other adhesion-mediated phenomena are associated with disease pathogenesis (discussed in section 1.3).

To complete the life cycle, a proportion of parasites must be taken up into a mosquito, and for this purpose a small proportion of merozoites differentiate into sexual stage parasites called gametocytes upon erythrocyte invasion, rather than into further

asexual trophozoites. Commitment to gametocytogenesis is thought to occur at the previous invasion cycle as all gametocytes from a particular schizont are male or female (Smith *et al.* 2000c). A stressed environment within the host is thought to trigger gametocytogenesis, which can be stimulated by culturing in partially spent media after a sudden increase in haematocrit *in vitro* (Carter *et al.* 1993; Sharp *et al.* 2006). These gametocytes can be readily taken up into the mosquito through the blood meal during feeding. Once inside the mosquito midgut, female gametocytes are fertilised by male gametocytes after DNA replication and exflagellation, forming a zygote. Triggers for gametocyte activation include a drop in temperature, or presence of xanthurenic acid (Muhia *et al.* 2001). Differentiation of the zygote occurs, resulting in a motile ookinete, which migrates through the midgut wall to settle on the basal lamina and form an oocyst. Here extensive replication occurs, producing 2000-8000 haploid nuclei after 12-18 days, which are released as sporozoites into the haemocoel as the oocyst bursts (Sinden 2002). The sporozoites migrate to the salivary glands of the mosquito, where they are prepared for invasion the next time the mosquito bites. The *P. falciparum* life cycle is summarised in Fig. 1.2.

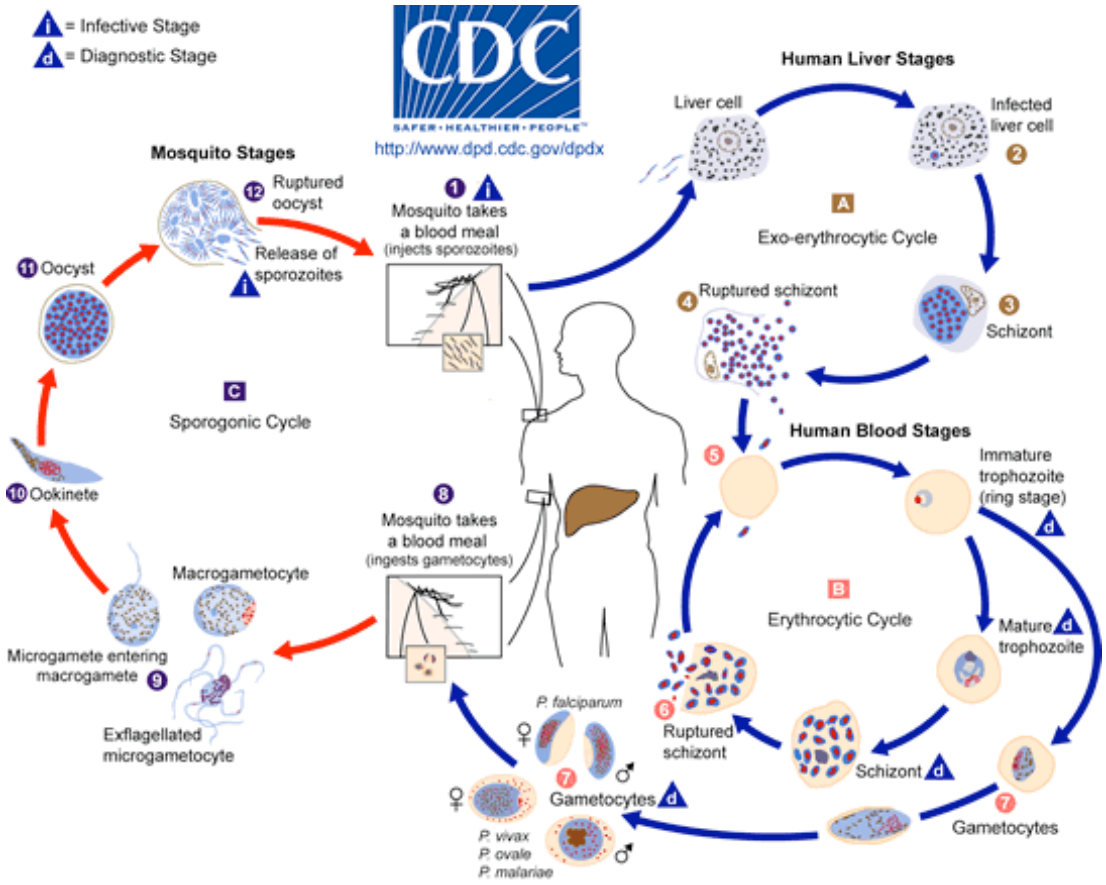

Fig. 1.2. *Plasmodium falciparum* life cycle. Reproduced from Center for Disease Control & Prevention Division of Parasitic Diseases Parasite Image Library http://www.dpd.cdc.gov/dpdx/HTML/Image_Library.htm. A human host is inoculated with sporozoites during an *Anopheles* mosquito bite (1). The sporozoites reach the liver (2) where they mature into liver stage schizonts (3). Rupture of this schizont results in the release of merozoites into the bloodstream (4), completing the exo-erythrocytic cycle (A). These infect new erythrocytes (5), entering the erythrocytic cycle (B). Ring stage trophozoite parasites mature to pigmented trophozoites, and then to schizonts, which rupture (6) releasing merozoites for another round of asexual propagation. A proportion of the merozoites enter the sexual stage, forming gametocytes (7) which can be taken up by the mosquito (8). Within the mosquito the sporogenic cycle (C) occurs. Male gametocytes exflagellate and enter female gametocytes (9) forming a zygote. The zygote become motile and elongated, now an

ookinete (10), and invades the midwall gut of the mosquito for maturation into an oocyst (11). Growth and rupture of the oocyst results in release of sporozoites (12) which are deposited in the salivary gland of the mosquito.

1.1.3 Antigenic variation

The ability to evade the host immune system is crucial for the survival of the parasites. Certain parasite-derived proteins must be inserted into the erythrocyte membrane to enable processes such as sequestration to avoid clearance by the spleen. This causes parasite-derived proteins to be exposed to the extracellular environment and thus to be vulnerable to antibody-mediated immunity. To avoid providing consistent targets for the host immune system, the *P. falciparum* genome encodes several large hypervariable polymorphic gene families called the variant surface antigens (VSA). Each member of a VSA family can be expressed individually and function independently but can become replaced by a novel VSA variant before a successful antibody response can be elicited. Cross-reactivity of antibodies between members of the hypervariable gene families is low to avoid recognition by any previously induced antibodies within the host, and exposed proteins are under a high level of divergent evolution (Hughes and Hughes 1995; Bockhorst *et al.* 2007). However, certain functional or structural constraints result in a number of shared epitopes (Joergensen *et al.* 2006) which eventually allows the host to develop protective immunity to clinical disease. Expression of these polymorphic gene families can be simplified as waves of expression of different members of the family over the course of an infection. Switching occurs before an immune response builds up, each time keeping one step ahead of the immune system (Fig. 1.3), although in a

natural infection the dynamics of immune response and VSA expression may become more complex.

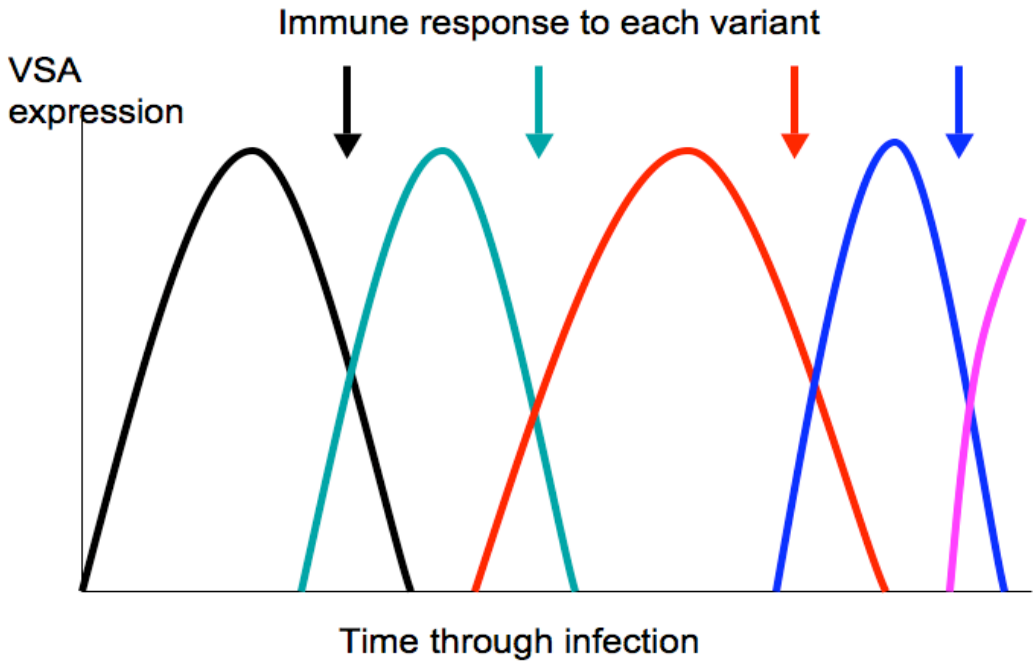

Fig. 1.3. Simplified schematic diagram of the theory of antigenic variation. VSA are expressed for a limited period and then switched to a new variant prior to a successful immune response. Waves of different VSA variants are indicated by colour. Different switching rates result in different duration of expression for the different variants.

1.2 PfEMP1 and *var* genes

1.2.1 PfEMP1 repertoire

The most well-studied *P. falciparum* VSA family involved in antigenic variation is the polymorphic *var* gene family which encodes the *Plasmodium falciparum* erythrocyte membrane protein 1 family (PfEMP1) (Biggs *et al.* 1991; Baruch *et al.* 1995; Smith *et al.* 1995; Su *et al.* 1995). Each parasite has a diverse repertoire of 50-60 *var* genes, and a correspondingly diverse array of PfEMP1 molecules (Gardner *et al*. 2002; Kraemer *et al*. 2007). Only one PfEMP1 variant is displayed on the host erythrocyte surface in a single cell cycle, and this is controlled at the level of *var* gene transcription (Smith *et al.* 1995; Scherf *et al.* 1998). However, PfEMP1 expression can be switched at each reinvasion cycle during an infection to avoid host recognition (Roberts *et al*. 1992; Chen *et al*. 1998b; Gatton *et al*. 2003). The genomic *var* gene repertoire of different isolates is thought to be largely non-overlapping, apart from a small number of well-conserved subfamilies, *var1csa, var2csa* and the type 3 *var* genes. However, estimations of the extent of global *var* gene diversity are confused by different levels of conservation and recombination in *var* genes in different geographic areas (Fowler *et al.* 2002; Tami *et al.* 2003; Albrecht *et al.* 2006; Barry *et al.* 2007). Other multigene families involved in antigenic variation in *P. falciparum* include rifins (Petter *et al.* 2007) and the smaller gene families of stevors and Pfmc-2TM (Lavazec *et al.* 2007).

1.2.2 *Var* gene structure

Var genes have 2 exons separated by a 0.8-1.2 kb intron (Fig. 1.4) (Su *et al*. 1995). The extracellular portion of PfEMP1 molecules is encoded by the highly polymorphic exon 1 (4-10 kb). This extracellular domain comprises several domains: an N-terminal segment, cysteine-rich interdomain region (CIDR), constant 2 (C2) domains and Duffy-binding-like (DBL) domains, named because of their homology to the duffy binding protein of *P. vivax*. DBL domains can be subclassified by consensus motifs into 5 well-defined groups (DBLα-ε), plus a sixth heterogeneous group, DBL-X (Smith *et al.* 2000; Gardner *et al.* 2002).

Var genes sequenced to date have between 2 and 7 DBL domains and up to 2 CIDR domains (Gardner *et al*. 2002; Kraemer *et al*. 2007). DBLα domains are always N-terminal, and occur in most known *var* gene types. There are two forms of DBLα domain, DBLα1 and DBLα0 (also sometimes just called DBLα). These are defined by presence/absence of three conserved cysteines, and conserved hydrophobic residues summarised in Fig. 1.5. (Kraemer and Smith 2003; Lavstsen *et al*. 2003; Robinson *et al*. 2003). There are three main CIDR types, α, β, and γ. CIDR α domains are further classified as CIDRα, which always occur in tandem with DBLα0 domains, or CIDRα1, which always occur with DBLα1 domains, though a DBLα1 domain can occur without a CIDRα1 domain (Robinson *et al*. 2003; Kraemer *et al*. 2007). The tandem pairing of DBLβ2-C2 is also well conserved.

The central region of the intron is AT-rich and contains a bi-directional promoter which produces a 'sterile' (untranslated) transcript (Calderwood *et al.* 2003). The conserved intracellular acidic terminal sequence and the transmembrane domain are

encoded by the highly conserved exon 2 (1.5 kb). The relationship between *var* genes and PfEMP1 is summarised in Fig. 1.4.

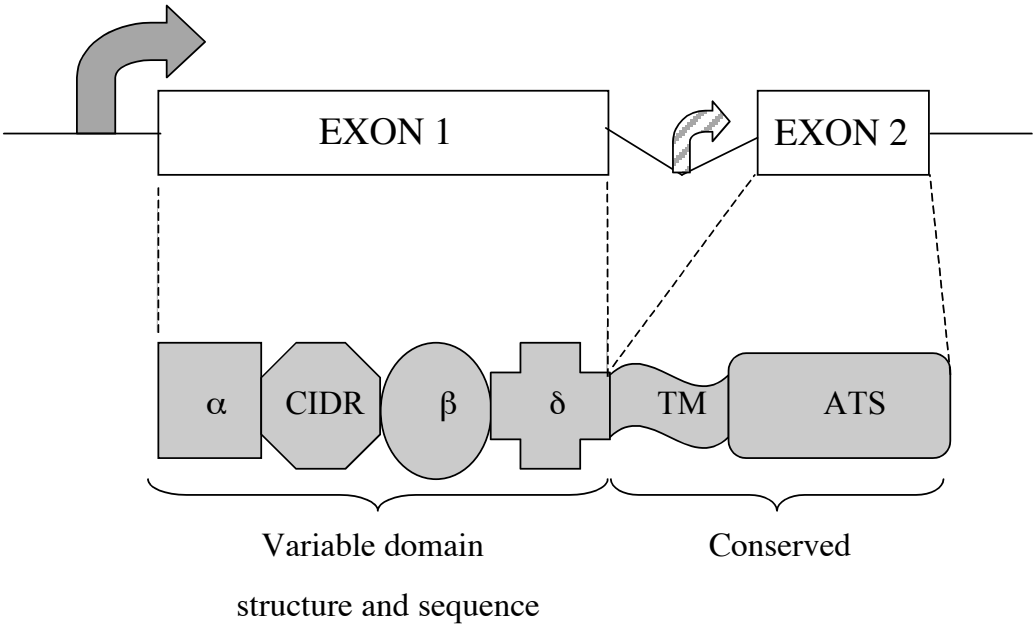

Fig. 1.4. *Var* gene/PfEMP1 structure. *Var* gene exon 1 encodes DBL and CIDR domains; exon 2 encodes transmembrane region (TM) and acidic terminal sequence (ATS). The *var* gene promoter (grey) and intronic promoter (diagonal stripes) are indicated.

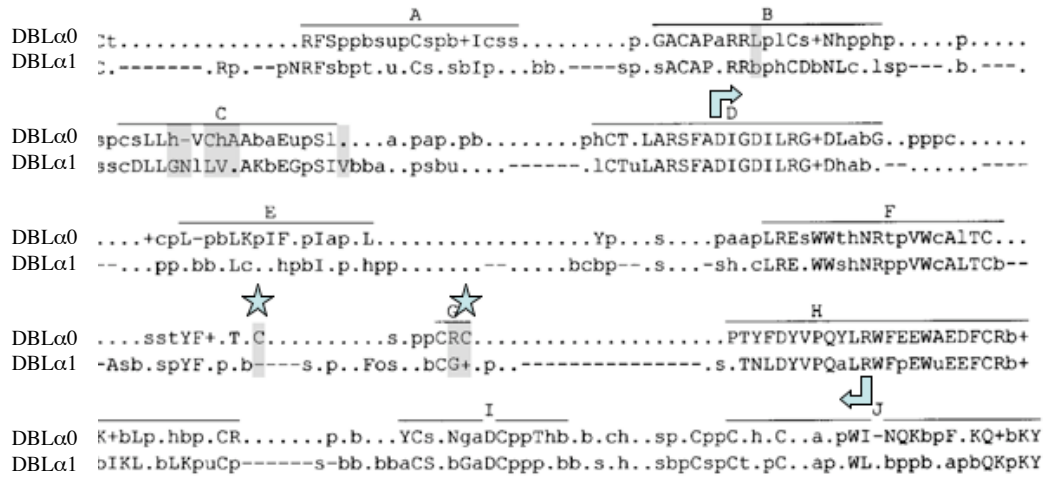

Fig. 1.5. Consensus residue features of the DBL_0 and DBLα1 subtype, adapted from Robinson *et al*. (2003), showing results from a multiple alignment of 57 DBL_0 and nine DBL_1 subtype sequences from the 3D7 genome and other parasite genotypes. The entire DBLα domain is included. The 80% consensus for each type is shown with conserved residues indicated by capital letters of the single amino acid code. Residues that were conserved for similar amino acid character are indicated as: c, charge: D, E, H, K, R; +, positive: H, K, R; h, hydrophobic: A, C, F, I, L, M, V, W, Y; p, polar: C, D, E, H, K, N, Q, R, S, T; s, small: A, C, D, G, N, P, S, T, V; u, tiny: A, G, S; b, big: E, K, R, I, L, N, S, Y, W. Within the alignment, periods represent positions that were not conserved and dashes (–) indicate gaps that were introduced to maintain the alignment. Shaded residues were highly discriminatory and present in at least 80% of one type of sequences but absent or present in less than 5% of the other type. Previously defined DBL homology blocks defined by Smith *et al.*, 2000 are overlined and labelled A to J. Block arrows show the tag section of DBLα amplified by the Taylor primers discussed in chapter 3 (Taylor *et al*. 2000a; Bull *et al*. 2005a). Stars show the two cysteines within this block that can be used to classify amplified sequences as DBLα0 or DBLα1 within the amplified tag.

1.2.3 *Var* gene groups

Many of the v*ar* genes of sequenced laboratory isolates are situated close to the telomeres, often in tandem with another *var* gene or with a *rif* gene, the rest being centromerically located (Gardner *et al*. 2002; Kraemer *et al*. 2007). *Var* genes have been classified into three major groups (A, B and C) and two intermediate groups (B/A and B/C), defined by the gene's position and orientation within the chromosome (Voss *et al.* 2000; Gardner *et al.* 2002; Vazquez-Macias *et al.* 2002; Kraemer and Smith 2003; Lavstsen *et al.* 2003), summarised in Table 1.1. The groupings are based on the 3D7 *var* gene repertoire, but the same groupings are observed in *var* genes from the recently sequenced *P. falciparum* isolates HB3 and IT (Kraemer *et al*. 2007) and the group classification is applicable to all *var* genes. Group A, B and C *var* genes can be found in *P. reichenowi*, which diverged from *P. falciparum* approximately 5-7 million years ago (Escalante *et al.* 1995; Trimnell *et al.* 2006), suggesting an ancient origin for the *var* gene groups.

Group A *var* genes are subtelomeric and transcribed towards the telomere. They have a semi-conserved upstream sequence (UpsA) and typically encode large PfEMP1 with four or more DBL domains. They contain an N-terminal DBLα1 domain (Kraemer and Smith 2003; Lavstsen *et al.* 2003; Robinson *et al.* 2003). The group A *var* gene group includes members of the conserved *var* gene family *var1csa* (PFE1640w in 3D7). *Var1csa var* genes have an "UpsA2" upstream sequence, which is a variation on the UspA sequence with unique 60 bp and 150 bp repeated motifs, and was formerly referred to as UpsD (Vazquez-Macias *et al*. 2002; Kraemer and Smith 2003; Lavstsen *et al*. 2003; Kraemer *et al*. 2007). The UpsA2 upstream sequence has only been seen in one non-*var1csa var* gene, found in HB3 (Kraemer *et al*. 2007). A

var1csa homologue is present in most strains of *P. falciparum* (Rowe *et al*. 2002a; Salanti *et al*. 2002; Kyes *et al*. 2003; Winter *et al*. 2003), and forms a highly conserved *var* gene family. In laboratory strain 3D7 *var1csa* is a pseudogene due to a truncation, and it lacks the exon 2 (Gardner *et al*. 2002; Rowe *et al*. 2002a). The type 3 *var* genes are also group A *var* genes, see section 1.2.4.

Group B *var* genes are also mostly telomerically located, but have a different upstream sequence type (UpsB) and are transcribed towards the centromere. Group B/A genes have an UpsB upstream region with an N-terminal DBLα0 domain, or a hybrid DBLα0/α1 domain that is DBLα0-like at the N-terminus, but DBLα1-like in the expressed sequence tag region (such as PF08_0140 and MAL6P1.316 in 3D7) and have a group A-type complex domain structure. Essentially they are group B *var* genes that have group A *var* gene-like characteristics. The precise definition of these B/A *var* genes is currently under debate, and as more *var* gene sequences are available for examination (Kraemer *et al.* 2007).

Group C *var* genes are centromeric and have a third upstream sequence type (UpsC). Group B and C *var* genes tend to be shorter, with two DBL domains and two CIDR domains, and their DBLα domain is of the DBLα0 type. Group B and C *var* genes are similar in architecture, mostly type 1 (DBLα-CIDRα-DBLδ-CIDR"not-α" (usually β or γ)-ATS) in HB3 and 3D7 (Gardner *et al*. 2002; Kraemer *et al*. 2007). Group B/C *var* genes resemble group C genes in chromosomal location, but have an UpsB upstream region.

A conserved *var* gene family, *var2csa* (PFL0030c in 3D7), has a distinct upstream region (UpsE) which has with little similarity to Ups A, B or C sequences (Kraemer and Smith 2003; Lavstsen *et al*. 2003; Kraemer *et al*. 2007). Most strains have a *var2csa* homologue (Trimnell *et al.* 2006), which is central to sequestration in the placenta during infection of pregnant women (more detail in section 1.4.5).

Var gene group	Upstream Sequence	No. of genes in 3D7	No. of DBL domains	Position	Orientation	DBLα0/α1	No. of cysteines in amplified tag
A	UpsA	10	2-7	Subtelomeric	Telomeric	DBLα1	2
Including:							
var1csa	UpsA2	1	7			DBLα $_{var1csa}$	
type 3 *var*	UpsA	3	2			DBLα$_{type3}$	
B/A	UpsB	4	4-7	Subtelomeric	Centromeric	DBLα1 or	2
						DBLα0	4
B	UpsB	21	2-3	Subtelomeric	Centromeric	DBLα0	4
B/C	UpsB	10	2-3	Central	Telomeric	DBLα0	4
C	UpsC	13	2-3	Central	Telomeric	DBLα0	4
var2csa	UpsE	1	6	Subtelomeric	Telomeric	None	-

Table 1.1. Characteristics of *P. falciparum var* gene groups. Type 3 *var* gene family and the *var1csa var* gene homologues are indicated as conserved subgroups of group A *var* genes. DBLα $_{var1csa}$: *var1csa* homologues have a conserved DBLα1 domain (Rowe *et al*. 2002a). DBLα$_{type3}$: type 3 *var* genes have a semi-conserved DBLα1 domain (see chapter 5).

1.2.4 Type 3 *var* genes

The type 3 genes are the smallest *var* genes and are highly conserved (Gardner *et al*. 2002; Trimnell *et al*. 2006). The extracellular portion has only two DBL domains: N-terminal DBLα domain, followed by a DBLε domain (Smith *et al.* 2000; Gardner *et al.* 2002). They are the only genes in 3D7 apart from PFL0030c (*var2csa*) not to have a CIDR domain. Their high sequence conservation indicates that recombination is restricted to within the type 3 *var* gene family. Of the few *P. falciparum* strains studied so far, most have 1-2 type 3 *var* gene homologues, though HB3 has none and 3D7 has 3 (Gardner *et al*. 2002; Trimnell *et al*. 2006). The type 3 *var* genes in 3D7, pfa0015c, pfi1820w and mal6p1.314 (renamed pff0020c), are telomerically located and transcribed towards the telomere in 3D7. The upstream region is UpsA-type and there are no distinguishing features to the type 3 upstream region (Trimnell *et al*. 2006). They also have group A type ATS domain and 3' downstream untranslated region. They are thus classified as group A *var* genes even though other group A *var* genes are longer with a more complex domain structure (Gardner *et al*. 2002; Kraemer and Smith 2003) as shown in Fig. 1.6. More detail on the type 3 *var* genes and PfEMP1 is given in chapter 5.

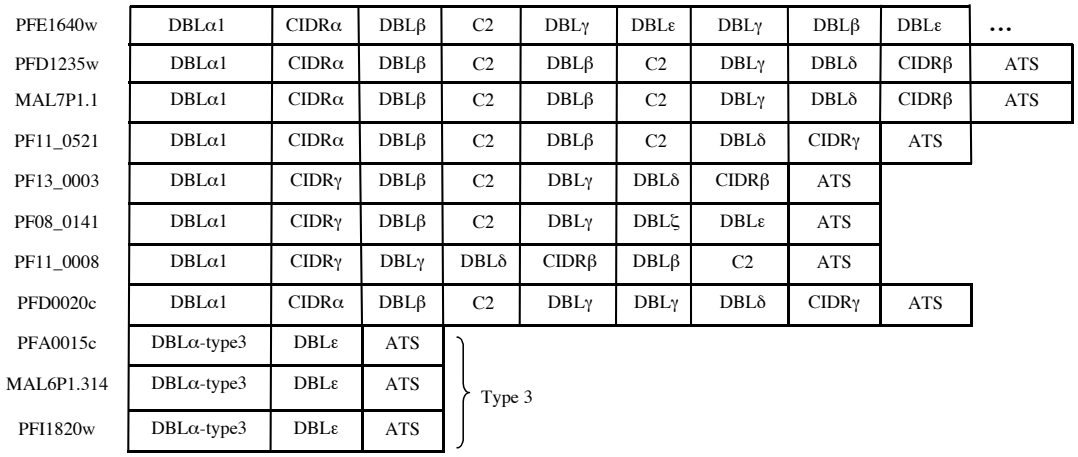

Fig. 1.6. Domain structure of Group A *var* genes of 3D7 (adapted from Lavstsen *et al.* 2003). The three type 3 *var* from 3D7 are indicated. DBLζ are a subset of DBLX.

The DBLα of the type 3 *var* genes is DBLα1-type, consistent with other group A *var* genes. The first portion of type 3 DBLα1 domains is indistinguishable from that of other DBLα1 domains. However, the type 3 DBLα1 domain sequence then diverges after around 480 nucleotides from other group A DBLα1 domains, and all known type 3 DBLα domains end in a highly conserved sequence. The DBLε domains of type 3 *var* genes are also very highly conserved (further details in chapter 5).

The type 3 *var* genes probably originated after the split from *P. reichenowi*, which does not appear to contain a type 3 *var* gene homologue (Trimnell *et al.* 2006). This may indicate specificity for infection of humans rather than other primates. Little has previously been reported about type 3 *var* gene transcription or type 3 PfEMP1

protein expression timing or prevalence in *P. falciaprum* laboratory strains or field isolates.

1.2.5 *Var* gene recombination

Recombination of *var* genes occurs within and between isolates. It is thought to occur during sexual stage development within the mosquito, and probably also during mitosis within the asexual cell cycle (Freitas-Junior *et al*. 2000; Taylor *et al*. 2000b). Small or large recombination events can occur, which contribute to the mosaic-nature of *var* genes, and play a role in *var* gene evolution (Ward *et al.* 1999; Freitas-Junior *et al.* 2000; Kaestli *et al.* 2004; Bull *et al.* 2005a; Trimnell *et al.* 2006; Barry *et al.* 2007; Kraemer *et al.* 2007). Telomeric clustering is believed to facilitate recombination between *var* genes, which preferentially occurs between *var* genes with a similar upstream region and orientation (Kraemer and Smith 2003). Thus, group B and C *var* genes appear to recombine separately from the group A *var* genes. The three laboratory strains sequenced to date indicate that the distinct *var* gene groups are of similar proportions in all in *P. falciparum* isolates (Gardner *et al.* 2002; Kraemer *et al.* 2007). As with the type 3 *var* gene family, conserved gene families *var1csa* and *var2csa* also recombine separately from other *var* genes (Kraemer *et al.* 2007). This has allowed them to be maintained in most *P. falciparum* genomes since evolutionary separation from *P. reichenowi*, which also contained a *var1csa* and a *var2csa* homologue (Trimnell *et al.* 2006).

Genes arise through gene duplication and diversifying selection. There are two sets of duplicated genes in 3D7, PFD1235w and MAL8P1.207.

1.2.6 Timing of *var* gene expression

Var genes cluster in telomeric "bouquets", caused by crosslinking of telomeres at the nuclear periphery (Freitas-Junior *et al.* 2000; Marty *et al.* 2006). Expression is controlled by a mutually exclusive expression, so that only one PfEMP1 is expressed during each asexual growth cycle (Smith *et al.* 1995; Scherf *et al.* 1998; Dzikowski *et al.* 2006).

Var gene transcripts are detectable by RT-PCR during ring and trophozoite stage, though the single full length *var* gene transcript is often only detectable by Northern blot at ring stage, up to 20 hr post invasion (Chen *et al.* 1998b; Scherf *et al.* 1998; Kyes *et al.* 2000; Kyes *et al.* 2003; Dahlback *et al.* 2007). The same *var* gene transcripts can be detected by RT-PCR at ring and trophozoite stage of parasite growth *in vitro* and in infected human volunteers (Peters *et al.* 2002; Dahlback *et al.* 2007). The *var1csa* gene is transcribed later, present only at trophozoite stage (Kyes *et al.* 2003) and may not be counted in the mutually exclusive expression system, as it appears to be constitutively expressed in many field isolates (Winter *et al.* 2003). *Var1csa* can be transcribed in 3D7 even though it is a pseudogene and so cannot produce functional PfEMP1 (Kyes *et al.* 2003; Kyes *et al.* 2007). Some studies have reported multiple *var* gene transcripts within a single parasite (Duffy *et al.* 2002), though it is hard to distinguish between *var* genes from different parasites, and this phenomenon is controversial. No data on timing of transcription or protein expression of the type 3 *var* genes has been published to date.

Gametocytes also express PfEMP1 early in development (stages I and II) and commonly express UpsC *var* genes (Sharp *et al.* 2006). Whether this is a switch on

commitment to gametocytogenesis, or a reflection of UpsC *var*-expressing parasites being more likely to undergo gametocytogenesis is unclear. Gametocytes sequester specifically in spleen and bone marrow (Smalley 1976; Rogers *et al.* 2000), but it is unclear whether this sequestration is PfEMP1-mediated. As gametocytes are the transmitted form of the parasite, the molecules causing sequestration and gametocytogenesis may be involved in determining transmission rates and parasite virulence.

1.2.7 Activation and silencing of *var* genes

DNA rearrangement is not required for *var* gene activation, which is controlled by an *in situ* gene activation, causing trancription initiation via RNA polymerase II (Kyes *et al.* 2007). Physical movement of *var* genes to a distinct location along the nuclear periphery may be required for expression (Ralph *et al*. 2005).

It appears to be crucial for the parasite to only express one *var* gene at a time, thus requiring the remaining *var* genes to be transcriptionally silent. For example, silencing of the remaining *var* genes is crucial for maintaining the reserve *var* repertoire for immune evasion. Perhaps suprprisingly, the activity of the intronic promoter located between the two *var* gene exons (Fig. 1.4) has been shown to be required for a *var* gene to remain silenced, though the precise role of the promoter or "sterile" transcript is not yet understood (Deitsch 2001; Calderwood *et al.* 2003; Frank *et al.* 2006). The late transcription pattern seen for *var1csa,* may be due to lack of a regulatory intronic promoter (Gardner *et al*. 2002; Winter *et al*. 2003).

Chromatin modifications, including methylation and acetylation of histones, appear to be involved in *var* gene silencing, though this is not yet fully understood. Histone acetylation is controlled by a homologue of the yeast Sir2 (silent information regulator), called PfSir2 (Duraisingh *et al*. 2005; Freitas-Junior *et al*. 2005). PfSir2 co-localises with telomeric bouquets, binding to transcriptionally repressed chromosomes, and disruption of PfSir2 results in aberrant *var* gene transcription of certain *var* genes (Duraisingh *et al*. 2005). The methylation state of particular histones, such as histone H3 at lysine K9, is also involved in transcription control (Chookajorn *et al*. 2007). Recently, histone methylation has also been shown to be involved in the "memory" process by which new ring stage parasites are able to re-express the *var* gene which was expressed by the parent parasite at the previous invasion cycle (Lopez-Rubio *et al*. 2007).

However, *var* genes can be active in an otherwise transcriptionally silent region of the chromosome, and in tandem with silent *var* or *rif* genes (Ralph *et al.* 2005; Marty *et al.* 2006). Silencing of *var* genes thus appears to be controlled independently for each individual gene rather than simply packaging vast swathes of chromatin into a generally repressed state.

1.2.8 *Var* gene switching

Var genes need to switch fast enough to evade host immune response without running out of novel PfEMP1 variants before uptake by mosquito. The order of *var* gene expression is complex; there is no predetermined order of *var* gene expression, but the expression order does not appear to be entirely random. *Var* genes have a range of switching rates, though switching rate is an intrinsic property of each particular *var*

gene (Horrocks *et al*. 2004b). Estimates of switching rates vary from 2% per generation *in vitro* (Roberts *et al*. 1992) up to 16% *in vivo* (Peters *et al*. 2002), though the rate differs for different *var* genes (Horrocks *et al*. 2004a). In one study, Ups C (centromeric) *var* showed slower "off rates" than group A *var* genes and were thus transcribed for longer in culture (Dzikowski *et al*. 2006). The different *var* gene groups appear to be controlled separately. For example, silencing of UpsA and E genes is dependent on the histone deacetylase activity of Pfsir2, whereas Ups B and C genes remained silenced after Pfsir2 knock out (Duraisingh *et al*. 2005). This may be a mechanism directing *var* gene choice in response to a particular situation, though this is not fully understood.

Recent computer modelling of *var* gene expression switching in culture has suggested that *var* genes may use intermediate *var* genes during switching. This is the "single to many to single" hypothesis" (A. Serazin and C. Newbold personal communication) and comes from observations of cultures expressing a predominant *var* gene activating transcription of several different *var* genes which are all rapidly silenced again as the culture as a whole switches to expression of a second predominant *var* gene. It is possible different switching mechanisms are utilised by different *var* genes in different situations.

1.3 *P. falciparum* and adhesion

1.3.1 *P. falciparum* adhesion phenotypes

P. falciparum has the unique property of adhesion among human-infective *Plasmodia*. The major role for adhesion in *P. falciparum* is sequestering to avoid host clearance by the spleen (Chotivanich *et al.* 2002). This leads to adhesion phenotypes associating with pathology and virulence (Fig. 1.7).

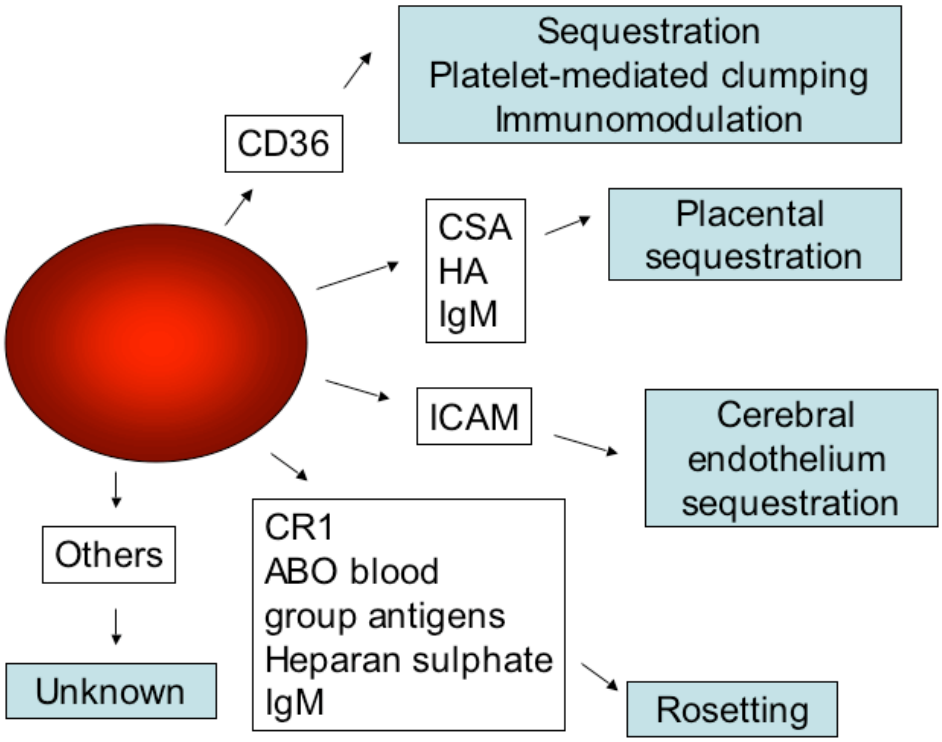

Fig. 1.7. Common host ligands *P. falciparum* infected erythrocytes and associated adhesion phenotypes.

PfEMP1 mediates adhesion of *P. falciparum* infected erythrocytes. Export into knobs allows efficient adhesion of the PfEMP1 to its various ligands (Baruch *et al.* 1995;

Crabb *et al.* 1997; Horrocks *et al.* 2005). PfEMP1 are sensitive to cleavage by trypsin, and trypsinisation of infected erythrocytes correlates with decreased cytoadherence properties (Leech *et al.* 1984).

1.3.2 PfEMP1-mediated adhesion phenotypes: cytoadhesion

Many host ligands are potential adhesion sites for PfEMP1-mediated sequestration, as detailed in Table 1.2.

CD36 is an endothelial scavenger receptor, present on the peripheral vasculature endothelium, on many components of the blood, including monocytes, platelets and erythrocytes, and in organs such as liver and spleen, but is not present on cerebral endothelium (Turner *et al.* 1994; Serghides *et al.* 2003). CD36 can act as a ligand for infected erythrocytes (Handunnetti *et al*. 1992; Udomsangpetch *et al*. 1997; Urban *et al*. 1999; Heddini *et al*. 2001; Pain *et al*. 2001; Robinson *et al*. 2003) and binding to CD36 is the major adhesion phenotype for infected erythrocytes. Affinity for CD36 is a property of group B, C or B/C PfEMP1 via the CIDRα domain and the majority of PfEMP1 (49/60 in 3D7) bind to the CD36 (Robinson *et al*. 2003). However, CD36-binding appears to mediate sequestration of infected erythrocytes away from vital organs such as the brain, and adhesion to CD36 is inversely associated with severe malaria (Rogerson *et al.* 1999; Serghides *et al.* 2003).

CSA is a clinically important ligand for cytoadhesion, in the specific case of placental malaria, where CSA on the placenta offers a novel ligand for sequestration of infected erythrocytes (Fried and Duffy 1996; Reeder *et al*. 2000). Hyaluronic acid (Beeson and

Brown 2004) and IgM binding (Creasey *et al.* 2003) have also been associated with placental parasites (see section 1.4.4 and chapter 4 for more detail).

Intracellular adhesion molecule 1 (ICAM-1) is another clinically important adhesion phenotype of *P. falciparum* field isolates. Upregulation of ICAM-1 has been reported during *P. falciparum* cerebral malaria (Turner *et al.* 1994; Silamut *et al.* 1999), and as such sequestration via ICAM-1 has been associated with cerebral malaria. However, ICAM-1 upregulation is not seen in all cerebral malaria patients and can occur prior to parasitisation of the cerebral microvasculature, and has even be reported to occur in infected individuals without cerebral sequestration (Brown *et al.* 1999; Silamut *et al.* 1999). Adhesion to ICAM-1, via a tandem pairing of DBLβ and C2 domains, can be selected for *in vitro* and has been observed in field isolates (Smith *et al*. 2000a; Chattopadhyay *et al*. 2004; Springer *et al*. 2004). E-selectin has also been reported to be upregulated in cerebral endothelium during parasite sequestration, but affinity for E-selectin in field isolates of laboratory strains has not been commonly reported and consistent link with cerebral malaria is unconfirmed (Turner *et al*. 1994; Silamut *et al*. 1999).

Adhesion can be a cooperative process. For example, P-selectin can mediate temporary adhesion, which allows rolling across endothelium and platelets, promoting firm adhesion through other ligands such as CD36 (Roberts *et al*. 1985; Senczuk *et al*. 2001). Adhesion to ICAM and CD36 also appears to be synergistic (McCormick *et al*. 1997).

Other host ligands that may support cytoadhesion include vascular cell adhesion molecule (VCAM), thrombospondin and platelet endothelial cell adhesion molecule (PECAM-1). Affinity to multiple ligands is correlated with malaria severity in *P. falciparum* field isolates (Heddini *et al*. 2001). Adhesion to complement receptor 1 (CR1) (Rowe *et al*. 1997), ABO blood sugars (Carlson and Wahlgren 1992; Barragan *et al*. 2000), and heparan sulfate (Ockenhouse *et al*. 1992) on uninfected erythrocytes can mediate binding to uninfected erythrocytes, in a process called rosetting (see section 1.3.3).

A link between the cytoadhesion properties of the expressed PfEMP1 of an isolate and clinical disease is logical. Parasites from different organs within a patient show differential *var* gene expression (Montgomery *et al*. 2007), despite reports suggesting sequestered masses are genotypically identical (Dembo *et al*. 2006; Montgomery *et al*. 2006) suggesting a link between PfEMP1 (or other VSA) and site of cytoadhesion. In addition, parasites from cerebral malaria field isolates do not tend to be genetically more similar to each other than those causing uncomplicated malaria (Ferreira *et al*. 2002), supporting the hypothesis that it is the expressed VSA that affects disease pathology.

Host ligand	Description	Location	PfEMP1 domain	Associated phenotype	References
CD36 (Platelet glycophorin IV)	Globular glycoprotein scavenger receptor (88 kDa)	Endothelial cells (except cerebral) Platelets Dendritic cells Mature monocytes	CIDRα1	Sequestration Platelet-mediated clumping Immunomodulation	Handunnetti *et al.* 1992; Udomsangpetch *et al.* 1997; Urban *et al.* 1999; Heddini *et al.* 2001; Pain *et al.* 2001; Robinson *et al.* 2003
ICAM-1	Ig family adhesion molecule 80-110 kDa	Endothelial cells including cerebral endothelium with inducible upregulation.	DBLβ/C2	Expression reported to increase in cerebral malaria and to co-localise with sequestration	Turner *et al.* 1994; Springer *et al.* 2004
CSA	Poly-sulfated matrix protein	Placental syncitiotrophoblasts Endothelial cells including cerebral Various blood cells	DBLγ *var1csa* DBLX *var2csa*	Placental malaria major role	Gamain *et al.* 2004; Duffy *et al.* 2005; Fried *et al.* 2006 Gamain *et al.* 2005
HA	Non-sulfated glycosaminoglycan	Placental syncitiotrophoblasts		Placental malaria minor role	Beeson *et al.* 2000; Duffy *et al.* 2005
IgG	Monomeric immunoglobulin	Blood plasma		Placental malaria	Flick *et al.* 2001
Non-specific IgM	Pentameric immunoglobulin	Blood plasma	DBLε	Placental malaria Rosetting	Creasey *et al.* 2003; Semblat *et al.* 2006
CR1	Immune adherence receptor	Erythrocytes	DBLα1	Rosetting	Rowe *et al.* 1997
Blood sugars ABO	O-linked glycoproteins	Erythrocytes		Rosetting	Carlson and Wahlgren 1992; Barragan *et al.* 2000
Heparan sulfate	Sulfated glycoconjugate	Erythrocytes		Rosetting	Ockenhouse *et al.* 1992
E-selectin	Selectin family adhesion molecule	Activated endothelial cells		Expression reported to increase in cerebral malaria and to co-localise with sequestration	Springer *et al.* 2004 Turner *et al.* 1994

Host ligand	Description	Location	PfEMP1 domain	Associated phenotype	References
VCAM	Ig superfamily adhesion molecule	Activated endothelial cells		Expression reported to increase in cerebral malaria	Ockenhouse *et al.* 1992
Thrombospondin	Glycoprotein	Platelets and secreted			Roberts *et al.* 1985
P-selectin	Selectin family adhesion molecule	Endothelial cells Activated platelets		"Rolling" enhanced adhesion via other ligands including CD36	Ho *et al.* 1998; Senczuk *et al.* 2001
PECAM-1	Transmembrane glycoprotein	Many blood cells including erythrocytes and platelets			Treutiger *et al.* 1997

Table 1.2. Host ligands supporting adhesion of *P. falciparum* infected erythrocytes: CD36, intracellular adhesion molecule 1 ICAM-1, chondroitin sulphate A CSA, hyaluronic acid HA, IgG, IgM, complement receptor 1 CR1, ABO Blood sugars, Heparan sulfate, E-selectin, vascular cell adhesion molecule VCAM, thrombospondin, P-selectin and platelet endothelial cell adhesion molecule PECAM-1.

1.3.3 PfEMP1-mediated adhesion phenotypes: rosetting

Rosetting is the spontaneous binding of an infected erythroctye to uninfected erythrocytes (Fig. 1.8).

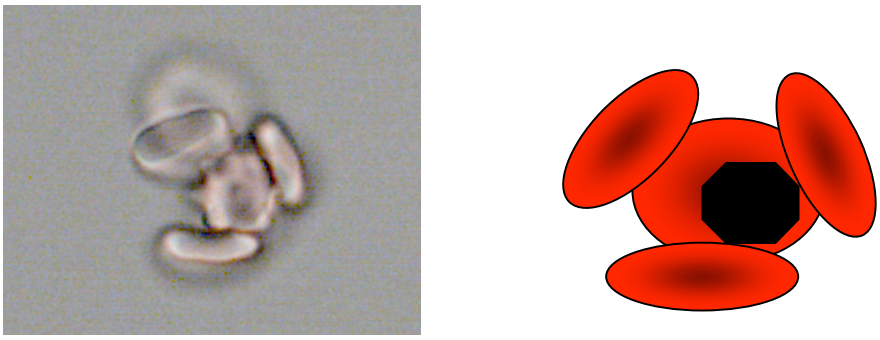

Fig. 1.8. Rosetting. A) Photograph showing a rosetting-TM284 infected erythrocyte. B) Schematic diagram representing a pigmented trophozoite-infected erythrocyte adhering to 3 uninfected erythrocytes.

All known human-infective *Plasmodia* can rosette (Udomsanpetch *et al.* 1995; Angus *et al.* 1996; Lowe *et al.* 1998), and rosettes have also been seen in rodent malaria strains including *P. chabaudi* (Mackinnon *et al.* 2002). Rosettes can be seen in the peripheral blood of patients infected with *P. vivax* (Chotivanich *et al.* 1998), but only very rarely in the peripheral blood of patients infected with *P. falciparum* as the mature stages are usually sequestered. In *P. falciparum* field isolate samples taken from peripheral blood, the ring stage parasites must be cultured *in vitro* to trophozoite stage to see rosettes form. The rosette frequency (RF) is the percentage of infected erythrocytes binding to 2 or more uninfected erythrocytes. The combination of sequestration and rosetting in *P. falciparum* field isolates may cause obstruction of the microvasculature (Kaul *et al.* 1991), which may contribute to the

association between rosetting and severe malaria (Carlson *et al.* 1990; Rowe *et al.* 1995; Rowe *et al.* 2002c).

Rosetting is a strain-specific property (Wahlgren *et al.* 1990). Rosetting isolates are relatively uncommon, though an estimated 25-50% of severe malaria isolates have a high rosette frequency (RF > 30%) (Rowe 2005). PfEMP1 is the major ligand for rosetting (Rowe *et al.* 1997; Chen *et al.* 1998a). A well-characterised rosetting interaction involves adhesion between the DBLα1 domain from R29R+*var1* of parasite clone R29, and CR1 on the uninfected erythrocyte surface (Rowe *et al.* 1997; Rowe *et al.* 2000; Mayor *et al.* 2005). Other erythrocyte ligands can also support rosetting including heparan sulfate-like molecules (Carlson *et al.* 1992) and ABO blood group antigens (Carlson and Wahlgren 1992; Chen *et al.* 1998a; Barragan *et al.* 2000). CD36 binding parasites do not usually support rosetting, except in the case of Malayan Camp (Handunnetti *et al.* 1992). Many diverse PfEMP1 support rosetting, and rosetting PfEMP1 can be considered a functional subgroup of PfEMP1, but no single consensus 'rosetting motif' has so far been identified by comparisons of different rosetting PfEMP1 (Normark *et al.* 2007). Rosetting PfEMP1 have been reported that include a DBLα1 domain (e.g. Rowe *et al.* 1997), or a DBLα0 domain (Chen *et al.* 1998a), though recent evidence from numerous laboratory isolates strongly suggests that most rosetting PfEMP1 gene are group A PfEMP1, and that group B and C PfEMP1 rarely support rosetting (J.A. Rowe, unpublished data).

The physical properties of the rosetting interactions allow certain molecules to effectively disrupt rosetting on a wide range of field and laboratory *P. falciparum* isolates. These molecules include glycoconjugate compounds such as heparin and fucoidan (Carlson *et al*. 1992; Rowe *et al*. 1994). However, their high anticoagulant activity induces bleeding (Munir *et al*. 1980; Rampengan 1991; Carlson *et al*. 1992), which prevents their use as rosetting-inhibiting drugs in the treatment of severe malaria (WHO 2000). Identification of effective rosette-inhibiting drugs without harmful side effects such as high anticoagulant activity would offer potential therapeutic benefit for severe clinical symptoms caused by rosette *P. falciparum* isolates.

It remains unclear what the advantage (if any) of rosetting is for the parasite. It does not appear to be linked with increased merozoite invasion (Deans and Rowe 2006). It may be a form of immune evasion, for example protecting the infected erythrocyte from the innate immune systems by preventing contact-dependent activation of natural killer cells (Artavanis-Tsakonas *et al.* 2003), or acting as a cloak to reduce phagocytosis by macrophages or neutrophils. It may be a by-product of evolution of adhesive phenotypes "intended" for sequestration, for example to endothelium. It remains possible that rosetting is an *in vitro* artefact.

1.3.4 PfEMP1-mediated adhesion phenotypes: platelet mediated clumping

CD36 binding also mediates platelet-mediated clumping (PMC), whereby platelets adhere to infected erythrocytes, bridging them together and causing them to clump

(Pain *et al.* 2001). Not all CD36-binding parasites support PMC in culture, and any additional interactions between the infected erythrocyte and the platelets are unknown at present. PMC is associated with high parasitaemia (Arman *et al.* 2007). Higher PMC levels are seen in patients with severe malaria (Pain *et al.* 2001), though as this category often has a high parasitaemia, PMC may not be associated with virulence *per se* (Arman *et al.* 2007). PMC is not usually seen in rosetting parasites, as the two binding mechanisms are both PfEMP1-mediated and appear to be mutually exclusive. The relevance and function of PMC *in vivo* remains unclear.

1.3.5 PfEMP1-mediated immunomodulation

Sequestration and associated adhesion phenotypes may not be the only active reason for affinity for host molecules; PfEMP1-mediated adhesion to cells of the immune system has been reported to cause modulation of the immune response. Binding of infected erythrocytes to dendritic cells halts dendritic cell maturation, prevents up-regulation of MHC class II molecules, inhibits T cell activation, and causes a switch in cytokine production towards immunosuppressive cytokine release (Urban *et al.* 1999; Urban *et al.* 2001). This interaction appears to be via CD36 (McGilvray *et al.* 2000; Urban *et al.* 2001), and is probably mediated by the CIDR domains of group B or C PfEMP1. Whether other domains from group A PfEMP1 can also fulfil this function is unclear. Binding to natural killer NK cells is contact dependent and can be mediated through PfEMP1 (Artavanis-Tsakonas *et al.* 2003; Baratin *et al.* 2007). Binding of infected cells to immune cells thus appears to be a parasite-driven attempt to halt an inflammatory immune response. However, in some studies, activation of dendritic cells due to *P. falciparum* infection, for example during schizont rupture, is

reported to stimulate an immune response (Pichyangkul *et al*. 2004). The stimulation and suppression of the immune system during a malaria infection is complex, and is probably dependent on previous malaria exposure, host genotypic factors and the infective parasite strain.

P. falciparum malaria disease manifestation

1.4.1 *P. falciparum* malaria disease manifestation in African children

P. falciparum malaria is the major cause of malaria disease in young children in endemic areas. Malaria disease is characterised by periodic fevers, with an asexual parasitaemia detectable by Giemsa staining of the peripheral blood. *P. falciparum* disease is heterogeneous, differing markedly from infection to infection and a variety of other symptoms commonly accompanies this classic fever. The range of clinical manifestations, from fever to increasingly severe complications, is outlined in Fig. 1.9 and Table 1.3. "Severe malaria" broadly refers to fever with at least one severe clinical complication due to *P. falciparum* infection. In Africa, severe anaemia is common in the youngest children (under 2 years old), with seizures and cerebral malaria predominating in slightly older children (Newton *et al.* 2000). In areas of lower transmission such as South East Asia, severe disease is commonly seen in adults, and multi-organ failure is the most common severe disease manifestation.

In malaria-endemic high transmission areas such as across sub-Saharan Africa, immunity to clinical disease is achieved by 5 years of age, followed by increased immunity to infection (Snow 1999; Breman 2001; Snow *et al.* 2005). Total immunity is not usually achieved, and an asymptomatic low parasitaemia is prevalent in

malaria-endemic communities, and is required to maintain the immunity to clinical disease. Severe malaria occurs in those with little previous exposure to malaria, and thus predominantly in young children in malaria endemic areas, but also in travellers, and in returning migrants. At present, development of these severe complications remains hard to predict, and the contribution of parasite genetic factors or virulence factors in the onset of severe complications is an area of great interest.

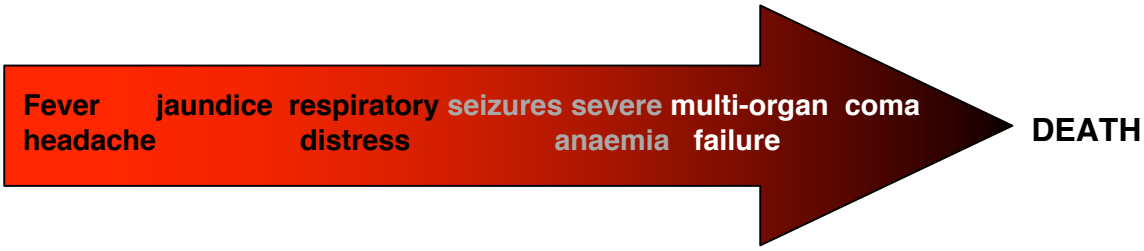

Fig. 1.9. Increasing severity of symptoms due to *P. falciparum* malaria.

Defining criteria of severe disease	
1. Cerebral Malaria	Unrousable coma
2. Severe normocytic anaemia	*Hae*matocrit < 15% or Hb < 5 g/dl
3. Renal failure	Urine output < 400 ml in 24 hr
4. Pulmonary failure/oedema	
5. Hypoglycaemia	Blood glucose < 40 mg/dl
6. Circulatory collapse, shock	Systolic blood pressure < 50 mm Hg
7. Spontaneous bleeding	E.g. from gums, nose, GI tract
8. Repeated generalized convulsions	> 2 convulsions within 24 hr
9. Acidaemia	Arterial pH < 7.25
10. Acidosis	Plasma bicarbonate < 15 mmol/litre
11. Malaria haemoglobinuria	
Other manifestations	
1. Imparied consciousness but rousable	
2. Prostration, extreme weakness	
3. Hyperparasitaemia	> 10% erythrocytes infected
4. Jaundice	Serum bilirubin > 3.0 mg/dl
5. Hyperpyrexia	Rectal temperature > 40°C.

Table 1.3. Severe malaria manifestions and complications of *P. falciparum* malaria in children. Adapted from World Health Organisation (2000).

1.4.2 Definitions of clinical childhood disease used in this analysis

i) Cerebral malaria

An unrousable coma (Blantyre coma score ≤ 2) in the presence of asexual parasitaemia, where all other causes of encephalopathy are excluded, defines cerebral malaria (WHO 2000). There are approximately half a million cases of cerebral malaria in African children every year, of which 10-30% are fatal and the pathology is associated with sequestration of parasitized erythrocytes in the cerebral microvasculature (MacPherson *et al.* 1985; White 1987; Brewster *et al.* 1990; Berendt *et al.* 1994a; Newton *et al.* 1998; Silamut *et al.* 1999). Sequestration is due to adhesion of infected erythrocytes to the cerebral microvasculature and mature trophozoites and schizonts are often seen at high concentration within the brain capillaries (MacPherson *et al.* 1985). In addition, due to the tightly packed nature of infected erythrocytes (in some areas of brain capillaries 100% erythrocytes can be infected), some young ring stage parasites can also become trapped within some vessels (Silamut *et al.* 1999). The coma is rapidly reversible, and only an estimated 7-12% patients are left with permanent neurological impairments. In these cases neural damage is possibly due to relatively rare development of focal lesions, or ring haemorrhages, within the cerebral hemisphere (Brewster *et al*. 1990; Newton *et al*. 1998). Widespread ischaemic damage appears to be avoided as the "sequestered" erythrocytes are not entirely static; the microvasculature obstruction is caused by "sludging" of a mass of infected cells which allows very slight oxygenation of the cerebral endothelium (White 1987). There is usually an absence of platelets and minimal fibrin deposition associated with the coma and large cerebral haemorrhages are uncommon (White 1987). Levels of inflammatory cytokines such as TNFα are

higher in cerebral malaria cases than uncomplicated cases in some studies, though the involvement of cytokines is inconsistent between reports, and immune damage is probably not significant in disease pathology in all cases (Kwiatkowski *et al.* 1990; Day *et al.* 1999; Newton *et al.* 2000). However, an increase in permeability of the blood brain barrier, due to activation of endothelial cells and activation of perivascular macrophages, may contribute to disease pathology in some cerebral malaria patients (Brown *et al.* 1999).

ii) Uncomplicated malaria

P. falciparum parasitaemia and fever with no signs or symptoms of severe disease (such as prostration, impaired consciousness or repeated convulsions, see Table 1.3), is defined as uncomplicated malaria. This condition is rarely fatal and recovery is rapid. This is a commonly used non-severe disease category in disease-association studies (Kirchgatter and Portillo Hdel 2002; Bull *et al*. 2005a; Kaestli *et al*. 2006; Rottmann *et al*. 2006).

iii) Hyperparasitaemia

If the parasite density of uncomplicated malaria (parasitaemia and fever with no signs or symptoms of severe disease) exceeds 500,000 parasites per microlitre of blood, the patient is classed as having hyperparasitaemia. This parasite density is equivalent to approximately 10% parasitaemia. Such an enormous parasite burden may be expected to cause severe disease manifestation, as severe malaria complications are associated with a high parasitaemia (WHO 2000; Rowe *et al*. 2002b). In Asia parasitaemia is directly correlated with severity and risk of death.

However, in Africa the prognosis for patients with hyperparasitaemia but no other symptoms of severe malaria is good (Lyke *et al*. 2003). Thus while high parasitaemia is associated with severe disease, hyperparasitaemia alone in Africa can be regarded as a form of uncomplicated malaria; perhaps such a high parasitaemia without other signs of severe disease indicates particularly non-virulent parasites. A comparison of cerebral and hyperparasitaemia patients is a more accurate comparison of parasite virulence than cerebral versus uncomplicated malaria, as there is no significant difference in parasitaemia. In this study uncomplicated malaria was thus defined as parasitaemia < 500,000 parasites/μl blood.

1.4.3 PfEMP1 and severe malaria in children

As PfEMP1 family proteins are surface exposed, and involved in immunomodulation, sequestration, and other adhesive phenotypes such as rosetting, they are prime candidates for involvement in disease manifestation.

Severe malaria has previously been associated with expression of a restricted and antigenically conserved subset of variant surface antigens (VSA) through field isolate agglutination studies (Bull *et al.* 1999; Bull *et al.* 2000; Nielsen *et al.* 2002). These reveal that VSA from isolates from patients with severe malaria (VSA severe malaria; VSA_{SM}) are commonly recognised by sera from semi-immune individuals. PfEMP1 associated with severe disease thus appear to be preferentially expressed in a naïve individual, thus being common targets for protective immunity. Increasing levels of VSA-specific antibodies are thought to then modulate the VSA repertoire available for expression in a semi-immune host.

This VSA_{SM} hypothesis was used to model severe malaria-phenotype parasites in a laboratory strain *in vitro*, by using bead-selection of parasites with sera from semi-immune children, and thus selecting for parasites expressing VSA that are commonly recognised (Jensen *et al*. 2004). Selecting 3D7 parasites in this fashion resulted in upregulation of many group A *var* genes, and downregulation of certain group C genes, suggesting an association of group A *var* genes and severe disease (Jensen *et al*. 2004). The pattern of *var* gene upregulation after selection on sera was similar to the level of upregulation seen after infection of volunteers with NF54 parasites (genotypically identical to 3D7), such that group A and B/A *var* genes expanded relatively quickly, and groups B, C, and B/C tended to be downregulated during the infection (Lavstsen *et al.* 2005).

Recent field isolate studies have so far failed to show a consistent link between *var* gene group and disease outcome, and data from different studies are conflicting, in part due to differences in disease classification and methods of analysis.

In Brazil, DBLα domains lacking 1-2 conserved cysteine residues (DBLα1 domains; probably group A PfEMP1) were more frequently expressed in patients with severe malaria than with uncomplicated malaria (Kirchgatter and Portillo Hdel 2002). Field isolates from Tanzania showed an upregulation of group A and B *var* gene transcription in severe malaria field isolates (Rottmann *et al*. 2006), while in Papua New Guinea, expression of group B *var* genes were associated with clinical malaria, both severe and mild (Kaestli *et al.* 2006). However, in Kenya no significant

association was found between *var* gene group and disease category, using DBLα domain sequence type as a marker of *var* gene group (Bull *et al.* 2005a). Thus there is a trend for group A PfEMP1 to be associated with severe malaria, and group C with asymptomatic parasitaemia. However, differences in the parasitaemia of the asymptomatic parasitaemia or "mild" disease field isolates with the severe malaria category make true associations with parasite virulence hard to determine. The diverse range of symptoms grouped in the different "severe malaria' categories confound the data making comparisons between studies difficult. In addition, disease manifestation differs between countries. For example, in South East Asia, multi-organ failure is relatively common, whereas cerebral malaria is not, and rosetting is not associated with severe disease (al-Yaman *et al.* 1995), possibly due to high prevalence of CR1 deficiency (Cockburn *et al.* 2004). PfEMP1 involvement in Asia may therefore be different from in Africa, where the association between rosetting and severe malaria is significant, and cerebral malaria is a common severe complication (Carlson *et al.* 1990; Rowe *et al.* 1995; Rowe *et al.* 2002c).

A consistent and compelling link between *var* group expression between *in vivo P. falciparum* infection and clinical disease manifestation has not previously been shown.

1.4.4 *P. falciparum* placental malaria

In malaria-endemic areas adults are usually clinically immune to malaria. However, pregnant women once again become susceptible to the disease, which is characterised by an accumulation of mature-stage erythrocytes in the placenta

(Beeson and Brown 2002). 50 million pregnancies are exposed to malaria each year (Steketee *et al*. 2001) and placental malaria is a major cause of infant morbidity and mortality, reduced birth weight and severe maternal anaemia, especially common in first pregnancies (Brabin *et al*. 1993). Pregnancy-associated immunosuppression was originally blamed for the susceptibility of pregnant women to the disease. However, it is now believed that the placenta provides a new niche for parasitic survival, which may be exploited by parasites that can display particular surface antigens. This is thought to be possible due to the presence of the glycosaminoglycan chondroitin sulfate A (CSA) displayed via the proteoglycan thrombomodulin on the syncytiotrophoblast cells of the placenta, which can act as a receptor for infected erythrocytes (Fried and Duffy 1996; Reeder *et al*. 2000). Infected placenta were observed to have higher CSA levels than uninfected, suggesting CSA-upregulation may occur, or that placenta with higher CSA levels are more likely to become infected (Muthusamy *et al.* 2007).

Resistance to placental malaria increases with gravidity alongside an increase in IgG which recognise erythrocytes displaying CSA-binding surface antigens (Fried *et al*. 1998; Ricke *et al*. 2000; Staalsoe *et al*. 2004). These antibodies also correlate with improved birth outcome (Duffy and Fried 2003; Staalsoe *et al*. 2004). Moreover, these antibodies recognise infected erythrocytes from different continents, suggesting there is a common mechanism for protection against placental malaria worldwide (Fried *et al*. 1998).

There has also been some evidence to suggest that other host molecules such as hyaluronic acid (HA) binding may also be an important placental receptor (Beeson and Brown 2004), though CSA is thought to be the major placental sequestration receptor (Fried *et al.* 2006; Muthusamy *et al.* 2007). Malaria during pregnancy thus comes about due to the placenta providing a new niche for parasitic survival, which may be exploited by the parasite by using a distinct repertoire of placenta-specific surface antigens.

1.4.5 PfEMP1 and placental malaria

The main candidates for binding to CSA are PfEMP1. Various DBLγ domains have been associated with CSA binding in placental isolates, and common DBLγ domain sequences have previously been reported within populations of pregnant women in Cameroon, Gabon and Kenya (Khattab *et al*. 2001; Fried and Duffy 2002; Khattab *et al*. 2003). Three main subfamilies of potential placenta-specific CSA-binding PfEMP1 have been identified: *var1csa* family (Buffet *et al*. 1999) (also called FCR3*var*CSA), *var2csa* (Salanti *et al*. 2003), and also the CS2*var* gene (Reeder *et al*. 1999), (reviewed in Rowe *et al.* 2004). *Var1csa*, is highly conserved (Rowe *et al*. 2002a; Salanti *et al*. 2002; Winter *et al*. 2003), and was initially a promising candidate for mediating CSA-binding, as antibodies raised to the DBL3γ domain were able to recognise many infected erythrocytes from CSA-binding parasite lines (Lekana Douki *et al*. 2002; Costa *et al*. 2003). However, transcription of *var1csa* (Fried and Duffy 2002; Winter *et al*. 2003) and CS2*var* (Duffy *et al.* 2006a) were not found to be consistently up-regulated in pregnancy-associated malaria, and CS2*var* is not well conserved between strains.

There is now strong evidence for *var2csa* playing a major role in placental malaria. *Var2csa* is expressed on the surface of CSA-selected parasites (Salanti *et al*. 2004) and directly binds CSA though its DBL3X domain, which is closely related to the 67 amino acid minimal CSA-binding region portion of FCR3-CSA DBL3-γ (Gamain *et al*. 2004; Gamain *et al*. 2005). VAR2CSA is consistently upregulated in laboratory isolates after selection for CSA-affinity, and VAR2CSA knock-out disrupts CSA-affinity (Salanti *et al*. 2003; Viebig *et al*. 2007). Interestingly, VAR2CSA does not contain a DBLγ domain (Gardner *et al*. 2002) which was surprising given the association of both VAR2CSA and DBLγ domains with placental malaria, though this can partially be explained by cross-reacting epitopes between VAR1CSA DBL3γ and VAR2CSA DBL3X (Bir *et al*. 2006).

A *var2csa* homologue has been identified in most strains and field isolates of *P. falciparum*; two *var2csa* homologues were found in HB3 (Trimnell *et al*. 2006; Kraemer *et al*. 2007).

The DBL6ε domain of VAR2CSA also binds non-specific IgM (Semblat *et al*. 2006), consistent with nonspecific IgM binding having a role in placental malaria (Flick *et al*. 2001; Creasey *et al*. 2003).

VAR2CSA is recognised by endemic plasma in a sex-specific and parity-dependent manner (Salanti *et al*. 2004) and *var2csa* transcription was detected in infected erythrocytes specifically from pregnant women from Senegal (Tuikue Ndam *et al*.

2005). Anti-VAR2CSA antibodies are present in pregnant women from East and West Africa (Salanti *et al*. 2004; Tuikue Ndam *et al*. 2006). Despite the antigenic variation between VAR2CSA from different isolates, these antibodies appear to be cross-reactive to different polymorphic versions of VAR2CSA, though are not always able to inhibit binding of diverse VAR2CSA to CSA (Beeson *et al*. 2006).

Literature to date thus consistently indicates an important role for VAR2CSA in placental malaria. However, there remains a lack of evidence of *var2csa* expression directly from field isolates, rather than from CSA-binding laboratory isolates. It is also unclear to what extent other PfEMP1 play a role in placental malaria. Field isolate data on relevance of *var2csa* in placental malaria is very important as *var2csa* is of great interest as a vaccine candidate against placental malaria.

1.5 Aims of the thesis

The general aim of the thesis was to investigate the role of conserved PfEMP1 subgroups as virulence factors in clinical disease in African field isolates from children (Mali and Kenya) and pregnant women (Malawi).

In the case of childhood disease, two approaches were taken to investigate PfEMP1 as a virulence factor. Firstly, transcribed *var* genes in childhood malaria field isolates from Mali were examined. *Var* gene groups were determined using DBLα domain transcript sequences as an indicator of *var* gene group of the transcribed *var* genes. The hypothesis was that there would be a difference in the pattern of transcription of *var* genes between the three clinical groups. It was hypothesised that there would be

a relatively higher level of group A *var* gene transcription in the cerebral malaria isolates compared to the hyperparasitaemia and uncomplicated malaria isolates, extrapolating from the *in vitro* work of Jensen *et al* (2004). The type 3 *var* gene family were not included in this analysis due to the primers used, and so were investigated separately in laboratory strains and field isolates. As they are also group A *var*, albeit atypically short and conserved, expression of type 3 *var* genes was also hypothesised to be different in the three clinical categories, with an expected association with cerebral malaria.

Secondly, a major contribution of PfEMP1 in severe disease in Africa is the binding of uninfected erythrocytes causing rosettes. Rosetting PfEMP1 form a functional subgroup of PfEMP1; they are predominantly group A (Rowe, JA, personal communication), and are possibly structurally conserved due to similar interactions with rosetting ligands. I spent two months in Kilifi, Kenya, examining rosetting field isolates. Unfortunately, there was insufficient material available to examine the expressed *var* genes responsible for rosetting in these field isolates. However, as well as understanding the molecular mechanism of rosetting, development of non-toxic compounds for rosette disruption is an important area of research. Attempts to identify rosette-disrupting compounds for auxiliary treatment of severe malaria complications caused by rosetting *P. falciparum* isolates have so far been troubled by the high anti-coagulant activity of candidate molecules. I was able to test the ability of a sulfated glycoconjugate compound, curdlan sulfate, to disrupt rosettes in a group rosetting *P. falciparum* field isolates.

In addition to work on childhood malaria isolates from Mali and Kenya, I also examined *var* gene transcription in a group of placental field isolates from Malawi. Specifically, I investigated transcription of DBLγ domains, and a well conserved *var* gene, *var2csa*. The hypothesis was that *var2csa* would be specifically and consistently transcribed in the placental isolates, but not in a comparison group of childhood malaria isolates, and that there might also be some differences in the sequence of DBLγ domain transcripts from placental and childhood malaria isolates.

My four results chapters address the following specific aims:

1. To compare *var* gene transcription in childhood malaria field isolates in three strictly defined clinical manifestation groups. DBLα domain transcripts, as indicators of *var* gene group, were analysed to test the hypothesis that a subset of *var* may influence clinical disease.
2. To analyse *var* gene transcription in placental malaria field isolates, investigating the involvement of a specific *var* gene, *var2csa*, and of conserved DBLγ domains in malaria during pregnancy.
3. To study *var* gene transcription and protein expression of the unusual, small and highly conserved type 3 *var* gene family.
4. To assess the anti-rosetting potential of a sulfated glycoconjugate compound, curdlan sulfate, on rosetting *P. falciparum* field isolates, as a potential therapeutic agent against severe malaria caused by rosetting *P. falciparum* strains.

Chapter 2

Materials and methods

2.1. Aim of chapter

This chapter describes general materials and methods that are relevant to more than one chapter of the whole thesis. Further detail of specific materials and methods used within each individual chapter is given within that chapter.

2.2 List of suppliers

All of the suppliers mentioned in this chapter and in the individual chapter specific material and methods sections are listed below.

Abcam, Cambridge, UK

Alpha Labs, Hampshire, UK

Ambion, Warrington, UK

Amersham, Buckinghamshire, UK

BDH, Poole, UK

Bio-Rad, Hertfordshire, UK

DNAstar, Inc, Madison, WI, USA.

Eurogentec, Seraing, Belgium

Gibco, now a division of Invitrogen, Paisely, UK

Invitrogen, Paisley, UK

MJ Research, Waltham, MA, USA

Pierce, Pierce Biotechnology Inc, Rockford, IL, USA

Promega, Southampton, UK

Qiagen, Sussex, UK

Roche, Hertfordshire, UK

Sigma, Dorset, UK

Vivascience, now Satorius Group, Surrey, UK.

2.3 Field isolate collection

2.3.1 Mali childhood malaria field isolates

Childhood malaria samples were collected as part of, and a gift from, the Bandiagara Malaria Project case-control study of severe malaria that has been described in detail previously (Lyke *et al*. 2003; Lyke *et al*. 2004). Blood samples were collected from children with malaria after informed consent from parents or guardians, and all protocols received institutional review board approval. Isolates were obtained from 26 patients with strictly defined disease criteria from the following 3 disease categories:

i) Cerebral malaria (9 isolates): Unrousable coma (Blantyre coma score ≤ 2) in the presence of asexual parasitaemia where other obvious causes of encephalopathy are excluded (WHO 2000).

ii) Uncomplicated malaria (9 isolates): *P. falciparum* parasitaemia and fever with no signs or symptoms of severe disease (such as prostration, impaired consciousness or repeated convulsions, see Table 1.3, introduction). In this study uncomplicated malaria patients were defined as having <500,000 parasites per microlitre of blood (approximately 10% parasitaemia), due to the hyperparasitaemia category (see below).

iii) Hyperparasitaemia (8 isolates): As uncomplicated but malaria parasite density exceeds 500,000 parasites per microlitre of blood.

The original isolate numbers were changed in the thesis for clarity. Appendix 1 provides a key for isolate reference numbers, and other isolate details.

2.3.2. Parasite cryopreservation of Mali field isolates

Parasites were prepared for freezing in Mali for long term storage in liquid nitrogen (Rowe, JA, Edinburgh). 1 volume glycerolyte (42.25% w/v glycerol, 0.1 M sodium lactate, 4 mM potassium chloride, 0.1 M sodium dihydrogen phosphate, pH 6.8) was added dropwise to 3 volumes packed cells, allowing cells to equilibrate osmotically for 5 minutes (min) at room temperature (RT) before dropwise addition of a further 4 volumes glycerolyte. Samples were incubated at –70ºC overnight (o/n) before storage in liquid nitrogen. A blood spot from each isolate was made on 3MM Whatman paper for genomic DNA extraction (see section 2.3.11). Frozen isolate samples and blood spots were then shipped to Edinburgh. Subsequent thawing of cryopreserved field isolate cultures was carried out by A. Raza, Edinburgh. Cells were thawed at 37ºC in a water bath, and 200 µl 12% NaCl was added dropwise over 5 min. After a further 5 min, 5 ml 1.8% NaCl was added dropwise, with gentle agitation of the cells, followed by 5 ml 0.9% NaCl with 0.2% glucose solution. Cells were then washed twice in incomplete RMPI: RPMI1640 medium (Invitrogen), supplemented with 25 mM HEPES, 20 mM glucose, 2 mM glutamine, 25 µg/ml gentamycin and 750 µl NaOH.

2.3.3 Mali field isolate maturation to pigmented-trophozoite stage

Field isolate ring stage parasite were cultured for 8–24 hours (hr) in complete RPMI: RPMI1640 medium (Invitrogen), supplemented with 25 mM HEPES, 20 mM glucose, 2 mM glutamine, 25 µg/ml gentamycin and 750 µl NaOH with 10% pooled normal human serum (Scottish Blood Transfusion Service, Edinburgh, UK). Flasks were gassed with 96% nitrogen, 3% carbon dioxide and 1% oxygen. The maturity of

the culture was regularly assessed by Giesma staining, until morphologically equivalent to 16-20 hr post-invasion in a laboratory strain.

2.3.4 Giemsa staining of thin blood smears

Approximately 10 µl of the culture at 20% haematocrit was placed onto a microscope slide and spread thinly with a clean microscope slide. Thin blood smears were air-dried, fixed with 100% methanol for 20 sec and air-dried again. Slides were immersed in 10% Giemsa stain solution (BDH) diluted in Giemsa buffer (prepared using Giemsa buffer tablets; BDH) for 15 min. Slides were then washed thoroughly with tap water and air-dried for light miscroscopy using a 40x and 100x objective lens under immersion oil (BDH).

2.3.5 Trizol treatment of parasites for RNA extraction

Parasites were pelleted (2000 rpm, 4 min), and as much supernatant as possible was aspirated away. Trizol reagent (Gibco) was warmed to room temperature, and 10 volumes of Trizol reagent was added to 1 volume packed cells. Cells were left at RT for 5 min, then stored at -70˚C.

2.3.6 Malawi placental field isolates

Mature sequestered placental parasites from pregnant women from Malawi were collected directly from *P. falciparum*-infected placenta on delivery, and stored immediately in Trizol before shipment to UK (gift from Stephen J. Rogerson). These were isolates P132, P134, P136, P143, P154 and CS294.

2.4 Molecular methods

2.4.1 RNA extraction

Parasites in Trizol reagent were thawed on ice. Two volumes chloroform were added per volume packed cells. The tube was shaken vigorously for 15 sec then left at RT for 3 min. The aqueous layer was separated from the phenol-chloroform phase by centrifugation (4000 rpm, 45 min, 4˚C). This upper aqueous layer was removed into a fresh tube and the RNA was precipitated by incubating with 0.5 ml isopropanol per ml of Trizol (RT, 10 min) before centrifugation to pellet the RNA (4000 rpm, 30 min, 4˚C). RNA was washed in 1 ml 70% ethanol prepared with DEPC-H_20 and precipitated again (4000 rpm, 10 min, 4˚C). The RNA pellet was air dried at RT for 10 min, redisolved in DEPC-H_20 (60˚C, 10 min) and stored at –70˚C. DEPC-H_20 was prepared by addition of 0.1% DEPC (diethyl pyrocarbonate) to high grade Millipore water overnight (o/n) at 37˚C then autoclaved to destroy the DEPC. Gloves were always worn and filter tips used when handling RNA.

2.4.2 DNase treatment

Any contaminating genomic (g) DNA in the RNA preparation was removed by treatment with 1.5 units DNase (Gibco) for 30 min at RT. 1.5 μl of 25 mM EDTA (10 min, 65 ˚C) was added to inactivate the DNase enzyme.

2.4.3 cDNA preparation

cDNA was then prepared using Superscript III First Strand Synthesis (Invitrogen) according to the manufacturer's instructions. 50 ng random hexamers, 1 nmol dNTP and 2 μl DEPC-H_20 was added to approximately 1 μg RNA. This was mixed gently,

and heated to 65ºC for 5 min. The mixture was left on ice for 2 min to cool. The mixture was split into two tubes: "Plus RT" (RT: reverse transcriptase) and "RT Contol" (to detect gDNA contamination in the RT-PCR reaction). 4 μl of 5x first strand synthesis buffer, 0.4 μmol DTT, 100 nmol $MgCl_2$ and 1 μl DEPC-H_20 was added to each, mixed gently and incubated (25˚C, 2 min). 0.5 μl Superscript III reverse transcriptase (RT) was added to each plus RT tube, or 0.5μl DEPC-H_20 added to control tubes. These were incubated at 25˚C for 10 min, 50˚C for 50 min and 85˚C for 15 min. The cDNA was then stored at –20˚C until use. cDNA from laboratory isolates (except 3D7) was a gift from JA Rowe.

2.4.4 PCR (polymerase chain reaction)

All PCR and RT-PCR reactions were carried out using amplitaq gold with 10x PCR Gold buffer (Promega) or Platinum taq and Platinum taq buffer (Invitrogen), with separate addition of $MgCl_2$ and dNTP as detailed in appropriate chapters. All PCR and RT-PCR reactions were performed in sterile 0.5 ml eppendorf tubes on a PCT-100 Peltier thermal cycler PCR machine (MJ Research). Primer sequences and amplification conditions are detailed in each chapter. For RT-PCR, samples without RT were used in all reactions to exclude gDNA contamination. A positive control (3D7 cDNA for RT-PCR and 3D7 gDNA for PCR, unless stated otherwise) and negative control (distilled water) were used in all PCR and RT-PCR reactions.

2.4.5 Agarose gel electrophoresis

All PCR and RT-PCR were examined by agarose gel eletrophoresis. Unless otherwise stated, 5 μl of PCR or RT-PCR products was loaded onto a 1.5% agarose

gel, prepared using 1.5 g electrophoresis grade agarose (Invitrogen), 10 ml UltraPure 10xTBE (1M Tris, 0.9 M Boric acid and 0.01M EDTA, Invitrogen) and 90 ml distilled water. DNA ladder, ϕX174 RF DNA/*Hae* fragments (Invitrogen), λ DNA/*Hin*DIII fragments (Invitrogen), or 100 bp DNA ladder (Invitrogen), was also loaded. Gels were run at 80 V for 45-60 min. After 25 min running time the gel was removed and stained in 0.5 μg/ml Ethidium Bromide (EtBr) for 5 min, before replacing in the gel tray for the remaining 20-40 min electrophoresis. DNA products were visualised under UV.

2.4.6 PCR/RT-PCR product purification

If only one band of the correct size was seen after agarose gel electrophoresis of a sample of the PCR/RT-PCR products, the rest of the reaction was purified using a QIAquick PCR Purification Kit (Qiagen). 5 volumes buffer PB was added to the PCR/RT-PCR products to promote binding to a QIAquick spin column. Non-bound liquid, salts and primers were washed through the column by spinning on a bench-top centrifuge (13,000 rpm, 1 min) and discarded. 750 μl wash buffer was added to the column to wash remaining impurities from the column upon spinning (13,000 rpm, 1 min). The flow-through was discarded and the column spun again to remove any residual ethanol. PCR/RT-PCR products were then collected in a fresh tube after addition of 50 μl elution buffer (10 mM Tris-Cl, pH 8.5) to the column and a final spin (13,000 rpm, 1 min).

If more than one band was seen, or primer dimers were also seen, PCR/RT-PCR products were purified using a QIAgen Gel Extraction Kit (Qiagen). A section of the

gel containing the correct PCR product was excised and melted in 3 volumes buffer QG Melted agarose, and then added to a spin column. Non-bound liquid, salts and primers were washed through the column by spinning on a bench-top centrifuge (13,000 rpm, 1 min) and discarded. Washing with wash buffer and elution was as for QIAquick PCR Purification Kit (Qiagen), described above.

2.4.7 Ligation and cloning

7 µl purified PCR product was ligated into 1 µl PCR II TA cloning vector (TA cloning kit, Invitrogen) using 4 units T4 DNA ligase and 1 µl ligation buffer (all from TA cloning kit, Invitrogen) o/n at 14°C. The resulting plasmids were used to transform One Shot TOP10F competent cells (Invitrogen). 2 µl ligated plasmid was mixed slowly into one vial of One Shot TOP10F competent cells, and the cells were incubated on ice for 30 min. Cells were heat shocked (30 sec, 42°C) followed by 2 min incubation on ice. Transformed cells were recovered in SOC media (Invitrogen), at 37°C for 1 hr with shaking. Plates prepared with Luria Bertani (LB) agar (Sigma) with 50 µl/ml ampicillin were covered in 40 µl each of 20 µg/ml X-gal and 20 µg/ml IPTG for blue/white screening. Transformed cells were plated out onto the LB agar plates and incubated o/n at 37°C. White colonies indicate an insert has disrupted the lacZ locus, whereas blue colonies indicate a re-ligated non-recombinant plasmid as the lacZ gene is active. Individual white colonies were selected for overnight culture in LB (Sigma) with 50 µl/ml ampicillin at 37°C.

2.4.8 Plasmid extraction

Plasmids were extracted from overnight cultures using a miniprep kit (Qiagen). Bacterial cells from overnight growth from individual plate colonies were pelleted (13,000 rpm, 3 min) and resuspended in 250 µl buffer P1. Cells were lysed 250 µl P2 buffer, and neutralised in 350 µl N3 buffer. Bacterial cell debris was removed by centrifugation (13,000 rpm, 10 min), and the supernatant containing the plasmid applied to a spin column. Spinning (13,000 rpm, 1 min) allowed non-bound liquid or remaining salts to flow through the column while the plasmid remained bound. Plasmids were washed in 750 µl wash buffer (13,000 rpm, 1 min). The flow-through was discarded and the column spun again to remove any residual ethanol. Plasmids were then collected in a fresh tube after addition of 50 µl elution buffer (10 mM Tris-Cl, pH 8.5) to the column and a final spin (13,000 rpm, 1 min).

2.4.9 *Eco*RI restriction enzyme digestion of plasmids

5 µl of the plasmid extraction in elution buffer was digested with 5 unit *Eco*RI (Promega) in a 10 µl reaction, containing 1 µl buffer H (Promega) and 0.2 5 µl BSA (Promega), which was incubated at 37°C for 1.5-2 hr. 5 µl of the digested plasmid preparation was visualised on a 1.5% agarose gel, prepared using 1.5 g electrophoresis grade agarose (Invitrogen), 10 ml UltraPure 10xTBE (1M Tris, 0.9 M Boric acid and 0.01M EDTA, Invitrogen) and 90 ml distilled water. Gels were run at 80 V for 45-60 min. After 25 min running time the gel was removed and stained in EtBr (0.5 µg/ml) for 5 min, before replacing in the gel tray for the remaining 20-40 min electrophoresis. DNA products were visualised under UV.

2.4.10 Sequencing

Plasmids containing an insert were sequenced. 5 μl of BigDye terminator reaction mix (Applied Biosciences) and 1.6 pmol sequencing vector VR1 (AGATGCATGCTCGAG CGG) or VF1 (ACGTCGGATCCACTAGTA) was added to 5 μl of the miniprep plasmid preparation containing an insert. The mix was incubated for 25 cycles of 96°C for 30 sec, 50°C for 15 sec and 60°C for 4 min in sterile 0.2 ml eppendorf strips on a PCT-100 Peltier thermal cycler PCR machine (MJ Research). Sequencing was carried out by the University of Edinburgh School of Biological Sciences Sequencing Service.

2.4.11 DNA extraction

For genotyping, parasite DNA was extracted from blood spots on filter paper using chelex-100 extraction (Plowe *et al.* 1995). A small square of blood spot filter paper was soaked in 0.5x saponin in PBS o/n at 37 ºC. This was centrifuged (6000 rpm, 3 min) and the liquid removed. The filter paper was washed with fresh 1x PBS and re-pelleted (6000 rpm, 3 min). The liquid was removed as this contains haem and other debris. 50 μl chelex suspension and 100 μl DEPC-H_20 was added. This was boiled (100ºC) for 8 min. The upper layer, above the chelex suspension contains the gDNA. Genomic DNA is also present in the RNA extract before DNase1 treatment. An aliquot of RNA was used for PCR of gDNA for PCR of upstream regions.

2.4.12 Genotyping

The minimum number of genotypes per isolate was estimated by genotyping PCR with primers to the size-variant genes MSP1 and MSP2 (Ranford-Cartwright *et al.*

1993). Each PCR was nested. Primer sequences for MSP1 outer PCR: O1 (CACATGAAAGTTATCAAGAACTTGTC) and O2 (GTACGTCTAATT CATTTGCACG). Primer sequences for MSP1 inner PCR: N1 (GCAGTATTGACAGGTTATGG) and N2 (GATTGAAAGGTATTTGAC). Primer sequences for MSP2 outer PCR: S2 (GAGGGATGTTGCTGCTCCACAG) and S3 (GAAGGTAATTAAAACATTGTC). Primer sequences for MSP2 inner PCR: S1 (GAGTATAAGGAGAAGTATG) and S4 (CTAGAACCATGCATATGTCC). All PCR reactions included 5 μl 10x PCR Gold buffer, 25 pmol each of forward and reverse primers and 0.2 μl Amplitaq Gold polymerase with a final concentration 1.875 mM $MgCl_2$, and 1.25 mM of each dNTP, and the volume adjusted to 50 μl after addition of template DNA. For outer PCRs, the DNA template was 5 μl chelex extracted gDNA. For inner (nested) PCRs, the DNA template was 3 μl of the outer PCR product. MSP1 outer and inner PCR cycle conditions were 94ºC 5 min, then 30 cycles of 94ºC for 25 sec, 50ºC for 35 sec, 68ºC for 90 sec, followed by a 10 min extension at 68ºC and cooling to 4ºC. MSP2 outer and inner PCR cycle conditions were 94ºC 5 min, then 30 cycles of 94ºC for 5 sec, 50ºC for 15 sec, 65ºC for 1 min, followed by a 10 min extension at 65ºC and cooling to 4ºC. PCR products were run 8% on Novex Pre-cast TBE Polyacrylamide gels (Invitrogen) at 200 V, 1 hr. with Novex TBE Running buffer (Invitrogen). Gels were soaked in EtBr (0.5 μg/ml) and visualised under UV.

2.5 Sequence analysis

2.5.1 Grouping of sequences into contigs

Sequences were analysed using Lasergene software (DNAstar, Inc). Contigs were

created with a minimum percentage match of 95% to classify sequences for each isolate using SeqMan (DNAstar, Inc). Nucleotide sequences were translated into amino acid sequence using EditSeq (DNAstar, Inc). Protein sequences were aligned using the ClustalW method within MegAlign (DNAstar, Inc) and the alignment converted into a nucleotide alignment with Tranalign (http://bioweb.pasteur.fr/docs/EMBOSS/tranalign.html). Phenograms were then created from nucleotide or amino acids sequences within MegAlign (DNAstar, Inc). The sequences were also aligned using Muscle (Edgar, *et al*, 2004) for creation of the network (Graham Stone, Appendix 2). All phenograms are intended to give a measure of sequence similarity rather than to suggest evolutionary descent.

2.5.2 Homology searches

Homology searches were performed using nucleotide-nucleotide BLAST search of the NCBI database (http://www.ncbi.nlm.nih.gov/BLAST). Default parameters were used, apart from restricting the taxon to *P. falciparum* (taxon 5833). The Sanger *P. falciparum* Blast server http://www.sanger.ac.uk/cgibin/blast/submitblast/p_falciparum, Plasmodb *Plasmodium* genome resource http://www.plasmodb.org/plasmo/home.jsp and the Broad Institute HB3 and Dd2 sequencing data http://www.broad.mit.edu were also used.

2.5.3 Amino acid sequence identity analysis

Each set of sequenced domains (DBLα in chapter 3, DBLγ/var2csa DBL3X in chapter 4 and type 3 DBLα and DBLε in chapter 5) were aligned at the amino acids level using clustal W within Megalign (DNAstar, Inc). The percentage sequence

identity was recorded into a table. The sequence identity figures within the table were colour-coded into the following groups; 0-30, 30-39.9, 40-49.9, 50-59.9, 60-69.9 70-99.9 and 100% amino acid identity. Sequences were split into various sub-categories, such as disease manifestation, or DBLα0 versus DBLα1, and the figures were repeated. This provided a pictorial illustration of general trends of the level sequence similarities between and within the different groups of *var* gene domains. Histograms and box plots of percentage sequence identity were then created in Statview, using the amino acid identity data from MegAlign (2.5.3).

2.6 Long term culture and manipulation of *P. falciparum*

2.6.1 Culture procedures

All processes were carried out in a laminar flow hood, which was regularly cleaned with detergent and 70% ethanol. Aseptic techniques were used throughout, and all plastics and slides used in the handling of parasites were decontaminated with 1% virkon (Alpha Labs). Parasites were cultured in complete RPMI: RPMI1640 medium (Invitrogen) containing 25 mM HEPES, supplemented with 20 mM glucose, 2 mM glutamine, 25 μg/ml gentamycin and 750 μl 1M NaOH with 10% pooled normal human serum (Scottish blood Transfusion service, Edinburgh, UK). Flasks were gassed with 96% nitrogen, 3% carbon dioxide and 1% oxygen. Cultures were maintained at 1-10% parasitaemia by addition of fresh group O blood cells approximately every 48 hours as appropriate. Blood was prepared firstly through removal of white blood cells and buffy coat by centrifugation (4000 rpm, 15 min) and washing twice in incomplete RPMI: RPMI1640 medium (Invitrogen) containing 25 mM HEPES, supplemented with 20 mM glucose, 2 mM glutamine, 25 μg/ml

gentamycin and 750 µl 1M NaOH, before resuspension at 50% haematocrit in incomplete RMPI. Blood was stored at 37ºC until required and was used for up to 10 days. Cultures were maintained at 2% haematocrit at 37ºC in complete RPMI and were regularly assessed by Giemsa stained thin films (section 2.2.4). This culture method is standard (Trager and Jensen 1976). Preparation for long-term storage in liquid nitrogen was carried out as outlined in section 2.2.2 on cryopreservation.

2.6.2 Sorbitol synchronization of *P. falciparum* infected erythrocytes

Cultures were regularly synchronised using sorbitol (Sigma) to lyse the mature stages by osmotic lysis (Lambros and Vanderberg 1979). Parasites younger than 20 hr post invasion are resistant to sorbitol lysis as they are impermeable to sorbitol. Thus sorbitol treatment leaves only ring stage parasites in the culture. Parasite cultures were pelleted (2000 rpm, 4 min). Culture medium was removed and the cell pellet resuspended in 5 ml of 5% (w/v) D-sorbitol (Sigma) and incubated at 37˚C for 15 min. Cells were then pelleted again (2000 rpm, 4 min), and washed twice with 10 ml of RPMI 1640 medium and returned to standard culture conditions.

2.6.3 Enrichment of pigmented trophozoite and schizont infected erythrocytes

Pigmented trophozoite and schizont stages were enriched by gradient separation using using Percoll (colloidal silica particles coated with polyvinylpyrrolidone) which creates smooth, isometric gradients (Sigma, UK). Cell cultures were pelleted (2000 rpm, 4 min) and resuspended in a 5 ml of RPMI 1640 medium without serum, and carefully layered on top of 5 ml 30% percoll in a 15 ml falcon tube. The tube

was centrifuged (4000 rpm, 15 min). Pigmented trophozoite and schizont infected erythrocytes form a clear layer above the sediment of uninfected and ring stage parasite infected erythroctyes, which fall to the bottom of the tube. The upper layer containing pigmented trophozoite and schizont infected erythrocytes was transferred to a fresh tube, washed twice with 10 ml of RPMI-1640 and re-pelleted (2000 rpm, 4 min), and returned to standard culture condition with fresh complete RPMI and washed group O erythrocytes.

2.6.4 Enrichment of rosetting pigmented trophozoite and schizont infected erythrocytes

Pigmented trophozoite infected erythrocyte cultures were selected for high rosetting parasites by gradient separation using using Percoll (Sigma, UK). Cell cultures were pelleted (15 min, 4000 rpm) and resuspended in a 5 ml of RPMI 1640 medium without serum, and carefully layered on top of 5 ml 30% percoll in a 15 ml falcon tube. The tube was centrifuged (5 min, 1800 rpm). Non-rosetting pigmented trophozoite infected erythrocytes form a clear layer above the sediment of uninfected and rosetting pigmented trophozoite stage infected erythroctyes, which fall to the bottom of the tube. The upper layer containing pigmented trophozoite and schizont infected erythrocytes was removed by aspiration. The lower layer of rosetting and non-infected erythrocytes was washed twice with 10 ml of RPMI-1640, re-pelleted (2000 rpm, 4 min), and returned to standard culture condition with fresh complete RPMI and washed group O erythrocytes.

2.6.5 Gametocyte preparation

Gametocytogenesis was induced in a culture of 6% rings, by increasing the haematocrit to 5% and incubating in partially spent complete RPMI media (2:3 ratio fresh:used complete RPMI) followed by incubating at 37 ºC for 32 hr. After 32 hr the media was changed for fresh complete RPMI. The media was changed again after a further 48 hr. After a further 24 hr, gametocyes were present at 0.5-1% at stage II-IV by microscopy. Gametocytes were purified using a gradient of percoll (52.5%, 45%, and 30% percoll in incomplete RPMI) in a 15 ml corex glass tube, which was spun at 10,000 rpm, 10 min, RT. Gametocytes form a separate layer above the uninfected cells and ring stage-infected erythrocytes, and the fraction containing the gametocytes was collected. Most schizont and pigmented trophozoite-infected erythrocytes also form a separate layer from the gametocytes. Remaining schizont and pigmented trophozoite-infected erythrocytes in the gametocyte fraction were destroyed by sorbitol lysis. Trizol was added to the gametocye preparation and RNA extracted as section 2.2.5.

2.6.6 Laboratory isolates used in this study

Laboratory strains are single genotype parasite clonal populations, which have been adapted to culture *in vitro*. For the majority of *P. falciparum* laboratory strain analysis, strain 3D7 was used as it has been fully sequenced and annotated, available from http://www.plasmodb.org. All other *P. falciparum* strains used are listed (Table 2.2). Isogenic strains are indicated.

Strain	Origin
NF54 [a]	Schipol Airport
3D7[a]	NF54
FCR3[b]	SE Asia
IT[b]	SE Asia
R29[b]	SE Asia

A1R[b]	SE Asia
Palo Alto[b]	SE Asia
TM267[b]	SE Asia
TM180	Thailand
HB3	Honduras
Malayan Camp	Thai-Malaysian border
Dd2	Indochina
7G8	Brazil
Muz12	Papua New Guinea

Table 2.2. Laboratory strains used in this thesis and worldwide origin (Mu *et al.* 2005). [a]3D7 and NF45 are isogenic. [b] FCR3, IT, R29, A1R, Palo Alto and TM267 are also isogenic.

2.7 Statistical methods

Stastistical analysis was done with StatView 5.0.1 software. Student's t-tests were used to compare normally distributed data from two groups with roughly equal variance, including parasitaemia of isolates and age of patients at time of the infection. ANOVA were also used to back up t-test results when multiple t-tests were used to compare different data sets from a single experiment. Chi-squared tests were used to compare distribution of observed data compared to a null hypothesis, such as DBLα1/DBLα0 expression. Kruskal Wallis (non-parametric) tests were used to compare non-normal data such as rosette frequency. Correlations were assessed by Spearman Rank correlation.

Chapter 3

Var gene transcription and childhood malaria disease manifestation

Some of the results presented in this chapter were published as

Kyriacou, HM *et al*. (2006). Differential *var* gene transcription in *Plasmodium falciparum* isolates from patients with cerebral malaria compared to hyperparasitaemia. Molecular and Biochemical Parasitology 150(2):211-8.

3.1 Abstract

P. falciparum field isolates from Mali were used to test the hypothesis that transcription of a subset of the total *var* gene repertoire was associated with severe clinical disease outcome. Using DBLα domain as an indicator of *var* gene group, an association was found between group A *var* gene transcription and disease manifestation. Children with cerebral malaria disease (coma) showed significantly higher levels of group A *var* gene transcription than a control group of children with equally high parasite burden but no signs or symptoms of severe disease. This provides evidence for the importance of expressed PfEMP1 in disease pathogenesis. The link demonstrated here between DBLα1-type DBLα domains and severe disease also has potential implications in future drug and vaccine design, for example suggesting that DBLα1 rather than DBLα0 may provide a better target for vaccine development to tackle severe malaria disease.

3.2 Introduction

3.2.1 *P. falciparum* severe disease in Africa

Children under 5 years old in sub-Saharan Africa bear the majority of disease and mortality due to *P. falciparum* malaria infection (WHO 2000), and many distinct severe disease syndromes can develop upon infection (discussed in chapter 1). Cerebral malaria, coma due exclusively to *P. falciparum* infection associated with sequestration of parasitized erythrocytes in the cerebral microvasculature, is a relatively common severe disease manifestation in Africa, occurring in approximately half a million children per year with a 10-30% mortality (MacPherson *et al.* 1985; White 1987; Brewster *et al.* 1990; Berendt *et al.* 1994a; Newton *et al.* 1998; Silamut *et al.* 1999). During the rainy season in malaria-endemic areas, over 70% of children can be infected with an asymptomatic parasitaemia (Bejon *et al.* 2007). Malaria fever without severe complications is defined as "uncomplicated" malaria disease, and is commonly used as a control population for severe disease-association studies (Kirchgatter and Portillo Hdel 2002; Bull *et al.* 2005a; Kaestli *et al.* 2006; Rottmann *et al.* 2006). In addition, some children in Africa have been observed to withstand a surprisingly high parasitaemia (10% erythrocytes infected), with no severe disease complications. This condition is rare in low transmission areas such as Asia or South America, where disease severity is linked more directly with parasitaemia. Parasite isolates from these children provide a good control group for a study of parasite virulence in severe clinical disease isolates, with any effect of parasitaemia being removed.

3.2.2 PfEMP1 and severe disease

The surface-exposed multigene polymorphic PfEMP1 protein family, encoded by *var* genes mediate immunomodulation, sequestration, and other adhesive phenotypes, and are key candidates for modulating pathology of an infection. PfEMP1 are classified into three main groups A-C and two intermediate groups B/A and B/C (see chapter 1). This classification is based on chromosomal position, direction of transcription, and the upstream region of the *var* genes, and so potentially separates genes on the basis of different promoter regions. The classification also splits genes into two broad groups. Group A and B/A tend to have a complex domain structure with 4-7 DBL domains and a CIDRα1 domain which does not have affinity for CD36 (Robinson *et al.* 2003). Group B, C or B/C PfEMP1 in general are shorter commonly with only 2 DBL domains and 2 CIDR domains, including a CIDRα which typically has affinity for CD36 (Gardner *et al.* 2002; Robinson *et al.* 2003; Kraemer *et al.* 2007).

Restricted and antigenically conserved subsets of variant surface antigens (VSA) have previously been associated with severe disease through field isolate agglutination studies, termed VSA "severe malaria", VSA_{SM} (Bull *et al.* 1999; Bull *et al.* 2000; Nielsen *et al.* 2002). PfEMP1 family variants are obvious targets for investigation of this observation.

A link between group A PfEMP1 and severe disease was suggested by Jensen *et al* (2004) through transcription analysis of severe malaria-phenotype parasites produced by bead selection of parasites on sera from semi-immune children. A link between

group A *var* gene expression and severe disease was also indicated by a small field isolate study in Brazil (Kirchgatter and Portillo Hdel 2002), though other studies in Papua New Guinea, Tanzania and Kenya have shown conflicting results (Bull *et al*. 2005a; Kaestli *et al*. 2006; Rottmann *et al*. 2006). These differences may be partly explained by differences in disease classification and methods of analysis, as well as differences in disease manifestation (see introduction for more detail). This study set out to examine *var* gene transcription in three carefully defined disease manifestation groups.

3.2.3 *Var* gene DBLα domain analysis

The PfEMP1 DBLα domain is the most well conserved DBL domain type. Almost all sequenced *var* genes to date contain a DBLα domain, including 59 of the 60 3D7 *var* genes, the exception being members of the *var2csa* family (Gardner *et al*. 2002). Two relatively conserved sections flanking a 400 bp highly polymorphic stretch allowed primers to be designed to recognise and amplify most DBLα domains through polymerase chain reaction (PCR) (Taylor *et al*. 2000a; Bull *et al*. 2005a). In 3D7, 56/59 DBLα domains are recognised by these primers with an unbiased distribution. Unfortunately, type 3 *var* genes cannot be amplified by these primers as the reverse primer site is not recognised (see chapter 5). Reverse transcriptase (RT)-PCR of these primers on RNA from an isolate should amplify all of the non-type 3 DBLα domain transcripts present.

PfEMP1 domain sequences can be aligned and compared phylogenetically, using a phylogenetic tree building progam (Smith *et al.* 2000b; Kraemer and Smith 2003;

Lavstsen *et al.* 2003). DBLα sequences can also be split into the two groups DBLα0 and DBLα1, on the basis of 2 conserved cysteines in the amplified tag (Table 1.1, introduction). In addition, domains can be further sub-classified into 6 DBLα groups (Table 3.1, Fig. 3.1) (Bull *et al.* 2005a; Bull *et al.* 2007).

Group	Cysteines in tag	PoLV1	PoLV2	DBLα type
1	2	MFK*	Non-*REY	DBLα1
2	2	Non-MFK*	*REY	DBLα1
3	2	Non-MFK*	Non-*REY	DBLα1
4	4	ND	Non-*REY	DBLα0
5	4	ND	*REY	DBLα0
6	≠ 2 or 4	ND	ND	-

Table 3.1. DBLα group definitions from Bull *et al.* (2005). PoLV; position of limited variation. *Any amino acid. ND: Not defined at this position. Group 6 includes DBLα0 and DBLα1 domains.

In addition, the upstream region sequence can be used to identify *var* gene group (see section 3.5.5). The three methods of *var* gene analysis/classification used in this chapter are represented in Fig. 3.1.

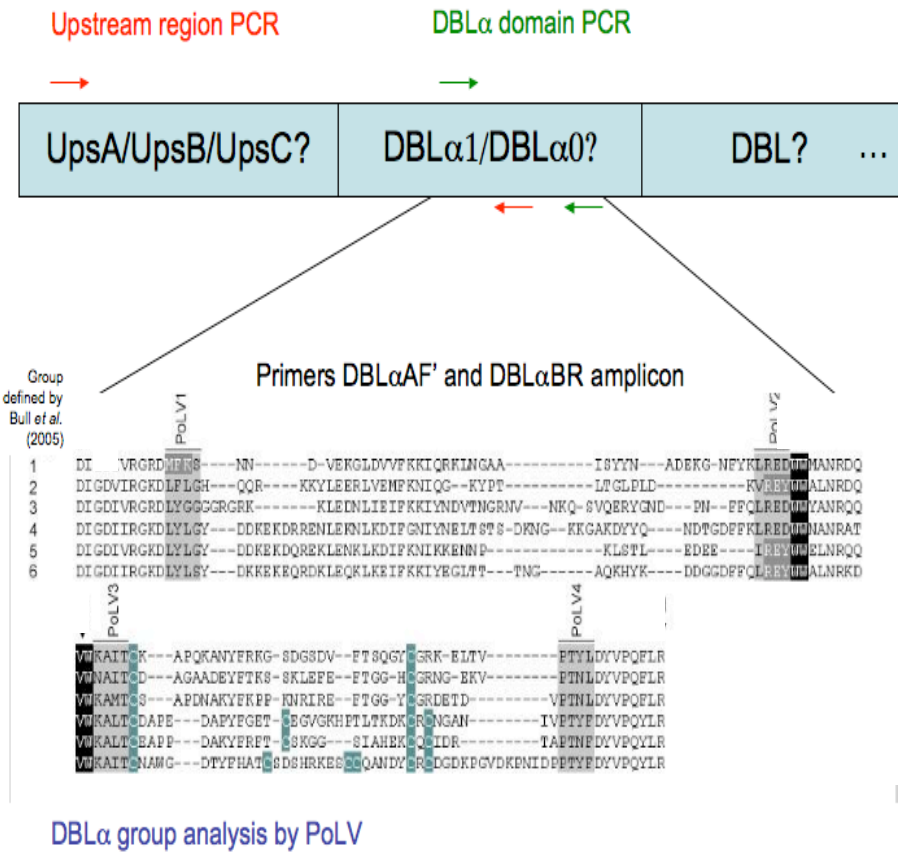

Fig. 3.1. The three methods of *var* gene analysis/classification. Green: DBLα sequence analysis from PCR using degenarate primers DBLαAF' and DBLαBR (Taylor *et al*. 2000a; Bull *et al*. 2005a) to amplify a variable section of the DBLα domain. Blue: DBLα sequence grouping into DBLα groups 1-6 using positions of limited variation (PoLV) (Bull *et al.* 2005a; Bull *et al.* 2007). PoLV1-4 are indicated within the DBLαAF' and DBLαBR amplicon; adapted from Bull *et al*. (2007). Red: Upstream sequence analysis from PCR of upstream region (UpsA, UpsB or UpsC) from PCR using a generic upstream region forward primer and DBLα domain-specific reverse primer; more detail given in section 3.5.5.

3.2.4 *Var* gene analysis: DBLα domains as indicator of *var* gene group

The 3D7 genome and the recently sequenced HB3 and IT genomes provide data on common *var* gene structures, allowing assumptions to be made about the architecture of a *var* gene on the basis of DBL domains present (Gardner *et al.* 2002; Kraemer *et al.* 2007). In this chapter, analysis of DBLα domain sequence, and subsequent classification of the domains into DBLα1 domain or DBLα0 domain, allows assumptions to be made on the group of *var* gene transcribed, and thus PfEMP1 group expressed. Presence of a DBLα1 domain indicates a group A or B/A PfEMP1. Conversely, presence of a DBLα0 domain indicates a group B, C or B/C PfEMP1, see chapter 1 for more details.

3.3 Aim of chapter

Variable surface antigens are prime candidates for influencing the pathogenesis of infection, as they mediate immuno-modulation and sequestering within the host. This chapter focuses on a *var* gene transcription profiling study of *P. falciparum* childhood malaria field isolates, with the aim of indentifying if there was a link between expressed *var* gene group and disease manifestation.

3.4 Materials and methods

Materials and methods that are specific to chapter 3 are listed below. General materials and methods and a list of suppliers are given in chapter 2.

3.4.1 Field isolate collection

Childhood malaria samples from cerebral malaria (9), uncomplicated malaria (9) and hyperparasitaemia (8) were collected as part of, and a gift from, the Bandiagara Malaria Project case-control study of severe malaria (Lyke *et al*. 2003; Lyke *et al*. 2004) as described in chapter 2. Cerebral malaria is defined as unrousable coma (Blantyre coma score ≤ 2) in the presence of asexual parasitaemia where all other causes of encephalopathy are excluded (WHO 2000). Uncomplicated malaria and hyperparasitaemia are both defined as *P. falciparum* parasitaemia and fever with no signs or symptoms of severe disease (such as prostration, impaired consciousness or repeated convulsions, see Table 1.3, introduction). However, hyperparasitaemia is additionally defined as parasite density exceeding 500,000 parasites per microlitre of blood (approximately 10% parasitaemia), thus in this study uncomplicated malaria patients were defined as having <500,000 parasites per microlitre of blood.

Parasites were cryopreserved in Mali, thawed in Edinburgh, and cultured for 8-24 hr, to early pigmented trophozoite stage as described in chapter 2. RNA was extracted and cDNA prepared as described in chapter 2.

3.4.2 RT-PCR conditions

Reverse-transcriptase (RT)-PCR was used to amplify a region of 300-400 bp of the *var* DBLα domain using unbiased degenerate primers DBLα AF' GCACG(A/C)AGTTT(C/T)GC and DBLαBR GCCCATTC(G/C)TCGAACCA (Taylor *et al*. 2000a; Bull *et al*. 2005a). These primers are capable of amplifying the entire *var* gene repertoire of 3D7 apart from the strain-transcending *var2CSA* gene

implicated in malaria in pregnancy as this gene has no DBLα domain (detailed discussion in chapter 4), and the 'type 3' *var* gene family members, which have atypical DBLα1 domains, of which there are three in 3D7 (detailed discussion in chapter 5). Amplification used 5 µl 10x PCR Gold buffer, 25 pmol each of DBLαAF' and DBLαBR primers and 0.2 µl Amplitaq Gold polymerase with a final concentration 2 mM $MgCl_2$, and 1.25 mM of each dNTP, and the volume adjusted to 50 µl after addition of 2 µl cDNA (or distilled water). Amplification conditions were as described (Taylor *et al.* 2000a; Bull *et al.* 2005a) with a hot start (95˚C, 5 min) followed by 35 cycles of 95˚C, 20 sec; 42˚C, 20 sec; 60˚C, 1 min. Samples without RT were used in all reactions to exclude gDNA contamination. 2 µl 3D7 cDNA was used as a positive control, and distilled water as a negative control.

See chapter 2 for details of ligation, cloning, transformation, and sequencing of RT-PCR products. In brief, RT-PCR products were visualised by electrophoresis on 1.5% agarose gels. RT-PCR products were purified and ligated into PCR II TA cloning vector (Invitrogen) and ligated plasmids were used to transform *E. coli*. Transform *E. coli* was grown overnight under ampicillin selection and blue/white colony screening. Individual colonies were selected for overnight growth and the plasmids extracted for sequencing. Presence of an insert in the extracted plasmid preparations was verified by *Eco*RI restriction digestion prior to sequencing. Sequencing was carried out by the University of Edinburgh School of Biological Sciences Sequencing Service.

3.4.3 Transcript sequence analysis

Transcript sequences from each isolate were grouped into contigs of >95% nucleotide identity using the SeqMan programme within the DNAstar software package. Consensus sequences from each isolate were defined as sequence A, B, C etc from that isolate as EditSeq files (DNAstar software package), and protein sequences were obtained by translating the DNA sequences using the Editseq translation function. Nucleotide and protein sequences were then compared within and between isolates using MegAlign (DNAstar software package). Alignments and phenograms were produced using the clustal W alignment programme within MegAlign, using default settings. Sequence distances were calculated using MegAlign, and colour-coded in Excel into the following groups; 0-30, 30-39.9, 40-49.9, 50-59.9, 60-69.9, 70-99.9 and 100% amino acid identity for production of sequence distance figures. Homology searches were performed using nucleotide-nucleotide BLAST search of the NCBI database (http://www.ncbi.nlm.nih.gov/BLAST). Pie charts were created in Excel. Phenograms were laid out in Adobe Illustrator. Histograms and boxplots were created in Statview.

3.4.4 *Var* gene upstream region PCR

Upstream PCRs were carried out on gDNA with each of 4 upstream primers, UpsA TATTYHATKTATTAYATTTGTTGTA, UpsB GTTAGAACATTTAAAATTATA, UpsC1 AVAGAWATATGRTAGATAYAG and UpsC2 ACAAACATAGTGAC TACC based on sequences from 3D7, and a gene-specific reverse primer (Table 3.2) for each isolate dominant *var* gene DBLα domain, and for laboratory isolates Palo Alto, TM180 and A1R. Amplification used 5 μl 10x PCR Gold buffer, 25 pmol of an

upstream primer, 25 pmol of a downstream primer and 0.2 µl Amplitaq Gold polymerase with a final concentration 2 mM $MgCl_2$, and 1.25 mM of each dNTP, and the volume adjusted to 50 µl after addition of 0.5 µl gDNA from the RNA preparation (or distilled water). Amplification conditions were 35 cycles of 94˚C, 5 sec; 46˚C, 15 sec; 60˚C, 2 min. 0.25 µl gDNA (3D7 unless otherwise stated) was used as a positive control, and distilled water as a negative control. RT-PCR products were obtained for 22 isolates. The remaining 4 isolates (Hyp6, HYP8, U1 and U4) were not studied due to lack of parasite material. PCR product were purified, ligated into PCR II vector (Invotrogen) and used to transform *E. coli* for colony picking, plasmid extraction and sequencing as described chapter 2. The upstream sequence of the predominant *var* gene from 9 isolates was studied. The remaining upstream sequences were not obtained due to problems with cross-reactivity of the "specific" primer with other DBLα domains (13 isolates).

Isolate/strain	Isolate predominant domain	Upstream PCR domain specific reverse primer sequence
CM1	CM1A	CTT ACT TTA GGT AGT GG
CM2	CM2A	AAC AAT CGT TGT ATT ACT CGC
CM3	CM3A	TTT GAA TGG GCT TGA TTT
CM4	CM4A	TGT ATT AGT CGA AGA TGT TCC
CM5	CM5A	ATG AAT TCC CCT GTT GTT
CM6	CM6A	ACC ATC ATA ATC ACT TAT TTG
CM7	CM7A	AAC TCC ATT TGG TTT ATA TAC
CM8	CM8A	CTT GAC TTG TAA AAA CAT CAC
CM9	CM9A	CAC CAT TTT TAT CTT GGT
HYP1	HYP1A	TTT TTC AGT CCA ACT ATC GTT
HYP2	HYP2A	TTT CCA CCA TTT TTA TCT TGG
HYP3	HYP3A	TTT CAC ATA TTT AGC TAC TCC
HYP4	HYP4A	TTG GTC TCT ATT AGC GTT
HYP5	HYP5A	GTC CTT CGT CAA ATC ACC
HYP6	HYP6A	ND
HYP7	HYP7A	TTC ATC CTG AAT CTT CTG

HYP8	HYP8A	ND
U1	U1A	ND
U2	U2A	TCT AGC CAT AGA TGG ACT TTC
U3	U3A	ACC ATC ATA ATC ACT TAT TTG
U4	U4A	ND
U5	U5A	GAA TAT ATA TCA CCT TGC TCT
U6	U6A	CCT TTG GAG CTT TG
U7	U7A	TTT TTG TCA TTG TCA TTG TAG
U8	U8A	CTG CTA GCC TGT TGT CGT
U9	U9A	TTG AGC ATC TTT TAG CTT GTT
Palo Alto	PARvar1	GTT CTT GTA CTT TAG GTG A
TM180	TM180var1	TAA ATT GGT AAG AAC GGC TCC TTG
A1R	A1Rvar1	CAT TCT TCC CTC TCG T

Table 3.2. Reverse primer sequences for upstream regions PCR for the predominant gene from each isolate. ND: Not designed due to lack of parasite material.

3.4.5 Statistical analysis

Statistical analysis was done with StatView 5.0.1 software. Student's t-tests were used to compare normally distributed data from two groups with roughly equal variance (patient age, isolate parasitaemia, number of genotypes in each isolate). Kruskal Wallis (non-parametric) tests were used to compare non-normal data (isolate rosette frequency and transcription frequency of the six DBLα groups in the different clinical categories). Chi-squared tests were used to compare distribution of observed data with a null hypothesis, such as DBLα1/DBLα0 expression levels. Fisher's Exact Test was used to compare the predominant gene per isolate for DBLα1/DBLα0 type. A 3x6 contingency table was used to compare the number of transcripts classified into the 6 DBLα domains groups proposed by Bull *et al.* (2005) in each clinical manifestation group. Correlations between DBLα1% and age, parasitaemia and rosette frequency were assessed by Spearman Rank correlation.

3.5. Results 1: DBLα domain transcription analysis in Malian childhood field isolates

3.5.1 Malian childhood malaria field isolate details

Field isolates were obtained from 26 children with strictly defined conditions of uncomplicated (9) or cerebral malaria (9), or hyperparasitaemia (8) from Bandiagara, Mali, as part of a case-control trial study (Lyke *et al.* 2003; Lyke *et al.* 2004). The aim of the study was to examine *var* gene transcription within these isolates, using degenerate primers to DBLα domains to amplify DBLα domain transcripts by RT-PCR.

Before this was done it was important to assess the 26 field isolates to check that there were no significant differences in age and parasitaemia between the groups which may influence the data. No significant difference in patient age was seen across the three clinical categories (Fig. 3.2A, Table 3.3; t-test, $p > 0.45$), probably due to age matching in the study group from which these isolates were taken. Cerebral and hyperparasitaemia isolates did not differ significantly in parasitaemia (t-test, $p = 0.83$). Both had significantly higher parasitaemia than the uncomplicated isolates (Fig. 3.2B, Table 3.3; $p > 0.001$).

In addition to age and parasitaemia, data on the rosette frequency and level of platelet-mediated clumping within each isolate was also available. Cerebral isolates showed significantly higher rosette frequency than both other categories (Fig. 3.2C, Table 3.3; $p = 0.03$), as expected in isolates from Africa (Carlson *et al.* 1990; Rowe *et al.* 1995; Rowe *et al.* 2002b). Only 4 isolates showed platelet-mediated clumping

(PMC; Fig. 3.2D), including the only cerebral isolate in which there were no rosettes, CM8 (PMC 53%, RF 0). Low PMC levels meant that comparison of the disease categories was not significant, though the data has been analysed elsewhere, showing an association between parasitaemia and PMC levels, though not with disease severity *per se* (Arman *et al*, 2007).

Furthermore, field isolates can comprise multiple infections. To assess the number of genotypically distinct infecting parasite strain within each isolate, the number of distinct genotypes in each isolate was estimated by PCR of size-variant genotype markers MSP1 and MSP2 (see materials and methods). Multiple distinct genotypes were present in many isolates (range 1-5, Table 3.4). There was no significant difference in number of genotypes between the three clinical categories (t-tests, $p > 0.48$, Table 3.3).

This data is also shown in Appendix 1, which shows a table of all data regarding the Mali childhood isolates discussed in the thesis.

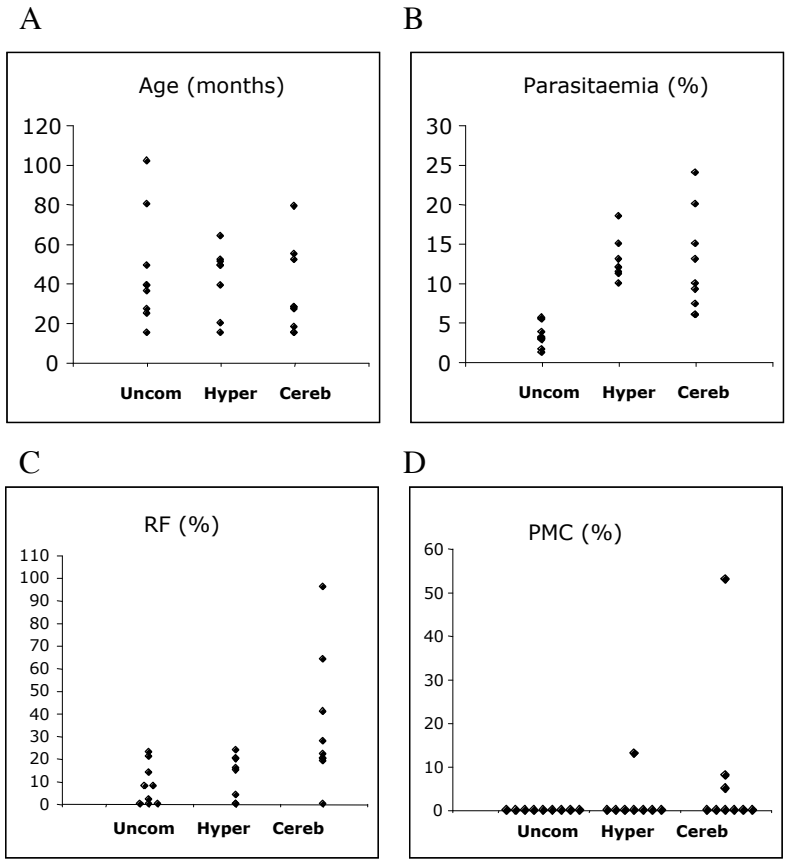

Fig. 3.2. Individual isolate details for the 26 Malian childhood *P. falciparum* malaria field isolates studied showing A) age, B) parasitaemia, C) rosette frequency (RF; percentage of infected erythrocytes bound by ≥ 2 uninfected erythrocytes) and D) platelet-mediated clumping frequency (PMC; percentage of infected erythrocytes bound by ≥ 2 uninfected erythrocytes upon addition of platelets).

Malaria disease category	Age (months) (mean ± SD)	Parasitaemia (%) (mean ± SD)	Rosette frequency [a] (%) (median: 25th, 75th percentiles)	Genotypes (mean:range)
Uncomplicated	45.8 ± 28.0	3.3 ± 1.5	8.0 : 0, 15.8	2.4 (1-4)
Hyperparasitaemia	42.5 ± 16.9	11.9 ± 3.9	9.5 : 0, 18.0	2.6 (1-4)
Cerebral	35.2 ± 22.0	12.3 ± 6.3	22.0 : 19.8, 46.8	2.2 (1-5)
P values	P > 0.45[b]	P = 0.83 H:C [c] P < 0.001 U:C/H	P = 0.03 [d]	P > 0.48 [e]

Table 3.3. Combined data from all isolates within each disease category

[a]% of mature-stage infected erythrocytes that bind 2 or more uninfected erythrocytes.

[b]Uncomplicated:cerebral p = 0.46, uncomplicated:hyperparasitaemia p = 0.72, cerebral:hyperparasitaemia p = 0.68, t-test.

[c] H: hyperparasitaemia; C: cerebral malaria; U: uncomplicated malaria. t-test.

[d]Kruskal Wallis test.

[e]Uncomplicated:cerebral p = 0.72, uncomplicated:hyperparasitaemia p = 0.72, cerebral:hyperparasitaemia p = 0.49, t-test.

Uncomplicated isolates		Cerebral isolates		Hyperparasitaemia isolates	
Isolate	Genotypes	Isolate	Genotypes	Isolate	Genotypes
U1	4	CM1	1	HYP1	4
U2	3	CM2	3	HYP2	3
U3	3	CM3	3	HYP3	1
U4	3	CM4	5	HYP4	2
U5	3	CM5	1	HYP5	3
U6	1	CM6	3	HYP6	3
U7	3	CM7	1	HYP7	3
U8	1	CM8	1	HYP8	2
U9	1	CM9	2		
Range Mean	1 to 4 2.4	Range Mean	1 to 5 2.2	Range Mean	1 to 4 2.6

Table 3.4. Estimated number of distinct genotypes present per isolate for each isolate on the basis of PCR of size-variant markers MSP1 and MSP2.

3.5.2 DBLα RT-PCR technique

The aim of this chapter was to investigate the transcribed *var* genes in Malian *P. falciparum* malaria field isolate by examining the sequence and relative frequency of transcribed DBLα domains by RT-PCR. There was not enough parasite material to perform real-time RT-PCR for quantitative analysis of the DBLα domain transcripts in each isolate, so RT-PCR was quantified by colony analysis.

RNA was extracted from the 26 field isolates, and cDNA was prepared. DBLα transcripts were amplified from cDNA by RT-PCR using degenerate primers to DBLα domains (Taylor *et al*. 2000a; Bull *et al*. 2005a). An aliquot of products from

each RT-PCR reaction was visualised on a 1.5% agarose gel. Fig. 3.3 shows a representative gel; the amplified DBLα RT-PCR products from isolates HYP1, HYP3 and HYP5 are seen as bands of approximately 400 bp. Multiple bands can be seen, representing multiple DBLα domain transcripts of slightly different length.

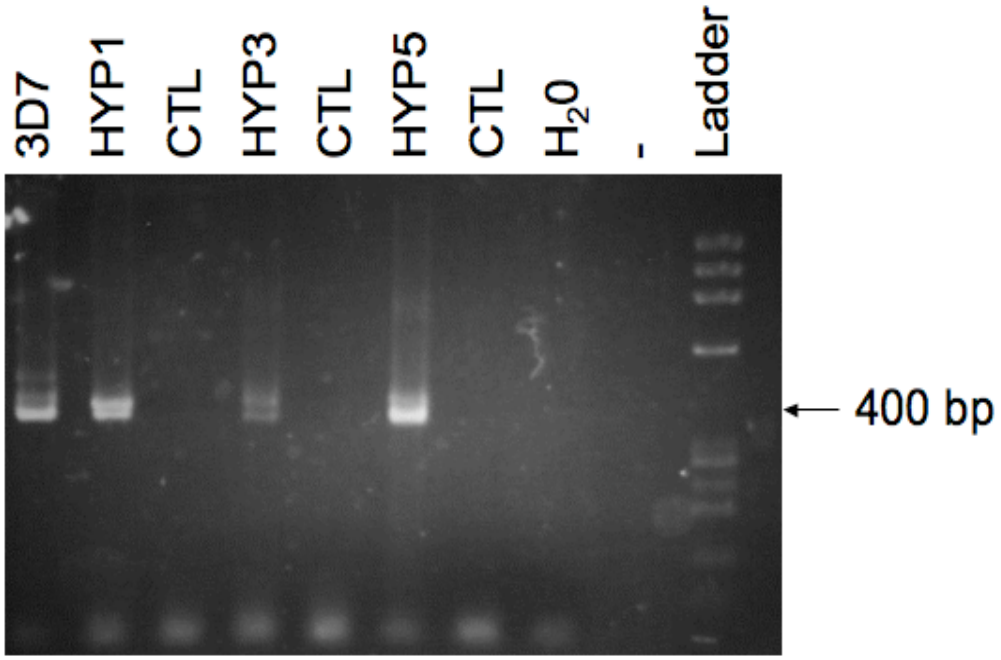

Fig. 3.3. Representative gel of DBLα domain RT-PCR products from Mali field isolates. RT-PCR products from amplification of DBLα domains from cDNA from Mali field isolates HYP1, HYP3 and HYP5, with primers DBLαAF' and DBLαBR, were visualised by electrophoretic separation on a 1.5% agarose gel. Reverse transcriptase negative cDNA preparation control (CTL) for each isolate reveal PCR products from gDNA contamination, and are next to the cDNA amplification for each isolate. These lanes remain blank indicating there is no gDNA contamination in the cDNA preparation. 3D7 cDNA was used for a positive control, and distilled water as a negative control for the PCR reaction. DNA ladder was ϕX174 RF DNA/*Hae* fragments (Invitrogen).

These DBLα RT-PCR products were then purified and ligated into plasmids. These recombinant plasmids were used to transform *E. coli*, which were plated onto LB agar/ampicillin plates and grown up overnight at 37°C. Ampicillin in the plates selected for growth of transformed bacteria, and blue-white screening allowed bacterial colonies containing a recombinant plasmid to be selected. 14-19 white bacterial colonies were selected for expansion in LB broth at 37°C, and after approximately 18 hours a number of recombinant plasmids from colonies from each RT-PCR were extracted using a QIAgen miniprep kit. The presence of an insert of the correct length was confirmed by enzymatic digestion of the multiple cloning site using restriction enzyme *Eco*RI of a sample of each extracted plasmid. Digested plasmids were visualised on 1.5% agarose gels, and plasmids containing an insert were marked by presence of an approximately 400 bp band. Fig. 3.4 shows a typical gel.

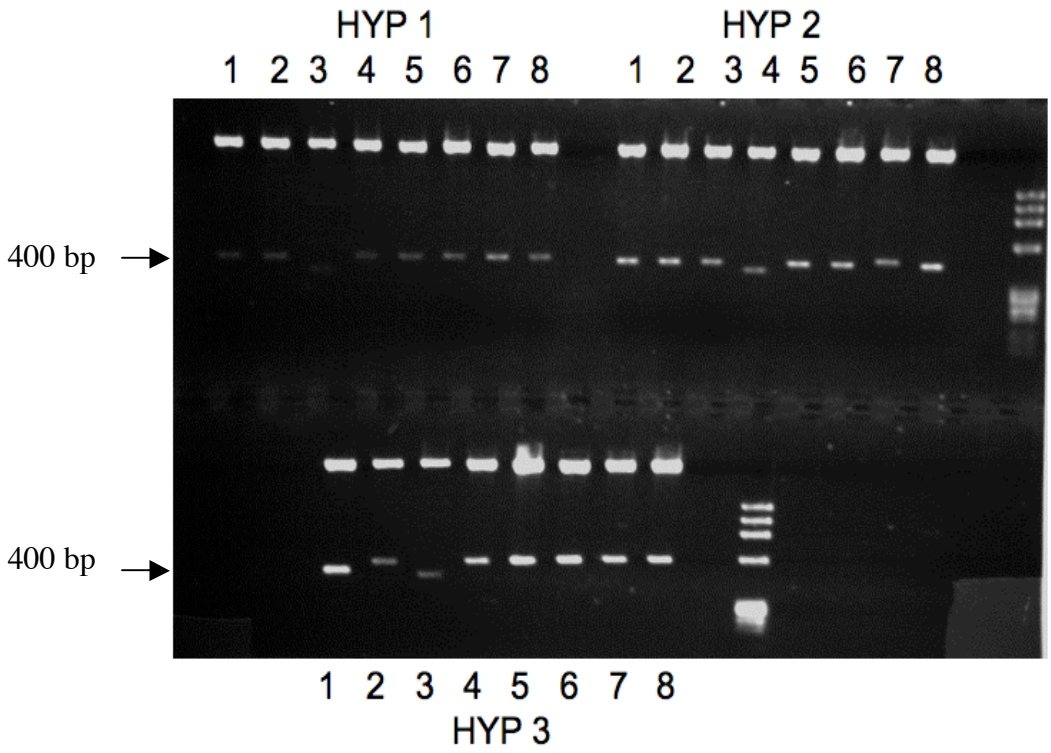

Fig. 3.4. A typical 1.5% agarose gel of *Eco*RI digests products of plasmids extracted from a set of minipreps. Plasmid preparations were digested in *Eco*RI for 1.5-2 hr at 37ºC. In this case 8 minipreps from 3 isolates HYP1, HYP2 and HYP3 are shown, all of which had inserts of approximately 400 bp. DNA ladder was ϕX174 RF DNA/*Hae* fragments (Invitrogen).

The inserted DBLα domain tags in purified plasmids from each isolate RT-PCR transformation were sequenced, using a primer site just upstream of the multiple cloning site on the vector.

The RT-PCR colony picking analysis technique described above is summarised in Fig. 3.5.

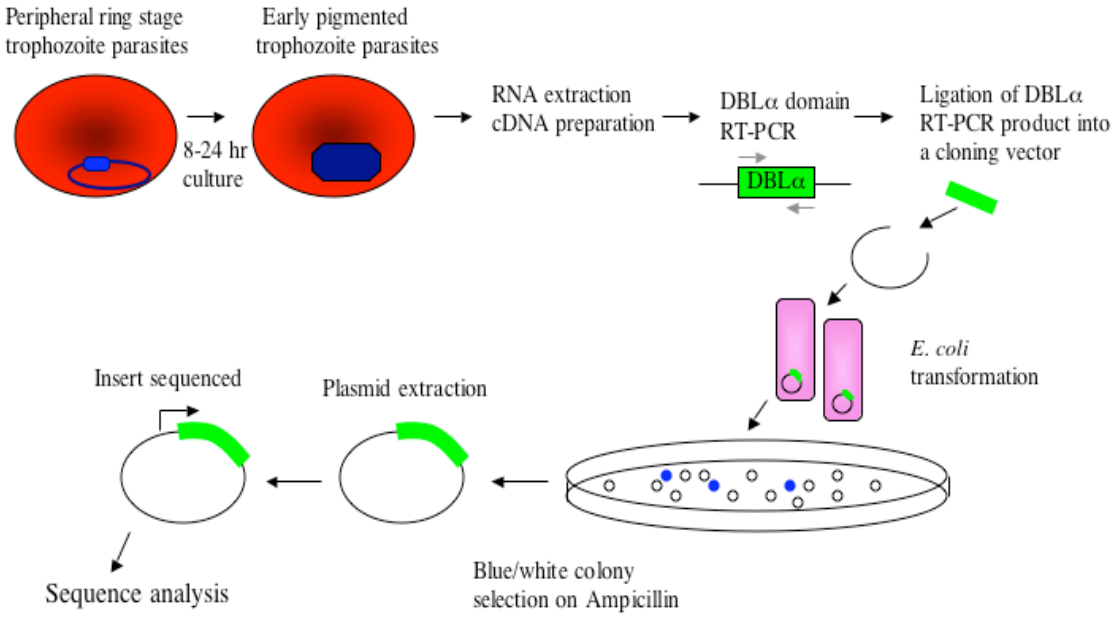

Fig. 3.5. Schematic diagram of RT-PCR colony picking analysis technique.

3.5.3 DBLα RT-PCR validity

In the first instance, I investigated the validity of my approach by sequencing inserts in 16-17 "blue" colonies derived from each of 3 field isolate. To determine if sampling a larger number of plasmids would influence the results of the study, colony picking was repeated, picking 50 further colonies for two of the isolates, CM7 and CM9 (Fig. 3.6, colony pick repeat column). In addition, to determine whether the RT-PCR results were representative and repeatable, RT-PCR, cloning and sequencing was repeated from a separate RT-PCR reaction from the same RNA extraction from three isolates, CM4, CM7 and CM9 (Fig. 3.6, RT-PCR repeat column).

In all cases, the same predominant sequence was obtained from the second amplification, supporting RT-PCR analysis from a lower number of sequences. For CM9, the same two sequences were obtained in similar ratio in all three analyses (15:1, 42:8 and 14:1 respectively). For CM4, the dominant domain was seen at a similar frequency in both RT-PCR (15:1:1 and 12:1), but a different minor sequence was seen in the second RT-PCR reaction. For CM7, a more complex pattern of gene expression was seen, with a total of 10 different minor domains obtained, though the dominant sequence remained consistent, and there was some overlap in the minor domain transcripts (Fig. 3.6; colours represent the same sequence).

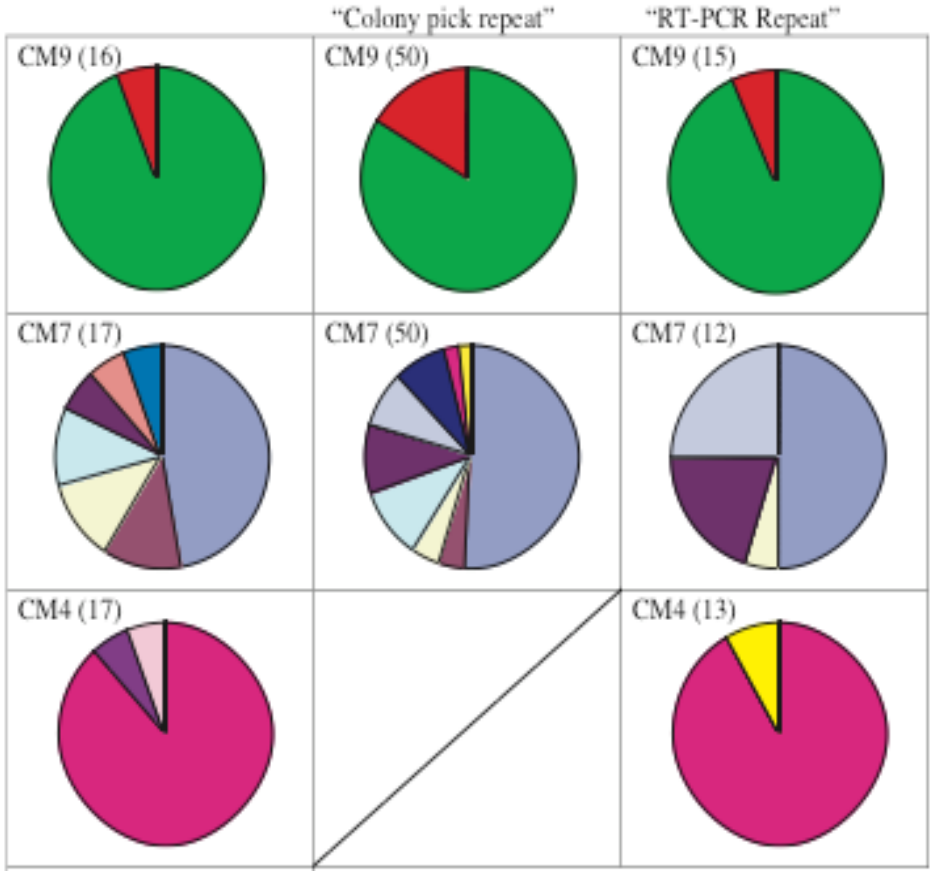

Fig. 3.6. RT-PCR validation. The pie charts represent the frequency of transcripts sequenced from miniprep plasmids from three isolates, CM9, CM7 and CM4. For each isolate the same colour represents the same unique sequence. Left: 16-17 plasmids sequenced from bacteria transformed with ligation products from an RT-PCR reaction. Middle: a further 50 plasmids were sequenced from the same plate of bacteria transformed with the ligation products from the original RT-PCR reaction. Right: 12-15 plasmids were sequenced from bacteria transformed with ligated plasmids from a new RT-PCR reaction from the orignial cDNA preparation.

3.5.4 Transcribed DBLα domains in childhood malaria field isolates

Having established that the technique was valid, 14-19 minipreps from plates of transformed bacteria carrying plasmids representing DBLα *var* gene transcript from each of the remaining 23 Malian childhood field isolates were sequenced. Sequences from each isolate were compared using SeqMan software. Identical or almost identical sequences from the same isolate (>95% identity) were defined as isolate sequence A, B, C etc in order of abundance (Genbank accession numbers DQ367086-DQ367226).

The relative abundance of the different DBLα sequences for each isolate is shown in Fig. 3.7. Here, pie charts represent the total repertoire of DBLα transcripts detected by RT-PCR, with the area of the pie slices representing the relative levels of abundance of each DBLα sequence from colony picking analysis. The number of colonies picked for plasmid sequencing is also shown.

In addition, DBLα domains can be defined as either DBLα1 or DBLα0 on the basis of conserved cysteines (DBLα1-like genes have 2 cysteines in the amplified tag, and DBLα0-like genes have 4 cysteines in the amplified tag; Table 1.1). Sequences are coloured as DBLα1 (white) or DBLα0 (black) in Fig. 3.7.

UNCOMPLICATED	CEREBRAL	HYPERPARASITAEMIA
U1 (15) 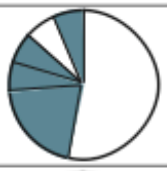	CM1 (18) 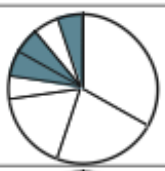	HYP1 (15) 
U2 (15) 	CM2 (14) 	HYP2 (15) 
U3 (17) 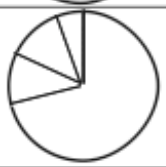	CM3 (14) 	HYP3 (18) 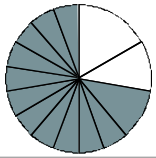
U4 (15) 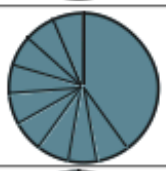	CM4 (17) 	HYP4 (15) 
U5 (19) 	CM5 (18) 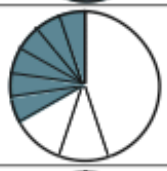	HYP5 (15) 
U6 (19) 	CM6 (17) 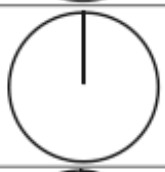	HYP6 (16) 
U7 (16) 	CM7 (17) 	HYP7 (16) 
U8 (18) 	CM8 (19) 	HYP8 (17) 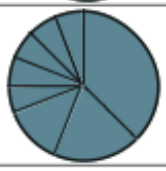
U9 (14) 	CM9 (16) 	

Fig. 3.7. Frequencies of distinct DBLα sequences in each isolate. The pie charts represent the relative number of different DBLα sequences detected in each isolate by RT-PCR, cloning and analysis of 14-19 mini-prep clones per isolate. For each isolate, each pie-slice represents a different sequence, and the size of each pie-slice represents relative abundance of transcript. Isolate name is in the top left corner of each box. Bracketed numbers indicate the exact number of mini-prep clones sequenced for each isolate. Shading indicates DBLα0-like (grey) or DBLα1-like (white) sequences.

The number of sequences per isolate varied between 1 and 14 (Fig. 3.7). There was no significant difference in the number of distinct DBLα sequences per isolate detected in each clinical category (cerebral malaria: median 5, range 1-9; hyperparasitaemia: median 6.5, range 2-14; uncomplicated malaria: median 4, range 2-10, $p = 0.72$, Kruskal-Wallis test).

The frequency of DBLα1-like *var* gene transcripts within each clinical manifestation group was analysed (Fig. 3.8). There was a highly significant difference in the frequency of DBLα1-like *var* gene transcripts within the cerebral malaria isolates (80.1%) compared to the hyperparasitaemia isolates (25.7%; $p < 0.001$, Chi-squared test). 40.5% of the sequences from the uncomplicated malaria patients were DBLα1-like. The frequency of DBLα1-like *var* gene transcripts in both cerebral and hyperparasitaemia was significantly different from in uncomplicated isolates ($P < 0.005$, Chi-squared test) which showed intermediate DBLα1-like *var* gene transcription.

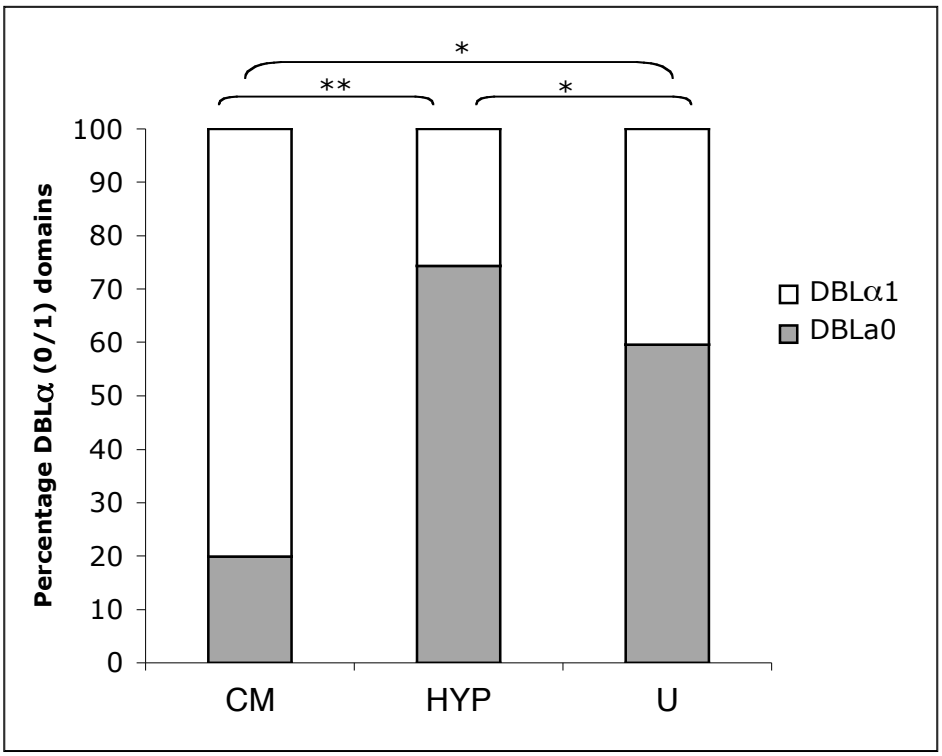

Fig. 3.8. Percentage of DBLα0 (grey) and DBLα1 (white) transcripts detected across the 26 Malian field isolates separated by disease category cerebral (C), hyperparasitaemia (HYP) and uncomplicated malaria (U). *There is a significant difference in DBLα1 proportion between cerebral and uncomplicated isolates, and between hyperparasitaemia and uncomplicated isolates (both $p < 0.005$, Chi-squared test). ** There is also a significant difference in DBLα1 proportion between cerebral and hyperparasitaemia isolates ($P < 0.001$, Chi-squared test).

If only the predominant gene from each isolate was examined, a marked difference remained between the cerebral malaria and hyperparasitaemia isolates. The predominant gene in 8/9 isolates from cerebral malaria patients was DBLα1-like, whereas the predominant gene in 6/8 hyperparasitaemia isolates was DBLα0-like (Fig. 3.9, DBLα0- specific cysteines boxed). This difference is significant (Fisher's Exact test, p = 0.013). For uncomplicated malaria isolates, the predominant gene was DBLα1-like in 5/9 isolates and DBLα0-like type in 4/9 isolates, not significantly different from the cerebral or hyperparasitaemia isolates (U:HYP, P=0.29; U:CM P=0.13, Fisher's exact test).

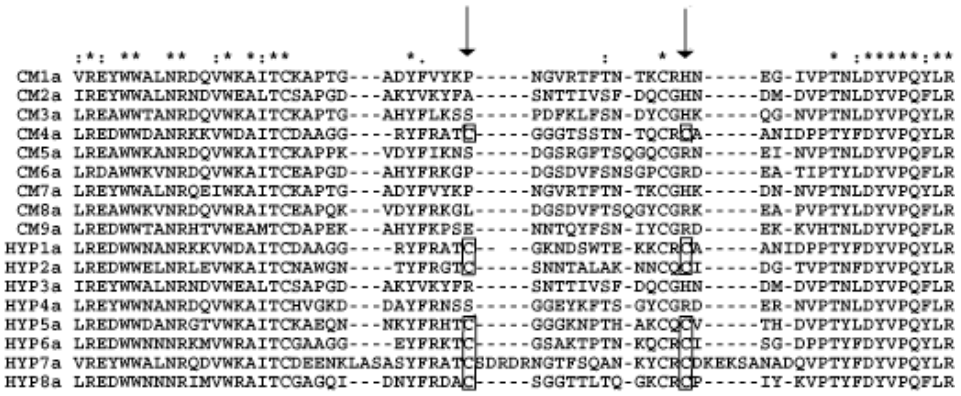

Fig. 3.9. Clustal W alignment of the predominant DBLα domains gene transcript in *P. falciparum* isolates CM1-9 from cerebral malaria patients and HYP 1-8 from hyperparasitaemia patients. The second half of the expressed sequence tag is shown and the position of the residues that distinguish DBLα0-like domains (cysteines present) from DBLα1-like domains (cysteines missing) are arrowed, and the cysteine residues are boxed. Symbols: * indicates conserved residues; : indicates conservative substitution; . indicates semi-conservative substitution.

DBLα domains can be separated into 6 groups according to sequence motifs in the expressed sequence at positions of limited variation as well as the number of cysteine residues (Bull *et al.* 2005a), as described in Table 3.1. Group 1 domains have 2 cysteines in the amplified tag and the sequence MFK* at a particular locus defined as PoLV1. Group 2 domains also have 2 cysteines in the amplified tag and have *REY at a second locus defined as PoLV2. Group 3 domains contain neither MFK* or *REY, but also have 2 cysteines in the amplified tag. Group 4 and 5 domains have 4 cysteines in the amplified tag. Group 4 domains do not contain *REY at PoLV2 whereas group 5 domains do. Group 6 domains have 1,3,5 or more cysteines in the amplified tag.

Under these definitions, DBLα1 domains are Bull groups 1-3 and DBLα0 domains are groups 4 and 5. Group 6 are atypical domains with 1, 3, or >5 cysteines in the amplified tag and can be DBLα1 or DBLα0 domains. Examination of the Mali sequences classified into these six DBLα domain sequence groups did not reveal any further differences between the three disease categories (Fig. 3.10). As expected, most of the genes transcribed in the isolates from cerebral malaria patients are in groups 1-3 (DBLα1), and isolates from hyperparasitaemia patients mostly transcribe *var* genes in groups 4 and 5 (DBLα0). The isolates from uncomplicated malaria patients show an intermediate pattern with 4 isolates mostly transcribing groups 1-3 (DBLα1) and 5 isolates mostly transcribing groups 4 and 5 (DBLα0). Transcription frequencies of the six different DBLα groups in the different clinical categories are significant (P = 0.049, Kruskal Wallis test). A 3x6 contingency table was also used

to compared the number of transcripts classified into the 6 DBLα groups. For data in the three clinical groups combined, the distribution of reads in each group is significantly different (P<0.001). Seven group 6 sequences described by Bull *et al* (number of cysteines ≠ 2 or 4) were detected, none of which were transcribed at high level, and all of which could be classified as either DBLα1 or DBLα0. Neither of the extra 2 cysteines found in DBLα0 was ever present alone.

A

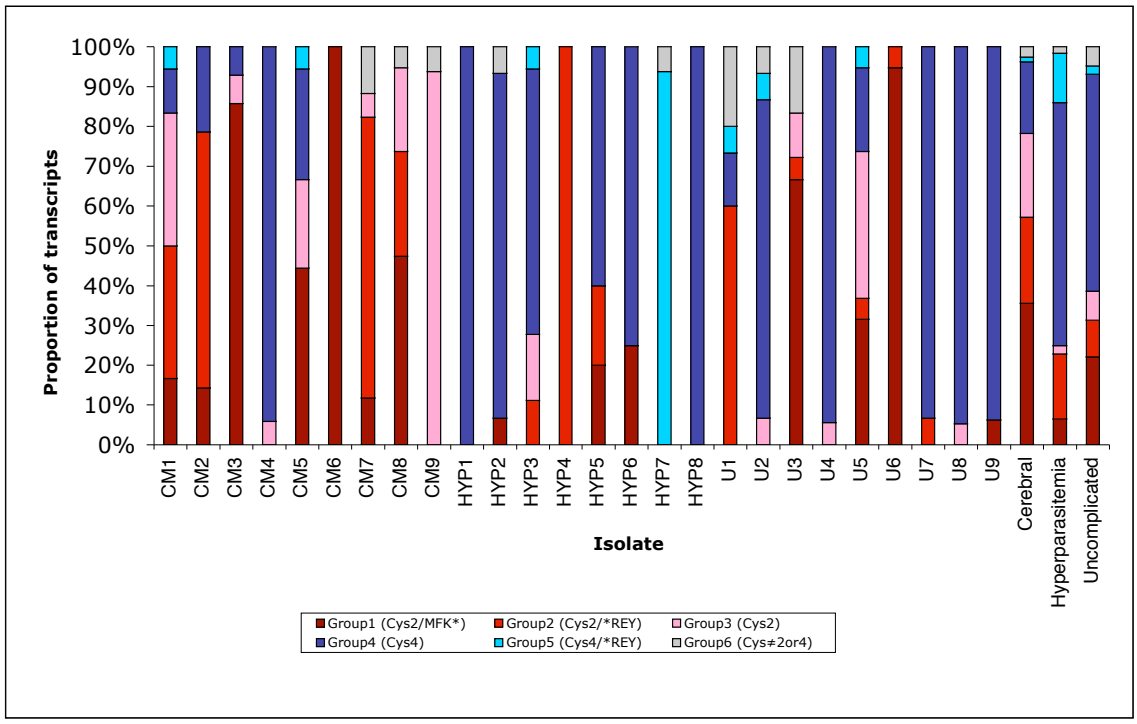

B

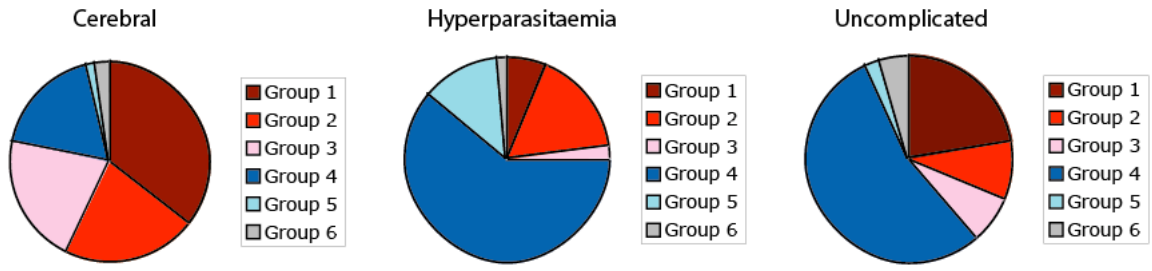

Fig. 3.10. The transcribed *var* genes domain sequences from each isolate, and for all cerebral, hyperparasitaemia and uncomplicated malaria isolate sequences grouped, were separated into 6 DBLα sequence types (Bull *et al*. 2005a). Group 1-3 domains have 2 cysteines in the amplified tag (DBLα1). In addition, group 1 domains have MFK* at a particular locus defined as PoLV1, group 2 domains have *REY at a second locus defined as PoLV2 and group 3 domains contain neither MFK* or *REY. Group 4 and 5 domains have 4 cysteines in the amplified tag (DBLα0). Group 4 domains do not contain *REY at PoLV2 whereas group 5 domains do. Group 6 domains have 1,3,5 or more cysteines in the amplified tag. A) Proportion of transcript in all isolates in the 6 DBLα sequence groups, and combined data for the three clinical manifestation groups as a bar chart. B) Data for three disease manifestation groups combined as pie charts.

3.5.5 Upstream sequence analysis for predominant DBLα domain transcripts

In the sequenced laboratory strains 3D7, IT and HB3 and in other published *var* genes, DBLα1 domains are exclusively seen in group A or B/A *var* genes while DBLα0 domains are found in group B, C or B/C *var* genes (Gardner *et al*. 2002; Lavstsen *et al*. 2003; Kraemer *et al*. 2007). Thus, DBLα(0/1) domain sequences are indicators of *var* gene group. The association of DBLα1 domain transcription with cerebral malaria described above could be simplified as an association between transcription of group A or B/A *var* with cerebral malaria. To validate using DBLα(0/1) domain to denote groups of transcribed *var* genes, the different *var* gene group upstream region sequences were examined.

Degenerate primers were designed to recognise type A, B or C upstream regions, using an alignment of published upstream sequences, to allow classification of the upstream regions of the detected DBLα domains sequences by PCR. These were designed to amplify the specific upstream regions from laboratory isolate gDNA (gift from A Raza and JA Rowe) when paired with a gene-specific reverse primer (Fig. 3.11). These primers successfully amplified the upstream region of a specific *var* gene from gDNA from three parasite strains PAR+, TM180 and AIR only when the appropriate upstream group primer (Ups A, B or C) was used (Fig. 3.12).

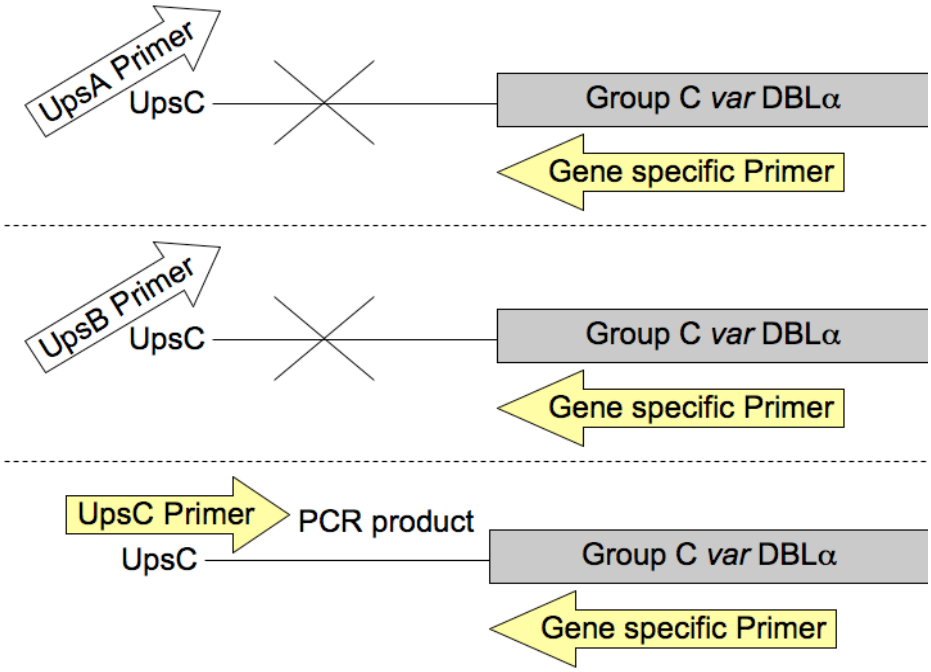

Fig. 3.11. Strategy for specific amplification of transcribed DBLα domain for gDNA. Degenerate primers recognising Ups A, B and C regions were used in PCR reactions with a specific primer to the domain of interest. Only the reaction with the appropriate upstream region primer resulted in PCR product, which was then sequenced to verify amplification of the correct DBLα domain and to obtain upstream sequence data.

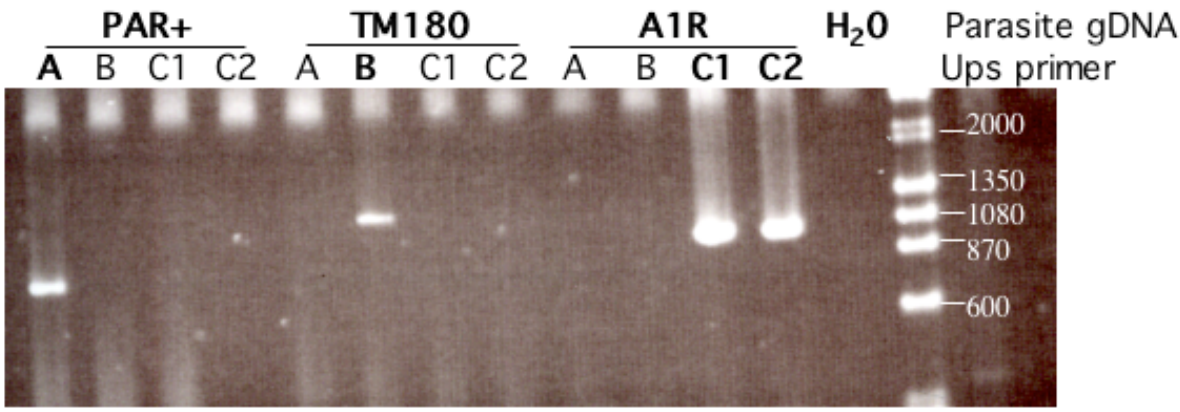

Fig. 3.12. PCR gel showing domain amplification of Ups A, B and C upstream regions. Specific primers to *var* genes PARvar1 (Strain: It/Palo Alto [PAR+]; UpsA), TM180var1 (Strain TM180; UpsB) and A1Rvar1 (Strain A1R; UpsC) were used with specific primers for UpsA, UpsB and two different UpsC primers C1 and C2, and with the appropriate gDNA. PCR product is only seen with the expected upstream primer. DNA ladder was λ DNA/*Hin*DIII fragments (Invitrogen).

Specific primers to the dominant DBLα domain sequence tag from the field isolate were designed (Table 3.2). These specific primers were used with each of the upstream primers to amplify the upstream region of the predominant domains in each isolate. PCR product was obtained and fully sequenced from nine isolates. This gave the expected result that all of the examined field isolate *var* genes with DBLα1 domains had UpsA-type or UpsB-type upstream regions whereas all of the field isolate *var* genes with DBLα0 domains had UpsB-type or UpsC-type upstream regions as is seen in 3D7 laboratory strain (Lavstsen *et al*. 2003). Upstream sequence group and predicted *var* gene groups are shown in Table 3.5. Other domains could

not be sequenced due to cross recognition of other DBL domains with the "specific" primer, or lack of parasite material.

Manifestation	Domain	DBLα1/0	Ups sequence	Predicted *Var* group
Cerebral Malaria	CM2A	DBLα1	A	A
	CM3A	DBLα1	A	A
	CM6A	DBLα1	A	A
	CM8A	DBLα1	A	A
Hyperparasitaemia	HYP1A	DBLα0	B	B
	HYP4A	DBLα1	B	B/A
	HYP5A	DBLα0	B	B
Uncomplicated Malaria	U2A	DBLα0	C	C
	U8A	DBLα0	B	B

Table 3.5. Ups sequence and predicted *var* groups for the dominant domain in 9 isolates with successful upstream region. Upstream regions were amplified with specific primers for UpsA, UpsB and UpsC upstream regions and a reverse gene specific primer for the predominant DBLα gene for each isolate.

3.5.6 Phylogenic analysis of DBLα domain transcripts

The association between disease phenotype and *var* gene expression was explored by mapping symptoms across a phylogeny of the DBLα sequences. A phenogram was created from a clustal W alignment of protein sequences. Phenograms depict genetic relationships without assumptions of evolutionary history. EBA175 was added as a root, as it is a common ancestor of DBL domains, and forms a clear outgroup (Adams *et al*. 1992). For reference, a selection of DBLα sequences from the three major groups A, B and C from the fully sequenced *P. falciparum* laboratory clone 3D7 (Gardner *et al*. 2002) were included, plus four 3D7 genes with intermediate characteristics (B/A or B/C) (Fig. 3.13).

There is a pronounced split as DBLα1-like form a separate clade from DBLα0-like sequences in the phenogram. All sequences above the node where the two clades split (marked *, Fig. 3.13) are DBLα0-like and all below are DBLα1-like. The DBLα0-like upper clade is comb-like, indicating a high level of recombination or an explosive gene duplication event of these sequences. The DBLα1-like lower clade has a more complex branch structure, suggesting more directed evolution.

The phenogram was also coloured according to the 6 DBLα groups classified by Bull *et al* (2005), Fig. 3.14. Group 4 and 5 sequences cluster separately from groups 1-3. Group 2 sequences form an outgroup of DBLα1 sequences, in general clustering separately from group 1 and 3 sequences. There is no obvious pattern to the position of group 6 sequences.

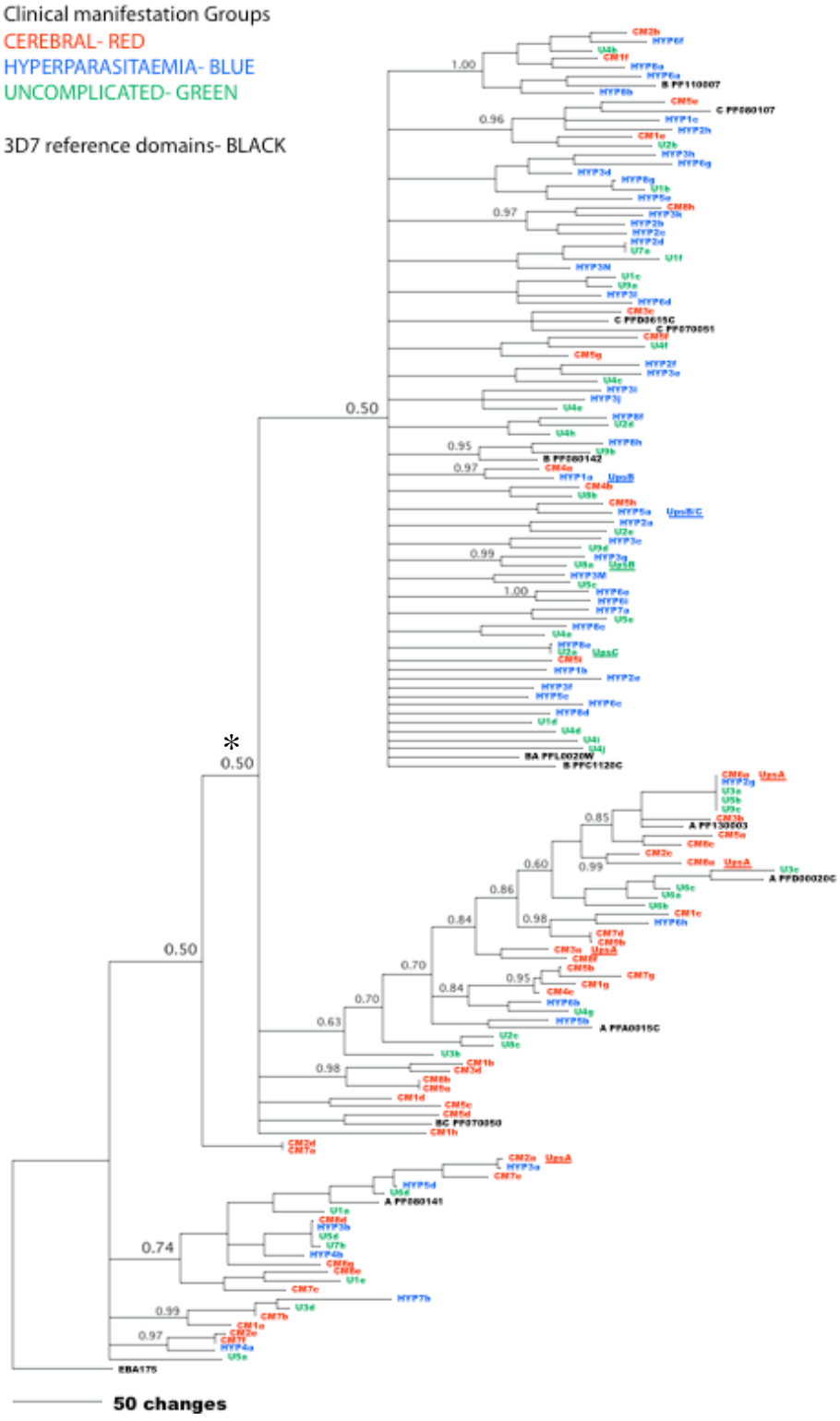
Clinical manifestation Groups
CEREBRAL- RED
HYPERPARASITAEMIA- BLUE
UNCOMPLICATED- GREEN
3D7 reference domains- BLACK
1.00
0.96
0.97
0.50
0.95
0.97
0.99
1.00
*
0.50
0.85
0.60
0.99
0.86
0.84
0.98
0.70
0.95
0.84
0.70
0.63
0.98
0.50
0.74
0.99
0.97
EBA175
50 changes

Fig. 3.13**.** Phenogram produced from an amino acid alignment using Clustal W, and the tree-building program in MegAlign (DNA star lasergene software). Sequences transcribed by isolates from African children with cerebral malaria (CM, red), hyperparasitaemia (HYP, blue), and uncomplicated malaria (U, green) are compared to a selection of *var* genes from the laboratory clone 3D7. For the 3D7 genes, the gene name is preceded by A, B, C, BA or BC to indicate the group to which the gene belongs. The sequences fall into 2 major clades, which split at the asterisked node (*) with the DBLα1-like sequences in the higher clade and the DBLα0-like sequences lie in the lower clade. For the predominant gene from 9 of the Malian isolates, the *var* gene upstream region was determined by PCR and is indicated after the appropriate domain (UpsA, UpsB or UpsC). Bootstrap values were calculated by Graham Stone through 1000 repeat iterations of the tree and superimposed onto the phenogram.

DBLα groups
1 (DBLα1)
2 (DBLα1)
3 (DBLα1)
4 (DBLα0)
5 (DBLα0)
6 (DBLα1/α0)

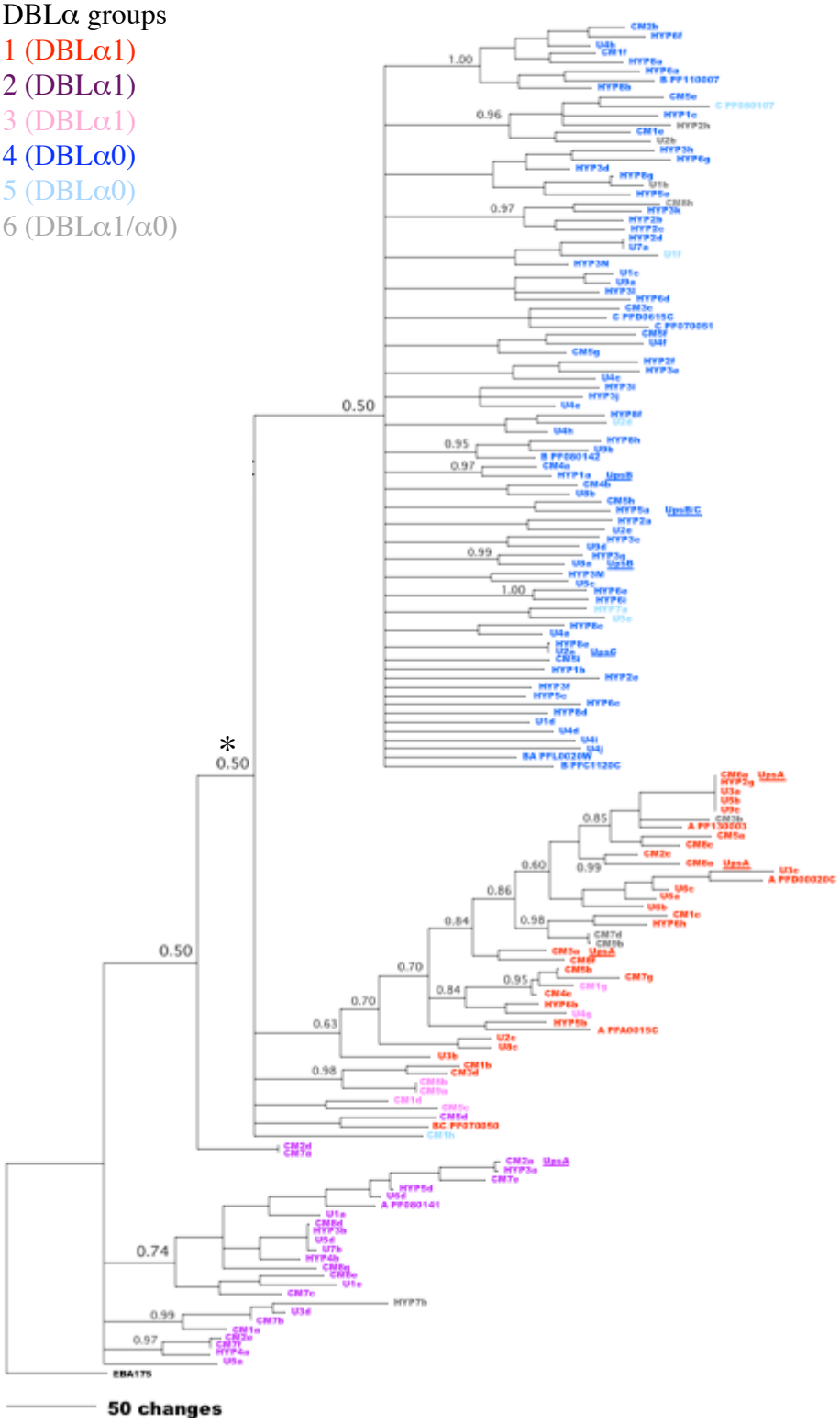

Fig. 3.14**.** Phenogram was produced as for Fig. 3.13. Amino acid sequences were alignmened in Clustal W, and the phenogram was created tree-building program in MegAlign (DNA star lasergene software). Sequences transcribed by isolates from African children with cerebral malaria (CM), hyperparasitaemia (HYP), and uncomplicated malaria (U) are compared to a selection of *var* genes from the laboratory clone 3D7. For the 3D7 genes, the gene name is preceded by A, B, C, BA or BC to indicate the group to which the gene belongs. The sequences fall into 2 major clades, which split at the asterisked node (*) with the DBLα1-like sequences in the higher clade and the DBLα0-like sequences lie in the lower clade. For the predominant gene from 9 of the Malian isolates, the *var* gene upstream region was determined by PCR and is indicated after the appropriate domain (UpsA, UpsB or UpsC). Sequences are coloured according to the DBLα group classification of Bull *et al*. 2005: DBLα1 groups: group 1: red, group 2: purple, group 3: pink. : DBLα0 groups: group 4: dark blue, group 2: light blue. Group 6 sequences are in grey. Bootstrap values were calculated by Graham Stone through 1000 repeat iterations of the tree and superimposed onto the phenogram.

The phenogram successfully separates the domains on the basis of sequence. However, recombination can generate conflicting signals during the process of tree-building, potentially causing a significant source of error (Huson and Bryant 2006). Phylogenetic networks take recombination into account better than traditional phenogram building algorithms. As *var* genes are subject to a high level of recombination (Freitas-Junior *et al*. 2000; Taylor *et al*. 2000b; Kraemer *et al*. 2007) a network was considered more accurate. A network (Appendix 2) was created by Dr Graham Stone (University of Edinburgh) to replace the phenogram. The network was produced from an initial Clustal W alignment of the amino acid sequences, converted to a nucleotide alignment. The network (Appendix 2) recapitulates the split of DBLα1 versus DBLα0 sequences seen in the phylogenetic tree. Sequences from the cerebral malaria patients (red in network; Appendix 2) are significantly concentrated into a 'cerebral malaria clade' ($P < 0.001$, chi-squared test), while sequences from the hyperparasitaemia patients (blue) are significantly concentrated in a 'hyperparasitaeima clade' ($P < 0.025$, chi-squared test). Sequences from the uncomplicated malaria patients (green) showed no bias in distribution between the two main clades of the network.

3.6 Results 2: Sequence conservation between *var* gene DBLα domain transcripts

3.6.1 Sequence identity between DBLα domain transcripts

Identical sequences from different isolates (branch length zero in Fig. 3.13, or parallel branches in network, Appendix 2) were rare, reflecting minimal overlap in *var* gene repertoires between isolates. Only 12 of the 142 unique sequence tags were present as identical or almost identical (>95% nucleotide identity) in more than 1 isolate. The mean amino acid sequence identity between sequences was 42.2% (SE 0.2%), SD 8.6% (Fig. 3.15).

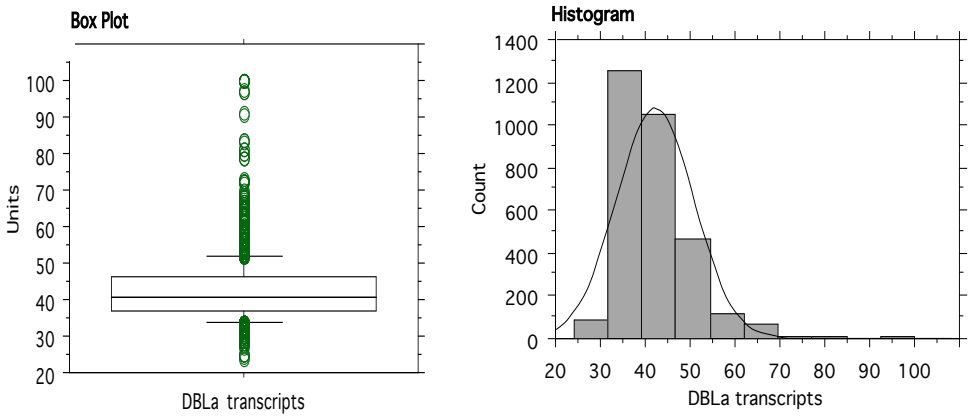

Fig. 3.15. The percentage amino acid identity between all DBLα transcripts from the Mali field isolates is displayed as a box plot (showing 10th, 25th, 50th, 75th and 90th percentiles; values <10th percentile and >90th plotted separately) and as a histogram. Amino acid sequences were created from nucleotide sequences in EditSeq, and percentage identity was calculated using MegAlign. Histograms and box plots of sequence identity were then created in Statview.

3.6.2 Sequence identity between *var* gene DBLα domain transcripts in disease categories

The level of amino acid identity between different Mali DBLα sequence domain transcripts in each clinical category was also determined. The mean amino acid identity between transcripts was surprisingly similar between the three disease categories. Cerebral isolate transcripts showed mean 42.9% (SE 0.26%), and hyperparasitaemia isolate transcripts showed mean 42.8% (SE 0.27%). The mean percentage sequence identity uncomplicated isolate transcripts, 40.9% (SE 0.27%), was slightly lower from that of hyperparasitaemia and cerebral isolate transcripts, and this difference was significant (t-test, $p < 0.005$). There was no significant difference in transcript identity between hyperparasitaemia and cerebral isolate sequences (t-test, $p = 0.89$). The variance of amino acid identity in the three categories was similar (SD: cerebral 8.6%, hyperparasiteamia 8.8%, uncomplicated, 8.1%). Fig. 3.16 shows histograms and a box plot of the data.

The level of amino acid identity between different Mali DBLα sequence domain transcripts in each clinical category was also illustrated pictorially (Fig. 3.17). Amino acid identity between 2 domains was colour coded such that darker shading reflects higher amino acid identity.

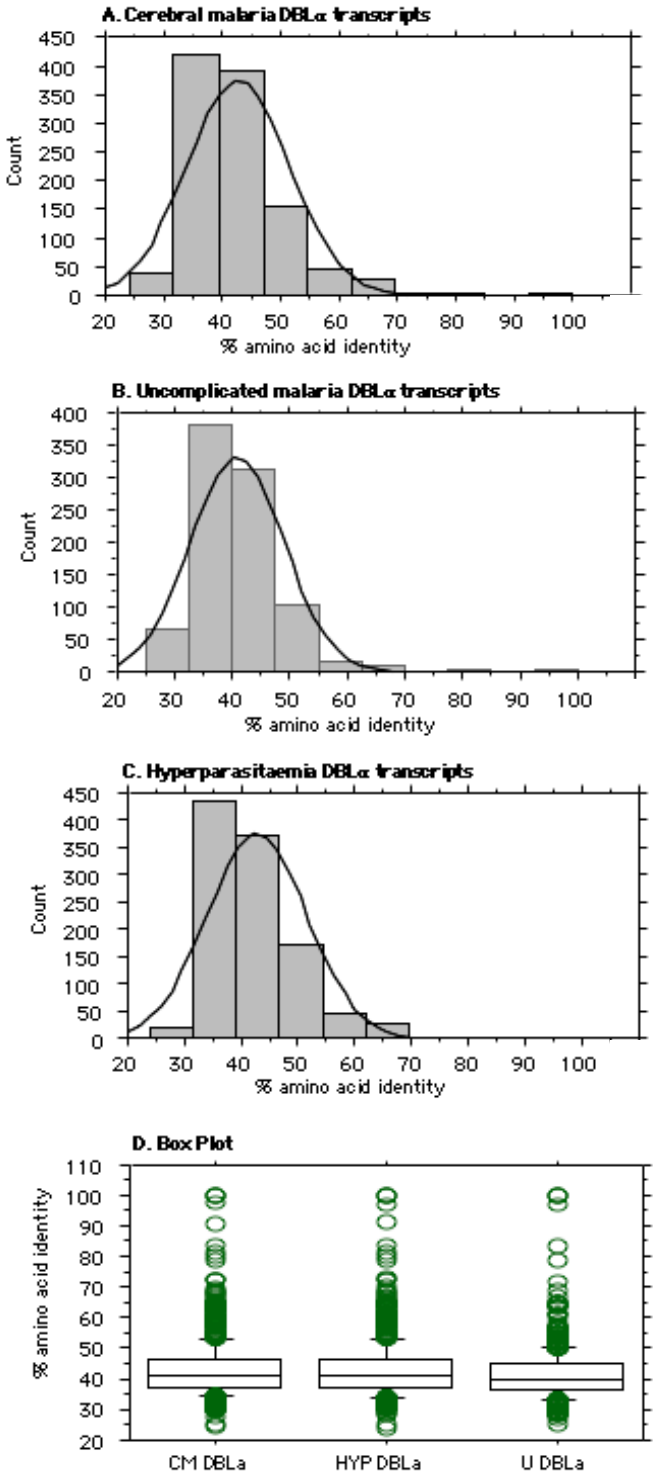
A. Cerebral malaria DBLα transcripts
Count
% amino acid identity
B. Uncomplicated malaria DBLα transcripts
Count
% amino acid identity
C. Hyperparasitaemia DBLα transcripts
Count
% amino acid identity
D. Box Plot
% amino acid identity
CM DBLa
HYP DBLa
U DBLa

Fig. 3.16. Histograms and box plots (showing 10th, 25th, 50th, 75th and 90th percentiles; values <10th percentile and >90th plotted separately) of percentage amino acid identity between cerebral, hyperparasitaemia and uncomplicated malaria DBLα transcripts. Sequences transcribed in cerebral, hyperparasitaemia or uncomplicated malaria isolates were considered separately. Amino acid sequences were created from nucleotide sequences in EditSeq, and percentage identity was calculated using MegAlign. Histograms and box plots of identity were then created in Statview.

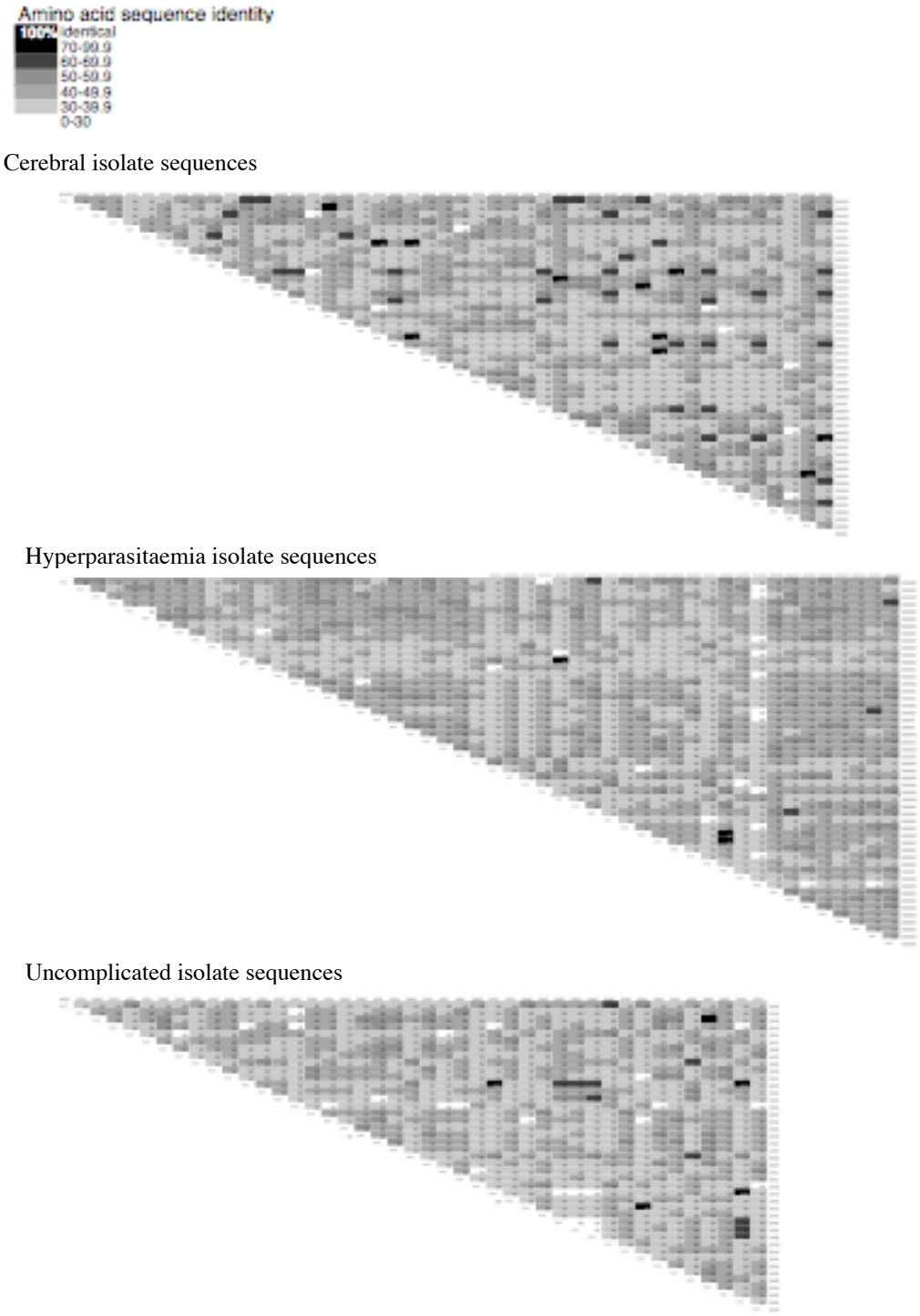

Fig. 3.17. Amino acid sequence distance charts showing percentage amino acid identity between domains separated by disease classification. Sequences transcribed in cerebral, hyperparasitaemia or uncomplicated malaria isolates were considered

separately. Amino acid sequences were created from nucleotide sequences in EditSeq, and percentage identity was calculated using MegAlign. Darkness of shading indicates level of identity between domains.

3.6.3 Sequence identity between *var* gene DBLα domain transcripts in DBLα(1/0) groups

The sequence identity of the DBLα1-like and DBLα0-like transcripts separately was also calculated. The mean amino acids identity between DBLα0–like transcripts was 46.0% (SE 0.2%) slightly higher than that for DBLα1-like transcripts 45.6% (SE 0.1%). Though a small difference, because of the large sample size this difference is significant (t-test, $p < 0.005$). The standard deviation of the DBLα1 sequences (10.5%) is much greater than for DBLα0 sequences (5.5%), seen as a broader curve in the histogram (Fig. 3.18). Both DBLα1 sequences and DBLα0 sequences are more similar to each other than sequences separated by disease category, due to the definitions of DBLα1 and DBLα0 sequences. This is equivalent to DBLα1 and DBLα0 sequences clustering separately on the phenogram (Fig. 3.13) and network (Appendix 2). Fig. 3.19 shows the results pictorially.

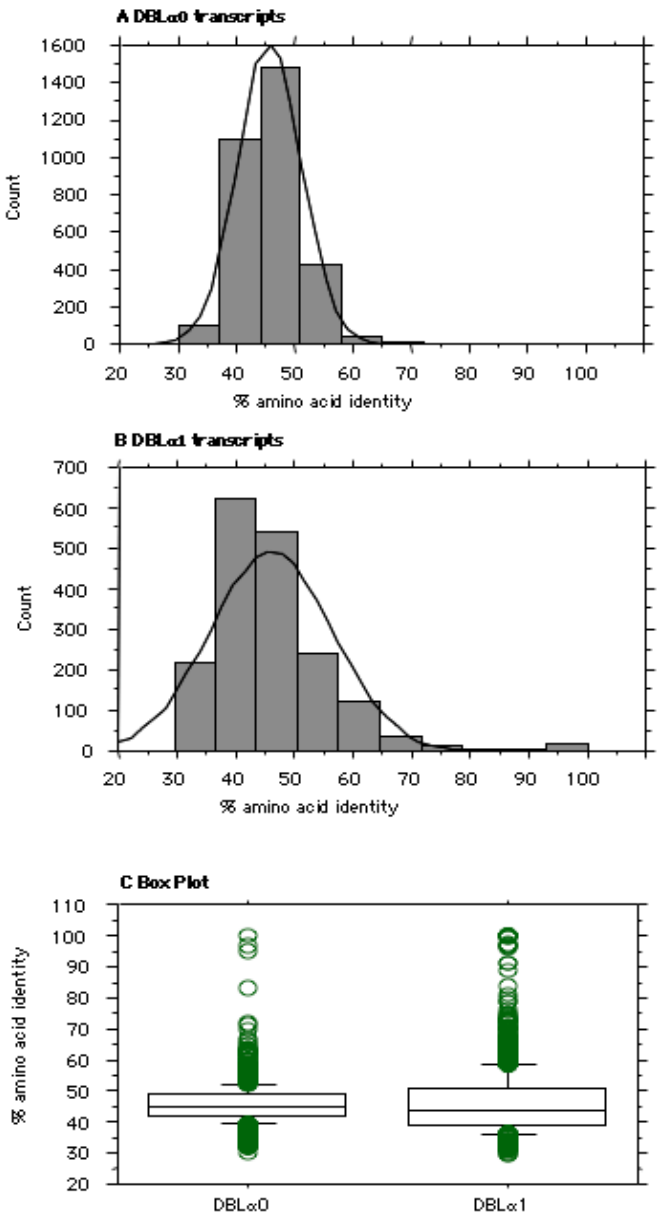

Fig. 3.18. Histograms and box plot (showing 10th, 25th, 50th, 75th and 90th percentiles; values <10th percentile and >90th plotted separately) of percentage amino acid identity between all DBLα0 domain and DBLα1 domain transcripts. Amino acid sequences were created from nucleotide sequences in EditSeq, and percentage identity was calculated using MegAlign. Histograms and box plots of identity were then created in Statview.

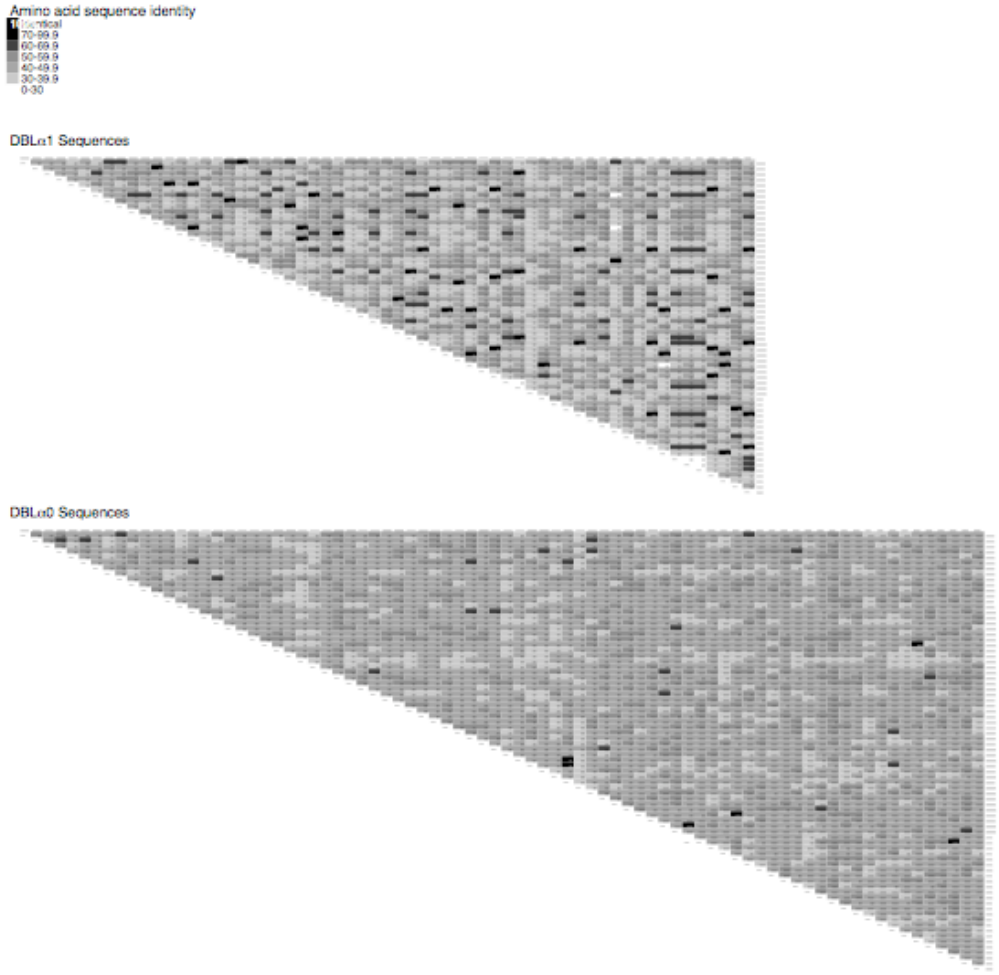

Fig. 3.19. Amino acid sequence distance charts showing percentage amino acid identity between domains separated by DBLα0/1 classification. Darkness of shading indicates level of identity between domains. DBLα1 and DBLα0 transcript sequences were considered separately. Amino acid sequences were created from nucleotide sequences in EditSeq, and percentage identity was calculated using MegAlign.

3.6.4 Evidence for conserved *var* genes

To examine the extent of conservation of these genes to other published global *var* genes, sequences were entered in to NCBI BLAST homology search. Database matches (> 95% nucleotide identity and > 95% sequence coverage) to the Mali sequence described in this study as of August 2007 are given in Table 3.6.

The most common sequence found in the Mali sequences (CM6A) was present in 5 isolates (CM6, U3, U5, U9 and HYP2), and was the only *var* transcript detected in isolate CM6. Nine further non-*var1csa* Mali sequences were common to 2 isolates (>95% identity): CM9A:CM8B (100% identity), CM7A:CM2D (100%), CM9B:CM7D (100%), U7A:HYP2D (100%), CM2E:CM7F (99%), HYP8E:U2A (99%), U1B:HYP8G (98%), CM2A:HYP3A (98%), U3D:CM7B (96%). One of these (CM7D/CM9B) was identical to a DBLα domain from IT/FCR3 family laboratory strain family (Accession number DQ408000). This domain belongs to the PfEMP1 PARvar1, which is responsible for rosetting in the Palo Alto form of this strain (J.A. Rowe, unpublished data). None of the other 8 sequences found in multiple isolates in Mali (CM6A group, or the 8 transcripts found in 2 isolates) showed any highly homologous database matches.

Of the non-*var1csa* sequences found in multiple isolates, most (7/10) involved cerebral isolate transcripts, and almost half (4/10) were exclusive to cerebral isolates. No transcript was exclusive to uncomplicated or hyperparasitaemia isolates. In addition, of the non-*var1csa* sequences found in multiple isolates, most (7/10) were DBLα1-like. The group 4 var (Jensen *et al.* 2004) were not amplified in any of the

isolates. A similar proportion of DBLα1/0 sequences had no database matches (35% DBLα1, 28% DBLα0 sequences).

Seven *var1csa* homologues were also found; CM8D, HYP3B, U5D, U7B were 3D7 *var1csa* homologues and CM1G, CM4C, CM5B were FCR3 *var1csa* homologues, as shown in Table 3.7.

Mali field isolate DBLα sequences					**Database matches (>95% identity, >95% coverage)**	
Name	**Accession Number**	**Freq.**	**DBLα0/1**	**Group**	**Accession Number (Origin)**	**Nucleotide identities (%)**
CM1 A	DQ367086	6/18	1	2	-	
CM1 B	DQ367087	4/18	1	3	-	
CM1 C	DQ367088	3/18	1	1	AM115620 (Kenya)[1]	336/352 (95%)
CM1 D	DQ367089	1/18	1	3	AY054749 (Dd2, Thailand)[2] AM115928 (Kenya)[1] L40609 (FCR3 strain)[3] DQ135195 (Gabon)[4]	394/394 (100%) 394/394 (100%) 394/394 (100%) 394/395 (99%)
CM1 E	DQ367090	1/18	0	4	-	
CM1 F	DQ367091	1/18	0	4	-	
CM1 G	DQ367092	1/18	1	3	DQ408100 (V1S, SE Asia)[5] AM115158 (Kenya)[1] DQ135232 (Gabon)[4] DQ135233 (Muz12, PNG)[6] DQ135235 (AME24, PNG)[6] AY054896 (PH1, Philipines)[2] AY054771 (Dd2, Thailand)[2] AM115319 (Kenya)[1] AJ420411 (TM180, Thailand)[7] AY462740 (PNG)[8]	347/352 (98%) 347/352 (98%) 346/352 (98%) 346/352 (98%) 346/352 (98%) 346/352 (98%) 346/352 (98%) 346/352 (98%) 346/352 (98%) 345/352 (98%) …
CM1 H	DQ367093	1/18	0	5	-	
CM2 A	DQ367094	7/14	1	2	DQ367144 (HYP3a, Mali)*	333/338 (98%)
CM2 B	DQ367095	3/14	0	4	-	
CM2 C	DQ367096	2/14	1	1	AF221828 (Kenya)[9]	340/340 (100%)
CM2 D	DQ367097	1/14	1	2	DQ367116 (CM7a, Mali)*	358/358 (100%)
CM2 E	DQ367098	1/14	1	2	DQ367121 (CM7f, Mali)*	325/329 (98%)
CM3 A	DQ367099	10/14	1	1	-	
CM3 B	DQ367100	2/14	1	1	AF528110 (Gabon)[10] DQ135381 (PNG)[6] DQ135380 (Sierra Leone)[6]	330/336 (98%) 328/336 (97%) 326/336 (97%)
CM3 C	DQ367101	1/14	0	4	-	

Mali field isolate DBLα sequences					Database matches (>95% identity, >95% coverage)	
Name	**Accession Number**	**Freq.**	**DBLα0/1**	**Group**	**Accession Number (Origin)**	**Nucleotide identities (%)**
CM3 D	DQ367102	1/14	1	3	-	
CM4 A	DQ367103	15/17	0	4	-	
CM4 B	DQ367104	1/17	0	4	-	
CM4 C	DQ367105	1/17	1	3	DQ265587 (W Amazon)[11] AJ536728 (Venezuela)[12] AJ536698 (Venezuela)[12] AF411601 (202, Sudan)[13] AY054879 (Solomon Island)[2] AF221773 (Vanuatu)[8] AJ420412 (TM284, Thailand)[7] AY054854 (Solomon Island)[2] AF528129 (Gabon)[10] AF221800 (Kenya)[9]	349/349 (100%) 349/349 (100%) 348/349 (99%) 347/349 (99%) 347/349 (99%) 347/349 (99%) 347/349 (99%) 346/349 (98%) 345/349 (98%) 345/349 (98%) …
CM5 A	DQ367106	8/18	1	1	-	
CM5 B	DQ367107	2/18	1	3	AY054944 (Philippines)[2] AM115051 (Kenya)[1] AF528153 (Gabon)[10] AM115381 (Kenya)[1] DQ135231 (Gabon)[4] DQ135230 (Gabon)[4] DQ135228 (Gabon)[4] AY054969 (Africa)[2] AM116420 (Kenya)[1] AM115598 (Kenya)[1]	349/349 (100%) 349/349 (100%) 348/348 (100%) 348/349 (99%) 346/349 (99%) 345/350 (98%) 344/350 (98%) 344/350 (98%) 335/359 (95%) 335/359 (95%) …
CM5 C	DQ367108	2/18	1	3	-	
CM5 D	DQ367109	1/18	0	5	-	
CM5 E	DQ367110	1/18	0	4	-	
CM5 F	DQ367111	1/18	0	4	-	
CM5 G	DQ367112	1/18	0	4	-	
CM5 H	DQ367113	1/18	0	4	AJ319683 (It)[14] AJ429520 (FCR3)[16] AF275870 (Brazil)[15] EF143944[17]	369/370 (99%) 352/354 (99%) 364/369 (98%) 351/353 (99%)
CM5 I	DQ367114	1/18	0	4	-	
CM6 A	DQ367115	16/16	1	1	DQ367210 (U5b, Mali)* DQ367225 (U9c, Mali)* DQ367195 (U3a, Mali)* DQ367142 (HYP2g, Mali)*	340/340 (100%) 340/340 (100%) 340/340 (100%) 340/340 (100%)
CM7 A	DQ367116	8/17	1	2	DQ367097 (CM2d, Mali)*	358/358 (100%)
CM7 B	DQ367117	2/17	1	6	DQ367198 (U3d, Mali)*	316/329 (96%)
CM7 C	DQ367118	2/17	1	2	-	
CM7 D	DQ367119	2/17	1	1	DQ367132 (CM9b, Mali)* DQ408000 (FCR3)[5]	352/352 (100%) 352/352 (100%)
CM7 E	DQ367120	1/17	1	2	DQ407961 (TM180, SE Asia)[5] DQ407945 (Tm90, SE Asia)	342/343 (99%) 341/343 (99%)
CM7 F	DQ367121	1/17	1	2	DQ367098 (CM2e, Mali)*	325/329 (98%)
CM7 G	DQ367122	1/17	1	3	AM116525 (Kenya)[1]	342/343 (99%)

Mali field isolate DBLα sequences					Database matches (>95% identity, >95% coverage)	
Name	**Accession Number**	**Freq.**	**DBLα0/1**	**Group**	**Accession Number (Origin)**	**Nucleotide identities (%)**
					AM116344 (Kenya)[1] AF528113 (Gabon)[10]	342/343 (99%) 341/342 (99%)
CM8 A	DQ367123	5/19	1	1	AM115191 (Kenya)[1]	346/346 (100%)
CM8 B	DQ367124	4/19	1	3	DQ367131 (CM9a, Mali)*	373/373 (100%)
CM8 C	DQ367125	3/19	1	1	-	
CM8 D	DQ367126	3/19	1	2	PFE1640w (Var1CSA, 3D7)[18] DQ367212 (U5d, Mali)* DQ367145 (HYP3b, Mali)* DQ408101 (M5, W Africa)[5] AF221823 (Kenya)[9] AF547158 (Cameroon)[19] AJ420400 (Malawi)[7] AF528109 (Gabon)[10] AF528107 (Gabon)[10] DQ135187 (Sierra Leone)[6]	330/331 (99%) 330/331 (99%) 330/331 (99%) 330/331 (99%) 330/331 (99%) 330/331 (99%) 330/331 (99%) 330/331 (99%) 330/331 (99%) 328/331 (99%) …
CM8 E	DQ367127	1/19	1	2	-	
CM8 F	DQ367128	1/19	1	1	-	
CM8 G	DQ367129	1/19	1	2	AM115921 (Kenya)[1]	327/329 (99%)
CM8 H	DQ367130	1/19	0	6	-	
CM9 A	DQ367131	15/16	1	3	DQ367124 (CM8b, Mali)*	373/373 (100%)
CM9 B	DQ367132	1/16	1	6	DQ367119 (CM7d, Mali)* DQ408000 (FCR3)[5]	352/352 (100%) 352/352 (100%)
HYP1 A	DQ367133	13/15	0	4	-	
HYP1 B	DQ367134	1/15	0	4	-	
HYP1 C	DQ367135	1/15	0	4	-	
HYP2 A	DQ367136	6/15	0	4	DQ135692 (Zimbabwe)[6]	335/343 (97%)
HYP2 B	DQ367137	3/15	0	4	-	
HYP2 C	DQ367138	1/15	0	4	-	
HYP2 D	DQ367139	1/15	0	4	DQ367218 (U7a, Mali)*	415/415 (100%)
HYP2 E	DQ367140	1/15	0	4	-	
HYP2 F	DQ367141	1/15	0	4	-	
HYP2 G	DQ367142	1/15	1	1	DQ367115 (CM6a, Mali)* DQ367210 (U5b, Mali)* DQ367225 (U9c, Mali)* DQ367195 (U3a, Mali)*	340/340 (100%) 340/340 (100%) 340/340 (100%) 340/340 (100%)
HYP2 H	DQ367143	1/15	0	6	-	
HYP3 A	DQ367144	3/18	1	2	DQ367094 (CM2a, Mali)*	333/338 (98%)
HYP3 B	DQ367145	2/18	1	2	PFE1640w (Var1CSA, 3D7)[18] DQ367212 (U5d, Mali)* DQ408101 (M5, W Africa)[5] AF221823 (Kenya)[9] AF547158 (Cameroon)[19] AJ420400 (Malawi)[7] AF528109 (Gabon)[10] AF528107 (Gabon)[10] AF528101 (Gabon)[10] DQ367126 (CM8d, Mali)*	331/331 (100%) 331/331 (100%) 331/331 (100%) 331/331 (100%) 331/331 (100%) 331/331 (100%) 331/331 (100%) 331/331 (100%) 331/331 (100%) 330/331 (99%)

Mali field isolate DBLα sequences					Database matches (>95% identity, >95% coverage)	
Name	**Accession Number**	**Freq.**	**DBLα0/1**	**Group**	**Accession Number (Origin)**	**Nucleotide identities (%)**
						…
HYP3 C	DQ367146	2/18	0	4	-	
HYP3 D	DQ367147	1/18	0	4	-	
HYP3 E	DQ367148	1/18	0	4	-	
HYP3 F	DQ367149	1/18	0	4	-	
HYP3 G	DQ367150	1/18	0	4	-	
HYP3 H	DQ367151	1/18	0	4	-	
HYP3 I	DQ367152	1/18	0	4	-	
HYP3 J	DQ367153	1/18	0	4	-	
HYP3 K	DQ367154	1/18	0	4	-	
HYP3 L	DQ367155	1/18	0	4	-	
HYP3 M	DQ367156	1/18	0	4	-	
HYP3 N	DQ367157	1/18	0	4	-	
HYP4 A	DQ367158	14/15	1	2	-	
HYP4 B	DQ367159	1/15	1	2	-	
HYP5 A	DQ367160	4/15	0	4	-	
HYP5 B	DQ367161	3/15	1	1	-	
HYP5 C	DQ367162	3/15	0	4	-	
HYP5 D	DQ367163	3/15	1	2	AJ536742 (Venezuela)[12] AJ536726 (Venezuela)[12] DQ135226 (Gabon)[4] AM116429 (Kenya)[1]	328/328 (100%) 328/328 (100%) 321/329 (97%) 311/326 (95%)
HYP5 E	DQ367164	2/15	0	4	-	
HYP6 A	DQ367165	5/16	0	4	-	
HYP6 B	DQ367166	3/16	1	1	DQ134477 (PNG)[6]	337/339 (99%)
HYP6 C	DQ367167	2/16	0	4	-	
HYP6 D	DQ367168	1/16	0	4	-	
HYP6 E	DQ367169	1/16	0	4	AM115543 (Kenya)[1]	399/405 (98%) 399/405 (98%)
HYP6 F	DQ367170	1/16	0	4	-	
HYP6 G	DQ367171	1/16	0	4	-	
HYP6 H	DQ367172	1/16	1	1	-	
HYP6 I	DQ367173	1/16	0	4	-	
HYP7 A	DQ367174	15/16	0	5	-	
HYP7 B	DQ367175	1/16	0	6	-	
HYP8 A	DQ367176	6/16	0	4	DQ135512 (Gabon)[4] DQ135513 (Gabon)[4] DQ135514 (Gabon)[4] DQ135515 (Gabon)[4]	343/356 (96%) 343/356 (96%) 343/356 (96%) 343/356 (96%)
HYP8 B	DQ367177	3/16	0	4	-	
HYP8 C	DQ367178	2/16	0	4	-	
HYP8 D	DQ367179	1/16	0	4	-	
HYP8 E	DQ367180	1/16	0	4	DQ367190 (U2a, Mali)*	411/415 (99%)
HYP8 F	DQ367181	1/16	0	4	-	
HYP8 G	DQ367182	1/16	0	4	DQ367185 (U1b, Mali)*	399/407 (98%)
HYP8 H	DQ367183	1/16	0	4	-	
U1 A	DQ367184	8/15	1	2	-	
U1 B	DQ367185	3/15	0	6	DQ367182 (HYP8g, Mali)*	399/407 (98%)
U1 C	DQ367186	1/15	0	4	-	

Mali field isolate DBLα sequences					Database matches (>95% identity, >95% coverage)	
Name	**Accession Number**	**Freq.**	**DBLα0/1**	**Group**	**Accession Number (Origin)**	**Nucleotide identities (%)**
U1 D	DQ367187	1/15	0	4	-	
U1 E	DQ367188	1/15	1	2	AY462831 (PNG)[8]	337/344 (97%)
U1 F	DQ367189	1/15	0	5	-	
U2 A	DQ367190	11/15	0	4	DQ367180 (HYP8e, Mali)*	411/415 (99%)
U2 B	DQ367191	1/15	0	6	-	
U2 C	DQ367192	1/15	1	3	-	
U2 D	DQ367193	1/15	0	5	-	
U2 E	DQ367194	1/15	0	4	-	
U3 A	DQ367195	12/17	1	1	DQ367115 (CM6a, Mali)* DQ367210 (U5b, Mali)* DQ367225 (U9c, Mali)* DQ367142 (HYP2g, Mali)*	340/340 (100%) 340/340 (100%) 340/340 (100%) 340/340 (100%)
U3 B	DQ367196	2/17	1	3	-	
U3 C	DQ367197	2/17	0	6	AY462743 (PNG)[8]	338/345 (97%)
U3 D	DQ367198	1/17	1	2	DQ367117 (CM7b, Mali)*	316/329 (96%)
U4 A	DQ367199	6/15	0	4	-	
U4 B	DQ367200	1/15	0	4	-	
U4 C	DQ367201	1/15	0	4	-	
U4 D	DQ367202	1/15	0	4	-	
U4 E	DQ367203	1/15	0	4	-	
U4 F	DQ367204	1/15	0	4	-	
U4 G	DQ367205	1/15	1	3	-	
U4 H	DQ367206	1/15	0	4	-	
U4 I	DQ367207	1/15	0	4	DQ135614 (Gabon)[6]	384/400 (96%)
U4 J	DQ367208	1/15	0	4	-	
U5 A	DQ367209	7/19	1	3	-	
U5 B	DQ367210	6/19	1	1	DQ367115 (CM6a, Mali)* DQ367225 (U9c, Mali)* DQ367195 (U3a, Mali)* DQ367142 (HYP2g, Mali)*	340/340 (100%) 340/340 (100%) 340/340 (100%) 340/340 (100%)
U5 C	DQ367211	4/19	0	4	-	
U5 D	DQ367212	1/19	1	2	PFE1640w (Var1CSA, 3D7)[18] DQ367145 (HYP3b, Mali)* DQ408101 (M5, W Africa)[5] AF221823 (Kenya)[9] AF547158 (Cameroon)[19] AJ420400 (Malawi)[7] AF528109 (Gabon)[10] AF528107 (Gabon)[10] AF528101 (Gabon)[10] DQ367126 (CM8d, Mali)*	331/331 (100%) 331/331 (100%) 331/331 (100%) 331/331 (100%) 331/331 (100%) 331/331 (100%) 331/331 (100%) 331/331 (100%) 331/331 (100%) 330/331 (99%) …
U5 E	DQ367213	1/19	0	5	-	
U6 A	DQ367214	10/19	1	1	-	
U6 B	DQ367215	7/19	1	1	-	
U6 C	DQ367216	1/19	1	1	-	
U6 D	DQ367217	1/19	1	2	AM116429 (Kenya)[1] AM115135 (Kenya)[1]	315/325 (96%) 319/331 (96%)
U7 A	DQ367218	14/15	0	4	DQ367139 (HYP2d, Mali)*	415/415 (100%)

Mali field isolate DBLα sequences					Database matches (>95% identity, >95% coverage)	
Name	**Accession Number**	**Freq.**	**DBLα0/1**	**Group**	**Accession Number (Origin)**	**Nucleotide identities (%)**
U7 B	DQ367219	1/15	1	2	DQ135187 (Sierra Leone)[6] AF368950 (Brazil)[20] AF547159 (Cameroon)[18] AM116007 (Kenya)[1] AJ420383 (Malawi)[7] AF528103 (Gabon)[10] AJ420408 (CS294, Malawi)[7] AJ420387 (P136, Malawi)[7] PFE1640w (Var1CSA, 3D7)[18] DQ367212 (U5d, Mali)* …	328/331 (99%) 328/331 (99%) 328/331 (99%) 328/331 (99%) 327/331 (99%) 327/331 (99%) 327/331 (99%) 327/331 (99%) 326/331 (98%) 326/331 (98%)
U8 A	DQ367220	17/19	0	4	-	
U8 B	DQ367221	1/19	0	4	DQ134996 (Gabon)[10]	372/373 (99%)
U8 C	DQ367222	1/19	1	3	EF158105 (It)[21]/AJ319704 (A4)[14] AM116392 (Kenya)[1] AM116205 (Kenya)[1] DQ135454 (PNG)[6]	342/346 (98%) 340/346 (98%) 340/346 (98%) 333/336 (99%)
U9 A	DQ367223	13/16	0	4	-	
U9 B	DQ367224	1/16	0	4	-	
U9 C	DQ367225	1/16	1	1	DQ367115 (CM6a, Mali)* DQ367210 (U5b, Mali)* DQ367195 (U3a, Mali)* DQ367142 (HYP2g, Mali)*	340/340 (100%) 340/340 (100%) 340/340 (100%) 340/340 (100%)
U9 D	DQ367226	1/16	0	4	-	

Table 3.6. NCBI database homologues for Mali isolate DBLα transcripts described in this study. Accession number, frequency (number of clones sequenced per isolate with identical sequence), DBLα0/1 classification and group (Bull *et al.* 2007) are given. Up to 10 database matches (>95% identity, >95% sequence coverage, http://www.ncbi.nlm.nih.gov/BLAST) are also described (accession number, country of origin, and% nucleotide identity). Multiple database matches from the same strain or isolate but entered multiply on the NCBI database multiple times are not repeated in the table.

… more than 10 database matches were found.

- no database matches were found.

[1](Bull *et al*. 2005a), [2](Fowler *et al*. 2002), [3](Su *et al*. 1995), [4] Barry *et al*. 2005 (unpublished), [5](Trimnell *et al*. 2006), [6](Barry *et al*. 2007), [7](Rowe *et al*. 2002a), [8](Kaestli *et al*. 2004), [9](Taylor *et al*. 2000b), [10](Winter *et al*. 2003), [11](Albrecht *et al*. 2006), [12](Tami *et al*. 2003), [13](Salanti *et al*. 2002), [14](Horrocks *et al*. 2002), [15](Duffy *et al*. 2002), [16](Fernandez *et al*. 2002), [17]Ozarkar, et al unpublished, [18](Hall *et al*. 2002), [19](Khattab *et al*. 2003), [20](Kirchgatter *et al*. 2000), [21](Kraemer *et al*. 2007), *this study/(Kyriacou *et al*. 2006).

Mali field isolate DBLα sequences	***Var1csa* homologue**	**Nucleotide identities (%)**
CM8D	3D7 *var1csa*	330/331 (99%)
HYP3B	3D7 *var1csa*	331/331 (100%)
U5D	3D7 *var1csa*	331/331 (100%)
U7B	3D7 *var1csa*	326/331 (98%)
CM1G	FCR3 *var1csa*	321/357 (89%)
CM4C	FCR3 *var1csa*	322/353 (91%)
CM5B	FCR3 *var1csa*	325/353 (92%)

Table 3.7. Details of homology of the Mali isolate DBLα transcripts described in this study to the two forms of *var1csa* described in Rowe *et al*. (2002a). Nucleotide identity to 3D7 *var1csa,* PFE1640w, (Hall *et al.* 2002) or FCR3 *var1csa*, AJ133811, (Scherf *et al*. 1998) is shown.

3.7 Results 3: Correlations of DBLα1 domain transcript frequency and isolate characteristics

3.7.1 DBLα1 domain transcription correlates with high rosetting

Rosette frequency (RF) was significantly higher in the cerebral malaria isolates than in the hyperparasitaemia or uncomplicated malaria isolates (Table 3.3; p = 0.035), in agreement with consistent observations that rosetting is a virulence factor in Africa (Carlson *et al*. 1990; Rowe *et al*. 1995; Rowe *et al*. 2002b). Group A *var* genes are associated with rosetting, and *var* genes responsible for rosetting in 8 rosetting laboratory isolates (unpublished data, Rowe JA) are all group A with DBLα1 domains that cluster within the 'cerebral'/DBLα1-like portion of the tree (data not shown).

In my isolates, DBLα1-like gene expression was also associated with rosetting (Spearman Rank correlation Rho = 0.52, p = 0.009; Fig. 3.20). This is in accordance with the association of group A *var* genes and rosetting (unpublished data, Rowe JA), and of rosette frequency and malaria severe/cerebral malaria in Africa (Carlson *et al*. 1990; Rowe *et al*. 1995; Rowe *et al*. 2002b). Colouring the points according to disease manifestation shows that the correlation is driven by high RF levels in the cerebral malaria isolates which also have high DBLα1% transciprtion levels (red in Fig. 3.20), and by low RF levels in the hyperparasitaemia malaria isolates which showed low DBLα1% transciprtion levels (blue in Fig. 3.20).

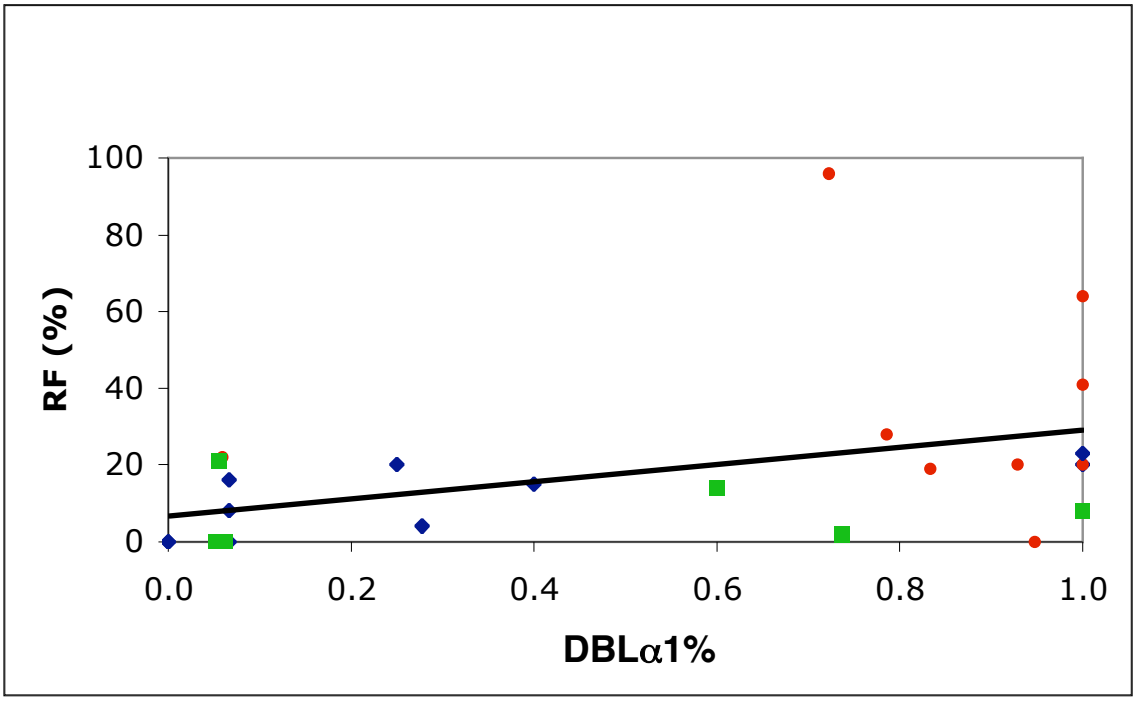

Fig. 3.20. Correlation between isolate rosette frequency (RF) and proportion of DBLα1-like domain transcripts detected. Spearman Rank correlation: Rho = 0.52, p = 0.009. Red cirles: cerebral malaria isolates, green squares: uncomplicated malaria isolates, blue diamonds: hyperparasitaemia isolates.

Splitting the sequences into the DBLα groups 1-5 (Bull *et al.* 2005a) (there were not enough group 6 domains to examine) reveals that DBLα1 groups 1 and 3 positively correlate with rosetting, but only group 1 reaches significance ($P < 0.05$) (Fig. 3.21). This is consistent with laboratory rosetting lines that are often groups 1 or 3 (Alex Rowe, personal communication) although Bull *et al.* (2005) found group 2 to be most strongly correlated with rosetting.

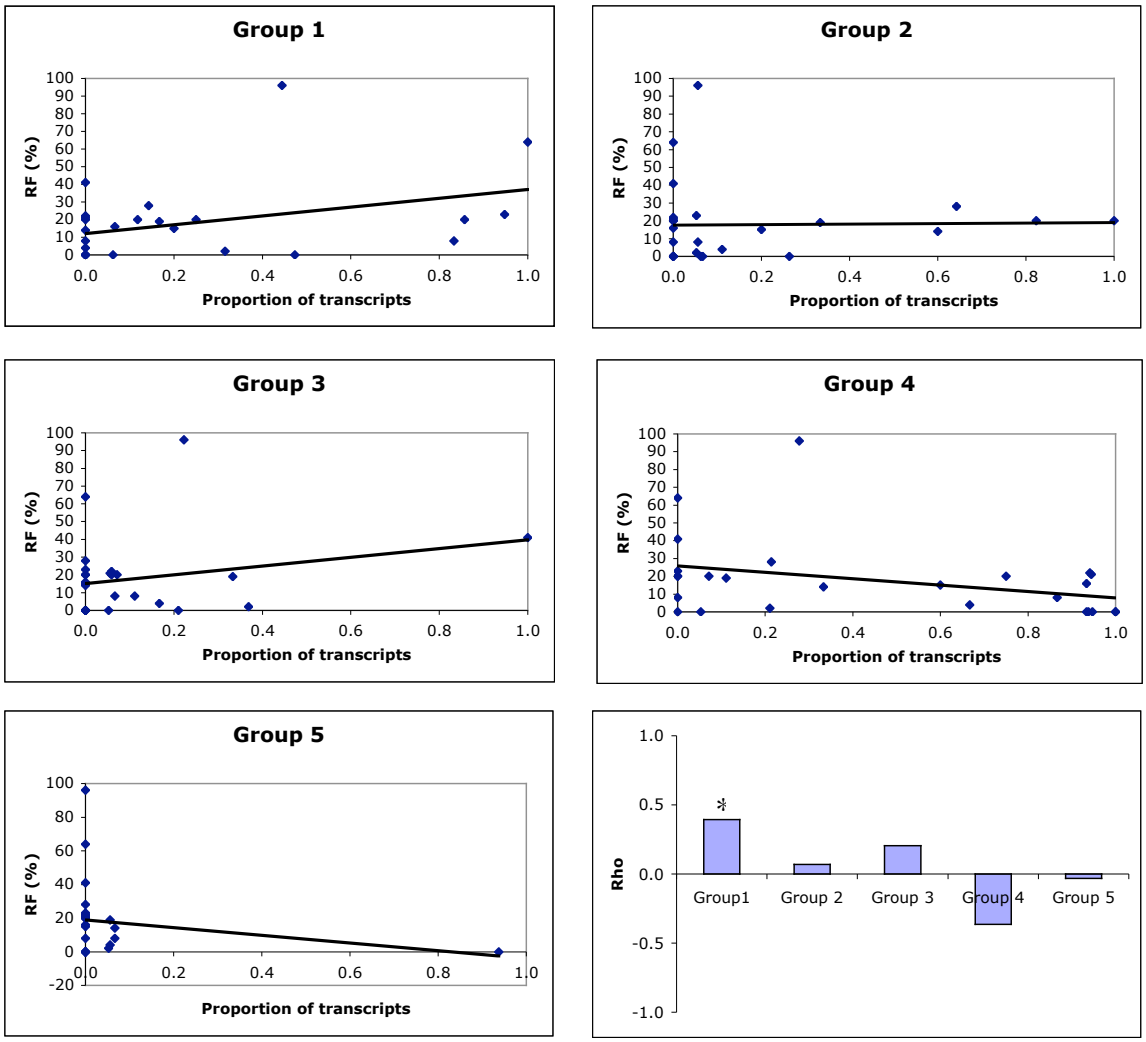

Fig. 3.21. Spearman Rank correlations between isolate rosette frequency (RF) and proportion of DBLα group 1-5 domain transcripts detected (Bull *et al.* 2005a). Groups 1 and 3 show positive Rho (Spearman Rank correlation) for association with rosette frequency. *Only group 1 association with rosette frequency is significant (Rho = 0.394; p = 0.049). There was a tendency for group 4 to be negatively associated with rosette frequency, but this was not significant (Rho = -0.365; p = 0.068).

3.7.2 DBLα1 domain transcription does not correlate with age

There was no significant correlation of any of the groups with age (Fig. 3.22), though there was a tendency for Bull group 4 transcripts to be associated with age (Rho = 0.385; p = 0.055, Fig. 3.23). All other groups showed (not significant) negative association with age (all p > 0.1) (Fig. 3.23).

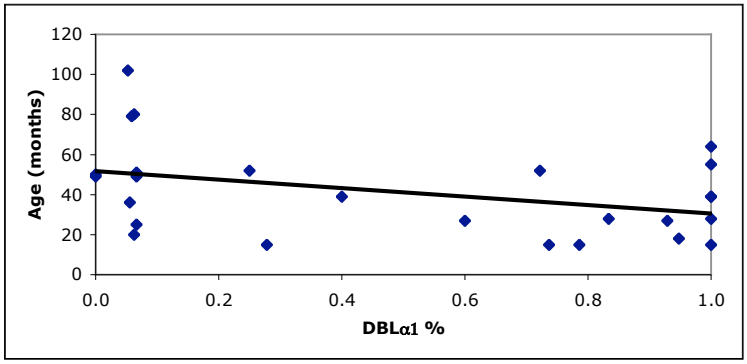

Fig. 3.22. No significant correlation was found between age (months) and proportion of DBLα1-like domain transcripts detected in the isolate. Spearman Rank correlation: Rho = -0.30, p = 0.14.

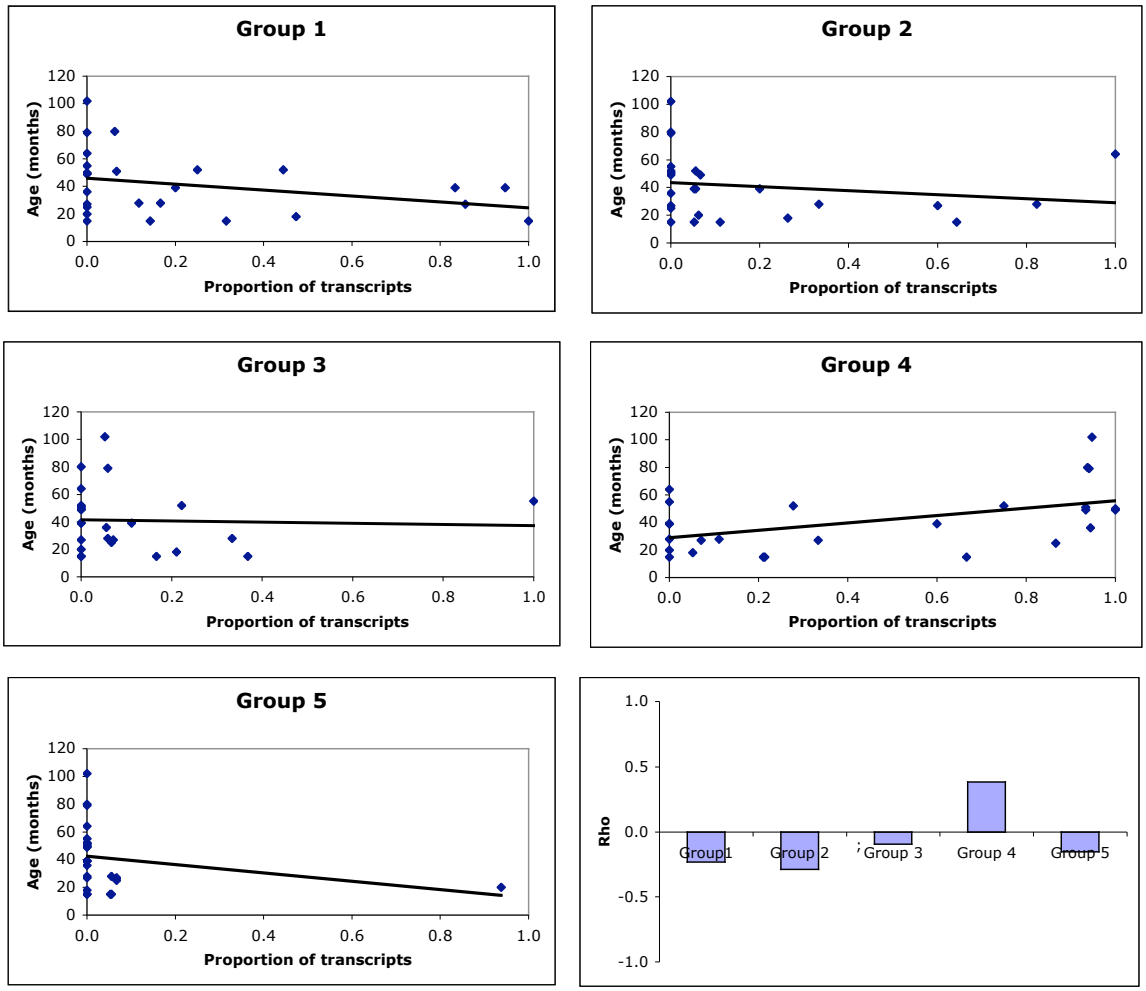

Fig. 3.23. Spearman Rank correlations between age and proportion of DBLα group 1-5 domain transcripts detected in the isolate (Bull *et al*. 2005a). No correlation produced a significant p value (all $p > 0.1$).

3.7.3 DBLα1 domain transcription does not correlate with parasitaemia

There was also no significant correlation of any of the groups with parasitaemia (in all groups $p > 0.1$) (Figs 3.24 and 3.25).

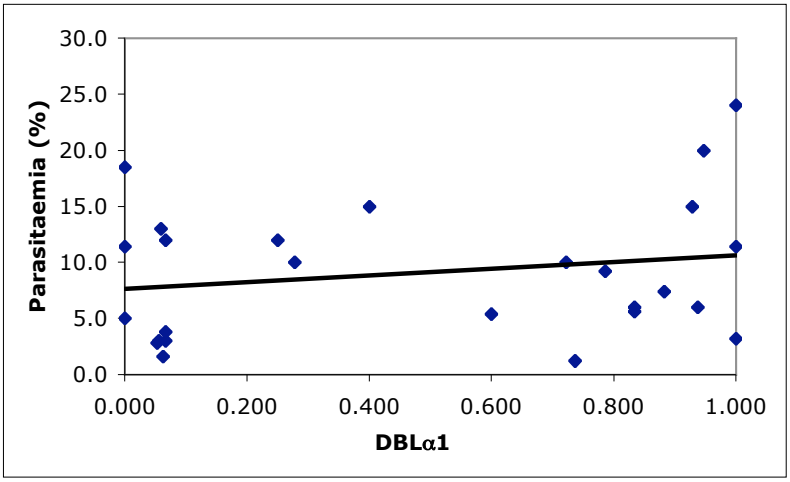

Fig. 3.24. No significant correlation was found between parasitaemia (%) and proportion of DBLα1-like domain transcripts detected in the isolate. Spearman Rank correlation: Rho = 0.35, p = 0.18.

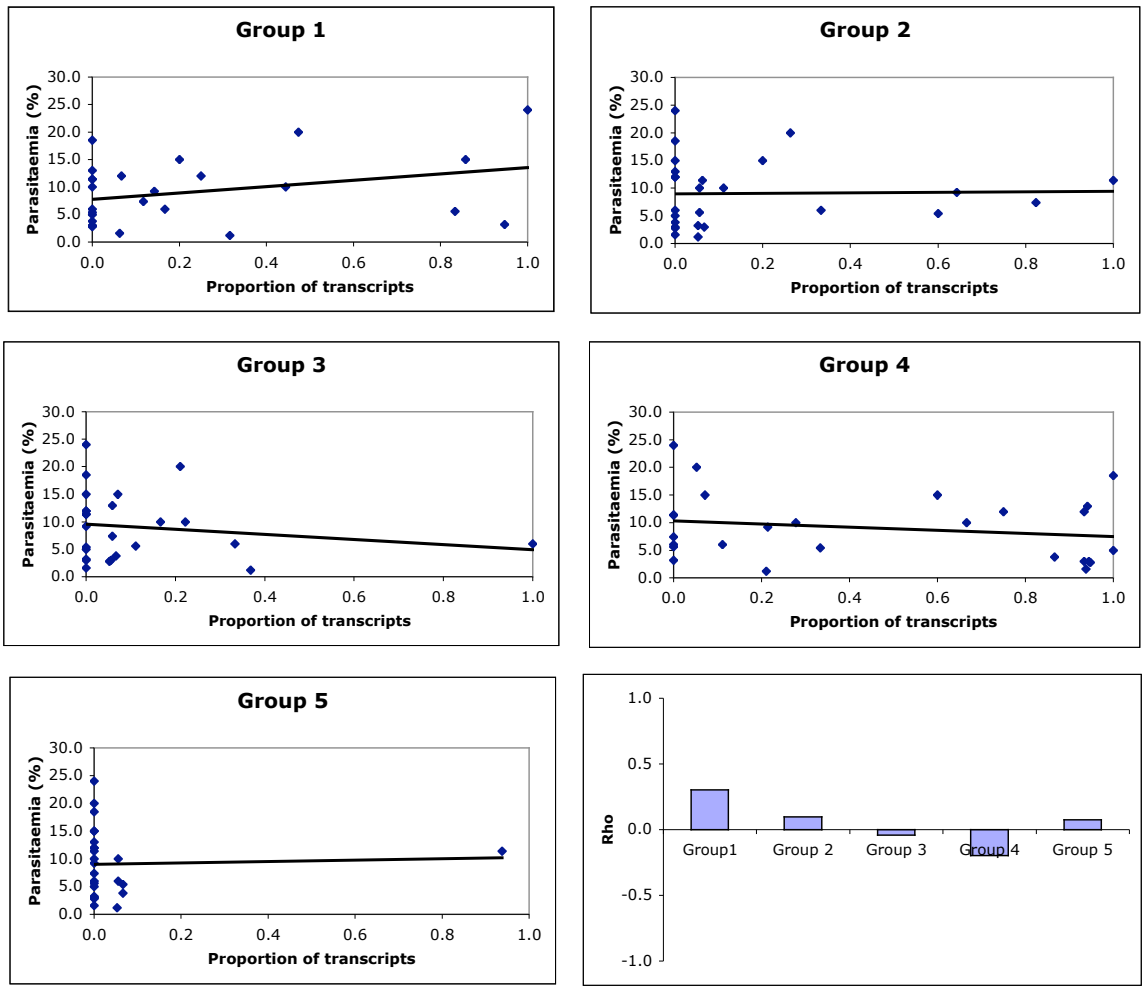

Fig. 3.25. Spearman Rank correlations between parasitaemia and proportion of DBLα groups 1-5 transcripts detected in the isolate (Bull *et al*. 2005a). No correlation produced a significant p value (all $p > 0.1$).

3.8 Discussion

The major finding presented in this chapter was that a higher level of DBLα1 domain transcription was observed in cerebral malaria isolates compared to hyperparasitaemia isolates. This indicates an association of group A *var* transcription with cerebral malaria, and therefore an association of group A PfEMP1 and malaria severity. This study of clinical isolates provides evidence to support *in vitro* work reporting a link between group A *var* gene transcription and "severe malaria phenotype parasites," parasites selected on semi-immune plasma pools (Jensen *et al.* 2004). I will recap my findings and then discuss my data in the context of other relevant studies.

Transcription profiling of 26 Malian field isolates revealed a marked difference in DBLα(0/1) transcription level in the three disease manifestation groups, with significantly higher frequency of DBLα1-like domain transcripts detected in cerebral malaria isolates compared to hyperparasitaemia isolates ($P < 0.001$, Chi-squared test). In the majority of cerebral malaria isolates the predominant transcript was DBLα1-like, significantly different to the hyperparasitaemia group, where the predominant transcript in the majority of isolates was DBLα0-like ($P = 0.013$, Fisher's Exact test). The majority of isolates possessed multiple genotypes (18/26), and thus different subpopulations of parasites had different genetic repertoires of *var* gene available to express. Expression of different *var* genes from subpopulations of parasites from the same genotype was also expected, due to switching of the expressed *var* gene. Most isolates (17/26) displayed expression of DBLα1-like and DBLα0-like domains. Of the remaining isolates, 6 exhibited 100% DBLα1-like

domain expression (U3, U6, CM6, CM7, CM9 and HYP4) and 3 had 100% DBLα0-like domain expression (U4, HYP1 and HYP8). No cerebral isolate exhibited 100% DBLα0-like domain expression. It is tempting to speculate that CM4 may be particularly susceptible to cerebral malaria, only having 1/17 DBLα1-like sequences. It is also possible that HYP4 may be protected from the cerebral malaria which might be expected from 100% DBLα1-like domain expression, for instance by having a protecting genetic polymorphism.

Younger host age and increased severity of disease has previously been associated with parasite expression of *var* sequences which are more frequently recognised by plasma from semi-immune children (Bull *et al*. 1999; Bull *et al*. 2000; Nielsen *et al*. 2002; Lindenthal *et al*. 2003). This suggested that *var* genes associated with severe disease, and young host age, are more common within a parasite population. This may suggest certain *var* genes being more commonly found in the genome of distinct parasites. Alternatively, certain PfEMP1 may be more frequently expressed, or commonly elicit a particularly successful immune response. The data in this chapter show that group A *var* genes are linked with severe disease, and group A *var* genes appear to be more 'common' in terms of sequence homology as most transcripts appearing in multiple isolates were group A. This fits with the hypothesis that surface antigens involved in severe disease can be recognised by plasma from high numbers of people within a population (Bull *et al*. 1999; Bull *et al*. 2000; Nielsen *et al*. 2002; Lindenthal *et al*. 2003).

A number of previous studies support the findings reported here. A small Brazilian study reported a link between severe malaria and expression of genes lacking 1-2 cysteines (those subsequently defined as missing in DBLα1 domains). However, only eight such sequences in total were found, across only six severe malaria patients (Kirchgatter and Portillo Hdel 2002). The association of group C *var* and non-severe disease was also seen in Tanzania (Rottmann *et al*. 2006) and Papua New Guinea (Kaestli *et al*. 2006), consistent with the data presented in this study. However, in Tanzania both group A and B were increased in the severe malaria group, and in Papua New Guinea, only group B was associated with clinical disease. Both studies used upstream region PCR to define *var* gene group (Kaestli *et al*. 2006; Rottmann *et al*. 2006). It is possible that some of the group B transcripts associated with severe malaria are group B/A (UpsB region with group A-like domain structure).

Previous studies used a broad definition of severe disease, grouping patients with very different severe complications, and presumably very different underlying pathologies and molecular mechanisms (Kirchgatter and Portillo Hdel 2002; Bull *et al*. 2005a; Kaestli *et al*. 2006; Rottmann *et al*. 2006). Uncomplicated malaria was commonly used as the comparison to severe malaria, resulting in studies comparing groups with disease severity and also highly different parasitaemia. Controlling for parasite burden by using hyperparasitaemia as the comparative non-severe malaria group was an important contributing factor to allow a clear result to be found from this study. Transcription from the uncomplicated malaria isolates showed an intermediate distribution across the DBLα(0/1) spectrum. However, analysis of the parasites causing the "uncomplicated" low parasitaemia disease must be treated with

caution. On presentation at hospital, these patients received treatment and thus it was not possible to follow disease progression to the natural end point of severe clinical symptoms, hyperparasitaemia or parasite clearance. The data from this study is consistent with the uncomplicated isolates representing an earlier time point in disease pathogenesis, where disease progression may be predestined but not yet clinically evident.

The success of this study relied on a precise and accurate disease definition for cerebral malaria of Blantyre score ≤ 2 with an asexual *P. falciparum* parasitaemia and no other possible cause of coma. Due to the high prevalence of low level asymptomatic parasitaemia in the general population, post-autopsy investigation revealed that *P. falciparum* was not the genuine cause of coma and/or death in up to 23% of patients diagnosed with cerebral malaria in Malawi (Taylor *et al.* 2004; Milner *et al.* 2005). In this study it was not possible to confirm cerebral diagnosis by autopsy, and as such it is theoretically possible that some of the cerebral malaria cases were incorrectly diagnosed. This could explain isolate CM4, unique in the cerebral malaria group with such a high frequency of DBLα0-like domain transcription (16/17 sequences). A strict definition of cerebral malaria was used in diagnosis of the isolates obtained for this study and the clear pattern of gene expression that emerged suggests that the diagnoses were as accurate as possible, although problems of misdiagnoses in a small proportion of cases remains a possibility in studies of field isolate disease manifestation and should be taken into consideration. This study and other reports (Kurtzhals *et al.* 2001; Nacher *et al.* 2001) emphasise the need for strictly defined disease criteria and carefully chosen

control groups in studies examining the molecular basis for malaria disease outcome. It is likely that this study was successful due to use of a strictly defined severe disease category with a precise pathology, and an appropriate control group.

In *P. falciparum* malaria, mature parasites sequester to avoid splenic clearance (Chotivanich *et al.* 2002) and cerebral malaria is characterised by sequestration of infected erythrocytes in the microvasculature of the brain (Berendt *et al.* 1994b; Silamut *et al.* 1999). Ideally, sequestered parasites, for example from postmortem brain, would be examined (Taylor *et al.* 2004; Milner *et al.* 2005). These parasites would be mature trophozoites, in contrast to the younger rings found in peripheral blood. Although once controversial (Chen *et al.* 1998b; Noviyanti *et al.* 2001; Duffy *et al.* 2002), the recent data strongly indicates that a single *var* gene is transcribed at ring stage and this corresponds to the PfEMP1 protein on the surface at trophozoite stage (Dahlback *et al.* 2007). This *var* gene transcript appears to remain present at high enough concentration for RNA extraction and RT-PCR in the mature trophozoite, and studies comparing *var* gene transcription across a cell cycle report the same *var* gene transcripts are present in ring and trophozoite parasites for a given culture (Peters *et al.* 2002; Montgomery *et al.* 2007). However, taking the RNA too late in the cell cycle may result in gaining relatively increased proportions of *var1csa,* which is transcribed throughout trophozoite stages (Kyes *et al.* 2003). A detailed study of *var* gene transcription in laboratory isolate NF54 suggests collection of parasites for *var* gene transcription studies at ring stage and pigmented trophozoite stage provides a good representation of *var* gene transcription for that invasion cycle (Dahlback *et al.* 2007). The report also confirmed that *var* gene

transcripts collected at ring stage are reflective of PfMEP1-mediated adhesion properties of the mature parasite. In this work and other similar studies (e.g.(Bull *et al*. 2005b), ring stage parasites were obtained from peripheral blood, carrying the assumption that the population of peripheral ring parasites directly reflects the sequestered mature population. Genotypically, peripheral parasites reflect the sequestered parasites (Dembo *et al*. 2006; Montgomery *et al*. 2006).

Sequestered parasite populations in different organs of the same patient show differential *var* gene expression, supporting a link between cytoadhesion and pathology (Montgomery *et al*. 2007). Although peripheral rings were not directly examined in this study, the assumption from previous studies is that the peripheral ring population reflects the sequestered parasite mass, which is then sequestered upon PfEMP1 expression at maturity in whichever organ best suits its particular cytoadhesive properties (Dembo *et al*. 2006; Montgomery *et al*. 2006). However, an absolute correlation between *var* gene transcript range in peripheral rings and sequestered erythrocyte PfEMP1 remains an assumption.

In addition, within an infection, *var* gene transcription is highly dynamic (Peters *et al*. 2002; Kaestli *et al*. 2004). Each *var* gene has its own intrinsic switching rate (Horrocks *et al*. 2004b), ranging from <0.025% per generation to at least 16% in experimentally infected individuals (Peters *et al*. 2002; Horrocks *et al*. 2004b). *Var* gene switching and silencing is very complex and is controlled at multiple levels. This involves tight transcriptional control with a silencing role of internal promoters and epigenetic chromatin modifications (Horrocks *et al*. 2004b; Duraisingh *et al*.

2005; Frank *et al*. 2006). At present it is not possible to predict the order of *var* gene expression as switching is not completely understood, but it is clear that the order of *var* gene transcription is far from random. *In vitro,* telomeric *var* genes (group A, B or A/B) have faster "off" rates than centromeric *var* genes (group C) (Frank *et al*. 2007). Upon adaptation to culture, parasites from infected individuals rapidly reduce the relative level of group A *var* gene transcription compared to group B or C (Peters *et al*. 2007). Laboratory strains tend to revert to group C *var* gene expression during long term culture (Frank *et al*. 2007). In contrast to fast "off" rates *in vitro,* group A and B genes expand more rapidly than group C genes in experimentally infected human volunteers (Lavstsen *et al*. 2005). It is possible that the activation of group A or B/A requires an additional stimulus from an infection, such as a detection of a signal from cerebral endothelium. Little is known about transcription factors which promote *var* gene activation, but it is possible that differences in the upstream region of the group A *var* genes may be involved in selection for group A *var* gene expression. For example, the mechanism of silencing appears to be different between the group A and B or C *var* genes, as silencing of group A, but not B or C, *var* genes is dependent on PfSir2 (Duraisingh *et al*. 2005).

In many studies (e.g. Kirchgatter *et al*. 2002), low parasitaemia isolates are cultured for a few cycles before RNA extraction. Combining the data showing that group A *var* genes are more likely to be switched off, and the fact that it is most often the uncomplicated malaria isolates that show low parasitaemia, suggests an unfair bias in the reporting of lower group A transcription levels in uncomplicated isolates. In this study, RNA was collected from all isolates at ring stage and was processed and

stored immediately. Isolates were not cultured through to the next cell cycle, and so no *var* gene switching could occur. However, even taking this extra precaution, the *var* gene expressed at collection may have been switched on since development of severe disease symptoms, and thus the currently expressed *var* gene may not be responsible for the clinical condition. Collecting field isolates as close as possible to onset of clinical symptoms, and avoiding culturing where possible, will increase confidence of a direct correlation between detected *var* gene transcription and disease outcome.

In addition to parasite isolates, the choice of DBLα domain to investigate was advantageous. Good primers were available (Taylor *et al*. 2000a; Bull *et al*. 2005a), and the vast majority of *var* genes contain a DBLα domain (Gardner *et al*. 2002). Though there was not enough parasite material for quantitative real-time RT-PCR, the RT-PCR colony picking technique used proved accurate and reproducible and has been used in many previous studies (e.g. Kirchgatter *et al*. 2002; Bull *et al,* 2005). A recent study comparing RT-PCR and real-time RT-PCR of *var* gene transcripts found RT-PCR gave very similar results to a real-time RT-PCR, with the same dominant transcript being detected with both approaches in the majority of isolates (Gatton *et al*. 2006). Though a clear distinction in DBLα(0/1) domain transcription levels between cerebral malaria and hyperparasitaemia isolates was discovered, the study could be reinforced and strengthened by sequencing more transcripts per isolate, the inclusion of more isolates from each group, and the addition of further clinical disease categories.

The disparity in DBLα (0/1) domain transcription levels between the two isolate groups suggests there might be a functional difference between DBLα0 and DBLα1 domains. The only known adhesive and well-characterised property of DBLα domains is rosetting, for example mediated via interaction of a PfEMP1 DBLα1 domain with CR1 on non-infected erythrocytes (Rowe *et al.* 1997). The association of rosetting with severe malaria in Mali and group A *var* genes in this present study was expected, as rosetting has been repeatedly linked to severe malaria in Africa (Carlson *et al.* 1990; Rowe *et al.* 1995; Bull *et al.* 2005a; Rowe 2005; Kaestli *et al.* 2006). In these Malian isolates, DBLα groups 1 and 3 correlated with rosette frequency (RF), in contrast to the correlation between DBLα group 2 and RF reported in a recent Kenyan study (Bull *et al.* 2005a). This could be a genuine difference between the Mali and Kenya isolates. Unlike DBLα groups 1 and 3, the proportion of DBLα group 2 sequences is not significantly different between cerebral and hyperparasitaemia isolates in this study. Interestingly, a link between DBLα1 domains in general and rosetting, but not group 2 DBLα domains and rosetting was also reported in a recent study of Ugandan field isolates (Normark *et al.* 2007). The functional significance of this DBLα grouping (1-6) compared to the broader grouping of DBLα(0/1) remains to be confirmed, though the classification is a useful tool for DBLα domain analysis. Although results associating sequences separated into the DBLα groups with RF are conflicting, the association of DBLα1 in general with rosetting is supported in both geographic locations and in laboratory isolates (Rowe, JA, unpublished data). The association of rosetting and severe malaria demonstrated in these field isolates, and in many other studies, highlights rosetting as a key target of clinical intervention to control parasite-mediated

phenomena associated with severe disease complications (see chapter 6 for discussion of rosette inhibition in severe malaria).

Though DBLα0 domains have been reported to support rosetting (Chen *et al.* 1998a), rosetting in laboratory strains appears to be predominantly via DBLα1 domains (Rowe, JA, unpublished data), suggesting that there is a steric restriction on the conformation of DBLα1 domain that can retain affinity for CR1 or other rosetting ligands. Perhaps the two extra cysteines found in DBLα0 domains form a disulfide bond that fundamentally alters the DBLα domain structure. Recent structural predictions of DBLα domain structure based on the known structures of EBA175 and *P. knowlsei* DBLα, suggest that DBLα0 domains have a GAG-binding motifs, which mimic the carbohydrate-binding pocket of EBA-175 (Tolia *et al.* 2005; Singh *et al.* 2006; Normark *et al.* 2007). In the DBLα1 domains, some of these GAG motifs disappear with the loss of the two cysteines, supporting this hypothesis. Motifs and predicted structural features present in rosetting PfEMP1 include an alpha helix that appears to be conserved between rosetting PfEMP1 DBLα domains (Normark *et al.* 2007).

Conversely, it may not be the DBLα1 domains *per se*, but other features of the group A *var* genes that is involved in cerebral malaria pathogenesis. Group A and B/A PfEMP1 are in general larger, with a more complex domain structure than PfEMP1 from group B, C and B/C. The plethora of other domains available in the group A and B/A PfEMP1 may have clinically relevant binding potential. For example, the majority of DBLγ domains, some of which were originally implicated in CSA

binding (see chapter 4) are found in group A or B/A *var* (12/14 in 3D7), as are the majority of DBLε domains (11/12 in 3D7), some of which enable binding to naturally occurring IgM anibodies (Semblat *et al*. 2006). There is also evidence that certain PfEMP1 have affinity for molecules on the cerebral endothelium such as ICAM1, mediated by a tandem array of DBLβ and C2 domain (Smith *et al*. 2000a; Springer *et al*. 2004). Perhaps surprisingly, ICAM-binding DBLβ/C2 tandem arrays do not appear to be associated with particular PfEMP1 groups (Smith, JD, personal communication).

Whilst DBLα1 domain transcripts are indicative of a group A, B/A PfEMP1, identification of DBLα0 domains is indicative of a group B, C or B/C PfEMP1. These typically possess a DBLα0-CIDRα type semi-conserved head structure (Gardner *et al*. 2002; Kraemer *et al*. 2007) and are capable of CD36-binding (Robinson *et al*. 2003). Though the DBLα0 domain itself does not have affinity for CD36, its presence suggests expression of PfEMP1 with affinity for CD36.

CD36-binding is the most common known adhesive property of malaria isolates, with the majority of field isolates having affinity for CD36 (Udomsangpetch *et al*. 1997). The role of CD36 in malaria pathogenesis is complex (reviewed in Serghides *et al*. 2003) and not fully understood. CD36 is a scavenger receptor expressed on erythrocytes, platelets, and many other cellular components of the blood, in many tissues including endothelium and muscle, and on organs such as liver and spleen, but not on the cerebral endothelium (Turner *et al*. 1994; Serghides *et al*. 2003). CD36-binding is thus associated with sequestration of infected erythrocytes in areas

such as skin and muscle away from vital organs such as the brain (Serghides *et al.* 2003). The lack of CD36-binding in infected erythrocytes coated in group A PfEMP1 may access cerebral endothelium, as they are less likely to be sequestered elsewhere. Earlier studies reported CD36 binding being associated with non-severe malaria without reference to PfEMP1 (Rogerson *et al.* 1999; Traore *et al.* 2000). It is tempting to speculate these results came about because of expression of group B, C or B/C PfEMP1 in these mild malaria patients.

CD36 binding also mediates platelet mediated clumping, a phenomenon originally associated with severe malaria (Pain *et al.* 2001). The only isolate with high PMC was a cerebral malaria isolate (CM8), with high parasitaemia (20%), but with low group B/C expression (only 1/19 DBLα0-like transcripts). The *in vivo* relevance of PMC remains unclear and the phenomenon is now thought to be associated with high parasitaemia but not severe malaria *per se* (Arman *et al*, in press).

Finally, CD36 promotes non-opsonic (non-inflammatory) phagocytic clearance (McGilvray *et al.* 2000) and phagocyosis of *Plasmodium* infected erythrocytes by human macrophages can by reduced by 50% by blocking CD36-dependent interactions (Smith *et al.* 2003). However, CD36-binding parasites are also able to cause inhibition of dendritic cells (Urban *et al.* 1999). These data suggest a complex relationship between CD36-binding and sequestration and immune response. In general, the data indicate a low immunopathological burden where CD36-binding parasites dominate. This is a good strategy for a parasite that does not benefit from host death, and is consistent with the association presented here between group B, C

or B/C *var* genes and hyperparasitaemia. However, the extent of CD36-binding in parasites not expressing a CD36 binding PfEMP1, through other proposed ligands such as modified band 3, sequestrin and CLAG9, is unclear (Serghides *et al*. 2003).

There was also no significant correlation of any of the DBLα groups with parasitaemia. The lack of association of any group with parasitaemia supports the idea that a particular *var* gene group does not encourage an expansion of parasitaemia, but the *var* gene group expressed plays a role in determining whether a severe clinical manifestation will develop. The lack of association of DBLα group with parasitaemia is also reflected in the sequences from uncomplicated malaria patients being distributed across the phenogram and network.

The relative proportion of DBLα1 *var* genes detected in this study is similar to the relative proportion of DBLα1 *var* genes in parasite genomes seen in published strains and other reports, at around 20-30% (Fowler *et al*. 2002; Gardner *et al*. 2002; Albrecht *et al*. 2006; Kraemer *et al*. 2007). If the proportion of DBLα1 *var* genes in an isolate is relative stable, as appears to be the case from 3D7, IT and HB3 genomes, this suggests that there is no general bias of expression towards DBLα1 or DBLα0 *var* genes, though the gDNA repertoire of DBLα *var* gene sequences within these particular isolates would have to be examined to confirm this.

Roughly one third of the transcript sequences were unique with no database matches, while others showed a high level of conservation. Interestingly, a non-*var1csa* highly conserved sequence, CM6A, was found in 5 isolates. Extended sequencing of the

CM6A domain from the *var* genes from which these sequences belong would reveal whether the entire gene is conserved between these isolates, or just the DBLα domain. It would be interesting to screen for the presence of this domain in other isolates to identify to what extent this is a strain transcending *var* gene in addition to the *var1csa, var2csa* and type 3 *var* gene family. Expression of this domain *in vitro* would be a useful starting point for the examination of any particular roles for which this sequence has been conserved, for example through a series of binding studies. The identification of a domain identical to the DBLα1 of Palo Alto rosetting *var* gene *PARvar1* in 2 rosetting cerebral malaria isolates (CM7, RF 20% and CM9, RF 41%) is also intriguing, suggesting this may be a conserved rosetting *var* gene family. It would be very interesting to examine the prevalence of this gene in other isolates, and investigate whether the homology to *PARvar1* extends throughout the entire *var* gene or is confined to the DBLα domain. These domains suggest that *var1csa*, *var2csa* and the type 3 *var* genes may not be the only *var* genes which are common to many different isolates.

The immunity achieved against *P. falciparum* infection by adulthood in malaria-endemic areas suggests a finite global diversity of *var* genes and other VSA, or at least a high enough level of cross-reactive epitopes for antibody-mediated immunity (Bull *et al.* 2000). Certain geographic locations appear have a limited *var* gene repertoire with a relatively stable *var* gene repertoire and considerable interstrain *var* gene overlap, including Brazil (Afonso Nogueira *et al.* 2002; Albrecht *et al.* 2006) and West Pacific (Fowler *et al.* 2006), while data from other areas suggests a lower sequence overlap globally (Fowler *et al.* 2002; Bull *et al.* 2005a; Trimnell *et al.*

2006). Though a study of the domains of 3D7 predicts that cross-reactive epitopes are relatively uncommon, antibodies directed at group A PfEMP1 show higher levels of cross-reactivity between domains than those directed at group B or C PfEMP1 (Joergensen *et al*. 2006). This is consistent with my findings that group A *var* genes tend to be more common in terms of conserved sequences between isolates and database matches, and with the original agglutination studies showing high frequency of recognition of parasites causing severe disease (e.g. Bull *et al*. 1999). The high level of diversifying selection on PfEMP1 (Lavstsen *et al*. 2003), and recombination between *var* genes within and between isolates, will continue to drive expansion of the global *var* gene repertoire.

The data presented in this chapter is of relevance to the exploration of PfEMP1 as a potential vaccine target. For example, as the majority of *var* genes contain DBLα0 domains these might be considered to provide a more comprehensive or universal target than DBLα1 domains. However, a DBLα0 domain vaccine, even if it was very effective at protecting against parasites expressing DBLα0 domains, may select for parasites expressing DBLα1 domains. In this study, DBLα1 domains are associated with cerebral malaria, and thus a DBLα0 domain vaccine may have the potential to select for cerebral malaria-causing PfEMP1-expressing parasites. Thus, a general DBLα0 domain vaccine would not necessarily be useful in protecting against severe disease. Analysis of this kind is critical to avoid creation of a vaccine which may actually be detrimental to those at risk of infection. Secondly, database analysis of the domains sequenced here highlight the huge global range of DBLα domains. Even from parasites collected from a small geographic location at a particular time

relatively little overlap between domains was seen. However, the presence of some very common DBLα1 domains such as the three described in this chapter could be exploited. Of course, sequence data is not enough to provide evidence for cross-reactive epitopes, as cryptic (conformational) epitopes are also possible (Joergensen *et al*. 2006).

In conclusion, the data presented in this study show a strong association of group A *var* gene transcription and cerebral malaria. This is consistent with previous work, and provides further evidence for the importance of PfEMP1 in clinical complications due to *P. falciparum* infection. The study was successful due to carefully chosen severe disease criteria and a suitable control group. As with any multifactorial disease, other factors such as household factors (Mackinnon *et al*. 2005) as well as polymorphisms in human genes such as CR1 (Cockburn *et al*. 2004) or blood group (Rowe *et al*. 2007) may also affect or modulate parasite virulence. However, the data strongly suggest that group A PfEMP1 play a critical role in cerebral malaria pathogenesis. As described, these findings have implications for future work on vaccine or drug design against PfEMP1, and increase our understanding of the molecular pathogenesis of parasite genetics contributing to cerebral malaria.

Chapter 4

Var gene transcription in placental malaria field isolates

Some of the results presented in this chapter were published as

Duffy, MF *et al*. (2006) Transcribed *var* genes associated with placental malaria in Malawian women. Infection and Immunity, 74: 4875-4883.

4.1 Abstract

P. falciparum placental malaria field isolates from Malawi were used to test the hypothesis that *var2csa* and/or conserved DBLγ domains are commonly transcribed in placental malaria field isolates. *Var2csa* transcription was detected in all placental isolates examined by RT-PCR, but not in a control group of childhood malaria isolates also analysed. Many DBLγ domain transcripts were also detected in these placental and childhood isolates, but no DBLγ domain features were found to be specific to placental isolates compared to the childhood isolates through phylogenetic analysis. This data strengthens the growing body of evidence pointing to *var2csa* as crucial for placental malaria pathogenesis, and confirms non-*var2csa var* genes are also expressed in placental field isolates.

4.2 Introduction

Malaria during pregnancy is the most common manifestation of clinical malaria in adults in malaria-endemic countries, where adults are typically immune to clinical disease (Brabin 1993; Brabin *et al.* 2004). Immunity to clinical disease increases through childhood with increasing episodes of disease, probably through cross-reactive immune responses developed from previously employed VSA variants. Parasite-infected erythrocytes depend on sequestration to avoid clearance in the spleen (Chotivanich *et al.* 2002), and once immunity is achieved, parasites have effectively exhausted the supply of novel sequestration receptors. However, upon pregnancy, the placenta becomes a novel niche for parasitic sequestration. As placental sequestration is a novel process in terms of disease episodes for an individual, adhesion is thought to require fresh VSA variants, which are not

expressed in malaria in childhood, and to which there is thus no protective immunity in the first pregnancy. These infected erythrocytes are unusual in their high affinity for chondroitin sulfate A (CSA). CSA is a sulfated glycosaminoglycan, present on the intervillous spaces and on syncitiotrophoblasts, which is where placental adhesion occurs (Achur *et al*. 2000; Valiyaveettil *et al*. 2004). Though CSA is also present on other cell types including cerebral endothelium and erythrocytes, CSA is not commonly a ligand for infected erythrocytes in non-placental field isolates. Affinity for CSA has thus provided a starting point for studies on placental malaria-phenotype parasites, and CSA-binding infected erythrocytes have become synonymous with placental malaria-type parasites. Though there is evidence that other adhesion phenotypes also play a minor role in placental sequestration, for example adhesion to hyaluronic acid (HA) (Beeson *et al*. 2000), CSA appears to be the major sequestration receptor in the placenta (Duffy *et al*. 2006b; Muthusamy *et al*. 2007). Some data regarding HA-mediated adhesion has been confused due to the possibility of contaminating CSA in the HA preparations used (Valiyaveettil *et al*. 2004; Fried *et al*. 2006).

As with childhood malaria, the PfEMP1 family are key suspects for mediating adhesion during pregnancy. PfEMP1 mediating placental adhesion would be expected to bind CSA, to be transcribed in the majority of placental field isolates and to be expressed exclusively in placental malaria field isolates (not for example in childhood malaria isolates). At the time of the study design, the conserved features which define *var* gene DBLγ domains were the only *var* gene sequences associated with expression in placental malaria (Khattab *et al*. 2001; Lekana Douki *et al*. 2002;

Costa *et al*. 2003; Khattab *et al*. 2003). In particular, transcription of well-conserved gene *var1csa* which contains 2 DBLγ domains was associated with placental malaria field isolates and with adhesion to CSA (Buffet *et al*. 1999; Rowe *et al*. 2002a; Gamain *et al*. 2004). Other DBLγ-containing *var* genes have been implicated in placental malaria: *CS2var* (Reeder *et al*. 1999) and *varPAM732* (Khattab *et al.* 2001; Badaut *et al.* 2007). The pan-reactivity of antibodies to DBLγ-containing *var* genes to placental malaria isolate worldwide suggested a small set of epitopes common to DBLγ domains was responsible for placental sequestration (Lekana Douki *et al*. 2002; Costa *et al*. 2003).

It was not logical to suspect all DBLγ domains would be involved in placental malaria, as DBLγ domain variants are common in the group A PfEMP1 which can be expressed in childhood malaria. Involvement of *var* genes in placental malaria which are also common in childhood infection is inconsistent with the novel placental-specific *var* gene hypothesis. It was hypothesised that only a subset of DBLγ domains may be involved in placental adhesion. The study thus was originally designed to amplify transcribed DBLγ domains from parasites taken directly from infected placenta, to explore any association of particular sequences with placental sequestration in field isolates. However, since the outset of the study two major advances altered the direction of the chapter.

Firstly, evidence for *var1csa* involvement in placental malaria was losing momentum. In 2003, Winter *et al*. reported that *var1csa* is commonly expressed in childhood isolates, and since then many other field isolate studies (including chapter

3 RT-PCR data) have supported this observation of *var1csa* expression in children and men. If *var1csa* plays a role in placental isolates, it is certainly not the major contributor.

Secondly, there was increasingly convincing evidence for involvement of another strain transcending *var* gene, *var2csa*, in placental malaria (Salanti *et al.* 2003; Salanti *et al.* 2004). VAR2CSA has since been shown to support adhesion to CSA through adhesion and knock out studies (Salanti *et al.* 2003; Salanti *et al.* 2004; Gamain *et al.* 2005; Viebig *et al.* 2005; Viebig *et al.* 2007) and to be expressed in infected erythrocytes in pregnant women from Senegal (Tuikue Ndam *et al.* 2005). Conservation of *var2csa* in the majority of field isolates examined, and in laboratory strains 3D7, HB3 and IT also suggests a strong selective pressure to retain a *var2csa* copy in the genome (Trimnell *et al.* 2006; Kraemer *et al.* 2007). The high conservation of this gene also indicated that it may provide a promising vaccine candidate, to mimic the natural immunity to placental malaria which increases with subsequent pregnancies (Fried *et al.* 1998; Duffy and Fried 2003), if it was proved that *var2csa* was essential for, or at least a common contributor to, placental sequestration.

As it became apparent that VAR2CSA may play a crucial role in placental malaria, the RT-PCR strategy adopted in this chapter was enhanced to also amplify the DBL3X domain of *var2csa* family *var* genes homologues. The primers still retained the ability to also amplify any transcribed DBLγ domains, as the primer sites were designed to recognise an area of homology between *var2csa* and DBLγ domains in

general. It was considered important to also detect DBLγ domain-containing transcribed *var* genes in the placental isolates firstly as a comparative set of *var* gene transcripts to *var2csa*, and secondly as the extent to which other *var* genes contribute to the placental malaria phenotype is still unclear. The panel of field isolates was also increased to include a range of childhood isolates for comparison.

4.3 Aim of chapter

The aim of this chapter was to test the hypothesis that a conserved *var* gene, *var2csa*, and/or conserved DBLγ domains are commonly and specifically transcribed in placental malaria field isolates.

4.4 Materials and methods

Materials and methods that are specific to chapter 4 are listed below. General materials and methods and a list of suppliers are given in chapter 2.

4.4.1 Field isolates

Placental malaria field isolates were obtained from Stephen J. Rogerson, from Blantyre, Malawi (Chapter 2).

4.4.2 RT-PCR conditions

RT-PCR was used to amplify approximately 500 bp of the *var* gene DBLγ domains, using unbiased primers; 1st set (DBLγ amplification only, designed by S.J. Rogerson, Melbourne, Australia): D3F (CCTCCWAGRAGAMAAAAATTAT) and D3R2 (CCATCKNAR AAATTGNGGTY), and second set (DBLγ/*var2csa*DBL3X

amplification) D3F as above and D3R1.2 (ACAAWANTSNTCDBMCCATTC, designed by J.A. Rowe). Neither of these pairs were nested. Amplification conditions were a hot start, 95˚C, 5 min, followed by 40 cycles of 95˚C, 20 sec; 42˚C, 30 sec; 60˚C, 30 sec finishing with 60˚C, 10 min. 25 pmol of each primer, 2.5 mM $MgCl_2$ and 0.125 units Platinum taq (Invitrogen) were used in each 50 µl reaction. 2 µl cDNA or H20, or 0.5 µl gDNA were used in the amplification reaction. Samples without RT were used in all reactions to exclude DNA contamination.

4.4.3 Primer bias calculation

The instrinsic bias for D3F and D3R1.2 primer pair had previously been calculated as < 2% for the most frequently detected sequence (S.J. Rogerson, Melbourne). The instrinsic bias for D3F and D3R1.2 primer pair was calculated using excel BIOMONDIST as < 2% for the most frequently detected sequence. The most frequently detected sequence was counted 9 times when only 5 counts would be expected in 37 minipreps. This is a bias of (9/5)^(1/35) over 35 cycles = 1.017, i.e. a 1.7% bias per cycle.

Details of ligation, cloning, transformation, and sequencing of RT-PCR products are given in chapter 2. In brief, RT-PCR products were visualised by electrophoresis on 1.5% agarose gels. RT-PCR products were purified and ligated into PCR II TA cloning vector (Invitrogen) and ligated plasmids were used to transform TOP10F *E. coli*. Transformed *E. coli* was grown overnight under ampicillin selection and blue/white colony screening. Individual white colonies were selected for overnight growth and the plasmids extracted for sequencing. Presence of an insert in the

extracted was verified by *Eco*RI restriction digestion prior to sequencing. Sequencing was carried out by the University of Edinburgh School of Biological Sciences Sequencing Service (details in chapter 2).

4.4.4 Transcript sequence analysis

Transcripts sequences from each isolate were grouped into contigs of >95% nucleotide identity using the SeqMan programme within DNAstar software package. Consensus sequences from each isolate were saved as sequence A, B, C etc from that isolate as EditSeq files (DNAstar software package), and protein sequences were obtained by translating the DNA sequences using EditSeq translation function. Nucleotide and protein sequences were then compared within and between isolates using MegAlign (DNAstar software package). Alignments and phenograms were produced using the clustal W alignment programme within MegAlign, using default settings. Sequence distances were calculated using MegAlign, and colour-coded into the following groups; 0-30, 30-39.9, 40-49.9, 50-59.9, 60-69.9 70-99.9 and 100% amino acid identity for production of sequence distance figures. Where nucleotide identity levels were not normally distributed, a non-parametric test (Mann-Whitney Test) as used rather than a t-test for comparisons between groups. Homology searches were performed using nucleotide-nucleotide BLAST search of the NCBI database (http://www.ncbi.nlm.nih.gov/BLAST). Pie charts were created in Excel. Phenograms were laid out in Adobe Illustrator.

4.5 Results 1: Preliminary DBLγ transcription data with primer pair D3F and D3R2

4.5.1 RT-PCR to amplify transcribed DBLγ domains in placental malaria isolates

Six placental malaria field isolates (CS294, P132, P134, P136, P143, P154) were obtained from Queen Elizabeth Central Hospital in Blantyre (gift from Stephen J. Rogerson). These were mature pigmented trophozoites which had been extracted directly from placenta and stored immediately in Trizol. Isolates P132, P136, P143 and P154 had previously been genotyped using PCR of size-variant markers (MSP1, MSP2 and GLURP allelic forms), which revealed that each isolate showed multiple infections; six different parasite genotypes were detected in isolate P132 and three were detected in P136, P143 and P154 (Rowe *et al.* 2002a). The number of genotypes for P134 and CS294 was not determined.

RNA extraction from each isolate and cDNA preparation had previously been performed by Dr JA Rowe (Rowe *et al.* 2002a). In addition, cDNA from 2 parasite strains that had previously been panned for affinity to CSA, TM180CSA and TM284CSA was obtained (gift from Dr JA Rowe).

Degenerate primers to amplify the expressed DBLγ domains by RT-PCR were designed by Stephen J. Rogerson; Primers: D3F and D3R2. This primer pair amplifies an approximately 500 bp region of DBLγ domains (Fig. 4.1) and had previously been tested for unbiased recognition of DBLγ domains (Stephen J. Rogerson, personal communication). At this stage the importance of VAR2CSA was

not known, and the focus of research was on involvement of DBLγ domains. Thus these primers did not recognise the DBLX domain, and so could not amplify *var2csa* (Fig. 4.1; see section 4.7 for primers to also amplify *var2csa*).

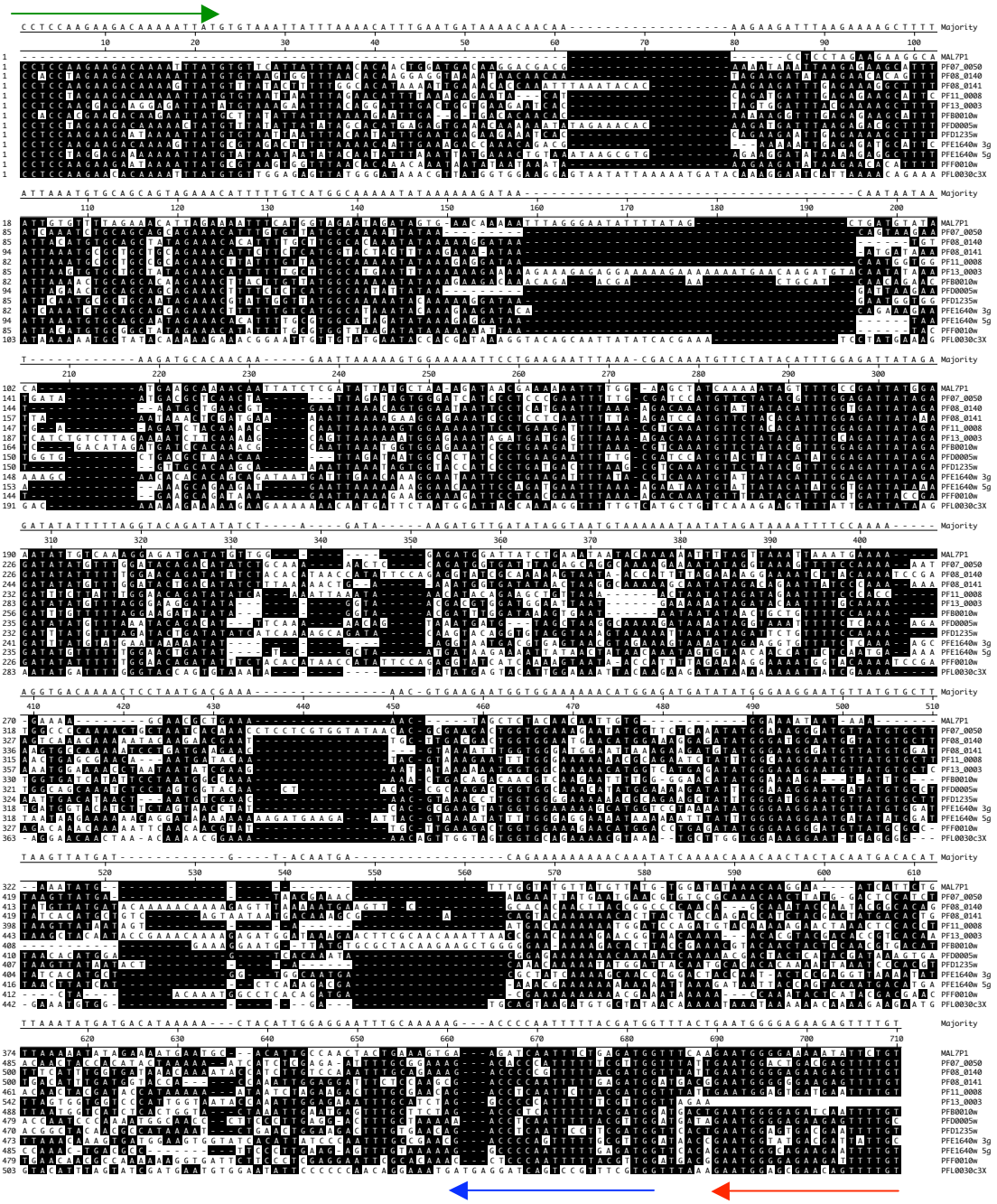

Fig. 4.1. Primer pairs to amplify DBLγ domains. A Clustal W aligment of 3D7 DBLγ domains and 3D7 *var2csa* DBL3X (PFL0030c3X) created in MegAlign is shown.

Primers D3F (green), D3R2 (blue) and D3R1.2 (red) are shown. Primer pair D3F/D3R2 recognises DBLγ domains only. Primer pair D3F/D3R1.2 also recognises *var2csa* (PFL0030c3X) see section 4.7.

4.5.2 RT-PCR to amplify transcribed DBLγ domains in placental malaria isolates: primer pair D3F and D3R2

DBLγ domain RT-PCR with primers D3F and D3R2 was carried out on the 6 placental isolates, and also the two parasite strains selected for CSA-affinity, TM180CSA and TM284CSA (Fig. 4.2). CS294, P132, P136, P143, P154 and TM180CSA gave RT-PCR product. P134 and TM284CSA did not give a RT-PCR product.

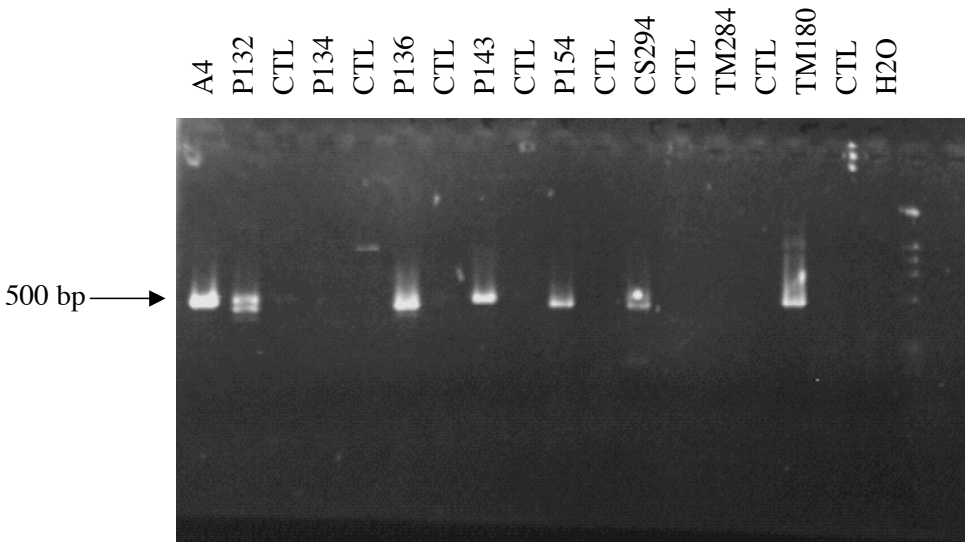

Fig. 4.2. 1.5% agarose gel of RT-PCR products from amplification of DBLγ domains from cDNA from Malawi placental field isolates CS294, P132, P143, P136, P143, P154, and laboratory strains TM180CSA and TM284CSA with primers D3F and D3R2. gDNA control (CTL) for each isolate, where the cDNA synthesis reaction is

performed without reverse transcriptase, is next to the cDNA amplification. These lanes remain blank indicating there is no gDNA contamination in the cDNA preparation. A4 gDNA was used for a positive control, and distilled water as a negative control. DNA ladder was ϕX174 RF DNA/*Hae* fragments (Invitrogen).

4.5.3 DBLγ domain transcripts detected by RT-PCR with primers D3F and D3R2

DBLγ domain RT-PCR products were purified by gel extraction and PCR products were used to transform *E. coli,* resulting in plates of colonies carrying plasmids with inserted copies of the DBLγ domains. A random selection of 12-17 of these colonies were picked and grown over night in LB broth at 37°C to allow growth and replication of the bacteria carrying the plasmid. After approximately 18 hours the recombinant plasmids were extracted. Presence of an insert of the correct length was confirmed by enzymatic digestion of the multiple cloning site using restriction enzyme *Eco*RI of a sample of each extracted plasmid. Digested plasmids were run out on 1.5% agarose gels, and plasmids containing an insert were marked by presence of an approximately 500 bp band. Fig. 4.3 shows a typical gel. Two bands were seen when the insert contained an *Eco*RI restriction site (GTTAAC, e.g. P143, digests 2, 4 and 7, Fig. 4.3).

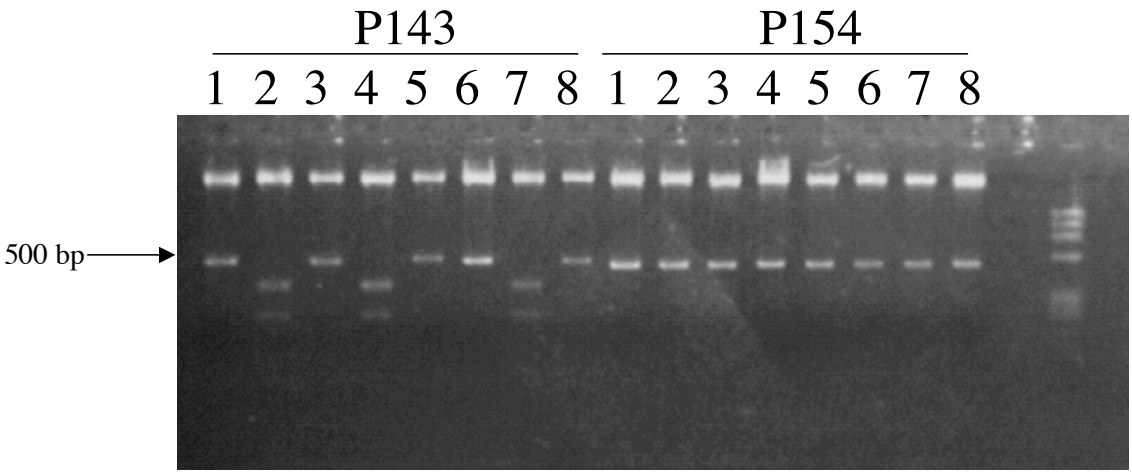

Fig. 4.3. A typical agarose gel of *Eco*RI digests products of plasmids extracted from a set of minipreps. In this case 8 plasmid extractions each from isolates P143 and P154 are shown, all of which had inserts of approximately 500 bp. DNA ladder was ϕX174 RF DNA/*Hae* fragments (Invitrogen).

The sequences obtained from each parasite isolate were compared for multiple copies of the same sequence (over 95% sequence identity), and defined as placental (Pl) *var* gene A, B, C… from each isolate. Up to five sequences were detected per isolate though the presence of more *var* gene transcripts cannot be excluded. Results were displayed as pie charts to indicate the relative abundance of distinct transcribed DBLγ domains (Fig. 4.4).

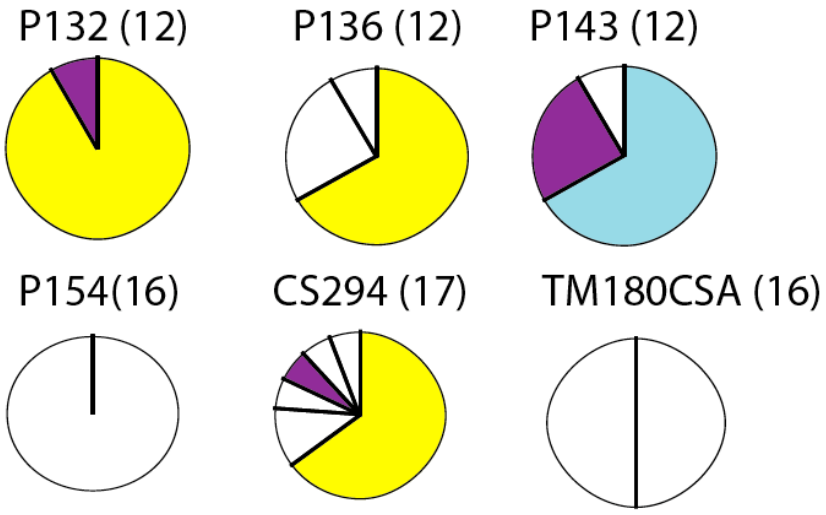

Fig. 4.4. Frequencies of distinct DBLγ sequences in each isolate. The pie charts represent the relative number of different DBLα sequences detected in each isolate by RT-PCR, cloning and analysis of 12-17 mini-prep clones per isolate. Each pie represents a different isolate, and the size of each pie-slice represents relative abundance of transcript. Isolate name given in bold and bracketed numbers indicate the exact number of plasmids sequenced for each isolate. Domains with homology to *var1csa* are shaded (3D7 *var1csa* DBL3γ; yellow. 3D7 *var1csa* DBL5γ; purple. FCR3 *var1csa* DBL3γ; blue).

All of the placental field isolates showed a predominant *var* gene. The predominant gene in three of the five isolates (CS294, P132 and P136) was almost identical (>97% homology). Nucleotide sequence comparisons revealed these sequences were highly homologous (>92% identity) to the DBL3γ of 3D7 *var1csa* (yellow in Fig. 4.4). Sequences homolgues to the DBL5γ of 3D7 *var1csa* were also seen (CS294PlvarD, P143PlvarB and P132PlvarB, > 87% homology to 3D7 *var1csa*

DBL5γ, purple in Fig. 4.4). The DBL3γ of FCR3 *var1csa* is slightly different to that of 3D7 (Rowe *et al.* 2002a), and the predominant gene of P143 was a FCR3-like *var1csa* homologue (97% homology, blue in Fig. 4.4).

Var1csa is a highly conserved sequence (Khattab *et al.* 2001), and has previously been reported in many placental isolates worldwide, including from Cameroon (Fried and Duffy 2002), Kenya (Khattab *et al.* 2003) and from Gabon (Kyes *et al.* 2003), but is also seen in childhood malaria field isolates (Winter *et al.* 2003, and discussed in chapter 3). The finding of *var1csa* in these placental isolates, collected as trophozoites and schizonts, is unsurprising as *var1csa* has an unusual transcription profile, being expressed at trophozoite stage (Kyes *et al.* 2003), rather than at ring stage, as for other *var* genes (Khattab *et al.* 2001; Salanti *et al.* 2004).

4.5.4 Sequence similarities between transcripts detected by RT-PCR with primers D3F and D3R2

Sequence identity between domains was 27.8-100% (mean 47.7%, s.d. 13.6%). Two sequences P154PlvarA and CS294PlvarB were identical, as were CS294PlvarA and P132PlvarB the *var1csa* DBL3γ homogues discussed above.

4.5.5 Phylogenetic analysis of transcript sequences detected by RT-PCR with primers D3F and D3R2

A phenogram was constructed to compare the DNA sequences from Malawi (red) and from laboratory CSA-selected strain TM180CSA (blue), with published DBLγ mRNA sequences from pregnancy-associated malaria in Gabon, Cameroon and

Kenya, and also with *var1csa* gene DBL3γ and DBL5γ domains from 3D7 and FCR3 (Beeson *et al*. 1999; Buffet *et al*. 1999; Reeder *et al*. 1999; Reeder *et al*. 2000; Khattab *et al*. 2001; Fried and Duffy 2002; Khattab *et al*. 2003; Salanti *et al*. 2003; Gamain *et al*. 2005). This was intended to examine the extent of the similarities between the DNA sequences, rather than to suggest phylogenetic evolution, and to display how the Malawi sequences were distributed in relation to DBLγ domains from other placental isolates. The predominantly expressed *var* gene from each of the isolates was marked with an arrow (←) (Fig. 4.5).

The Malawi sequences were distributed throughout the extent of the tree. There is no marked distinction between the different groups of sequences dependent on country of origin (Fig. 4.5).

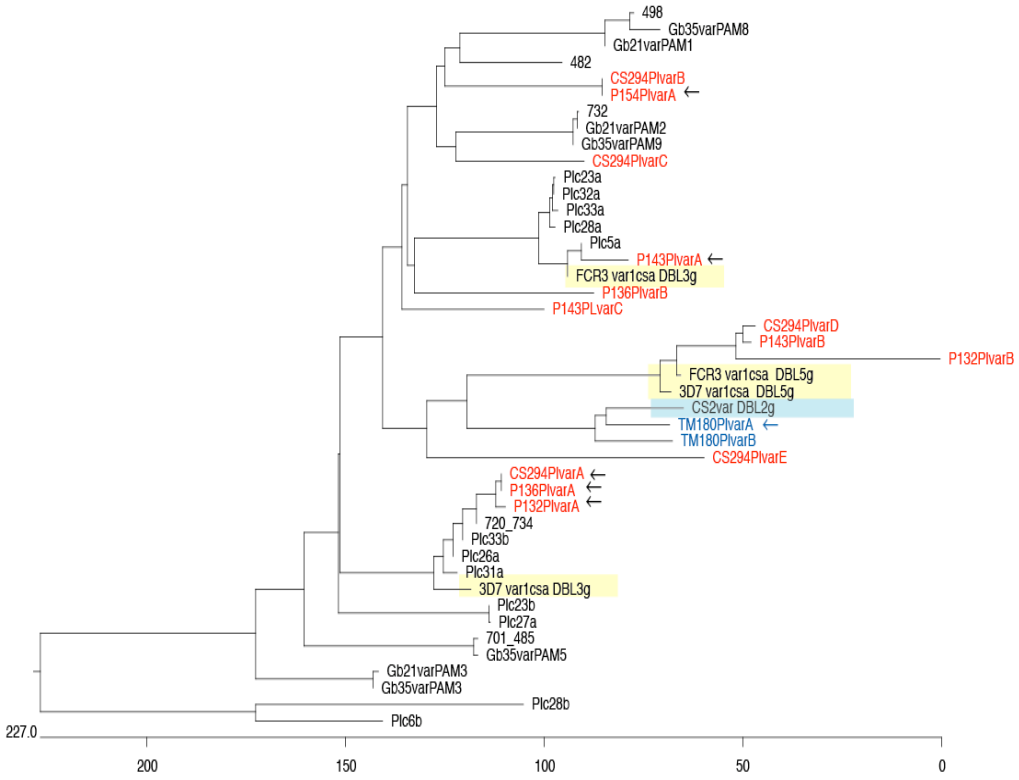

Fig. 4.5. Phenogram displaying transcribed DBLγ domains in *P. falciparum* placental field isolates from Malawi (this study; red) amplified with primers D3F and D3R2, with transcribed DBLγ domains in *P. falciparum* placental field isolates from Cameroon (498,482,732 and 720/734), Kenya (Plcx) and Gabon (Gbx). Transcribed DBLγ domains from CSA-binding laboratory strain TM180CSA (this study: blue) and the DBLγ domains of *var1csa* (FCR3 and 3D7; shaded in yellow) and *CS2var* (shaded in blue) are also included. The predominant transcript from each Malawi placental isolate and TM180CSA is marked with an arrow (←).

4.5.6 Limitation of transcription analysis using D3F and D3R2

Literature at the time of this study was emerging which strongly implicated *var2csa* as a (if not "the") major CSA-binding PfEMP1 (Salanti *et al.* 2003; Salanti *et al.* 2004; Tuikue Ndam *et al.* 2005; Viebig *et al.* 2005; Beeson *et al.* 2006). Unfortunately, *var2csa* could not be amplified with this primer pair, which became an obvious limitation of the study. The DBL3X domain of *var2csa,* which has been shown to support CSA binding (Gamain *et al.* 2005; Dahlback *et al.* 2006) has similarity to a DBLγ domain, and it was possible to design a primer pair to extend the range of DBL domains amplified to include the *var2csa* DBL3-X domain, without losing specificity for PfEMP1 DBLγ domains (section 4.6). It was decided to proceed with a second primer pair which would include *var2csa* in the RT-PCR analysis, rather than to extend the analysis with primer pair D3F and D3R2. Unfortunately, this meant that DBLγ domains from non-placental malaria isolates were not studied with D3F and D3R2.

4.6 Results 2: DBLγ/*var2csa* transcription analysis using a second set of primers D3F and D3R1.2

4.6.1 PCR on 3D7 genomic DNA to determine bias of a second set of primers D3F and D3R1.2

A second set of degenerate primers was designed (Dr JA Rowe) to amplify *var2csa* DBL3X domains as well as PfEMP1 DBLγ domains (D3F and D3R1.2; Fig. 4.1 and 4.6).

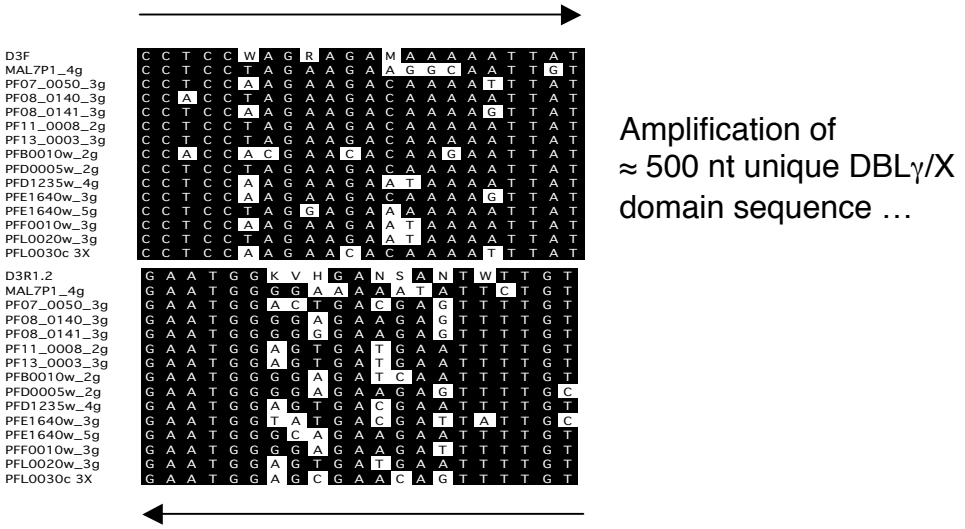

Fig. 4.6. Primer sites of D3F and D3R1.2 on a clustal W alignment of 3D7 DBLγ domains and *var2csa* DBL3X (PFL0030c 3X).

The degree of bias in this primer pair (D3F and D3R1.2) was determined by amplification of 3D7 genomic DNA. 3D7 genomic DNA was amplified with D3F and D3R1.2. The PCR products were cloned and 38 recombinant plasmids were sequenced. 12/16 gamma domains were represented in the sequences from the plasmids from 38 minipreps (Fig. 4.7). The primers showed acceptable primer bias (<2%) of amplification of 3D7 DBLγ domains (Gardner *et al*. 2002), in line with other published degenerate primers (Taylor *et al*. 2000a; Duffy *et al*. 2006a). *Var2csa* (PFL0030c 3X) was amplified with average frequency (Fig. 4.6.)

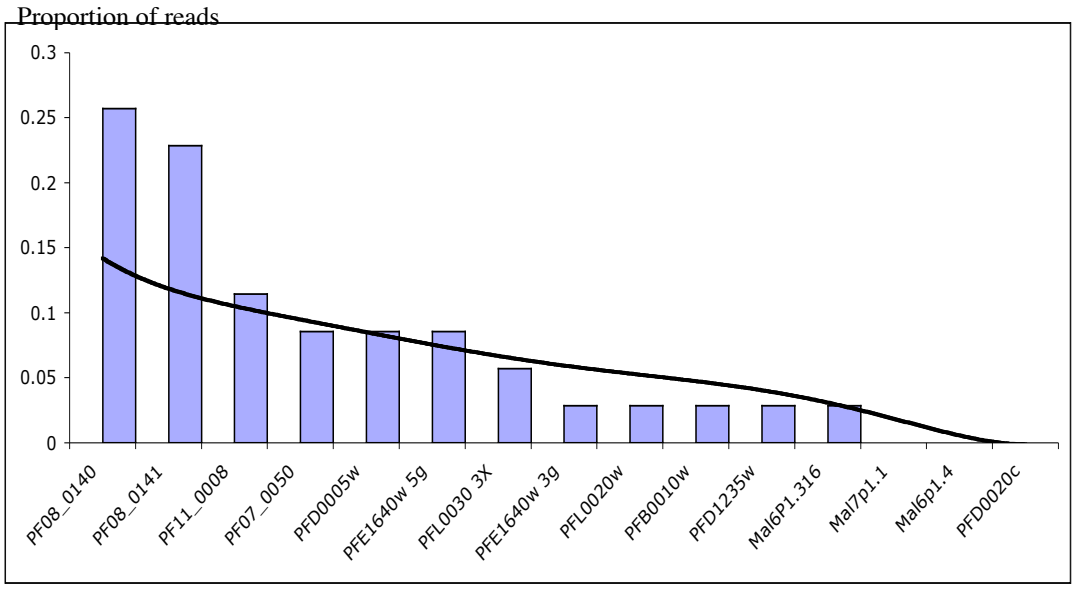

Fig. 4.7. Amplification of 3D7 gDNA using primer pair D3F and D3R1.2. Bars indicated frequency of amplification of the DBLγ domain/*var2csa*DBL3X transcripts. Black line shows expected bionomial distribution of frequencies as a polynomial trendline. This shows a bias of < 2% for the most frequently detected sequence.

4.6.2 DBLγ/*var2csa* DBL3X transcript sequences detected in Malawian placental malaria field isolates by RT-PCR with primers D3F and D3R1.2

RT-PCR was carried out with the new primer pair D3F amd D3R1.2 for the six placental isolates CS294, P132, P134, P136, P143, P154. Transcripts from TM180CSA and TM284 were not amplified as the focus of the study was transcription in placental isolates not laboratory strains. RT-PCR products were obtained for all six isolates and were purified, ligated and cloned as before. 11-19 colonies were picked at random for growth overnight in LB broth, and the plasmids were extracted as before for sequencing.

The sequences obtained with primer pair D3F and D3R1.2 from parasite isolates CS294, P132, P134, P136, P143, P154 were compared for multiple copies of the same sequence (over 95% sequence identity), and again defined as placental (Pl) *var* gene A-H from each isolate. Pie charts were then created to show frequency of different domains for the D3F/D3R1.2 primer pair (Fig. 4.8). *Var1csa* was present in 5/6 isolates with these primers (shaded in yellow, Fig. 4.8). All of the parasite isolates expressed at least one *var* gene with strong homology to *var2csa* (shaded in grey, Fig. 4.8).

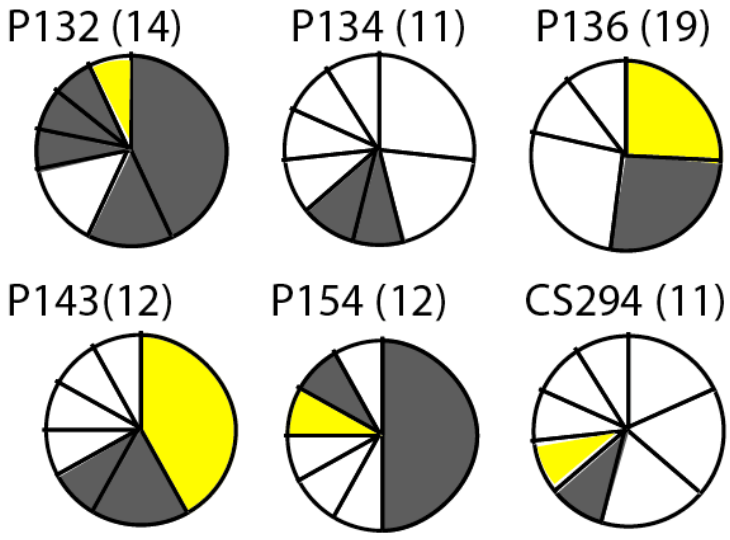

Fig. 4.8. Proportions of DBLγ/*var2csa* domains in 6 placental malaria isolates. Pie charts represent the relative number of different DBLγ/X sequences as detected by RT-PCR. Bracketed number is the number of cloned sequences for the isolate, and the isolate name is shown in bold. Sequences with homology to *var2csa* are shaded in grey, and with homology to *var1csa* in yellow.

Some sequences amplified with D3F and D3R2 were amplified again D3F and D3R1.2 (Fig. 4.9). Where a sequence was amplified that had already been identified from the first amplification, the original name was kept, e.g. P136PlvarA was amplified with both primer sets. Though some of the same sequences were amplified, the predominant transcript with D3F/D3R2 was not predominant when amplified with D3F/D3R1.2 in any isolate. With these primers, a wider range of domains was amplified, and a predominant gene was less clear.

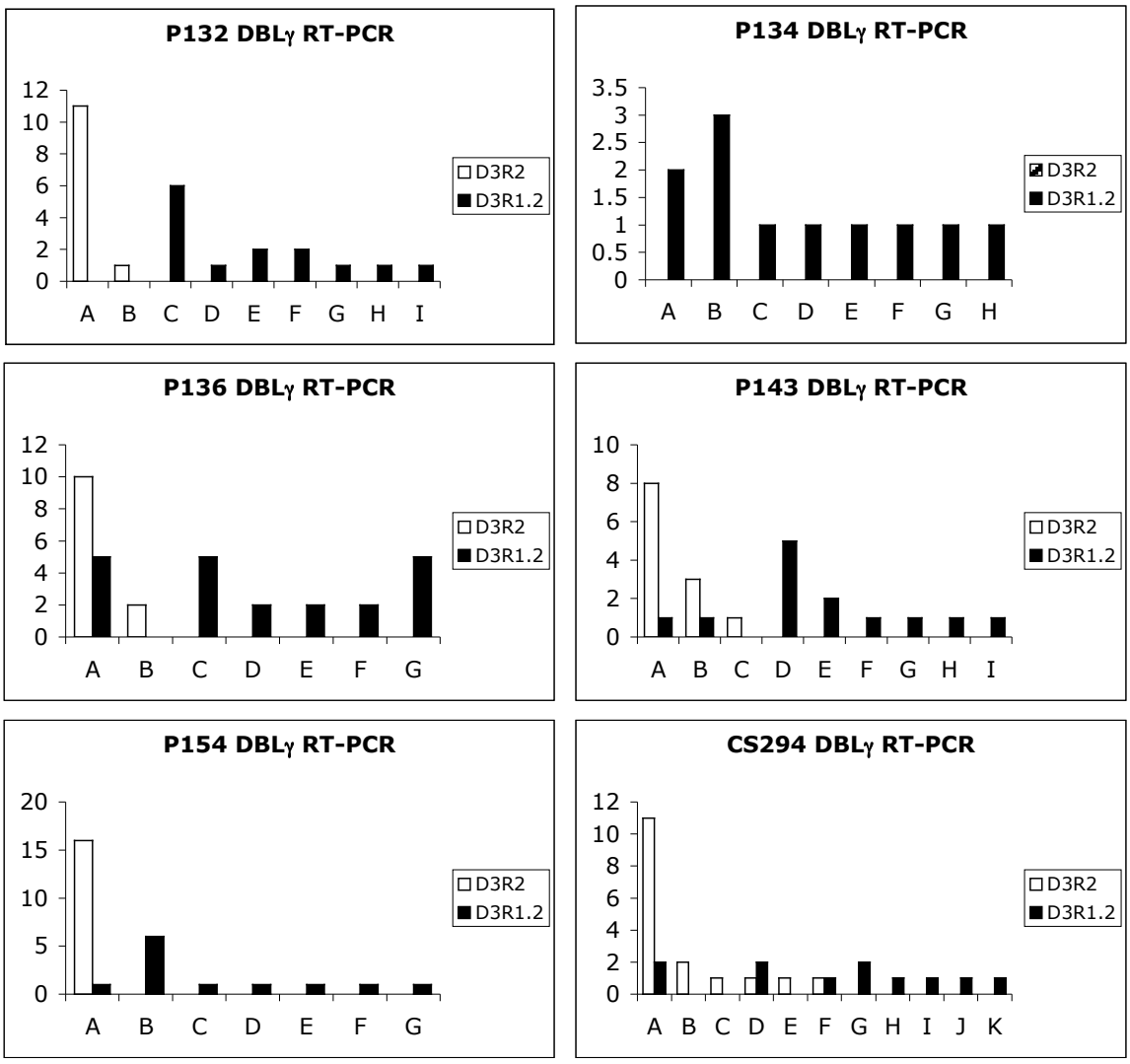

Fig. 4.9. DBLγ/*var2csa* RT-PCR on placental isolates P132, P134, P136, P143, P154 and CS294. Both amplifications used forward primer D3F. Y-axis shows frequency of RT-PCR products relating to transcripts A, B, C etc for each isolate with products with reverse primer D3R2 (striped) and D3R1.2 (black). There was no RT-PCR product for P134 with primer pair D3F/D3R2.

4.6.3 Phylogenetic analysis of transcript sequences detected by RT-PCR with primers D3F and D3R1.2

A phenogram was constructed to give an indication of sequence similarity of the *var* genes expressed from the difference isolates from the second set of primers, D3F and D3R1.2 (Fig. 4.10), and together sequences amplified from D3F and D3R2 primer pair (Fig. 4.11) with the published sequences from Gabon, Cameroon and Kenya, and also with *var1csa* DBL3γ and DBL5γ domains from 3D7 and FCR3 and *var2csa* DBL3X domain from 3D7 (Beeson *et al.* 1999; Buffet *et al.* 1999; Reeder *et al.* 1999; Reeder *et al.* 2000; Khattab *et al.* 2001; Fried and Duffy 2002; Khattab *et al.* 2003; Salanti *et al.* 2003; Gamain *et al.* 2005).

Fig. 4.10 and Fig. 4.11 both highlight the striking clustering of some transcripts from the placental malaria isolates discussed in this chapter around *var2csa* DBL3X. Only sequences from the second set of primers, D3F and D3R1.2 cluster here, due to primer specificity. The non-*var2csa* transcripts amplified with D3F and D3R1.2 are spread evenly throughout the rest of the tree. There was no obvious separation of transcripts from the two different primer sets, or from the Malawian isolates examined here compared to the published sequences.

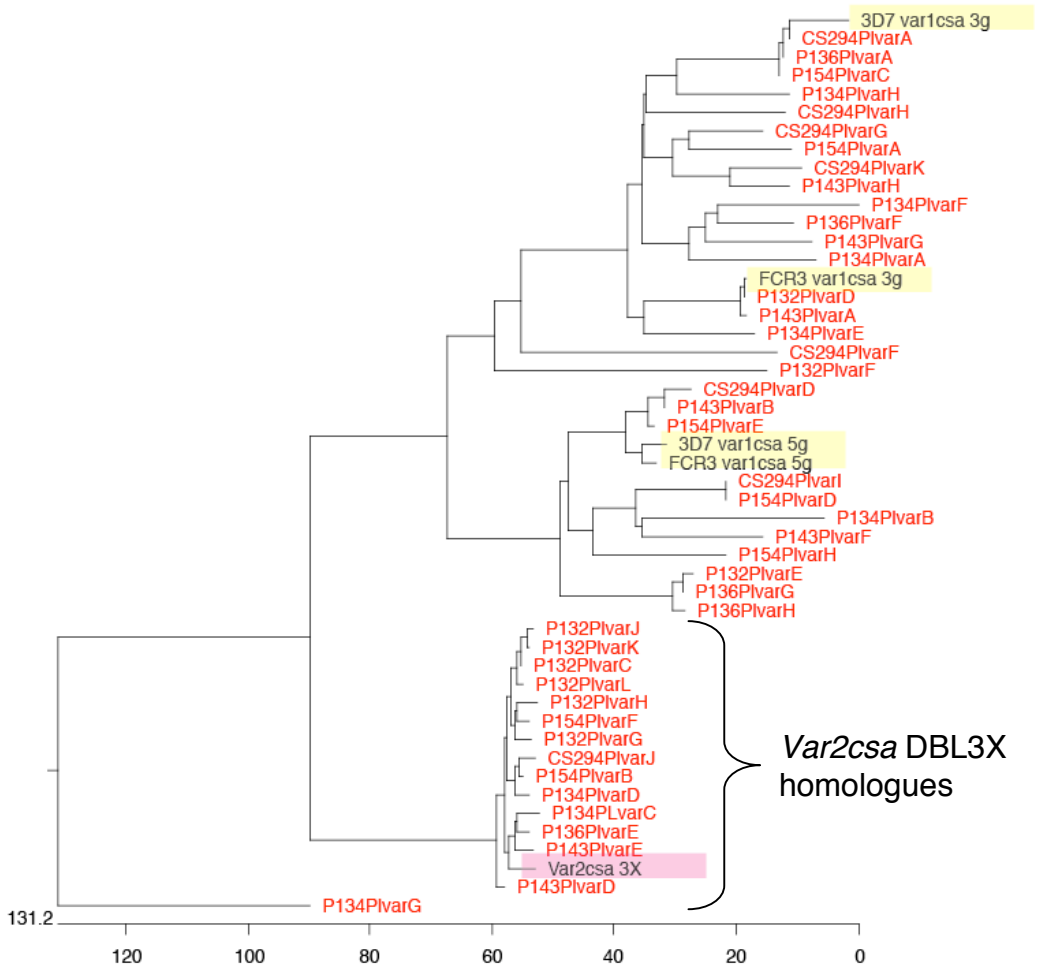

Fig. 4.10. Phenogram showing expressed DBLγ sequences from *P. falciparum* isolates of placental malaria from females in Malawi (red), alongside the DBLγ domains of *var1csa* (FCR3varCSA 3/5γ and 3D7Chr5var 3/5γ, yellow), and the DBL-3X domain of *var2csa* (pink). The phenogram was created using a clustal W alignment of amino acid sequences.

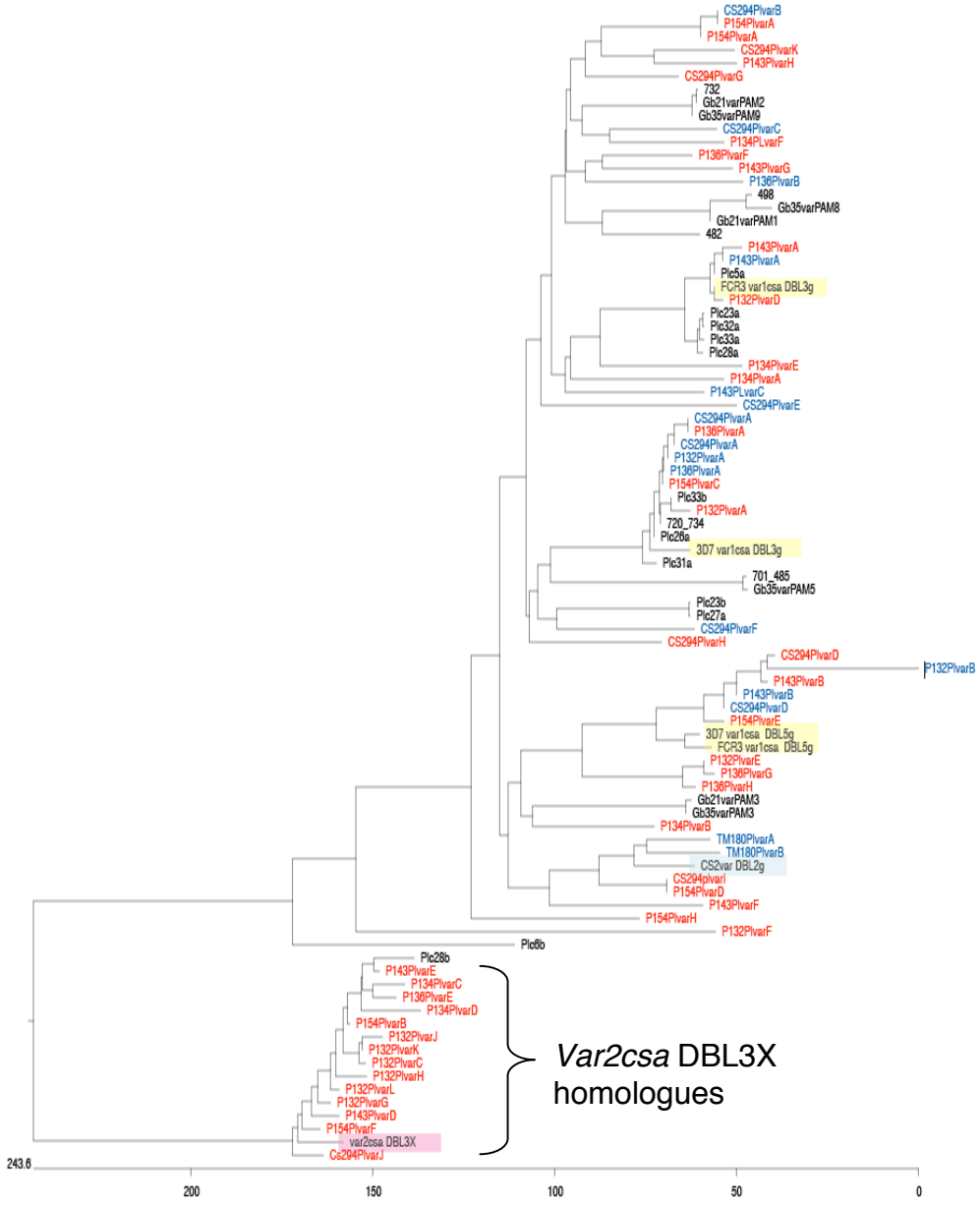

Fig. 4.11. Phenogram displaying transcribed DBLγ domains in *P. falciparum* placental field isolates from Malawi (this study) in relation to other DBLγ domains. Red: transcribed DBLγ domains in *P. falciparum* placental field isolates from Malawi amplified with D3F and D3R1.2. Blue: transcribed DBLγ domains in *P. falciparum* placental field isolates from Malawi amplified with primers D3F and D3R2 (some of these were also amplified with D3F and D3R1.2) and transcribed

DBLγ domains from CSA-binding laboratory strain TM180CSA with primers D3F and D3R2. Black: transcribed DBLγ domains in *P. falciparum* placental field isolates from Cameroon (498,482,732 and 720/734), Kenya (Plcx) and Gabon (Gbx). The DBLγ domains of *var1csa* (FCR3 and 3D7; shaded in yellow), the DBLγ domain of *CS2var* (shaded in blue) and the DBL3X domain of *var2csa* (shaded in pink) are also included.

4.6.4 DBLγ domain RT-PCR of childhood isolates using primers D3F and D3R1.2

It is not possible to assess whether *var2csa* transcription is specific for placental malaria field isolates without comparing the placental transcription pattern to that of non-pregnant individuals, such as non-pregnant women, men or children. The childhood malaria samples described in chapter 3 were available and so these were used for a comparison. RT-PCR, cloning and sequencing were then used to create transcription profiles for a subset of the childhood isolates examined for DBLα expression (Chapter 3). Five cerebral and five uncomplicated isolates were chosen at random.

As with the DBLα domains, a range of transcripts were detected per isolate. There was no significant difference in the number of sequences detected within the three disease categories (Kruskal Wallis test, P=0.48), and a predominant DBLγ domain was seen in most isolates (Fig. 4.12). *Var1csa* transcripts were detected in 8/10 childhood isolates; 4/5 cerebral isolates and 4/5 uncomplicated malaria isolates (yellow in Fig. 4.12). *Var2csa* transcripts were not detected in any childhood isolate

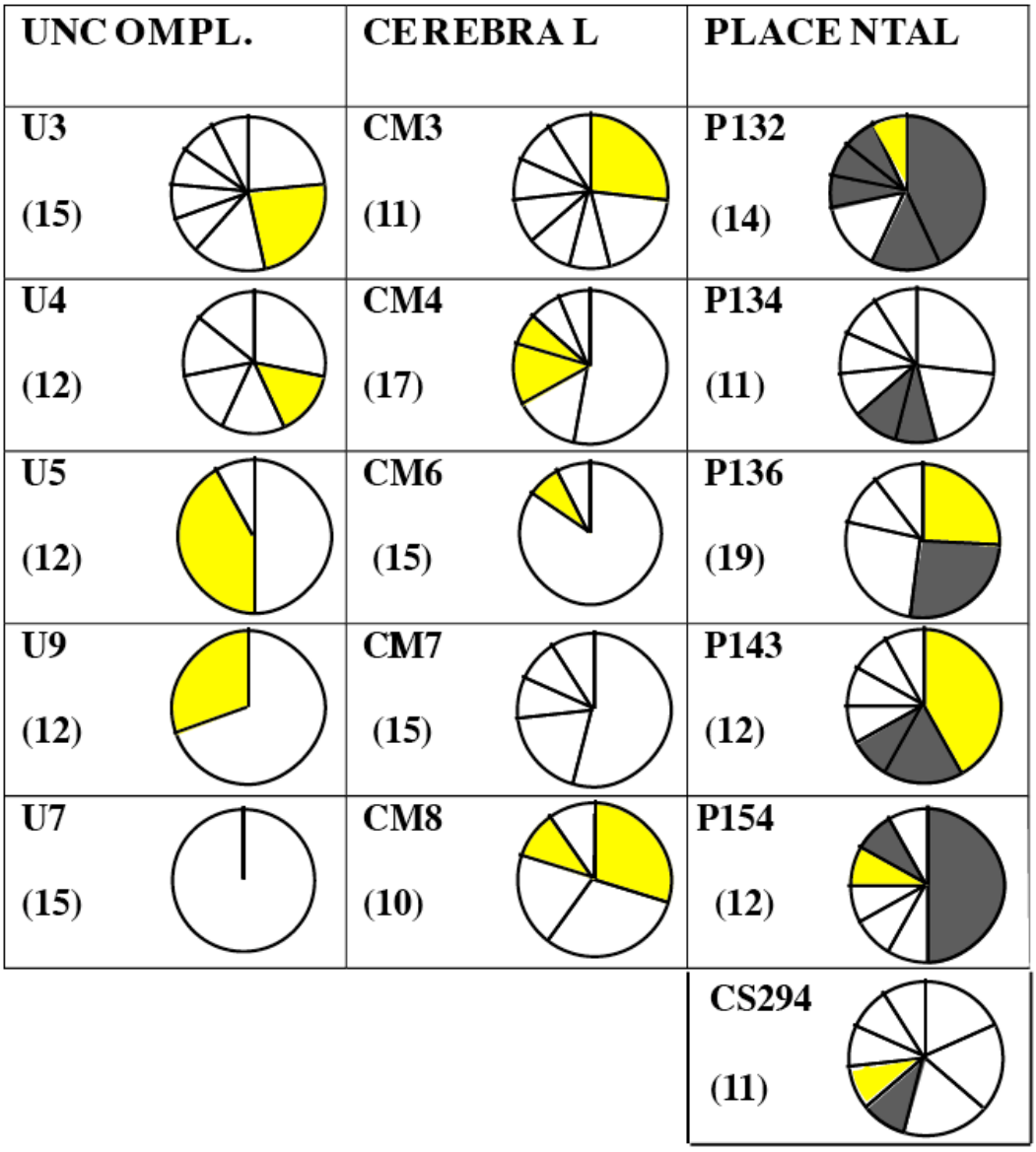

Fig. 4.12. Proportions of DBLγ/*var2csa* domains in 5 isolates from 3 disease categories; uncomplicated childhood malaria, cerebral childhood malaria, and placental malaria. Pie charts represent the relative number of different DBLγ/X sequences as detected by RT-PCR with D3F and D3R1.2. Bracketed number is the number of cloned sequences for the isolate, and the isolate name is shown in bold. Sequences with homology to *var2csa* are shaded in grey, and with homology to *var1csa* in yellow.

A phenogram was constructed, incorporating all sequences amplified from both the primer pairs from all 16 isolates (Fig. 4.13). There was no difference in distribution of the cerebral versus uncomplicated malaria DBLγ sequences. However, there was a very marked clustering of placental sequences around *var2csa* DBL3X domain, as *var2csa* is present at a high abundance in placental isolates from Malawi, but is not present in any of the childhood isolates from Mali. Using only sequences amplified from the second primer pair did not alter the overall shape of the tree (data not shown).


CM8g C
U3g C
CS294PvarK
P143PvarH
P154PvarA
CS294PvarB
P154PvarA
CM7g E
498
Gb35varPAM8
Gb21varPAM1
CM4g E
P136PvarF
P143PvarG
CM4g B
U4g E
482
Gb21varPAM2
Gb35varPAM9
732
CS294PvarC
P134PLvarF
CS294PvarG
U7g A
P136PvarB
P132PvarD
FCR3 var1csa DBL3g
Plc5a
P143PvarA
Plc23a
Plc32a
Plc33a
Plc28a
P134PvarA
P134PvarE
CM4g C
P143PLvarC
CM3g E
U3g F
U3g E
CM3g C
U3g H
CM8g B
U3g D
CM7g G
CS294PvarH
P136PvarA
P154PvarC
CS294PvarA
CM6g B
U4g B
720_734
3D7 var1csa DBL3g
Plc26a
CM8g A
U5g B
Plc31a
P132PvarA
Plc33b
701_485
Gb35varPAM5
Plc28b
Plc27a
CM3g H
CM4g D
CS294PvarF
TM180PvarA
Cs2var DBL2g
TM180PvarB
CS294pvarI
P154PvarD
CM3g B
U3g A
CM7g A
U4g F
CM3g G
U3g I
U5g A
CM3g D
CM3g F
U3g G
CM7g D
U10g A
CM4g A
U4g D
P143PvarF
CM7g B
U4g I
CM7g F
CM3g A
CM8g D
U3g B
P132PvarE
P136PvarG
P136PvarH
CS294PvarD
P143PvarB
P154PvarE
P132PvarB
3D7 var1csa DBL5g
FCR3 var1csa DBL5g
U4g G
Gb21varPAM3
Gb35varPAM3
CM7g C
CM6g A
CM6g C
P134PvarB
P154PvarH
CS294PvarE
P132PvarF
U4g C
U4g H
U5g C
Plc6b
var2csa DBL1X
var2csa DBL2X
P136PvarC
P132PvarK
P136PvarE
Plc28b
P143PvarE
P154PvarB
P134PvarD
P132PvarC
var2csa DBL3X
P154PvarF
P132PvarL
P132PvarH
P132PvarJ
P143PvarD
P132PvarG
Cs294PvarJ
P134PvarC
288.9
200
150
100
50
0
Nucleotide Substitutions (x100)
Var2csa DBL3X homologues

Fig. 4.13. Phenogram displaying transcribed DBLγ/*var2csa* transcripts in *P. falciparum* placental field isolates from *P. falciparum* isolates of childhood cerebral (purple) and uncomplicated (green) malaria from Mali and from placental isolates from Malawi (red) amplified with primers D3F and D3R21.2. Transcribed DBLγ domains in *P. falciparum* placental field isolates from Cameroon (498,482,732 and 720/734), Kenya (Plcx) and Gabon (Gbx), and from CSA-binding laboratory strain TM180CSA (blue), the DBLγ domains of *var1csa* (FCR3 and 3D7; yellow) and *CS2var* (blue) and the DBL3X domain of *var2csa* (pink) are also included. *Var2csa* DBL1X and DBL2X are also included for reference, but are in grey as they could not be amplified by these primers. Phenogram was constructed from a clustal W alignment of amino acid sequences.

A phenogram only including the childhood DBLγ transcripts amplified from the second primer pair from all 16 isolates (Fig. 4.14) also shows clearly there was no difference in distribution of the cerebral versus uncomplicated DBLγ sequences.

Unfortunately there was not enough parasite material to perform real-time RT-PCR for these samples, which would have been useful to quantify relative amounts of *var* gene transcripts detected in these isolates.

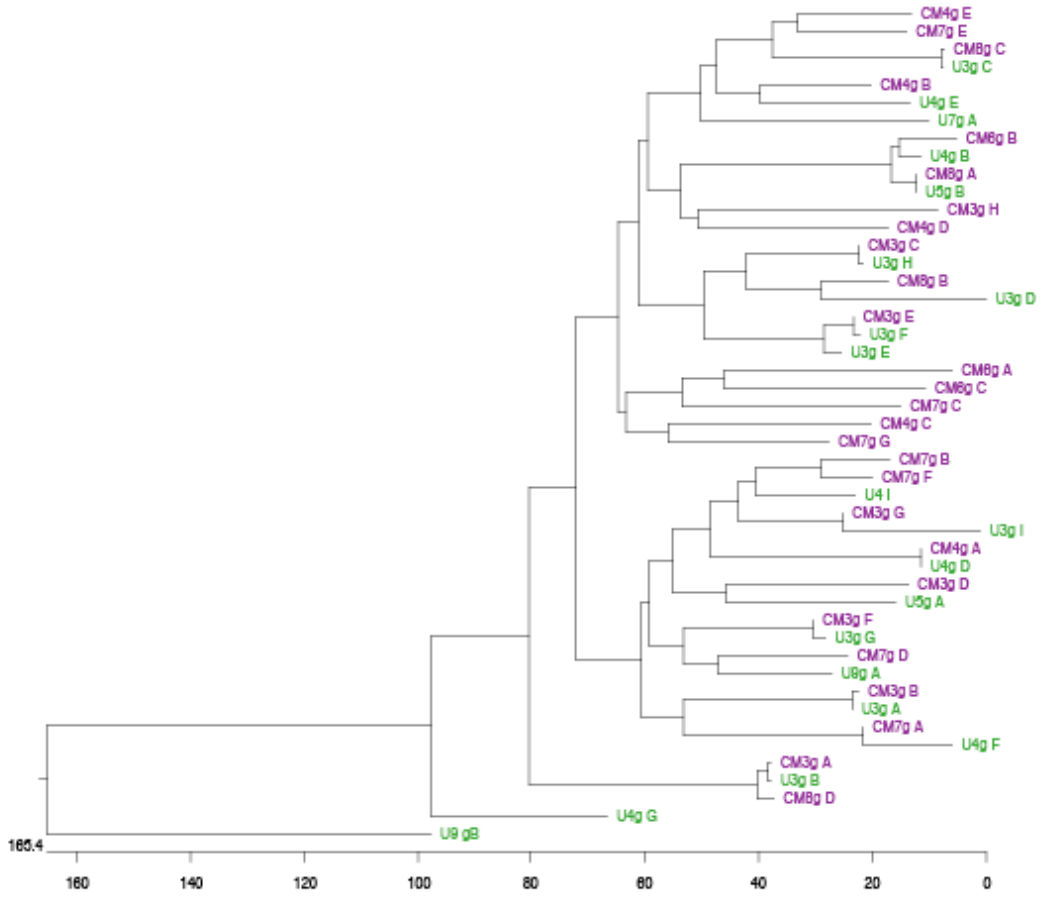

Fig. 4.14. Phenogram displaying transcribed DBLγ/*var2csa* transcripts in *P. falciparum* placental field isolates from *P. falciparum* isolates of childhood cerebral (purple) and uncomplicated (green) malaria from Mali amplified with primers D3F and D3R1.2. Phenogram constructed from a clustal W alignment of amino acid sequences.

4.7 DBLγ transcript analysis

4.7.1 Sequence diversity of DBLγ domain transcripts

The level of amino acid identity between different DBLγ sequence domain tags was calculated. Amino acid identity of the DBLγ transcripts separated by disease category indicates a significantly higher level of amino acid in the placental malaria group (median 33.1%) than in childhood malaria (median 30.1% Mann-Whitney Test <0.001) as shown by box plots and histograms (Fig. 4.15). The level of amino acid identity between different Malawi DBLγ sequence domain tags was calculated and also illustrated pictorially (Fig. 4.16). Percentage amino acid identity between 2 DBLγ/*var2csa* domains is colour coded such that darker shading reflects higher amino acid identity.

V*ar2csa* homologues are comparatively highly conserved and the *var2csa* transcripts amplified in these isolates shared 64-96% nucleotide identity, median 88.3% (Fig. 4.15 and 4.16). Removing the *var2csa* homologues decreased the similarity between placental isolates sequences (median 29.5%) though this act did not significantly change the distribution of sequence identities (Mann-Whitney test, placental "all sequences" versus placental "non-*var2csa* sequences", P=0.358). The was still a significant difference between placental DBLγ (non-*var2csa*) and childhood DBLγ sequences (Mann-Whitney test P=0.019).

Var2csa homologues were significantly more similar to each other than the DBLγ transcripts from childhood of placental malaria isolates both Mann-Whitney Test P<0.001).

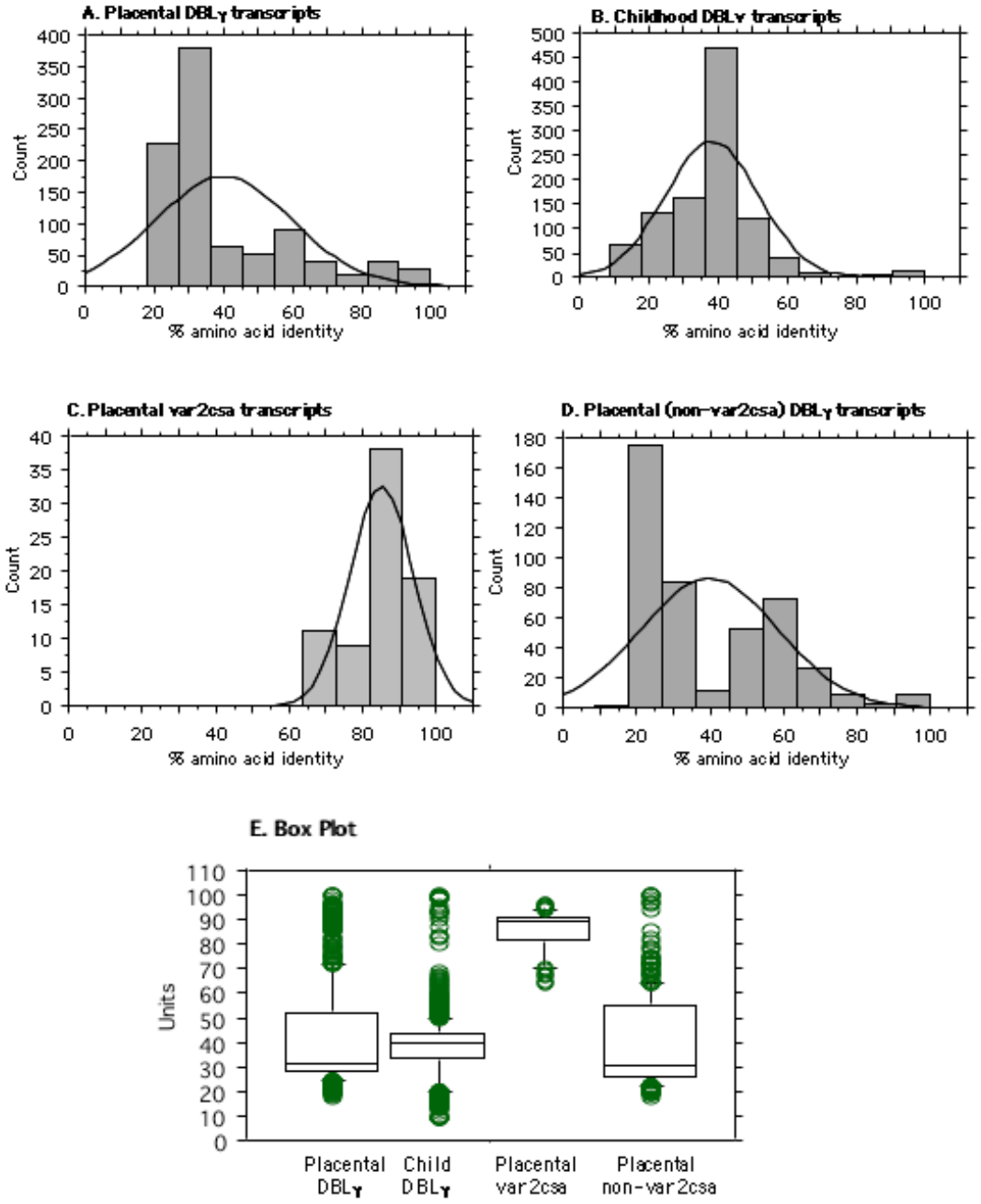

Fig. 4.15. Histograms and box plots of percentage amino acid identity between all DBLγ domain transcripts from placental, childhood, placental (*var2csa* only) and placental (non-*var2csa* only) DBLγ transcripts. Box plots show 10th, 25th, 50th, 75th and 90th percentiles; values <10th percentile and >90th plotted separately.

A

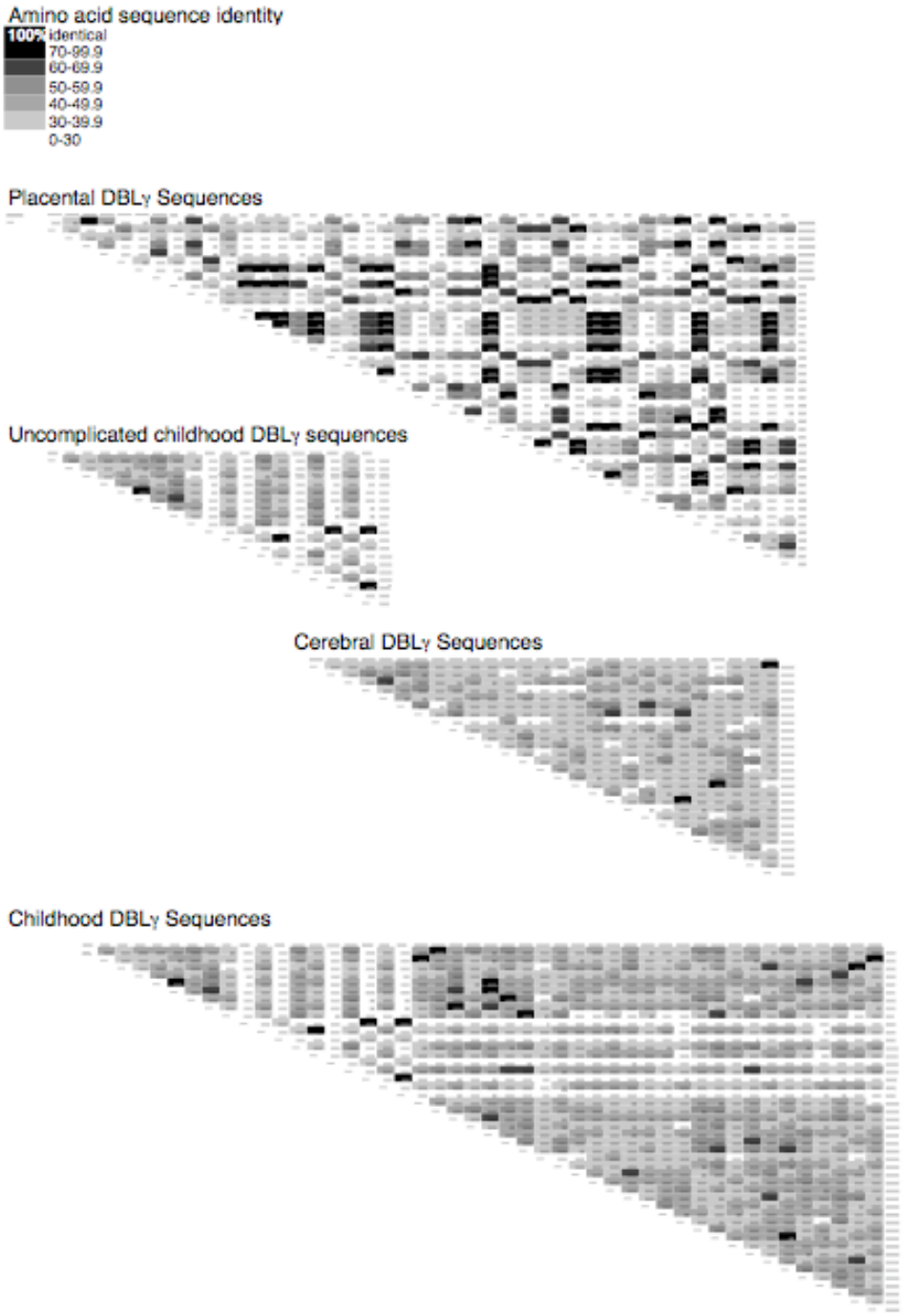
Amino acid sequence identity
100% identical
70-99.9
60-69.9
50-59.9
40-49.9
30-39.9
0-30
Placental DBLγ Sequences
Uncomplicated childhood DBLγ sequences
Cerebral DBLγ Sequences
Childhood DBLγ Sequences

B

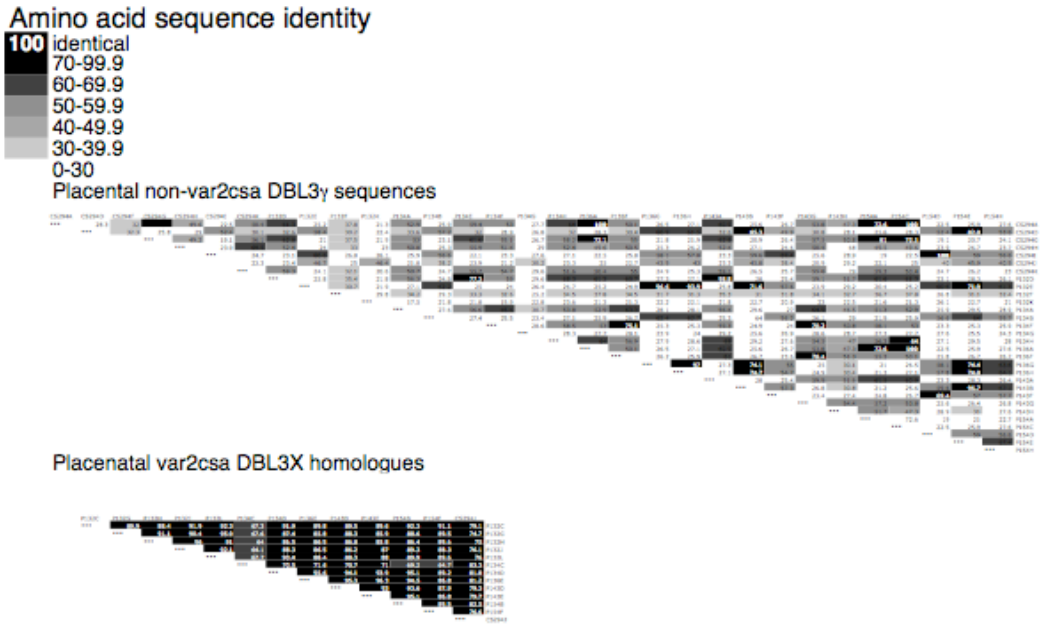

Fig. 4.16. Amino acid sequence distance charts showing percentage amino acid identity between domains for DBLγ/*var2csa* domains. A) Placental malaria, cerebral malaria, uncomplicated malaria, and all childhood isolate DBLγ/*var2csa* sequences. B) Placental *var2csa* homologues and non-*var2csa* homologues separately. Darkness of shading indicates level of identity between domains.

Although relatively highly conserved, the *var2csa* homologues retain some polymorphicity. Variability between the *var2csa* homologues is concentrated towards the end of the amplified tag, with a relatively more conserved region in the middle (alignment amino acids 78-122; Fig. 4.17).

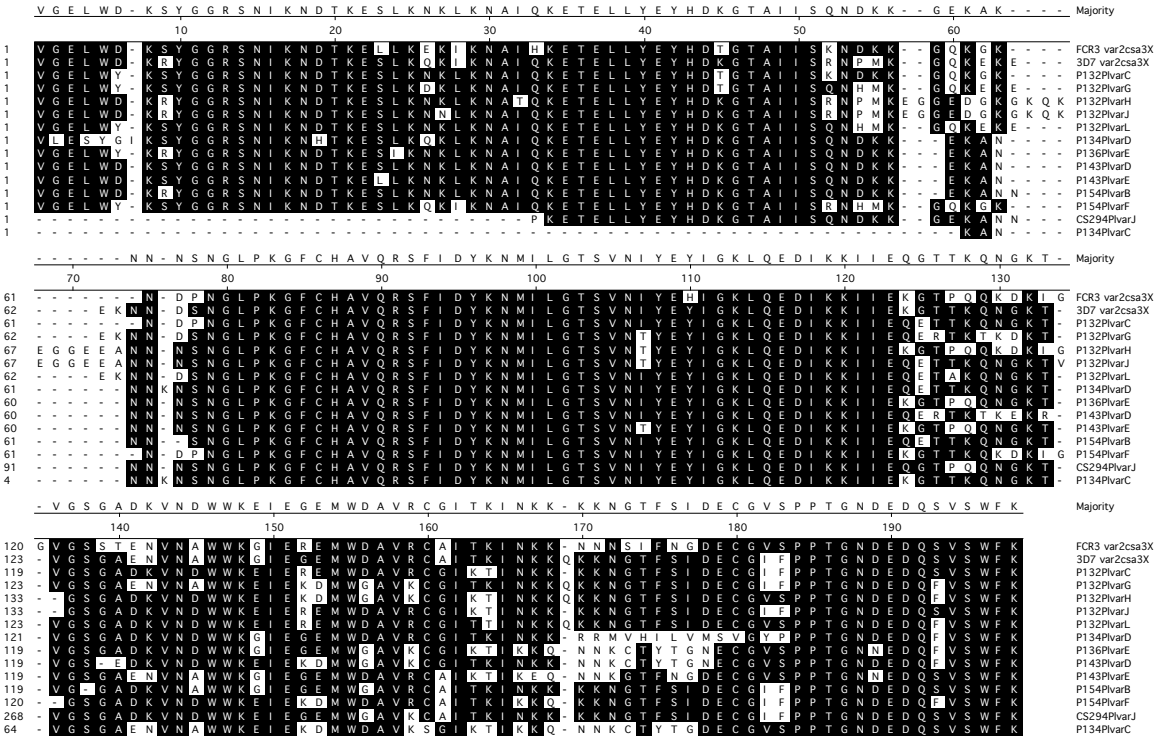

Fig. 4.17. Alignment of *var2csa* in this study and *var2csa* DBL3X from FCR3 and 3D7, produced from a clustal W alignment of protein sequences.

4.7.2 Conservation of DBLγ domain transcripts detected

A BLAST homology search performed for sequences not homologous to *var1csa* or *var2csa* on the NCBI database, indicated no other highly conserved DBLγ were present (Table 4.1). There is much less similarity between DBLγ domains than DBLα domains (Table 3.3, chapter 3) though this may reflect the fewer DBLγ domains on NCBI database, see discussion.

DBLγ transcript		Database matches	
Name	**Accession Number**	**Accession Number Origin**	**Nucleotide identities (%)**
P134varA	DQ306273	-	
P134varB	DQ306274	AF547151 gDNA[1]	456/474 (96%)
P134varE	DQ306277	-	
P134varF	DQ306278	-	
P134varG	DQ306279	-	
P134varH	DQ306280	-	
P136varB	-	-	
P136varC	-	-	
P143varC	-	-	
P143varF	DQ306290	-	
P143varG	DQ306291	-	
P143varH	DQ306292	-	
P154varA	DQ306293	Placental mRNA, Malawi CS294varB	450/450 (100%)
P154varD	DQ306296	DQ306305 placental mRNA, Malawi (CS294varI)*	488/488 (100%)
P154varH	DQ306299		
CS294varB	-	DQ306293 placental mRNA, Malawi (P154varA)*	450/450 (100%)
CS294varC	-	-	
CS294varE	-	DBLγ2 IT_var18[2]	458/492 (92%)
CS294varG	DQ306303	-	
CS294varH	DQ306304	-	
CS294varI	DQ306305	DQ306297 placental mRNA, Malawi (P154varD)*	488/488 (100%)
CS294varK	DQ306307	-	
U3A	-	-	
U3B	-	-	
U3C	-	-	
U3D	-	DBLγ2 IT_var22[2]	419/508 (82%)
U3E	-	-	
U3F	-	-	
U4D	-	-	
U4E	-	-	
U4F	-	-	
U5A	-	-	
U5C	-	-	
U9A	-	-	
U7A	-	-	
CM3B	-	-	
CM3C	-	-	
CM3D	-	-	

DBLγ transcript		Database matches	
Name	**Accession Number**	**Accession Number Origin**	**Nucleotide identities (%)**
CM3E	-	-	
CM3F	-	-	
CM3G	-	-	
CM4A	-	-	
CM4B	-	-	
CM4E	-	-	
CM4F	-	-	
CM6A	-	-	
CM6B	-	-	
CM7A	-	-	
CM7B	-	3D7 var Pff0010w DBLγ domain[3]	393/434 (90%)
CM7C	-	-	
CM7D	-	-	
CM7E	-	MC_var4 DBLγ domain[2]	392/452 (86%)
CM8B	-		
CM8C	-		
CM8D	-		
CM8E	-		

Table 4.1. Homology of Malawi isolate non-*vass1csa* or *var2csa* DBLγ transcripts described in this study compared to sequences on NCBI database. Database matches > 85% identity, >85% sequence coverage, http://www.ncbi.nlm.nih.gov/BLAST are also described (accession number, origin, and% nucleotide identity). - no database matches were found. [1]Khattab *et al*. 2003, [2]Kraemer *et al*. 2007, [3]Gardner *et al*. 2002, *This study/(Duffy *et al*. 2006a).

4.8 Analysis of DBLα domain transcripts detected in placental isolates P132, P136, P143, P154 and CS294, from Rowe *et al.* (2002a)

As most DBLγ are from Group A or B/A *var* (12/15 in 3D7, 12/18 in HB3 and 12/25 in IT) amplification of DBLγ domains in this study was expected to result in detection predominantly of group A or B/A *var* gene transcripts. If the 3D7 gene repertoire is typical, DBLγ domain amplification should detect 91% of non-type 3 group A or B/A *var* genes, but only 7% of group B, C or B/C *var* genes. If the HB3 or IT genomes are more typical, more group B,C or B/C *var* genes would be amplified by DBLγ domain RT-PCR.

To examine the relative proportions of group A and B/C *var* expressed in these isolates, DBLα(0/1) RTPCR transcription data on isolates P132, P136, P143, P154 and CS294, which already been published (Rowe *et al*. 2002a) was reanalysed. This paper had used the primers from Taylor *et al*. (2000a) and the method described in chapter 3. The DBLα domain transcripts were downloaded from NCBI database and classified as DBLα0 or DBLα1, on the basis of number of cysteines in the amplified tag (Table 1.1). Pie charts were created to show the relative proportions of the two subtypes of DBLα domain (DBLα0 shaded black, DBLα1 in white; Fig. 4.18). *Var1csa* homologues are indicated (yellow). This revealed higher DBLα0 than DBLα1 transcription in these placental isolates. Only 3 non-*var1csa* DBLα1 transcripts were detected.

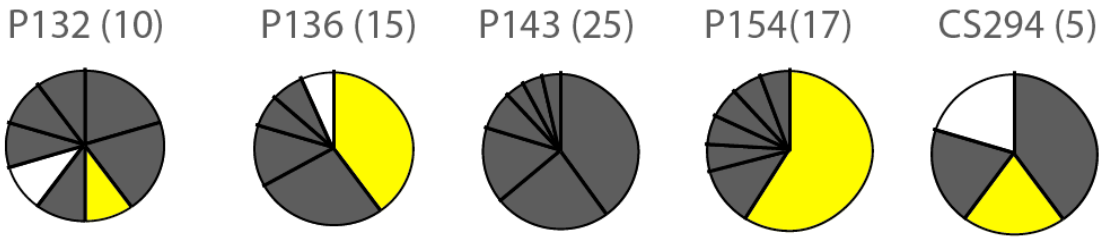

Fig. 4.18. DBLα domain RT-PCR data on isolates P132, P136, P143, P154 and CS294 taken from Rowe *et al.* (2002). Pie charts indicate relative abundance of DBLα domains (DBLα0 grey, DBLα1 white, *var1csa* homologues in yellow).

4.9 Discussion

The results presented in this chapter highlight the exclusive nature of transcription of a particular *var* gene, *var2csa*, in placental malaria isolates. This study of clinical isolates supports the growing body of evidence from studies of field and laboratory strains of *P. falciparum* advocating VAR2CSA as a major contributor to the opportunistic placental sequestration that commonly occurs during pregnancy in malaria-endemic areas. The data obtained will be discussed alongside current developments concerning the role of VAR2CSA in placental malaria.

In this study, transcription of at least one *var2csa* homologue was detected by RT-PCR in all six Malawian placental isolates available, but in none of the 10 Malian childhood isolates also examined. Other recent studies have also found *var2CSA* transcripts to be present in the majority of placental isolates but rarely detected in childhood or non-placental isolates, confirming this strong association specifically

with placental malaria (Salanti *et al*. 2004; Tuikue Ndam *et al*. 2005; Duffy *et al*. 2006a; Francis *et al*. 2007; Fried *et al*. 2007). Furthermore, VAR2CSA PfEMP1 protein is recognised by natural antibodies from endemic areas in a sex-specific and parity-dependent manner (Salanti *et al*. 2003; Salanti *et al*. 2004; Tuikue Ndam *et al*. 2006), again emphasising the link between *var2csa* and pregnancy reported in this study.

Placental isolates possess a unique binding phenotype with a consistently high affinity for CSA (Fried and Duffy 1996; Fried *et al*. 2006; Fried *et al*. 2007; Muthusamy *et al*. 2007). This is consistent with expression of VAR2CSA as VAR2CSA binds to CSA when expressed on the surface of an infected erythrocyte and is consistently upregulated in laboratory isolates after selection for CSA-affinity (Salanti *et al*. 2003; Avril *et al*. 2004; Salanti *et al*. 2004; Gamain *et al*. 2005; Duffy *et al*. 2006b; Beeson *et al*. 2007a; Francis *et al*. 2007; Fried *et al*. 2007). In certain strains *var2csa* disruption irreversibly ablates CSA-affinity, suggesting this protein mediates the majority of CSA-binding (Gamain *et al*. 2005; Viebig *et al*. 2005; Duffy *et al*. 2006b). Most field isolates are predicted to contain a *var2csa* homologue (Trimnell *et al*. 2006). If all *var2csa* homologues retain affinity for CSA, then it is likely that all parasite isolates have the potential to cause placental malaria.

The relative sequence homology between the VAR2CSA DBL3X domains identified in the placental field isolates in this study was 64-96%, similar to the range of homology published in Trimnell *et al*. 2006 (54-94%). *Var2csa* homologues are conserved by *var* gene standards, composed of blocks of highly conserved stretches,

separated by regions of high interclonal diversity (Beeson *et al*. 2006; Duffy *et al*. 2006a; Trimnell *et al*. 2006; Barfod *et al*. 2007; Bockhorst *et al*. 2007). Presence of a *var2csa* homologue in *P. reichenowi* suggests a strong evolutionary advantage for CSA-binding ability (Trimnell *et al*. 2006; Bockhorst *et al*. 2007). *Var2CSA* is under a high level of diversifying selection which appears to be driven by immune pressure (Dahlback *et al*. 2006; Barfod *et al*. 2007; Bockhorst *et al*. 2007). Whether all of the VAR2CSA homologues retain CSA-affinity is not obvious from the sequence.

None of the childhood isolates in this study showed evidence of *var2csa* transcription, consistent with a role for *var2csa* specifically in placental malaria. In other studies, *var2csa* homologues have infrequently been detected in non-pregnant individuals (Duffy *et al*. 2006a; Francis *et al*. 2007), though these do not always appear to have the characteristic CSA-binding ability (Fried *et al*. 2007). Low levels of antibodies with reactivity to VAR2CSA have also recently been detected in plasma from some men and children from various malaria-endemic areas (Beeson *et al*. 2007b). It may be that these VAR2CSA have a subtly different structure resulting in a different binding phenotype.

CSA is present in other parts of the body, including on the cerebral vasculature (Robert *et al*. 1995). However, VAR2CSA does not appear to be involved in any other sequestration, such as during cerebral malaria, and *var2csa* was not seen in these cerebral malaria isolates. CSA is hugely heterogeneous, composed of tandem repeats of glucuronic acid and N-acetylgalactosamine-4-sulfate, and subtleties in the structure of CSA in the placenta may be critical for adhesion here. Infected

erythrocytes adhere most efficiently to CSA in a low sulfation state, and this form is common in the intervillous spaces of the placenta (Achur *et al*. 2000). The origin of CSA in the placenta is foetal, not maternal (Muthusamy *et al*. 2007), possibly presenting a slightly different binding site for PfEMP1 interaction than maternal-derived CSA, for example on host erythrocytes, and providing the specificity for CSA-adhesion only in the placenta.

Upregulation of CSA upon infection may also be important; Muthusamy *et al*. (2007) observed infected placentas had higher CSA levels than uninfected placentas. It is also possible that CSA-binding has another function other than as a receptor for sequestration. For example CSA-binding placental parasites have recently been shown to escape non-opsonic phagocytosis compared to CD36-binding parasites (Serghides *et al*. 2006), though this may be due to loss of CD36-binding rather than gain of CSA-affinity. As placental CSA may be unique in structure, using placental cryosections (Avril *et al*. 2004) rather than bovine CSA (Fried and Duffy 1996; Ricke *et al*. 2000) for *in vitro* adhesion studies may give a more accurate reflection of clinically important *in vivo* interactions.

The childhood isolates used for comparison in this study were from Mali not Malawi and so have a different geographic origin from the placental isolates. However, the *var* gene repertoire of isolates in Mali appears to be typical of isolates across Africa and the world (chapter 3), and *var2csa* expression is seen in placental malaria isolates worldwide (Salanti *et al*. 2003; Avril *et al*. 2004; Salanti *et al*. 2004; Gamain *et al*. 2005; Duffy *et al*. 2006a; Beeson *et al*. 2007a; Francis *et al*. 2007). Ideally,

isolates from men or non-pregnant women, matched for age, geographic location and socioeconomic group would have been used for comparison. It would also have been interesting to also examine DBLγ transcription in the hyperparasitaemia isolates described in chapter 3 for comparison.

As *var2csa* has been associated with placental malaria, this study reveals expression of a perhaps surprisingly high number of non-*var2csa var* genes in placental isolates. The parasites studied were expelled directly from the placenta, raising the question whether these PfEMP1 were also involved in placental sequestration, alongside VAR2CSA. If this were the case it might be possible to detect a particularly "placental" sequence or motif. Antibodies to the DBL3γ domain of FCR3 VAR1CSA recognise 40-60% of placental isolates and block CSA adhesion, suggesting cross-reacting DBLγ domain epitopes are commonly expressed in placental malaria isolates (Lekana Douki *et al.* 2002; Costa *et al.* 2003). However, there was no particular clustering in the phenogram of placental isolate DBLγ transcript sequences compared to those from childhood malaria isolates. Furthermore, comparison to sequences on the NCBI database suggested there is not anything particularly "placental" about the DBLγ transcripts detected in the placental isolates in this study compared to the overall *var* gene repertoire. Of the 9 transcripts with highly homologous database matches, 4 matches were DBLγ transcripts, all from placental malaria isolates. No database matches to childhood malaria isolate transcripts were found. However, this may be misleading as DBLγ domains are most commonly studied in relation to placental malaria, and this may be reflected in the DBLγ RNA sequences represented in the NCBI database. Alternatively, some *var*

gene transcripts detected in these placental isolates may simply be from an incidental sub-symptomatic chronic infection that had expanded due to pregnancy-associated immunomodulation (reviewed in(Ndam and Deloron 2007), and have no direct role in placental sequestration.

The only DBLγ domain transcript seen in multiple isolates was *var1csa*, detected in 5 of the 6 placental isolates examined here. *Var1CSA* is commonly detected in placental isolates including those from Cameroon (Khattab *et al.* 2001), Kenya (Fried and Duffy 2002) and Gabon (Khattab *et al.* 2003), and VAR1CSA can mediate CSA binding (Buffet *et al.* 1999; Rowe *et al.* 2002a; Gamain *et al.* 2004; Badaut *et al.* 2007), though the *in vivo* relevance of this interaction in infection is unclear. *Var1csa* disruption in laboratory strain FCR3 was reported to knock out CSA-binding (Andrews *et al.* 2003), but CSA-affinity was regained as the parasite switched on *var2csa* (Gamain *et al.* 2005). The mechanism of VAR1CSA-mediated binding to CSA appears to be very similar to that of VAR2CSA. The minimal (67 amino acid) region of FCR3 VAR1CSA required for CSA binding has high homology to the CSA-binding domain of VAR2CSA (Gamain *et al.* 2004; Gamain *et al.* 2005), with cross-reacting epitopes (Bir *et al.* 2006), suggesting a common mechanism of adhesion, and overlapping binding sites. It might thus be expected that *var1csa* expression in an infection would elicit an antibody response which could be protective against VAR2CSA subsequent infections. However, as *var1csa* is commonly expressed in non-pregnant and childhood isolates (Fried and Duffy 2002; Rowe *et al.* 2002a; Winter *et al.* 2003), including 8/10 childhood isolates in this study, and incidents of placental malaria are high with estimates of infection in up

two-thirds of pregnancies in malaria-endemic sub-Saharan countries (Broen *et al.* 2007), it seems unlikely a protective antibody repertoire is created and maintained.

It is possible the association of *var1csa*, transcribed at trophozoite stage (Kyes *et al.* 2003), with placental isolates is a result of studying mature parasites extracted directly from the placental at delivery in this and many other studies (Khattab *et al.* 2001; Fried and Duffy 2002; Khattab *et al.* 2003; Duffy *et al.* 2006a). To avoid this, trophozoite parasites could be cultured to ring stage before RNA extraction. However, culturing risks *var* gene switching, as discussed in chapter 3. Alternatively, peripheral ring stage parasites could be studied. Peripheral ring stage parasites matured *in vitro* to pigmented-trophozoite stage tend to show the same binding phenotype as mature trophozoite parasites collected directly from the placenta from the same isolate (Francis *et al.* 2007). This suggests the parasites are from the same population, as observed in comparisons of sequestered and peripheral parasite populations in childhood isolates (Dembo *et al.* 2006; Montgomery *et al.* 2006). Whichever parasites are studied, it is clear *var1csa* expression is neither necessary nor sufficient for placental sequestration of infected erythrocytes.

In addition to *var1csa* and *var2csa,* other PfEMP1 are capable of binding to CSA and may prove to be conserved mediators of placental sequestration. Distinct DBLγ domains with affinity for CSA have been identified from placental isolates (Khattab *et al.* 2001; Khattab *et al.* 2003), including the semi-conserved varPAM732 which specifically binds to immobilised CSA (Chia *et al.* 2005), and to CSA on placental cryosections (Badaut *et al.* 2007). CS2*var* also has affinity for CSA (Reeder *et al.*

1999). Expression of *CS2var* rescued the CSA-binding phenotype of a *var2csa* knock-out parasite (Duffy *et al*. 2006b) and a placental isolate from Malawi expressed *CS2var* as the major transcript (Duffy *et al*. 2006a). However, *CS2var* is not commonly conserved between isolates nor expressed at higher levels in placental isolates compared to non-pregnant hosts, so a crucial role in placental malaria is unlikely (reviewed in(Rowe and Kyes 2004). Neither CS2*var* nor varPAM732 DBLγ domains transcripts were seen in these placental isolates.

As most DBLγ are from group A or B/A *var,* amplification of DBLγ domains in this study was expected to result in detection predominantly of group A or B/A *var* gene transcripts. Examining mainly group A and B/A *var* genes may be a limitation of the study, as most group B and C *var* genes would have been overlooked. This prompted analysis of DBLα(0/1) RTPCR data using the primers described in chapter 3 (data from Rowe *et al*. 2002) revealed higher DBLα0 than DBLα1 transcription in these placental isolates. The low level of transcription of DBLα1 domains in these isolates is consistent with the association of DBLα1 domains/group A PfEMP1 with severe childhood disease, and young immunologically naive hosts.

As syncitiotrophoblasts do not express CD36 (Sartelet *et al*. 2000), and placental isolates do not tend to show affinity for CD36 (Fried *et al*. 2007; Muthusamy *et al*. 2007), group B, C or B/C PfEMP1 expression was not expected. The high frequency of DBLα0 domains in Rowe *et al*. 2002 is thus surprising. If the association of DBLγ and group A (DBLα1 domains) is true for field isolates, the DBLα0 domains amplified here are unlikely to 'belong' to the DBLγ domain transcripts detected in

this chapter. The high presence of DBLα0 domains suggests even more non-*var2csa* *var* genes are being transcribed in these field isolates than would be predicted from the DBLγ analysis alone. Unfortunately, these primers cannot recognise *var2csa*, and so comparisons of abundance of DBLα(0/1) and *var2csa* transcription would not be possible unless quantitative real-time RT-PCR analysis was performed.

Results in chapter 3 showed cerebral isolates expressed a higher proportion of group A or B/A *var* genes than uncomplicated isolates. In this analysis, no difference was seen in the number or clustering of DBLγ/*var2csa* domain transcripts in the cerebral and uncomplicated childhood malaria groups. However, there is no data on the relative levels of transcription in the different isolates. Though a similar level of diversity of DBLγ transcripts per isolate was detected, this does not necessarily equate to a similar level of overall DBLγ transcription as non DBLγ-containing *var* genes are neglected. This data does not therefore conflict with the results of chapter 3.

Non-*var2csa* transcripts were found in each placental isolate, with no detectably "placental" features. There is no reason to assume they have affinity for CSA. However, they may bring about placental sequestration through other interactions. Binding to hyaluronic acid has previously been implicated in placental malaria (Beeson *et al*. 2000). Although subsequent studies have shown this interaction is not as important as CSA interaction (Muthusamy *et al*. 2007), it may still have a minor role. Binding to IgM is a characteristic of many placental isolates (Creasey *et al*. 2003), and can be mediated by PfEMP1 including *var1CSA* and *var2csa* (Semblat *et*

al. 2006). IgG binding may also be involved (Flick *et al*. 2001). ICAM1 also appears to be upregulated in placenta upon *P. falciparum* infection, (Sartelet *et al*. 2000) which provide a target for adhesion via certain PfEMP1 (Smith *et al*. 2000a; Springer *et al*. 2004). The complete binding phenotype of placental parasites is probably still not fully understood.

The clear association of *var2csa* with placental malaria have inevitably led research towards the development of a vaccine against placental malaria, though unfortunately this challenge has so far proved difficult. Assessments of the cross-reactivity of anti-*var2csa* protection are conflicting (Elliott *et al*. 2005; Beeson *et al*. 2006; Barfod *et al*. 2007) and the true level of involvement of other PfEMP1, or other proteins, is unclear. Recently a number of non-PfEMP1 proteins have been associated with placental malaria (Francis *et al*. 2007; Fried *et al*. 2007; Gowda *et al*. 2007; Mok *et al*. 2007). If other proteins have the potential to cause placental sequestration then a placental malaria vaccine directed exclusively at *var2csa* is unlikely to be successful. Seeking to inhibit parasite protein-mediated adhesion to host cells is not a problem confined to placental malaria. Rosetting, a phenomenon association with malaria severity in Africa (Carlson *et al*. 1990; Rowe *et al*. 1995; Rowe *et al*. 2002b) is brought about through interactions via many different PfEMP1 with uninfected erythrocytes. In the case of rosetting, interactions with host erythrocyte ligands via many different PfEMP1 can be universally inhibited by certain glycosaminoglycan drugs, rather than trying to target each interaction independently (Havlik *et al*. 2005; Kyriacou *et al*. 2007), see chapter 6 for details of curdlan sulfate as a rosette inhibiting drug. A similarly broad approach could be

useful in the case of placental malaria of trying to protect the placenta against a wide range of different mechanisms of placental-sequestration, rather than focussing on a single interaction, although this may not be feasible.

In conclusion, the data presented in this chapter are indicative of *var2csa* being important in placental malaria, an association which has become increasingly convincing in the light of recent supporting studies. In the case of placental malaria a clearer picture of *var* gene involvement has emerged than in childhood cerebral malaria, with one specific *var* gene rather than a whole subgroup being involved. This reflects a simpler mechanism of sequestration, whereby a single *var* gene has high affinity for a novel ligand. It follows that defining conserved sequences that contribute specifically to placental malaria is pivotal in the development of effective drugs and vaccines to combat this disease.

Chapter 5

Type 3 *var* genes and PfEMP1

5.1 Abstract

This chapter examined type 3 *var* gene transcription in laboratory strains and field isolates. Type 3 *var* genes are group A *var* genes, and it was hypothesised that their transcription would be associated with cerebral malaria, following the link between other group A *var* genes and cerebral malaria discussed in chapter 3. Type 3 *var* gene transcripts were detected in the majority (23/26) of field isolates examined, and were highly conserved. Transcription of the type 3 *var* genes was not associated with cerebral malaria, however, there was an increased diversity of transcripts in the hyperparasitaemia isolates compared to cerebral malaria isolates, possibly suggesting a higher frequency of type 3 *var* gene transcription. Phylogenetic analysis of the type 3 *var* gene sequences obtained revealed 6 highly conserved subgroups of type 3 DBLα domain. Type 3 DBLε domains were highly homologous across the entire length of the amplified tag. Transcription of type 3 *var* genes in *P. falciparum* laboratory isolates revealed transcription occurs in asexual parasites, in ring stage, pigmented trophozoite stage and schizont stages, of laboratory isolate 3D7. No association with binding phenotype in laboratory isolates (rosetting or IgM affinity) was observed. An attempt was also made to raise a type 3-specific polyclonal antibody.

5.2 Introduction

5.2.1 Type 3 *var* gene/ PfEMP1 structure

The type 3 *var* genes are the shortest of the *var* family, being approximately 4 kb in length (3.948, 3.984 and 3.978 kb in 3D7). The type 3 *var* genes thus encode the smallest PfEMP1 (approximately 153 kDa). Type 3 PfEMP1 have no CIDR domains and only two extracellular DBL domains; an N-terminal DBLα domain (further referred to as $DBL\alpha_{type3}$), and a membrane-proximal DBLε domain ($DBL\varepsilon_{type3}$) (Fig. 5.1, Fig. 5.2). The DBL domains are followed by a transmembrane region and ATS, typical for PfEMP1 (Fig. 5.1, Fig. 5.2).

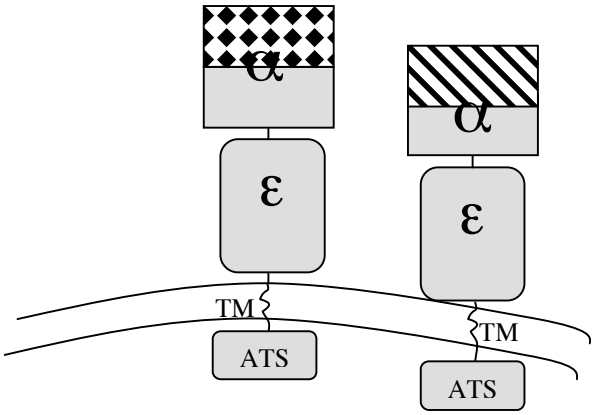

Fig. 5.1. Diagram of type 3 PfEMP1s showing $DBL\alpha_{type3}$, $DBL\varepsilon_{type3}$, transmembrane region (TM) and ATS region. Hatched and striped N-terminal region of $DBL\alpha_{type3}$ domains are variable, light grey shaded area of $DBL\alpha_{type3}$ and $DBL\varepsilon_{type3}$domains, as well as TM and ATS regions, are conserved between different type 3 variants.

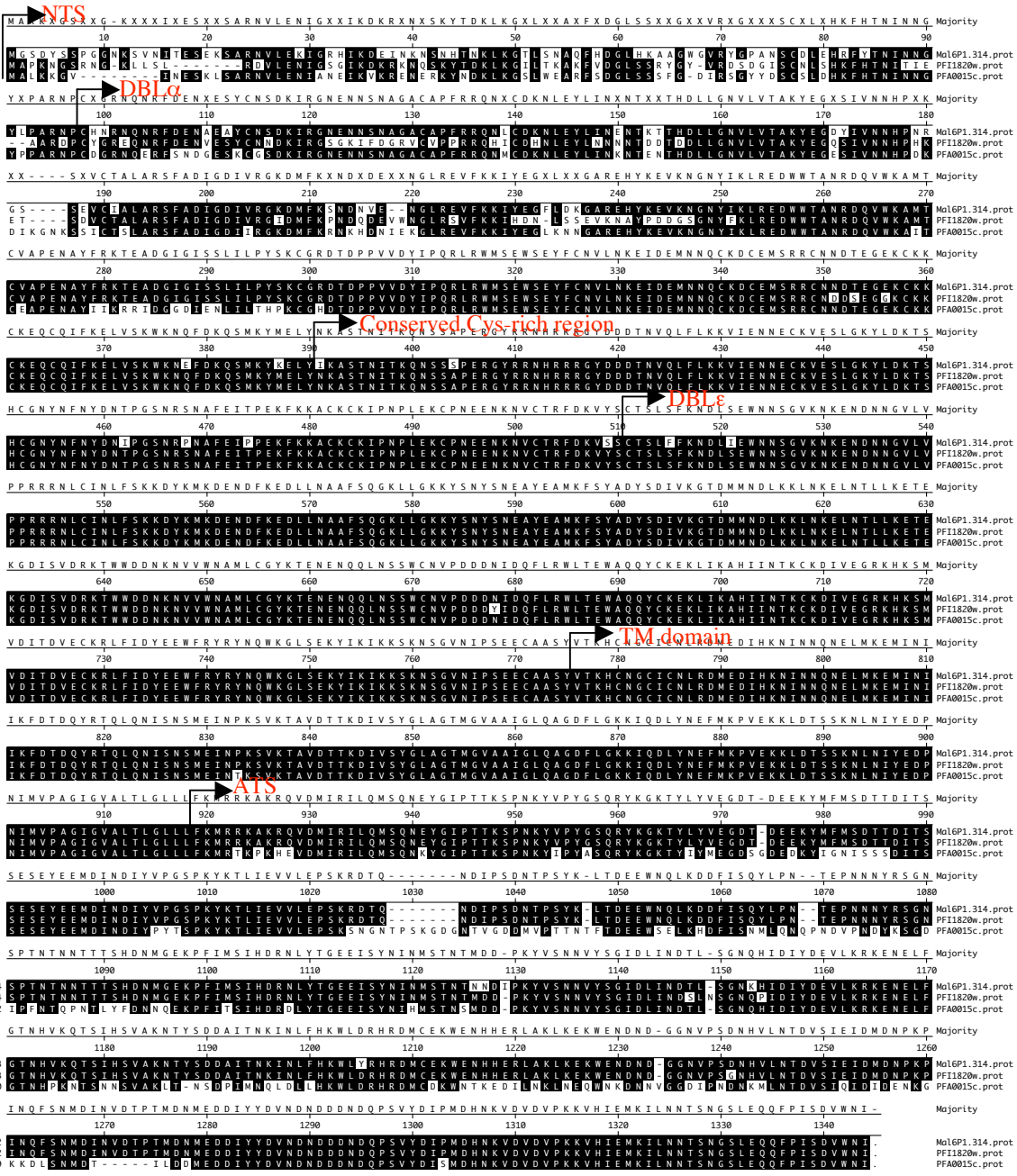

Fig. 5.2. Annotated clustal W alignment of the three 3D7 type 3 PfEMP1 amino acid sequences showing NTS region, DBLα domain, conserved cysteine-rich region, DBLε domain, transmembrane (TM) domain and ATS region. Arrows indicate beginning of each domain type.

5.2.2 Type 3 *var* genes are atypical group A *var* genes

Type 3 *var* genes are interesting due to their unusual domain structure, containing only two well-conserved extracellular DBL domains. The data presented in chapter 3 revealed an association between group A *var* gene transcription and cerebral malaria. However, transcription of type 3 *var* genes could not be analysed with the primers used in chapter 3. Type 3 *var* genes are group A genes; as well as having a DBLα1-type DBLα domain, the type 3 *var* genes have UpsA-type upstream regions and are telomerically located with transcription towards the telomere in 3D7 (Smith *et al.* 2000b; Gardner *et al.* 2002; Kraemer and Smith 2003; Lavstsen *et al.* 2003). However, the other group A *var* genes are characterised by having many extracellular domains. The type 3 *var* genes encode atypical group A PfEMP1, without the complex domain architecture of the other group A PfEMP1. It is possible that they have different properties to classic group A PfEMP1, and their transcription may not be associated with severe disease.

5.2.3 Type 3 *var* gene DBLα1 domains

The nucleotide sequence of first half of the $DBL\alpha_{type3}$ domains is variable, and $DBL\alpha_{type3}$ domains are indistinguishable from other DBLα1domains (Fig. 5.3). However, the $DBL\alpha_{type3}$ domains become increasingly similar until the final ≈ 336 nucleotides of each $DBL\alpha_{type3}$ domain, which form a highly conserved $DBL\alpha_{type3}$-specific region, and $DBL\alpha_{type3}$ cluster separately in a phenogram from other DBLα1 domains (Fig. 5.4).

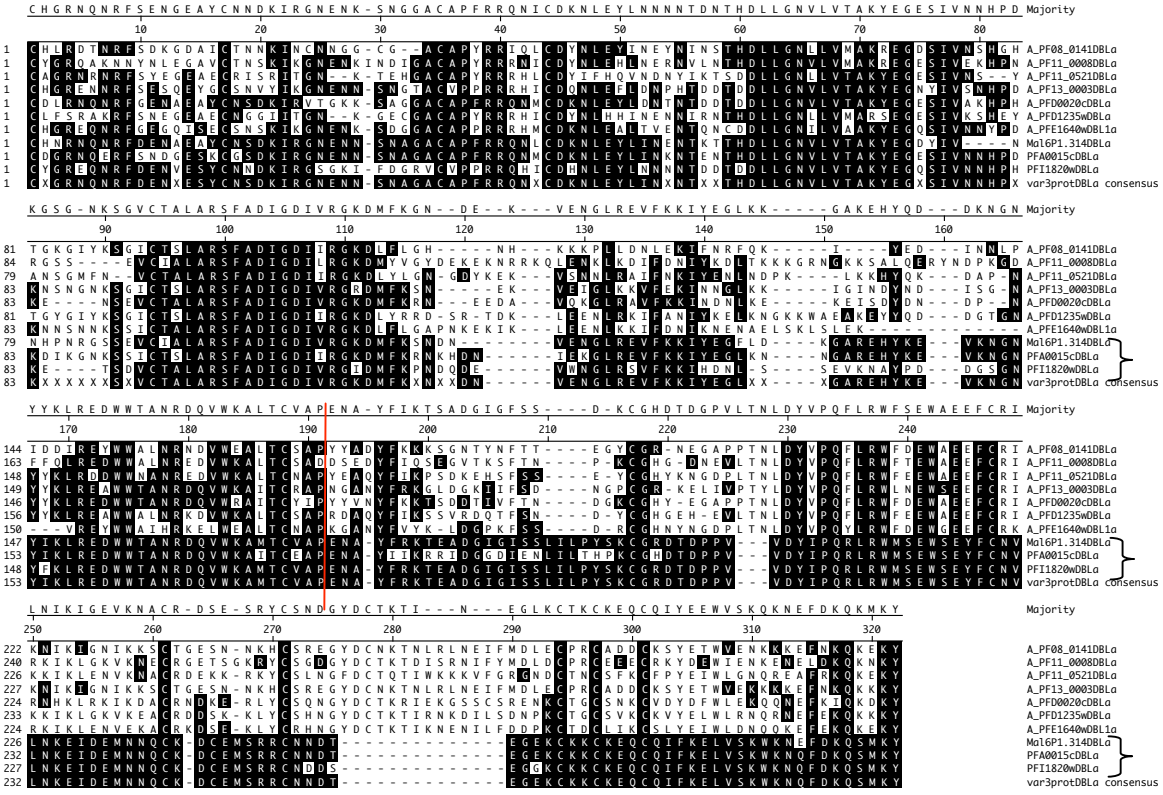

Fig. 5.3. Clustal W amino acid alignment of DBLα1 domains from 3D7. The consensus sequence from an alignment of the three DBLα_{type3} domains in 3D7 is shown and identical residues shaded. DBLα_{type3} domains are indicated (}). Red line (amino acid 191 in this alignment) indicates the start of the type 3-specific portion.

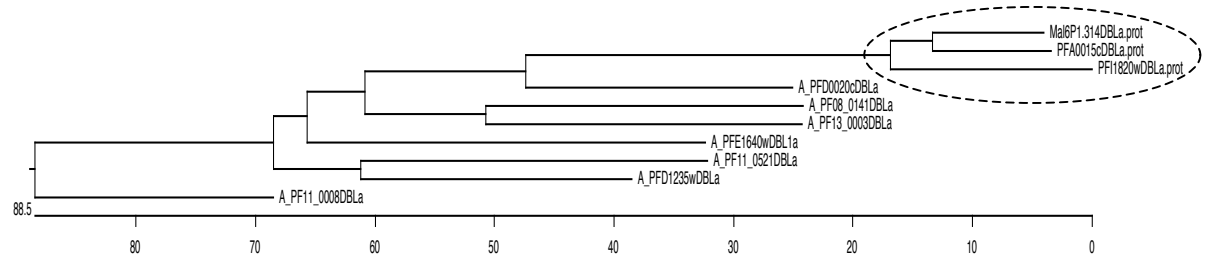

Fig. 5.4. Phenogram of 3D7 group A DBLα1 domains; DBLα_{type3} domains (circled) cluster separately.

5.2.4 Type 3 *var* gene DBLε domains

Similarly, Type 3 epsilon domains ($DBL\varepsilon_{type3}$) are extremely conserved; the three $DBL\varepsilon_{type3}$ in 3D7 have only 4 nucleotide differences, and they cluster separately from other epsilon domains after phylogenetic analysis (Fig. 5.5 and Fig. 5.6).

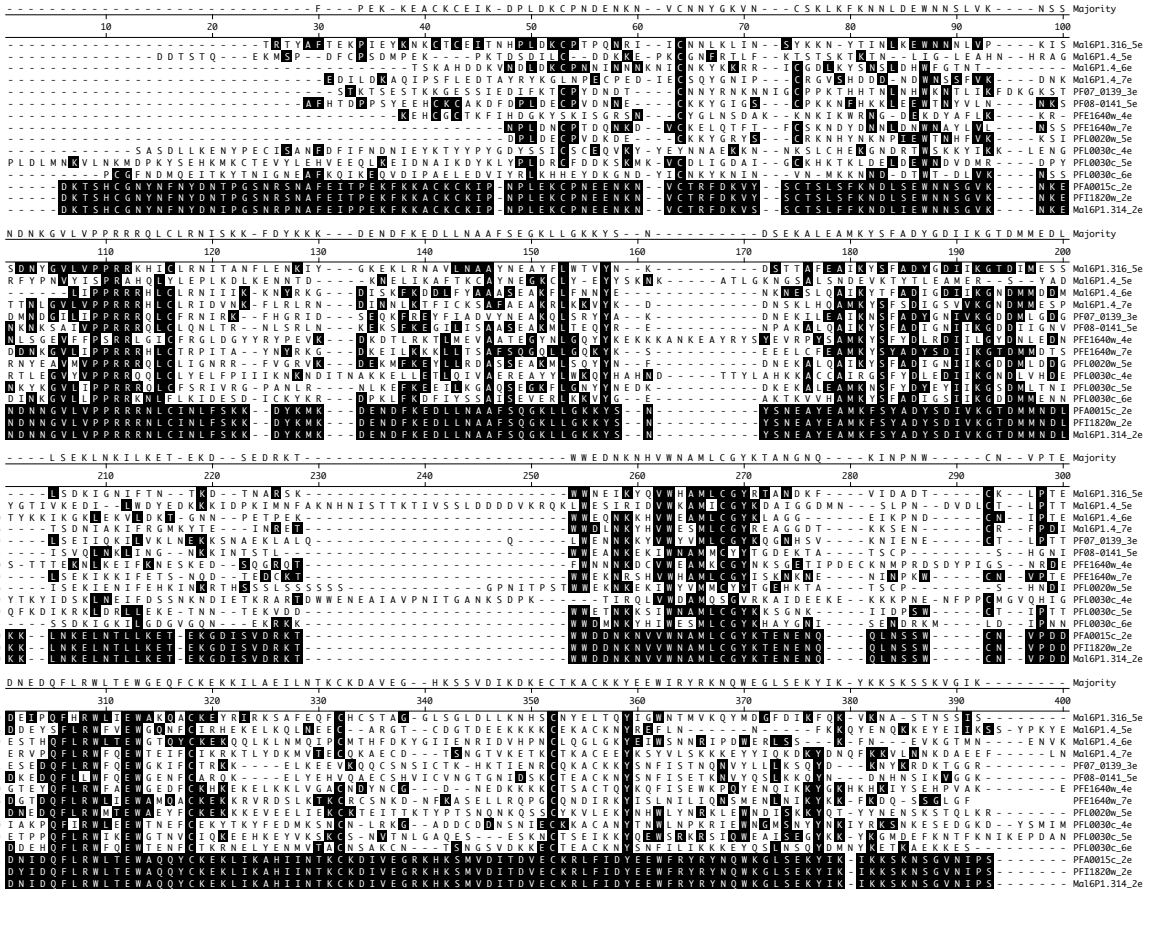

Fig. 5.5. Clustal W amino acid aligment of all 3D7 epsilon domains; type 3 epsilon domains indicated ({}) Shading indicates $DBL\varepsilon_{type3}$ domain residues.

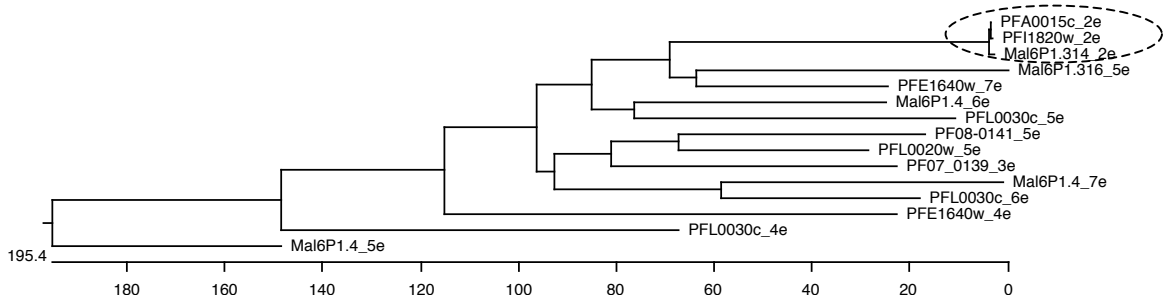

Fig. 5.6. Phenogram of 3D7 epsilon domains; DBLε_{type3} domains (circled) cluster separately.

5.2.5 Type 3 *var* gene intron

Retrieval of data from plasmboDB database revealed Pfa0015c, Pfi1820w and Mal6P1.314 have introns of 158, 171 and 150 bp respectively. These introns are much shorter than those of other *var* genes, which are usually 0.8-1.2 kb (Su *et al.* 1995). They do not contain the conserved repeat elements which make up the promoter initiator element, described by Calderwood *et al.* (2003). Pfi1820w and Mal6P1.314 do not contain the Inr-like initiator sequence (TCATA). Pfa0015c does contain this sequence, but as it is not in the correct context within the initiator element it is unlikely to act as a promoter (Calderwood *et al.* 2003). This has implicatons for regulation, as the intron promoter regulates *var* gene silencing (Deitsch 2001; Calderwood *et al.* 2003; Frank *et al.* 2006).

5.2.6 Type 3 *var* gene ATS region

The ATS region of the type 3 *var* genes in 3D7 cluster with the ATS region of the other 3D7 group A *var* genes in a distance tree of the ATS domains by Lavstsen *et al*. 2003. Mal6P1.314 and Pfi1820w ATS regions are almost identical and form a slight outgroup from other group A ATS regions (Lavstsen *et al*. 2003).

5.2.7 Type 3 *var* gene transcription

At present there is little published data on type 3 *var* gene expression in laboratory or field isolates. Two papers discuss type 3 *var* gene transcription in relation to disease severity. Firstly, Jensen *et al.* (2004) report type 3 *var* gene transcription (pfa0015c) at relatively high levels in unselected 3D7, and a decrease in expression after selection on semi-immune sera. This suggests type 3 PfEMP1 are not associated with severe disease and are not common targets for an immune response. Secondly, Rottman *et al.* (2006) reported a small (non-significant) upregulation of type 3 *var* gene transcription in severe malaria compared to uncomplicated or asymptomatic malaria isolates, but in this study there was an increase in all *var* gene groups in severe malaria compared to the control groups, suggesting an increase in overall *var* gene transcription in the severe malaria cohort, possibly due to the higher parasitaemia.

5.2.8 Type 3 *var* gene/PfEMP1 hypotheses

The intention of the chapter was to examine type 3 *var* gene transcription in a range of laboratory and field isolates. Due to the association of group A *var* gene transcription with cerebral malaria isolates discussed in chapter 3, it was

hypothesised that type 3 *var* gene transcription may be more common in cerebral malaria isolates than in hyperparasitaemia isolates. However, as type 3 *var* genes are not typical group A *var* genes, the association found between group A *var* genes and cerebral malaria disease in chapter 3 could not be extended to the type 3 *var* genes without specifically examining this link.

It was thought possible that the timing of expression could be regulated differently to other *var* genes due to the small intron and therefore lack of regulatory promoter (Deitsch 2001; Calderwood *et al.* 2003; Frank *et al.* 2006). It was also thought possible that the lack of the regulatory promoter may promote type 3 *var* gene expression outside the mutually exclusive *var* gene expression system (Smith *et al.* 1995; Scherf *et al.* 1998; Dzikowski *et al.* 2006), and that type 3 *var* gene transcripts could be constitutively expressed.

The high conservation of type 3 PfEMP1 led me to doubt prolonged exposure of type 3 PfEMP1 on the erythrocyte surface, and so an antibody was designed to specifically recognise type 3 PfEMP1, to allow protease experiments with immunofluorescence and Western blot to investigate type 3 PfEMP1 expression and determine whether it is surface expressed.

5.3 Aim of chapter

In this chapter, transcription of type 3 *var* genes in *P. falciparum* laboratory and field isolates was examined. Data was obtained on the frequency of expression, timing of expression, and sequence conservation of the type 3 *var* genes in laboratory strains and field isolates. In addition, to study protein expression of the type 3 PfEMP1, a type-3 specific anti-peptide polyclonal antibody was designed and raised in chicken. This antibody was then used to examine protein expression of type 3 PfEMP1 in *P. falciparum* laboratory strain 3D7.

5.4 Materials and methods

Materials and methods that are specific to chapter 5 are listed below. General materials and methods and a list of suppliers are given in chapter 2.

5.4.1 Type 3 *var* gene PCR/RT-PCR

Field isolate cDNA prepared as detailed for DBLα analysis was used (see chapter 2 and 3). Laboratory strains used were 3D7, NF54, Dd2, HB3, TM180, TM284, FCR3/It, 7G8, Muz12, TM267 and Malayan Camp all from JA Rowe/A Raza except 3D7. Type 3 *var* gene sequence taken from 3D7 were pfa0015c, pfi1820w and mal6p1.314 (also renamed pff0020c) (Gardner *et al*. 2002; Hall *et al*. 2002). Type 3 *var* gene sequences DQ408041-DQ408070 were taken from Trimnell *et al*. 2006.

5.4.2 Type 3 DBLα domain amplification

PCR/RT-PCR was used to amplify a region of the type 3 *var* gene DBLα domain using forward primer αAF3_type3F; GCAMGAAGTTTTGC modification of DBLαAF' (GCACGMAGTTTYGC) (Bull *et al*. 2005a) and reverse primer Type3alphaR1; CAGAAATATTCAG (PCR product 420 bp) or Type3alphaR2 ATATTTCATTGATTGTTTATC (PCR product 580 bp). Amplification used 5 μl 10x PCR Gold buffer, 25 pmol each of DBLαAF' and DBLαBR primers and 0.2 μl Amplitaq Gold polymerase with a final concentration 2 mM $MgCl_2$, and 1.25 mM of each dNTP, and the volume adjusted to 50 μl after addition of 2 μl cDNA, 0.25 μl gDNA, or distilled water. Amplification conditions were as described for DBLα RT-PCR (Taylor *et al*. 2000a; Bull *et al*. 2005a) with a hot start (95˚C, 5 min) followed by 35 cycles of 95˚C, 20 sec; 42˚C, 20 sec; 60˚C, 1 min. Samples without RT were used in all reactions to exclude gDNA contamination.

5.4.3 Type 3 DBLε domain amplification

PCR/RT-PCR was used to amplify a region of 726 bp of the type 3 *var* gene DBLε domain using forward primer Type3epsF GACAATAATGGTGTGTTAGTTCCTC and reverse primer Type3epsR GTATGATGCAGCACATTCCTCA. This pair was unbiased on 3D7 gDNA. Amplification conditions were as for DBLα domain RT-PCR; hot start (95˚C, 5 min) followed by 35 cycles of 95˚C, 20 sec; 42˚C, 20 sec; 60˚C, 1 min. Samples without RT were used in all reactions to exclude gDNA contamination. Amplification conditions and mix were as for type 3 *var* gene DBLα domain RT-PCR.

5.4.4 Tubulin gene amplification

PCR/RT-PCR was used to amplify 389 bp of the 3D7 *P. falciparum* β-tubulin gene using forward primer Tub3' GATCCAAGTGGTACCTAT and reverse primer Tub5' GGATACTCCTCTCTTAT. Amplification used 5 μl 10x PCR Gold buffer, 25 pmol each of Tub3' and Tub5' primers and 0.2 μl Amplitaq Gold polymerase with a final concentration of 2.25 mM $MgCl_2$, and 1.25 mM of each dNTP, and the volume adjusted to 50 μl after addition of 1 μl cDNA, 0.25 μl gDNA, or distilled water. Amplification conditions were a hot start (95˚C, 5 min) followed by 35 cycles of 95˚C, 10 sec; 50˚C, 15 sec; 62˚C, 1 min. Samples without RT were used in all reactions to exclude gDNA contamination.

5.4.5 Sequence analysis

See chapter 2 for details of ligation, cloning, transformation, and sequencing of RT-PCR products. In brief, RT-PCR products were visualised by electrophoresis on 1.5% agarose gels. RT-PCR products were purified and ligated into PCR II TA cloning vector (Invitrogen) and ligated plasmids were used to transform TOP10F *E. coli*. Transformed *E. coli* was grown overnight under ampicillin selection and blue/white colony screening. Individual white colonies were selected for overnight growth and the plasmids extracted for sequencing. Presence of an insert in the extracted plasmids was verified by *Eco*RI restriction digestion prior to sequencing. For Mali isolate gDNA type 3 *var* gene PCR only, plasmids were sequenced directly from transformed *E. coli* colonies. Colonies were grown at 37°C o/n in LB broth with 8% glycerol. Sequencing was then carried out by the University of Edinburgh School of Biological Sciences Sequencing Service.

Transcript sequences from each isolate were grouped into contigs of >95% nucleotide identity using the SeqMan programme within the DNAstar software package. Consensus sequences from each isolate were saved as sequence A, B, C etc from that isolate as EditSeq files (DNAstar software package), and protein sequences were obtained by translating the DNA sequences using the EditSeq translation function.

Nucleotide and protein sequences were then compared within and between isolates using MegAlign (DNAstar software package). Alignments and phenograms were produced using the clustal W alignment programme within MegAlign, using default settings. Sequence distances were calculated using MegAlign, and colour-coded into the following groups; 0-30, 30-39.9, 40-49.9, 50-59.9, 60-69.9 70-99.9 and 100% amino acid identity for production of sequence distance figures. Homology searches were performed using nucleotide-nucleotide BLAST search of the NCBI database (http://www.ncbi.nlm.nih.gov/BLAST). Phenograms were laid out in Adobe Illustrator.

5.4.6 Northern blot methods

1.2 g of agarose was disolved in 80 ml of distilled water with 10 ml of 10x MOPS (110 mM MOPS, 25 mM Na-Acetate, 5 mM EDTA pH 7.0) and 3 ml of 37% formaldehyde. 1 μg RNA, 9 μl formamide, 3 μl formaldehyde (37%), 2 μl 10x MOPS was heated to 65°C for 5 min and loaded immediately onto the gel with 2 μl of RNA gel loading buffer (1x MOPS with 0.01% Bromophenol blue, 10% glycerol,

30% formaldehyde, 3.33% formamide). Millennium Markers (Ambion) were also loaded. Gel was run at 150 volts in 1x MOPS running buffer for 90 min. Gel was stained with final concentration 0.5 μg/ml EtBr in 200 ml of 1x MOPS for 30 min on shaker at RT and destained twice with water for 30 min on shaker at room temperature to visualize RNA and photograph markers. To transfer the RNA to nitrocellulose, the gel was placed on top of a wick of wet MME paper in 10x SSC (1.5 M NaCl, 0.15 M Tri Sodium Citrate) covering the gel tray. Nylon membrane (Roche) prewetted in 10x SSC was placed on top of the gel, followed by 2x MME papers the size of gel prewet in 2x SSC, and then 2 inches of paper towel. A weight (old catalogue) was placed on top of the assembly. Next day the nylon membrane was removed and air-dried before cross-linking the RNA by UV (1.2 sec) in a Stratalinker. PCR for riboprobe used the primers as described in Table 5.1.

Probe	Forward Primer	Reverse Primer	Sequence (3D7)	Hybridisation
Type 3 DBLα	type3probeF: ccccctgttgttg	Type3alphaR2	PFA0015c	60°C
Type 3 DBLε	Type3epsF	Type3epsR	PFA0015c	60°C
Var gene exon2	Exon2F: aaaaaaccaaagca tctgttggaaatttat	Exon2R: gtgttgtttcgact aggtagtaccac	PF07_0048	50°C
MSP-1	NI	N2	MSP-1	60°C

Table 5.1 PCR primers for riboprobe design.

Amplification used 5 µl 10x PCR Gold buffer, 25 pmol each of DBLαAF' and DBLαBR primers and 0.2 µl Amplitaq Gold polymerase with a final concentration 2 mM $MgCl_2$, and 1.25 mM of each dNTP, and the volume adjusted to 50 µl after

addition of 2 μl cDNA, 0.25 μl gDNA, or distilled water. Amplification conditions were as described for DBLα RT-PCR (Taylor *et al*. 2000a; Bull *et al*. 2005a) with a hot start (95˚C, 5 min) followed by 35 cycles of 95˚C, 20 sec; 42˚C, 20 sec; 60˚C, 1 min. Samples without RT were used in all reactions to exclude gDNA contamination. PCR products were purified as described in chapter 2 and were cloned into PCR II vector (Invitrogen) and plasmids obtained by miniprep (QIAgen) and insert size verified by *Eco*RI digestion (details in chapter 2).

All materials for riboprobe production and Northern blot analysis were from Roche (Northern starter kit). For riboprobe transcription and DIG incorporation, 2μl NTP Mix, 1 μl RNase inhibitor, 2 μl 10xTansription Buffer, 40 units SP6 polymerase and DTT (final concentration 5 μM) was added to 1 μg template plasmid, and water added to give a final volume of 20 μl. Mix was incubated at 37°C for 2 hr. 2 μl of DNaseI was added (37°C, 15 min) to remove any DNA template, and the DNase reaction stopped by the addition of 2 μl of 200 mM EDTA, pH 8.0. The riboprobe was precipitated at –70°C for 2 hr, using 2.5 μl of 4 M LiCl and 75 μl of cold 100% ethanol, pelleted (13,000 rpm, 15 min, at 4°C) and washed with 50 μl 70% cold ethanol. The RNA pellet was air dried for 10 min and resuspended in 50 μl of DEPC-H_20 with 1 μl of RNase inhibitor.

Nylon membranes (Roche) were prehybridised in 10 ml hybridisation solution (Maleic acid buffer: 100 mM Maleic acid, 150mM NaCl, pH 7.5 with DIG Easy Hyb granules: Roche) for 1 hr at the hybridisation temperature (DBLαtype3, DBLεtype3 and MSP1 probe at 60 ˚C, exon 2 probe at 50˚C). 2 μl probe was boiled in 100 μl

hybridisation solution for 5 min and added to membrane with fresh hybridisation solution, and incubated at hybridisation temperature, with rotation, o/n. The membrane was then washed twice for 30 min at "hyb temp + 5˚C" in 0.2x SSC/0.1% SDS. Membrane was washed for 1 min in Maleic acid buffer (100 mM Maleic acid, 150mM NaCl, pH 7.5) and blocked for 1 hour in 20 ml Northern blocking buffer (18 ml of Maleic acid buffer with 2 ml of 10% Northern block buffer, Roche). Membrane was then incubated for 30 min in 20 ml blocking buffer + 2 µl Anti-DIG antibody (Roche), before two further 15 min washes in Maleic acid buffer with 0.3% Tween 20. Membrane was soaked for 2 min in Detection buffer (100 mM Tris-HCl, 100 mM NaCl pH 9.5) before incubating with 1 ml CDP-Star (Roche) 5 min, RT. Membrane was exposed to X-ray film.

5.4.7 Transcription time course

For the time course RT-PCR and for the Northern blots, RNA was extracted from a fresh culture of laboratory strain 3D7 by chloroform extraction and isopropanol precipitation as detailed in chapter 2. For the time courses, 200 µl packed cell volume was extracted for each time point and immediately stored in Trizol at -70˚C, and the rest of the culture re-gassed and incubated at 37˚C. A Giemsa slide was also prepared to assess parasite maturity at each time point. RNA extraction and cDNA preparation for each time point was carried out at the same time.

5.4.8 DBL domain structural modelling

The published structures of the EBA175 DBL domain (Tolia *et al.* 2005) and a *P. knowlesi* DBL domain (Singh *et al.* 2006) were downloaded from the Research Collaboratory for Structural Bioinformatics (RCSB) Protein Data Bank (http://www.pdb.org), PDB ID 1zrl and 2c6j, for modelling of type 3 protein structures. The mal6p1.314 DBLα domain amino acid sequence was aligned to the amino acid sequence of EBA175 and *P. knowlesi* DBLα by clustal W. The aligned amino acid sequence was then mapped onto the published structures using Cn3d structural modelling software (http://www.ncbi.nlm.nih.gov/Structure/CN3D/cn3d.shtml). Secondary structure colouring shortcuts, and worm and spacefill rendering shortcuts, were used. Regions of interest were highlighted in the structure by selection of the corresponding amino acid sequence.

5.4.9 Protean software

Protean/Lasergene software (DNAstar, Inc) was used to analyse features of the pfa1820w, pfa0015c and mal6P1.314 type 3 *var* gene DBLα domain protein sequences to aid peptide choice. Alpha helical and beta sheet regions were predicted by Garnier-Robson, Chou-Fasman and Eisenberg plots. These are based on statistical preferences of different amino acids to have particular secondary structure types in known protein structures. Kyte-Doolitle plots were used to predict hydrophobicity. Amino acids are given a hydrophobicity score between -4.6 (hydrophobic) and 4.6 (hydrophilic), and the hydrophobicity plot shows the averaged score over stretches of 9 amino acids. Karplus-Schulz plots show flexible regions based on the characteristics of neighbouring residues. The Emini plot predicts surface exposure

probability, based on values of surface accessibility averages over 6 amino acid stretches. The Jameson-Wolf index predicts antigenicity of a given region, through a complex algorithm combining hydrophobicity, surface probability, flexibility, and alpha/beta regions predictions.

5.4.10 Peptide antibody production

Final peptides were chosen after consultation with peptide.design@eurogentec.com. Peptide synthesis, hen immunization and yolk collection was all performed by Eurogentec, UK. Briefly, peptides DTDPPVVDYIPQC (peptide 1) and CNVLNKEIDEMNNQ (peptide 2) were synthesized by solid phase Fmoc chemistry by Eurogentec, Belgium. Peptides were analysed by MADLI-TOF mass spectrometry and reversed phase analytical HPLC for weight and purity at Eurogentec, Belgium. Peptides alone are not immunogenic, thus conjugation to a carrier is required to elicit an immune response. Keyhole Limpet Hemocyanin (KLH) carrier was linked to the thiol group of the terminal cysteines of each peptide using m-Maleimidobenzoyl-N-hydroxysuccinimide ester (MBS). Hens PO41 and PO42 were immunised under the Eurogentec Double XP protocol. Eggs were collected on days 51-98 after immunisation and pooled as follows: days 51-57, 58-66, 72-78 79-85, 86-92 and 93-98 (Table 5.2). Pooled yolks were sent to Edinburgh at 4°C for IgY extraction and purification.

Hen PO41

Day	Egg collection date (2007)	Pooled yolk volume	Pre-affinity purification [IgY]	Post-affinity purification [IgY]	Final [IgY] after purification and buffer exchange
51 – 57	28/3 – 04/04	48 ml	2.37 mg/ml	IgY stored @ -20˚ C	
58 – 66	04/04 – 11/04	60 ml	2.32 mg/ml	IgY stored @ -20˚ C	
66 - 71	11/08 – 18/04	Yolks stored @ -20˚ C			
72 - 78	18/04 – 25/04	Yolks stored @ -20˚ C			
79 - 85	25/04 – 02/05	100 ml	3.87 mg/ml	undetectable	Approx 1 mg/ml
86 - 92	02/05 – 09/05	50 ml	3.13 mg/ml	IgY stored @ -20˚ C	
93 - 98	09/05 – 14/05	Yolks stored @ -20˚ C			

Hen PO42

Day	Egg collection date (2007)	Pooled yolk volume	Pre-affinity purification [IgY]	Post-affinity purification [IgY]	Final [IgY] after purification and buffer exchange
51 - 57	28/3 – 04/04	60 ml	2.74 mg/ml	IgY stored @ -20˚ C	
58 - 66	04/04 – 11/04	66 ml	3.12 mg/ml	IgY stored @ -20˚ C	
66 - 71	11/08 – 18/04	Yolks stored @ -20˚ C			
72 - 78	18/04 – 25/04	Yolks stored @ -20˚ C			
79 - 85	25/04 – 02/05	100 ml	2.72 mg/ml	undetectable	Approx 1 mg/ml
86 - 92	02/05 – 09/05	30 ml	2.55 mg/ml	IgY stored @ -20˚ C	
93 - 98	09/05 – 14/05	Yolks stored @ -20˚ C			

Table 5.2. Egg collection and yolk processing schedule.

5.4.11 IgY Extraction

IgY extraction was performed using EggStract kit (Promega, Madison, WI) according to manufacturer's guidelines. Yolks were warmed to RT. 3 volumes precipitation solution A was added slowly and stirred for 5 min to precipitate the lipids. The mixture was centrifuged (10,000 rpm, 15 min), and the supernatant

collected into a graduated cylinder through gauze. The supernatant was stirred at RT while 1/3 volume solution B was added slowly to precipitate the IgY. The mixture was centrifuged (10,000 rpm, 15 min), and the supernatant discarded. The precipitated IgY was resuspended in PBS. IgY precipitation was repeated to increase the purity of extracted IgY. IgY was stored at -20˚C.

5.4.12 Determining IgY concentration

Absorbance at 280 was read on a spectrophotometer. The protein extinction coefficient of IgY is 13.3. This is the absorbance ($A280_{nm}$) value for 1% (i.e. 1 g/100ml) solution, measured in a 1 cm cuvette. Thus for concentration at mg/ml (0.1 % solution), absorbance at 280 nm must be divided by 1.33.

5.4.13 IgY affinity purification

A sample of the extracted IgY from immunised hen eggs was affinity-purified against the peptide using the SulfoLink Immobilization Kit (Pierce, IL, USA), according to manufacturer instructions. Briefly, 0.5 mg of each peptide was reduced using Tris(2-carboxyethyl)phosphine (TCEP) and both peptides immobilized concurrently on the SulfoLink Resin via the free sulfhydryl groups on the terminal cysteines. The internal methionine of peptide 2 will also stabilise immobilisation on the column. Extracted IgY (4-8 mg) was applied to the column. After washing, bound antibody eluted was in 3 x 2 ml 0.2 M glycine HCl (pH 2.5) and neutralised in 50 µl 1 M Tris HCl (pH 8.5) per ml elution. The full 6 ml elution was then concentrated using a vivaspin column (Vivascience, UK), molecular weight cut off 10 kDa, and buffer exchanged into 500 µl PBS containing 0.05% azide. Affinity-

purified and concentrated antibody was then aliquoted and stored at –20°C. Affinity purification was also carried out with the two peptides separately.

5.4.14 Enzyme-Linked ImmunoSorbent Assay (ELISA)

Microtest III assay plates (Falcon) were coated 150 ml PBS with 10 μg/ml peptide 1, 10 μg/ml peptide 2, 1% BSA or PBS alone, at 4°C, o/n. Plates were washed three times with PBS, blocked for 2 hr at 37°C with 150 μl 2% milk with 0.5% Tween 20 and washed three times with PBS before adding primary IgY 1:100 in blocking solution (150 μl) to each well, for 2 hr at 37°C. Plates were washed a further three times with PBS, before incubation with 150 μl of peroxidase conjugated goat anti-chicken IgG diluted 1:1000, 1hr RT, then washed a final 3 times with PBS. For detection, 100 ml TMB Substrate Reagent (BD OptEIA) was added to each well and the plate was left to develop for 30 min at RT, in the dark, before the reaction was stopped with 50 μl 2M H2SO4 per well. Absorbance measurements were made on an ELISA plate reader at 450 nm. These are shown as mean ± standard error (SE).

5.4.15 Detergent extraction of proteins

Infected erythrocytes (IE) or non-infected erythrocytes were washed twice with PBS. If trypsinisation was required, cells were incubated with 5 volumes 0.1 or 1 mg/ml trypsin (Sigma), or mock treated with PBS, for 5 min at RT. Trypsinisation was stopped by addition of trypsin inhibitor (Sigma) for 5 min at RT. Cells were then pelleted (4000 rpm, 3 min) and washed in RPMI. All cell preparations were then lysed on ice with 5 volumes of NETT buffer (150 mM NaCl, 5 mM EDTA, 50 mM tris pH8.0, 1% triton-X100 (w/v)) plus complete mini protease inhibitor cocktail

(Roche). Cell lysates were then centrifuged (13,000 rpm, 10 min at 4°C). Supernatants were removed. These are now referred to as triton-X100 soluble (TS) fractions. The triton-X100 insoluble pellet was resuspended in a Tris saline (20 mM tris-HCl pH 8.0, 150 mM HCl, 2% (w/v) SDS) plus complete mini protease inhibitor cocktail (Roche). The solubilised TI fraction was repeatedly pipetted and vortexed to disrupt the parasite DNA. Samples were centrifuged (13,000 rpm, 10 min, RT) to pellet the remaining insoluble fraction, seen as a brown pigment in the infected erythrocyte sample. The soluble TI fractions were removed and transferred to a fresh tube. All samples were stored at –80°C.

5.4.16 SDS-PAGE

SDS-PAGE was performed using the Novex precast gel system (all reagents from Invitrogen). Samples were prepared according to the NuPAGE Novex Tri-acetate mini Gel protocol with NuPAGE LDS sample buffer and NuPAGE reducing agent, and heated to 70°C for 10 min. Samples were then run on 3-8% Tris-acetate gradient gels using Tris-acetate SDS running buffer for 1 hr at 150 V. Pre-stained precision protein molecular weight markers (10-250 kDa; Bio-rad) were used in all gels.

5.4.17 SimplyBlue staining

To visualise all loaded proteins on the acrylamide gel, gels were washed 3x 5 min in distilled water and then soaked in SimplyBlue safe stain (Invitrogen) for 1 hr, and destained 1hr to overnight in distilled water.

5.4.18 Western blotting

Proteins were electrophoretically transferred from SDS-PAGE gels to polyvinylidene difluoride (PVDF) membrane (Invitrogen) using a NuPAGE transfer buffer (Invitrogen) (30 V, 1 hr, RT). PVDF membranes were activated in 100% methanol for 30 sec prior to transfer. Membranes were washed briefly in PBS before incubating in blocking buffer (PBS/5% milk) for 30-60 min RT with rocking, and then o/n at 4°C. Membrane was then incubated for 1 hr in primary antibody or sera was diluted to 1 in 1000 unless otherwise stated in PBS/5% milk with rocking at RT. Blots were washed 3 x 10 min with PBST (PBS with 0.5% Tween-20). Incubation in secondary antibody (1 in 1000 HRP-conjugated goat anti-chicken H&L IgY, Abcam) was for 1 hr. Blots were then washed 2 x 10 min with PBST and 1 x 10 min in PBS alone prior to visualisation with an enhanced chemiluminescence (ECL) detection kit (Amersham). Chemiluminescence was detected using Hyperfilm™ ECL (Amersham).

5.4.19 Immunoflourescence assay (IFA)

For live IFA, cultures at 2% haematocrit were incubated with primary antibody (chicken pre-immune IgY extract (1:10), rabbit preimmune serum (1:10) or immune IgY (1:10) in PBS/1%BSA) for 1 hr on ice. Cells were then washed three times in PBS/1%BSA, and incubated with alexa488-conjugated goat anti-chicken or anti-rabbit secondary antibody (1:1000) in PBS/1%BSA for 1 hr on ice in the dark. Cells were washed a further three times in PBS/DAPI/1%BSA and mounted onto a glass slide with flouromount. Live cells were viewed under fluorescence at 100x magnification.

For fixed IFA, *P. falciparum* cultures were smeared onto slides and fixed with acetone. Slides were incubated for 1 hour in preimmune IgY, immune IgY extract affinity purified against peptides 1 and 2 together (both 1:10 in PBS/1% BSA), or PBS/1%BSA alone. The culture was then washed and the slides were incubated in alexa 488 conjugated secondary antibody 1:1000 and PBS/DAPI/BSA1% for 1 hour in the dark. Secondary incubation was washed off and the fixed cells were viewed under fluorescence at 100x magnification.

5.5 Results 1: Type 3 *var* gene analysis

5.5.1 Type 3 *var* gene DBLα domain amplification: DBLα primer design 1

To examine whether type 3 *var* genes were transcribed in laboratory and field isolates, I designed a type 3-specific primer pair for use in PCR and RT-PCR. The primers were designed to specifically recognise all type 3 DBLα domains, but not recognise other DBLα domains or other sequences. The DBLαAF' forward primer from the Taylor primer pair described in section 1.3 recognises $DBL\alpha_{type3}$ domains, but the DBLαBR reverse primer does not amplify type 3 *var* genes. To amplify the type 3 DBLα domains a new primer pair was designed.

The forward primer was a modification of the DBLαAF' forward primer from Taylor *et al*. (2000a), which had increased specificity for the type 3 group A DBLα domains (αAF3_type3F; GCAMGAAGTTTTGC modification of DBLαAF'; GCACGMAGTTTYGC, Fig. 5.7); degeneracy at positions 6 (M) and 12 (Y) is unnecessary as all known type 3 DBLα domains have an A and T at these positions. However, degeneracy at position 4 was an improvement, as some type 3 DBLα domains (4/17 published sequences) have an A rather than a C here.

A reverse primer was designed to specifically amplify the $DBL\alpha_{type3}$ domains (primer: Type3alphaR1; CAGAAATATTCAG). This recognises a conserved section just before the end of the $DBL\alpha_{type3}$ domain, and results in a 420 bp PCR product (Fig. 5.8).

Both primer sequences recognised all published type 3 domains, and neither primer sequence showed homology to any genes other than type 3 *var* genes (NCBI Blast database search).

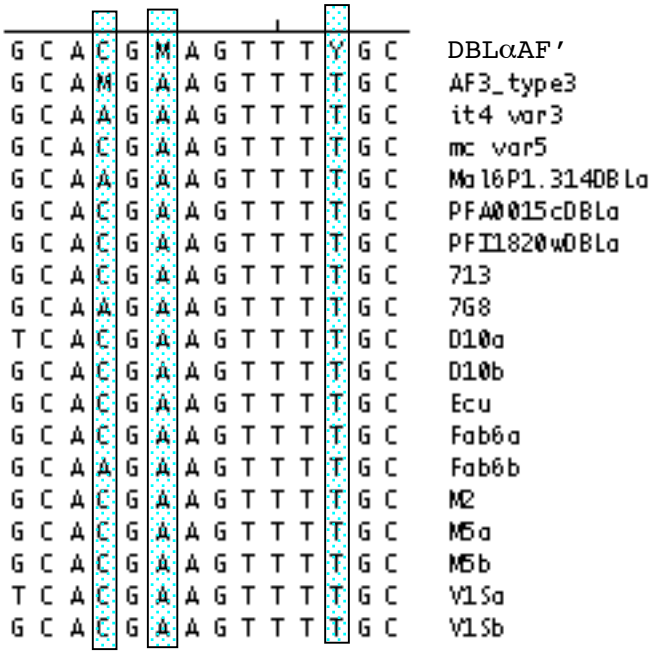

Fig. 5.7. Forward primers for amplification of type 3 DBLα domains. The forward primer GCAMGAAGTTTTGC (αAF3_type3) is a modification of the generic forward primer used for DBLα domain amplification in chapter 3 (DBLαAF' GCACGMAGTTTYGC Taylor *et al*. 2000a; Bull *et al*. 2005a) which is better suited to amplification of type 3 DBLα domains. Forward primers αAF3_type3 and DBLαAF' are shown with the primer binding sites from published type 3 DBLα domains from IT, MC, 3D7 and other *P. falciparum* isolates 713, 7G8, D10, Ecu, Fab6, M2, M5, V1S. Altered residues in αAF3_type3 compared to DBLαAF' are boxed.

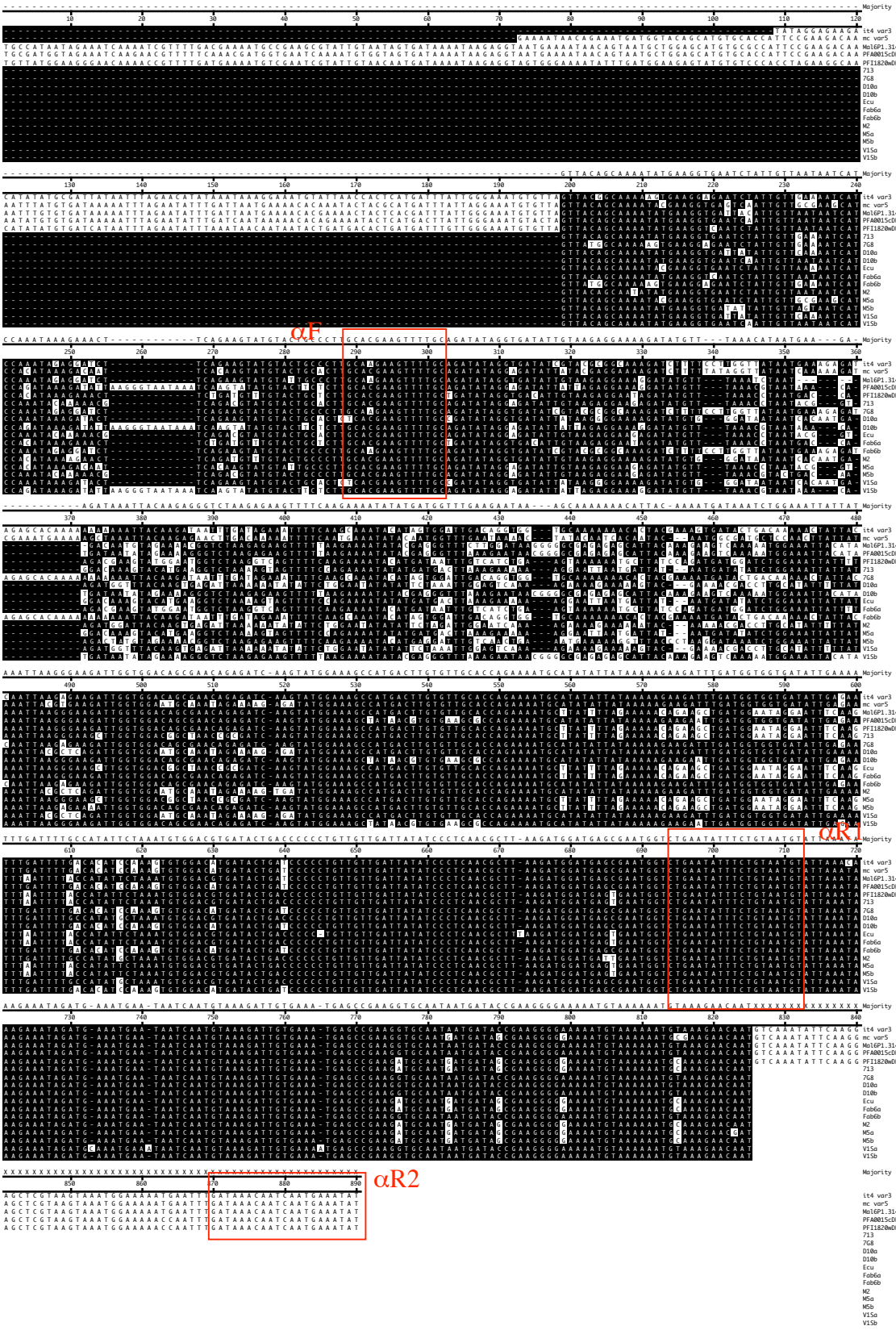
αF
αR1
αR2

Fig. 5.8. Alignment of published type 3 *var* genes from strains 3D7 (mal6p1.314, pfa0015c and pfi1820w), FCR3 (it4var3), Malayan Camp (mc var5), 713, 7G8, D10, Ecu, Fab6, M2, M5, V1S, showing primer sites for AF3_type3F (F), Type3alphaR1 (R1) and Type3alphaR2 (R2; (see section 5.5.3).

5.5.2 Testing primer pair AF3_type3F and Type3alphaR1 on 3D7 gDNA

The primer pair AF3_type3F and Type3alphaR1 were tested on 3D7 gDNA. Amplification resulted in a PCR product of the correct size for type 3 DBLα domain amplification with this primer pair (420 bp) (Fig. 5.9).

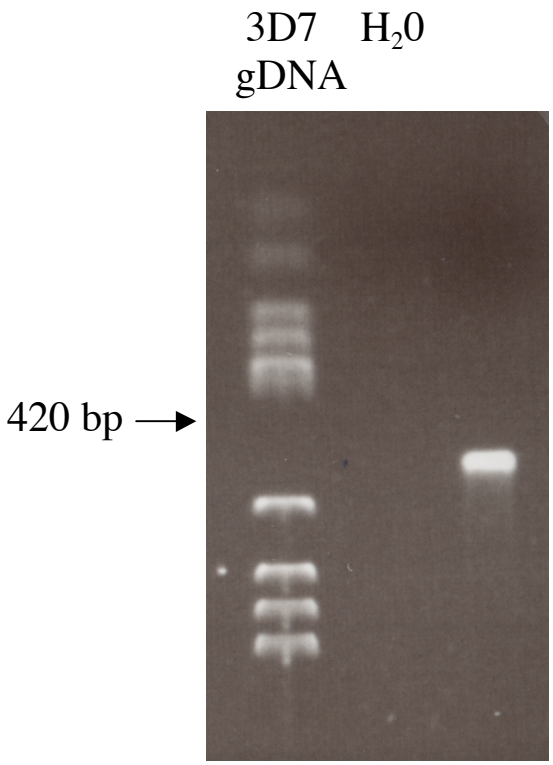

Fig. 5.9. Amplification of type 3 DBLα domains from 3D7 gDNA using primer pair AF3_type3F and Type3alphaR1. An aliquot (5 μl) of PCR product was run on a 1.5% agarose gel. Distilled water was used as a negative control for the PCR reaction. DNA ladder was ϕX174 RF DNA/*Hae* fragments (Invitrogen).

Products from the PCR of type 3 DBLα domains from 3D7 gDNA using primer pair AF3_type3F and Type3alphaR1 were purified and ligated into the TA cloning vector for transformation of *E. coli*, which were then grown overnight (details in chapter 2). 30 colonies were selected for overnight growth, and the plasmids extracted and an aliquot digested with *Eco*RI to verify an insert of the correct length was present (Fig. 5.10).

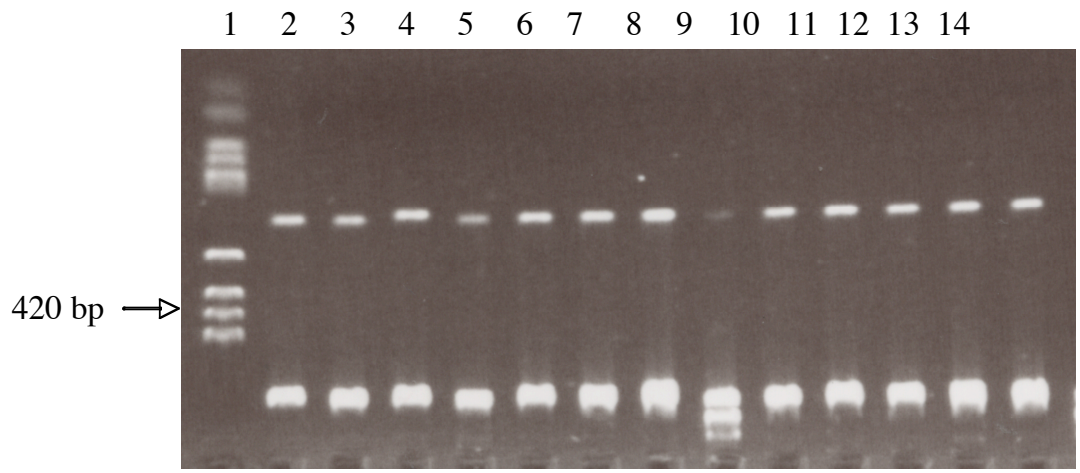

Fig. 5.10. 1.5% agarose gel of 5 μl of *Eco*RI digests products of plasmids extracted from a set of 14 minipreps from RT-PCR of 3D7 gDNA using primer pair AF3_type3F and Type3alphaR1. DNA ladder was ϕX174 RF DNA/*Hae* fragments (Invitrogen).

Plasmids containing an insert were sequenced to assess the frequency of the three 3D7 DBLα domain amplified by RT-PCR, which was expected to be approximately even. However, primer validation on 3D7 gDNA showed a bias in recognition of Pfi1820w and Pfa0015c DBLα domains compared to Mal6P1.314 (Fig. 5.11). This

bias was repeated with a further 21 colonies. This was surprising as the primer sites showed 100% identity to all 3D7 sequences, and products would be the same length.

The DBLα_{type3} domain from the single type 3 *var* gene from R29/IT strain laboratory isolate was also successfully amplified using the primer pair AF3_type3F and Type3alphaR1. No other genes, such as non-type 3 *var* genes were amplified with this primer pair.

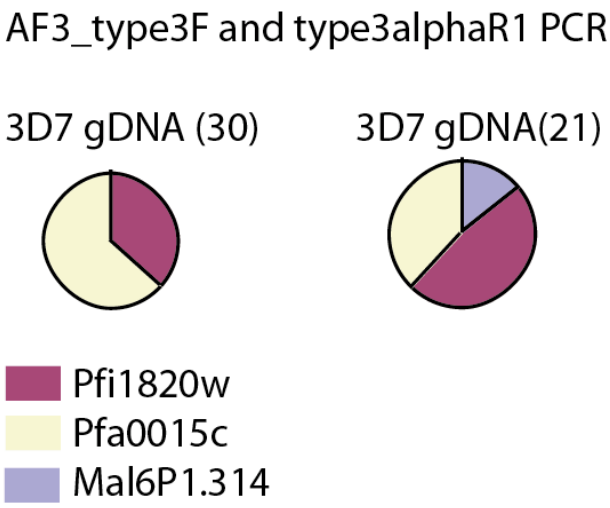

Fig. 5.11. Pie charts showing relative proportions of DBLα domains from the 3D7 type 3 *var* genes Pfi1820w, Pfa0015c and Mal6P1.314 after PCR on 3D7 genomic gDNA with primer pair AF3_type3F and Type3alphaR1.

5.5.3 Type 3 *var* gene DBLα domain amplification: DBLα primer design 2

A new reverse primer was designed to specifically amplify the $DBL\alpha_{type3}$ domains in order to achieve a more even amplification of the 3D7 type 3 DBLα domains. Primer Type3alphaR2 (ATATTTCATTGATTGTTTATC) recognises the end of the $DBL\alpha_{type3}$ domain, giving a 580 bp PCR product (Fig. 5.12). Type3alphaR2 recognises all published type 3 domains, and does not show homology to any genes other than type 3 *var* genes (NCBI Blast database search).

PCR products were obtained from PCR of 3D7 gDNA (Fig. 5.12A). These were purified, ligated and a random selection of 27 and 22 transformed plasmids sequenced as for the previous primer pair. Plasmids were digested by *Eco*RI to confirm presence of an insert prior to sequencing (Fig. 5.12B).

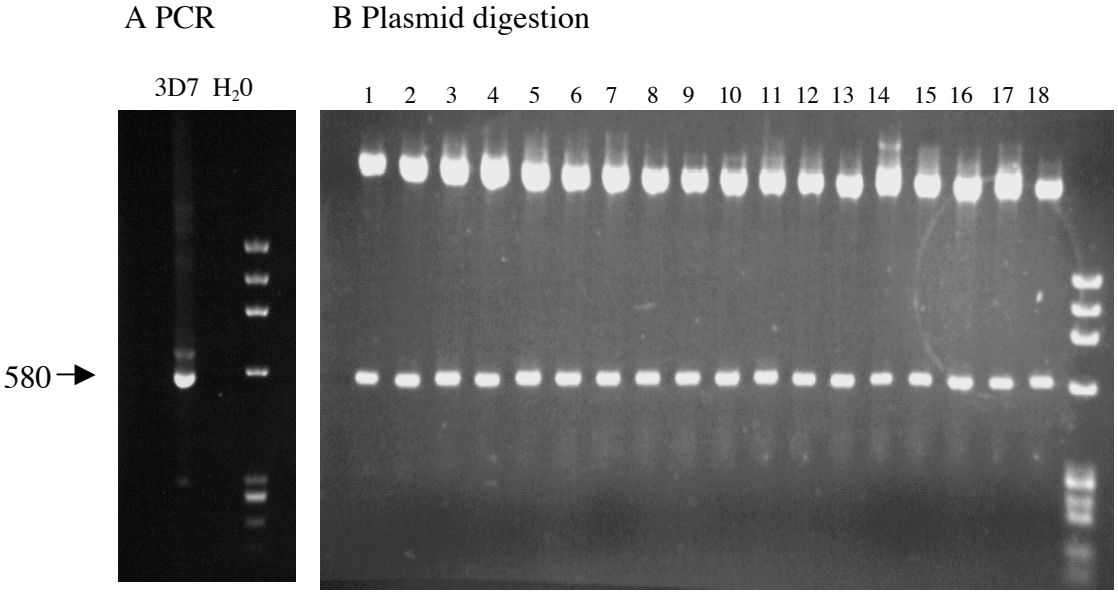

Fig. 5.12. Amplification of type 3 DBLα domains from 3D7 gDNA using primer pair AF3_type3F and Type3alphaR2. A) An aliquot (5 μl) of PCR product was run

on a 1.5% agarose gel. Distilled water was used as a negative control for the PCR reaction. DNA ladder was ϕX174 RF DNA/*Hae* fragments (Invitrogen). B) *Eco*RI digests products of plasmids extracted from a set of 18 minipreps from RT-PCR of 3D7 gDNA using primer pair AF3_type3F and Type3alphaR2. DNA ladder was ϕX174 RF DNA/*Hae* fragments (Invitrogen).

This pair was less biased on 3D7 gDNA, recognising all three domains in both sets of sequencing (Fig. 5.13). The primers were also used to amplify type 3 domains from NF54, and 18 plasmids were also sequenced from transformed *E. coli*. Mal6P1.314 was still amplified less frequently than the other 3D7 type 3 *var* genes, however the distribution of the three type 3 DBLα domains was not significantly different from expected in the two 3D7 amplifications or the NF54 amplification (Chi-squared P>0.3).

The DBLα_{type3} domain from the single type 3 *var* gene from R29/IT strain laboratory isolate was also successfully amplified with primer pair AF3_type3F and Type3alphaR2. No other genes, such as non-type 3 *var* genes were amplified from 3D7, NF54 or R29.

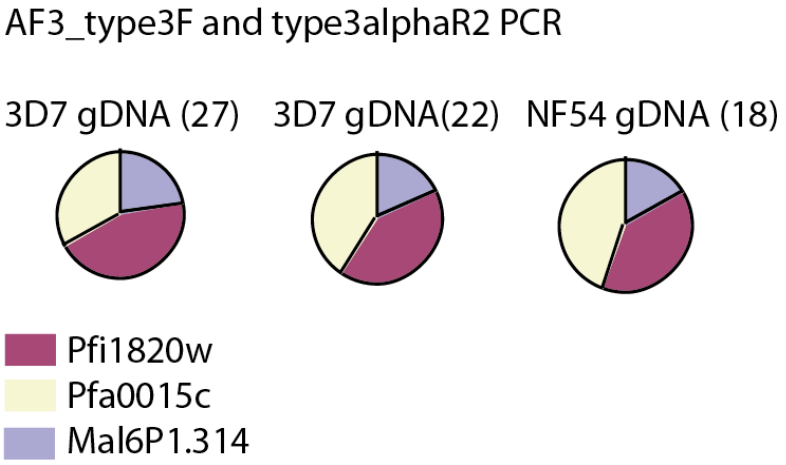

Fig. 5.13. Pie charts showing relative proportions of DBLα domains from the 3D7 type 3 *var* genes Pfi1820w, Pfa0015c and Mal6P1.314 after PCR on 3D7 genomic gDNA with primer pair AF3_type3F and Type3alphaR2.

5.5.4 Type 3 *var* gene DBLε domain amplification: DBLε primer design

A primer pair was also designed to amplify $DBL\varepsilon_{type3}$ domains, Type3epsF GACAATAATGGTGTGTTAGTTCCTC and type3epsR GTATGATGCAGC ACATTCCTCA (Fig. 5.14). These primers recognise the published type 3 epsilon domains and do not recognise any other genes (NCBI database homology search).

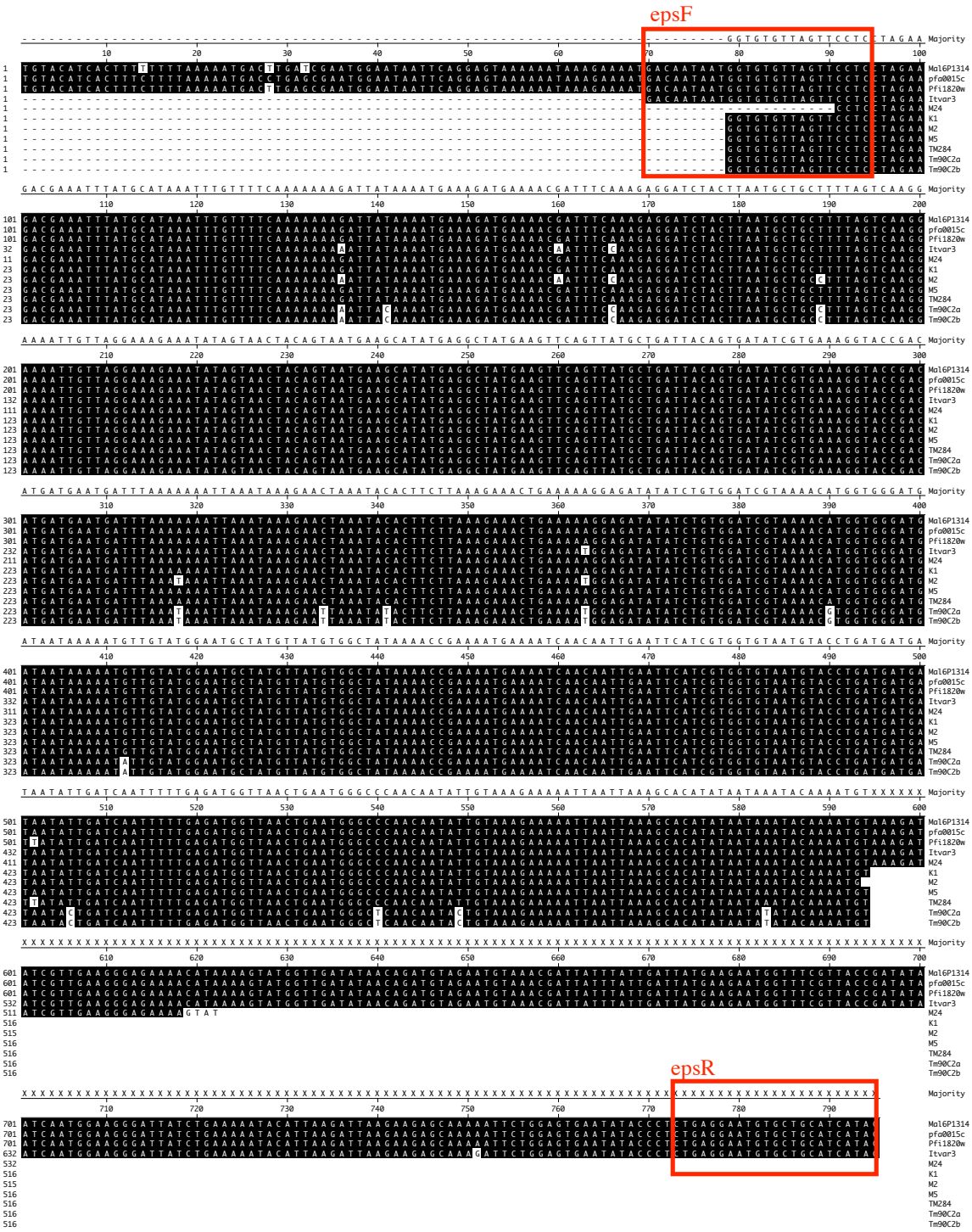

Fig. 5.14. Alignment of published type 3 *var* genes showing primer sites for Type3epsF and Type3epsR.

The primer pair Type3epsF and Type3epsR gave a PCR product of 726 bp when used with 3D7 gDNA (Fig. 5.15A). The PCR products were purified and ligated into the topo cloning vector for transformation of *E. coli*, which were grown overnight. 10 colonies were selected for overnight growth, and the plasmids extracted and an aliquot digested with *Eco*RI to verify an insert of the correct length was present (Fig. 5.15B). Type 3 epsilon domains contain an *Eco*RI site, the PCR product (726 bp) is seen as two smaller products (399 and 327 bp) after digestion (Fig. 5.15B).

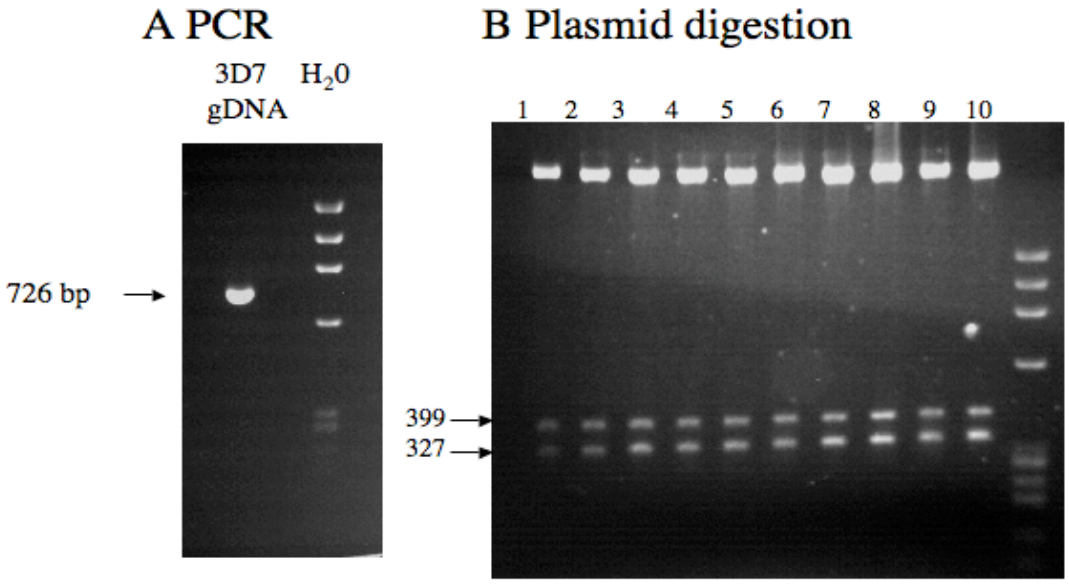

Fig. 5.15. Amplification of type 3 DBLα domains from 3D7 gDNA using primer pair Type3epsF, and Type3epsR. A) An aliquot (5 μl) of PCR product was run on a 1.5% agarose gel. Distilled water was used as a negative control for the PCR reaction. B) *Eco*RI digests products of plasmids extracted from a set of 10 minipreps from RT-PCR of 3D7 gDNA using primer pair Type3epsF and Type3epsR. DNA ladders were ϕX174 RF DNA/*Hae* fragments (Invitrogen).

Cloning and sequencing showed they specifically amplified the three DBLε domains from 3D7, and all three domains could be amplified (ratio 3,3,4, Fig. 5.16). This distribution of sequences was not significantly different from expected: $p > 0.99$, Chi-squared test. The $DBL\varepsilon_{type3}$ domain from the single type 3 *var* gene from R29/IT strain laboratory isolate was also successfully amplified using the epsilon primers Type3epsF and Type3epsR.

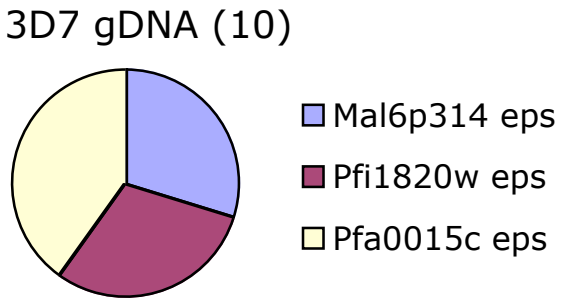

Fig. 5.16. Pie charts showing relative proportions of DBLε domains from the 3D7 type 3 *var* genes Pfi1820w, Pfa0015c and Mal6P1.314 after PCR on 3D7 genomic gDNA with primer pair Type3epsF and Type3epsR.

5.5.5 Type 3 *var* gene PCR from laboratory strains gDNA

Little data on the frequency of type 3 *var* gene occurring in *P. falciparum* genomes is available; at the time of the start of the study only 3D7 had been shown to contain a type 3 *var* gene, though subsequent sequencing has revealed a type 3 *var* gene in IT, but not in Dd2 or HB3. To assess the prevalence of type 3 *var* genes in strains other than 3D7, gDNA from 10 further strains was examined. Genomic DNA was

available from FCR3, TM267, TM284, Malayan Camp, Dd2, TM180, 7G8, Muz12 and HB3 (gift from JA Rowe/A Raza). Type 3 DBLα domains were amplified by primer pair AF3_type3F and Type3alphaR2. Type 3 DBLε domain was amplified by primer pair Type3epsF and Type3epsF. All PCR products were cloned and sequenced to verify type 3 domains had been amplified. Type 3 alpha and epsilon domains were amplified from 3D7, TM284, FCR3/IT, TM267 and Malayan Camp, but not from Dd2, HB3, TM180, 7G8 or Muz12 (Fig. 5.17 and Table 5.3). 7G8 gave a PCR product with the DBLα primer pair (AF3_type3F and Type3alphaR2), however, this was longer than expected for a type 3 *var* gene DBLα domain and sequencing proved that this was not a type 3 *var* gene DBLα domain. A summary of the type 3 domains detected in the laboratory isolates is given in Table 5.3.

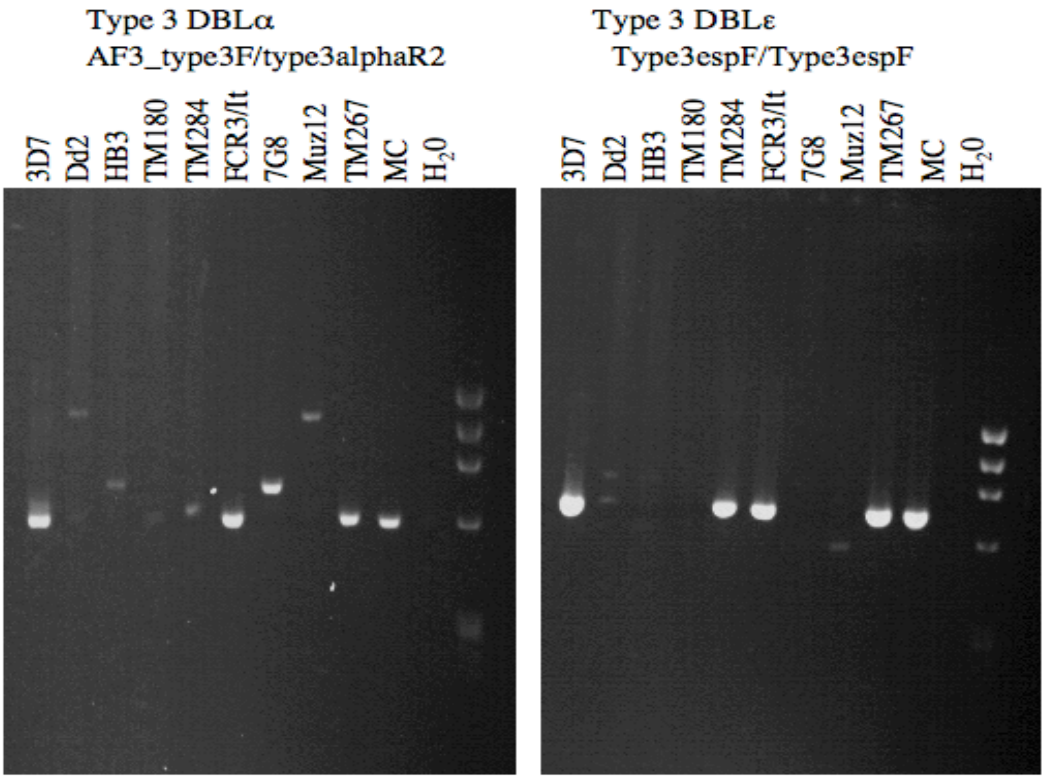

Fig. 5.17. PCR of type3 domains from lab strains 3D7, Dd2, HB3, TM180, TM284, FCR3/IT, 7G8, Muz12, TM267, Malayan Camp (MC). Left) Type 3 DBLα domains were amplified by primer pair AF3_type3F and Type3alphaR2. Right) Type 3 DBLε domain was amplified by primer pair Type3epsF and Type3epsF. A 5µl aliquot of all PCR products was run on 1.5% agarose gels. Distilled water was used as a negative control for the PCR reaction. The DNA ladder was ϕX174 RF DNA/*Hae* fragments (Invitrogen).

	Type 3 DBLα domain	Type 3 DBLε domain
	AF3_type3F Type3alphaR2	Type3epsF Type3epsR
3D7	✓	✓
FCR3/IT	✓	✓
TM267	✓	✓
TM284	✓	✓
Malayan Camp	✓	✓
Dd2	✗	✗
TM180	✗	✗
7G8	✗	✗
Muz12	✗	✗
HB3	✗	✗

Table 5.3. PCR for type 3 DBLα and DBLε domains was carried out on laboratory strains 3D7, FCR3/IT, TM267, TM284, Malayan Camp, Dd2, TM180, 7G8, Muz12 and HB3. Tick (✓) indicates a PCR product was obtained, and the sequence was confirmed as a type 3 domain. Cross (✗) indicates no type 3 PCR product was obtained, or was not the correct domain (7G8 DBLα).

Therefore 4/9 genetically distinct laboratory strains have a single detectable type 3 *var* gene (5/10 tested laboratory strains, but TM267 is isogenic with FCR3/IT). The three type 3 *var* genes from 3D7 and the one type 3 *var* gene from FCR3/IT/TM267 have been published and discussed previously, and the sequences amplified here match these sequences perfectly. The TM284 DBLα domain had not previously been published. The type 3 DBLεdomain amplified from TM284 is identical to the TM284 type 3 DBLε domain sequence submitted by Trimnell *et al.* (2006) over the length of the previously submitted sequence, but the sequence is longer as the PCR primers used in this chapter are further apart than those used by Trimnell *et al.*

(2006). The type 3 *var* gene from Malayan Camp had also not previously been published.

Type 3 *var* gene domains were not found in Dd2 by PCR using these conditions. Though Trimnell *et al*. found a type 3 *var* gene in Dd2 (epsilon domain only), subsequent publishing of the Dd2 genome sequence suggests Dd2 does not contain a type 3 *var* gene. The epsilon domain published as from Dd2 does not correspond with any contigs from the Dd2 genome published so far by the Broad Institute Sequencing Program. Trimnell *et al*. also found an epsilon domain, but not alpha domain, in TM180. Neither was found in my experiments by PCR. The negative PCR result for type 3 *var* gene domains in HB3 here are in agreement with those of Trimnell *et al*. and the Broad Institute Sequencing Program,

A type 3 *var* gene DBLα domain from 7G8 has been published by Trimnell *et al.* (2006), accession number DQ408045. A PCR product was detected from amplification of 7G8 gDNA with primers AF3_type3F and Type3alphaR2 but agarose gel electrophoresis (Fig. 5.17) suggested this was too long to be a type 3 DBLα domain and sequencing proved this PCR product was not a type 3 *var* gene, and was an epsilon domain with 57% identity to the published 7G8 type 3 DBLα domain. No PCR product was obtained from 7G8 gDNA with the epsilon primer pair Type3epsF/Type3epsR. Amplification of the DBLα domain was also attempted with the other primer pair AF3_type3F/Type3alphaR1, but no PCR product was obtained. These PCR suggest 7G8 does not have a type 3 *var* gene. The 7G8 sequence

published in Trimnell *et al* 2006 is identical to that of another *P. falciparum* strain examined in that paper, Fab6.

5.5.6 Type 3 *var* gene transcription: laboratory strains

Little data is currently available on the transcription of type 3 *var* genes in laboratory strains or field isolates. The aim of this section was to assess the frequency of type 3 *var* gene transcription in the laboratory strains available, and investigate any association with rosetting and IgM binding. In addition, it was necessary to identify a laboratory strain which was transcribing a type 3 *var* gene in order to investigate the timing of type 3 *var* gene transcription more precisely.

Early pigmented trophozoite culture cDNA from 7 laboratory strains (3D7, Palo Alto, TM267, A1R, A4R, R29 and TM284) was available for RT-PCR (gift from JA Rowe/A Raza). For 5 of the above strains (Palo Alto, TM267, A1R, A4R and R29), cDNA was also available from cultures that had been selected for high rosette frequency (> 70% RF). 3D7 could not be selected for high rosetting, but cDNA was available from parasites selected for IgM binding (Gift from JP Semblat). The transcription patterns of the above strains are presented below in sections 5.5.5a-d and summarised in section 5.5.5e.

5.5.6a Type 3 *var* gene transcripts are present in rosetting and non-rosetting TM267

RT-PCR amplified DBLα and DBLε domain transcripts from rosetting (R+) and non-rosetting (R-) TM267 (Fig. 5.18). This suggests type 3 *var* gene transcription does not influence rosetting in TM267.

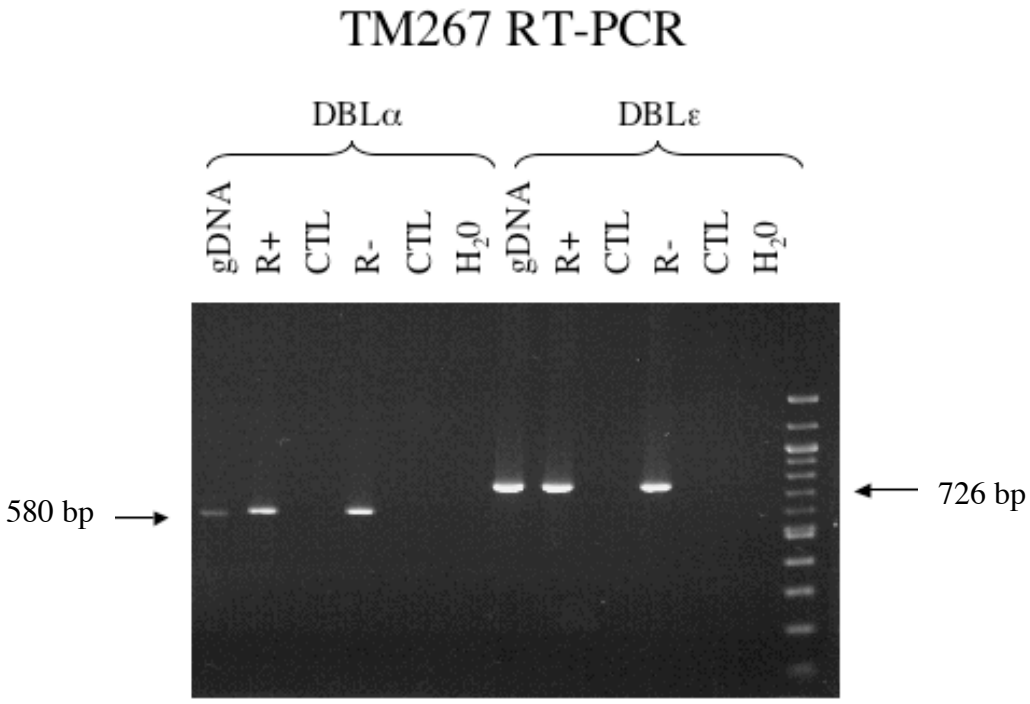

Fig. 5.18. Type 3 transcripts are present in rosetting and non-rosetting TM267 by RT-PCR. Type 3 DBLα domain transcripts were amplified by primer pair AF3_type3F and Type3alphaR2. Type 3 DBLε domain transcripts were amplified by primer pair Type3epsF and Type3epsF. PCR show gDNA, rosetting (R+) and non-rosetting (R-) cDNA, and distilled water as a negative control. A 5 μl aliquot of all RT-PCR products was run on a 1.5% agarose gel. CTL lanes (without reverse transcriptase, to control for gDNA contamination) were negative, indicating there was no gDNA contamination. DNA ladder was 100 bp ladder.

5.5.6b Type 3 *var* gene transcripts are present in rosetting and non-rosetting Palo Alto

The Palo Alto DBLε_{type3} domain was detected by RT-PCR from this cDNA but the DBLα_{type3} domain could not be amplified with the primer pair AF3_type3F and Type3alphaR2 (Fig. 5.19A). The DBLα primers recognise perfectly the Palo Alto DBLα_{type3} domain, and amplification of gDNA from the same Palo Alto culture shows that the alpha domain primers can still bind in this strain. To resolve this, amplification was carried out using the forward primer alpha primer and reverse epsilon primer, to span both the alpha and epsilon domain (1672 bp). This amplification gave PCR product in Palo Alto gDNA and cDNA (R+ and R-). Sequencing of these PCR/RT-PCR products gave the Palo Alto type 3 DBLα and DBLε domains separated by the published Palo Alto type 3 interdomain region (Broad Institute), confirming both DBL domains were linked as expected and were transcribed (Fig. 5.19B).

The RT-PCR amplification of the type 3 *var* gene in rosetting and non-rosetting Palo Alto suggests that type 3 *var* gene transcription does not influence rosetting in Palo Alto, as was seen with TM267. Palo Alto and TM267 are both clones of IT and are thus genetically identical. In addition, Palo Alto and TM267 express the same predominant *var* gene, and are thus essentially identical strains (JA Rowe, unpublished data). The detection of type 3 *var* gene transcripts in these two clones of IT, is consistent with these two strains being transcriptionally very similar.

Palo Alto RT-PCR

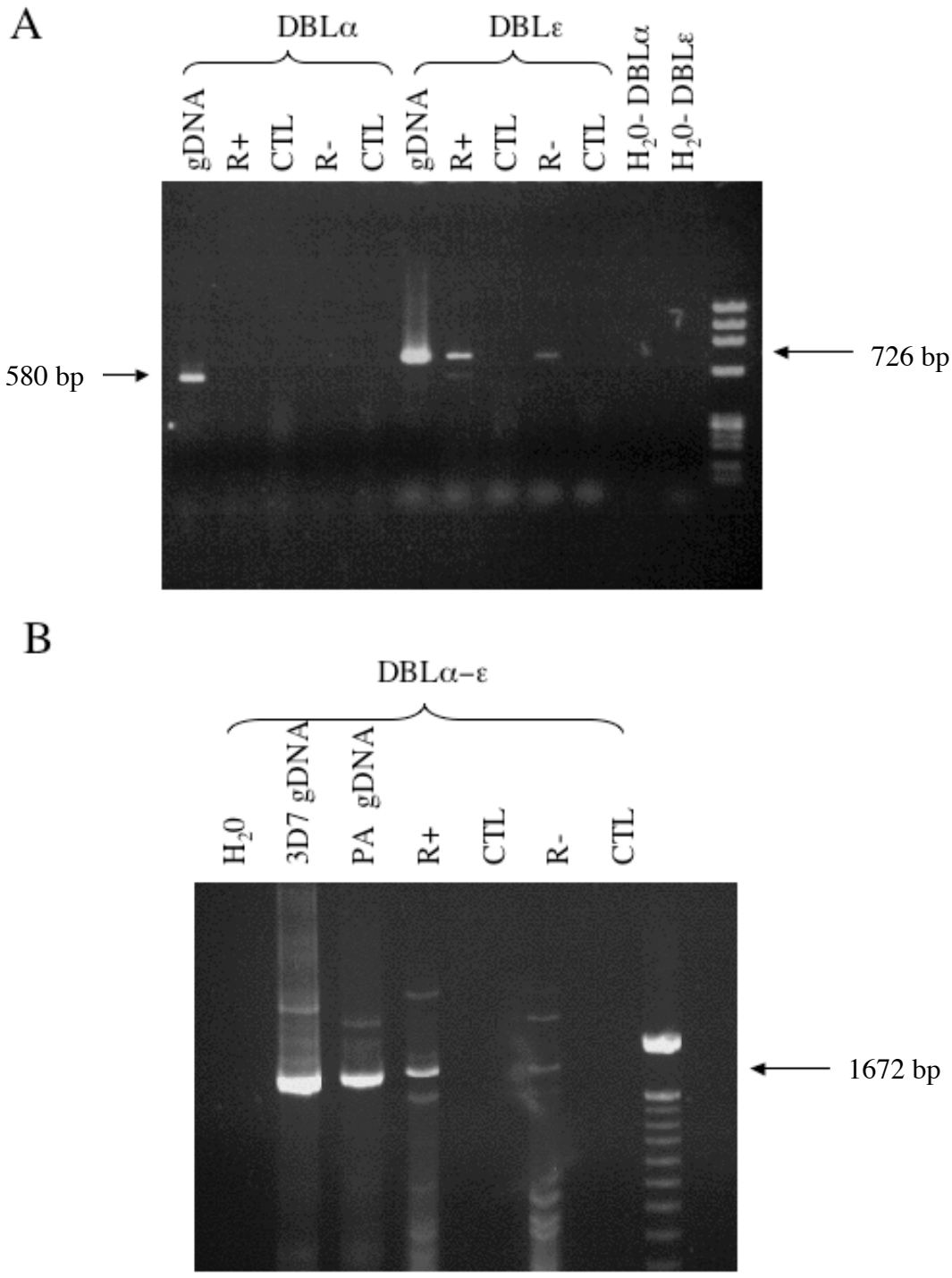

Fig. 5.19. Type 3 transcripts are present in rosetting and non-rosetting Palo Alto by RT-PCR. A) Type 3 DBLα/ε domain amplification from Palo Alto gDNA, and

cDNA from rosetting (R+) and non-rosetting (R-) Palo Alto using primer pair AF3_type3F and Type3alphaR2, or Type3epsF/R. B) Type 3 DBLα–ε domain transcripts were amplified from Palo Alto gDNA, and cDNA from rosetting (R+) and non-rosetting (R-) Palo Alto using primer pair AF3_type3F and Type3epsR. Distilled water was used as a negative control. A 5 μl aliquot of all RT-PCR products was run on a 1.5% agarose gel. CTL lanes (without reverse transcriptase, to control for gDNA contamination) were clean, indicating there was no gDNA contamination. DNA ladder was ϕX174 RF DNA/*Hae* fragments (Invitrogen).

5.5.6c Type 3 *var* gene transcripts are not present in rosetting or non-rosetting strains of A1R, A4R, R29 or in TM284

Type 3 *var* gene transcripts were not detected in either in the rosetting or non-rosetting subpopulations of the remaining 3 laboratory strains tested (R29, A1R, A4R; all IT-derived clones). Genomic DNA controls were positive for PCR product in all cases indicating PCR was successful. A representative gel is given in Fig. 5.20 for R29. The cDNA was a gift from JA Rowe/A Raza and had been used successfully for non-type 3 *var* gene RT-PCR (data not shown).

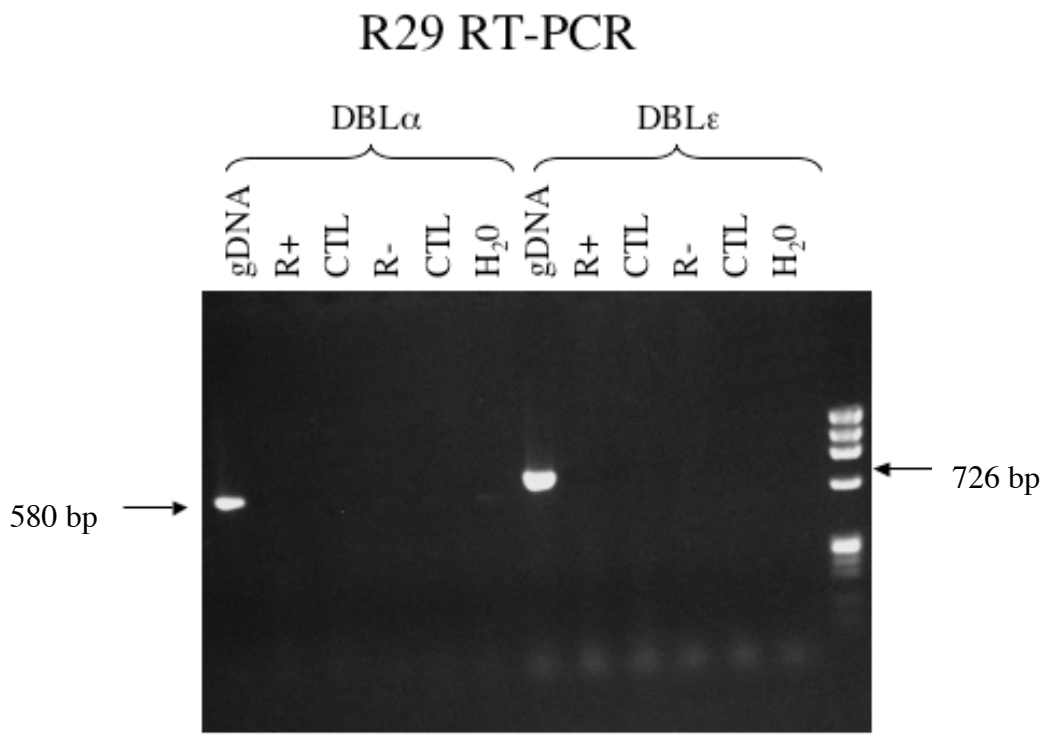

Fig. 5.20. Type 3 transcripts are not present in rosetting or non-rosetting R29. No type 3 DBLα/ε domain transcripts were amplified using primer pair AF3_type3F and Type3alphaR2 or Type3epsF and Type3epsF. Templates used were R29 gDNA, and cDNA from rosetting (R+) and non-rosetting (R-) R29, each with control (CTL) for gDNA contamination. A 5 μl sample of all RT-PCR products was run on a 1.5% agarose gel. Genomic DNA controls were positive for PCR product in all cases indicating PCR was successful. No cDNA lanes were positive indicating type 3 *var* genes were not being transcribed. DNA ladder was ϕX174 RF DNA/*Hae* fragments (Invitrogen).

5.5.6d Type 3 *var* gene transcripts are present in IgM-binding and non-IgM binding 3D7

RT-PCR amplified DBLα domain transcripts from IgM-bnding and non-IgM binding 3D7; RT-PCR reaction was carried out by JP Semblat (Fig. 5.21).

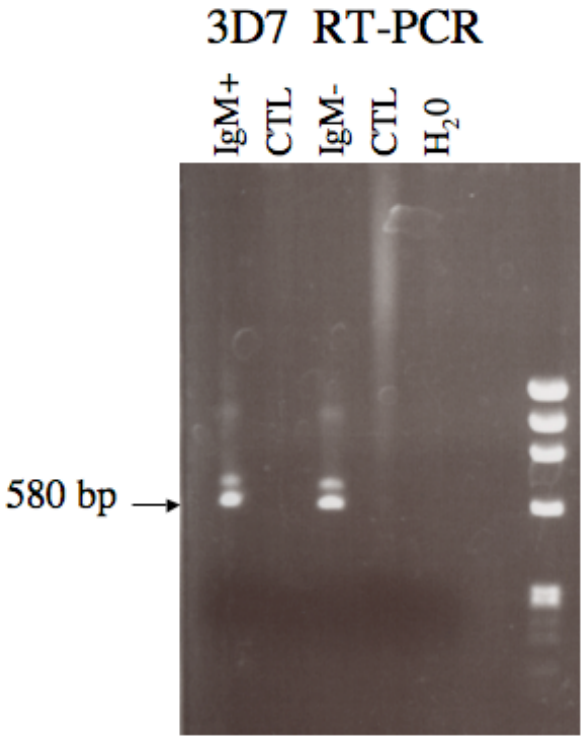

Fig. 5.21. Type 3 transcripts are present in IgM-bnding and non-IgM binding 3D7 by RT-PCR. Type 3 DBLα domain transcripts were amplified by primer pair AF3_type3F and Type3alphaR2 by JP Semblat. A 5µl aliquot of all RT-PCR products was run on 1.5% agarose gels. Distilled water was used as a negative control for the PCR reaction. DNA ladder was ϕX174 RF DNA/*Hae* fragments (Invitrogen).

RT-PCR products (gift from JP Semblat) were purified, ligated and cloned, and 15 or 16 miniprep plasmid extracts were sequenced. All three versions of the type 3 *var*

gene (pfa0015c, Pfi1820w and Mal6p1.314) DBLα_{type3} and DBLε_{type3} domains were amplified by RT-PCR from the 3D7 cDNA. There was a slight bias towards Pfi1820w, and away from Pfa0015c in the unselected parasites but this change in distribution was not significant (Chi-squared test, P=0.93, Fig. 5.22).

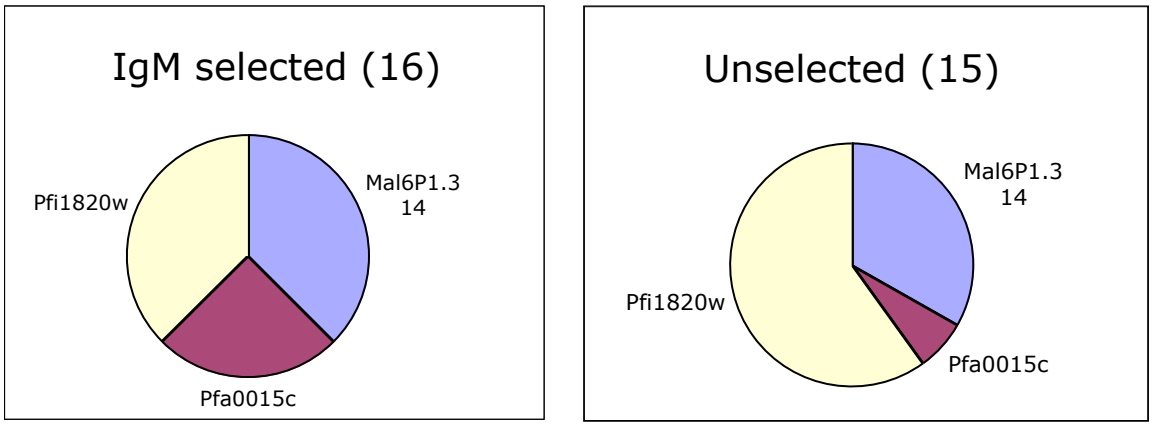

Fig. 5.22. Type 3 transcripts are present in IgM-bnding and non-IgM binding 3D7 by RT-PCR. Type 3 DBLα domain transcripts were amplified by primer pair AF3_type3F and Type3alphaR2. Pie charts represent distribution of the three 3D7 type 3 DBLα domain transcripts in IgM-binding and non-IgM binding strains from 16/15 purified plasmid extracts.

5.5.6e Type 3 *var* gene transcription in laboratory strains: summary

These results, summarised in Table 5.4, demonstrate that some but not all strains express a type 3 *var* gene, and that this expression is not associated with IgM binding in 3D7 or rosetting in TM267, Palo Alto, A1R, A4R or R29. RT-PCR results were the same in rosetting as for the non-rosetting isogenic strains. Amplification across the whole alpha and epsilon domains together using the forward alpha primer and reverse epsilon primer gave PCR product in the cDNA from rosetting Palo Alto.

Detection of type 3 *var* gene transcripts in Palo Alto and TM267, but not in other IT-derived clones (R29, A1R and A4R), suggests that type 3 *var* genes can be switched on and off in genetically identical parasites, and are thus not constitutively on as the lack of an intronic promoter suggested.

Non-rosetting/ Non-IgM binding	RT-PCR	
	$DBL\alpha_{type3}$	$DBL\varepsilon_{type3}$
3D7(IgM-)	✓	✓
Palo Alto^{IT} (R-)	✓	✓
TM267^{IT}(R-)	✓	✓
A1R^{IT}(R-)	×	×
A4R^{IT}(R-)	×	×
R29^{IT}(R-)	×	×
TM284	×	×

Rosetting/ IgM-binding	RT-PCR	
	$DBL\alpha_{type3}$	$DBL\varepsilon_{type3}$
3D7(IgM+)	✓	
Palo Alto^{IT} (R+)	✓	✓
TM267^{IT} (R+)	✓	✓
A1R^{IT} (R+)	×	×
A4R^{IT} (R+)	×	×
R29(R+)	×	×

Table 5.4. Summary of type 3 RT-PCR results for 7 laboratory *P. falciparum* strains, including rosetting (R+) and non-rosetting (R-) subpopulations of Palo Alto, TM267, A1R, A4R, R29 and IgM binding (IgM+) and non-binding (IgM-) subpopulations of 3D7. Palo Alto, TM267, A1R, A4R, R29 are all IT-derived clones as indicated. In addition, rosetting Palo Alto and TM267 also express the same predominant non-type 3 *var* gene, PARvar1 (JA Rowe, unpublished data).

5.5.7 Type 3 *var* gene transcription time course in laboratory strain 3D7

The 3D7 laboratory strain consistently expressed type 3 *var* genes in the above RT-PCR experiments. Thus, 3D7 was used for investigation of the timing of transcription of the type 3 *var* genes. Little data is currently available on timing of

transcription of type 3 *var* genes, apart from a report of type 3 *var* gene transcripts at "ring; 30 hr post invasion" and "trophozoite/schizont; 36-48 post invasion" 3D7 (Jensen *et al*. 2004), though relative levels of transcription were not measured. To examine the timing of transcription of the type 3 *var* genes, 3D7 parasite schizonts were purified using a percoll, and were incubated with fresh erythrocytes for 6 hours for invasion. After 6 hours, the remaining schizonts were destroyed by sorbitol lysis. RNA was collected from early rings, late rings, trophozoites, schizonts and gametocytes from a culture of laboratory strain 3D7 (Fig. 5.23). RT-PCR using the type 3 DBLα primers AF3_type3F and Type3alphaR2, and DBLε primers Type3epsF and Type3epsF, indicated that type 3 *var* gene transcripts were present at all asexual cell stages, but were not present in gametocyte RNA (Fig. 5.24). Non-type 3 DBLα domains were amplified with the DBLαAF'/DBLαBR primers from Taylor *et al*. discussed in chapter 3. All 3D7 cultures showed expression of non-type 3 *var* genes. Tubulin transcripts were present in all samples demonstrating that the cDNA preparation was successful.

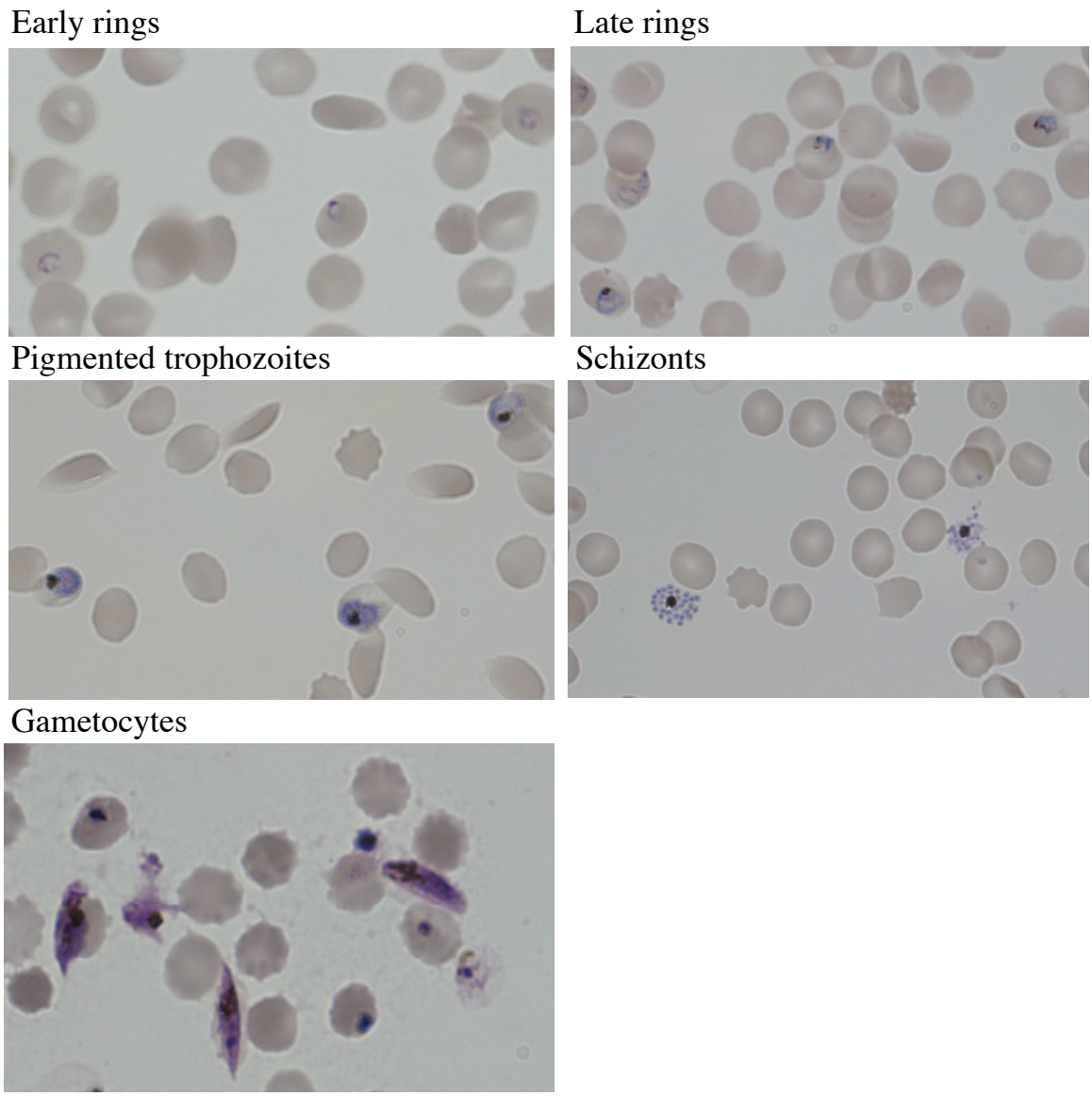

Fig. 5.23 Synchronised 3D7 culture, showing early rings (0-6 hr post-invasion), late rings (12-18 hr), pigmented trophozoites (24-30 hr), schizonts (36-42 hr) and gametocytes (stage II-IV). Parasites were stained with Geimsa. Images taken at 100x magnification.

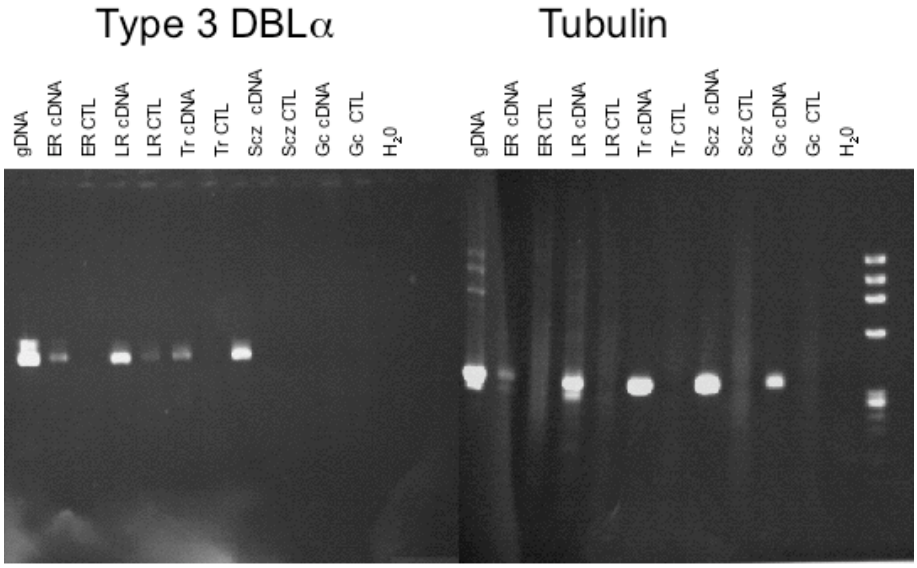

Fig. 5.24. RT-PCR analysis for synchronised 3D7 strain parasites for type 3 DBLα (left) and tubulin (right) was used for amplification for early rings (ER), late rings (LR), trophozoite (Tr), schizonts (Scz), gametocytes (Gc). CTL (control); no reverse transcriptase was used, providing a control for gDNA contamination. Amplifications for type 3 DBLα domains (primers AF3_type3F and Type3alphaR2) and tubulin (primers tubulin 3' and tubulin 5') are shown. A 5 μl sample of all RT-PCR products was run on a 1.5% agarose gel, and products were visualised under UV after staining in 0.5 μg/ml EtBr. Genomic DNA controls were positive for PCR product in all cases indicating PCR was successful. All asexual stages, but not gametocytes, were positive for type 3 DBLα domain RT-PCR (left). All cDNA lanes were positive for tubulin RT-PCR (right). DNA ladder was ϕX174 RF DNA/*Hae* fragments (Invitrogen).

5.5.8 48 hour type 3 *var* gene transcription time course in laboratory strain 3D7

For a more precise analysis of timing of expression, laboratory strain 3D7 parasites were tightly synchronised by purifying schizonts with percoll, and allowing only 1 hour for invasion of rings, before remaining schizonts were removed by sorbitol lysis. Parasite samples were taken regularly for RNA extraction and cDNA preparation until the first new rings were seen 42-43 hours post-invasion (Fig. 5.25).

RT-PCR analysis showed type 3 *var* gene transcripts were present across all time points (Fig. 5.26A). This transcription pattern was different from that observed for the non-type 3 DBLα domains, transcription of which was more easily detectable in rings than pigmented trophozoites. The strongest RT-PCR product for the non-type 3 DBLα domains was seen at late ring/early trophozoite stage (Fig. 5.26B). RT-PCR for tubulin (Fig. 5.26C) confirmed cDNA had been made successfully for each RNA extraction and tubulin transcription increased with maturity of the parasites. Unfortunately, despite repeated treatment with DNase, and repeated RNA collection and extraction, genomic DNA contamination remained a problem in these cDNA preparations (bands in RT-control lanes, Fig, 5.26 right panels). To resolve this issue, a fresh time course was undertaken from the same frozen parasite aliquots for Northern blot analysis.

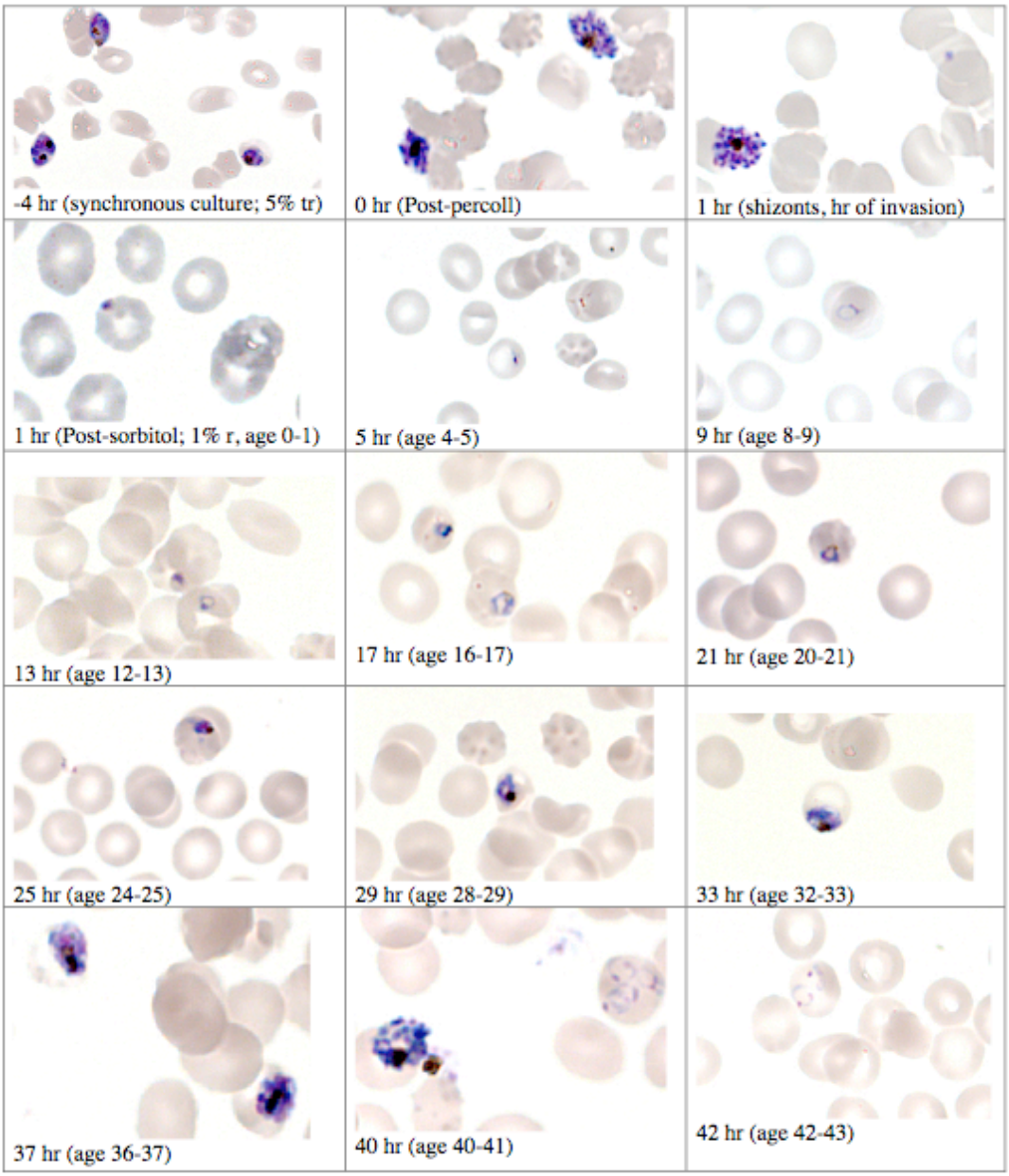

Fig. 5.25. Synchronised 3D7 culture for RT-PCR time course. Images taken 4 hr before percoll treatment (-4 hr), after percoll treatment (0 hr), after 1hr of invasion, and after a further 1, 5, 9, 13, 17, 21, 25, 29, 33, 37, 40 and 42 hr after sorbitol treatment. Parasites were stained with Giemsa and images were taken at 100x magnification.

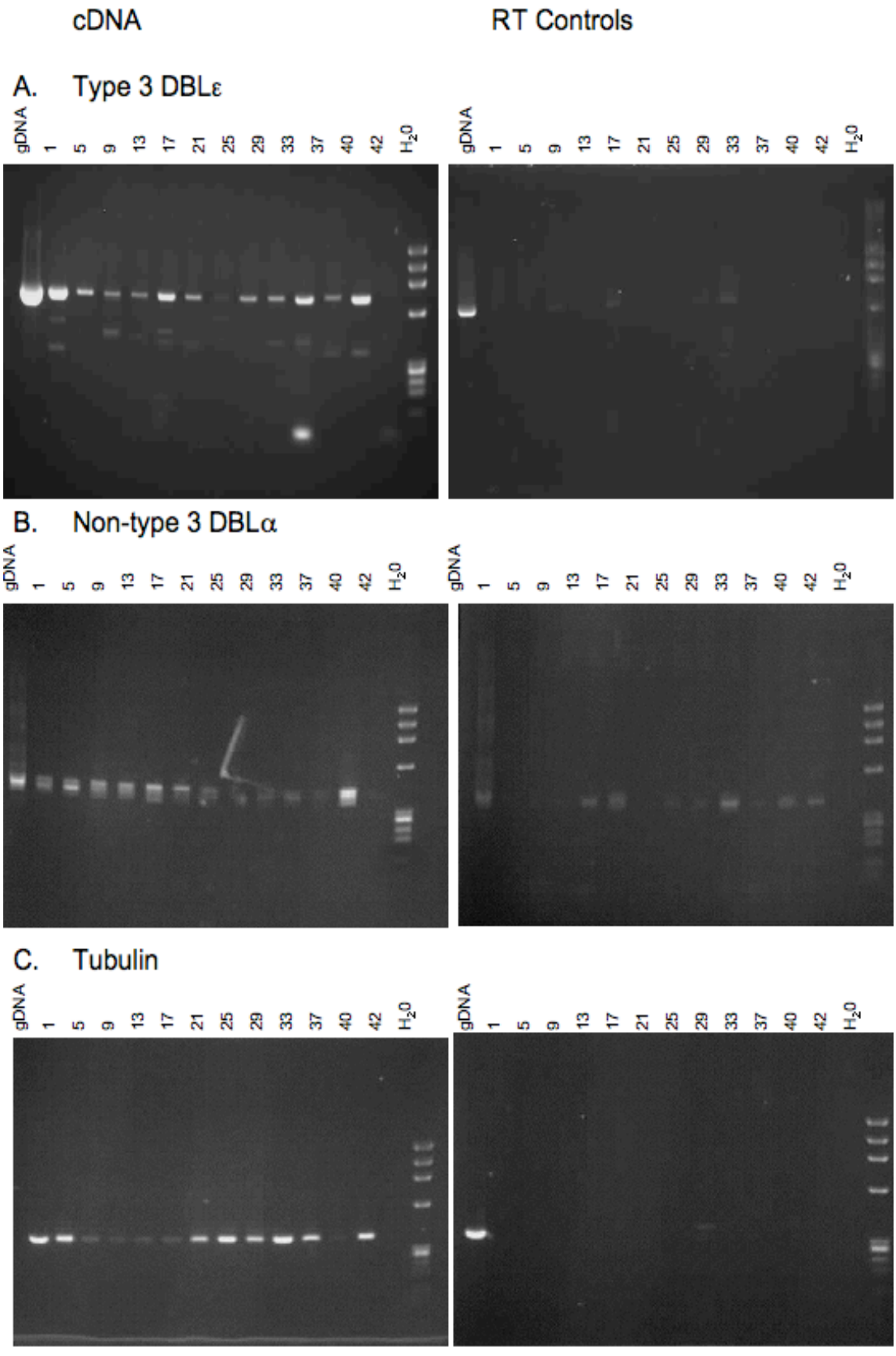
cDNA
RT Controls
A. Type 3 DBLε
B. Non-type 3 DBLα
C. Tubulin
gDNA
1
5
9
13
17
21
25
29
33
37
40
42
H2O

Fig. 5.26. RT-PCR analysis for synchronised 3D7 strain parasite time course. cDNA (left panels) or RT control samples (right panels) were used for amplification. Time points were 1, 5, 9, 13, 17, 21, 25, 29, 33, 37, 40 and 42 hr post invasion. 3D7 gDNA was used as a positive control and distilled water as a negative control. A) Type 3 DBLε *var* gene transcription: RT-PCR with primers Type3epsF and Type3epsF. B) Non-type 3 DBLα *var* transcription: RT-PCR with primers DBLαAF'/DBLαBR primers (Taylor *et al*. 2000a; Bull *et al*. 2005a). C). Tubulin transcription RT-PCR with primers Tub3' and Tub5'. DNA ladder was ϕX174 RF DNA/*Hae* fragments (Invitrogen).

5.5.9 Northern blot analysis: probe design

Probes were designed to recognise type 3 DBLα domain, type 3 DBLε domain, exon 2 and MSP1. Both type 3 domain probes were designed against pfa0015c. The type 3 DBLα domain probe spans only the type 3-specific section of the type 3 DBLα domain (Fig. 5.27). The type 3 DBLε domain probe covers the whole of the type 3 DBLε domain, and the PCR primers Type3epsF/R (section 5.5.3) were used. The exon 2 probe spans the first 310 nucleotides of the exon 2 of pfa0005w, and has 60.8-100% homology to the exon 2 of 3D7 *var* genes (mean homology 70.5%, S.D. 10.4%). The MSP probe spans 553 bp of the *P. falciparum* 3D7 MSP1.

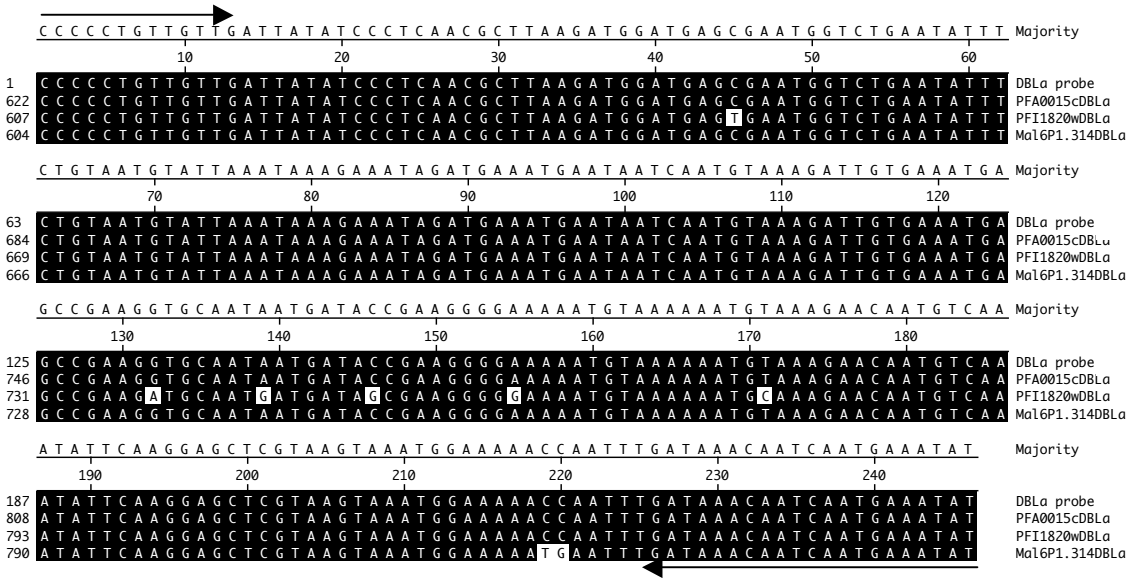

Fig. 5.27. Clustal W nucleotide sequence alignment of the DBLα probe sequence (identical to pfa0015c) with the homologous stretch of the three type 3 DBLα domains from 3D7. Primers type3probeF (forwards arrow) and Type3alphaR2 (backwards arrow) are indicated. Shading indicates nucleotides identical to the probe sequence.

PCR products were purified with a spin column and ligated into a PCR II vector. The vector was used to transform *E. coli*, and after overnight growth and plasmid extraction, the insert was sequenced to verify the sequence before probe production. The insert was then amplified using the specific forward primer and M13R/M13F primer sites within the vector to assess the direction of the insert (Fig. 5.28). All inserts were amplified with M13R (Fig. 5.29), and therefore SP6 polymerase was used for the reverse transcription reaction. SP6 polymerase was used to create a single stranded RNA complementary to the coding sequence for each insert.

Digoxigenin (DIG) label was attached to the uracil (dUTP) in the dNTP mix, and was thus incorporated into the RNA probe. This allows the probe to be detected using an antibody with affinity for the DIG label, overcoming the need for radioactivity (Fig. 5.28).

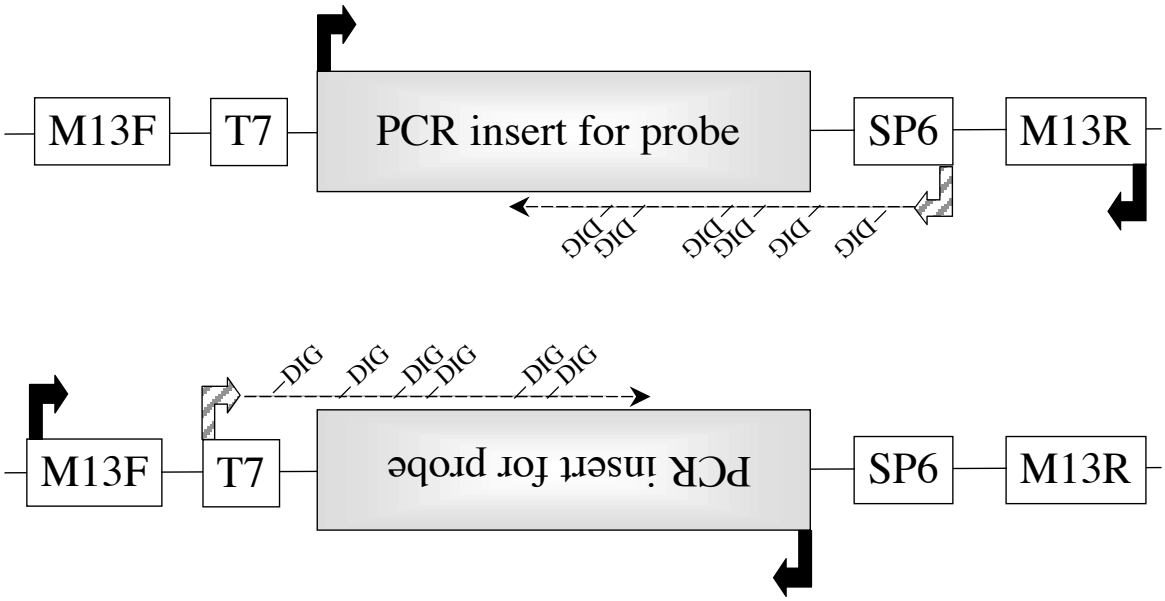

Fig. 5.28. Schematic of amplification for probe reverse transcription. PCR amplification using the specific forward primer and M13R/M13F primer sites within the vector was used to assess the direction of the insert. If the PCR with M13R is successful (upper panel), the insert is forwards, and thus the SP6 promoter is required for reverse transcription of the complementary strand with respect to the coding sequence for the probe. If the PCR with M13F is successful (lower panel), reverse transcription requires the T7 promoter. Digoxigenin (DIG) is incorporated into the probe during polymerisation.

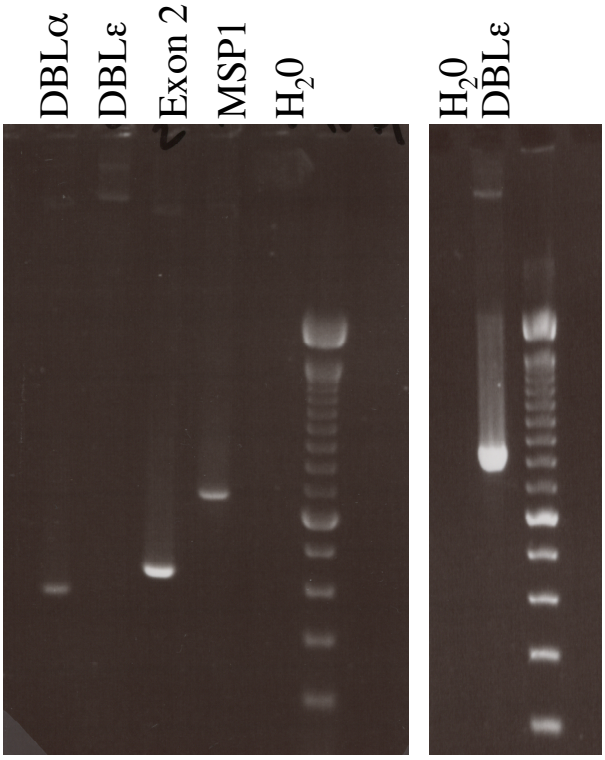

Fig. 5.29. PCR amplification using the specific forward primer and M13R was successful for all ligated vectors. Forward primers used were DBLα: type3probeF, DBLε: Type3epsF, exon2: exon2F, MSP1: N2, water control lane: N2. DBLε PCR was unsucssessful for the first ligation (left hand panel), and so the ligation was repeated (right hand panel).

DIG-labelled probes for DBLα, DBLε, Exon2 and MSP1 were diluted to 1:40, 1:400, 1:4000 and 1:40,000, along with a 1:10 dilution series DIG-labelled control probe for actin (starting concentration 10 ng/μl). 1 μl of each diluted probe was spotted onto nylon membrane, and fixed with UV. The membrane was washed briefly in Maleic acid buffer and blocked (1hr) before incubation with anti-DIG antibody (CDP-Star, Roche), to visualise the probe spots (Fig. 5.30).

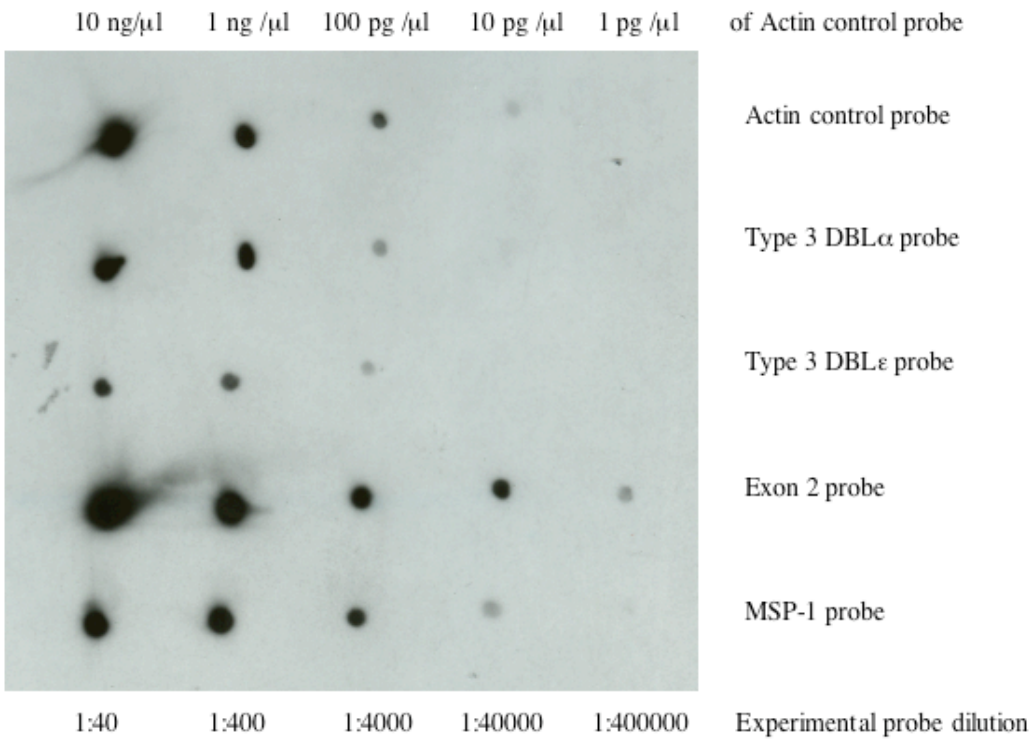

Fig. 5.30. DIG-labelled probes for DBLα, DBLε, Exon2 and MSP1 were diluted to 1:40, 1:400, 1:4000, 1:40,000 and 1:400,000, along with a 1:10 dilution series of a DIG-labelled control probe for actin (start concentration 10 ng/µl). 1 µl of each diluted probe was spotted onto nylon membrane, and fixed with UV. Probes were then incubated with anti-DIG antibody (CDP-Star), and probe spots visualised after exposure to X-ray film.

Comparisons to the actin probe of known concentration allowed estimation of the concentrations of the new probes. Estimated probe concentrations:

DBLα probe: 1:40 dilution ≈ 1 ng/µl ∴ probe 40 µg/ml

DBLε probe: 1:40 dilution ≈ 100 pg/µl ∴ probe 4 µg/ml

Exon 2 probe: 1:400 dilution ≈ 10 ng/µl ∴ probe 4000 µg/ml

MSP1 probe: 1:40 dilution ≈ 5 ng/µl ∴ probe 200 µg/ml

5.5.10 Northern blot analysis: presence of type 3 *var* gene transcript in laboratory strain 3D7

A Northern blot was used to verify the presence of type 3 *var* gene transcripts in laboratory strain 3D7. RNA prepared from a 9% mixed stage culture of 3D7 (4% ring, 4% pigmented trophozoite, 1% schizont). RNA was separated by agarose gel electrophoresis on a 1.2 % agarose/formamide gel, and the RNA was transferred to nylon membrane. The membrane was hybridised overnight at a range of temperatures (60ºC–68ºC) with the type 3 DBLα domain probe. The membrane was then washed in 0.5x SSC/0.2% SDS (see materials and methods), and was incubated in blocking buffer before incubation with an anti-DIG secondary antibody, which binds to the DIG label in the probe. Unbound antibody was washed away with Maleic acid wash buffer. The membrane was then processed in an X-ray developer.

Hybridisation with the type 3 DBLα domain probe at 60ºC resulted in detection of a 3.98 kb transcript corresponding to a type 3 *var* gene (Fig. 5.31A). The probe also cross-reacted strongly to a band at approx 6.5 kb, and faintly to longer *var* gene transcripts (> 9 kb). Increasing the stringency of the washing (longer time and a range of SSC/SDS concentrations) did not reduce the strength of the 6.5 kb band compared to the 3.98 kb transcript. Hybridisation at higher temperatures resulted in loss of any recognition of RNA by the probe.

To confirm the 3.98 kb transcript detected with the DBLα probe was a *var* gene, a probe generated against *var* gene exon 2 probe was also used. This generic *var* gene exon 2 probe was used to probe fresh nylon membranes from the same RNA

preparation from the mixed stage 3D7 culture. Hybridisation at 50ºC resulted in recognition of a type 3 *var* gene length (3.98 kb) transcript (Fig. 5.31B). Non-type 3 *var* genes (> 9kb) are also clearly recognised by the generic exon 2 probe. The 6.5 kb transcript (Band X in Fig. 5.31B) is again recognised, although only very faintly. Hybridisation at temperatures above 50ºC resulted in loss of transcript recognition.

Hybridisation was attempted with the type 3 epsilon probe with various temperature and washing conditions, but no DIG labelled probe was ever detected upon development of the membrane. This may be due to the low concentration of the probe, or an unsuccessful labelling reaction (faint spots, Fig. 5.30).

A homology search of the 3D7 genome database (http://www.plasmodb.org) suggests the only gene which was any homology to the probe is *var1csa* (PFE1640w); the DBLα probe has 60% homology with nucleotides 8165–8470 of the 9.45 kb *var1csa* transcript (Fig. 5.32). This may also be the faint upper band in Fig. 5.31, but the identity of the 6.5 kb transcript (band X) is unclear.

A DBLα probe B Exon 2 probe

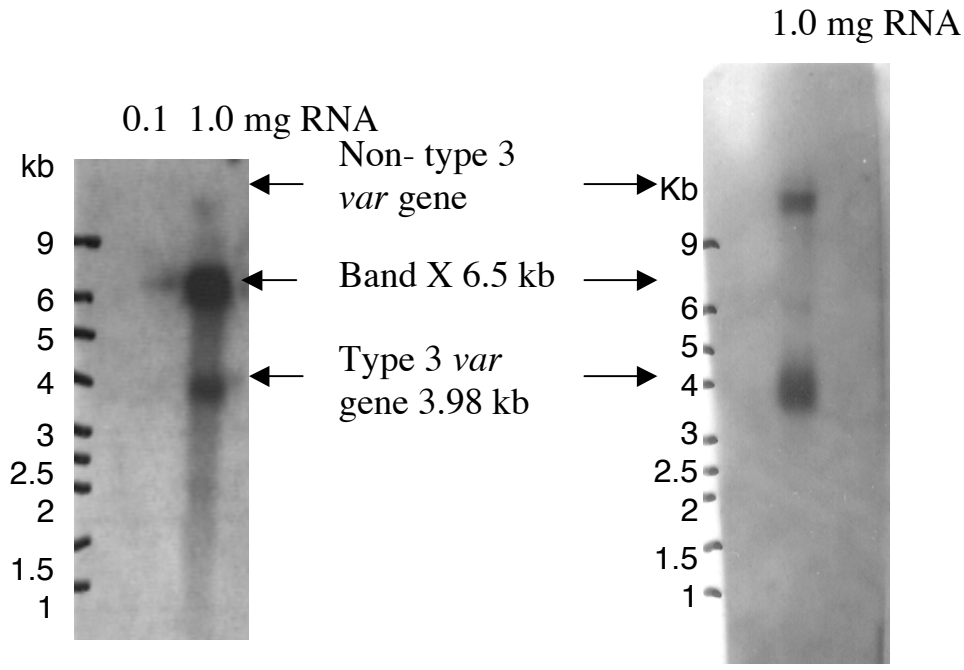

Fig. 5.31. Northern blot showing RNA from 9% mixed stage 3D7 culture (4% ring, 4% pigmented trophozoite, 1% schizont). RNA was separated by agarose gel electrophoresis on a 1.2 % agarose gel, and the RNA was transferred to nylon membrane. A) The membrane was hybridised overnight (60ºC) with a type 3 *var* gene DBLα domain probe. RNA corresponding to the type 3 DBLα *var* transcript (3.98 kb) is marked with an arrow (←). The probe cross reacts strongly to a band at approx 6.5 kb, and faintly to longer *var* gene transcripts (> 9 kb). B) The membrane was hybridised overnight (50ºC) with the *var* gene exon 2 probe. RNA corresponding to the type 3 DBLα *var* transcript (3.98 kb) is marked with an arrow (←). Longer *var* gene transcripts (> 9 kb) are also present and recognised by the probe.

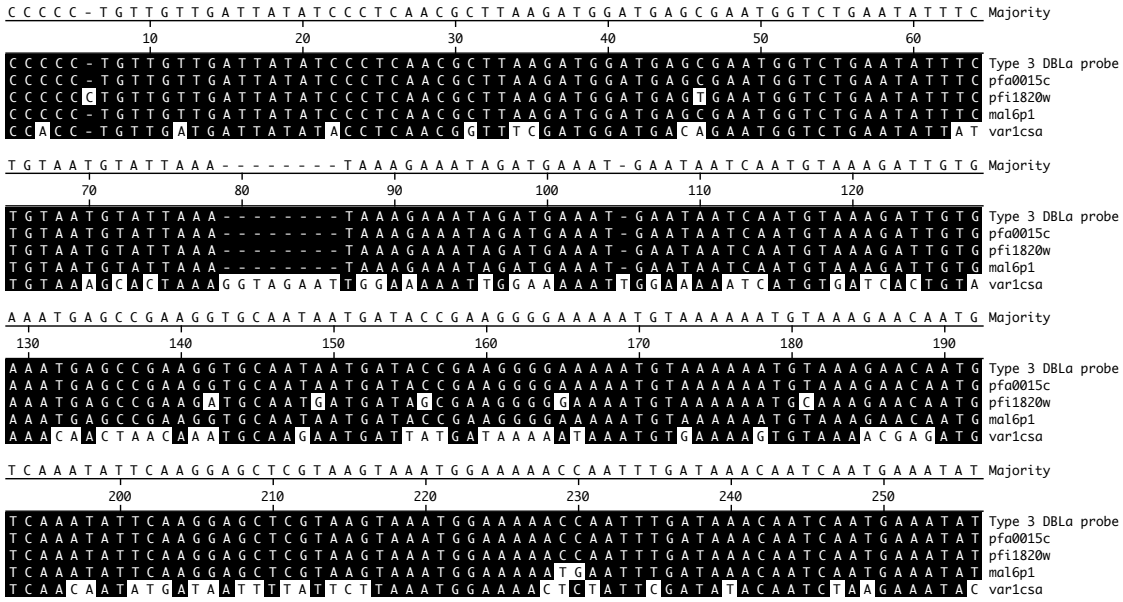

Fig. 5.32. Alignment showing the type 3 DBLα probe and the sections of transcripts recognised by it in 3D7; pfa0015c (nucleotides (nt) 886-1132, 100% homology), pfi1182w (nt 864-1120, 99.2% homology), mal6p1.314 (685-1141, 97.6% homology), and *var1csa* (nt 8165–8470 59.8% homology).

The RNA from the RT-PCR time courses were processed through the Northern blot analysis method describe above. Unfortunately, this was not successful for DBLα domain, DBLε domain or exon 2 probes. The MSP1 probe recognised the schizont extract at 42 hr post invasion only, suggesting the Northern blot method used was successful (Fig. 5.33). This suggests the gel, transfer and detection procedures were successful, and the buffers were correctly made. Failure to detect RNA with the other probes (type 3 DBLα/ε and exon 2) may have been due to the hybridisation or washing being sub-optimal for the other probes.

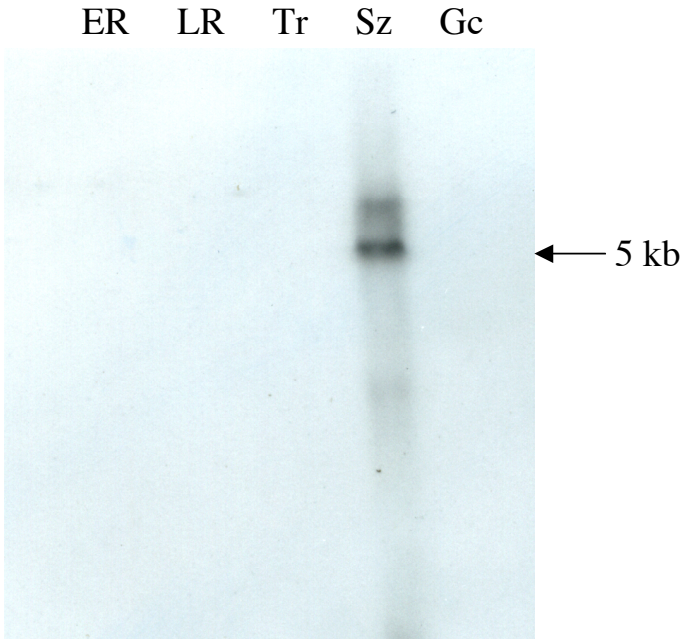

Fig. 5.33 MSP1 Northern blot of 3D7 time course. RNA samples were as Fig. 5.24 early rings (ER), late rings (LR), trophozoite (Tr), schizonts (Scz), gametocytes (Gc). RNA was separated by agarose gel electrophoresis on a 1.2 % agarose gel, and the RNA was transferred to nylon membrane. The membrane was hybridised overnight (60ºC) with the MSP1 probe. RNA corresponding to the MSP1 transcript (5.12 kb) is marked with an arrow (←).

5.5.11 Type 3 *var* genes in Mali field isolates

The aim of this section was to determine whether type 3 *var* genes were commonly transcribed in *P. falciparum* field isolates, using gDNA and cDNA from the 26 field isolates from the Mali study sites examined for non-type 3 DBLα transcription discussed in chapter 3 (Lyke *et al.* 2004). Data is presented for type 3 *var* gene presence in Mali field isolate gDNA (section 5.5.11), type 3 *var* gene DBLα/ε domain transcript detection by RT-PCR (sections 5.5.12 and 13 respectively), and finally a summary of type 3 *var* genes in the Mali isolates (section 5.5.14). Section 5.5.15 will then discuss the sequences phylogenetically.

5.5.12 PCR of type 3 gDNA *var* genes from Mali field isolate gDNA

Firstly, type 3 DBLα domain amplification on gDNA from each isolate was performed to assess whether type 3 *var* genes were present in the Mali isolates. PCR was performed using the alpha domain primer pair AF3_type3F and Type3alphaR2. Type 3 *var* gene DBLα domain PCR product was detected in all isolates (Fig. 5.34).

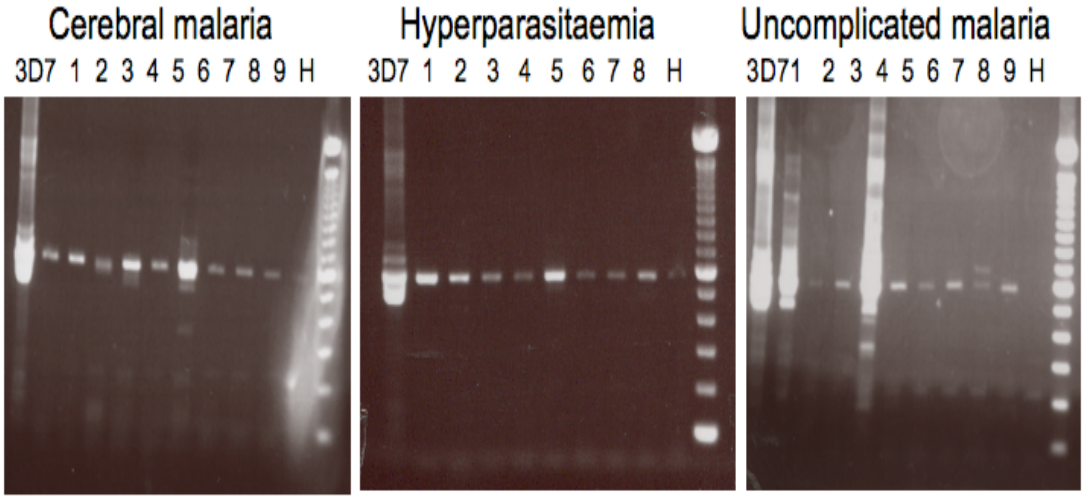

Fig. 5.34 Type 3 DBLα domains were amplified from gDNA from the 26 Malian field isolates (9 cerebral malaria, 8 hyperparasitaemia and 9 uncomplicated malaria) using primer pair AF3_type3F and Type3alphaR2. A 5 µl sample of all RT-PCR products was run on a 1.5% agarose gel. G: gDNA controls were positive for PCR product in all cases indicating PCR was successful. H: water control lanes. DNA ladder was 100 bp ladder.

For 10 isolates with a good PCR product (HYP1, HYP2, HYP5, HYP6, HYP7, CM1, CM4, CM6, U1 and U4) the PCR products were cloned and used to transform *E. coli*. The ligated plasmids from 24 colonies were extracted and sequenced from each of these isolates. The number of distinct (>95% identity) DBLα transcripts per isolate ranged from 1-4 from 5-22 miniprep plasmid sequences per isolate (Table 5.5). On average there were 0.86 type 3 DBLα domains per genotype, but more isolates would need to be studied to confirm these proportions.

Clinical disease category	Isolate	Minipreps sequenced	Distinct type 3 DBLα domains in gDNA PCR	Distinct genotypes detected	gDNA type3 per genotype
Hyperpara- Sitaemia	HYP1	22	2	4	0.50
	HYP2	14	3	3	1.00
	HYP5	15	3	4	0.75
	HYP6	5	2	3	0.67
	HYP7	19	2	3	0.67
Cerebral Malaria	CM1	11	2	1	2.00
	CM4	10	1	5	0.20
	CM6	10	3	3	1.00
Uncomplicated malaria	U1	10	2	4	0.50
	U4	11	4	3	1.33
				Average	0.86

Table 5.5. Table showing the number of distinct DBLα domains detected by PCR of gDNA using the type 3 alpha domain primer pair AF3_type3F and Type3alphaR2, with the number of miniprep plasmids sequenced. Also shown is the number of genotypes detected in these isolates (details in chapter 3), the relative number of type 3 *var* genes detected per genotype for each isolate, and the average number of detected DBLα domains per genotype.

5.5.13 Type 3 *var* gene transcription in Mali field isolates: Type 3 DBLα domain RT-PCR

Having established that the isolates all appeared to contain type 3 *var* genes at the gDNA level, RT-PCR was used to assess how frequently these were transcribed. Type 3 DBLα domain RT-PCR using AF3_type3F and Type3alphaR2 was performed on cDNA from each of the 26 Mali field isolates (prepared in chapter 3). PCR products were obtained for 15/26 isolates; 8/8 hyperparasitaemia isolates, 3/9 cerebral malaria isolates and 4/9 uncomplicated malaria isolates. The PCR products

were purified, cloned and sequenced, to assess the number of distinct type 3 DBLα domain transcripts per isolate. There was a significantly higher number of type 3 DBLα domain transcripts seen in the hyperparasitaemia isolates compared to cerebral malaria isolates (t-test, P=0.003). Table 5.6 shows the number of distinct type 3 DBLα transcripts detected per isolate.

Clinical disease category	Isolate name	Type 3 RT-PCR	
		Minipreps	Distinct type 3 DBLα domains
Hyperparasitaemia	HYP1	7	1
	HYP2	6	2
	HYP3	14	4
	HYP4	9	1
	HYP5	15	2
	HYP6	6	2
	HYP7	9	2
	HYP8	5	1
Cerebral malaria	CM1	7	1
	CM2	-	0
	CM3	-	0
	CM4	-	0
	CM5	-	0
	CM6	-	0
	CM7	11	2
	CM8	7	1
	CM9	-	0
Uncomplicated malaria	U1	4	2
	U2	-	0
	U3	-	0
	U4	4	1
	U5	10	2
	U6	7	1
	U7	-	0
	U8	9	3
	U9	-	0

Table 5.6: Presence and number of transcribed type 3 DBLα domains detected by RT-PCR using primers AF3_type3F and Type3alphaR2 in 8 hyperparasitaemia, 9 cerebral malaria and 9 uncomplicated malaria field isolates, with the number of minipreps sequenced.

5.5.14 Type 3 *var* gene transcription in Mali field isolates: Type 3 DBLε domain RT-PCR

Type 3 DBLε domain transcripts were also amplified by RT-PCR from the same cDNA preparations, using primers Type3epsF and Type3epsR. PCR products were obtained for 16/26 isolates; 6/8 hyperparasitaemia isolates, 6/9 cerebral malaria isolates and 4/9 uncomplicated malaria isolates. As before, the PCR products were purified, cloned and sequenced, to assess the number of distinct DBLε domain transcripts detected per isolate, shown in Table 5.7.

Clinical disease category	Isolate name	Type 3 RT-PCR	
		Minipreps	Distinct type 3 DBLε domains
Hyperparasitaemia	HYP1	5	1
	HYP2	3	1
	HYP3	6	1
	HYP4	-	0
	HYP5	6	1
	HYP6	6	1
	HYP7	6	1
	HYP8	-	0
Cerebral Malaria	CM1	4	1
	CM2	4	1
	CM3	3	1
	CM4	3	1
	CM5	4	1
	CM6	3	1
	CM7	-	0
	CM8	-	0
	CM9	-	0
Uncomplicated malaria	U1	6	1
	U2	-	0
	U3	-	0
	U4	4	1
	U5	5	1
	U6	-	0
	U7	6	1
	U8	-	0
	U9	-	0

Table 5.7: Presence and number of transcribed epsilon domains detected by RT-PCR using primers type 3 DBLα in 8 hyperparasitaemia, 9 cerebral malaria and 9 uncomplicated malaria field isolates, with the number of minipreps sequenced.

Epsilon domains were very similar (>92% amino acid identity, see section 5.5.15) and no isolates showed multiple DBLε domain transcripts.

5.5.15 Type 3 *var* gene transcription in Mali field isolates: Summary

In total, evidence of type 3 *var* gene transcription was detected in 23/26 isolates; all 8 hyperparasitaemia isolates, 8/9 cerebral isolates and 7/9 uncomplicated isolates (Table 5.8). The observation of epsilon but not alpha product in 7 isolates, including 5/9 cerebral isolates, was puzzling. RT-PCR was repeated on all of the cerebral isolates (except CM7 due to cDNA running out) with the first pair of type 3 DBLα domain primers (αAF3_type3F and Type3alphaR1, section 5.5.1). Only CM1 showed a PCR product with these primers. RT-PCR was also repeated on all of the cerebral isolates (except CM7 due to cDNA running out) with the forward type 3 DBLα domain primer and reverse epsilon domains primer (αAF3_type3F and Type 3epsR). Again, only CM1 showed a PCR product with these primers. The lack of product indicates the type 3 DBLα domains are either not present, or at very low concentration, in the cerebral malaria isolates. The type 3 DBLε domains are more highly conserved and there is no degeneracy in the forward primer, unlike the forward primer for the type 3 DBLα domains. Thus it is possible that a very low level of type 3 *var* gene transcription would be picked up by the epsilon but not the alpha domain primers, as the epsilon primers may be a more powerful primer pair

(see discussion). It is also possible the alpha domain primers could not amplify the alpha domain, though product was seen in the gDNA PCR for all cerebral isoates.

Clinical disease category	Isolate name	Type 3 RT-PCR		Estimated transcribed type 3 repertoire	Genotypes*	DBLα1%*
		α	ε			
Hyperpara-sitaemia	HYP1	1	1	1	4	0
	HYP2	2	1	2	3	0.07
	HYP3	4	1	4	1	0.28
	HYP4	1	0	1	2	1.00
	HYP5	2	1	2	3	0.40
	HYP6	2	1	2	3	0.25
	HYP7	2	1	2	3	0.06
	HYP8	1	0	1	2	0.00
Cerebral malaria	CM1	1	1	1	1	0.83
	CM2	0	1	1	3	0.79
	CM3	0	1	1	3	0.93
	CM4	0	1	1	5	0.06
	CM5	0	1	1	1	0.72
	CM6	0	1	1	3	1.00
	CM7	2	0	2	1	1.00
	CM8	1	1	1	1	0.95
	CM9	0	0	0	2	1.00
Uncomplicat ed malaria	U1	2	1	2	4	0.60
	U2	0	0	0	3	0.07
	U3	0	1	1	3	1.00
	U4	1	1	1	3	0.06
	U5	2	1	2	3	0.74
	U6	1	0	1	1	1.00
	U7	0	1	1	3	0.07
	U8	3	0	3	1	0.05
	U9	0	0	0	1	0.06

Table 5.8: Presence and number of transcribed type 3 alpha and epsilon domains detected by RT-PCR in 8 hyperparasitaemia, 9 cerebral malaria and 9 uncomplicated malaria field isolates, and the estimated (minimum) repertoire of transcribed type 3 *var* gene in each isolate. *Genotypes and DBLα1% data was taken from chapter 3.

There was no significant difference in the proportion of isolates showing type 3 *var* gene transcription in the three isolate groups (Chi-squared, p = 0.37). The relative levels of transcription between isolates cannot be directly compared, as the RT-PCR was not quantitative. However, there was a significantly higher number of type 3 transcripts seen in the hyperparasitaemia isolates compared to cerebral malaria isolates (t-test, p = 0.02; Fig. 5.35A). This difference is even greater if only the number of distinct DBLα_{type3} transcripts detected is compared (t-test, p = 0.003). This is in contrast to the findings of chapter 3 which showed an increase in non-type 3 DBLα1 transcripts in the cerebral versus hyperparasitaemia isolates, and shows an association between type 3 transcription and non-cerebral malaria.

There was no correlation between number of estimated transcribed type 3 *var* genes and DBLα1% as calculated in chapter 3 (Spearman Rank correlation: Rho = -0.03, p = 0.89; Fig. 5.35B). There was also no correlation between number of estimated transcribed type 3 *var* genes and number of genotypes estimated in chapter 3 (Spearman Rank correlation: Rho = 0.18, p = 0.38; Fig. 5.35C).

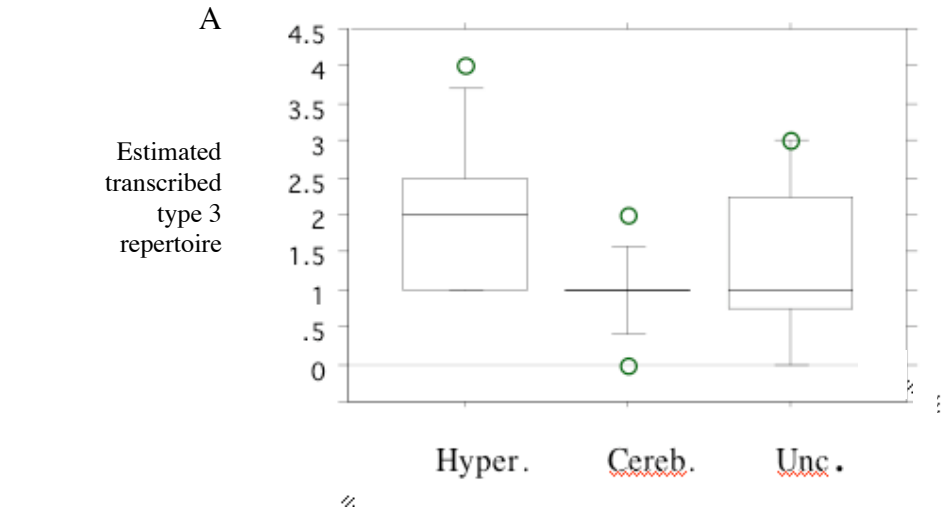

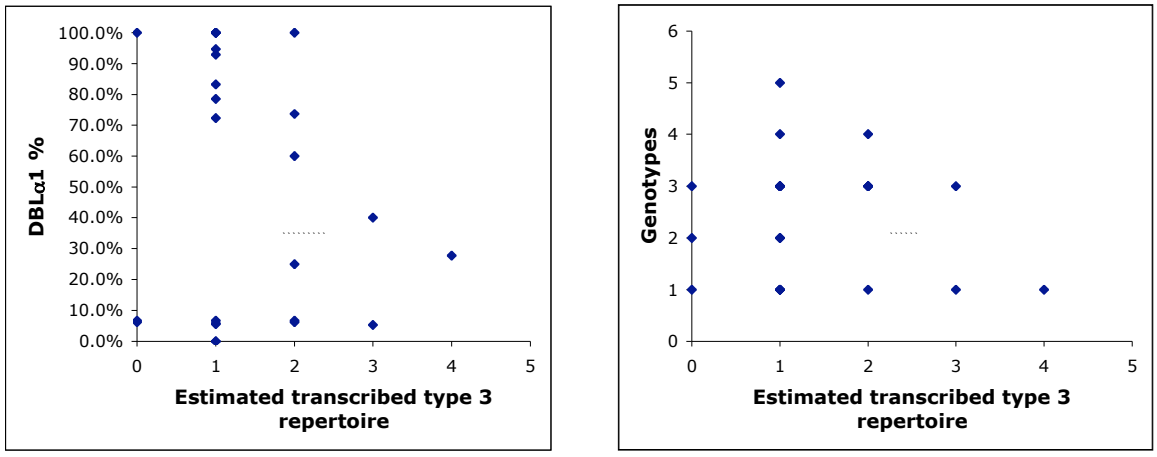

Fig. 5.35. A) Estimated transcribed type 3 *var* repertoire for the three isolate clinical categories. Hyperparasitaemia isolates showed significantly higher diversity of type 3 *var* genes than cerebral malaria isolates (t-test p = 0.02). B) Spearman Rank correlation DBLα1% and estimated transcribed type 3 repertoire (Rho = -0.03, p = 0.89). C) Spearman Rank correlation number of genotypes and estimated transcribed type 3 *var* gene repertoire (Rho = 0.18, p = 0.38).

Comparing the estimated number of transcribed and encoded type 3 *var* genes, approximately 50-70% percent of the type 3 *var* genes are transcribed (Table 5.9).

Clinical disease category	Isolate	Distinct type 3 DBLα domains in gDNA PCR	Distinct type 3 DBLα domains transcribed	Estimated type 3 *var* genes transcribed	Transcribed: gDNA ratio type 3 DBLα	Transcribed: gDNA ratio type 3 *var* gene
Hyperpara-sitaemia	HYP1	2	1	1	0.50	0.50
	HYP2	3	2	2	0.67	0.67
	HYP5	3	2	2	0.67	0.67
	HYP6	2	2	2	1.00	1.00
	HYP7	2	2	2	1.00	1.00
Cerebral Malaria	CM1	2	1	1	0.50	0.50
	CM4	1	0	1	0.00	1.00
	CM6	3	0	1	0.00	0.33
Uncomplicated malaria	U1	2	2	2	1.00	1.00
	U4	4	1	1	0.25	0.25
				Average	0.56	0.69

Table 5.9. Table showing the number of distinct DBLα domains detected by PCR of gDNA using the type 3 alpha domain primer pair AF3_type3F and Type3alphaR2, with the number distinct DBLα transcripts detected, and estimated number of type 3 *var* genes transcribed per isolate. The ratio of transcribed:encoded type 3 *var* genes, and the average of these for all 10 isolates is given.

The lack of product in CM9, U2 and U9 for alpha and epsilon domain RT-PCR indicates no, or little, type 3 *var* gene transcription. It is unlikely the RT-PCR reaction "failed" due to a poor cDNA preparation, as amplification of non-type 3 DBLα domains had been successful (chapter 3).

The low number of minipreps sequenced per isolate for alpha and epsilon RT-PCR mean that it is possible that other type 3 domain transcripts were also present. The

estimated number of type 3 transcripts in each isolate is included in the table of Mali isolate data (Appendix 1).

5.5.16 Type 3 *var* gene diversity in Mali field isolates

The type 3 domains showed a similarly high level of conservation as previously published type 3 *var* genes, with amino acid identities of 58.3-100% for the alpha domains (mean 76.3%, SE 0.4%, SD 0.2%) and 94.2-100% for the epsilon domains (mean 97.8%, SE 0.3%, SD 0.002%) as shown in Fig. 5.36 (histograms and box plot) and illustrated pictorially in Fig. 5.37.

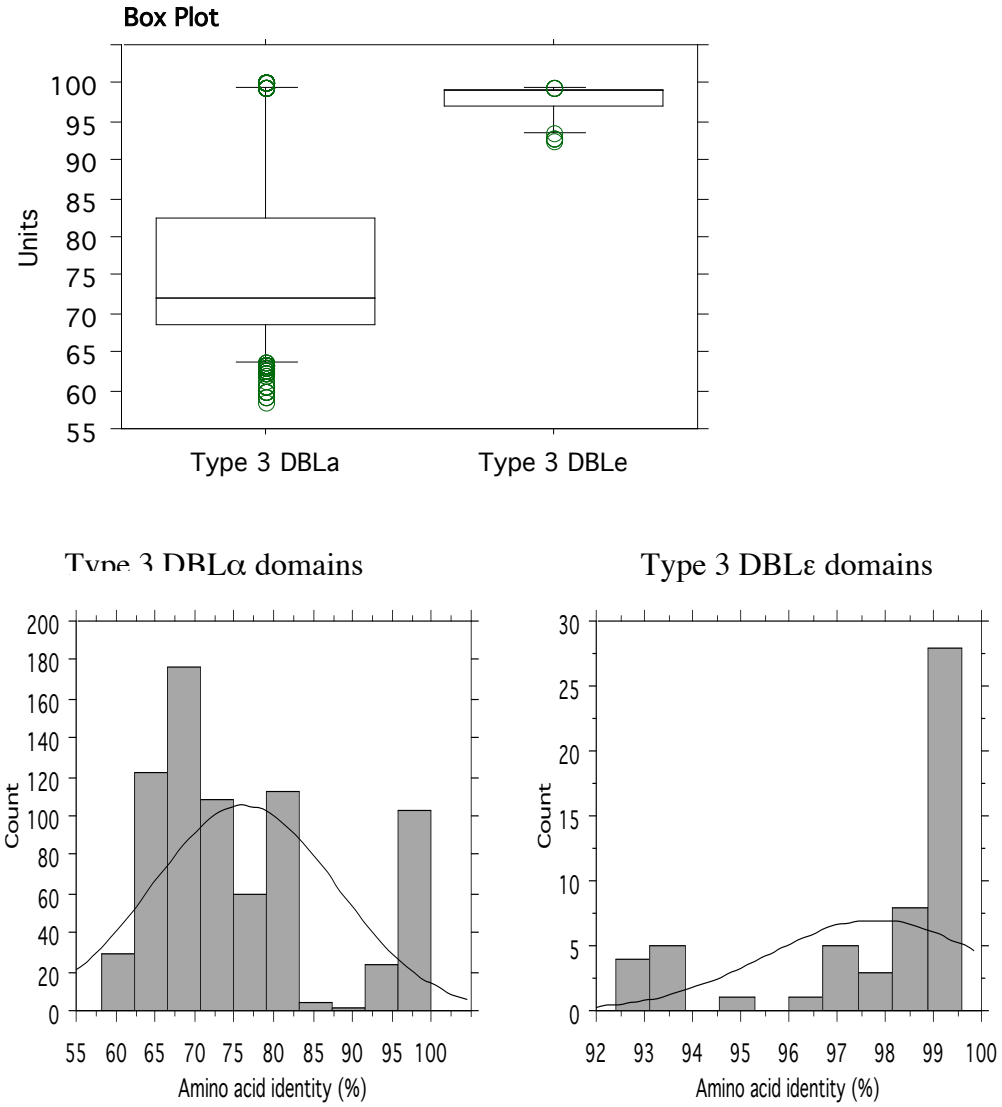

Fig. 5.36. Box plot (displaying 10th, 25th, 50th, 75th and 90th percentiles; values <10th percentile and >90th plotted separately) and histograms of percentage amino acid identity between cerebral, hyperparasitaemia and uncomplicated malaria type 3 DBLα and DBLε domains. Percentage identity was calculated using MegAlign. Histograms and box plots of identity were then created in Statview. Note the scale for amino acid identity on the histograms are different.

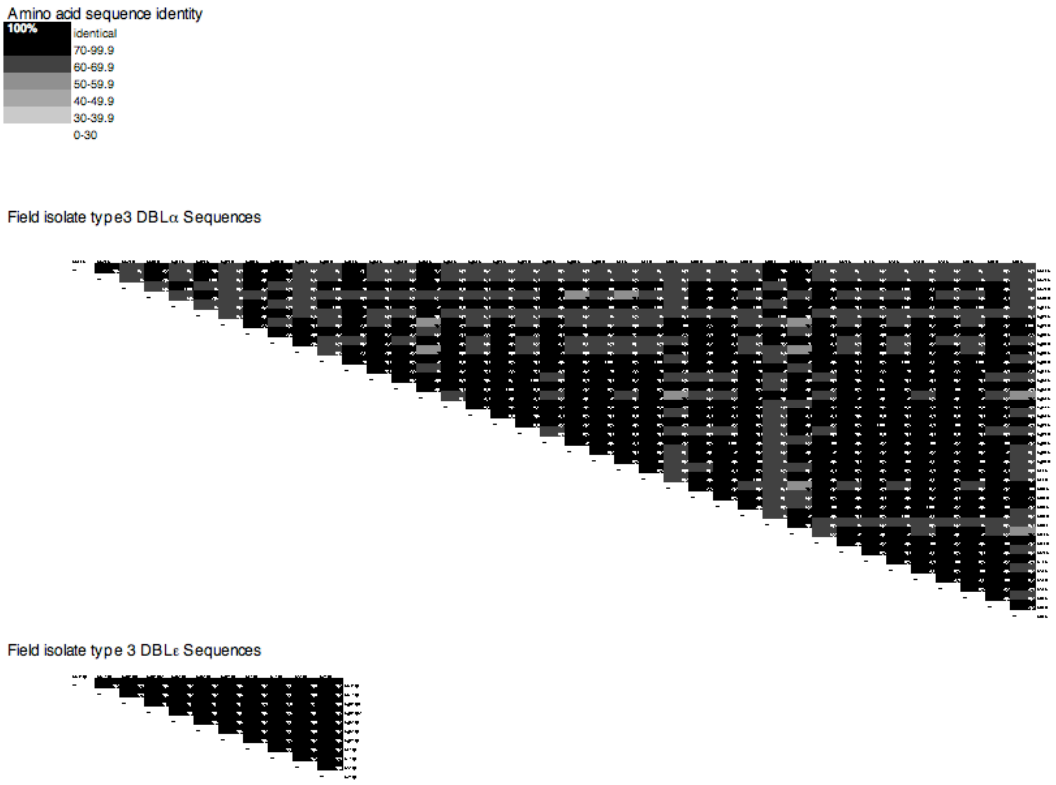

Fig. 5.37. Amino acid sequence distance charts showing percentage amino acid identity between Mali field isolate DBLα_{type3} and DBLε_{type3} domains. Darkness of shading indicates level of identity between domains. Amino acid sequences were created from nucleotide sequences in EditSeq, and percentage identity was calculated using MegAlign.

5.5.17 Phylogenetic analysis of DBLα type 3 domains from Mali field isolates

The DBLα_{type3} domains were aligned using clustal W and phenograms were created (Fig. 5.38). As expected from a subgroup of domains with such high sequence similarities, the DBLα_{type3} domains cluster separately from the non-type 3 DBLα domains of 3D7 (Fig. 5.38). The DBLα_{type3} domains clustered into 6 distinct clades, representing 6 highly conserved DBLα_{type3} domains groups DBLα_{type3} A-F of >95% nucleotide sequence identity (Fig. 5.38). The consensus sequence for these groups was defined as Type 3 DBLα_{type3} A-F so homology comparisons to different sequences could be made. Mal6p1.314 did not fall into one of these groups (nearest homology was 94% to type 3 group C).

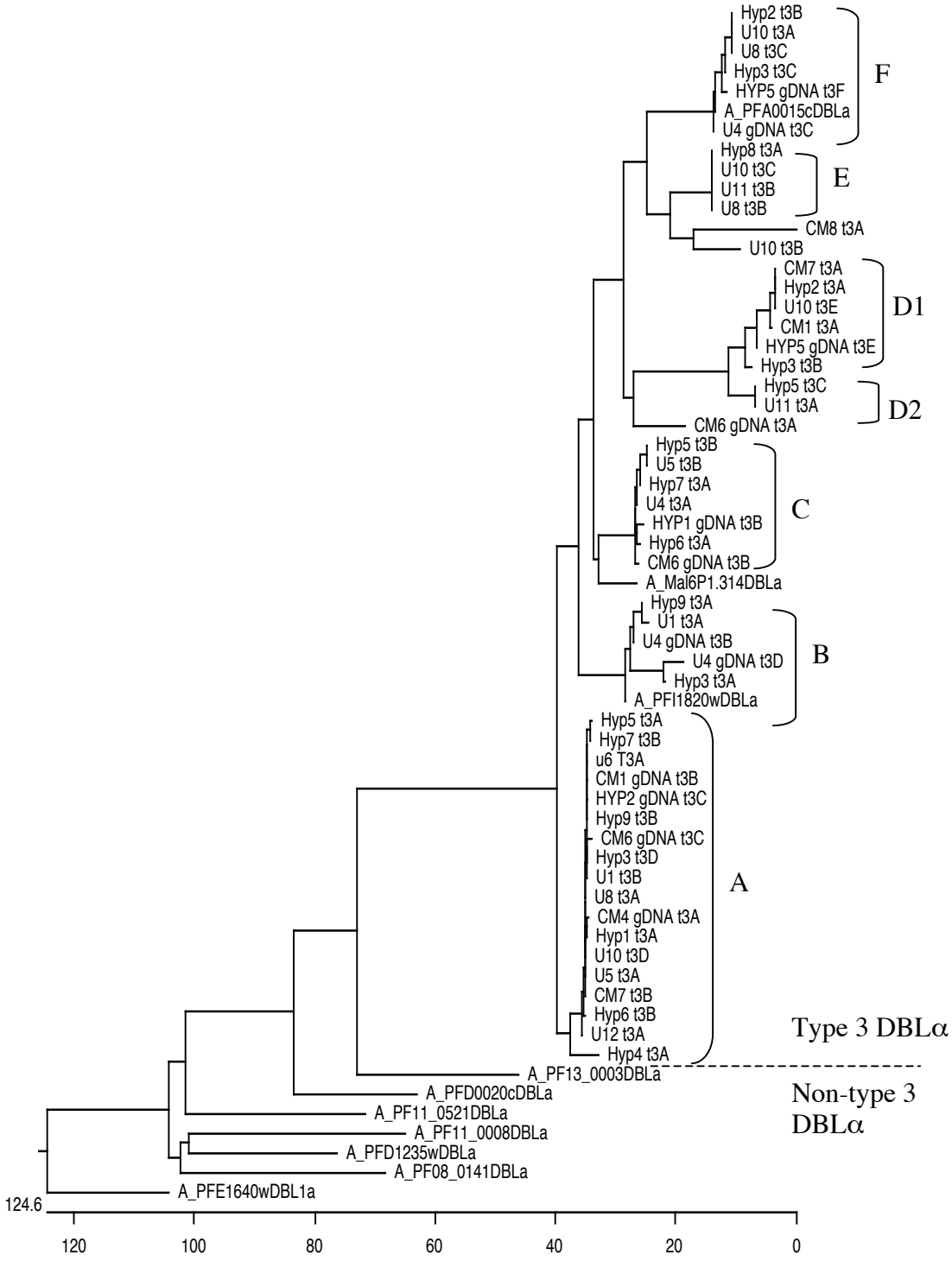

Fig. 5.38. Phenograms of field isolate Type 3 DBLα domains created from a clustal W alignment of sequences. Type 3 DBLα domains from the Mali isolates, transcribed or gDNA only are included, with 3D7 DBLα1 domains for comparison. Sequences are grouped into consensus group (>95% identity) A-F. Type 3 DBLα domains are above dotted line. Non-type 3 DBLα domains are below the line. D1

and D2 are defined as a subset of group D, as the sequences of group D2 fall just outside the 95% homology cut-off, but are very similar (94% identity) to those of group D1.

DBLα_{type3} were also amplified from gDNA from 6 Kenyan field isolates (gift from Pete Bull, Kilifi, Kenya), resulting in a further 8 DBLα_{type3} sequences. It was not possible to count the number of genotypes within each sample, as only a few microlitres cDNA was available, however a range of 1-5 is expected from previous work in this area (Bull *et al*. 1999). Five of these sequences fell into the strictly defined 6 subgroups A-F of DBLα_{type3} (>95% nucleotide sequence identity). In addition, 9 other sequences from various global locations (Trimnell *et al*. 2006) also showed high homology to the defined DBLα_{type3} subgroups (Fig. 5.39). DBLα_{type} group A is particularly highly conserved, with 19 sequences belonging to this group with >99% homology including sequences from vastly different geographic areas (East Africa, West Africa and South America), and a further 2 sequences with >95% homology. One sequence Kilifi gDNA5D was identical to the alpha domain of Mal6p1.314 (Fig. 5.39). A summary of the type 3 DBLα groups A-F is given in Table 5.10.

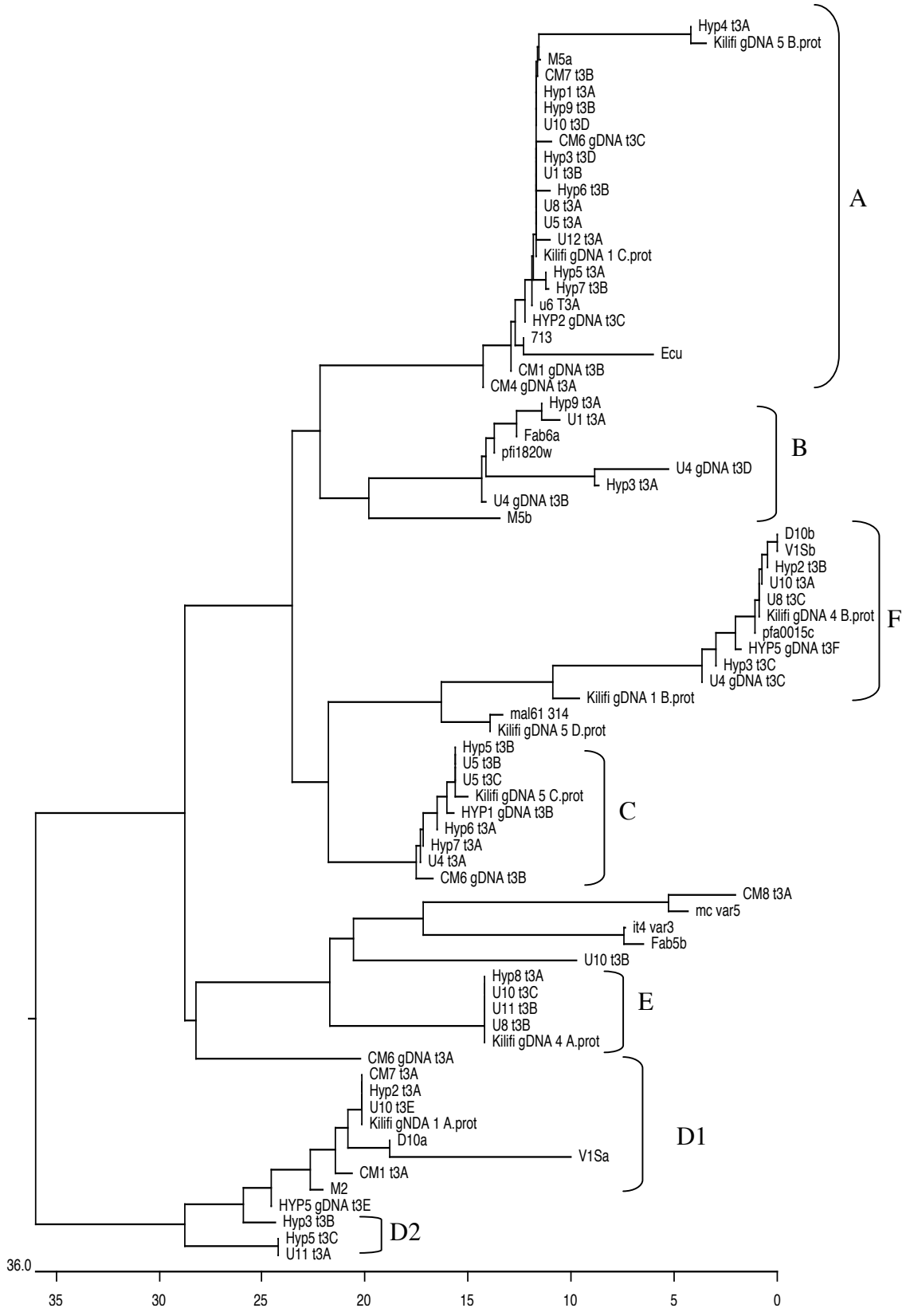

Fig. 5.39. Phenograms of field isolate Type 3 DBLα domains created from a clustal W alignment of sequences. A) Type 3 DBLα domains from the Mali isolates,

transcribed or gDNA only are included, with Kenya isolates sequences and other published type 3 DBLα domain sequences. Sequences are grouped into consensus group (>95% identity) A-F, including D1 and D2 separately as before.

Type 3 DBLα domain group (>95% indentity)	Mali type 3 DBLα domains (% identity to group)	Kilifi type 3 DBLα domains (% identity to group)	Published type 3 DBLα domains (% identity to group)
A	U1B (100%) U5A (100%) U6A (100%) U8A (100%) U12A (99%) HYP1A (100%) HYP3D (100%) HYP4A (96%) HYP5A (99%) HYP6B (99%) HYP7B (99%) HYP2C gDNA (99%) CM1B gDNA (100%) CM4A gDNA (99%) CM6C gDNA (99%) CM7B (100%)	K1C (99%) K5B (95%)	713. W Africa (100%) M5a, W Africa (99%) Ecu, S America (99%)
B	U1A (99%) HYP3A (96%) HYP5D gDNA (100%) HYP9A (96%)	None	pfi1820w, 3D7 (100%) Fab6a, S Africa (100%)
C	U4A (100%) U5B (100%) HYP1B gDNA (98%) HYP5B (100%) HYP6A (99%) HYP7A (100%) CM6A gDNA (98%)	K5C (99%)	None
D1	HYP2A (97%) HYP3B (95%) HYP5E gNDA (96%) CM1A (98%) CM7A (99%)	K1A (99%)	M2, W Africa (98%) D10a, PNG (97%) V1Sa, SE Asia (96%)
D2 (94% homology to D1)	U11A (100%) HYP5C (100%)		
E	U5C (99%) U8B (99%) U11B (99%) HYP8A (100%)	None	None
F	U4C gDNA (100%) U8C (99%) U10A (99%) HYP2B (100%) HYP3C (99%) Hyp5F gDNA (98%)	K1B (95%) K4B (100%)	Pfa0015c, 3D7 (100%) D10b, PNG (100%) V1Sb, SE Asia (100%)

Table 5.10. Six distinct groups of conserved (>95% identity) DBLα_{type3} domains A-F, showing the percentage identity of each sequence to the group consensus. Mali field isolate RT-PCR and gDNA sequences, Kilifi gDNA sequences and domains obtained from the NCBI database. Percentage nucleotide homology the defined DBLα_{type} group A-G consensus sequence is given in brackets. D1 and D2 are defined as a subset of group D, as the sequences of group D2 fall just outside the 95% homology cut-off, but are very similar (94% identity) to those of group D1. For published sequences geographic origin is also given.

5.5.18 Phylogenetic analysis of DBLε type 3 domains from Mali field isolates

The DBLε_{type3} domains also cluster separately from non-type 3 domains, forming just one tight group in the phenogram clearly distinct from the non-type 3 epsilon domains from 3D7 (Fig. 5.38). As they all show such high homology to each other they cannot be separated into more distinct subgroups. All type 3 epsilon domains found on NCBI database showed >97% nucleotide homology to this group. This is also reflected in the high sequence homology across the whole repertoire of amplified DBLε_{type3} domains (Fig. 5.40).

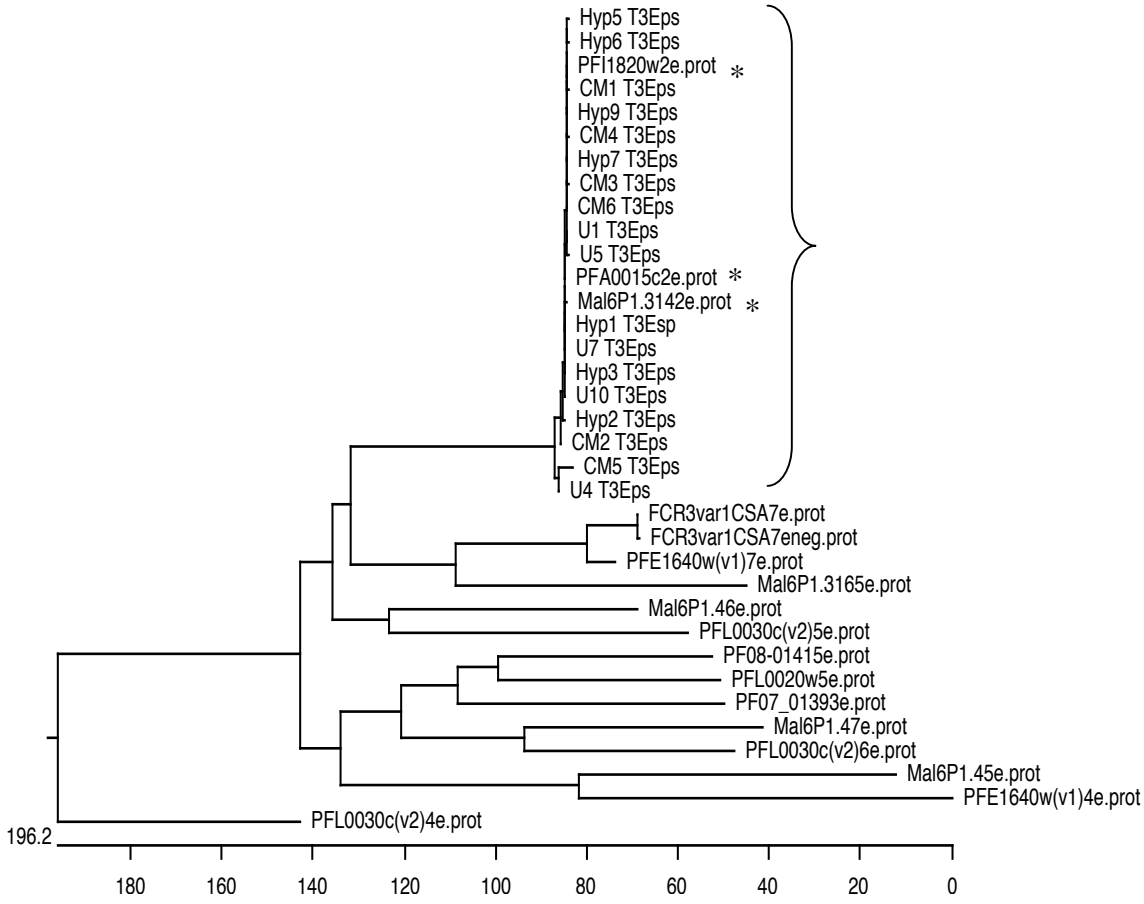

Fig. 5.40 Phenogram of field isolate DBLε_{type3} domains (bracketed) with 3D7 epsilon domains for comparison created from a clustal W amino acid alignment. *3D7 type 3 epsilon domains are marked with an asterisk.

5.6 Results 2: Type 3 PfEMP1 protein analysis

5.6.1 Type 3-specific anti-peptide polyclonal antibody production: DBLα domain structure

As one hypothesis of this chapter was that there might be an association of type 3 DBLα1 domain expression with cerebral malaria, it was decided to raise an antibody to the type 3 DBLα domain. This was intended to be a useful tool for confirming whether the type 3 PfEMP1 is translated, and would be used to determine if the type 3 PfEMP1 were surface exposed, using immunofluorescence, and Western blotting with protease treatment of the surface exposed proteins using trypsin. In the future, a type 3 DBLα domain could potentially be used to determine type 3 DBLα1 domain function; for example if binding assays suggested the type 3 DBLα1 domain had affinity for certain ligands, the antibody could be used to block binding, and show specificity of the interaction. It could also be used in culture, for example to determine whether the type 3 DBLα1 domain has any role in processes such as invasion, or for selection of type 3 PfEMP1-expressing parasites. These future experiments are outside the scope of this chapter (see discussion for further details).

The type 3 DBLε domains could also have been chosen as the target of a type 3 specific antibody as they are also very highly conserved. However, as they are more membrane proximal they might not be as accessible to antibody for example in live cell immunoflourescence assays.

As described in the introduction, $DBL\alpha_{type3}$domains contain a specific and conserved subdomain, comprising the second half of the domain (Fig. 5.41). Therefore it was

useful to model the structure of the type 3 specific subdomain to predict any structural feature which may influence antibody design, and to predict surface exposed regions.

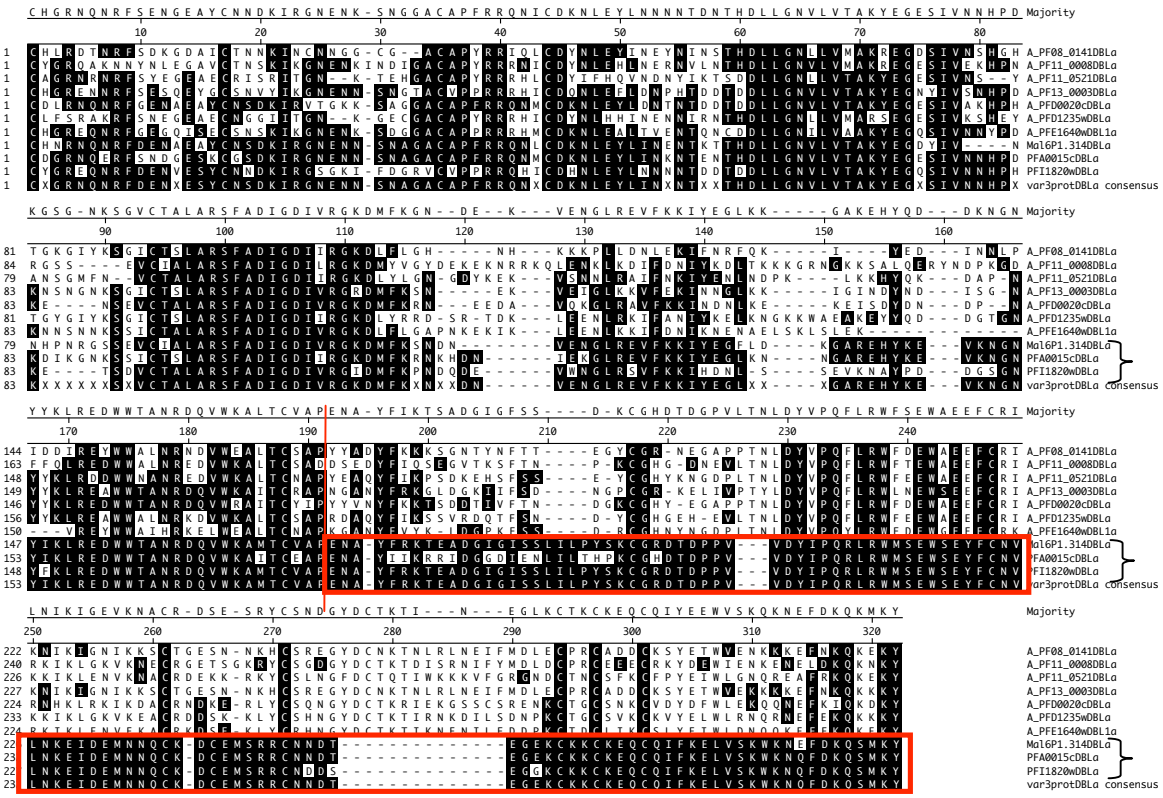

Fig. 5.41. Alignment of 3D7 group A *var* gene DBLα domains. Type 3-specific and conserved region is boxed in red.

The structure of the DBL domains of EBA175 had previously been published (Tolia *et al.* 2005). In comparison to EBA175 RII monomer F2 domains (Tolia *et al.* 2005), the type three specific portion of a DBLα_{type3} domain is equivalent to the F2 subdomain 2. The switch from generic DBLα1 domain to type 3 specific conserved

part of the DBLα_{type3} domain occurs between the two subdomains, specifically between helices T and U as described in Tolia *et al.* (2005) (Fig. 5.42). This is equivalent to between subdomains 2 and 3 of the *P. knowlesi* DBL as defined by Singh *et al.* (2006); subdomains 1 and 2 of the *P. knowlesi* DBL as defined by Singh are equivalent to the first subdomain of the RII EBA175 monomer F2 DBL domain, defined by Tolia.

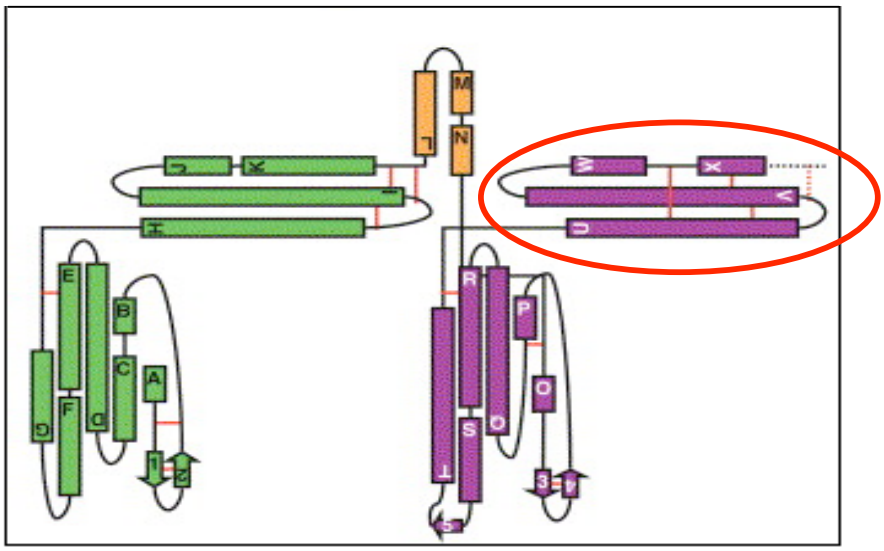

Fig. 5.42. The EBA175 RII monomer F1 (green) and F2 (purple) subdomains showing alpha helices (rectangles) and disulfide bridges (red lines), adapted from Tolia *et al.* (2005). The conserved type 3-specific region corresponds to the second half of the DBLα domain sequence, corresponding to the second subdomain (circled in red) within domain F2 (purple) of the eba174 RII monomer (Tolia *et al.* 2005). The first subdomain of the F2 DBL domain as defined by Tolia is equivalent to subdomains 1 and 2 of *Pk*DBL as defined by Singh *et al.* 2006 and the second Tolia subdomain is equivalent to Singh subdomain 3.

To analyse the structure of the type 3-specific DBLα domain sequence more closely, the structures of EBA175 and the *P. knowlesi* DBL were downloaded from the Research Collaboratory for Structural Bioinformatics (RCSB) Protein Data Bank (http://www.pdb.org). The 3D7 type 3 *var* gene mal6p1.314 sequence was used in structural modeling as a representative type 3 DBLα domain. The mal6p1.314 DBLα domain amino acid sequence was aligned to the amino acid sequence of EBA175 and *P. knowlesi* DBLα by clustal W. The aligned amino acid sequence was then mapped onto the published structures using Cn3d structural modelling software (http://www.ncbi.nlm.nih.gov/Structure/CN3D/cn3d.shtml). This programme superimposes aligned amino acids sequences but does not attempt to model novel structural features, or resolve unaligned sequences. Thus resulting structures are not definitive, but gross features, such as long alpha helices can be confidently positioned. The two DBL structures map very closely onto each other using this technique, showing a high degree of structural identity between these two domains, suggesting there might be a high structural similarity between other DBL domains.

Structural modelling of the type 3-specific subdomain using published structures of EBA175 and *P. knowlesi* DBL (Tolia *et al.* 2005; Singh *et al.* 2006) as a scaffold, suggests the type 3-specific region is a disordered stretch, followed by two long helices separated by another unstructured region (Fig. 5.43).

A B

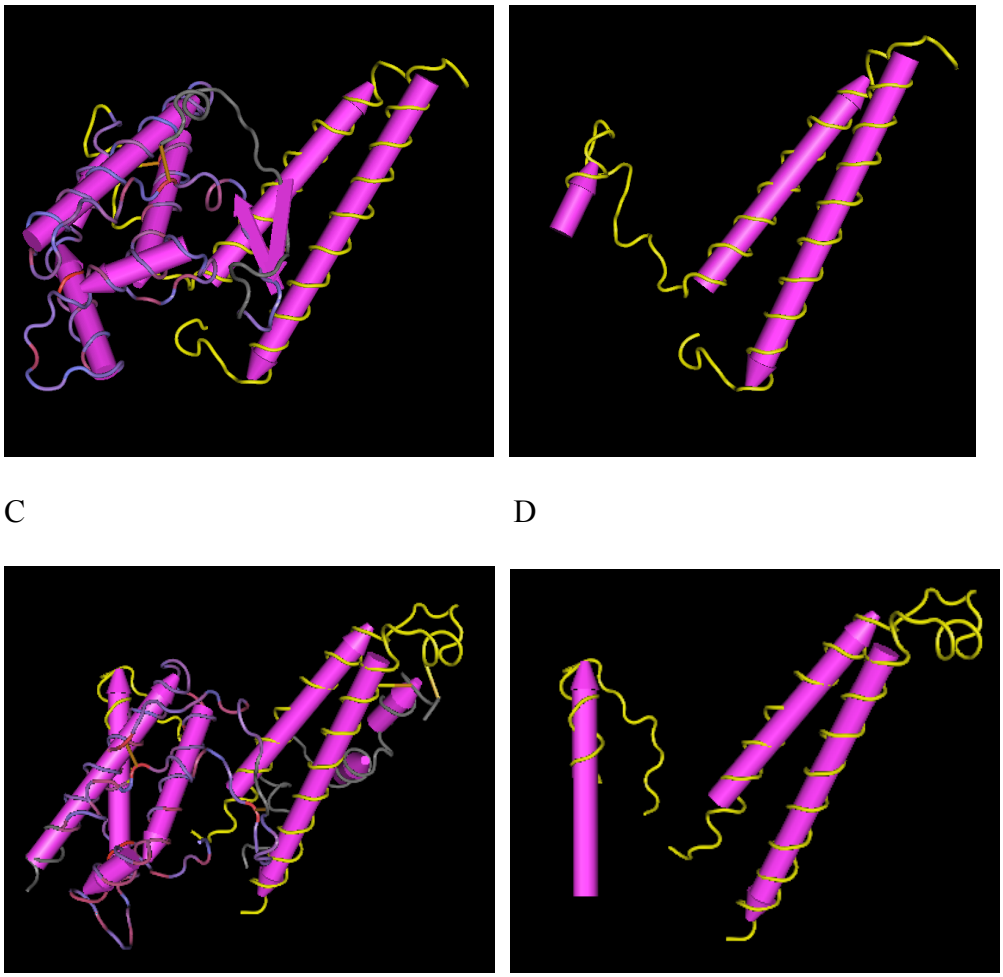

C D

Fig. 5.43. Cn3D generated image of Mal6P.314 amino acid sequences mapped onto known DBL structures. A and B (upper panel) show Mal6P1.314 mapped onto EBA175 F2 domain (PDB ID 1ZRL; Tolia *et al.* 2005). C and D (lower panel) show Mal6P1.314 mapped onto *P. knowlesi* DBL structure (PDB ID 2c6j; Singh *et al.* 2006). A and C (left) show the whole DBLα domain. B and D (right) show only the type 3 conserved region. Type 3 conserved regions are highlighted in yellow, showing disordered residues followed by two predicted long alpha helices.

5.6.2 Type 3-specific anti-peptide polyclonal antibody production: peptide choice

Peptides for anti-peptide antibodies should be 12-16 amino acids long (advice from peptide.design@eurogentec.com) with no internal cysteines as these are used for conjugation to the carrier. For production of an anti-peptide antibody for global recognition of all type 3 domains, peptides were chosen that are well conserved in all known type 3 domains but do not occur in other DBLα1 domains or any other parasite or host proteins. The peptides must also be highly antigenic to increase the chance of successful and specific antigen production in the host animal.

Protean software analysis was used to aid peptide design (Fig. 5.44). Alpha helical regions predicted by structural modelling (Fig. 5.43) are also supported by Garnier Robson analysis (Fig. 5.44). Alpha helical regions suggest a conserved structure, and thus potentially a conserved structural epitope for antigen recognition. Helical peptides are good antigenic targets for recognition of proteins in native states, such as by immunoflourescence, as it is likely that the peptide may also form a helix, and thus have a similar conformation to the native protein. However, denatured proteins have lost secondary structure, so antibodies to helices are not necessarily helpful for recognition of denatured proteins by Western blot analysis.

After analysis with Protean/Lasergene, and consulation with the company Eurogentec (peptide.design@eurogentec.com), three peptides were identified as the most promising epitopes:

1) DTDPPVVDYIPQ

2) CNVLNKEIDEMNNQ

3) LVSKWKN(E/Q)FDK

Kyte-Doolittle plots of these amino acids show the hydrophillicity of the regions is high, suggesting that these amino acids are probably surface exposed, in agreement with the Emini surface probability plot (Fig. 5.44). The Jameson-Wolf analysis also shows high antigenic index for most of this region (Fig. 5.44). These peptides are shown on an amino acid alignment of type 3 DBLα domains (Fig. 5.45) and highlighted in a DBL$\alpha_{type\ 3}$ domain structure model (Fig. 5.46). Blast search of the NCBI database suggested these epitopes do not occur in other proteins.

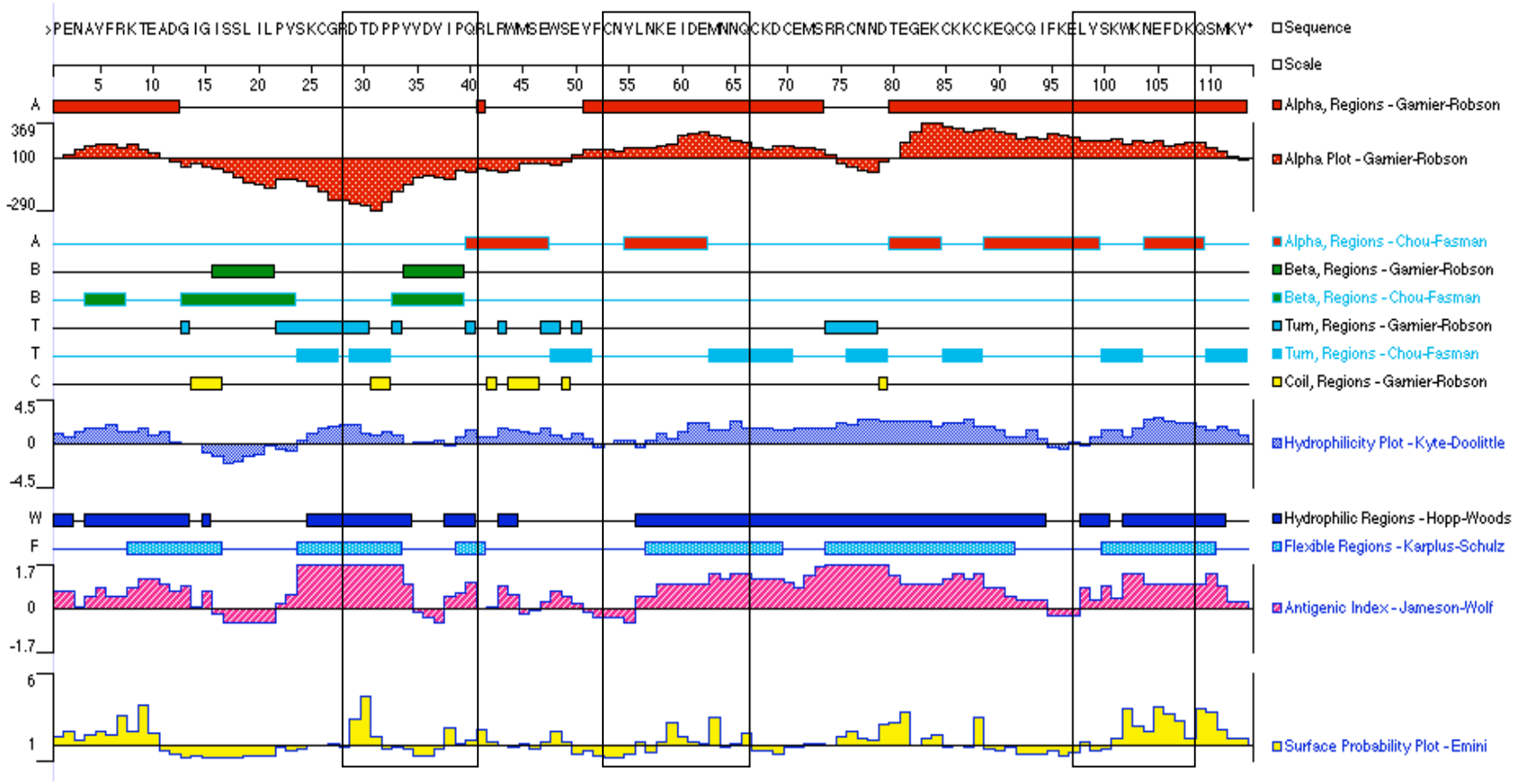
>PENAYFRKTEADGIGISSLILPYSKCGRDTDPPYVDVIPQRLRMMSEWSEYFCNYLNKEIDEMNNQCKDCEMSRRCNNDTEGEKCKKCEQCQIFKELYSKWKNEFDKQSMKY*
Sequence
Scale
Alpha, Regions - Gamier-Robson
Alpha Plot - Gamier-Robson
Alpha, Regions - Chou-Fasman
Beta, Regions - Gamier-Robson
Beta, Regions - Chou-Fasman
Turn, Regions - Gamier-Robson
Turn, Regions - Chou-Fasman
Coil, Regions - Gamier-Robson
Hydrophilicity Plot - Kyte-Doolittle
Hydrophilic Regions - Hopp-Woods
Flexible Regions - Karplus-Schulz
Antigenic Index - Jameson-Wolf
Surface Probability Plot - Emini

Fig. 5.44. Analysis of the final 133 amino acids of Mal6p1.314 DBLα domain using Protean/Lasergene software (DNAstar, Inc), showing predictions of alpha helical and beta sheet regions (Garnier-Robson, Chou-Fasman and Eisenberg plots), hydrophobicity (Kyte-Doolitle plot), flexible regions (Karplus-Schulz plot), antigenicity (Jameson-Wolf index) and surface exposure probability (Emini plot). Potential peptides for immunisation (DTDPPVVDYIPQ) (CNVLNKEIDEMNNQ) and (LVSKWKN(E/Q)FDK) are boxed.

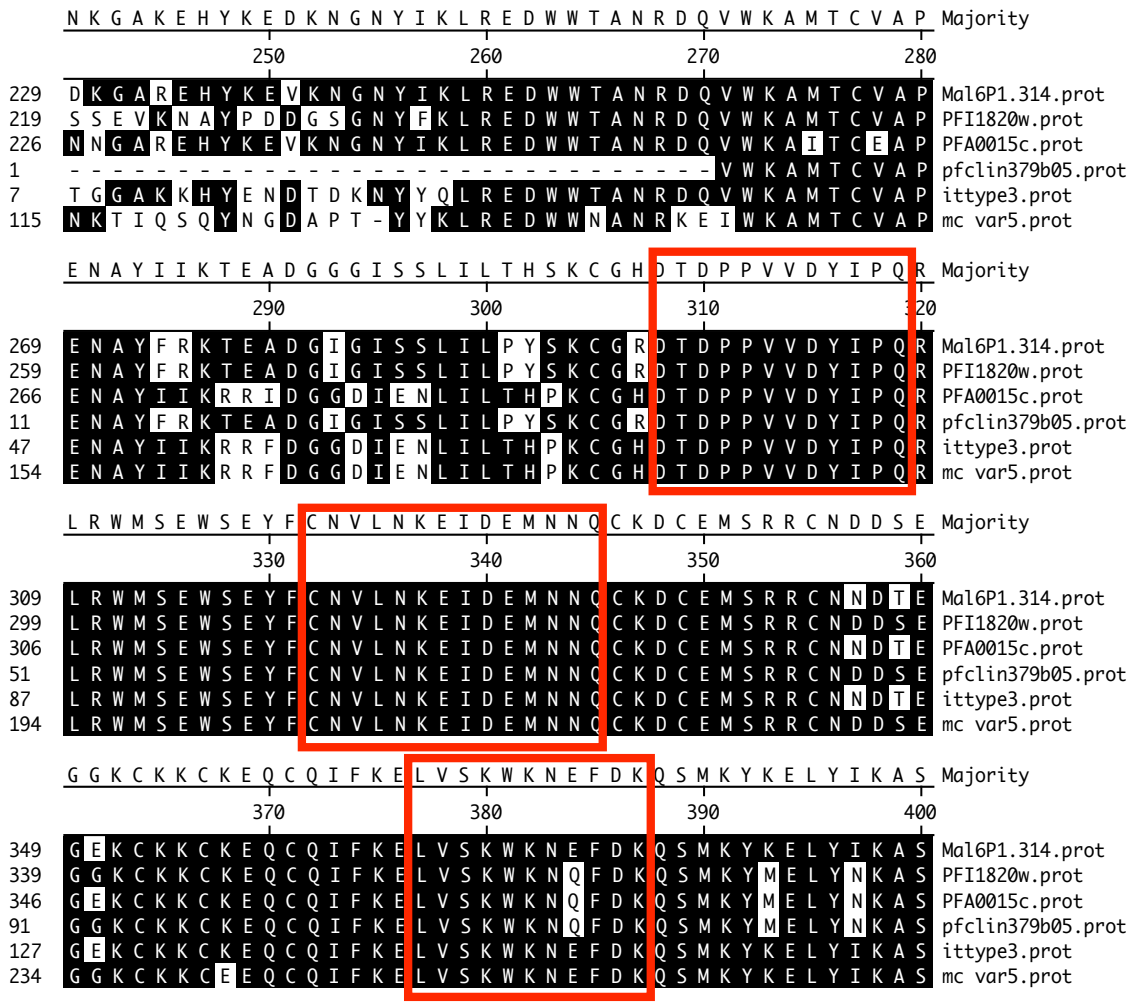

Fig. 5.45. Position of three potential immunogenic peptides (DTDPPVVDYIPQ) (CNVLNKEIDEMNNQ) and (LVSKWKN(E/Q)FDK) (boxed) on clustal W alignment of type3 amino acid sequences; mal6p1.314, pfi1820w and pfa0015c from 3D7, pfclin379b05 from Ghanaian clinical isolate (www.sanger.ac.uk), ittype3.pot from IT/FCR3 strain and mc *var5* from Malayan Camp.

A B

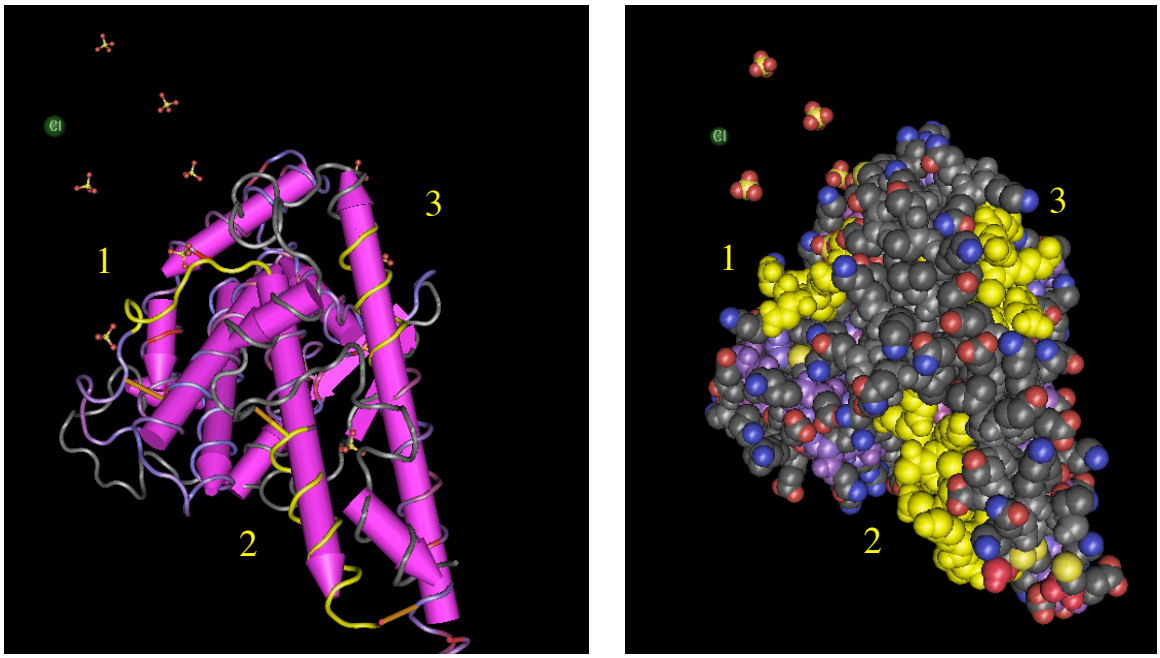

Fig. 5.46. Cn3D generated worm (A) and spacefill (B) images of Mal6P.314 amino acid sequences mapped onto the known structure of EBA175 F2 domain (PDB number 1ZRL) (Tolia *et al.* 2005). Peptides DTDPPVVDYIPQ (1), CNVLNKEIDEMNNQ (2) and LVSKWKN(E/Q)FDK (3) are indicated in yellow.

Two peptides are better than one for raising polyclonal antigen as this increases the immunization success rate of obtaining antibodies that recognize the protein from 75% to 95% (reference http://uk.eurogentec.com). Due to the E/Q discrepancy in the third peptide LVSKWKN(E/Q)FDK, the two peptides chosen were:

Peptide 1. DTDPPVVDYIPQ

Peptide 2. CNVLNKEIDEMNNQ

As described, both peptides are totally conserved in all available published type 3 DBLα domains, including the three from 3D7, and showed no homology to any other proteins (*P. falciparum*, human, or otherwise) by NCBI blast homology search. Both are hydrophilic with a high antigenic index (Jameson-Wolf and Kyte-Doolittle plots; Fig. 5.44), and are thus likely to be surface exposed with good antigenic potential. Peptide 2 is likely to resemble native protein secondary structure, as is it predicted helical by structural modelling and Garnier-Robinson prediction. As such, antibodies recognising this peptide are likely to recognise native protein such as in immunoflourescence. Peptide 1 is less likely to resemble native protein conformation as it is predicted to be disordered by Protean analysis. Antibodies recognising this epitope will potentially recognise denatured proteins such as in a Western blot. A terminal cysteine would be added to peptide 1 to facilitate coupling to the carrier (final sequence DTDPPVVDYIPQ +C).

5.6.3 Preimmune sera analysis

Two host animals were required for immunisation. The more commonly used and appropriate host species were hen and rabbit. To decide which species would be used, 5 preimmune hen egg yolks and 5 preimmune rabbit sera were obtained from Eurogentec (Belgium), and the preimmune antibody repertoire from the animals was tested for recognition of infected and uninfected red blood cells.

Preimmune hen egg samples from 5 candidate hens were obtained as fresh yolk. Preimmune hen yolk IgY purification was carried out using the Promega Eggstract

kit. Extracted IgY concentration (2-4 mg/ml) was within the expected concentration of IgY from yolk (Eggstract kit manual).

To determine how pure the sample was, the 1 µl (2-4 µg) of the IgY extractions was run on a reducing SDS-PAGE gel and either stained with SimplyBlue (Fig. 5.47A) or transferred onto a PVDF membrane and probed with a goat anti-chicken HRP-conjugated secondary antibody (Fig. 5.47B). The heavy (67 kDa) and light (27 kDa) IgY chains were detected by SimplyBlue and by goat anti-chicken HRP-conjugated secondary antibody probing. Fig. 5.47 shows that the purified IgY extract was successful and was relatively pure.

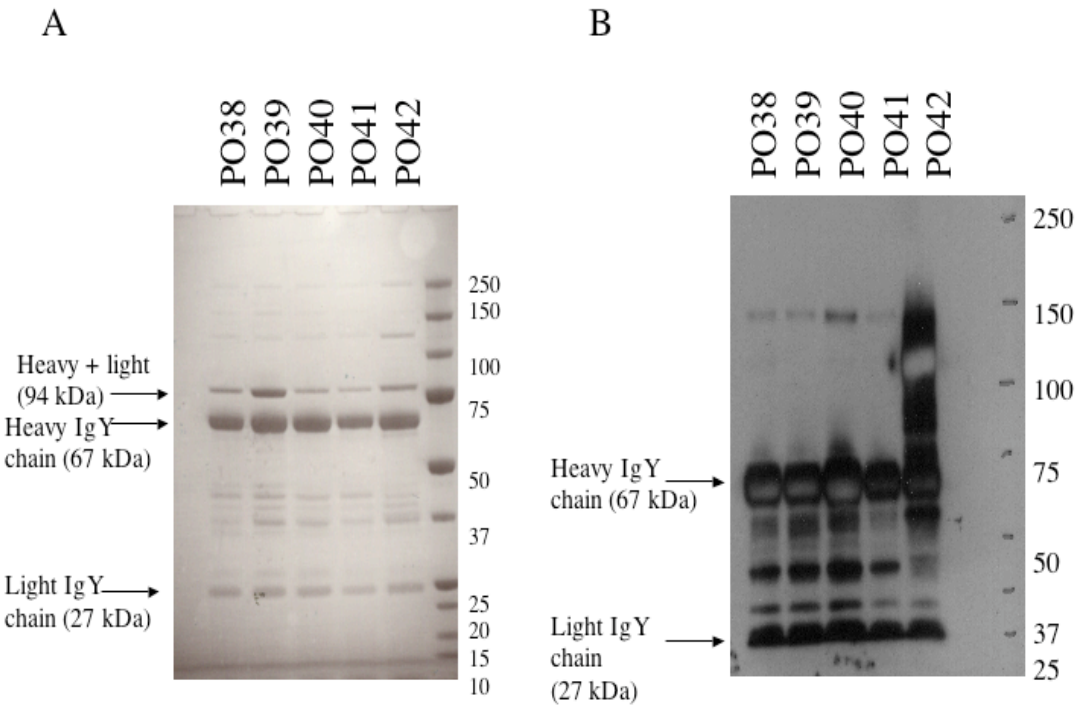

Fig. 5.47. IgY extractions (PO38-42). A) 1 µl of each IgY extract (2-4 mg/ml) was run out on a gradient 3-8% reducing tris-acetate SDS-PAGE gel and all proteins were visualized by staining with SimplyBlue. B) Proteins transferred to PVDF membrane and detected with an anti-chicken HRP- conjugated secondary antibody

(1:1000, 1 hr incubation). IgY was visualised using enchanced chemiluminescence and exposure to X-ray film. The protein ladder was a pre-stained precision protein molecular weight marker (Bio-Rad).

5.6.4 Preimmune recognition of IE proteins by Western blot

Western blots were used to determine whether the antibodies in the preimmune sera or yolk extract recognised proteins from infected erythrocytes (IE). Proteins extracted from an asynchronous culture of 3D7 were run on a 3-8% reducing acrylamide gel. The proteins were transferred to PVDF membrane. The membrane was cut into strips for incubation in the sera at 1:100 dilution. The appropriate secondary antibody (anti-chicken or anti-rabbit) conjugated to HRP was used to detect primary antibody binding.

Each IgY extract showed some recognition of IE proteins (Fig. 5.48). PO40 IgY bound the IE proteins the most strongly and PO41 and PO42 showed the least binding in the 155-270 kDa range. The Western blot was repeated to try to improve the quality of protein detection but this was not successful. It was decided to rely on affinity purification to reduce background antibody affinity for IE proteins.

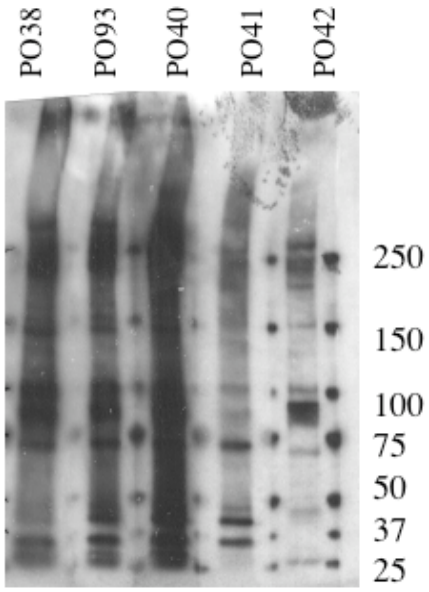

Fig. 5.48. Western blot of an asynchronous culture of 3D7 (gift from JP Semblat) using preimmune IgY extracts. Extracted IE proteins were separated by reducing SDS-PAGE on a 3-8% tris-acetate gel (1 hr, 150 V). Proteins were transferred to PVDF membrane (1 hr, 30V) and the membrane was cut into strips. Each strip of membrane was blocked overnight in milk and then incubated in the IgY extract (PO38-42) at 1:100 dilution for 1 hr. HRP-conjugated anti-chicken secondary antibody (1:1000, 1 hr incubation) was used to bind IgY. Bands were visualised using enchanced chemiluminescence and exposure to X-ray film. The protein ladder was a pre-stained precision protein molecular weight marker (Bio-Rad).

Each preimmune rabbit sera also showed some recognition of IE proteins, with strong recognition of proteins in the PfEMP1 size (155-270 kDa) range (Fig. 5.49). Rabbit S170 showed the lowest levels of host protein recognition. All rabbits serum recognized proteins around size of known type 3 PfEMP1 (153 kDa), and strong recognition of proteins around 100 kDa and 250 kDa.

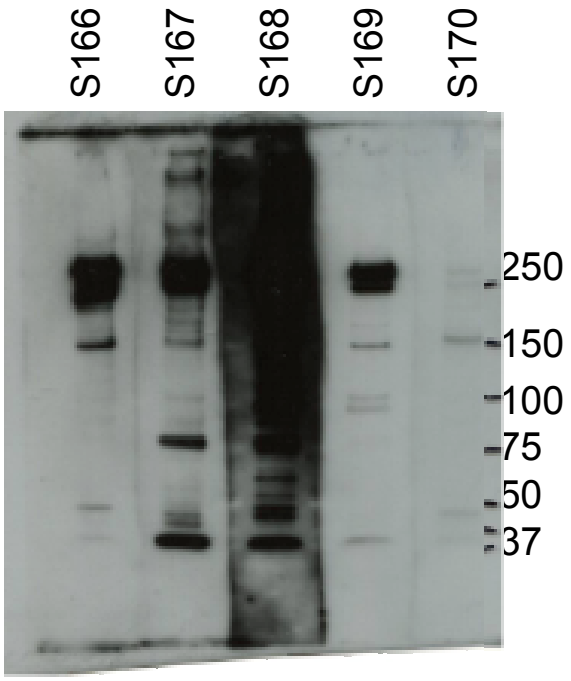

Fig. 5.49. Western blot of an asynchronous culture of 3D7 (gift from JP Semblat) using preimmune rabbit sera. Extracted IE proteins were separated by reducing SDS-PAGE on a 3-8% tris-acetate gel (1 hr, 150 V). Proteins were transferred to PVDF membrane (1 hr, 30V) and the membrane was cut into strips. Each strip of membrane was blocked overnight in milk and then incubated in the preimmune rabbit sera (S166-S170) at 1:100 dilution for 1 hr. HRP-conjugated anti-rabbit secondary antibody (1:1000, 1 hr incubation) was used to detect bond IgG. Bands were visualised using enchanced chemiluminescence and exposure to X-ray film. The protein ladder was a pre-stained precision protein molecular weight marker (Bio-Rad).

5.6.5 Preimmune recognition of IE proteins on live cells in immunoflourescence assay (IFA)

Samples of *P. falciparum* culture were used to assess whether the preimmune sera or yolk IgY would recognise native proteins in an immunoflourescence assay (IFA). As many parasite proteins that are exported to the surface of the erythrocyte are seen on the surface at pigmented trophozoite stage (e.g. PfEMP1), the IFAs were performed when the culture contained a majority of parasites at the pigmented trophozoite stage (4%), although some ring stage parasites were also present (1%). As such any recognition of host erythrocyte proteins, or *plasmodium* protein on the IE suface at ring or pigmented trophozoite stage, should be detected.

A TM284 *P. falciparum* culture (gift from A Raza) was incubated for 1 hour in preimmune sera (1:10) or preimmune IgY (1:10) in PBS/1% BSA. The IgY was then washed off and the cells were incubated in alexa 488 conjugated secondary antibody 1:1000 and PBS/DAPI/BSA1% for 1 hour in the dark. Secondary incubation was washed off and the live cells were viewed under fluorescence at 100x magnification.

Representative images from each of the IFA are shown in Fig. 5.50 and a summary is given in Table 5.11. Where recognition occurred, DAPI staining revealed fluorescing cells were not specifically infected or uninfected.

A

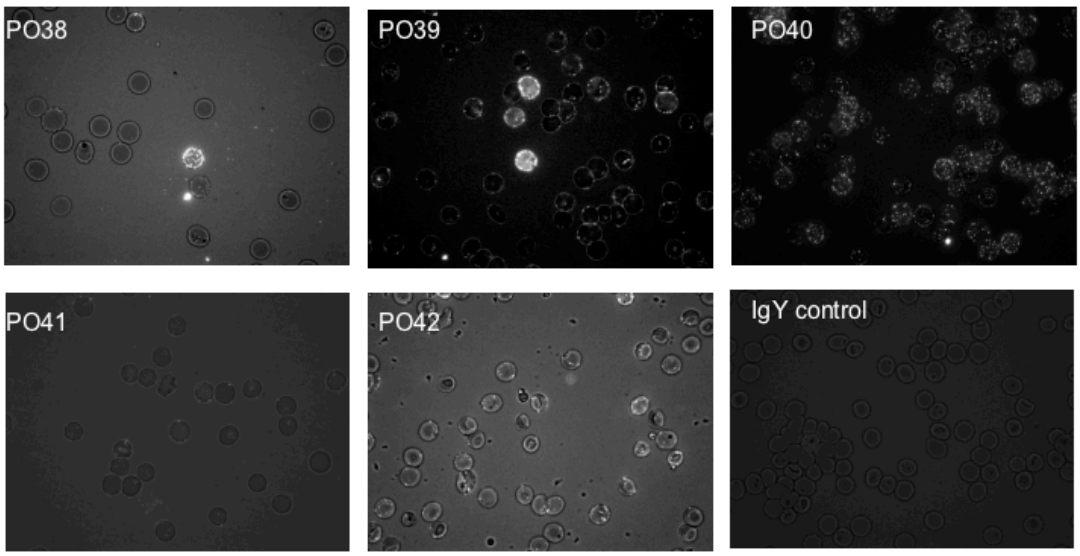

B

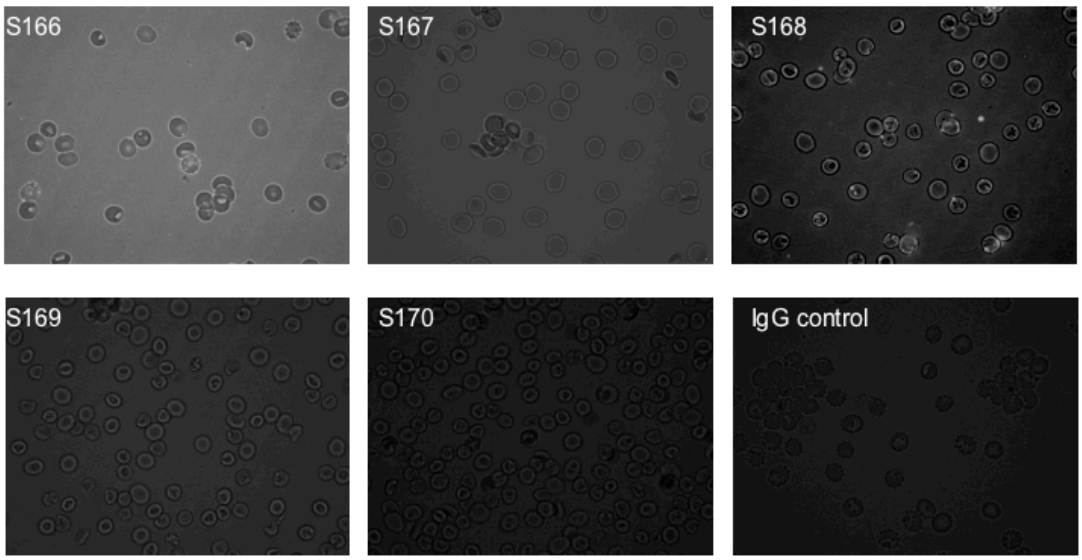

Fig. 5.50. Representative images of immunoflourescence assays (IFA) on TM284 infected IE. Cells at 2% haematocrit and cultures at 4% trophozoite, 1% ring stage. A) Cells were incubated with chicken pre-immune IgY extract (1:10) and then with alexa488-conjugated goat anti-chicken secondary antibody (1:1000). B) Cells were incubated with rabbit preimmune serum (1:10) and then with alexa488-conjugated goat anti-rabbit secondary antibody (1:1000).

Sample	Preimmune sera	Immunofluorescence observed
Hen egg IgY extracts	PO38	Occasional cells fluoresced strongly plus occasional speckles in other cells.
	PO39	Occasional cells fluoresced strongly plus moderate speckles in most cells.
	PO40	All cells fluoresced strongly.
	P041	Rare fluorescence of a few speckles per cell.
	PO42	Moderate speckling in every cell.
Rabbit Sera	S166	Occasional fluorescence of few speckles per cell.
	S167	No fluorescence.
	S168	Occasional fluorescence of few speckles per cell.
	S169	No fluorescence.
	S170	No fluorescence.
Secondary controls	Chicken control	No fluorescence.
	Rabbit control	No fluorescence.

Table 5.11 Preimmune IFA summary.

5.6.6 Animal choice and justification

Chickens were chosen for immunization. Yolk have more IgY than rabbit sera has IgG and more yolk volume is received from chicken than sera from rabbits. Thus chicken immunization provides more antibody per animal. Avian antibody is expected to be less cross-reactive to mammalian proteins than rabbit antibody. Although the immunofluorescence data suggested rabbit preimmune sera showed lower recognition of IE proteins, all rabbit preimmune sera showed a high level of recognition of proteins around the size of type 3 PfEMP1 (153 kDa).

Chickens SH19 and SH20 were chosen because they showed the lowest levels of preimmune recognition of infected erythrocyte proteins in Western blot and

immunofluorescence. This suggested they might yield specific antibody with low background of non-specific signal. Any remaining non-specific recognition in the post-immunisation polyclonal antibody mix will be reduced by affinity purification against the two immunizing peptides.

5.6.7 Generation of affinity-purified polyclonal antibody

Chickens PO41 and PO42 were immunised with peptides DTDPPVVDYIPQC (peptide 1) and CNVLNKEIDEMNNQ (peptide 2) by Eurogentec (Belgium).

Eggs were collected in weekly batches, and received as fresh pooled yolk. IgY was extracted from days 51-98 post immunization, and extracted IgY reconstituted in PBS to the original yolk volume for each weekly pool (Table 5.2). Affinity purification against a mixture of the two peptides was perfomed using the Sulfolink technology (Promega) for 4/7 pools. This exploits the free sulfhydryl groups on the terminal cysteines of the peptides to immobilize the peptides on a SulfoLink Resin (see Fig. 5.51 and materials and methods). IgY was eluted in 6 ml elution buffer, due to its low pH, then buffer exchanged into 0.5 ml PBS.

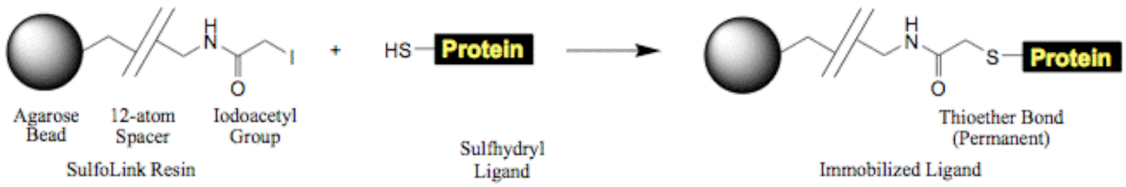

Fig. 5.51. SulfoLink Resin affinity purification method. Diagram taken from Sulfolink kit 20325 manual, Pierce.

Affinity-purified IgY from days 79-85 (dates 25/04-02/05) were used in all following experiments, unless stated otherwise.

5.6.8 Affinity-purified antibody recognises target peptides by ELISA

To determine whether the pre-immune, post-immune and affinity-purified antibodies had affinity for the peptides, an ELISA was performed. Peptides were immobilised onto ELISA plate wells overnight at 4ºC. Antibody was incubated in the plates and non-bound antibody was removed by washing before incubation with 150 µl of peroxidase conjugated goat anti-chicken IgG diluted 1:1000, for 1 hour. TMB Substrate was added to each well and the plate was left to develop for 30 min in the dark, before the reaction was stopped with sulfuric acid. The concentration of bound antibody was assessed by absorbance at 450 nm. These are shown as mean ± standard error (SE), Fig. 5.52.

The ELISA data (Fig. 5.52) showed preimmune sera had low affinity for the peptides, and immunisation resulted in IgY with affinity for both peptides. The pool of antibodies from the immune yolks also has increased affinity for BSA and milk block compared to IgY extracted from the yolks of the hens pre-immunisation. However, after affinity purification, the resulting antibody pools from both hens had increased specificity for both peptides, and greatly reduced affinity for BSA and milk block. Both pools of affinity-purified antibodies had equally high affinity for the 2 peptides, suggesting that both peptides had elicited a successful immune response in each hen.

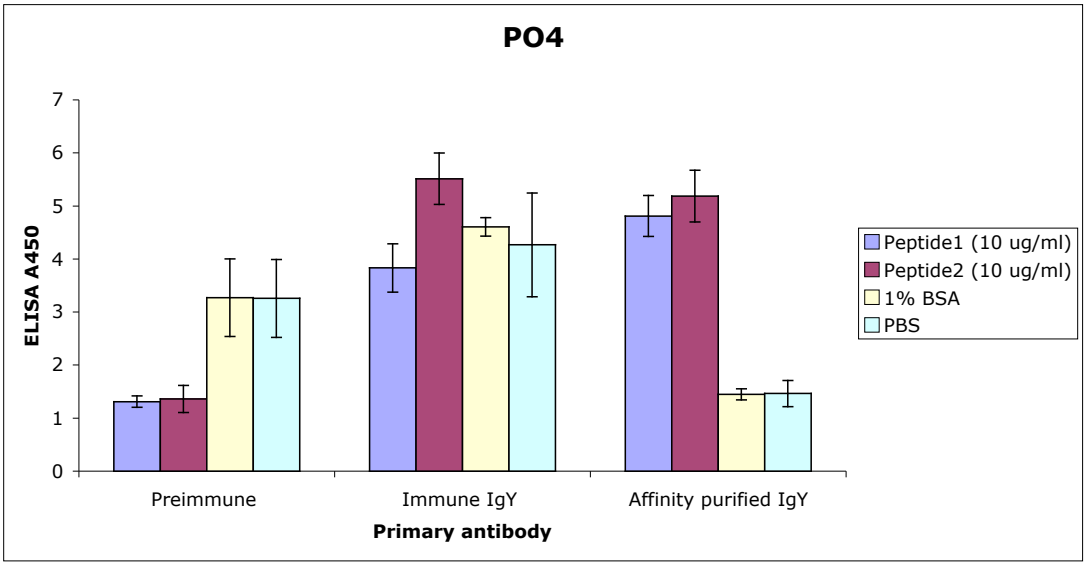

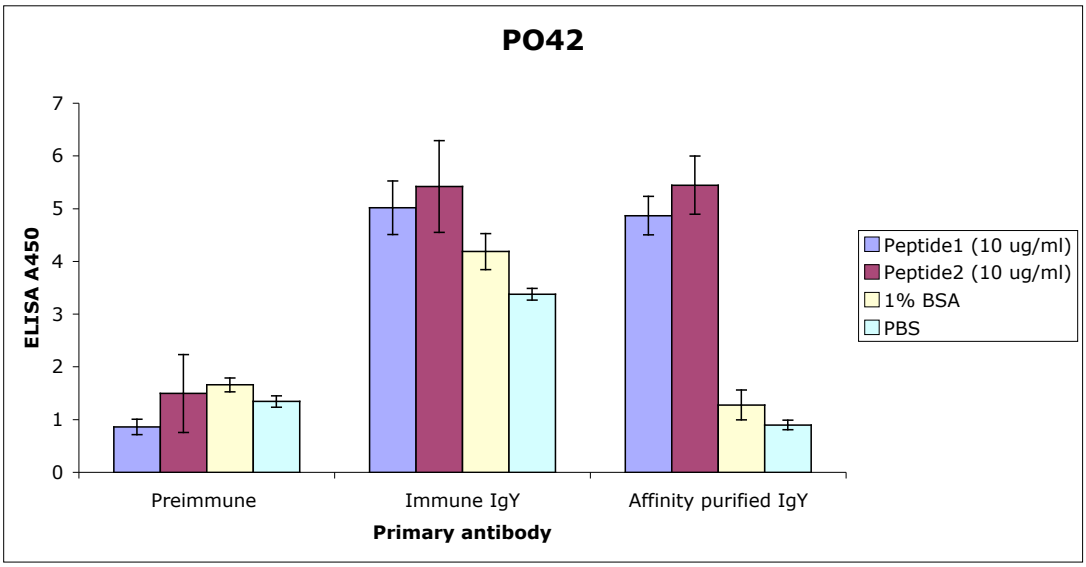

Fig. 5.52. ELISA showing affinity of preimmune, post immune IgY and affinity-purified IgY, purified against both peptides simultaneously. Antibody was incubated in ELISA plate wells coated (overnight at 4ºC) with 10 μg/ml peptide 1, 10 μg/ml peptide 2, 1% BSA in PBS or PBS alone. Non-bound antibody was removed by washing before incubation with 150 μl of peroxidase conjugated goat anti-chicken IgG diluted 1:1000. Detection was measured as absorbance at 450 nm after incubation with TMB Substrate then sulfuric acid. These are shown as mean ± standard error (SE).

5.6.9 Affinity purified antibody recognises band of approximately 150 kDa

To assess whether the antibody recognised type 3 PfEMP1 in a protein extract of 3D7 culture. 6.5 μl of protein extract was separated by denaturing SDS-PAGE on a 3-8% tris-acetate gel, and the proteins were transferred to PVDF membrane. The membrane was blocked overnight in milk. At the same time, 1:100 dilution of the immune IgY or affinity purified IgY from chickens PO41 and PO42 was pre-incubated overnight in blocking buffer with a small strip of PVDF membrane to remove antibodies that bound non-specifically to the membrane. The blocked membrane was incubated for 1 hour with the immune or affinity purified IgY. Non-bound antibody was then removed by washing, and bound antibody detected by incubation with secondary HRP-conjugated anti-chicken antibody followed by enchanced chemiluminescence and exposure to X-ray film.

The pre-purification immune IgY from both chickens showed a high level of non-specific affinity to many proteins IE proteins (Fig. 5.53) as was predicted by ELISA (Fig. 5.52). The affinity-purified antibody from hen PO41 did not show any strong protein recognition; a faint band at approximately 150 kDa may be type 3 PfEMP1. The affinity-purified antibody from hen PO42 recognised a protein of approximately 150 kDa on SDS-PAGE by Western blot that is specific to infected erythrocytes and may be type 3 PfEMP1. The three type 3 PfEMP1 in 3D7, Mal6p1.314 (153.3 kDa), Pfa0015c (153.3 kDa) and pfi1820w (152.0 kDa), are all too close in size to differentiate these by migration. There is also a strong band at approximately (180 kDa).

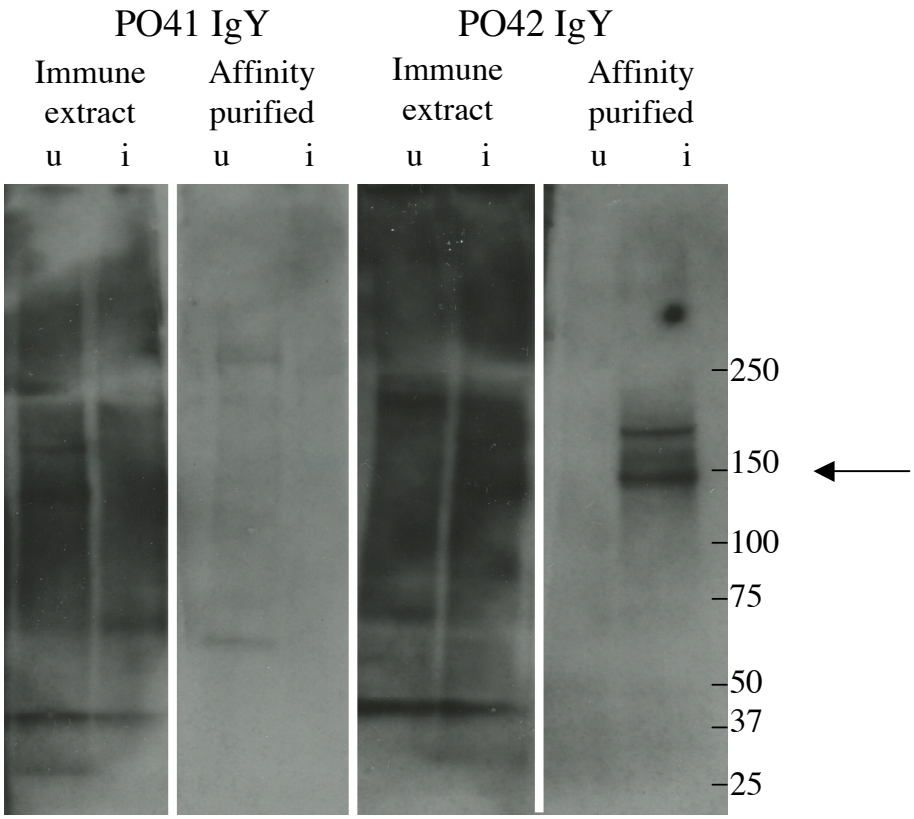

Fig. 5.53. Western blot of an asynchronous culture of 3D7 using immune IgY extract and affinity-purified IgY from PO41 (left) or PO42 (right). Triton soluble protein extraction from uninfected erythrocytes (u) and erythrocytes infected with a 10% mixed stage culture of 3D7 (i) were run on a reducing SDS-PAGE on a 3-8% tris-acetate gel (1 hr, 150 V). Proteins were transferred to PVDF membrane (1 hr, 30V) and the membrane was cut into 4 strips. Each strip of membrane was blocked overnight in milk and then incubated with immune IgY extract or affinity-purified IgY from PO41 (left) or PO42 (right) at 1:100 dilution for 1 hr and 1 hr secondary incubation with HRP-conjugated anti-chicken secondary antibody (1:1000). Bands were visualised using enhanced chemiluminesence and exposure to X-ray film. An approximately 150 kDa protein, the size of a type 3 PfEMP1, is indicated (arrow). The ladder was pre-stained precision protein molecular weight marker (BioRad).

5.6.10 Affinity purification against peptides separately

Affinity purification was also carried out on the two peptides separately for immune IgY from chicken PO42. Only chicken PO42 IgY was used as the PO42 IgY affinity purified against both peptides showed higher recognition of the band of 150 kDa, which was thought to be the type 3 PfEMP1, than the PO41 IgY affinity purified against both peptides. Affinity purification was performed as before using Sulfolink resin affinity purification method. The purified antibody showed recognition of the appropriate peptide, and low affinity for PBS/BSA (Fig. 5.54). Purification with peptide 2 and both peptides together were successful, with enriched IgY with affinity for the appropriate wells. Purificationagainst peptide 1 separately was less successful, with low specific affinity for peptide 1.

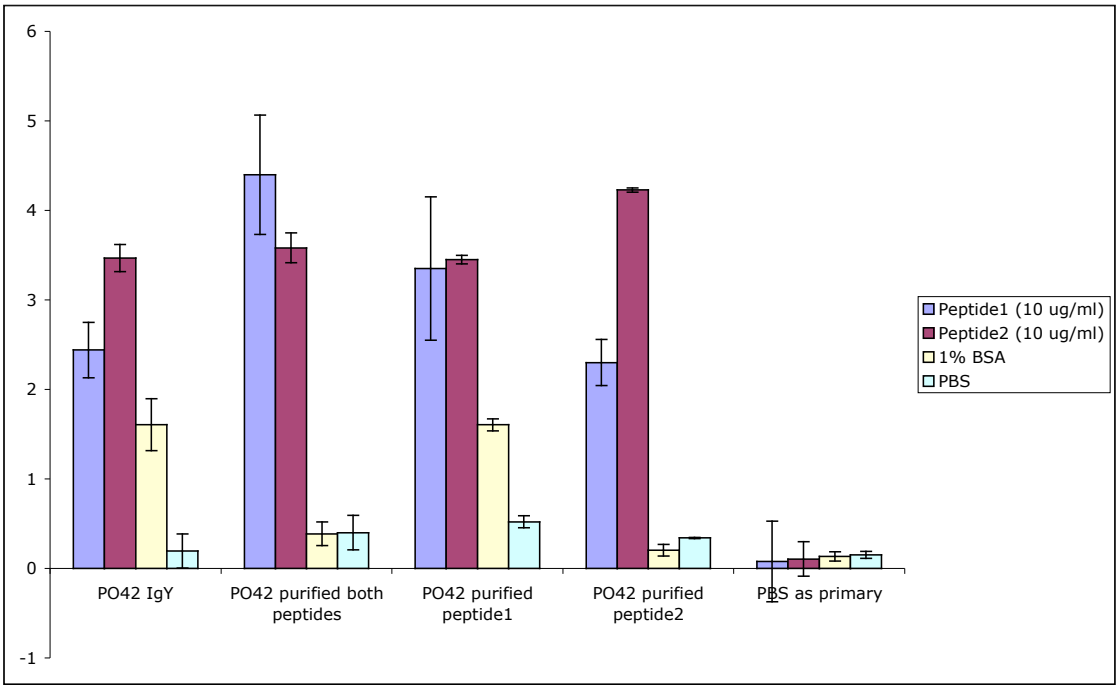

Fig. 5.54. ELISA showing affinity of post immune non-purified PO42 IgY and PO42 IgY purified with both peptide, or peptides 1 or 2 separately. Antibody was incubated in ELISA plate wells coated (overnight at 4ºC) with 10 µg/ml peptide 1, 10 µg/ml peptide 2, 1% BSA in PBS or PBS alone. Non-bound antibody was removed by washing before incubation with 150 µl of peroxidase conjugated goat anti-chicken IgG diluted 1:1000. Detection was measured as absorbance at 450 nm after incubation with TMB Substrate then sulfuric acid. These are shown as mean ± standard error (SE).

To assess the recognition specificity for IE proteins of the peptide1- and peptide 2-purified antibodies a Western blot was performed. The 3D7 culture protein extract used in Fig. 5.53 was separated again by denaturing SDS-PAGE on a 3-8% tris-acetate gel, and the proteins were transferred to fresh PVDF membrane. The membrane was blocked overnight in milk. At the same time, 1:100 dilution of chicken PO42 immune IgY affinity purified against peptide 1 or peptide 2 was pre-incubated overnight in blocking buffer with a small strip of PVDF membrane to remove antibodies that bound non-specifically to the membrane. The blocked membrane was incubated for 1 hour with the affinity purified IgYs. Non-bound antibody was then removed by washing, and bound antibody detected by incubation with secondary HRP-conjugated anti-chicken antibody followed by enchanced chemiluminescence and exposure to X-ray film (Fig. 5.55).

Antibody purified against both peptides independently recognised a 150 kDa protein in *P. falciparum* protein extract but not in the uninfected erythrocyte controls (Fig. 5.55). Antibody affinity purified against peptide 1 showed weak recognition of type 3 protein, and also cross reacted with a host cell-derived protein at 240 and 260 kDa (possibly spectrin). Antibody affinity purified against peptide 2 gave a much stronger recognition of the type 3 protein at 150 kDa, but also cross-reacted with a parasite-derived protein at approx 270 - 300 kDa, possibly non-type3 PfEMP1. Recognition of the triton-soluble fraction by the antibody purified against both peptides (Fig. 5.53, above) more closely resembles that purified against peptide 2 only. Thus, it is likely that the majority of IgY in the purified antibody pool recognises peptide 2.

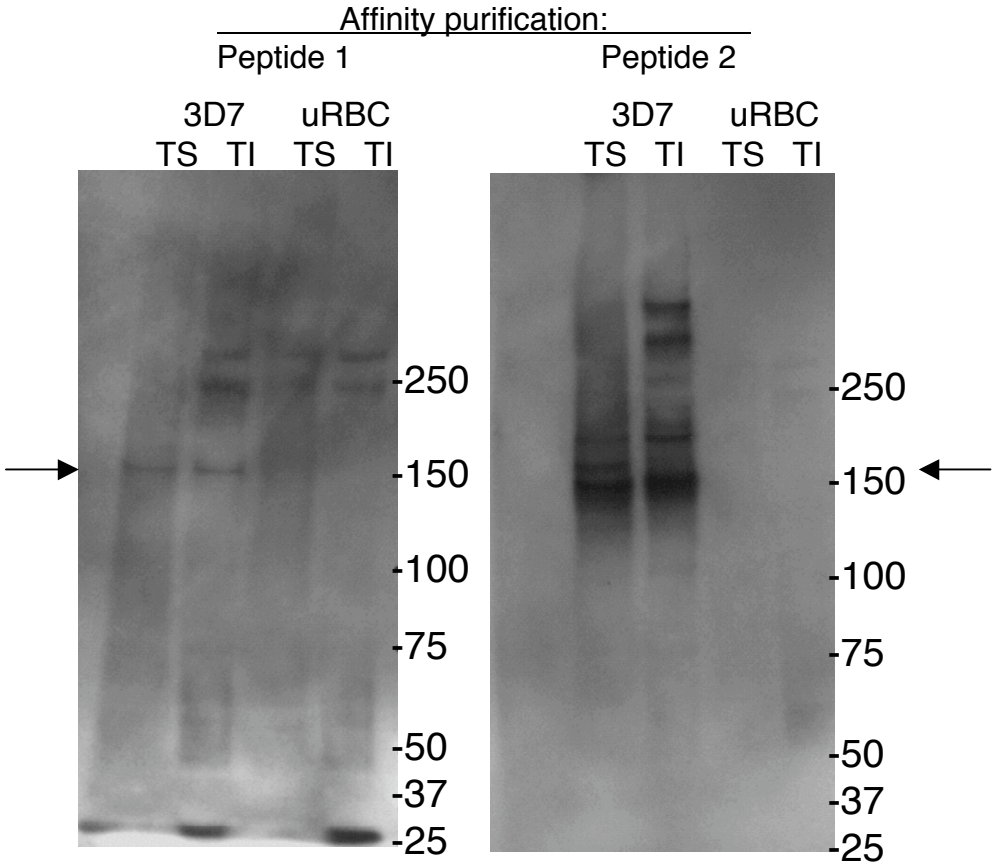

Fig. 5.55. Triton soluble (TS) and Triton insoluble (TI) protein extractions from erythrocytes infected with a 6% trophozoite stage culture of 3D7 and uninfected erythrocytes control were run on a reducing 3-8% tris-acetate gel SDS-PAGE and proteins were transferred to PVDF membrane. The membrane was blocked overnight in milk and probed with 1:1000 dilution of PO42 IgY affinity-purified against peptide 1 (left) or peptide 2 (right). Secondary incubation was with HRP-conjugated anti-chicken secondary antibody (1:1000). Bands were visualised using enhanced chemiluminesence and exposure to X-ray film. A protein of the correct size for a type 3 PfEMP1 (153 kDa) is indicated (arrow). The protein ladder was a pre-stained precision protein molecular weight marker (Bio-Rad).

5.6.11 The 150 kDa band detected with the antibody appears to be trypsin insensitive

The pigmented trophozoite culture was treated with 0.1-1mg/ml trypsin for 5 min, and then treated with trypsin inhibitor for 5 min, before protein extraction. The 150 kDa band detected with the antibody appears to remain trypsin insensitive, indicating it may be internal (Fig. 5.56).

In an attempt to verify the trypsin worked, the blot was repeated and probed for non-type 3 PfEMP1 with an antibody with affinity for the ATS region and complement receptor 1 which are expected to be trypsin sensitive at >10 μg/ml (Miller *et al.* 1977; Sharling *et al.* 2007). Unfortunately the Western blots were unsuccessful due to high background (PfEMP1 ATS) or no signal (CR1). However, the type 3 antibody cross-reacts with bands in the 270-300 kDa range in the 3D7 triton insoluble protein extracts which may be non-type 3 PfEMP1. These bands are reduced on addition of the trypsin at 1 mg/ml (Fig. 5.56), suggesting that the trypsinisation was effective.

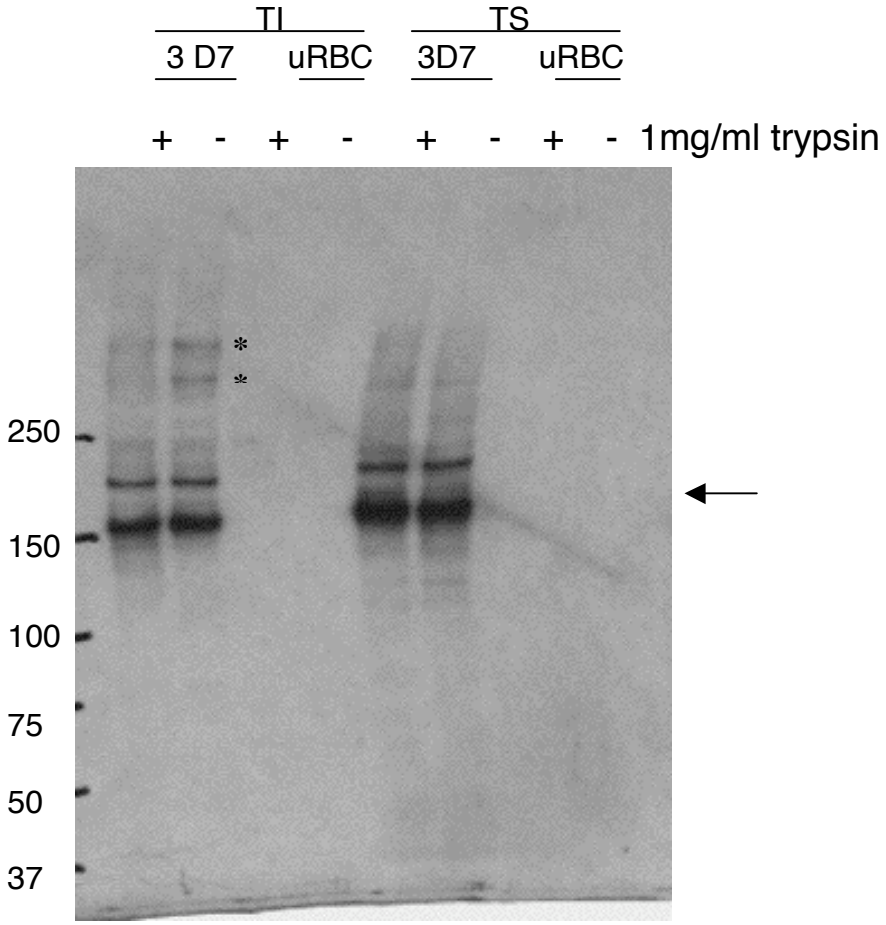

Fig. 5.56. Triton soluble (TS) and Triton insoluble (TI) protein extractions from uninfected erythrocytes (uRBC) and erythrocytes infected with a 6% trophozoite stage 3D7 culture (3D7) were run on a denaturing SDS-PAGE and probed with affinity-purified anti-type 3 antibody. Samples marked (+) were incubated with 1mg/ml trypsin for 5 min before protein extraction. The 153 kDa protein is marked with an arrow. Bands thought to correspond to non-type 3 PfEMP1, which reduce in intensity after trypsinisation, are indicated (*).The protein ladder was a pre-stained precision protein molecular weight marker (Bio-Rad).

5.6.12 Antibody recognises a protein of 150 kDa in HB3; a strain without a type 3 PfEMP1

The recent whole genome sequencing of parasite strain HB3 revealed that this strain was a natural knock-out for the type 3 PfEMP1. This explains "failure" of the type 3 alpha and epsilon PCR in HB3 gDNA in section 5.5.4.

HB3 parasites were cultured and protein samples collected from a culture of 7% trophozoites. Proteins were loaded on to four reducing 3-8% tris-acetate acrylamide gels, separated by SDS-PAGE, and transferred to PVDF membrane for Western blot (3 gels), or stained in SimplyBlue to record total protein loaded (1 gel). The three PVDF membranes were probed with preimmune IgY, immune IgY affinity purified against peptide 1, or immune IgY affinity purified against peptide 2. Probing with immune IgY affinity purified against peptide 2 showed strong recognition of a 150 kDa protein in HB3, as well as in 3D7 rings and pigmented trophozoites (Fig. 5.57). This suggests the 150 kDa band is specific to infected erythrocytes, but may not be specific to a type 3 PfEMP1.

In order to see if this cross reactivity was a problem due to using reducing SDS-PAGE, the Western blot with the same antibody preparation was repeated using native (non-reducing) gels. No proteins were recognized by the antibody after membrane were probed with preimmune IgY or immune IgY affinity purified against peptide 1 or 2.

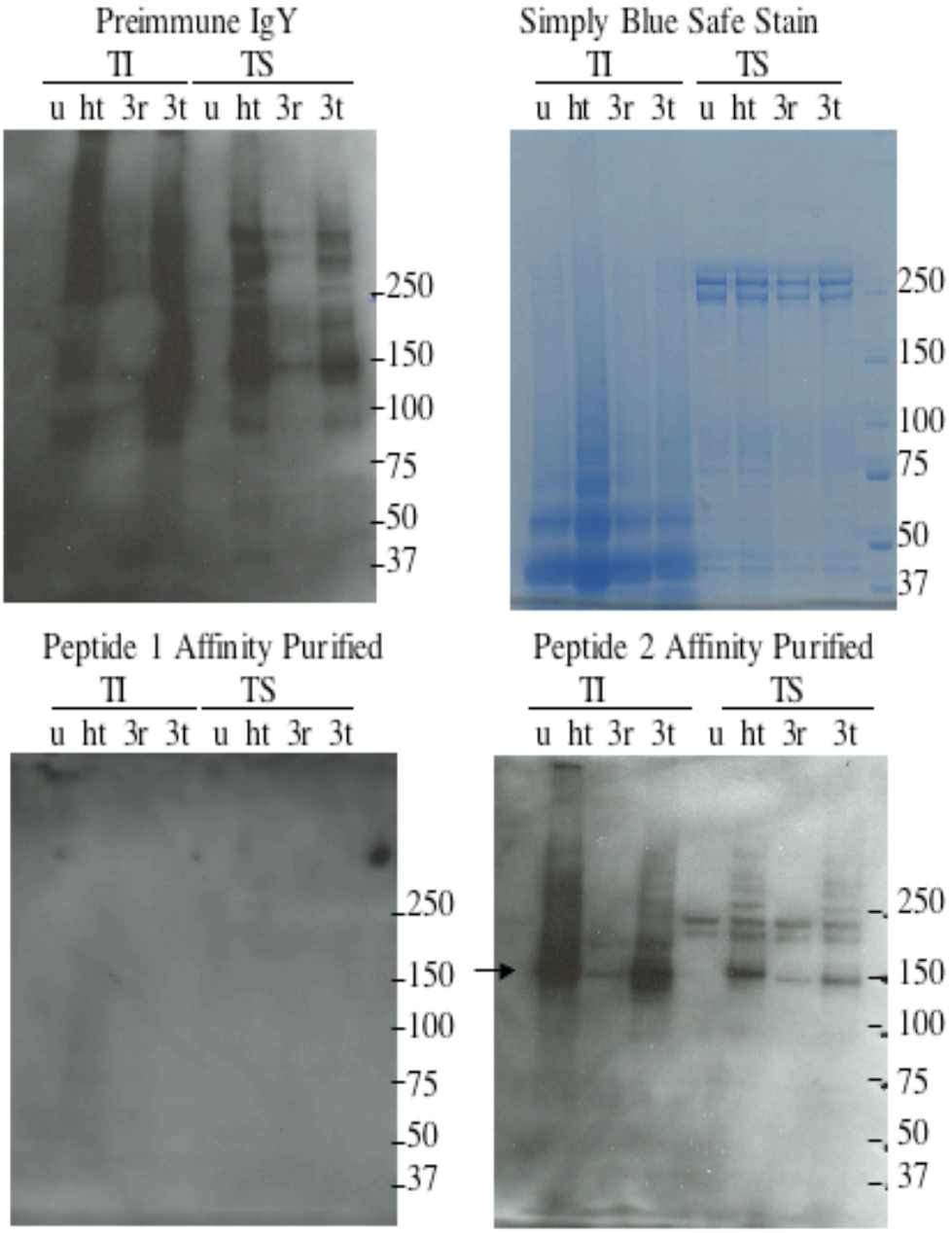

Fig. 5.57. Triton soluble (TS) and Triton insoluble (TI) protein extractions from uninfected erythrocytes (U), HB3 culture 7% trophozoites (ht), 3D7 culture 6% rings (3r) and 3D7 culture 6% pigmented trophozoites (3t) were loaded onto reducing 3-8% tris-acetate acrylamide gels, separated by SDS-PAGE, and transferred to PVDF membrane for Western blot or stained in SimplyBlue (top right) to record total

protein loaded. Membranes were blocked in 5% milk o/n and probed with preimmune IgY (top left), immune IgY affinity purified against peptide 1 (bottom left), or immune IgY affinity purified against peptide 2 (bottom right) for 1 hr. After washing, secondary incubation was with HRP-conjugated anti-chicken secondary antibody (1:1000). Bands were visualised using enhanced chemiluminesence and exposure to X-ray film. A protein of 153 kDa is recognised in all infected erythrocyte lanes, including HB3, by peptide 2-affinity purified antibody (indicated with an arrow). The protein ladder was a pre-stained precision protein molecular weight marker (Bio-Rad).

5.6.13 Antibody recognises a protein on HB3 by fixed IFA

A fixed IFA was used to assess whether the antibody would recognise uninfected erythrocytes, and erythrocytes infected with 3D7 or HB3. 3D7 and HB3 *P. falciparum* cultures were smeared on to a glass slide and fixed with acetone. The slides were incubated for 1 hour with preimmune IgY or immune IgY (affinity purified against both peptides) both 1:10 in PBS/1% BSA, or with PBS/1% BSA alone. Unbound antibody was then washed off and the slides were incubated in alexa 488 conjugated secondary antibody 1:1000 and PBS/DAPI/1%BSA for 1 hour in the dark. Secondary incubation was washed off and the fixed cells were viewed under fluorescence at 100x magnification. The IFA on 3D7 revealed the affinity-purified antibody recognized infected erythrocytes only (Fig. 5.58). However, repeating the IFA on HB3-infected erythrocytes also resulted in recognition of IE by the affinity-purified antibody (Fig. 5.58). For both 3D7 and HB3 cultures, uninfected erythrocytes did not fluoresce with preimmune IgY or PBS/1%BSA alone (Fig.

5.58). As only infected erythrocytes were recognised by the affinity purified antibody, the cross reactivity must be to a parasite-derived protein, as seen with the Western blot (Fig. 5.58). It is likely there is cross reactivity to high molecular weight PfEMP1, as suggested by faint bands (>250 kDa (*), Fig. 5.56), as well as with the band of 150 kDa in HB3, which is also likely to exsist in 3D7. All erythrocytes, infected and uninfected, fluoresced with immune IgY in live IFA (data not shown). Whether there is any specific recognition of the type 3 PEMP1 in 3D7 is not clear.

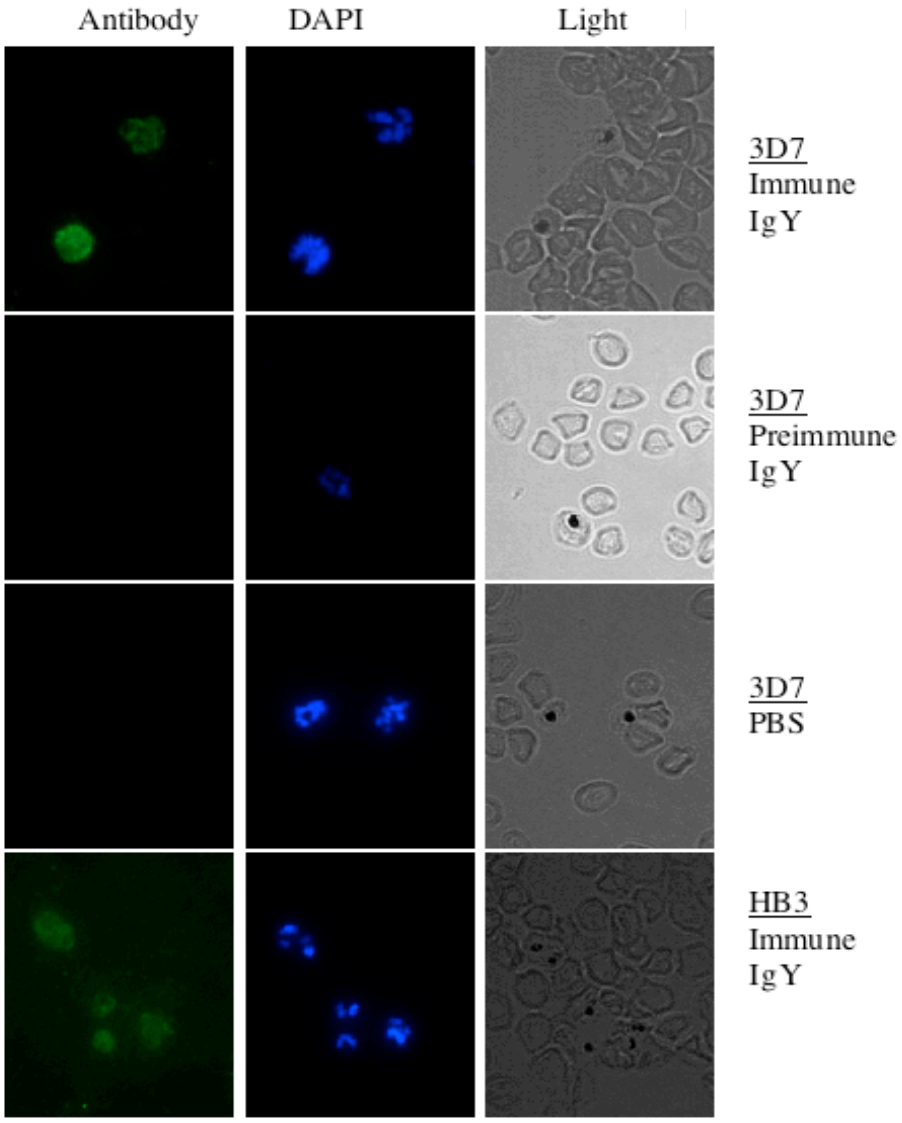

Fig. 5.58. *P. falciparum* cultures of 3D7 (6% pigmented trophozoites; upper 3 panels) and HB3 (7% pigmented trophozoites; bottom) were smeared onto slides and fixed with acetone. Slides were incubated for 1 hour in preimmune IgY, immune IgY extract affinity purified against peptides 1 and 2 together (all 1:10 in PBS/1% BSA), or PBS/1%BSA alone. The culture was then washed and the slides were incubated in alexa 488 conjugated secondary antibody 1:1000 and PBS/DAPI/1/%BSA for 1 hour in the dark. Secondary incubation was washed off and the fixed cells were viewed under fluorescence at 100x magnification. Representative images of 3D7 with preimmune IgY, affinity purified immune IgY extract and PBS/1%BSA alone, and HB3 with affinity purified immune IgY extract are shown. HB3 did not fluoresce with preimmune IgY or PBS/1%BSA alone.

5.7 Discussion

This chapter examined the type 3 *var* genes and PfEMP1 in a range of laboratory and field isolates. The hypotheses to be examined in this chapter were threefold. Firstly, that there would be a high level of conservation in all type 3 *var* genes in laboratory strains and field isolates, but that the timing of expression may be unusual due to the lack of a regulatory intronic promoter which controls the silencing of other *var* genes (Deitsch 2001; Calderwood *et al.* 2003; Frank *et al.* 2006). Secondly that there might be a link between type 3 *var* gene transcription and cerebral malaria, due to the association of group A *var* transcription with cerebral malaria isolates discussed in chapter 3. Thirdly, due to the high conservation of type 3 PfEMP1 it was hypothesised that type 3 PfEMP1 may not be surface exposed, and design of a type

3-specific antibody was attempted to address this question. The data obtained in answer to the above hypotheses will be discussed.

PCR of gDNA revealed 4 of the 9 laboratory isolates examined encode a type 3 *var* gene. Transcripts were only detected in TM267, Palo Alto and 3D7, suggesting expression was not constitutive, as had been hypothesised due to the lack of regulatory intron (Deitsch 2001; Calderwood *et al.* 2003; Frank *et al.* 2006). Another conserved *var* gene family, *var1csa,* also lacks the regulatory intron, and appears to be regulated uniquely, possibly outside of the mutually exclusive *var* gene promoter system (Kyes *et al*. 2003; Winter *et al*. 2003; Kyes *et al*. 2007). Transcription of type 3 *var* genes was not associated with rosetting in TM267 or Palo Alto, or with IgM binding in 3D7.

RT-PCR data for laboratory strain 3D7 suggests that type 3 *var* genes are expressed in both ring and trophozoite stages of erythrocytic development. Northern blot confirmed the presence of the type 3 *var* gene transcript in a mixed stage culture, but due to technical difficulties a precise Northern blot time course could not be completed. There was no evidence for a unique mechanism of transcriptional control. No type 3 transcripts were detected in gametocytes, in agreement with a previous study (Sharp *et al*. 2006).

The type 3 DBLα domains were omitted in the field isolate transcription profiling study (chapter 3) as in many similar *var* gene studies (Fowler *et al*. 2002; Bull *et al*. 2005a; Albrecht *et al*. 2006; Barry *et al*. 2007; Kraemer *et al*. 2007), due to disparity

between type 3 and non-type 3 reverse primer site sequences (Taylor *et al*. 2000a; Bull *et al*. 2005a). Most (23/26) of the field isolates examined in this study show evidence of type 3 *var* gene transcription, supporting recent observations that the vast majority of isolates contain a type 3 *var* gene (Trimnell *et al*. 2006). Type 3 *var* sequences show an extremely high level of conservation within and between isolates. The almost total conservation of the second half of DBLα_{type3} domains suggests a very particular and conserved function. The first half of the DBLα_{type3} domain sequence, though not entirely conserved, appears to be constrained in sequence, and six conserved subgroups of DBLα_{type3} domain (A-F) were defined. This indicates a functional constraint on the type 3 PfEMP1 alpha domain, and suggests that there may be a limited repertoire of DBLα_{type3} sequences. DBLε_{type3} domains are also highly conserved, with nucleotide sequence homology >97% across the whole domain. DBLε_{type3} domains are so similar that different domains from different type 3 *var* genes may not easily be distinguished, and no isolate showed multiple distinct epsilon transcripts in the RT-PCR analysis.

The high similarity of DBLε_{type3} domain sequences partially explains the discrepancy between the number of alpha and epsilon domains detected by RT-PCR. However, why some isolates showed DBLα_{type3} domain but not DBLε_{type3} domain transcription, or *vice versa*, cannot easily be explained. It is formally possible DBLα and DBLε domains are regulated alternately, though this would be very unusual and unexpected. Alternatively, it could be a PCR artefact. The most likely explanation is that there is a very low level of type 3 *var* gene transcript in these isolates, and the alpha domain PCR is less powerful than the epsilon domain PCR due to the

degeneracy of the forward primer, and so cannot efficiently amplify the type 3 DBLα domain transcript by RT-PCR. Type 3 transcription in field isolates could be studied in more detail, especially where alpha and epsilon data were inconsistent, to explore this observation more thoroughly.

The second hypothesis, that there would be a strong correlation between type 3 DBLα1 domain transcription and cerebral malaria, did not appear to be true for type 3 DBLα1 domains. Type 3 *var* gene transcripts were not more commonly detected in cerebral malaria isolates. Though type 3 *var* gene DBLε domain transcripts were detected in 8/9 cerebral isolates, type 3 *var* gene DBLα domain transcripts could not be detected, suggesting a low level of transcription. Furthermore, all 8 hyperparasitaemia isolates and 7/9 uncomplicated isolates showed evidence of type 3 *var* gene DBLε domain transcription, with type 3 *var* gene DBLα domain transcripts also detectable in all hyperparasitaemia and 5/7 of these uncomplicated malaria isolates. The data suggests a correlation between increased diversity of type 3 *var* gene transcription with hyperparasitaemia. As the total RT-PCR product was not quantifiable, it was not possible to directly compare abundance of type 3 transcripts in different isolates, and so it is not possible to conclude an overall higher level of type 3 *var* gene transcription in hyperparasitaemia isolates compared to cerebral malaria isolates. It is intriguing that the uncomplicated malaria isolates fall between the hyperparasitaemia and cerebral malaria isolates in the diversity of type 3 *var* gene transcripts observed. This is reminiscent of the level of DBLα1 domain transcription in uncomplicated malaria isolates falling between that of cerebral malaria isolates and hyperparasitaemia malaria isolates reported in chapter 3. This

strengthens the observation of a discrepancy in diversity of type 3 *var* gene transcripts in the two other groups, as uncomplicated malaria can be considered an earlier stage in disease progression, before expansion to hyperparasitaemia, or development of severe symptoms, as discussed in chapter 3.

It is interesting that genes with the same upstream region (group A type 3 *var* genes versus group A non-type 3 *var* genes; both UpsA) appear to be regulated differently in terms of level of expression in field isolates. It may be possible that parasite populations in an infection tend to have a certain proportion of parasites activating group A *var* gene expression; when this is a non-type 3 group A *var* gene, severe symptoms are common, but when this is a type 3 group A *var* gene, severe symptoms are less likely, and hyperparasitaemia can develop. There was not a significant negative correlation between type 3 group A *var* gene transcript diversity and non-type 3 DBLα1 domain transcription proportion, though data on absolute type 3 *var* gene versus non-type 3 group A transcription level is not available.

This association between the DBLα1-type 3 domain with hyperparasitaemia may indicate that only DBLα1(non-type3) are involved in severe disease pathology, for example through processes such as rosetting (Rowe *et al.* 1995; Russell *et al.* 2005), which tend to be mediated through non-type 3 DBLα1 domains (Rowe, JA, unpublished data). Alternatively, it could be the large variety of domains in the long and complex group A PfEMP1 that are crucial to disease pathology, rather than the DBLα1 domain directly. The reduced number of extracellular domains in the type 3 PfEMP1 may result in reduced adhesive potential. This is supported by *in vitro* data

that no type 3 *var* genes were upregulated when parasites were selected for adhesion to a human bone marrow endothelial cell line (Jensen *et al.* 2004). Type 3 *var* gene transcription was not found to be associated with rosetting or IgM binding in this study, and the type 3 epsilon domain is not capable of IgM binding (Semblat, JP *et al. in prep*). In addition, and unlike many other group A *var* genes, the type 3 *var* genes were not increased in transcription after selection for "severe malaria phenotype" by affinity for pools of semi immune plasma (Jensen *et al.* 2004). These observations suggest that type 3 *var* genes are not likely to be specifically involved in severe disease pathogenesis, though very little data on type 3 *var* transcription *in vivo* is available. Parasites from experimentally infected volunteers expressed type 3 *var*, though transcription levels were low, and tended to decrease with time of infection, unlike many non-type 3 group A *var* genes (Lavstsen *et al.* 2005). In a subsequent study, type 3 *var* gene transcription was found to be significantly higher in severe malaria cases than in asymptomatic malaria, though this increase may simply reflect the 7 fold higher parasitaemia in the severe malaria group (Rottmann *et al.* 2006). It would have been interesting to compare this severe malaria type 3 *var* gene transcription to an appropriate hyperparasitaemia patient group with similar parasitaemia.

The third hypothesis examined type 3 PfEMP1 and possible surface exposure. The high level of conservation of the type 3 *var* genes (for example all epsilon domains share > 97%, and the 6 groups of highly conserved type 3 DBLα domains) appears to be at odds with its membership of a family of variant surface antigens. Of the two other well-conserved PfEMP1 families, VAR2CSA is conserved due to a crucial role

of CSA-binding in placental malaria (discussed in chapter 4), but the role of VAR1CSA is still uncertain. It is generally believed that conserved proteins are selected for a particular purpose, thus the conservation and frequency of the type 3 *var* genes between isolates indicates an important function, although this study identified 5 laboratory strains in which a type 3 *var* could not be amplified from gDNA (Muz12, Dd2, HB3, TM180 or 7G8) suggesting they cannot be essential. The role of the type 3 *var* genes cannot be determined without first studying the encoded proteins. At present there is no published data determining whether the type 3 PfEMP1 are expressed at a protein level, or if they are exported to the infected erythrocyte surface. It is conceivable such a conserved *var* gene family might be a liability to a strategy of immune evasion; if a copy was commonly expressed on the surface of every *P. falciparum* isolate antibodies might be raised which could recognise all other isolates on subsequent infections. It is possible such a conserved gene would remain internal.

To attempt to address this possibility, a polyclonal antibody to the type 3 *var* was designed and raised in chickens. The DBLα_{type3} domain was chosen for antibody production rather than the DBLε_{type3} domain. The type 3-specific portion of the DBLα_{type3} domain is highly conserved and so it was possible to identify type 3-specific peptide epitopes for immunisation. It would also have been possible to use peptide epitopes from the epsilon domain to create a type 3 PfEMP1-specific antibody. However, DBLα_{type3} domains also contain a variable region, whereas DBLε_{type3} domains are almost identical across the whole domain. Thus different DBLα_{type3} domains are more likely to have different binding properties than different

DBLε_{type3} domains. In addition, DBLα domains are more N-terminal and thus lie further away from the erythrocyte surface. Being more exposed they might have an increased binding potential. DBLα domains which bind host molecules have already been defined in the case of rosetting (Rowe *et al.* 1997; Russell *et al.* 2005), and so the interaction of conserved DBLα_{type3} domains with other proteins is not unlikely. Thus the binding properties of DBLα_{type3} domains appeared to be more interesting to study than that of DBLε_{type3} domains, especially due to the association between non-type 3 DBLα1 domains and cerebral malaria. Therefore an antibody raised against the DBLα_{type3} domains was considered potentially more useful.

Hens rather than rabbits were chosen for immunisation due to the better pre-immune sera data for hens, specifically for hens PO41 and PO42. Hen egg yolks also give an increased yield of antibody compared to rabbit sera. Avian antibodies are also less likely to cross react with mammalian erythrocyte proteins than rabbit antibodies.

After consultation with Eurogentec, 2 highly conserved type 3-specific peptides were chosen for immunisation. Structural modelling on EBA175 (Tolia *et al.* 2005) and *P. knowelsi* DBLα (Singh *et al.* 2006) allowed one helical and one disordered peptide to be chosen. This was to give a high chance of eliciting specific antibodies to recognise type 3 PfEMP1 in immunoflouresence (native state) and in Western blot (denatured state). ELISA confirmed a specific recognition of both peptides with affinity-purified antisera, though the level of recognition was not very high compared to non-specific binding to BSA/PBS in the immune serum prior to affinity purification. Affinity-purification against both peptides together gave a similar

affinity profile to antisera purified against peptide 2 only. This suggests peptide 2 elicited a more efficient immune response in the hens. The majority of antibodies in the resulting affinity-purified antisera thus probably recognise peptide 2.

The affinity-purified anti-peptide antisera recognised a protein of approximately 150 kDa on a Western blot in protein extracts from ring and pigmented trophozoite stages, indicating that type 3 PfEMP1 (153 kDa) may be recognised by the antibody at both ring and pigmented trophozoite stage. In general, PfEMP1 are expressed at ring stage and are packaged in single small vesicles and exported to Maurer's clefts under the erythrocyte plasma membrane (*Hae*ggstrom *et al*. 2004; Knuepfer *et al*. 2005; Frankland *et al*. 2006). If type 3 PfEMP1 acted as "normal" they woud be expected to appear at the erythrocyte surface, usually in knobs approximately 16 hours post-invasion (Horrocks *et al*. 2005). The mechanism of export of PfEMP1 is controversial, but appears to involve an N-terminal hydrophobic stretch and a PEXEL, motif or vacuolar transport signal (VTS), located within the first DBL domain (Hiller *et al*. 2004; Marti *et al*. 2004; Knuepfer *et al*. 2005). The PEXEL/VTS are present in the type 3 PfEMP1. This suggests trafficking of type 3 PfEMP1 is, at least in part, through a similar mechanism to other PfEMP1.

There is evidence that at least some type 3 PfEMP1 reaches the surface, as it can be labelled with sulfo-N-hydroxysuccinimide (NHS)-LC-biotin (Sharling *et al*. 2007). Sulfo-NHS-LC-biotin is an ester vitamin that reacts with and labels lysines and the N-termini of proteins via primary amino groups. Uptake of biotin through the novel permeation pathway (Baumeister *et al*. 2003) was prevented using furosemide (Kirk

et al. 1994; Sharling *et al*. 2007), thus the biotin labelling was specific to surface-exposed proteins. Surface proteins were separated by SDS-PAGE and a band of approximately 150 kDa was detected with HRP-conjugated streptavidin. Detection using a generic antibody to PfEMP1 ATS region suggested this protein was probably type 3 PfEMP1, suggesting the type 3 PfEMP1 was on the erythrocyte surface.

Surface-exposed PfEMP1 is sensitive to cleavage by trypsin at concentration 0.1 mg/ml (Leech *et al*. 1984; Sharling *et al*. 2004), and trypsinisation results in loss of PfEMP1-mediated adhesion in trypsin-sensitive PfEMP1 (Nielsen *et al*. 2007). This study suggested that 150 kDa band recognised by the type 3 antibody is resistant to trypsin at 0.1-1 mg/ml. Higher molecular weight proteins (> 270 kDa) in the triton insoluble fraction which cross reacted with the antibody and are probably non-type 3 PfEMP1, decreased in intensity in the trypsin-treated lanes. This suggests the trypsinisation was successful. In addition, type 3 PfEMP1 trypsin-insensitivity was also observed in a study of PfEMP1 biotinylation (Sharling *et al*. 2007). This indicates the type 3 PfEMP1 is resistant to trypsin cleavage, or is not exported to the erythrocyte surface.

If the type 3 PfEMP1 is surface-exposed, an alternative reason for trypsin insensitivity could be simply its length. The epsilon domain and second half of the alpha domain of type 3 PfEMP1 may be hidden. EBA175, a dimer of two DBL domains, has a predicted length of 8.6 nm, extrapolating from a Stoke's radius of 4.3 nm (Tolia *et al*. 2005). Thus, the extracellular portion of a type 3 PfEMP1, also having just two DBL domains, may be expected to have a similar length. The

glycocalyx, a network of polysaccharides on cellular components of the blood, has a mean thickness on erythroctyes of 5.9 nm (Linss *et al*. 1991). Speculatively, this fits well with the approximately 3/4 of the type 3 PFEMP1 being conserved, possibly leaving the N-terminal portion of the DBLα domain open to immune pressure and the resulting diversifying selection.

Unfortunately, these results were all questionable due to the antibody recognising a band of the same size in HB3, a strain without a type 3 *var* gene. Whether the antibody cross react with something in HB3, but also recognises the type 3 PfEMP1 in 3D7 is not clear. If the type 3 PfEMP1 is recognised, as suggested by recognition of the peptides through ELISA, then the intensity of the Western blot band should decrease if the type 3 PfEMP1 is sensitive to trypsin, even if the antibody also cross-reacts with another protein of a similar size. Affinity purifying the antibody against the type 3 PfEMP1 protein directly might be helpful.

The function of the type 3 PfEMP1 remains unclear. Their conserved sequence suggests an important function, although their absence in certain strains such as HB3 suggests they are not essential. As they appear to remain internal, a role in sequestration is unlikely. A role in invasion is possible, as invasion proteins would be expected only to be surface exposed at merozoite stage, such MSP-1 or AMA-1 (O'Donnell *et al*. 2000; Triglia *et al*. 2000). If affinity purification of the antibody against the type 3 PfEMP1 directly was successful, then future experiments could help elucidate the function of the type 3 PfEMP1. Using the antibody in a type 3 PfEMP1-expressing culture may reveal a function in processes such as invasion,

merozoite release or schizont rupture, or in binding phenotypes such as rosetting or platelet-mediated clumping. Binding-affinity in type 3 PfEMP1-expressing strains could also be tested through expression of DBLα_{type3} domains, or entire type 3 PfEMP1 in *in vitro* expression systems. Expression could be verified using the antibody, and type 3 PfEMP1-specific adhesion could be confirmed using additional antibody to reverse binding. The antibody may also help to address type 3 binding specificity by inhibiting adhesion of type 3-expressing parasites to ligand-coated plates.

In conclusion, the experiments outlined in this chapter revealed that type 3 *var* genes are commonly transcribed in laboratory strains and field isolates, and are highly conserved, largely falling into 6 highly conserved groups on the basis of sequence polymorphism in the first half of the alpha domain. Surprisingly, transcription was associated with hyperparasitaemia rather than cerebral malaria, as was the case for other non-type 3 DBLα1 domains in chapter 3, suggesting an altered regulation of this subpopulation of group A *var* genes. Unfortunately, attempts to raise an antibody to investigate type 3 PfEMP1 expression timing and protein location were unsuccessful due to cross-reactivity of the antibody produced. The type 3 *var* genes/PfEMP1 remain an intriguing and highly conserved family, and further investigation of these *var* genes/PfEMP1, for example with regard to function, would be of great interest in the future.

Chapter 6

Curdlan sulfate: potential for treatment of severe malaria symptoms caused by rosetting *P. falciparum* strains

Some of the results presented in this chapter were published as

Kyriacou, HM *et al.* (2006). *In vitro* inhibition of *Plasmodium falciparum* rosette formation by Curdlan Sulfate. Antimicrobial Agents and Chemotherapy 51, 1321-1326

6.1 Abstract

Gene sequence associations with severe malaria disease manifestation, such as the link between group A *var* gene transcription cerebral childhood malaria (discussed in chapter 3) and *var2csa* transcription placental malaria in pregnant women (discussed in chapter 4), provide information on the pathogenesis of the disease and offer data for informed drug and vaccine design to improve medical treatment available to infected individuals. Vaccines usually target conserved parasite antigens to elicit a protective immune response and drugs can be designed to disrupt processes associated with severe disease. The spontaneous binding of infected erythrocytes to uninfected erythrocytes to form rosettes is a property of some strains of *P. falciparum* that is linked to severe complications of malaria. Rosette disrupting drugs such as heparin and fucoidan have high anticoagulant activity, preventing their use as treatment, Curdlan sulfate (CRDS) is a sulfated glycoconjugate compound that is chemically similar to heparin but with much lower anticoagulant activity. CRDS has previously been shown to have antimalarial activity *in vitro* and is safe for clinical use. Previous work in the Rowe laboratory revealed that CRDS significantly inhibited rosetting in seven *P. falciparum* laboratory strains. In this chapter the ability of CRDS to inhibit rosetting in a group of 18 African clinical isolates was examined. CRDS disrupted rosettes *in vitro* in all 18 *P. falciparum* African field isolates examined. The kinetics of CRDS anti-rosetting action in laboratory strain Palo Alto was also examined, revealing fast action on rosettes (< 2 min) and reversibility of rosette disruption. The strong ability to inhibit rosetting suggests that CRDS has the potential to reduce the severe complications and mortality rates from

P. falciparum malaria among African children, supporting further clinical trials of CRDS.

6.2 Introduction

Despite decades of research, malaria still claims an estimated million lives per year in sub-Saharan Africa, and severe complications such as cerebral malaria remain relatively common (WHO 2000). Eradication of *Plasmodium* remains a long-term goal. Meanwhile, it is crucial to target factors that contribute to severe disease and reduce clinical complications of malaria. Rosetting, which is estimated to be a factor in 25-50% of severe malaria cases in sub-Saharan Africa (Rowe 2005), is one obvious target for therapy to reduce incidents of severe disease.

6.2.1 Molecular basis of rosetting

Rosetting is the spontaneous binding of non-infected erythrocytes by erythrocytes infected with mature asexual blood stage *Plasmodium* parasites (reviewed in Rowe 2005). The molecular basis of rosetting centres on PfEMP1, the high-molecular weight transmembrane protein, encoded by the *plasmodium var* multigene family, discussed in chapters 3-5. Rosetting is a strain-specific property (Wahlgren *et al.* 1990) and it is the N-terminal DBLα domain of a subset of PfEMP1 that mediates the rosetting interaction (Rowe *et al.* 1997; Chen *et al.* 2004). There is little sequence similarity between rosetting DBLα domains, though sequence analysis suggests the majority are DBLα1 domains, and that rosetting PfEMP1 are frequently Group A *var* genes (J.A.Rowe unpublished data; Bull *et al*. 2005a; Kyriacou *et al*. 2006; Normark *et al*. 2007 and as discussed in chapter 3).

Rosetting is a heterogeneous phenomenon, and a variety of molecules on the erythrocyte surface may participate in rosette formation, including heparan sulfate (HS)- like glycosaminoglycans (GAG) (Chen *et al.* 1998a; Barragan *et al.* 1999; Vogt *et al.* 2003), complement receptor 1 (Rowe *et al.* 1997), and the trisaccharide glycan of blood group A antigen (Barragan *et al.* 2000). CD36, a scavenger receptor on many host cells including erythrocytes (van Schravendijk *et al.* 1992), has also been shown to occasionally support rosetting, acting as the receptor for Malayan Camp strain rosettes (Handunnetti *et al.* 1992). Low molecular weight "rosettins" may also be involved, though there is little data on these (Helmby *et al*. 1993).

6.2.2 Rosette frequency (RF) is linked to severe disease in African field isolates

In African *P. falciparum* malaria field isolates, there is a compelling link between rosette frequency (RF) and severe disease (Carlson *et al*. 1990; Rowe *et al*. 1995), and higher rosetting was observed in the cerebral malaria compared to hyperparasitaemia or uncomplicated Malian field isolates discussed in chapter 3. Rosette-like aggregates have been observed in congested cerebral vessels (Riganti *et al*. 1990), but are infrequently reported in cerebral malaria postmortem. Rosettes are not observed in arterioles (high wall sheer stress), but rapidly reform in the venules (low wall sheer stress), demonstrating rapid reformation after disruption in an artificially perfused rat microvasculature model of *P. falciparum*–infected erythrocyte sequestration (Kaul *et al.* 1991).

However, an association between rosetting and severe malaria disease is not the case in Asia, where complement receptor 1 (CR1) deficiency is common. CR1 deficient erythrocytes show reduced RF with 5/5 laboratory isolates (Rowe *et al*. 1997), including Malayan Camp which rosettes through CD36- perhaps pointing to a synergistic interaction between CD36 and CR1.

All other members of human-infective *plasmodium* family also rosette, for example almost all *P. vivax* isolates show some degree of rosetting (Udomsanpetch *et al.* 1995; Angus *et al.* 1996; Chotivanich *et al.* 1998; Lowe *et al.* 1998). However, it is only in *P. falciparum* that rosetting is linked to severe disease, probably because of the additional cytoadhesion property which may act in concert with rosetting to cause vessel obstruction (Rowe 2005) as demonstrated in a rat model (Kaul *et al.* 1991). Human erythrocyte polymorphisms such as CR1 deficiency in Asia (Cockburn *et al.* 2004; Thomas *et al.* 2005) and blood group O (Rowe *et al*. 2007) in malaria-endemic areas have been postulated to be selected for because of their protective effect in malaria due to reduced rosetting, and a resulting inverse association with severe malaria. It has not so far been possible to prove a causative link between rosetting and severe malaria, but the evidence is compelling.

6.2.3 Rosette disruption by heparin and heparan sulfate (HS)

Heparan sulfate (HS) and heparin are members of the sulfated glycosaminoglycan (GAG) family. HS and heparin are both composed of alternating glycosamine and uronic acids, linked 1→3 or 1 → 4 (Fig. 6.1). The glucosamine can be N-sulfated or N-acetylated and can contain O-sulfate ester on the second carbon. The uronic acids

can be glucuronic acid or iduronic acid and may also be O-sulfated. Binding properties of distinct GAGs are associated with the sulfate and carboxyl groups. As sulfation states of heparin and HS vary, the two can be very similar, but in general heparin is a highly sulfated form of HS, with a more uniform sulfation across the molecule and more extensive modification. HS is found on almost all cells including endothelial cells, whereas heparin is only present in granules of connective tissue, mast cells and basophils. HS was reported to be present on erythrocytes in 2004 (Vogt *et al*. 2004), confirming HS as a potential rosetting receptor.

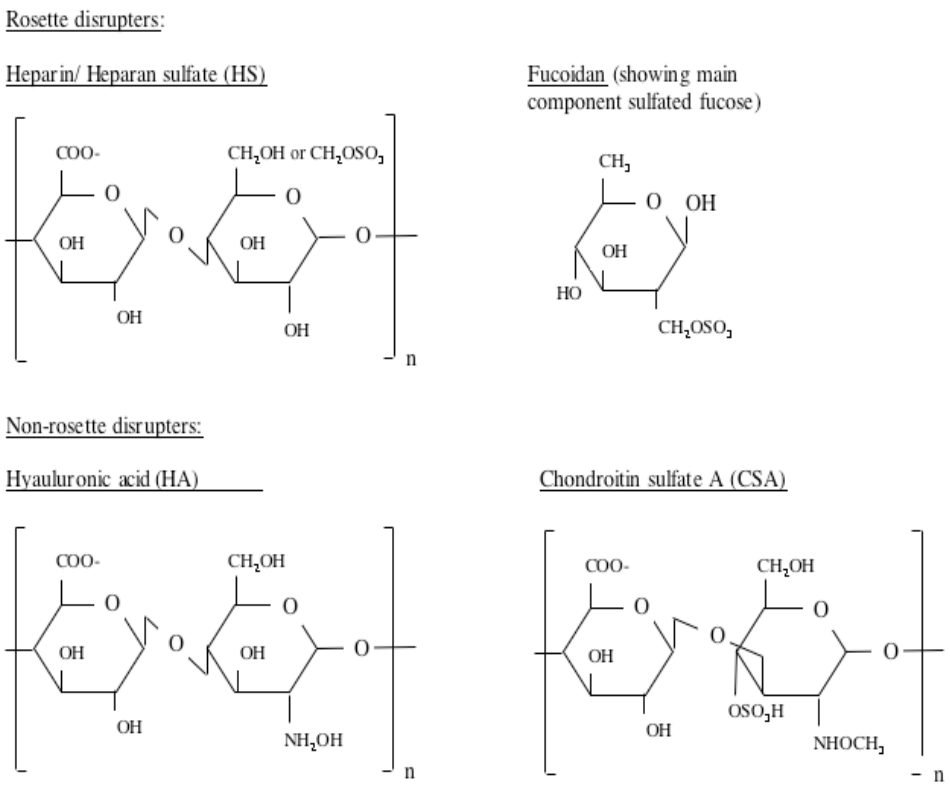

Fig. 6.1 Glycosaminoglycan (GAG) structures: Rosette disrupting GAGs; heparin/heparan sulfate (HS), and the main component of fucoidan, sulfated fucose.

Non-rosette disrupting GAGs; hyauluronic acid (HA) and chondroitin sulfate A (CSA).

Previous work has shown that rosettes can be disrupted by glycosaminoglycans or sulfated glycoconjugate compounds such as heparin and fucoidan in a strain dependent manner (Carlson *et al.* 1992; Rowe *et al.* 1994; Barragan *et al.* 1999). Heparin and HS consistently disrupt rosettes in approximately 50% of rosetting field isolates (Carlson *et al.* 1992; Rowe *et al.* 1994; Chen *et al.* 1998a; Barragan *et al.* 1999). Fucoidan has a more wide ranging action than heparin (9/10 isolates sensitive to fucoidan, compared to 5/10 sensitive to heparin in Rowe *et al.* 1994). Some isolates are more resistant to rosette disruption, e.g. PAR+ is more sensitive to heparin and fucoidan than TM284+ (Carlson *et al.* 1992; Rowe *et al.* 1994).

Heparin was a promising candidate for adjuvant therapy for severe disease, and clinical trials with heparin have shown some success (Munir *et al.* 1980; Rampengan 1991). However, a high level of heparin-induced intracranial bleeding has led to this treatment being discouraged and the anti-coagulant effects of these drugs prevent their use as treatment for severe malaria (WHO 2000).

6.2.4 Reducing anticoagulant activity of rosette disrupting compounds

The anticoagulant properties of GAGs are an intrinsic chemical property of each individual GAG, based on the chemical structure, size and modifications. The different members of the family show a range of anticoagulant activity, so it is possible to design molecules with reduced anticoagulant activity, whilst retaining

rosette disruption ability. A number of ways have been attempted to reduce the anticoagulant activity of heparin-based derivatives (Fig. 6.2).

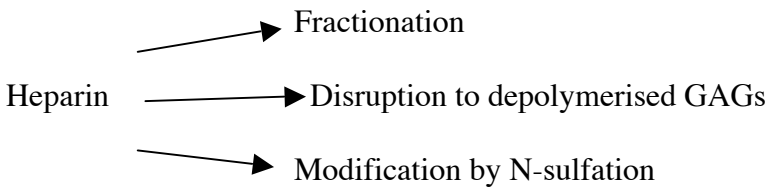

Fig. 6.2. Strategies for reducing anticoagulant activity of rosette disrupting heparin derivatives.

Firstly, fractionation can be used to separate heparin according to molecular weight or affinity for antithrombin III, resulting in heparin-derived fractions with varying rosette disruption ability and anticoagulant properties (Carlson and Wahlgren 1992). The rosette inhibition activity was not associated with anti-coagulant properties, suggesting it should be possible to find a fraction with the optimum combination of high anti-rosette activity but low anticoagulant nature.

Secondly, depolymerisation of heparin results in reduction to composite 'building blocks' of novel depolymerised glycosaminoglycans (dGAGs). These lack anti-coagulant activity but still disrupt rosettes and inhibit merozoite invasion (Vogt *et al.* 2006). Rosette disruption with small disaccharides as well as with monomer and long polymers had previously been reported (Barragan *et al.* 1999). There was evidence of

reduced sequestration in macaques and rats, but so far without convincing extrapolation to humans (Vogt *et al*. 2006).

Thirdly, modifications of heparin/HS based compounds can drastically alter their chemical properties. The N-sulfate groups on heparin/HS are important for rosette disruption activity and the extent of N-sulfation further increases rosette disruption activity (Barragan *et al*. 1999). This is supported by chemical data showing the sulfation state of polysaccharides is responsible for anti-coagulant activity (Chaidedgumjorn *et al*. 2002). All sulfated carbohydrate-based heparin derivatives have some degree of anti coagulant and antithrombin activity, but this differs between compounds, and is due to specific interactions rather than to the general anionic character (Alban and Franz 2000). 1 → 3 linked polysaccharides exhibit 75% reduction in plasma mediated antithrombin activity compared to heparin activity, and the 6-sulfate group largely determines the level of anticoagulant activity (Chaidedgumjorn *et al*. 2002).

6.2.5 Curdlan sulfate has low anticoagulant properties

Curdlan sulfate (CRDS, Fig. 6.3) is a sulfated 1->3 β-D glucan; MW: 402.329. CRDS was predicted to have rosette disruption properties (Havlik *et al*. 2005) due to its polyanionic nature and chemical similarities to other sulfated polysaccharides (Xiao *et al*. 1996), see structure in Fig. 6.1. CRDS has a much more favourable toxicity profile than heparin as it has 10-fold lower anticoagulant activity, measured as activated partial thromboplastin time (APTT) compared to heparin (Kaneko *et al.* 1990).

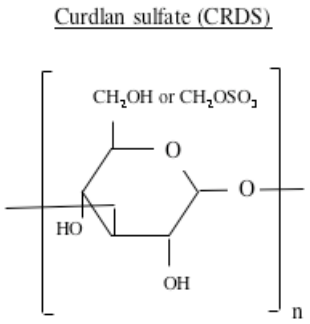

Fig. 6.3. Structure of curdlan sulfate (CRDS), a sulfated glycosaminoglycan with rosette disrupting potential.

The exact mechanism of CRDS anticoagulant activity is unclear. Unlike heparin, CRDS does not accelerate thrombin inactivation by anti-thrombin but there is evidence it may bind to fibrinogen, causing steric hindrance preventing interaction between thrombin and fibrinogen and preventing fibrin deposition (Alban and Franz 2000).

6.2.6 Curdlan sulfate is safe to use

CRDS is safe to use, and completed phase 1 clinical trials in HIV therapy over 10 years ago (Gordon *et al.* 1994; Gordon *et al.* 1997). In HIV, CRDS appears to block HIV adsorption on target CD4+ T cells (Kaneko *et al.* 1990; Aoki *et al.* 1992), via binding to the V3 loop of gp120 (Jagodzinski *et al.* 1994), therefore preventing virus invasion. A similar adsorption mechanism exists in merozoite invasion of *P. falciparum*, and CRDS almost completely blocks merozoite invasion (Havlik *et al.*

1994). CRDS may act as an analogue of the glycophorin sialic acid which is required for merozoite invasion (Orlandi *et al*. 1992; Evans *et al*. 1998). A similar mechanism may cause heparin-induced invasion disruption (Kulane *et al*. 1992). CRDS may also inhibit sporozoite invasion of hepatocytes, as reported for other sulfated glycans (Pancake *et al*. 1992). CRDS does not affect trophozoite maturation but does delay schizont rupture (Evans *et al*. 1998).

6.2.7 Curdlan sulfate and malaria

A clinical trial of the effect of CRDS in severe/cerebral *P. falciparum* malaria by Havlik *et al.* (2005) suggested that CRDS may be able to reduce disease severity, as fever clearance time was reduced as was coma resolution time, though the trial was not conclusive, probably due to the small number of patients in the trial (Havlik *et al.* 2005).

As CRDS inhibits merozoite invasion but does not affect trophozoite development (Havlik *et al.* 1994; Evans *et al.* 1998), it is likely that the CRDS modifies erythrocyte surface proteins. A role in rosette disruption has also been postulated, due to its polyanionic character (Havlik *et al.* 2005). Because of the chemical similarities between CRDS and heparin, and the 10 fold lower anticoagulant effects of CRDS (Kaneko *et al.* 1990), it was hypothesised that CRDS might be effective against *P. falciparum* rosetting and could form the basis of an adjunctive treatment for severe malaria (Havlik *et al.* 2005).

CRDS is also active against *Babesia*, a tick-borne parasite which is an economically important infection of cattle in the tropics and sub tropics. The mechanism is unclear but *Babesia* has a similar mechanism of infection as *P. falciparum* (Igarashi *et al.* 1998).

CRDS thus has the chemical properties that suggest it may disrupt rosettes and is safe for clinical use (Kaneko *et al.* 1990; Jagodzinski *et al.* 1994; Havlik *et al.* 2005). This study tested the ability of CRDS to inhibit rosetting in *P. falciparum* field isolates, and shows universal rosette inhibition at therapeutic doses of CRDS. CRDS disrupted rosettes in 18/18 *P. falciparum* field isolates tested in addition to 7/7 laboratory isolates previously examined in the laboratory. The combined data present CRDS as a strong candidate for adjunct therapy in severe malaria from rosetting *P. falciparum*.

6.3 Aim of chapter

The aim of the chapter was to assess the ability of curdlan sulfate (CRDS) to disrupt rosettes in field isolates of *P. falciparum*, to complement *in vitro* work on laboratory isolates carried out in the Rowe laboratory. The ultimate aim of this work was to examine CRDS as a potential therapeutic agent against severe malaria among African children caused by rosetting strains of *P. falciparum*.

6.4 Materials and methods

Materials and methods that are specific to chapter 6 are listed below. General materials and methods and a list of suppliers are given in chapter 2.

6.4.1 Parasites

Wild isolates were collected from Kilifi District Hospital, Kenya. Fresh isolates were cultured by standard methods (chapter 2) for at least 18 hours *in vitro* to the mature pigmented trophozoite stage. Frozen rings and trophozoites had been cryopreserved in glycerolyte and stored in liquid nitrogen, before thawing for either immediate use (frozen trophs), or culturing to the mature pigmented trophozoite stage (frozen rings). Cryopreservation of mature trophozoites does not affect the surface antigens of the trophozoite-infected erythrocytes (Kinyanjui *et al*. 2004). Thus the rosetting frequency of a single isolate does not change significantly pre-freezing and post-thawing (Kyriacou *et al*. 2007). Two sets of field isolates were used; those collected Jan-March 2006, and those which had been previously collected and cryopreserved (J.A. Rowe) in 1993. Summary of field isolates used: Collected Jan-March 2006: 6566Fztr, RF48; 6394Fztr, RF15; 6399Fztr, RF12; 6547Fztr, RF5; 6542Fztr, RF52; 6794Fzrng, RF33; 6921Fsh, RF27.5; 6962Fsh, RF24.5; 6908Fsh, RF27 and collected in 1993: KR1Fzr, RF53.5; KR7Fzr, RF68; KR9Fzr, RF14; KR10Fzr, RF25; KR11Fzr, 27; KR14Fzr, RF37.5, KR17Fzt, RF61; KR18Fzt, 28; KR20Fzr, RF6 (Fsh, fresh trophs; Fztr, frozen trophs, Fzrng, frozen rings. RF, pretreatment rosette frequency).

Rosetting laboratory strains used were TM284+, TM180, Muz12R+, HB3, R29, A4R and PAR+. Laboratory strains were cultured by standard methods and rosetting was regularly selected by percoll treatment (see chapter 2).

6.4.2 Assessment of Rosette Frequency

All rosette assays were performed on mature pigmented trophozoites, determined using a Giemsa smear (details in chapter 2). Rosette frequency (RF) varies from cycle to cycle, but is stable within a given cycle (Rowe *et al.* 1994). Parasites were resuspended at 1-2% haematocrit in complete binding medium (Bicarbonate-free RPMI, supplemented as RPMI), as this has a more stable pH when ungased. The culture suspension was pre-stained with ethidium bromide (EtBR), or acridine orange (AO), to identify infected erythrocytes. These staining methods did not alter rosette frequency (PAR+: EtBr staining: mean RF 69.0%, SE 1.1%; AO staining: mean RF 68.8%, SE 0.8%).

6.4.3 Curdlan sulfate drug rosetting inhibition assay

Curdlan suphate (CRDS) was dissolved in sterile phosphate buffered saline (PBS) and added to 18 μl pigmented trophozoites (RF > 50%) culture suspension to give final concentrations 0, 10, 50 and 100 μg/ml. Final concentrations of 100 μg/ml fucoidan and 100 μg/ml hyaluronic acid (both from Sigma, UK) were used as positive and negative controls for rosette inhibition (Rowe *et al.* 1994).

All aliquots of *P. falciparum* were incubated for 30 min. Field isolates were rotated for 30 min at room temperate. Laboratory isolates were incubated at 37 °C, and cells

were resuspended every 15 min by flicking the tubes. These methods do not alter the rosette frequency (PAR+: Incubation with EtBr 30 min rotation, RT, RF 69.0% SE 1.1; incubation with EtBr 30 min not rotating, but "flicking" at 0, 15 and 30 min, RF 68.5%, SE 0.65). Wet preparation slides of the parasites were prepared and viewed under fluorescence. Two hundred infected erythrocytes were counted, and scored for number of rosettes; at least two uninfected red blood cells bound constitutes a rosette. Rosette frequency was then expressed as a percentage of total infected erythrocytes. All slides were counted blind. For laboratory strains, data were collected at least three times for every culture and condition used. For field isolates, isolates were only counted once for each condition.

6.4.4 Kinetics of curdlan sulfate rosette disruption

CRDS was dissolved in sterile phosphate buffered saline (PBS) and added to 180 μl culture suspension of PAR+ or TM284+ pigmented trophozoites to give final concentration of 50 μg/ml or 0 μg/ml (PBS control). Cultures were incubated at 37°C, and RF recorded after 0, 2, 5, 30, 60 and 120 min. The assay was repeated 5 times.

6.4.5 Rosette reformation after curdlan sulfate rosette disruption

Two 36 μl aliquots of culture suspension of PAR+ pigmented trophozoites were incubated at 37°C with a final concentration of 50 μg/ml CRDS, 100 μg/ml fucoidan, 100 μg/ml hyaluronic acid or with 2 μl PBS. After 30 min one culture for each condition was washed 4 times with 750 μl incomplete binding media, to wash away the CRDS, fucoidan, hyauluronic acid or PBS, and the culture was resuspended in

complete binding media and incubated at 37 °C. RF was recorded after 0, 2, and 120 min (after washing) and 120 min (without washing). The assay was repeated 4 times.

6.4.6 Statistics

Relative rosette frequency was calculated as a proportion of post-treatment rosette frequency, and given as mean ± SD or SE as appropriate. Paired t-tests were used to compare RF in different treatment groups of time points as the data were normally distributed. Combined data for field isolate RF after treatment was also analysed using ANOVA.

6.5 Previous work: CRDS-mediated inhibition of rosetting in laboratory strains

The following laboratory work (section 6.5 only) was carried out by Ahmed Raza and Katie E Steen (Edinburgh), but data analysis, statistics and production of the figures was carried out personally.

The effect of CRDS was tested in eight different laboratory parasite strains. Cultures were pigmented trophozoites (RF > 50%). Three doses of CRDS were used (10, 50, 100 μg/ml), alongside a PBS control (i.e. 0 μg/ml CRDS). Positive and negative controls for rosette inhibition, fucoidan and hyaluronic acid, were also included. Rosette frequency was significantly reduced (t-test, $P<0.05$) by CRDS at the highest dose (100 μg/ml) in all parasites (7/7). At 50 μg/ml CRDS, rosetting was significantly reduced in all parasites apart from TM284+ (6/7). At 10 μg/ml CRDS,

rosette frequency was reduced (t-test, $P<0.05$) in 3/8 parasites. Data for each laboratory isolate is given in Fig. 6.4, and a summary table is shown in Fig. 6.5.

The mean RF for all parasites combined at each treatment were 62.3% for PBS (Standard Error (SE) 2.8), 21.9% for 10 μg/ml CRDS (SE:6.6), 14.6% for 50 μg/ml CRDS (SE:4.6) and 8.7% for 100 μg/ml CRDS (SE:2.7). As expected hyaluronic acid provided a reliable negative control for rosette inhibition (mean RF 65.2%, SE 2.8) and fucoidan a reliable positive control (mean RF 5.4%, SE 1.0).

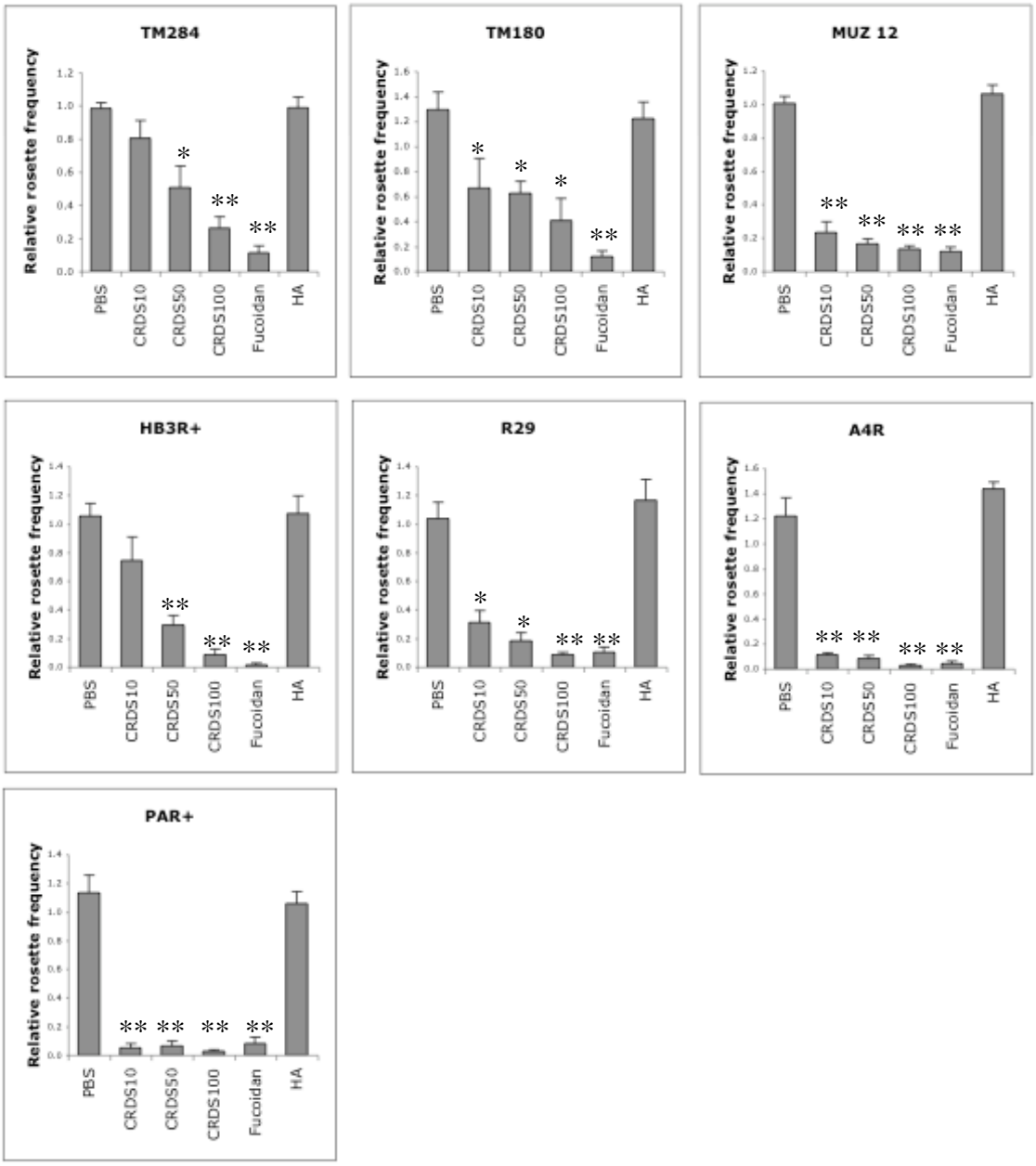

Fig. 6.4. Individual data for inhibition of rosette frequency in 7 laboratory strains of *P. falciparum* by 0, 10, 50 and 100 μg/ml CRDS in PBS. Each assay was counted blind and performed in triplicate. Post-treatment RF, calculated as proportion of pre-treatment RF, were logged to normalise the data then compared to pre-treatment RF using paired t-tests. p values are indicated with asterisks as *P<0.05 and **P<0.005.

P. falciparum strain	Origin	RF as proportion of pre-treatment RF after addition of CRDS:			
		0 μg/ml	10 μg/ml	50 μg/ml	100 μg/ml
TM284+	Thailand			*	**
TM180	Thailand		*	*	*
Muz12R+	PNG		**	**	**
HB3	Honduras			**	**
R29	SE Asia		*	*	**
A4R	SE Asia		**	**	**
PAR+	SE Asia		**	**	**

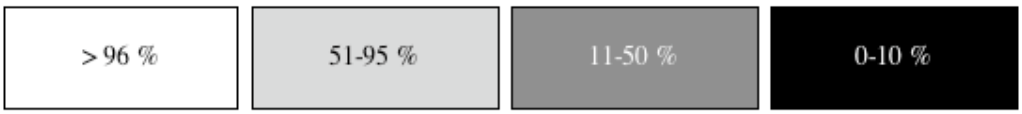

Fig. 6.5. Summary table for rosette disruption in laboratory strains of *P. falciparum* by 0, 10, 50 and 100 μg/ml CRDS in PBS. Each assay was counted blind and performed in triplicate. Post-treatment RF, calculated as proportion of pre-treatment RF, is indicated by shading as >96%, 51-95%, 11-50% and 0-10%. Post-treatment RFs were logged to normalise the data then compared to pre-treatment RF using paired t-tests. p values are indicated with asterisks as *P<0.05 and **P<0.005.

Parasites responded to CRDS in a dose dependent manner, though there was variation in the response of the parasite strains to CRDS. Some isolates, such as PAR+, are very sensitive to CRDS, with significant inhibition at only 10 μg/ml (Fig. 6.4, 6.5 and 6.6). This may be due to differences in the strength of the rosettes, depending on the precise molecular interactions involved, as seen for fucoidan and heparin fucoidan (Rowe *et al*. 1994).

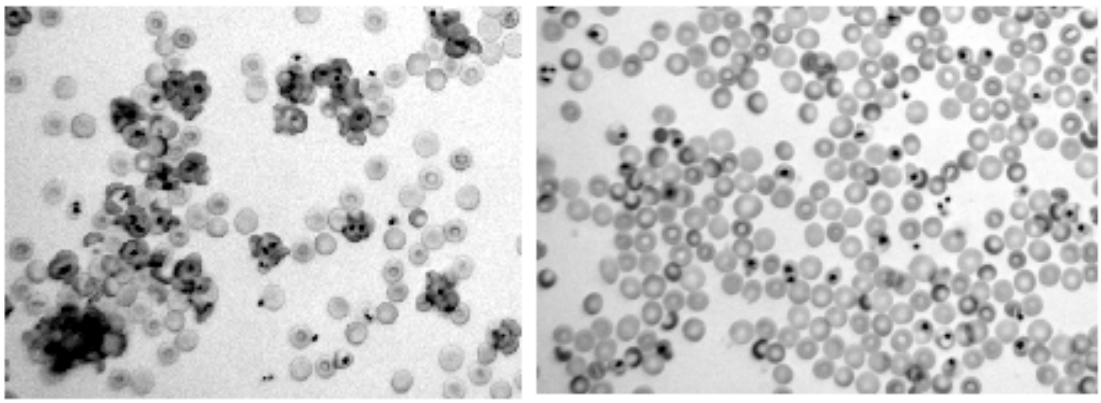

Control PAR+ culture. PAR+ culture treated with 10 μg/ml CRDS.

Fig. 6.6. 10μg/ml CRDS significantly reduced rosetting in *P. falciparum* laboratory strain PAR+ compared to a control culture. Live wet-preparation images taken with 40x objective lens on a bright field microscope. Infected erythrocytes can be identified by the presence of malaria pigment, seen as black dots within the erythrocytes. Images taken by Alex Rowe.

6.6 Results 1: CRDS inhibition of rosetting in laboratory strains

After the initial rosette disruption experiments described above (section 6.5), I wanted to further define the rosette-disrupting ability of CRDS.

6.6.1 CRDS inhibition of rosetting in laboratory strains: kinetics of CRDS

The kinetics of CRDS rosette disruption was assessed in PAR+ (very CRDS sensitive; Fig. 6.4) and TM284+ (less CRDS sensitive; Fig. 6.4) over 2 hr with 50 μg/ml CRDS.

PAR+ (mean RF 67.6%, SE:2.6%) was treated with 50 μg/ml CRDS and rosette frequency recorded over 2 hours. Rosettes were disrupted within 2 min (relative RF 11.9%, SE:3.3%). After 2 hr no rosettes were present in the CRDS treated samples (relative RF 0%, SE 0%). The PBS control samples showed high RF (relative RF 95.9%, SE 1.9%). Fig. 6.7A shows mean relative rosette frequencies for 5 repeats of the 6 time points.

TM284+ (mean RF 67.6%, SE:2.6%) was also treated with 50 μg/ml CRDS and rosette frequency recorded over 2 hours. Rosettes were also disrupted within 2 min, but to a lesser extent that for PAR+, reflecting the reduced sensitivity of TM284+ rosettes to CRDS treatment (at 2 min: relative RF 55.4%, SE:2.9%). Rosettes were still present in the CRDS treated samples after 2 hr (at 2 hr: mean RF 32.9%, SE 0.6%).Rosetting in the PBS control samples remained high (PBS at 2 hr: mean RF

87.3%, SE 6.7%). Fig. 6.7B shows mean relative rosette frequencies for 5 repeats of the 6 time points.

A

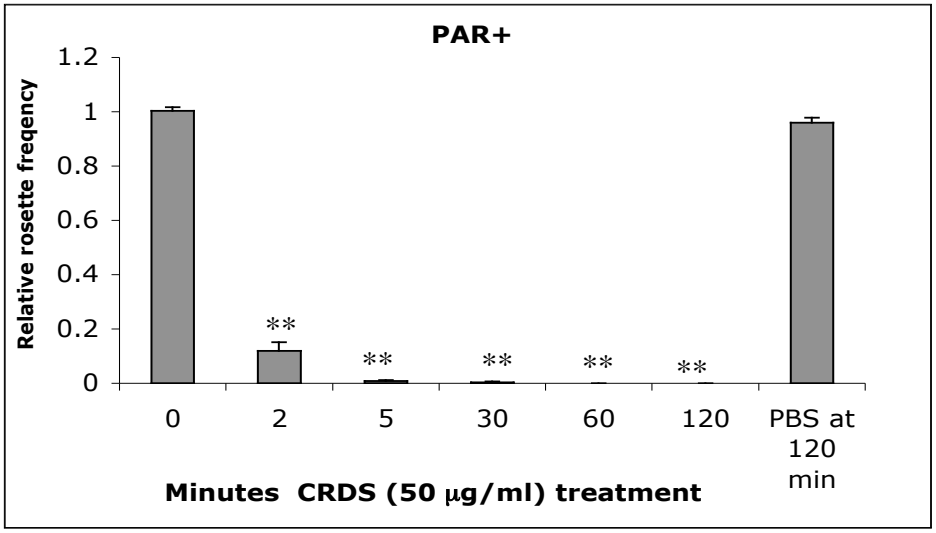

B

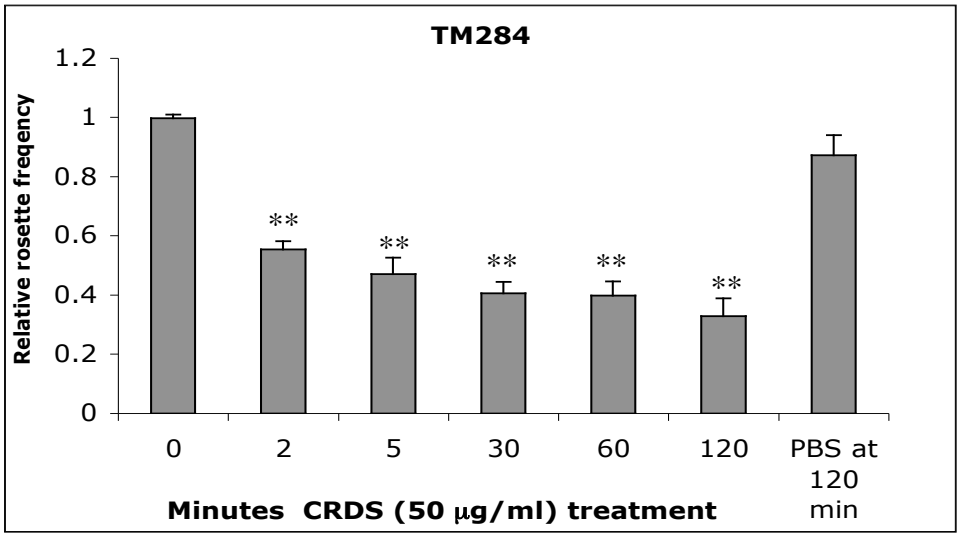

Fig. 6.7. Speed of action of CRDS. PAR+ parasites were treated with 0 or 50 μg/ml CRDS. The RF was assessed at 0, 2,5, 30, 60 and 120 min post treatment. RF given as proportion of pre-treatment RF, as mean ± SE for 5 repeats of the experiment.

Post-treatment RFs were compared to pre-treatment RF using paired t-tests. p values are indicated with asterisks as **P<0.005.

6.6.2 CRDS inhibition of rosetting in laboratory strains: Rosette reformation after CRDS treatment

The ability of rosettes to reform after CRDS disruption was also investigated. Rosette reformation assays were also carried out on PAR+ parasites. After 30 min CRDS treatment (maximum disruption), the CRDS was thoroughly washed out with incomplete binding medium (as binding medium, but with no added serum), and the erythrocytes re-suspended in fresh complete binding medium. Rosette frequency returned to 102% (SE:6.5%) original RF (Fig. 6.8). This shows similar kinetics to fucoidan (Rowe *et al*. 1994), which I found to return to 100% (SE:8.2%) original RF after washing.

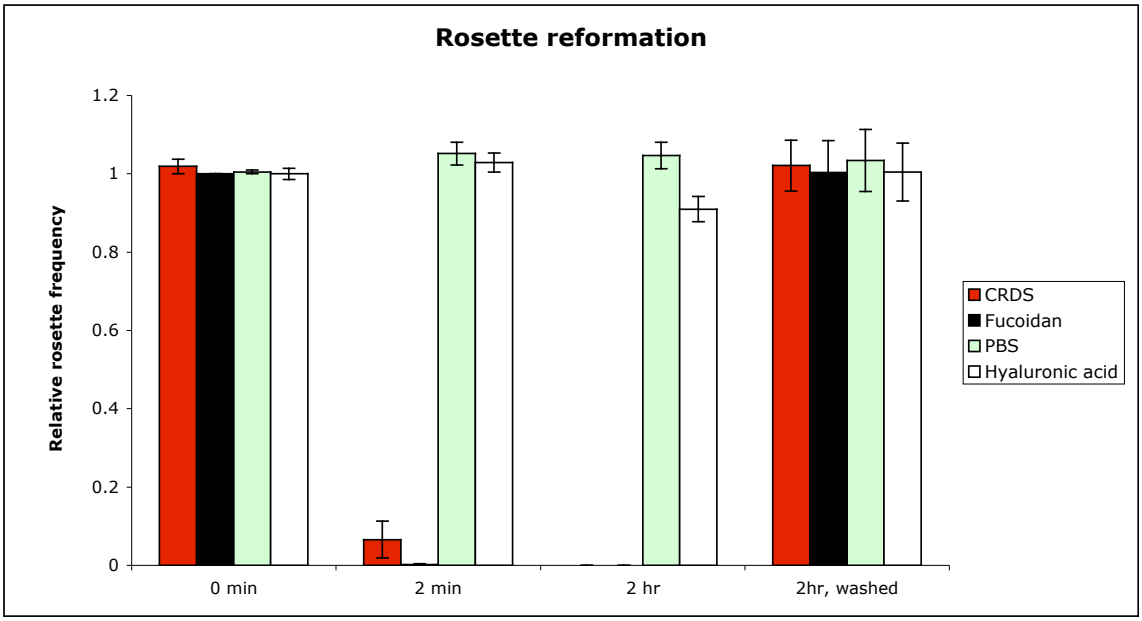

Fig. 6.8. Rosette reformation assay. PAR+ were incubated at 37°C with final concentration of 50 μg/ml CRDS, 100 μg/ml fucoidan, 100 μg/ml hyaluronic acid or with 2 μl PBS. After 30 min the drug treatment was washed out. RF was recorded after 0, 2, and 120 min (after washing) and 120 min (without washing). The assay was repeated 4 times. RF is given as proportion of pre-treatment RF as mean ± SE for 4 repeats of the experiment.

6.7 Results 2: CRDS-mediated rosette disruption in rosetting field isolates

To validate the use of CRDS in a clinical trial, the same four concentrations of CRDS (0, 10, 50 and100 μg/ml), alongside fuciodan and hyaluronic acid, were used on rosetting field isolates from Kilifi District Hosital, Kenya.

6.7.1 CRDS-mediated rosette disruption in rosetting field isolate samples from Kilifi, Kenya collected Jan-March 2006

Nine rosetting isolates were cultured to mature trophozoite stage. CRDS consistently disrupted rosetting in a concentration dependent manner in all parasites (Fig. 6.9). Fucoidan and hyaluronic acid were used for positive and negative controls for rosette inhibition in all isolates.

CRDS seems to be at least as effective at rosette disruption as fucoidan, reported to be active against 9/10 isolates in a previous study (Rowe *et al*. 1994), and to have a wider range of action than heparin, which was effective in only 50% isolates in that same study and in others (Carlson *et al*. 1992; Rowe *et al*. 1994; Chen *et al*. 1998a; Barragan *et al*. 1999).

As with laboratory isolates there is evidence for high and low responders to CRDS, with some isolates reacting strongly to a low dose, whereas others required the highest dose for effective rosette inhibition. This may have implications for dose needed for therapy.

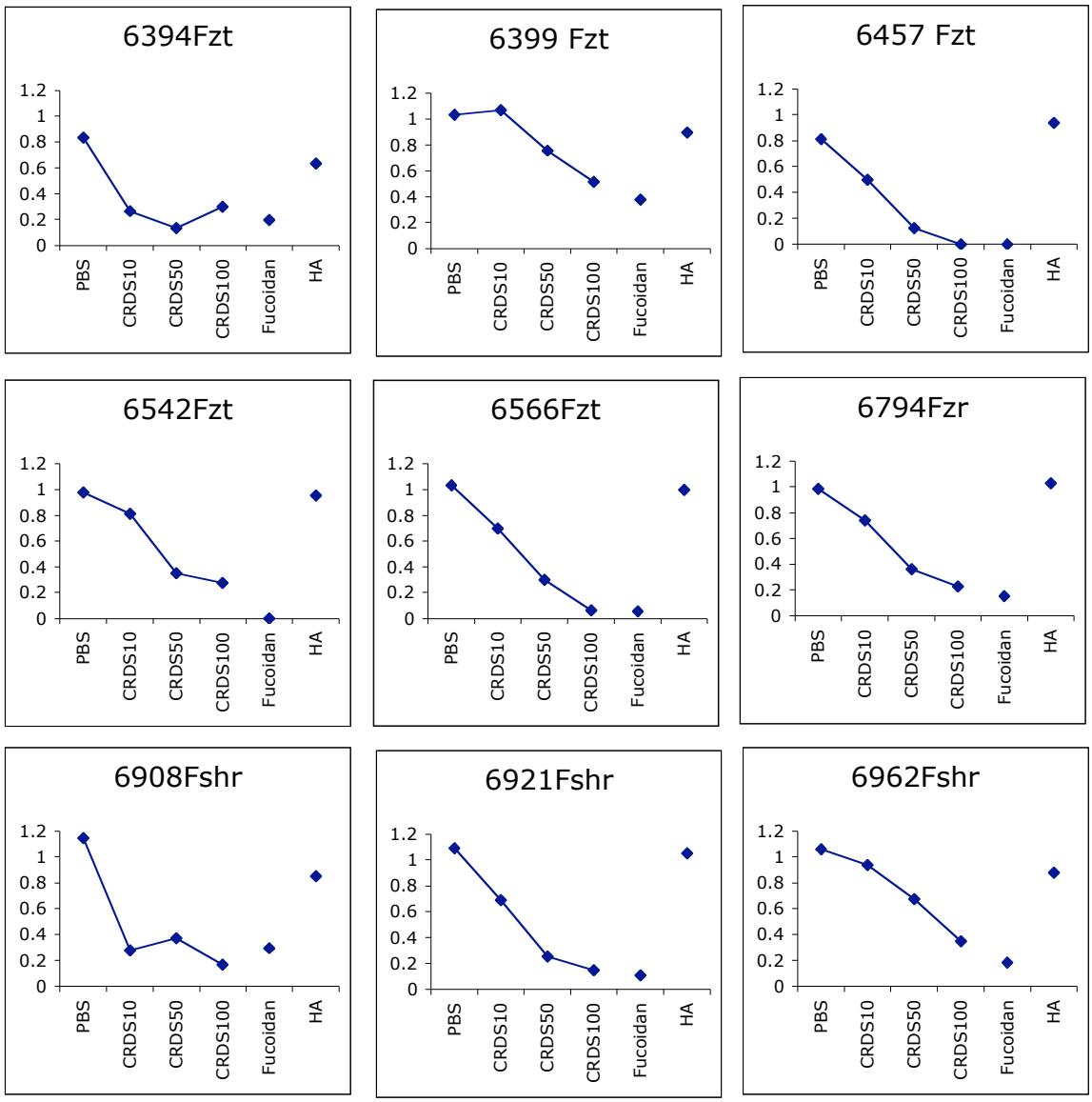

Fig. 6.9. CRDS-mediated rosette disruption in 9 rosetting field isolates from Kilifi, Kenya, collected Jan-March 2006. RF shown as proportion of pre-treatment RF for comparison: Relative rosette frequency, Y-axis. Summary of field isolates used: 6566Fztr, RF48; 6394Fztr, RF15; 6399Fztr, RF12; 6547Fztr, RF5; 6542Fztr, RF52; 6794Fzrng, RF33; 6921Fsh, RF27.5; 6962Fsh, RF24.5; 6908Fsh, RF27. (Number, Clinical Brady Number from Kilifi District Hospital; Fsh, fresh trophs; Fztr, frozen trophs, Fzrng, frozen rings. RF, pretreatment rosette frequency).

Rosette frequency was expressed relative to initial (pre-treatment) rosette frequency, so that all nine field isolates could be compared (Fig. 6.10). There was a significant inhibition ($P < 0.05$) across all field isolates combined at 10 μg/ml CRDS, and this rose in significance ($P < 0.005$) for 50 and 100 μg/ml CRDS conditions. Difference in RF compared to PBS control for all concentrations was significant by ANOVA ($P<0.0001$).

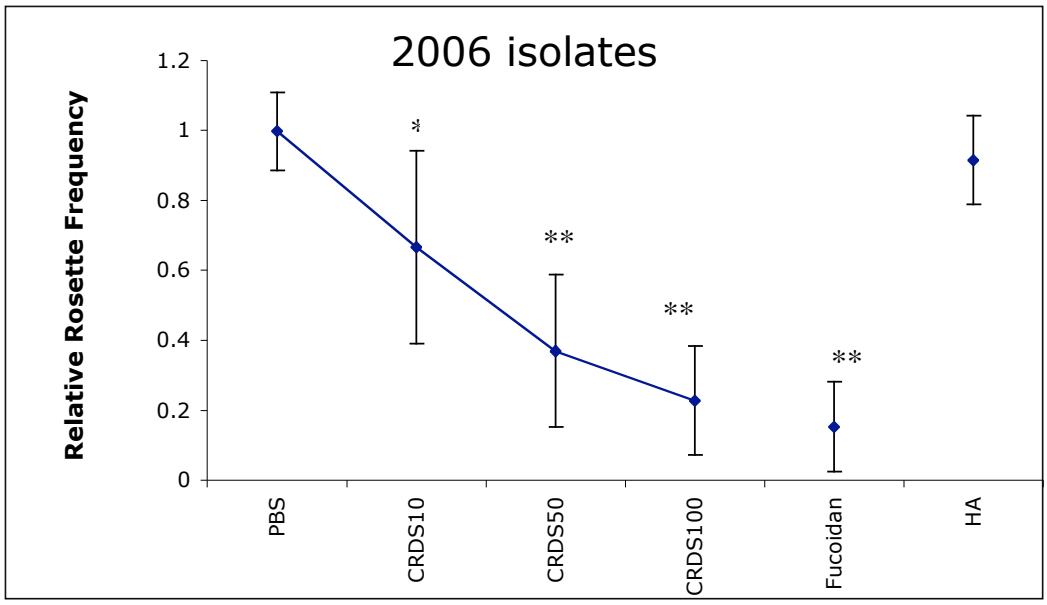

Fig. 6.10. Combined data for 9 field isolates of *P. falciparum* from Kilifi, Kenya, collected Jan-March 2006 treated with 0, 10, 50, 100 μg/ml CRDS in PBS, 100 μg/ml fucoidan or with 100 μg/ml hyaluronic acid. Mean ± SD is shown. * $p < 0.05$. ** $p < 0.005$ for paired t-tests compared to 0 μg/ml CRDS (PBS control). Relative rosette frequency was calculated as a proportion of each isolate's own pre-treatment rosette frequency.

6.7.2 CRDS-mediated rosette disruption in rosetting field isolate samples from Kilifi, Kenya 2- samples collected and cryopreserved in 1993

It was not possible to examine any more field isolate in Kenya due to the lack of malaria during Jan-March 2006 because of a severe drought. However, in order to increase the sample size, further field isolates from Kenya that had been frozen in 1993 (J.A. Rowe) were thawed and cultured to mature trophozoite stage as above.

Consistent with the previous Kenya field isolate samples (section 6.7.1), CRDS consistently disrupted rosetting in a concentration dependent manner in all parasites (Fig. 6.11), again showing evidence for high and low responders to CRDS.

As for the previous field isolate samples, rosette frequency was expressed relative to initial (pre-treatment) rosette frequency, so that all nine field isolates could be compared (Fig. 6.12). There was a significant inhibition ($P = 0.006$) across all field isolates combined at 10 μg/ml CRDS, and this rose to ($P < 0.005$) significance for 50 and 100 μg/ml CRDS conditions. Difference in RF compared to PBS control for all concentrations was significant by ANOVA ($P<0.0001$).

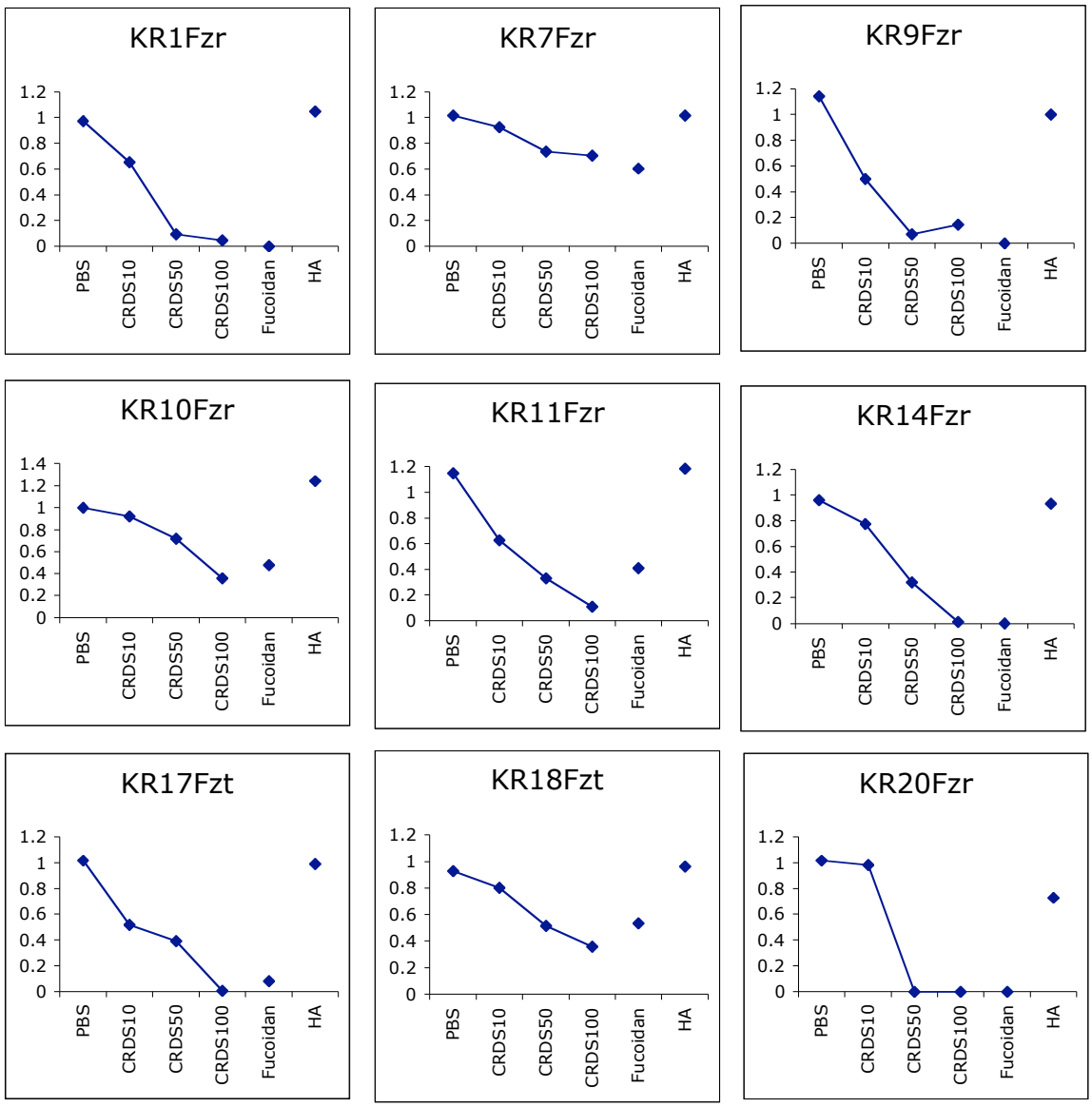

Fig. 6.11. CRDS-mediated rosette disruption in 9 rosetting field isolates from, Kilifi Kenya, collected 1993. RF shown as proportion of pre-treatment RF for comparison: Relative rosette frequency, Y-axis. Summary of field isolates used: KR1Fzr, RF53.5; KR7Fzr, RF68; KR9Fzr, RF14; KR10Fzr, RF25; KR11Fzr, 27; KR14Fzr, RF37.5, KR17Fzt, RF61; KR18Fzt, 28; KR20Fzr, RF63 (Fztr, frozen trophs, Fzrng, frozen rings. RF, pretreatment rosette frequency).

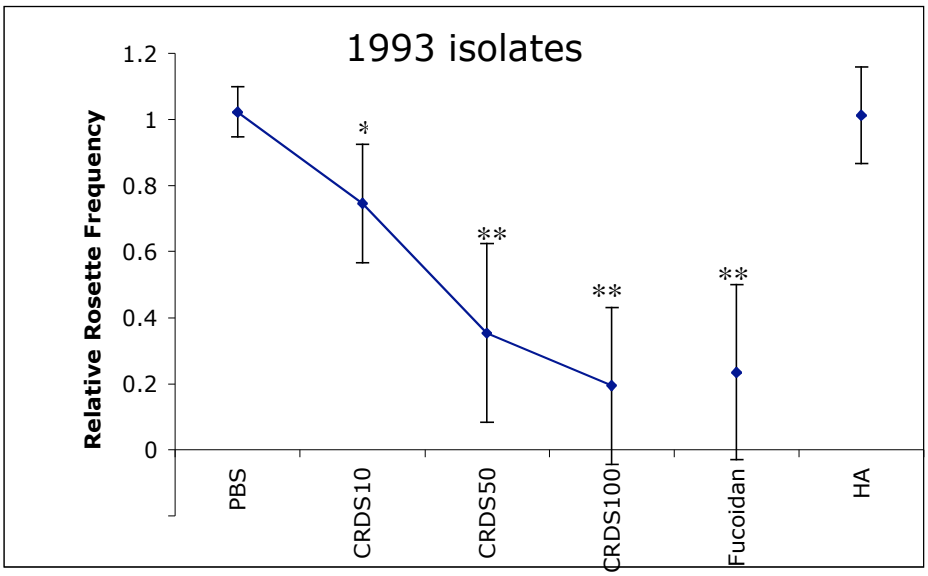

Fig. 6.12. Combined data for 9 field isolates of *P. falciparum* from Kilifi, Kenya collected in 1993 treated with 0, 10, 50, 100 μg/ml CRDS in PBS, 100 μg/ml fucoidan or with 100 μg/ml hyaluronic acid. Mean ± SD is shown. * $p < 0.05$. ** $p < 0.005$ for paired t-tests compared to 0 μg/ml CRDS (PBS control). Relative rosette frequency was calculated as a proportion of each isolate's own pre-treatment rosette frequency.

6.7.3 CRDS-mediated rosette disruption in rosetting field isolates: combined data

Rosette frequency was expressed relative to initial (pre-treatment) rosette frequency, so that all 18 field isolates could be compared (Fig. 6.13). There was a significant inhibition (P<0.005) across all field isolates combined at each CRDS condition compared to PBS. The effect of CRDS was also significant by ANOVA (P<0.0001).

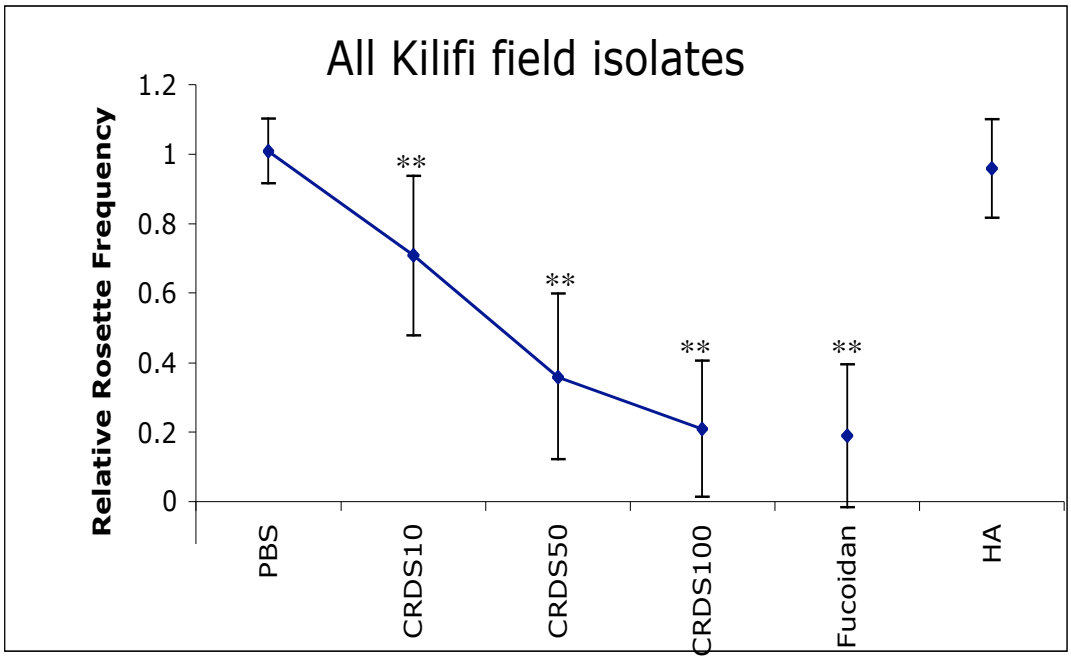

Fig. 6.13. Combined data for all 18 field isolates of *P. falciparum* from Kilifi, Kenya treated with 0, 10, 50, 100 μg/ml CRDS in PBS, 100 μg/ml fucoidan or with 100 μg/ml hyaluronic acid. Mean ± SD is shown. * $p < 0.05$. ** $p < 0.005$ for paired t-tests compared to 0 μg/ml CRDS (PBS control). Relative rosette frequency was calculated as a proportion of each isolate's own pre-treatment rosette frequency.

6.7.4 PfEMP1 expression in rosetting field isolates

Attempts were made to analyse the *var* gene transcription in the Kenyan rosetting field isolates, by separating the rosetting and non-rosetting infected erythrocytes using percoll (Fig. 6.14, details in chapter 2).

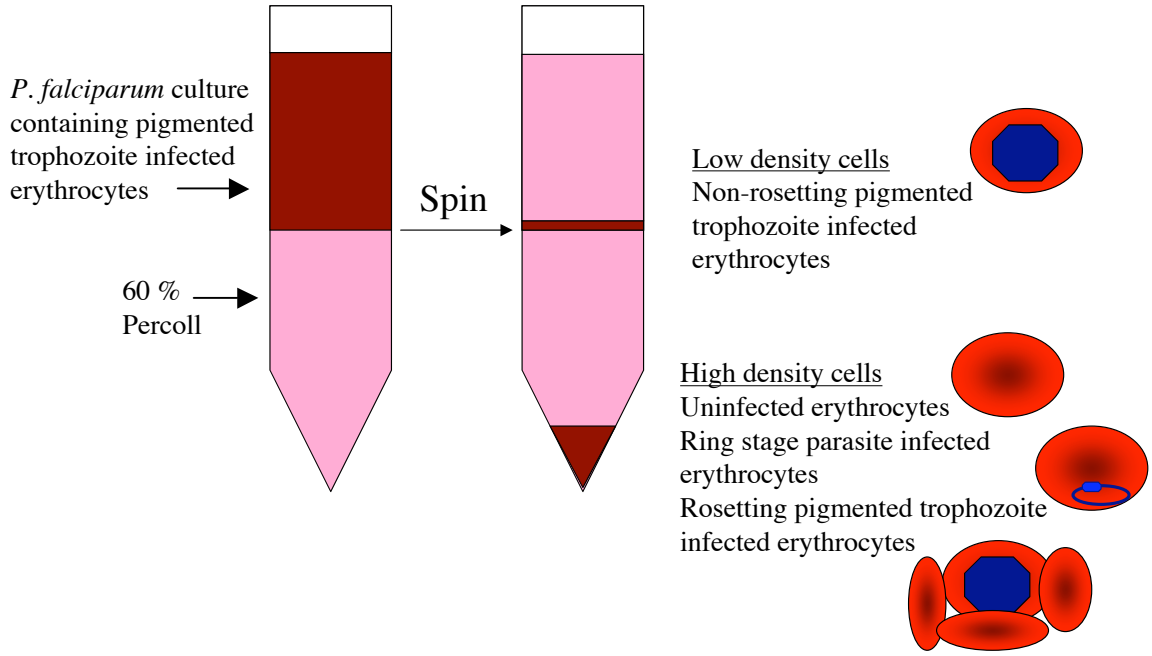

Fig. 6.14. Pigmented trophozoite infected erythrocytes can be separated from uninfected and ring stage parasite infected erythrocytes using a percoll gradient, as trophozoite infected erythrocytes have a lower density, and form a discrete layer above the 60% percoll after spinning (4000 rpm, 15 min). However, rosettes sink beneath the percoll due to the weight of uninfected erythrocytes, causing rosetting pigmented trophozoite infected erythrocytes to remain with the uninfected or ring stage infected cells. Rosetting and non-rosetting pigmented trophozoite infected erythrocytes can thus be separated.

Unfortunately, the small packed cell volume of the field isolates which was available meant that only a few microlitres of non-rosetting parasites were retrieved, and so there was not enough for RNA extraction, cDNA preparation and RT-PCR for a control (non-rosetting) set of *var* gene transcripts for comparison. Without this control group, analysis of the *var* gene transcripts from the remainder of the culture would be hard to interpret, as the contributions of the different PfEMP1 to rosetting would not be clear. An interesting follow-up study to this would be to examine the link between rosetting and expressed PfEMP1 in field isolates, and between expressed PfEMP1 and efficiency of CRDS action.

6.8 Discussion

CRDS was found to disrupt rosettes in 18/18 field isolates at doses suitable for clinical use, showing a significant effect on rosette frequency in two groups of Kenyan field isolates. The analysis of CRDS on field isolates discussed in this chapter complements data on laboratory clones (outlined in section 6.5), together showing that CRDS effectively and consistently disrupts rosettes in a wide range of strains.

At present we cannot prevent infection, or predict severe disease manifestation, so a key area of therapy is to reduce severe disease complications. High levels of rosetting (>30% RF) are estimated to occur in approximately 25% of severe malaria cases in Kenya, and around 50% of severe malaria cases in Mali (Alex Rowe, personal communication). If these figures are representative across the whole of sub-Saharan Africa, rosetting may play a role in an estimated 500,000 *P. falciparum*

malaria deaths per year in sub-Saharan Africa (Rowe 2005). Rosette inhibiting drugs could thus have a substantial impact on malaria mortality and morbidity. The strong ability to reduce rosetting suggests CRDS may be able to reduce the severe complications and lower mortality of *P. falciparum* malaria.

Who would CRDS therapy be for? A clinical trial of CRDS in severe and cerebral malaria reported a moderate decrease in fever and coma resolution time (Havlik *et al.* 2005). However, the patients studied were from Thailand, where rosetting is not associated with disease severity, possibly due to the CR1 deficiency across Asia (al-Yaman *et al.* 1995; Cockburn *et al.* 2004). Rosette disruption via CRDS treatment might not be appropriate in Asia. Rosette-disruption via CRDS therapy is also not relevant where *P. vivax* is the dominant infective *Plasmodium*. Although rosetting is a common property of *P. vivax* field isolates, and heparin (and therefore potentially also CRDS) reverses *P. vivax* rosettes, rosetting of *P. vivax* is not associated with severe disease (Chotivanich *et al*. 1998). As such there may not be any therapeutic benefit from disrupting the *P. vivax* rosettes.

However, in Africa, and especially in African children, there is compelling evidence that rosetting is involved in the pathogenesis of severe disease (Carlson *et al.* 1990; Rowe *et al.* 1995; Rowe *et al.* 2002c and also reported in chapter 3). In the case of cerebral malaria, parasitized erythrocytes adhering to the cerebral endothelium are associated with coma which is fatal in up to 30% of cases (MacPherson *et al.* 1985; White 1987; Brewster *et al.* 1990; Berendt *et al.* 1994a; Newton *et al.* 1998; Silamut *et al.* 1999). However, if the infected cells are cleared, a full recovery is made with

neurological impairment in only 12% of survivors (Brewster *et al.* 1990). As rosetting parasites are associated with cerebral malaria (Carlson *et al.* 1990; Rowe *et al.* 1995; Rowe *et al.* 2002c), it seems logical to conclude that the rosettes participate in the obstruction of the cerebral capillaries. Thus, disruption of rosettes may quicken the clearance of infected erythrocytes from the cerebral vasculature. This may reverse the coma more rapidly and reduce chance of focal lesions, or ring haemorrhages, within the cerebral hemisphere which can lead to neurological sequelae (Brewster *et al*. 1990; Newton *et al*. 1998). Ideally CRDS treatment could be targeted towards isolates with a high rosette frequency, though the 24 hr culturing required to mature peripheral ring parasites to pigmented trophozoites would be inappropriate for field situations. Furthermore, many patients do no have 24 hr to wait before treatment as most malaria deaths occur within 24 hr of admission (Jaffar *et al.* 1997), before standard anti-malarial drugs are effective. Thus there is an urgent need for drugs to tackle phenomena causing severe malaria disease symptoms within this short time window. As rosetting is consistently associated with all forms of severe disease in Africa (though not in Asia) (Carlson *et al.* 1990; al-Yaman *et al.* 1995; Rowe *et al.* 1995; Rowe *et al.* 2002b) CRDS could be given to all patients showing severe complications in Africa.

In addition to rosetting, it is possible CRDS may have a direct effect on sequestration. HS can also mediate sequestration, as HS is present on endothelial cells although the possibility of HS as a ligand for sequestration for infected erythrocytes has been controversial. Xiao *et al*. (1993) reported HS does not influence cytoadherence to HMEC or C2 melanoma cells, as heparinase treatment

did not abolish adhesion. However, the heparinase treatment used may not have completely digested the heparin, leaving enough HS chains on the endothelium to support IE adhesion. Vogt *et al*. (2003) reported adhesion of FCR3 and wild type clinical isolates to HUVEC and HLEC cells lines via hepain/HS, through a DBLα:HS interaction, and field isolates with affinity for HS have been reported (Heddini *et al*. 2001). Sporozoite invasion of hepatocytes is via CSP adhesion to heparan sulfate proteoglycans on the hepatocyte surface (Frevert *et al*. 1993). This may also be disrupted by CRDS.

Even if CRDS does not directly inhibit sequestration, removal of rosettes is likely to reduce vascular blockage. For example disruption of Malayan Camp rosettes dramatically decreased microvascular obstruction and cytoadherence in a rat mesocaecum vasculature model with *P. falciparum* infected sequestered erythrocytes (Kaul *et al*. 1991), though the rosetting ligand in this case was CD36, a common endothelial sequestration receptor, and not affected by CRDS (Evans *et al*. 1998). However, CD36 binding is associated with sequestration in non-vital organs, and with PfEMP1 expressed in non-severe malaria, as discussed in chapter 3.

Other ligands present on cell types such as endothelium or platelets, which may aid sequestration by bridging IE and activated endothelium, may also be affected by CRDS. Chondroitin sulfate A and hyaluronic acid, implicated in placental malarial sequestration, as discussed in chapter 4, are both sulfated glycoconjugates and thus chemically similar to heparin. Though these molecules do not inhibit rosetting (Rowe *et al*. 1994), it remains possible that CRDS may disrupt their use as adhesion

receptors for infected erythrocytes. Thus it is possible CRDS may also play a role in reversal of adhesion in placental malaria.

Further experiments characterising the effect of CRDS on laboratory isolates revealed that rosettes were able to reform after CRDS was removed. The short half-life (2-3 hr; Gordon *et al*. 1994) and rosette reformation after washing has implications for administration of drug, suggesting that the drug should be administered regularly throughout treatment. The effect on merozoite invasion was not examined in this study, but it has previously been reported that CRDS can inhibit merozoite invasion (Havlik *et al*. 1994; Evans *et al*. 1998), as can many sulfated glycoconjugates (Kulane *et al*. 1992; Xiao *et al*. 1996).

At present there is no data on whether GAGs influence commitment to gametocytogenesis, which is an important consideration for any drug administered to infected individuals, as reducing the asexual parasitaemia can sometimes be associated with an increase in sexual stage parasites, and thus an overall increase in transmission, such as has been observed with chloroquine (Buckling *et al*. 1999).

It is important to emphasise that CRDS has already been shown to be well tolerated in clinical trials and was able to reduce fever clearance time in a recent clinical trial of *P. falciparum* malaria (Havlik *et al*. 2005). CRDS is able to inhibit *P. falciparum* growth *in vitro,* through inhibiting merozoite invasion (Havlik *et al*. 1994; Evans *et al*. 1998). In addition CRDS has also been shown to down-modulate cytokine effects in HIV infection (Naito *et al*. 2001). This is promising for auxiliary therapy for

severe malaria treatment, as some of the clinical symptoms may be due to the immune response to infection (Grau *et al*. 1989; Kwiatkowski *et al*. 1990), making CRDS an even more potent agent against severe disease symptoms of clinical malaria. This data, together with previous reports, suggests that CRDS is a strong candidate for adjunctive therapy in severe malaria, and support further clinical trials of CRDS, especially in African children where rosetting is linked to severe disease.

Chapter 7

Discussion

Discussion

The general aim of the thesis was to investigate the hypothesis that PfEMP1 expression influences clinical malaria disease due to *P. falciparum* infection. The work presented in the thesis focussed on conserved PfEMP1 subgroups and clinical disease presentation in African field isolates, and development of a drug that could use this information to prevent onset of severe symptoms due to *P. falciparum* infection. In the case of childhood malaria, I have shown that there was a significantly higher frequency of group A *var* gene transcripts in cerebral malaria field isolates compared to isolates from children with equally high parasite burdens but no symptoms or signs of severe malaria (hyperparasitaemia), suggesting that group A *var* genes are important determinants of parasite virulence (chapter 3). In work on placental malaria, I detected *var2csa* transcripts in all 6 placental malaria field isolates examined, but not in a control group of 10 childhood malaria isolates, suggesting that *var2csa* expression is a critical factor in the onset of clinical malaria disease in pregnant women (chapter 4), consistent with other recent studies (Tuikue Ndam *et al.* 2005; Duffy *et al.* 2006a). I also found that type 3 *var* genes, an atypically small and conserved subset of group A *var* genes, were commonly transcribed in blood-stage parasites, showing a possible association with hyperparasitaemia rather than cerebral malaria field isolates, and sequence analysis confirmed a very high level of conservation across this *var* gene subfamily (chapter 5). In addition, I found a non-toxic compound, curdlan sulfate, to be effective at disrupting rosettes in all rosetting field isolates examined (chapter 6), suggesting potential for use in treatment of severe malaria due to rosetting *P. falciparum*

isolates. This final chapter aims to link together these findings and discuss the role of conserved PfEMP1 and clinical malaria disease.

The link between group A *var* gene expression and severe malaria (chapter 3) is consistent with data from previous field isolate studies (Kirchgatter and Portillo Hdel 2002; Rottmann *et al*. 2006) and with upregulation of group A *var* gene transcription in 3D7 after selection for severe malaria-type VSA (Jensen *et al*. 2004). Severe malaria has also been linked to "common" *var* genes through sera agglutination studies (Bull *et al*. 1999), and the resistance to severe malaria which develops throughout childhood suggests common epitopes are present in severe malaria-causing parasites, allowing protective cross-reactive antibodies to develop. Group A *var* genes tend to have more cross-reacting epitopes than group B or C (Joergensen *et al*. 2006), and transcripts that were present in multiple isolates in the chapter 3 analysis were more frequently DBLα1 than DBLα0. Thus the association between group A PfEMP1 and severe malaria is consistent with a link between "common" PfEMP1 and severe malaria.

Multiple adhesive phenotypes can be associated with severe malaria (Heddini *et al*. 2001). Group A PfEMP1 tend to have more domains than group B and C PfEMP1 (Gardner *et al*. 2002; Kraemer *et al*. 2007), and thus have an increased binding potential, for example for ligands such as ICAM-1 (Smith *et al*. 2000a; Springer *et al*. 2004) or IgM (Semblat *et al*. 2006). Furthermore, binding to molecules on uninfected erythrocytes, such as CR1 (Rowe *et al*. 1997; Rowe *et al*. 2000), ABO blood group antigens (Carlson and Wahlgren 1992; Chen *et al*. 1998a; Barragan *et*

al. 2000) or heparan sulfate (Carlson *et al*. 1992), causes rosetting, which is a phenomenon associated with severe malaria in African field isolates (Carlson *et al*. 1990; Rowe *et al*. 1995; Rowe *et al*. 2002c). Rosetting is more commonly a property of group A *var* genes (Rowe, JA, unpublished data), and many field studies observe a correlation of higher rosette frequency with group A/DBLα1 domain expression (chapter 3; Bull *et al*. 2005a; Kaestli *et al*. 2006; Rottmann *et al*. 2006; Normark *et al*. 2007). This provides another consistent link between group A PfEMP1 and severe disease.

Rosetting interactions may cause rosetting PfEMP1 to have conserved structural or sequence features which may provide common epitopes for recognition by cross-reactive antibodies. Natural rosetting-disrupting antibodies can form upon infection, and have been associated with protection from cerebral malaria (Carlson *et al*. 1990). Antibodies raised against the rosetting DBLα domains of FCR3S1.2 (the rosetting PfEMP1 of FCR3) disrupt FCR3 rosettes (Chen *et al*. 2004) and also show cross-reactive rosette disruption against R29 rosettes (Moll *et al*. 2007). These antibodies also showed recognition of a panel of Ugandan field isolates, with increased recognition of those causing severe disease (Normark *et al*. 2007) suggesting common antibody epitopes are present across diverse rosetting PfEMP1. The interaction of many diverse rosetting PfEMP1 with host rosetting ligands can also be inhibited by drugs such as heparin (Carlson *et al*. 1992; Rowe *et al*. 1994) and curdlan sulfate (chapter 6), also suggesting common features are present between many rosetting interactions.

Conversely, group B and C PfEMP1 are commonly expressed in non-severe malaria (this study chapter 3, Kaestli *et al*. 2006; Rottmann *et al*. 2006). Group B and C PfEMP1 commonly bind to CD36, which is associated with non-severe malaria, and with immunosuppression (Urban *et al*. 1999) and sequestration in non-vital organs (Serghides *et al*. 2003). Group B and C PfEMP1 are commonly expressed in individuals who have reached a high level of immunity to clinical disease (asymptomatic adults e.g. Kaestli *et al*. 2006, or hyperparasitaemia; this study) suggesting cross-reactive protective antibodies are rare. Parasites from clinically immune individuals, or patients with mild or asymptomatic malaria infection, are less likely to be agglutinated by heterologous sera (Bull *et al*. 2000), also indicating a lower level of epitope cross-reactivity. Cross-reactive epitopes between group B and C PfEMP1 of 3D7 are uncommon (Joergensen *et al*. 2006), and few DBLα0 were found in multiple isolates in the Mali childhood malaria isolates discussed in this thesis (chapter 3). Thus DBLα0 domains or group B and C PfEMP1, though present in the majority of PfEMP1, are not promising vaccine candidates, as they are associated with non-severe malaria and do not share a high number of cross-reactive epitopes.

If a vaccine were to be raised to PfEMP1, then this data suggests group A PfEMP1 should be targeted. Immunisation of Aotus monkeys with the CIDR domain of Malayan Camp caused protection against subsequent infection with the same strain, showing PfEMP1 domains can be immunogenic and elicit a protective antibody response (Baruch *et al*. 2002). As all known group A PfEMP1 have a DBLα1

domain, cross-reactive epitopes within DBLα1 domains might be a promising focus for vaccine design. DBLα0 domain immunisation in Sprague Dawley rats also elicited a protective immune response against rosetting and sequestration, with some degree of cross-reactivity to other strains, providing evidence that DBLα domain immunisation can be effective (Chen *et al.* 2004; Moll *et al.* 2007; Normark *et al.* 2007). Normark *et al.* (2007) also suggested certain motifs are common between PfEMP1 associated with rosetting and severe malaria isolates, and using structural modelling predicted that some of these motifs lie within a pocket of the DBLα1 domain that is homologous to the fold used by *Pk*-DBLα for DARC-recognition. This fold is also conserved in EBA-175 and may be a conserved area for receptor binding that could provide a cross-reactive structural antibody target. However, there was little overall cross-reactivity of antibodies raised against various domains of 3D7 (Joergensen *et al.* 2006) and the question remains whether PfEMP1 is too polymorphic to be an effective vaccine candidate.

The type 3 PfEMP1 are a special case of group A PfEMP1, having only 2 extracellular domains and an atypically short intron which appears to be without a regulatory promoter. Theoretically, the type 3 PfEMP1 subfamily makes an excellent vaccine candidate as type 3 PfEMP1 are highly conserved. However, though most or many *P. falciparum* strains encode a type 3 *var* gene, and most field isolates show type 3 *var* gene expression (chapter 5), there is no evidence that they are expressed on the infected erythrocyte surface, or that their expression is essential, and as such a vaccine might not be effective. Furthermore, the surprising observation of greater diversity of type 3 *var* gene expression in hyperparasitaemia isolates compared to

cerebral malaria isolates suggests that these atypical group A PfEMP1 may not be commonly involved in severe disease pathogenesis (chapter 5).

At present the only PfEMP1 which shows potential as a vaccine target is VAR2CSA specifically in the context of placental malaria, as discussed in chapter 4. There is a strong association between *var2csa* transcription and placental malaria field isolates (chapter 4, and e.g. Tuikue Ndam *et al*. 2005; Duffy *et al*. 2006a). In addition, VAR2CSA has affinity for CSA, which is associated with placental sequestration (Fried and Duffy 1996; Reeder *et al*. 2000; Muthusamy *et al*. 2007). The rise in anti-VAR2CSA antibodies, which coincides with protection from placental malaria upon subsequent pregnancies (Salanti *et al*. 2004; Tuikue Ndam *et al*. 2006), suggests a VAR2CSA vaccine could effectively mimic this natural immunity. Not all peptide stretches of VAR2CSA are targets of natural antibodies (Dahlback *et al*. 2006), and so high sequence homology appears to be insufficient to ensure an protective antibody response. A motif EIEKD within a variable region (V2) was noted by Dahlback *et al*. (2006) to be common in VAR2CSA from primigravidae and was predicted to lie within a surface exposed loop, and thus provide a promising vaccine target. The motif EIEKD is uncommon in multigravidae where GIEGE is found at this position (Dahlback *et al*. 2006). Although this suggests EIEKD-VAR2CSA variants may be more virulent or more efficient at sequestration and thus a good vaccine target, loss of these variants may simply result in selection of GIEGE-VAR2CSA variants and would not necessarily result in an overall decrease of placental infection. As discussed in chapter 4, there still remains some sequence diversity between *var2csa* homologues, and there is evidence of surprisingly low

cross-reactivity between antibodies raised against different VAR2CSA (e.g.(Bockhorst *et al.* 2007; Oleinikov *et al.* 2007). In addition, the contribution of other PfEMP1 is unclear, and there is evidence of a high number of non–*var2csa var* genes being transcribed at similar or higher frequency to *var2csa* (chapter 4). Furthermore, other (non-PfEMP1) proteins have also been associated with placental malaria (Francis *et al.* 2007). If VAR2CSA is not the only protein responsible for placental sequestration, then the relative contributions of other proteins must also be taken into account in order to determine the efficacy of an anti-VAR2CSA vaccine.

In addition to vaccines, drugs can also be used to target sequestration in malaria. At present there are no drugs designed to directly target sequestration of *P. falciparum*-infected erythrocytes. However, advances in the development of a drug to target rosetting (curdlan sulfate, as described in chapter 6) are promising. The benefits of a rosette-disrupting drug are that it is quick acting and may have an immediate effect in reducing microvascular obstruction due to rosetting and help to relieve symptoms of anaemia by releasing bound uninfected erythrocytes back into the circulation. Curdlan sulfate could be administered to all patients with severe malaria disease in Africa, where rosetting is associated with all forms of severe disease (Rowe *et al.* 1995; Rowe 2005), and so patients would not require expensive or time-consuming tests to assess rosette frequency before drug administration. As many parasite isolates do not rosette, there may be little pressure for drug resistance to develop against this anti-rosetting drug, as is seen with more conventional antimalarials, which aim to eradicate the parasite. Thus drug resistance to curdlan sulfate may be slow to build up in a population. The effect of curdlan sulfate on other

glycosaminoglycan interactions, such as sequestration to CSA in placental malaria, is at present unknown, and would be an interesting follow-up study. There is also recent evidence that CSA is involved in ookinete invasion in the *anopheles* mosquito (Dinglasan *et al*. 2007). In addition to disrupting placental sequestration via CSA, this may provide another opportunity for any drugs which can disrupt CSA-binding, whether developed from the VAR2CSA/placental malaria perspective, or from research on CSA/proteoglycans and rosetting.

The links between conserved PfEMP1 and clinical disease are not independent. Interactions between the major associations discussed above can be represented in a network of relationships between PfEMP1 group and clinical disease (Fig. 7.1). This highlights the connections between various factors associated with severe/cerebral clinical disease and group A PfEMP1, such as "commonness", rosetting and multiple-binding phenotypes, as distinct from factors associated with non-severe clinical disease/hyperparasitaemia, such as CD36-binding and group B or C PfEMP1. VAR2CSA, CSA-binding and placental malaria form a separate triangle, with a possible link to group A PfEMP1 due to DBLγ domain interactions. The possible therapeutic interventions with curdlan sulfate are also indicated in Fig. 7.1. These include rosette inhibition, a general role in severe malaria treatment for example through other roles such as merozoite inhibition (Havlik *et al*. 1994; Evans *et al*. 1998), and the possibility of inhibition of other interactions such as CSA-binding, as discussed in chapter 6. The putative link between type 3 PfEMP1 and non-severe malaria/hyperparasitaemia discussed in chapter 5 is also included.

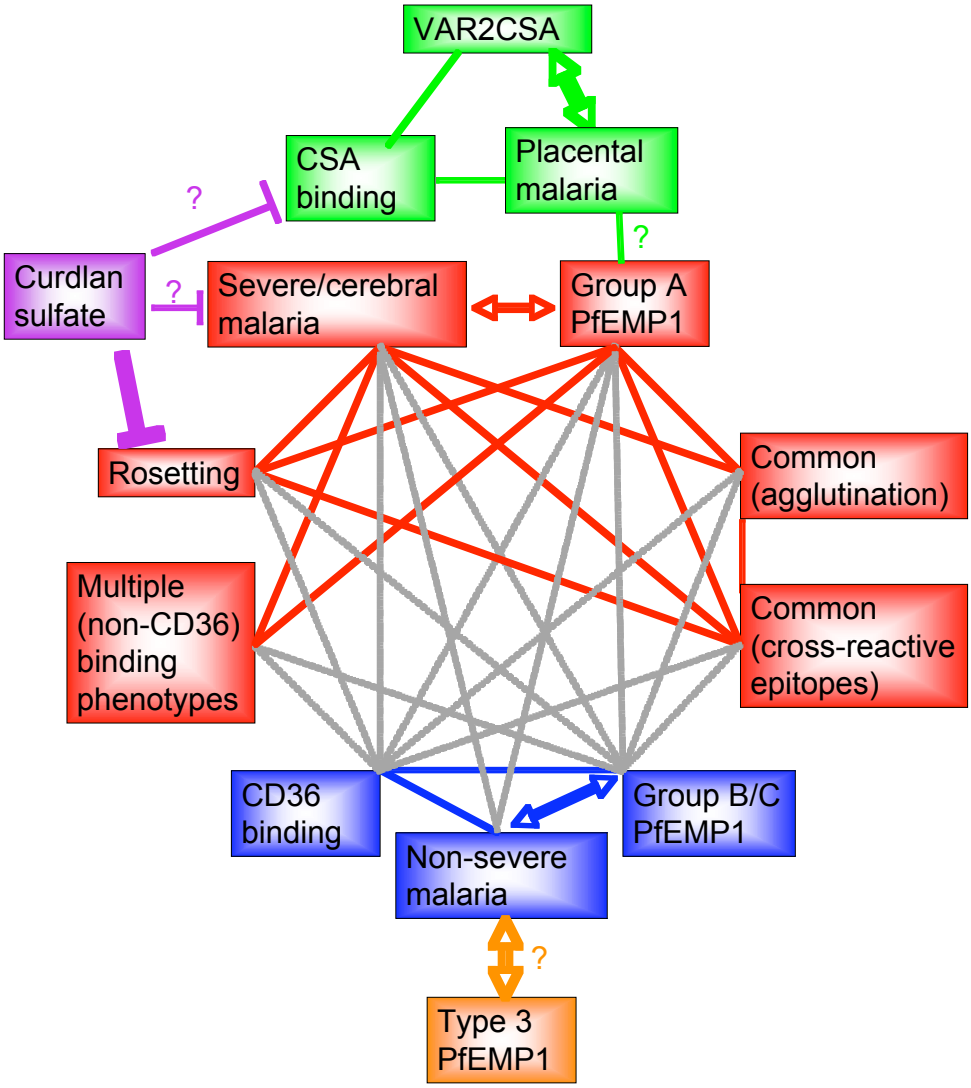

Fig. 7.1. Relationships between PfEMP1 group and clinical disease. Positive associations between factors associated with severe or clinical disease and group A PfEMP1 (red), between non-severe clinical disease/hyperparasitaemia and group B or C PfEMP1 (blue), between VAR2CSA, CSA binding and placental malaria (green) and possible therapeutic interventions with curdlan sulfate (purple) are indicated. Dotted lines show negative associations. Bold arrows between group A PfEMP1 and severe/cerebral malaria, between group B/C PfEMP1 and non-severe malaria, between VAR2CSA and placental malaria and between type 3 PfEMP1 (orange) and non-severe malaria, and the bold line between curdlan sulfate and rosette inhibition, indicate relationships based on data from this thesis.

This network highlights the associations between multiple factors and raises questions about intervention strategies. For example, does knocking out a bridging point between group A PfEMP1 and severe malaria (such as rosetting or other binding phenotypes) reduce the strength of the link between group A PfEMP1 expression and severe disease?

In conclusion, the data presented in this thesis demonstrate significant relationships between *var* gene/PfEMP1 expression and clinical outcome in *P. falciparum* malaria disease pathogenesis. Research on malaria is highly multidisciplinary, and benefits from all areas of research working collectively towards the common goal of malaria disease control and eradication. This work highlights the need for continued research on *var* gene/PfEMP1 expression involvement in clinical disease in the effort to reduce the severity of complications due to *P. falciparum* infection, in the fight against this devastating disease.

References

References

Achur, R. N., M. Valiyaveettil, A. Alkhalil, C. F. Ockenhouse and D. C. Gowda (2000). "Characterization of proteoglycans of human placenta and identification of unique chondroitin sulfate proteoglycans of the intervillous spaces that mediate the adherence of Plasmodium falciparum-infected erythrocytes to the placenta." J Biol Chem **275**(51): 40344-56.

Adams, J. H., B. K. Sim, S. A. Dolan, X. Fang, D. C. Kaslow and L. H. Miller (1992). "A family of erythrocyte binding proteins of malaria parasites." Proc Natl Acad Sci U S A **89**(15): 7085-9.

Afonso Nogueira, P., G. Wunderlich, M. Shugiro Tada, J. d'Arc Neves Costa, M. Jose Menezes, A. Scherf and L. H. Pereira-da-Silva (2002). "Plasmodium falciparum: analysis of transcribed var gene sequences in natural isolates from the Brazilian Amazon region." Exp Parasitol **101**(2-3): 111-20.

Aikawa, M., C. G. Huff and H. Sprinz (1967). "Fine structure of the asexual stages of Plasmodium elongatum." J Cell Biol **34**(1): 229-49.

al-Yaman, F., B. Genton, D. Mokela, A. Raiko, S. Kati, S. Rogerson, J. Reeder and M. Alpers (1995). "Human cerebral malaria: lack of significant association between erythrocyte rosetting and disease severity." Trans R Soc Trop Med Hyg **89**(1): 55-8.

Alban, S. and G. Franz (2000). "Characterization of the anticoagulant actions of a semisynthetic curdlan sulfate." Thromb Res **99**(4): 377-88.

Albrecht, L., E. F. Merino, E. H. Hoffmann, M. U. Ferreira, R. G. de Mattos Ferreira, A. L. Osakabe, R. C. Dalla Martha, M. Ramharter, A. M. Durham, J. E. Ferreira, H. A. Del Portillo and G. Wunderlich (2006). "Extense variant gene family repertoire overlap in Western Amazon Plasmodium falciparum isolates." Mol Biochem Parasitol **150**(2): 157-65.

Andrews, K. T., L. A. Pirrit, J. M. Przyborski, C. P. Sanchez, Y. Sterkers, S. Ricken, H. Wickert, C. Lepolard, M. Avril, A. Scherf, J. Gysin and M. Lanzer (2003). "Recovery of adhesion to chondroitin-4-sulphate in Plasmodium falciparum varCSA disruption mutants by antigenically similar PfEMP1 variants." Mol Microbiol **49**(3): 655-69.

Angus, B. J., K. Thanikkul, K. Silamut, N. J. White and R. Udomsangpetch (1996). "Short report: Rosette formation in Plasmodium ovale infection." Am J Trop Med Hyg **55**(5): 560-1.

Aoki, T., Y. Kaneko, T. Nguyen, M. S. Stefanski, R. C. Ting and M. M. Manak (1992). "Curdlan sulfate and HIV-1: II. In vitro long-term treatment of HIV-1 infection with curdlan sulfate." AIDS Res Hum Retroviruses **8**(5): 605-12.

Artavanis-Tsakonas, K., K. Eleme, K. L. McQueen, N. W. Cheng, P. Parham, D. M. Davis and E. M. Riley (2003). "Activation of a subset of human NK cells upon contact with Plasmodium falciparum-infected erythrocytes." J Immunol **171**(10): 5396-405.

Atkinson, C. T., M. Aikawa, G. Perry, T. Fujino, V. Bennett, E. A. Davidson and R. J. Howard (1988). "Ultrastructural localization of erythrocyte cytoskeletal and integral membrane proteins in Plasmodium falciparum-infected erythrocytes." Eur J Cell Biol **45**(2): 192-9.

Avril, M., B. Traore, F. T. Costa, C. Lepolard and J. Gysin (2004). "Placenta cryosections for study of the adhesion of Plasmodium falciparum-infected erythrocytes to chondroitin sulfate A in flow conditions." Microbes Infect **6**(3): 249-55.

Badaut, C., G. Faure, N. G. Tuikue Ndam, G. Bertin, A. Chaffotte, A. Khattab, M. Q. Klinkert, P. Deloron and G. A. Bentley (2007). "Receptor-binding studies of the DBLgamma domain of Plasmodium falciparum erythrocyte membrane protein 1 from a placental isolate." Mol Biochem Parasitol **151**(1): 89-99.

Bannister, L. H., J. M. Hopkins, R. E. Fowler, S. Krishna and G. H. Mitchell (2000). "A brief illustrated guide to the ultrastructure of Plasmodium falciparum asexual blood stages." Parasitol Today **16**(10): 427-33.

Baratin, M., S. Roetynck, B. Pouvelle, C. Lemmers, N. K. Viebig, S. Johansson, P. Bierling, A. Scherf, J. Gysin, E. Vivier and S. Ugolini (2007). "Dissection of the role of PfEMP1 and ICAM-1 in the sensing of plasmodium falciparum-infected erythrocytes by natural killer cells." PLoS ONE **2**(2): e228.

Barfod, L., N. L. Bernasconi, M. Dahlback, D. Jarrossay, P. H. Andersen, A. Salanti, M. F. Ofori, L. Turner, M. Resende, M. A. Nielsen, T. G. Theander, F. Sallusto, A. Lanzavecchia and L. Hviid (2007). "Human pregnancy-associated malaria-specific B cells target polymorphic, conformational epitopes in VAR2CSA." Mol Microbiol **63**(2): 335-47.

Barragan, A., P. G. Kremsner, M. Wahlgren and J. Carlson (2000). "Blood group A antigen is a coreceptor in Plasmodium falciparum rosetting." Infect Immun **68**(5): 2971-5.

Barragan, A., D. Spillmann, P. G. Kremsner, M. Wahlgren and J. Carlson (1999). "Plasmodium falciparum: molecular background to strain-specific rosette disruption by glycosaminoglycans and sulfated glycoconjugates." Exp Parasitol **91**(2): 133-43.

Barry, A. E., A. Leliwa-Sytek, L. Tavul, H. Imrie, F. Migot-Nabias, S. M. Brown, G. A. McVean and K. P. Day (2007). "Population genomics of the immune evasion (var) genes of Plasmodium falciparum." PLoS Pathog **3**(3): e34.

Baruch, D. I., B. Gamain, J. W. Barnwell, J. S. Sullivan, A. Stowers, G. G. Galland, L. H. Miller and W. E. Collins (2002). "Immunization of Aotus monkeys with a functional domain of the Plasmodium falciparum variant antigen induces protection against a lethal parasite line." Proc Natl Acad Sci U S A **99**(6): 3860-5.

Baruch, D. I., B. L. Pasloske, H. B. Singh, X. Bi, X. C. Ma, M. Feldman, T. F. Taraschi and R. J. Howard (1995). "Cloning the P. falciparum gene encoding PfEMP1, a malarial variant antigen and adherence receptor on the surface of parasitized human erythrocytes." Cell **82**(1): 77-87.

Baum, J., D. Richard, J. Healer, M. Rug, Z. Krnajski, T. W. Gilberger, J. L. Green, A. A. Holder and A. F. Cowman (2006). "A conserved molecular motor drives cell invasion and gliding motility across malaria life cycle stages and other apicomplexan parasites." J Biol Chem **281**(8): 5197-208.

Baumeister, S., T. Endermann, S. Charpian, J. Nyalwidhe, C. Duranton, S. Huber, K. Kirk, F. Lang and K. Lingelbach (2003). "A biotin derivative blocks parasite induced novel permeation pathways in Plasmodium falciparum-infected erythrocytes." Mol Biochem Parasitol **132**(1): 35-45.

Beeson, J. G., K. T. Andrews, M. Boyle, M. F. Duffy, E. K. Choong, T. J. Byrne, J. M. Chesson, A. M. Lawson and W. Chai (2007a). "Structural basis for binding of plasmodium falciparum erythrocyte membrane protein 1 to chondroitin sulfate and placental tissue and the influence of protein polymorphisms on binding specificity." J Biol Chem **282**(31): 22426-36.

Beeson, J. G. and G. V. Brown (2002). "Pathogenesis of Plasmodium falciparum malaria: the roles of parasite adhesion and antigenic variation." Cell Mol Life Sci **59**(2): 258-71.

Beeson, J. G. and G. V. Brown (2004). "Plasmodium falciparum-infected erythrocytes demonstrate dual specificity for adhesion to hyaluronic acid and chondroitin sulfate A and have distinct adhesive properties." J Infect Dis **189**(2): 169-79.

Beeson, J. G., G. V. Brown, M. E. Molyneux, C. Mhango, F. Dzinjalamala and S. J. Rogerson (1999). "Plasmodium falciparum isolates from infected pregnant women and children are associated with distinct adhesive and antigenic properties." J Infect Dis **180**(2): 464-72.

Beeson, J. G., E. J. Mann, T. J. Byrne, A. Caragounis, S. R. Elliott, G. V. Brown and S. J. Rogerson (2006). "Antigenic differences and conservation among placental Plasmodium falciparum-infected erythrocytes and acquisition of variant-specific and cross-reactive antibodies." J Infect Dis **193**(5): 721-30.

Beeson, J. G., F. Ndungu, K. E. Persson, J. M. Chesson, G. L. Kelly, S. Uyoga, S. L. Hallamore, T. N. Williams, J. C. Reeder, G. V. Brown and K. Marsh (2007b). "Antibodies among Men and Children to Placental-Binding Plasmodium falciparum-Infected Erythrocytes that Express var2csa." Am J Trop Med Hyg **77**(1): 22-28.

Beeson, J. G., S. J. Rogerson, B. M. Cooke, J. C. Reeder, W. Chai, A. M. Lawson, M. E. Molyneux and G. V. Brown (2000). "Adhesion of Plasmodium falciparum-infected erythrocytes to hyaluronic acid in placental malaria." Nat Med **6**(1): 86-90.

Bejon, P., J. A. Berkley, T. Mwangi, E. Ogada, I. Mwangi, K. Maitland, T. Williams, J. A. Scott, M. English, B. S. Lowe, N. Peshu, C. R. Newton and K. Marsh (2007). "Defining childhood severe falciparum malaria for intervention studies." PLoS Med **4**(8): e251.

Berendt, A. R., D. J. Ferguson, J. Gardner, G. Turner, A. Rowe, C. McCormick, D. Roberts, A. Craig, R. Pinches, B. C. Elford and et al. (1994a). "Molecular mechanisms of sequestration in malaria." Parasitology **108 Suppl**: S19-28.

Berendt, A. R., G. D. Tumer and C. I. Newbold (1994b). "Cerebral malaria: the sequestration hypothesis." Parasitol Today **10**(10): 412-4.

Biggs, B. A., L. Gooze, K. Wycherley, W. Wollish, B. Southwell, J. H. Leech and G. V. Brown (1991). "Antigenic variation in Plasmodium falciparum." Proc Natl Acad Sci U S A **88**(20): 9171-4.

Bir, N., S. S. Yazdani, M. Avril, C. Layez, J. Gysin and C. E. Chitnis (2006). "Immunogenicity of Duffy binding-like domains that bind chondroitin sulfate A and protection against pregnancy-associated malaria." Infect Immun **74**(10): 5955-63.

Bockhorst, J., F. Lu, J. H. Janes, J. Keebler, B. Gamain, P. Awadalla, X. Z. Su, R. Samudrala, N. Jojic and J. D. Smith (2007). "Structural polymorphism and

diversifying selection on the pregnancy malaria vaccine candidate VAR2CSA." Mol Biochem Parasitol **155**(2): 103-12.
Brabin, B. (1993). "An analysis of malaria in pregnancy in Africa." Bull. World Health Org. **61**: 1005-16.
Brabin, B., S. Maxwell, L. Chimsuku, F. Verhoeff, H. J. van der Kaay, R. Broadhead, P. Kazembe and A. Thomas (1993). "A study of the consequences of malarial infection in pregnant women and their infants." Parassitologia **35 Suppl**: 9-11.
Brabin, B. J., C. Romagosa, S. Abdelgalil, C. Menendez, F. H. Verhoeff, R. McGready, K. A. Fletcher, S. Owens, U. D'Alessandro, F. Nosten, P. R. Fischer and J. Ordi (2004). "The sick placenta-the role of malaria." Placenta **25**(5): 359-78.
Breman, J. G. (2001). "The ears of the hippopotamus: manifestations, determinants, and estimates of the malaria burden." Am J Trop Med Hyg **64**(1-2 Suppl): 1-11.
Brewster, D. R., D. Kwiatkowski and N. J. White (1990). "Neurological sequelae of cerebral malaria in children." Lancet **336**(8722): 1039-43.
Broen, K., K. Brustoski, I. Engelmann and A. J. Luty (2007). "Placental Plasmodium falciparum infection: causes and consequences of in utero sensitization to parasite antigens." Mol Biochem Parasitol **151**(1): 1-8.
Brown, H., T. T. Hien, N. Day, N. T. Mai, L. V. Chuong, T. T. Chau, P. P. Loc, N. H. Phu, D. Bethell, J. Farrar, K. Gatter, N. White and G. Turner (1999). "Evidence of blood-brain barrier dysfunction in human cerebral malaria." Neuropathol Appl Neurobiol **25**(4): 331-40.
Bryant, D. and V. Moulton (2004). "Neighbor-net: an agglomerative method for the construction of phylogenetic networks." Mol Biol Evol **21**(2): 255-65.
Buckling, A., L. C. Ranford-Cartwright, A. Miles and A. F. Read (1999). "Chloroquine increases Plasmodium falciparum gametocytogenesis in vitro." Parasitology **118 (Pt 4)**: 339-46.
Buffet, P. A., B. Gamain, C. Scheidig, D. Baruch, J. D. Smith, R. Hernandez-Rivas, B. Pouvelle, S. Oishi, N. Fujii, T. Fusai, D. Parzy, L. H. Miller, J. Gysin and A. Scherf (1999). "Plasmodium falciparum domain mediating adhesion to chondroitin sulfate A: a receptor for human placental infection." Proc Natl Acad Sci U S A **96**(22): 12743-8.
Bull, P. C., M. Berriman, S. Kyes, M. A. Quail, N. Hall, M. M. Kortok, K. Marsh and C. I. Newbold (2005a). "*Plasmodium falciparum* Variant Surface Antigen Expression Patterns during Malaria." PLoS Pathog **1**(3): e26.
Bull, P. C., M. Kortok, O. Kai, F. Ndungu, A. Ross, B. S. Lowe, C. I. Newbold and K. Marsh (2000). "Plasmodium falciparum-infected erythrocytes: agglutination by diverse Kenyan plasma is associated with severe disease and young host age." J Infect Dis **182**(1): 252-9.
Bull, P. C., S. Kyes, C. O. Buckee, J. Montgomery, M. M. Kortok, C. I. Newbold and K. Marsh (2007). "An approach to classifying sequence tags sampled from Plasmodium falciparum var genes." Mol Biochem Parasitol **154**(1): 98-102.
Bull, P. C., B. S. Lowe, M. Kortok and K. Marsh (1999). "Antibody recognition of Plasmodium falciparum erythrocyte surface antigens in Kenya: evidence for rare and prevalent variants." Infect Immun **67**(2): 733-9.

Bull, P. C., A. Pain, F. M. Ndungu, S. M. Kinyanjui, D. J. Roberts, C. I. Newbold and K. Marsh (2005b). "Plasmodium falciparum antigenic variation: relationships between in vivo selection, acquired antibody response, and disease severity." J Infect Dis **192**(6): 1119-26.

Calderwood, M. S., L. Gannoun-Zaki, T. E. Wellems and K. W. Deitsch (2003). "Plasmodium falciparum var genes are regulated by two regions with separate promoters, one upstream of the coding region and a second within the intron." J Biol Chem **278**(36): 34125-32.

Carlson, J., H. P. Ekre, H. Helmby, J. Gysin, B. M. Greenwood and M. Wahlgren (1992). "Disruption of Plasmodium falciparum erythrocyte rosettes by standard heparin and heparin devoid of anticoagulant activity." Am J Trop Med Hyg **46**(5): 595-602.

Carlson, J., H. Helmby, A. V. Hill, D. Brewster, B. M. Greenwood and M. Wahlgren (1990). "Human cerebral malaria: association with erythrocyte rosetting and lack of anti-rosetting antibodies." Lancet **336**(8729): 1457-60.

Carlson, J. and M. Wahlgren (1992). "Plasmodium falciparum erythrocyte rosetting is mediated by promiscuous lectin-like interactions." J Exp Med **176**(5): 1311-7.

Carter, R., L. Ranford-Cartwright and P. Alano (1993). "The culture and preparation of gametocytes of Plasmodium falciparum for immunochemical, molecular, and mosquito infectivity studies." Methods Mol Biol **21**: 67-88.

Cavanagh, D. R., D. Dodoo, L. Hviid, J. A. Kurtzhals, T. G. Theander, B. D. Akanmori, S. Polley, D. J. Conway, K. Koram and J. S. McBride (2004). "Antibodies to the N-terminal block 2 of Plasmodium falciparum merozoite surface protein 1 are associated with protection against clinical malaria." Infect Immun **72**(11): 6492-502.

Chaidedgumjorn, A., H. Toyoda, E. R. Woo, K. B. Lee, Y. S. Kim, T. Toida and T. Imanari (2002). "Effect of (1-->3)- and (1-->4)-linkages of fully sulfated polysaccharides on their anticoagulant activity." Carbohydr Res **337**(10): 925-33.

Chattopadhyay, R., T. Taneja, K. Chakrabarti, C. R. Pillai and C. E. Chitnis (2004). "Molecular analysis of the cytoadherence phenotype of a Plasmodium falciparum field isolate that binds intercellular adhesion molecule-1." Mol Biochem Parasitol **133**(2): 255-65.

Chen, Q., A. Barragan, V. Fernandez, A. Sundstrom, M. Schlichtherle, A. Sahlen, J. Carlson, S. Datta and M. Wahlgren (1998a). "Identification of Plasmodium falciparum erythrocyte membrane protein 1 (PfEMP1) as the rosetting ligand of the malaria parasite P. falciparum." J Exp Med **187**(1): 15-23.

Chen, Q., V. Fernandez, A. Sundstrom, M. Schlichtherle, S. Datta, P. Hagblom and M. Wahlgren (1998b). "Developmental selection of var gene expression in Plasmodium falciparum." Nature **394**(6691): 392-5.

Chen, Q., F. Pettersson, A. M. Vogt, B. Schmidt, S. Ahuja, P. Liljestrom and M. Wahlgren (2004). "Immunization with PfEMP1-DBL1alpha generates antibodies that disrupt rosettes and protect against the sequestration of Plasmodium falciparum-infected erythrocytes." Vaccine **22**(21-22): 2701-12.

Chia, Y. S., C. Badaut, N. G. Tuikue Ndam, A. Khattab, S. Igonet, N. Fievet, G. A. Bentley, P. Deloron and M. Q. Klinkert (2005). "Functional and immunological characterization of a duffy binding-like- gamma domain from

Plasmodium falciparum erythrocyte membrane protein-1 expressed by a placental isolate." J Infect Dis **192**(7): 1284-93.
Chookajorn, T., R. Dzikowski, M. Frank, F. Li, A. Z. Jiwani, D. L. Hartl and K. W. Deitsch (2007). "Epigenetic memory at malaria virulence genes." Proc Natl Acad Sci U S A **104**(3): 899-902.
Chotivanich, K., R. Udomsangpetch, R. McGready, S. Proux, P. Newton, S. Pukrittayakamee, S. Looareesuwan and N. J. White (2002). "Central role of the spleen in malaria parasite clearance." J Infect Dis **185**(10): 1538-41.
Chotivanich, K. T., S. Pukrittayakamee, J. A. Simpson, N. J. White and R. Udomsangpetch (1998). "Characteristics of Plasmodium vivax-infected erythrocyte rosettes." Am J Trop Med Hyg **59**(1): 73-6.
Cockburn, I. A., M. J. Mackinnon, A. O'Donnell, S. J. Allen, J. M. Moulds, M. Baisor, M. Bockarie, J. C. Reeder and J. A. Rowe (2004). "A human complement receptor 1 polymorphism that reduces Plasmodium falciparum rosetting confers protection against severe malaria." Proc Natl Acad Sci U S A **101**(1): 272-7.
Cortes, A., C. Carret, O. Kaneko, B. Y. Yim Lim, A. Ivens and A. A. Holder (2007). "Epigenetic silencing of Plasmodium falciparum genes linked to erythrocyte invasion." PLoS Pathog **3**(8): e107.
Costa, F. T., T. Fusai, D. Parzy, Y. Sterkers, M. Torrentino, J. B. Douki, B. Traore, S. Petres, A. Scherf and J. Gysin (2003). "Immunization with recombinant duffy binding-like-gamma3 induces pan-reactive and adhesion-blocking antibodies against placental chondroitin sulfate A-binding Plasmodium falciparum parasites." J Infect Dis **188**(1): 153-64.
Cowman, A. F. and B. S. Crabb (2006). "Invasion of red blood cells by malaria parasites." Cell **124**(4): 755-66.
Crabb, B. S., B. M. Cooke, J. C. Reeder, R. F. Waller, S. R. Caruana, K. M. Davern, M. E. Wickham, G. V. Brown, R. L. Coppel and A. F. Cowman (1997). "Targeted gene disruption shows that knobs enable malaria-infected red cells to cytoadhere under physiological shear stress." Cell **89**(2): 287-96.
Creasey, A. M., T. Staalsoe, A. Raza, D. E. Arnot and J. A. Rowe (2003). "Nonspecific immunoglobulin M binding and chondroitin sulfate A binding are linked phenotypes of Plasmodium falciparum isolates implicated in malaria during pregnancy." Infect Immun **71**(8): 4767-71.
Dahlback, M., T. Lavstsen, A. Salanti, L. Hviid, D. E. Arnot, T. G. Theander and M. A. Nielsen (2007). "Changes in var gene mRNA levels during erythrocytic development in two phenotypically distinct Plasmodium falciparum parasites." Malar J **6**: 78.
Dahlback, M., T. S. Rask, P. H. Andersen, M. A. Nielsen, N. T. Ndam, M. Resende, L. Turner, P. Deloron, L. Hviid, O. Lund, A. G. Pedersen, T. G. Theander and A. Salanti (2006). "Epitope mapping and topographic analysis of VAR2CSA DBL3X involved in P. falciparum placental sequestration." PLoS Pathog **2**(11): e124.
Day, N. P., T. T. Hien, T. Schollaardt, P. P. Loc, L. V. Chuong, T. T. Chau, N. T. Mai, N. H. Phu, D. X. Sinh, N. J. White and M. Ho (1999). "The prognostic and pathophysiologic role of pro- and antiinflammatory cytokines in severe malaria." J Infect Dis **180**(4): 1288-97.

Deans, A. M., K. E. Lyke, M. A. Thera, C. V. Plowe, A. Kone, O. K. Doumbo, O. Kai, K. Marsh, M. J. Mackinnon, A. Raza and J. A. Rowe (2006). "Low multiplication rates of African Plasmodium falciparum isolates and lack of association of multiplication rate and red blood cell selectivity with malaria virulence." Am J Trop Med Hyg **74**(4): 554-63.

Deans, A. M., S. Nery, D. J. Conway, O. Kai, K. Marsh and J. A. Rowe (2007). "Invasion pathways and malaria severity in Kenyan Plasmodium falciparum clinical isolates." Infect Immun **75**(6): 3014-20.

Deans, A. M. and J. A. Rowe (2006). "Plasmodium falciparum: Rosettes do not protect merozoites from invasion-inhibitory antibodies." Exp Parasitol **112**(4): 269-73.

Deitsch, K. W. (2001). "Gene silencing and antigenic variation in malaria parasites." ScientificWorldJournal **1**: 650-2.

Dembo, E. G., H. T. Phiri, J. Montgomery, M. E. Molyneux and S. J. Rogerson (2006). "Are Plasmodium falciparum parasites present in peripheral blood genetically the same as those sequestered in the tissues?" Am J Trop Med Hyg **74**(5): 730-2.

Dinglasan, R. R., A. Alaganan, A. K. Ghosh, A. Saito, T. H. van Kuppevelt and M. Jacobs-Lorena (2007). "Plasmodium falciparum ookinetes require mosquito midgut chondroitin sulfate proteoglycans for cell invasion." Proc Natl Acad Sci U S A **104**(40): 15882-7.

Duffy, M. F., G. V. Brown, W. Basuki, E. O. Krejany, R. Noviyanti, A. F. Cowman and J. C. Reeder (2002). "Transcription of multiple var genes by individual, trophozoite-stage Plasmodium falciparum cells expressing a chondroitin sulphate A binding phenotype." Mol Microbiol **43**(5): 1285-93.

Duffy, M. F., T. J. Byrne, S. R. Elliott, D. W. Wilson, S. J. Rogerson, J. G. Beeson, R. Noviyanti and G. V. Brown (2005). "Broad analysis reveals a consistent pattern of var gene transcription in Plasmodium falciparum repeatedly selected for a defined adhesion phenotype." Mol Microbiol **56**(3): 774-88.

Duffy, M. F., A. Caragounis, R. Noviyanti, H. M. Kyriacou, E. K. Choong, K. Boysen, J. Healer, J. A. Rowe, M. E. Molyneux, G. V. Brown and S. J. Rogerson (2006a). "Transcribed var genes associated with placental malaria in Malawian women." Infect Immun **74**(8): 4875-83.

Duffy, M. F., A. G. Maier, T. J. Byrne, A. J. Marty, S. R. Elliott, M. T. O'Neill, P. D. Payne, S. J. Rogerson, A. F. Cowman, B. S. Crabb and G. V. Brown (2006b). "VAR2CSA is the principal ligand for chondroitin sulfate A in two allogeneic isolates of Plasmodium falciparum." Mol Biochem Parasitol **148**(2): 117-24.

Duffy, P. E. and M. Fried (2003). "Antibodies that inhibit Plasmodium falciparum adhesion to chondroitin sulfate A are associated with increased birth weight and the gestational age of newborns." Infect Immun **71**(11): 6620-3.

Duraisingh, M. T., A. G. Maier, T. Triglia and A. F. Cowman (2003). "Erythrocyte-binding antigen 175 mediates invasion in Plasmodium falciparum utilizing sialic acid-dependent and -independent pathways." Proc Natl Acad Sci U S A **100**(8): 4796-801.

Duraisingh, M. T., T. S. Voss, A. J. Marty, M. F. Duffy, R. T. Good, J. K. Thompson, L. H. Freitas-Junior, A. Scherf, B. S. Crabb and A. F. Cowman (2005). "Heterochromatin silencing and locus repositioning linked to regulation of virulence genes in Plasmodium falciparum." Cell **121**(1): 13-24.

Dzikowski, R., M. Frank and K. Deitsch (2006). "Mutually exclusive expression of virulence genes by malaria parasites is regulated independently of antigen production." PLoS Pathog **2**(3): e22.

Elliott, S. R., M. F. Duffy, T. J. Byrne, J. G. Beeson, E. J. Mann, D. W. Wilson, S. J. Rogerson and G. V. Brown (2005). "Cross-reactive surface epitopes on chondroitin sulfate A-adherent Plasmodium falciparum-infected erythrocytes are associated with transcription of var2csa." Infect Immun **73**(5): 2848-56.

Escalante, A. A., E. Barrio and F. J. Ayala (1995). "Evolutionary origin of human and primate malarias: evidence from the circumsporozoite protein gene." Mol Biol Evol **12**(4): 616-26.

Evans, S. G., D. Morrison, Y. Kaneko and I. Havlik (1998). "The effect of curdlan sulphate on development in vitro of Plasmodium falciparum." Trans R Soc Trop Med Hyg **92**(1): 87-9.

Fernandez, V., Q. Chen, A. Sundstrom, A. Scherf, P. Hagblom and M. Wahlgren (2002). "Mosaic-like transcription of var genes in single Plasmodium falciparum parasites." Mol Biochem Parasitol **121**(2): 195-203.

Ferreira, M. U., S. Nair, T. V. Hyunh, F. Kawamoto and T. J. Anderson (2002). "Microsatellite characterization of Plasmodium falciparum from cerebral and uncomplicated malaria patients in southern Vietnam." J Clin Microbiol **40**(5): 1854-7.

Flick, K., C. Scholander, Q. Chen, V. Fernandez, B. Pouvelle, J. Gysin and M. Wahlgren (2001). "Role of nonimmune IgG bound to PfEMP1 in placental malaria." Science **293**(5537): 2098-100.

Fowler, E. V., M. Chavchich, N. Chen, J. M. Peters, D. E. Kyle, M. L. Gatton and Q. Cheng (2006). "Physical linkage to drug resistance genes results in conservation of var genes among West Pacific Plasmodium falciparum isolates." J Infect Dis **194**(7): 939-48.

Fowler, E. V., J. M. Peters, M. L. Gatton, N. Chen and Q. Cheng (2002). "Genetic diversity of the DBLalpha region in Plasmodium falciparum var genes among Asia-Pacific isolates." Mol Biochem Parasitol **120**(1): 117-26.

Francis, S. E., V. A. Malkov, A. V. Oleinikov, E. Rossnagle, J. P. Wendler, T. K. Mutabigwa, M. Fried and P. E. Duffy (2007). "Six genes are preferentially transcribed by the circulating and sequestered forms of Plasmodium falciparum parasites that infect pregnant women." Infect Immun.

Frank, M., R. Dzikowski, B. Amulic and K. Deitsch (2007). "Variable switching rates of malaria virulence genes are associated with chromosomal position." Mol Microbiol **64**(6): 1486-98.

Frank, M., R. Dzikowski, D. Costantini, B. Amulic, E. Berdougo and K. Deitsch (2006). "Strict pairing of var promoters and introns is required for var gene silencing in the malaria parasite Plasmodium falciparum." J Biol Chem **281**(15): 9942-52.

Frankland, S., A. Adisa, P. Horrocks, T. F. Taraschi, T. Schneider, S. R. Elliott, S. J. Rogerson, E. Knuepfer, A. F. Cowman, C. I. Newbold and L. Tilley (2006). "Delivery of the malaria virulence protein PfEMP1 to the erythrocyte surface requires cholesterol-rich domains." Eukaryot Cell **5**(5): 849-60.

Freitas-Junior, L. H., E. Bottius, L. A. Pirrit, K. W. Deitsch, C. Scheidig, F. Guinet, U. Nehrbass, T. E. Wellems and A. Scherf (2000). "Frequent ectopic

recombination of virulence factor genes in telomeric chromosome clusters of P. falciparum." Nature **407**(6807): 1018-22.

Freitas-Junior, L. H., R. Hernandez-Rivas, S. A. Ralph, D. Montiel-Condado, O. K. Ruvalcaba-Salazar, A. P. Rojas-Meza, L. Mancio-Silva, R. J. Leal-Silvestre, A. M. Gontijo, S. Shorte and A. Scherf (2005). "Telomeric heterochromatin propagation and histone acetylation control mutually exclusive expression of antigenic variation genes in malaria parasites." Cell **121**(1): 25-36.

Frevert, U., S. Engelmann, S. Zougbede, J. Stange, B. Ng, K. Matuschewski, L. Liebes and H. Yee (2005). "Intravital observation of Plasmodium berghei sporozoite infection of the liver." PLoS Biol **3**(6): e192.

Frevert, U., P. Sinnis, C. Cerami, W. Shreffler, B. Takacs and V. Nussenzweig (1993). "Malaria circumsporozoite protein binds to heparan sulfate proteoglycans associated with the surface membrane of hepatocytes." J Exp Med **177**(5): 1287-98.

Fried, M., G. J. Domingo, C. D. Gowda, T. K. Mutabingwa and P. E. Duffy (2006). "Plasmodium falciparum: chondroitin sulfate A is the major receptor for adhesion of parasitized erythrocytes in the placenta." Exp Parasitol **113**(1): 36-42.

Fried, M. and P. E. Duffy (1996). "Adherence of Plasmodium falciparum to chondroitin sulfate A in the human placenta." Science **272**(5267): 1502-4.

Fried, M. and P. E. Duffy (2002). "Two DBLgamma subtypes are commonly expressed by placental isolates of Plasmodium falciparum." Mol Biochem Parasitol **122**(2): 201-10.

Fried, M., K. K. Hixson, L. Anderson, Y. Ogata, T. K. Mutabingwa and P. E. Duffy (2007). "The distinct proteome of placental malaria parasites." Mol Biochem Parasitol **155**(1): 57-65.

Fried, M., F. Nosten, A. Brockman, B. J. Brabin and P. E. Duffy (1998). "Maternal antibodies block malaria." Nature **395**(6705): 851-2.

Gamain, B., J. D. Smith, M. Avril, D. I. Baruch, A. Scherf, J. Gysin and L. H. Miller (2004). "Identification of a 67-amino-acid region of the Plasmodium falciparum variant surface antigen that binds chondroitin sulphate A and elicits antibodies reactive with the surface of placental isolates." Mol Microbiol **53**(2): 445-55.

Gamain, B., A. R. Trimnell, C. Scheidig, A. Scherf, L. H. Miller and J. D. Smith (2005). "Identification of multiple chondroitin sulfate A (CSA)-binding domains in the var2CSA gene transcribed in CSA-binding parasites." J Infect Dis **191**(6): 1010-3.

Gardner, M. J., N. Hall, E. Fung, O. White, M. Berriman, R. W. Hyman, J. M. Carlton, A. Pain, K. E. Nelson, S. Bowman, I. T. Paulsen, K. James, J. A. Eisen, K. Rutherford, S. L. Salzberg, A. Craig, S. Kyes, M. S. Chan, V. Nene, S. J. Shallom, B. Suh, J. Peterson, S. Angiuoli, M. Pertea, J. Allen, J. Selengut, D. Haft, M. W. Mather, A. B. Vaidya, D. M. Martin, A. H. Fairlamb, M. J. Fraunholz, D. S. Roos, S. A. Ralph, G. I. McFadden, L. M. Cummings, G. M. Subramanian, C. Mungall, J. C. Venter, D. J. Carucci, S. L. Hoffman, C. Newbold, R. W. Davis, C. M. Fraser and B. Barrell (2002). "Genome sequence of the human malaria parasite Plasmodium falciparum." Nature **419**(6906): 498-511.

Gatton, M. L., J. M. Peters, E. V. Fowler and Q. Cheng (2003). "Switching rates of Plasmodium falciparum var genes: faster than we thought?" Trends Parasitol **19**(5): 202-8.

Gatton, M. L., J. M. Peters, K. Gresty, E. V. Fowler, N. Chen and Q. Cheng (2006). "Detection sensitivity and quantitation of Plasmodium falciparum var gene transcripts by real-time rt-PCR in comparison with conventional rt-PCR." Am J Trop Med Hyg **75**(2): 212-8.

Glushakova, S., D. Yin, T. Li and J. Zimmerberg (2005). "Membrane transformation during malaria parasite release from human red blood cells." Curr Biol **15**(18): 1645-50.

Gordon, M., S. Deeks, C. De Marzo, J. Goodgame, M. Guralnik, W. Lang, T. Mimura, D. Pearce and Y. Kaneko (1997). "Curdlan sulfate (CRDS) in a 21-day intravenous tolerance study in human immunodeficiency virus (HIV) and cytomegalovirus (CMV) infected patients: indication of anti-CMV activity with low toxicity." J Med **28**(1-2): 108-28.

Gordon, M., M. Guralnik, Y. Kaneko, T. Mimura, M. Baker and W. Lang (1994). "A phase I study of curdlan sulfate--an HIV inhibitor. Tolerance, pharmacokinetics and effects on coagulation and on CD4 lymphocytes." J Med **25**(3-4): 163-80.

Gowda, A. S., S. V. Madhunapantula, R. N. Achur, M. Valiyaveettil, V. P. Bhavanandan and D. C. Gowda (2007). "Structural basis for the adherence of Plasmodium falciparum-infected erythrocytes to chondroitin 4-sulfate and design of novel photoactivable reagents for the identification of parasite adhesive proteins." J Biol Chem **282**(2): 916-28.

Grau, G. E., T. E. Taylor, M. E. Molyneux, J. J. Wirima, P. Vassalli, M. Hommel and P. H. Lambert (1989). "Tumor necrosis factor and disease severity in children with falciparum malaria." N Engl J Med **320**(24): 1586-91.

Gruenberg, J., D. R. Allred and I. W. Sherman (1983). "Scanning electron microscope-analysis of the protrusions (knobs) present on the surface of Plasmodium falciparum-infected erythrocytes." J Cell Biol **97**(3): 795-802.

*Hae*ggstrom, M., F. Kironde, K. Berzins, Q. Chen, M. Wahlgren and V. Fernandez (2004). "Common trafficking pathway for variant antigens destined for the surface of the Plasmodium falciparum-infected erythrocyte." Mol Biochem Parasitol **133**(1): 1-14.

Hall, N., A. Pain, M. Berriman, C. Churcher, B. Harris, D. Harris, K. Mungall, S. Bowman, R. Atkin, S. Baker, A. Barron, K. Brooks, C. O. Buckee, C. Burrows, I. Cherevach, C. Chillingworth, T. Chillingworth, Z. Christodoulou, L. Clark, R. Clark, C. Corton, A. Cronin, R. Davies, P. Davis, P. Dear, F. Dearden, J. Doggett, T. Feltwell, A. Goble, I. Goodhead, R. Gwilliam, N. Hamlin, Z. Hance, D. Harper, H. Hauser, T. Hornsby, S. Holroyd, P. Horrocks, S. Humphray, K. Jagels, K. D. James, D. Johnson, A. Kerhornou, A. Knights, B. Konfortov, S. Kyes, N. Larke, D. Lawson, N. Lennard, A. Line, M. Maddison, J. McLean, P. Mooney, S. Moule, L. Murphy, K. Oliver, D. Ormond, C. Price, M. A. Quail, E. Rabbinowitsch, M. A. Rajandream, S. Rutter, K. M. Rutherford, M. Sanders, M. Simmonds, K. Seeger, S. Sharp, R. Smith, R. Squares, S. Squares, K. Stevens, K. Taylor, A. Tivey, L. Unwin, S. Whitehead, J. Woodward, J. E. Sulston, A. Craig, C. Newbold and B. G.

Barrell (2002). "Sequence of Plasmodium falciparum chromosomes 1, 3-9 and 13." Nature **419**(6906): 527-31.
Handunnetti, S. M., M. R. van Schravendijk, T. Hasler, J. W. Barnwell, D. E. Greenwalt and R. J. Howard (1992). "Involvement of CD36 on erythrocytes as a rosetting receptor for Plasmodium falciparum-infected erythrocytes." Blood **80**(8): 2097-104.
Harris, P. K., S. Yeoh, A. R. Dluzewski, R. A. O'Donnell, C. Withers-Martinez, F. Hackett, L. H. Bannister, G. H. Mitchell and M. J. Blackman (2005). "Molecular identification of a malaria merozoite surface sheddase." PLoS Pathog **1**(3): 241-51.
Havlik, I., S. Looareesuwan, S. Vannaphan, P. Wilairatana, S. Krudsood, P. E. Thuma, D. Kozbor, N. Watanabe and Y. Kaneko (2005). "Curdlan sulphate in human severe/cerebral Plasmodium falciparum malaria." Trans R Soc Trop Med Hyg **99**(5): 333-40.
Havlik, I., S. Rovelli and Y. Kaneko (1994). "The effect of curdlan sulphate on in vitro growth of Plasmodium falciparum." Trans R Soc Trop Med Hyg **88**(6): 686-7.
Heddini, A., F. Pettersson, O. Kai, J. Shafi, J. Obiero, Q. Chen, A. Barragan, M. Wahlgren and K. Marsh (2001). "Fresh isolates from children with severe Plasmodium falciparum malaria bind to multiple receptors." Infect Immun **69**(9): 5849-56.
Helmby, H., L. Cavelier, U. Pettersson and M. Wahlgren (1993). "Rosetting Plasmodium falciparum-infected erythrocytes express unique strain-specific antigens on their surface." Infect Immun **61**(1): 284-8.
Hiller, N. L., S. Bhattacharjee, C. van Ooij, K. Liolios, T. Harrison, C. Lopez-Estrano and K. Haldar (2004). "A host-targeting signal in virulence proteins reveals a secretome in malarial infection." Science **306**(5703): 1934-7.
Ho, M., T. Schollaardt, X. Niu, S. Looareesuwan, K. D. Patel and P. Kubes (1998). "Characterization of Plasmodium falciparum-infected erythrocyte and P-selectin interaction under flow conditions." Blood **91**(12): 4803-9.
Horrocks, P., S. Kyes, R. Pinches, Z. Christodoulou and C. Newbold (2004a). "Transcription of subtelomerically located var gene variant in Plasmodium falciparum appears to require the truncation of an adjacent var gene." Mol Biochem Parasitol **134**(2): 193-9.
Horrocks, P., R. Pinches, Z. Christodoulou, S. A. Kyes and C. I. Newbold (2004b). "Variable var transition rates underlie antigenic variation in malaria." Proc Natl Acad Sci U S A **101**(30): 11129-34.
Horrocks, P., R. Pinches, S. Kyes, N. Kriek, S. Lee, Z. Christodoulou and C. I. Newbold (2002). "Effect of var gene disruption on switching in Plasmodium falciparum." Mol Microbiol **45**(4): 1131-41.
Horrocks, P., R. A. Pinches, S. J. Chakravorty, J. Papakrivos, Z. Christodoulou, S. A. Kyes, B. C. Urban, D. J. Ferguson and C. I. Newbold (2005). "PfEMP1 expression is reduced on the surface of knobless Plasmodium falciparum infected erythrocytes." J Cell Sci **118**(Pt 11): 2507-18.
Hughes, M. K. and A. L. Hughes (1995). "Natural selection on Plasmodium surface proteins." Mol Biochem Parasitol **71**(1): 99-113.
Huson, D. H. and D. Bryant (2006). "Application of phylogenetic networks in evolutionary studies." Mol Biol Evol **23**(2): 254-67.

Igarashi, I., F. K. Njonge, Y. Kaneko and Y. Nakamura (1998). "Babesia bigemina: in vitro and in vivo effects of curdlan sulfate on growth of parasites." Exp Parasitol **90**(3): 290-3.

Jaffar, S., M. B. Van Hensbroek, A. Palmer, G. Schneider and B. Greenwood (1997). "Predictors of a fatal outcome following childhood cerebral malaria." Am J Trop Med Hyg **57**(1): 20-4.

Jagodzinski, P. P., R. Wiaderkiewicz, G. Kurzawski, M. Kloczewiak, H. Nakashima, E. Hyjek, N. Yamamoto, T. Uryu, Y. Kaneko, M. R. Posner and et al. (1994). "Mechanism of the inhibitory effect of curdlan sulfate on HIV-1 infection in vitro." Virology **202**(2): 735-45.

Jensen, A. T., P. Magistrado, S. Sharp, L. Joergensen, T. Lavstsen, A. Chiucchiuini, A. Salanti, L. S. Vestergaard, J. P. Lusingu, R. Hermsen, R. Sauerwein, J. Christensen, M. A. Nielsen, L. Hviid, C. Sutherland, T. Staalsoe and T. G. Theander (2004). "Plasmodium falciparum associated with severe childhood malaria preferentially expresses PfEMP1 encoded by group A var genes." J Exp Med **199**(9): 1179-90.

Joergensen, L., L. Turner, P. Magistrado, M. A. Dahlback, L. S. Vestergaard, J. P. Lusingu, M. Lemnge, A. Salanti, T. G. Theander and A. T. Jensen (2006). "Limited cross-reactivity among domains of the Plasmodium falciparum clone 3D7 erythrocyte membrane protein 1 family." Infect Immun **74**(12): 6778-84.

Kaestli, M., I. A. Cockburn, A. Cortes, K. Baea, J. A. Rowe and H. P. Beck (2006). "Virulence of malaria is associated with differential expression of Plasmodium falciparum var gene subgroups in a case-control study." J Infect Dis **193**(11): 1567-74.

Kaestli, M., A. Cortes, M. Lagog, M. Ott and H. P. Beck (2004). "Longitudinal assessment of Plasmodium falciparum var gene transcription in naturally infected asymptomatic children in Papua New Guinea." J Infect Dis **189**(10): 1942-51.

Kaneko, Y., O. Yoshida, R. Nakagawa, T. Yoshida, M. Date, S. Ogihara, S. Shioya, Y. Matsuzawa, N. Nagashima, Y. Irie and et al. (1990). "Inhibition of HIV-1 infectivity with curdlan sulfate in vitro." Biochem Pharmacol **39**(4): 793-7.

Kaul, D. K., E. F. Roth, Jr., R. L. Nagel, R. J. Howard and S. M. Handunnetti (1991). "Rosetting of Plasmodium falciparum-infected red blood cells with uninfected red blood cells enhances microvascular obstruction under flow conditions." Blood **78**(3): 812-9.

Keeley, A. and D. Soldati (2004). "The glideosome: a molecular machine powering motility and host-cell invasion by Apicomplexa." Trends Cell Biol **14**(10): 528-32.

Khattab, A., P. G. Kremsner and M. Q. Klinkert (2003). "Common surface-antigen var genes of limited diversity expressed by Plasmodium falciparum placental isolates separated by time and space." J Infect Dis **187**(3): 477-83.

Khattab, A., J. Kun, P. Deloron, P. G. Kremsner and M. Q. Klinkert (2001). "Variants of Plasmodium falciparum erythrocyte membrane protein 1 expressed by different placental parasites are closely related and adhere to chondroitin sulfate A." J Infect Dis **183**(7): 1165-9.

Kinyanjui, S. M., T. Howard, T. N. Williams, P. C. Bull, C. I. Newbold and K. Marsh (2004). "The use of cryopreserved mature trophozoites in assessing

antibody recognition of variant surface antigens of Plasmodium falciparum-infected erythrocytes." J Immunol Methods **288**(1-2): 9-18.
Kirchgatter, K., R. Mosbach and H. A. del Portillo (2000). "Plasmodium falciparum: DBL-1 var sequence analysis in field isolates from central Brazil." Exp Parasitol **95**(2): 154-7.
Kirchgatter, K. and A. Portillo Hdel (2002). "Association of severe noncerebral Plasmodium falciparum malaria in Brazil with expressed PfEMP1 DBL1 alpha sequences lacking cysteine residues." Mol Med **8**(1): 16-23.
Kirk, K., H. A. Horner, B. C. Elford, J. C. Ellory and C. I. Newbold (1994). "Transport of diverse substrates into malaria-infected erythrocytes via a pathway showing functional characteristics of a chloride channel." J Biol Chem **269**(5): 3339-47.
Knuepfer, E., M. Rug, N. Klonis, L. Tilley and A. F. Cowman (2005). "Trafficking of the major virulence factor to the surface of transfected P. falciparum-infected erythrocytes." Blood **105**(10): 4078-87.
Kraemer, S. M., S. A. Kyes, G. Aggarwal, A. L. Springer, S. O. Nelson, Z. Christodoulou, L. M. Smith, W. Wang, E. w. Levin, C. I. Newbold, P. J. Myler and J. D. Smith (2007). "Patterns of gene recombination shape var gene repertoires in Plasmodium falciparum: comparisons of geographically diverse isolates." BMC Genomics **8**: 45.
Kraemer, S. M. and J. D. Smith (2003). "Evidence for the importance of genetic structuring to the structural and functional specialization of the Plasmodium falciparum var gene family." Mol Microbiol **50**(5): 1527-38.
Kulane, A., H. P. Ekre, P. Perlmann, L. Rombo, M. Wahlgren and B. Wahlin (1992). "Effect of different fractions of heparin on Plasmodium falciparum merozoite invasion of red blood cells in vitro." Am J Trop Med Hyg **46**(5): 589-94.
Kurtzhals, J. A., B. Q. Goka, B. D. Akanmori and L. Hviid (2001). "The importance of strict patient definition in studies of malaria pathogenesis." Trends Parasitol **17**(7): 313-4.
Kwiatkowski, D., A. V. Hill, I. Sambou, P. Twumasi, J. Castracane, K. R. Manogue, A. Cerami, D. R. Brewster and B. M. Greenwood (1990). "TNF concentration in fatal cerebral, non-fatal cerebral, and uncomplicated Plasmodium falciparum malaria." Lancet **336**(8725): 1201-4.
Kyes, S., R. Pinches and C. Newbold (2000). "A simple RNA analysis method shows var and rif multigene family expression patterns in Plasmodium falciparum." Mol Biochem Parasitol **105**(2): 311-5.
Kyes, S. A., Z. Christodoulou, A. Raza, P. Horrocks, R. Pinches, J. A. Rowe and C. I. Newbold (2003). "A well-conserved Plasmodium falciparum var gene shows an unusual stage-specific transcript pattern." Mol Microbiol **48**(5): 1339-48.
Kyes, S. A., S. M. Kraemer and J. D. Smith (2007). "Antigenic Variation in Plasmodium falciparum: Gene Organization and Regulation of the var Multigene Family." Eukaryot Cell **6**(9): 1511-20.
Kyriacou, H. M., K. E. Steen, A. Raza, M. Arman, G. Warimwe, P. C. Bull, I. Havlik and J. A. Rowe (2007). "In vitro inhibition of Plasmodium falciparum rosette formation by Curdlan sulfate." Antimicrob Agents Chemother **51**(4): 1321-6.
Kyriacou, H. M., G. N. Stone, R. J. Challis, A. Raza, K. E. Lyke, M. A. Thera, A. K. Kone, O. K. Doumbo, C. V. Plowe and J. A. Rowe (2006). "Differential var

gene transcription in Plasmodium falciparum isolates from patients with cerebral malaria compared to hyperparasitaemia." Mol Biochem Parasitol **150**(2): 211-8.

Lambros, C. and J. P. Vanderberg (1979). "Synchronization of Plasmodium falciparum erythrocytic stages in culture." J Parasitol **65**(3): 418-20.

Lavazec, C., S. Sanyal and T. J. Templeton (2007). "Expression switching in the stevor and Pfmc-2TM superfamilies in Plasmodium falciparum." Mol Microbiol **64**(6): 1621-34.

Lavstsen, T., P. Magistrado, C. C. Hermsen, A. Salanti, A. T. Jensen, R. Sauerwein, L. Hviid, T. G. Theander and T. Staalsoe (2005). "Expression of Plasmodium falciparum erythrocyte membrane protein 1 in experimentally infected humans." Malar J **4**(1): 21.

Lavstsen, T., A. Salanti, A. T. Jensen, D. E. Arnot and T. G. Theander (2003). "Sub-grouping of Plasmodium falciparum 3D7 var genes based on sequence analysis of coding and non-coding regions." Malar J **2**(1): 27.

Leech, J. H., J. W. Barnwell, L. H. Miller and R. J. Howard (1984). "Identification of a strain-specific malarial antigen exposed on the surface of Plasmodium falciparum-infected erythrocytes." J Exp Med **159**(6): 1567-75.

Lekana Douki, J. B., B. Traore, F. T. Costa, T. Fusai, B. Pouvelle, Y. Sterkers, A. Scherf and J. Gysin (2002). "Sequestration of Plasmodium falciparum-infected erythrocytes to chondroitin sulfate A, a receptor for maternal malaria: monoclonal antibodies against the native parasite ligand reveal pan-reactive epitopes in placental isolates." Blood **100**(4): 1478-83.

Lindenthal, C., P. G. Kremsner and M. Q. Klinkert (2003). "Commonly recognised Plasmodium falciparum parasites cause cerebral malaria." Parasitol Res **91**(5): 363-8.

Linss, W., C. Pilgrim and H. Feuerstein (1991). "[How thick is the glycocalyx of human erythrocytes?]." Acta Histochem **91**(1): 101-4.

Lopez-Rubio, J. J., A. M. Gontijo, M. C. Nunes, N. Issar, R. Hernandez Rivas and A. Scherf (2007). "5' flanking region of var genes nucleate histone modification patterns linked to phenotypic inheritance of virulence traits in malaria parasites." Mol Microbiol **66**(6): 1296-305.

Lowe, B. S., M. Mosobo and P. C. Bull (1998). "All four species of human malaria parasites form rosettes." Trans R Soc Trop Med Hyg **92**(5): 526.

Lyke, K. E., D. A. Diallo, A. Dicko, A. Kone, D. Coulibaly, A. Guindo, Y. Cissoko, L. Sangare, S. Coulibaly, B. Dakouo, T. E. Taylor, O. K. Doumbo and C. V. Plowe (2003). "Association of intraleukocytic *Plasmodium falciparum* malaria pigment with disease severity, clinical manifestations, and prognosis in severe malaria." Am J Trop Med Hyg **69**(3): 253-9.

Lyke, K. E., A. Dicko, A. Kone, D. Coulibaly, A. Guindo, Y. Cissoko, K. Traore, C. V. Plowe and O. K. Doumbo (2004). "Incidence of severe Plasmodium falciparum malaria as a primary endpoint for vaccine efficacy trials in Bandiagara, Mali." Vaccine **22**(23-24): 3169-74.

Mackinnon, M. J., T. W. Mwangi, R. W. Snow, K. Marsh and T. N. Williams (2005). "Heritability of malaria in Africa." PLoS Med **2**(12): e340.

Mackinnon, M. J., P. R. Walker and J. A. Rowe (2002). "Plasmodium chabaudi: rosetting in a rodent malaria model." Exp Parasitol **101**(2-3): 121-8.

MacPherson, G. G., M. J. Warrell, N. J. White, S. Looareesuwan and D. A. Warrell (1985). "Human cerebral malaria. A quantitative ultrastructural analysis of parasitized erythrocyte sequestration." Am J Pathol **119**(3): 385-401.

Maier, A. G., M. T. Duraisingh, J. C. Reeder, S. S. Patel, J. W. Kazura, P. A. Zimmerman and A. F. Cowman (2003). "Plasmodium falciparum erythrocyte invasion through glycophorin C and selection for Gerbich negativity in human populations." Nat Med **9**(1): 87-92.

Malkin, E., C. A. Long, A. W. Stowers, L. Zou, S. Singh, N. J. MacDonald, D. L. Narum, A. P. Miles, A. C. Orcutt, O. Muratova, S. E. Moretz, H. Zhou, A. Diouf, M. Fay, E. Tierney, P. Leese, S. Mahanty, L. H. Miller, A. Saul and L. B. Martin (2007). "Phase 1 study of two merozoite surface protein 1 (MSP1(42)) vaccines for Plasmodium falciparum malaria." PLoS Clin Trials **2**(4): e12.

Malkin, E. M., D. J. Diemert, J. H. McArthur, J. R. Perreault, A. P. Miles, B. K. Giersing, G. E. Mullen, A. Orcutt, O. Muratova, M. Awkal, H. Zhou, J. Wang, A. Stowers, C. A. Long, S. Mahanty, L. H. Miller, A. Saul and A. P. Durbin (2005). "Phase 1 clinical trial of apical membrane antigen 1: an asexual blood-stage vaccine for Plasmodium falciparum malaria." Infect Immun **73**(6): 3677-85.

Marti, M., R. T. Good, M. Rug, E. Knuepfer and A. F. Cowman (2004). "Targeting malaria virulence and remodeling proteins to the host erythrocyte." Science **306**(5703): 1930-3.

Marty, A. J., J. K. Thompson, M. F. Duffy, T. S. Voss, A. F. Cowman and B. S. Crabb (2006). "Evidence that Plasmodium falciparum chromosome end clusters are cross-linked by protein and are the sites of both virulence gene silencing and activation." Mol Microbiol **62**(1): 72-83.

Mayor, A., N. Bir, R. Sawhney, S. Singh, P. Pattnaik, S. K. Singh, A. Sharma and C. E. Chitnis (2005). "Receptor-binding residues lie in central regions of Duffy-binding-like domains involved in red cell invasion and cytoadherence by malaria parasites." Blood **105**(6): 2557-63.

McCormick, C. J., A. Craig, D. Roberts, C. I. Newbold and A. R. Berendt (1997). "Intercellular adhesion molecule-1 and CD36 synergize to mediate adherence of Plasmodium falciparum-infected erythrocytes to cultured human microvascular endothelial cells." J Clin Invest **100**(10): 2521-9.

McGilvray, I. D., L. Serghides, A. Kapus, O. D. Rotstein and K. C. Kain (2000). "Nonopsonic monocyte/macrophage phagocytosis of Plasmodium falciparum-parasitized erythrocytes: a role for CD36 in malarial clearance." Blood **96**(9): 3231-40.

Miller, L. H., J. D. Haynes, F. M. McAuliffe, T. Shiroishi, J. R. Durocher and M. H. McGinniss (1977). "Evidence for differences in erythrocyte surface receptors for the malarial parasites, Plasmodium falciparum and Plasmodium knowlesi." J Exp Med **146**(1): 277-81.

Milner, D. A., Jr., C. P. Dzamalala, N. G. Liomba, M. E. Molyneux and T. E. Taylor (2005). "Sampling of supraorbital brain tissue after death: improving on the clinical diagnosis of cerebral malaria." J Infect Dis **191**(5): 805-8.

Mok, B. W., U. Ribacke, G. Winter, B. H. Yip, C. S. Tan, V. Fernandez, Q. Chen, P. Nilsson and M. Wahlgren (2007). "Comparative transcriptomal analysis of

isogenic Plasmodium falciparum clones of distinct antigenic and adhesive phenotypes." Mol Biochem Parasitol **151**(2): 184-92.

Moll, K., F. Pettersson, A. M. Vogt, C. Jonsson, N. Rasti, S. Ahuja, M. Spangberg, O. Mercereau-Puijalon, D. E. Arnot, M. Wahlgren and Q. Chen (2007). "Generation of cross-protective antibodies against Plasmodium falciparum sequestration by immunization with an erythrocyte membrane protein 1-duffy binding-like 1 alpha domain." Infect Immun **75**(1): 211-9.

Montgomery, J., D. A. Milner, Jr., M. T. Tse, A. Njobvu, K. Kayira, C. P. Dzamalala, T. E. Taylor, S. J. Rogerson, A. G. Craig and M. E. Molyneux (2006). "Genetic analysis of circulating and sequestered populations of Plasmodium falciparum in fatal pediatric malaria." J Infect Dis **194**(1): 115-22.

Montgomery, J., F. A. Mphande, M. Berriman, A. Pain, S. J. Rogerson, T. E. Taylor, M. E. Molyneux and A. Craig (2007). "Differential var gene expression in the organs of patients dying of falciparum malaria." Mol Microbiol **65**(4): 959-67.

Mu, J., P. Awadalla, J. Duan, K. M. McGee, D. A. Joy, G. A. McVean and X. Z. Su (2005). "Recombination hotspots and population structure in Plasmodium falciparum." PLoS Biol **3**(10): e335.

Muhia, D. K., C. A. Swales, W. Deng, J. M. Kelly and D. A. Baker (2001). "The gametocyte-activating factor xanthurenic acid stimulates an increase in membrane-associated guanylyl cyclase activity in the human malaria parasite Plasmodium falciparum." Mol Microbiol **42**(2): 553-60.

Munir, M., H. Tjandra, T. H. Rampengan, I. Mustadjab and F. H. Wulur (1980). "Heparin in the treatment of cerebral malaria." Paediatr Indones **20**(1-2): 47-50.

Muthusamy, A., R. N. Achur, M. Valiyaveettil, J. J. Botti, D. W. Taylor, R. F. Leke and D. C. Gowda (2007). "Chondroitin sulfate proteoglycan but not hyaluronic acid is the receptor for the adherence of Plasmodium falciparum-infected erythrocytes in human placenta, and infected red blood cell adherence up-regulates the receptor expression." Am J Pathol **170**(6): 1989-2000.

Nacher, M., P. Singhasivanon, F. Gay, U. Silachamroon and S. Looareesuwan (2001). "Case-control studies on host factors in severe malaria." Trends Parasitol **17**(6): 253-4.

Naito, T., M. Okada, H. Ogasawara, H. Kaneko, T. Hishikawa, T. Matsumoto, I. Sekigawa, H. Hashimoto and Y. Kaneko (2001). "Curdlan sulfate induces the downmodulation of chemokine receptors leading to suppression of HIV infection." J Acquir Immune Defic Syndr **26**(5): 512-3.

Ndam, N. T. and P. Deloron (2007). "Molecular Aspects of Plasmodium falciparum Infection during Pregnancy." J Biomed Biotechnol **2007**(5): 43785.

Nery, S., A. M. Deans, M. Mosobo, K. Marsh, J. A. Rowe and D. J. Conway (2006). "Expression of Plasmodium falciparum genes involved in erythrocyte invasion varies among isolates cultured directly from patients." Mol Biochem Parasitol **149**(2): 208-15.

Newton, C. R., T. T. Hien and N. White (2000). "Cerebral malaria." J Neurol Neurosurg Psychiatry **69**(4): 433-41.

Newton, C. R., T. E. Taylor and R. O. Whitten (1998). "Pathophysiology of fatal falciparum malaria in African children." Am J Trop Med Hyg **58**(5): 673-83.
Nielsen, M. A., M. Resende, M. Alifrangis, L. Turner, L. Hviid, T. G. Theander and A. Salanti (2007). "Plasmodium falciparum: VAR2CSA expressed during pregnancy-associated malaria is partially resistant to proteolytic cleavage by trypsin." Exp Parasitol **117**(1): 1-8.
Nielsen, M. A., T. Staalsoe, J. A. Kurtzhals, B. Q. Goka, D. Dodoo, M. Alifrangis, T. G. Theander, B. D. Akanmori and L. Hviid (2002). "Plasmodium falciparum variant surface antigen expression varies between isolates causing severe and nonsevere malaria and is modified by acquired immunity." J Immunol **168**(7): 3444-50.
Normark, J., D. Nilsson, U. Ribacke, G. Winter, K. Moll, C. E. Wheelock, J. Bayarugaba, F. Kironde, T. G. Egwang, Q. Chen, B. Andersson and M. Wahlgren (2007). "PfEMP1-DBL1alpha amino acid motifs in severe disease states of Plasmodium falciparum malaria." Proc Natl Acad Sci U S A **104**(40): 15835-40.
Noviyanti, R., G. V. Brown, M. E. Wickham, M. F. Duffy, A. F. Cowman and J. C. Reeder (2001). "Multiple var gene transcripts are expressed in Plasmodium falciparum infected erythrocytes selected for adhesion." Mol Biochem Parasitol **114**(2): 227-37.
O'Donnell, R. A., F. Hackett, S. A. Howell, M. Treeck, N. Struck, Z. Krnajski, C. Withers-Martinez, T. W. Gilberger and M. J. Blackman (2006). "Intramembrane proteolysis mediates shedding of a key adhesin during erythrocyte invasion by the malaria parasite." J Cell Biol **174**(7): 1023-33.
O'Donnell, R. A., A. Saul, A. F. Cowman and B. S. Crabb (2000). "Functional conservation of the malaria vaccine antigen MSP-119across distantly related Plasmodium species." Nat Med **6**(1): 91-5.
Ockenhouse, C. F., T. Tegoshi, Y. Maeno, C. Benjamin, M. Ho, K. E. Kan, Y. Thway, K. Win, M. Aikawa and R. R. Lobb (1992). "Human vascular endothelial cell adhesion receptors for Plasmodium falciparum-infected erythrocytes: roles for endothelial leukocyte adhesion molecule 1 and vascular cell adhesion molecule 1." J Exp Med **176**(4): 1183-9.
Oleinikov, A. V., E. Rossnagle, S. Francis, T. K. Mutabingwa, M. Fried and P. E. Duffy (2007). "Effects of sex, parity, and sequence variation on seroreactivity to candidate pregnancy malaria vaccine antigens." J Infect Dis **196**(1): 155-64.
Orlandi, P. A., F. W. Klotz and J. D. Haynes (1992). "A malaria invasion receptor, the 175-kilodalton erythrocyte binding antigen of Plasmodium falciparum recognizes the terminal Neu5Ac(alpha 2-3)Gal- sequences of glycophorin A." J Cell Biol **116**(4): 901-9.
Pain, A., D. J. Ferguson, O. Kai, B. C. Urban, B. Lowe, K. Marsh and D. J. Roberts (2001). "Platelet-mediated clumping of Plasmodium falciparum-infected erythrocytes is a common adhesive phenotype and is associated with severe malaria." Proc Natl Acad Sci U S A **98**(4): 1805-10.
Pancake, S. J., G. D. Holt, S. Mellouk and S. L. Hoffman (1992). "Malaria sporozoites and circumsporozoite proteins bind specifically to sulfated glycoconjugates." J Cell Biol **117**(6): 1351-7.

Peters, J., E. Fowler, M. Gatton, N. Chen, A. Saul and Q. Cheng (2002). "High diversity and rapid changeover of expressed var genes during the acute phase of Plasmodium falciparum infections in human volunteers." Proc Natl Acad Sci U S A **99**(16): 10689-94.

Peters, J. M., E. V. Fowler, D. R. Krause, Q. Cheng and M. L. Gatton (2007). "Differential changes in Plasmodium falciparum var transcription during adaptation to culture." J Infect Dis **195**(5): 748-55.

Petter, M., M. *Hae*ggstrom, A. Khattab, V. Fernandez, M. Q. Klinkert and M. Wahlgren (2007). "Variant proteins of the Plasmodium falciparum RIFIN family show distinct subcellular localization and developmental expression patterns." Mol Biochem Parasitol **156**(1): 51-61.

Pichyangkul, S., K. Yongvanitchit, U. Kum-arb, H. Hemmi, S. Akira, A. M. Krieg, D. G. Heppner, V. A. Stewart, H. Hasegawa, S. Looareesuwan, G. D. Shanks and R. S. Miller (2004). "Malaria blood stage parasites activate human plasmacytoid dendritic cells and murine dendritic cells through a Toll-like receptor 9-dependent pathway." J Immunol **172**(8): 4926-33.

Plowe, C. V., A. Djimde, M. Bouare, O. Doumbo and T. E. Wellems (1995). "Pyrimethamine and proguanil resistance-conferring mutations in *Plasmodium falciparum* dihydrofolate reductase: polymerase chain reaction methods for surveillance in Africa." Am J Trop Med Hyg **52**(6): 565-8.

Pradel, G., K. Hayton, L. Aravind, L. M. Iyer, M. S. Abrahamsen, A. Bonawitz, C. Mejia and T. J. Templeton (2004). "A multidomain adhesion protein family expressed in Plasmodium falciparum is essential for transmission to the mosquito." J Exp Med **199**(11): 1533-44.

Ralph, S. A., E. Bischoff, D. Mattei, O. Sismeiro, M. A. Dillies, G. Guigon, J. Y. Coppee, P. H. David and A. Scherf (2005). "Transcriptome analysis of antigenic variation in Plasmodium falciparum--var silencing is not dependent on antisense RNA." Genome Biol **6**(11): R93.

Rampengan, T. H. (1991). "Cerebral malaria in children. Comparative study between heparin, dexamethasone and placebo." Paediatr Indones **31**(1-2): 59-66.

Ranford-Cartwright, L. C., P. Balfe, R. Carter and D. Walliker (1993). "Frequency of cross-fertilization in the human malaria parasite Plasmodium falciparum." Parasitology **107**: 11-8.

Reeder, J. C., A. F. Cowman, K. M. Davern, J. G. Beeson, J. K. Thompson, S. J. Rogerson and G. V. Brown (1999). "The adhesion of Plasmodium falciparum-infected erythrocytes to chondroitin sulfate A is mediated by P. falciparum erythrocyte membrane protein 1." Proc Natl Acad Sci U S A **96**(9): 5198-202.

Reeder, J. C., A. N. Hodder, J. G. Beeson and G. V. Brown (2000). "Identification of glycosaminoglycan binding domains in Plasmodium falciparum erythrocyte membrane protein 1 of a chondroitin sulfate A-adherent parasite." Infect Immun **68**(7): 3923-6.

Ricke, C. H., T. Staalsoe, K. Koram, B. D. Akanmori, E. M. Riley, T. G. Theander and L. Hviid (2000). "Plasma antibodies from malaria-exposed pregnant women recognize variant surface antigens on Plasmodium falciparum-infected erythrocytes in a parity-dependent manner and block parasite adhesion to chondroitin sulfate A." J Immunol **165**(6): 3309-16.

Riganti, M., E. Pongponratn, T. Tegoshi, S. Looareesuwan, B. Punpoowong and M. Aikawa (1990). "Human cerebral malaria in Thailand: a clinico-pathological correlation." Immunol Lett **25**(1-3): 199-205.

Robert, C., B. Pouvelle, P. Meyer, K. Muanza, H. Fujioka, M. Aikawa, A. Scherf and J. Gysin (1995). "Chondroitin-4-sulphate (proteoglycan), a receptor for Plasmodium falciparum-infected erythrocyte adherence on brain microvascular endothelial cells." Res Immunol **146**(6): 383-93.

Roberts, D. D., J. A. Sherwood, S. L. Spitalnik, L. J. Panton, R. J. Howard, V. M. Dixit, W. A. Frazier, L. H. Miller and V. Ginsburg (1985). "Thrombospondin binds falciparum malaria parasitized erythrocytes and may mediate cytoadherence." Nature **318**(6041): 64-6.

Roberts, D. J., A. G. Craig, A. R. Berendt, R. Pinches, G. Nash, K. Marsh and C. I. Newbold (1992). "Rapid switching to multiple antigenic and adhesive phenotypes in malaria." Nature **357**(6380): 689-92.

Robinson, B. A., T. L. Welch and J. D. Smith (2003). "Widespread functional specialization of Plasmodium falciparum erythrocyte membrane protein 1 family members to bind CD36 analysed across a parasite genome." Mol Microbiol **47**(5): 1265-78.

Robson, K. J., U. Frevert, I. Reckmann, G. Cowan, J. Beier, I. G. Scragg, K. Takehara, D. H. Bishop, G. Pradel, R. Sinden and et al. (1995). "Thrombospondin-related adhesive protein (TRAP) of Plasmodium falciparum: expression during sporozoite ontogeny and binding to human hepatocytes." Embo J **14**(16): 3883-94.

Rogers, N. J., B. S. Hall, J. Obiero, G. A. Targett and C. J. Sutherland (2000). "A model for sequestration of the transmission stages of Plasmodium falciparum: adhesion of gametocyte-infected erythrocytes to human bone marrow cells." Infect Immun **68**(6): 3455-62.

Rogerson, S. J., R. Tembenu, C. Dobano, S. Plitt, T. E. Taylor and M. E. Molyneux (1999). "Cytoadherence characteristics of Plasmodium falciparum-infected erythrocytes from Malawian children with severe and uncomplicated malaria." Am J Trop Med Hyg **61**(3): 467-72.

Rottmann, M., T. Lavstsen, J. P. Mugasa, M. Kaestli, A. T. Jensen, D. Muller, T. Theander and H. P. Beck (2006). "Differential expression of var gene groups is associated with morbidity caused by Plasmodium falciparum infection in Tanzanian children." Infect Immun **74**(7): 3904-11.

Rowe, A., A. R. Berendt, K. Marsh and C. I. Newbold (1994). "Plasmodium falciparum: a family of sulphated glycoconjugates disrupts erythrocyte rosettes." Exp Parasitol **79**(4): 506-16.

Rowe, A., J. Obeiro, C. I. Newbold and K. Marsh (1995). "Plasmodium falciparum rosetting is associated with malaria severity in Kenya." Infect Immun **63**(6): 2323-6.

Rowe, J. A. (2005). Rosetting. Molecular Approaches to Malaria. I. W. Sherman. Washington, D.C., ASM Press**:** 416-426.

Rowe, J. A., I. G. Handel, M. A. Thera, A. M. Deans, K. E. Lyke, A. Kone, D. A. Diallo, A. Raza, O. Kai, K. Marsh, C. V. Plowe, O. K. Doumbo and J. M. Moulds (2007). "Blood group O protects against severe Plasmodium falciparum malaria through the mechanism of reduced rosetting." Proc Natl Acad Sci U S A.

Rowe, J. A. and S. A. Kyes (2004). "The role of Plasmodium falciparum var genes in malaria in pregnancy." Mol Microbiol **53**(4): 1011-9.
Rowe, J. A., S. A. Kyes, S. J. Rogerson, H. A. Babiker and A. Raza (2002a). "Identification of a conserved Plasmodium falciparum var gene implicated in malaria in pregnancy." J Infect Dis **185**(8): 1207-11.
Rowe, J. A., J. M. Moulds, C. I. Newbold and L. H. Miller (1997). "P. falciparum rosetting mediated by a parasite-variant erythrocyte membrane protein and complement-receptor 1." Nature **388**(6639): 292-5.
Rowe, J. A., J. Obiero, K. Marsh and A. Raza (2002b). "Short report: Positive correlation between rosetting and parasitemia in Plasmodium falciparum clinical isolates." Am J Trop Med Hyg **66**(5): 458-60.
Rowe, J. A., S. J. Rogerson, A. Raza, J. M. Moulds, M. D. Kazatchkine, K. Marsh, C. I. Newbold, J. P. Atkinson and L. H. Miller (2000). "Mapping of the region of complement receptor (CR) 1 required for Plasmodium falciparum rosetting and demonstration of the importance of CR1 in rosetting in field isolates." J Immunol **165**(11): 6341-6.
Rowe, J. A., J. Shafi, O. K. Kai, K. Marsh and A. Raza (2002c). "Nonimmune IgM, but not IgG binds to the surface of Plasmodium falciparum-infected erythrocytes and correlates with rosetting and severe malaria." Am J Trop Med Hyg **66**(6): 692-9.
Rug, M., S. W. Prescott, K. M. Fernandez, B. M. Cooke and A. F. Cowman (2006). "The role of KAHRP domains in knob formation and cytoadherence of p falciparum-infected human erythrocytes." Blood **108**(1): 370-8.
Russell, C., O. Mercereau-Puijalon, C. Le Scanf, M. Steward and D. E. Arnot (2005). "Further definition of PfEMP-1 DBL-1alpha domains mediating rosetting adhesion of Plasmodium falciparum." Mol Biochem Parasitol **144**(1): 109-13.
Salanti, A., M. Dahlback, L. Turner, M. A. Nielsen, L. Barfod, P. Magistrado, A. T. Jensen, T. Lavstsen, M. F. Ofori, K. Marsh, L. Hviid and T. G. Theander (2004). "Evidence for the Involvement of VAR2CSA in Pregnancy-associated Malaria." J Exp Med **200**(9): 1197-203.
Salanti, A., A. T. Jensen, H. D. Zornig, T. Staalsoe, L. Joergensen, M. A. Nielsen, A. Khattab, D. E. Arnot, M. Q. Klinkert, L. Hviid and T. G. Theander (2002). "A sub-family of common and highly conserved Plasmodium falciparum var genes." Mol Biochem Parasitol **122**(1): 111-5.
Salanti, A., T. Staalsoe, T. Lavstsen, A. T. Jensen, M. P. Sowa, D. E. Arnot, L. Hviid and T. G. Theander (2003). "Selective upregulation of a single distinctly structured var gene in chondroitin sulphate A-adhering Plasmodium falciparum involved in pregnancy-associated malaria." Mol Microbiol **49**(1): 179-91.
Sartelet, H., O. Garraud, C. Rogier, I. Milko-Sartelet, Y. Kaboret, G. Michel, C. Roussilhon, M. Huerre and D. Gaillard (2000). "Hyperexpression of ICAM-1 and CD36 in placentas infected with Plasmodium falciparum: a possible role of these molecules in sequestration of infected red blood cells in placentas." Histopathology **36**(1): 62-8.
Scherf, A., R. Hernandez-Rivas, P. Buffet, E. Bottius, C. Benatar, B. Pouvelle, J. Gysin and M. Lanzer (1998). "Antigenic variation in malaria: in situ switching, relaxed and mutually exclusive transcription of var genes during

intra-erythrocytic development in Plasmodium falciparum." Embo J **17**(18): 5418-26.
Semblat, J. P., A. Raza, S. A. Kyes and J. A. Rowe (2006). "Identification of Plasmodium falciparum var1CSA and var2CSA domains that bind IgM natural antibodies." Mol Biochem Parasitol **146**(2): 192-7.
Senczuk, A. M., J. C. Reeder, M. M. Kosmala and M. Ho (2001). "Plasmodium falciparum erythrocyte membrane protein 1 functions as a ligand for P-selectin." Blood **98**(10): 3132-5.
Serghides, L., S. N. Patel, K. Ayi and K. C. Kain (2006). "Placental chondroitin sulfate A-binding malarial isolates evade innate phagocytic clearance." J Infect Dis **194**(1): 133-9.
Serghides, L., T. G. Smith, S. N. Patel and K. C. Kain (2003). "CD36 and malaria: friends or foes?" Trends Parasitol **19**(10): 461-9.
Sharling, L., A. Enevold, K. M. Sowa, T. Staalsoe and D. E. Arnot (2004). "Antibodies from malaria-exposed pregnant women recognize trypsin resistant epitopes on the surface of Plasmodium falciparum-infected erythrocytes selected for adhesion to chondroitin sulphate A." Malar J **3**: 31.
Sharling, L., K. M. Sowa, J. Thompson, H. M. Kyriacou and D. E. Arnot (2007). "Rapid and specific biotin labelling of the erythrocyte surface antigens of both cultured and ex-vivo Plasmodium parasites." Malar J **6**: 66.
Sharp, S., T. Lavstsen, Q. L. Fivelman, M. Saeed, L. McRobert, T. J. Templeton, A. T. Jensen, D. A. Baker, T. G. Theander and C. J. Sutherland (2006). "Programmed transcription of the var gene family, but not of stevor, in Plasmodium falciparum gametocytes." Eukaryot Cell **5**(8): 1206-14.
Silamut, K., N. H. Phu, C. Whitty, G. D. Turner, K. Louwrier, N. T. Mai, J. A. Simpson, T. T. Hien and N. J. White (1999). "A quantitative analysis of the microvascular sequestration of malaria parasites in the human brain." Am J Pathol **155**(2): 395-410.
Sinden, R. E. (2002). "Molecular interactions between Plasmodium and its insect vectors." Cell Microbiol **4**(11): 713-24.
Singh, S. K., R. Hora, H. Belrhali, C. E. Chitnis and A. Sharma (2006). "Structural basis for Duffy recognition by the malaria parasite Duffy-binding-like domain." Nature **439**(7077): 741-4.
Smalley, M. E. (1976). "Plasmodium falciparum gametocytogenesis in vitro." Nature **264**(5583): 271-2.
Smith, J. D., C. E. Chitnis, A. G. Craig, D. J. Roberts, D. E. Hudson-Taylor, D. S. Peterson, R. Pinches, C. I. Newbold and L. H. Miller (1995). "Switches in expression of Plasmodium falciparum var genes correlate with changes in antigenic and cytoadherent phenotypes of infected erythrocytes." Cell **82**(1): 101-10.
Smith, J. D., A. G. Craig, N. Kriek, D. Hudson-Taylor, S. Kyes, T. Fagen, R. Pinches, D. I. Baruch, C. I. Newbold and L. H. Miller (2000a). "Identification of a Plasmodium falciparum intercellular adhesion molecule-1 binding domain: a parasite adhesion trait implicated in cerebral malaria." Proc Natl Acad Sci U S A **97**(4): 1766-71.
Smith, J. D., G. Subramanian, B. Gamain, D. I. Baruch and L. H. Miller (2000b). "Classification of adhesive domains in the Plasmodium falciparum

erythrocyte membrane protein 1 family." Mol Biochem Parasitol **110**(2): 293-310.
Smith, T. G., P. Lourenco, R. Carter, D. Walliker and L. C. Ranford-Cartwright (2000c). "Commitment to sexual differentiation in the human malaria parasite, Plasmodium falciparum." Parasitology **121 (Pt 2)**: 127-33.
Smith, T. G., L. Serghides, S. N. Patel, M. Febbraio, R. L. Silverstein and K. C. Kain (2003). "CD36-mediated nonopsonic phagocytosis of erythrocytes infected with stage I and IIA gametocytes of Plasmodium falciparum." Infect Immun **71**(1): 393-400.
Snow, R., Craig M., Deichmann, U. and Marsh, k. (1999). "Estimaing mortality, morbidity and disability due to malaria among Africa's non-pregnant population." Bull World Health Organ **77**(8): 624-640.
Snow, R. W., C. A. Guerra, A. M. Noor, H. Y. Myint and S. I. Hay (2005). "The global distribution of clinical episodes of Plasmodium falciparum malaria." Nature **434**(7030): 214-7.
Springer, A. L., L. M. Smith, D. Q. Mackay, S. O. Nelson and J. D. Smith (2004). "Functional interdependence of the DBLbeta domain and c2 region for binding of the Plasmodium falciparum variant antigen to ICAM-1." Mol Biochem Parasitol **137**(1): 55-64.
Staalsoe, T., C. E. Shulman, J. N. Bulmer, K. Kawuondo, K. Marsh and L. Hviid (2004). "Variant surface antigen-specific IgG and protection against clinical consequences of pregnancy-associated Plasmodium falciparum malaria." Lancet **363**(9405): 283-9.
Steketee, R. W., B. L. Nahlen, M. E. Parise and C. Menendez (2001). "The burden of malaria in pregnancy in malaria-endemic areas." Am J Trop Med Hyg **64**(1-2 Suppl): 28-35.
Su, X. Z., V. M. Heatwole, S. P. Wertheimer, F. Guinet, J. A. Herrfeldt, D. S. Peterson, J. A. Ravetch and T. E. Wellems (1995). "The large diverse gene family var encodes proteins involved in cytoadherence and antigenic variation of Plasmodium falciparum-infected erythrocytes." Cell **82**(1): 89-100.
Suwanarusk, R., B. M. Cooke, A. M. Dondorp, K. Silamut, J. Sattabongkot, N. J. White and R. Udomsangpetch (2004). "The deformability of red blood cells parasitized by Plasmodium falciparum and P. vivax." J Infect Dis **189**(2): 190-4.
Tami, A., R. Ord, G. A. Targett and C. J. Sutherland (2003). "Sympatric Plasmodium falciparum isolates from Venezuela have structured var gene repertoires." Malar J **2**(1): 7.
Tarun, A. S., K. Baer, R. F. Dumpit, S. Gray, N. Lejarcegui, U. Frevert and S. H. Kappe (2006). "Quantitative isolation and in vivo imaging of malaria parasite liver stages." Int J Parasitol **36**(12): 1283-93.
Taylor, H. M., S. A. Kyes, D. Harris, N. Kriek and C. I. Newbold (2000a). "A study of var gene transcription in vitro using universal var gene primers." Mol Biochem Parasitol **105**(1): 13-23.
Taylor, H. M., S. A. Kyes and C. I. Newbold (2000b). "Var gene diversity in Plasmodium falciparum is generated by frequent recombination events." Mol Biochem Parasitol **110**(2): 391-7.

Taylor, T. E., W. J. Fu, R. A. Carr, R. O. Whitten, J. S. Mueller, N. G. Fosiko, S. Lewallen, N. G. Liomba and M. E. Molyneux (2004). "Differentiating the pathologies of cerebral malaria by postmortem parasite counts." Nat Med **10**(2): 143-5.

Thomas, B. N., B. Donvito, I. Cockburn, T. Fandeur, J. A. Rowe, J. H. Cohen and J. M. Moulds (2005). "A complement receptor-1 polymorphism with high frequency in malaria endemic regions of Asia but not Africa." Genes Immun **6**(1): 31-6.

Tolia, N. H., E. J. Enemark, B. K. Sim and L. Joshua-Tor (2005). "Structural basis for the EBA-175 erythrocyte invasion pathway of the malaria parasite Plasmodium falciparum." Cell **122**(2): 183-93.

Trager, W. and J. B. Jensen (1976). "Human malaria parasites in continuous culture." Science **193**(4254): 673-5.

Traore, B., K. Muanza, S. Looareesuwan, S. Supavej, S. Khusmith, M. Danis, P. Viriyavejakul and F. Gay (2000). "Cytoadherence characteristics of Plasmodium falciparum isolates in Thailand using an in vitro human lung endothelial cells model." Am J Trop Med Hyg **62**(1): 38-44.

Treutiger, C. J., A. Heddini, V. Fernandez, W. A. Muller and M. Wahlgren (1997). "PECAM-1/CD31, an endothelial receptor for binding Plasmodium falciparum-infected erythrocytes." Nat Med **3**(12): 1405-8.

Triglia, T., J. Healer, S. R. Caruana, A. N. Hodder, R. F. Anders, B. S. Crabb and A. F. Cowman (2000). "Apical membrane antigen 1 plays a central role in erythrocyte invasion by Plasmodium species." Mol Microbiol **38**(4): 706-18.

Trimnell, A. R., S. M. Kraemer, S. Mukherjee, D. J. Phippard, J. H. Janes, E. Flamoe, X. Z. Su, P. Awadalla and J. D. Smith (2006). "Global genetic diversity and evolution of var genes associated with placental and severe childhood malaria." Mol Biochem Parasitol **148**(2): 169-80.

Tuikue Ndam, N. G., A. Salanti, G. Bertin, M. Dahlback, N. Fievet, L. Turner, A. Gaye, T. Theander and P. Deloron (2005). "High level of var2csa transcription by Plasmodium falciparum isolated from the placenta." J Infect Dis **192**(2): 331-5.

Tuikue Ndam, N. G., A. Salanti, J. Y. Le-Hesran, G. Cottrell, N. Fievet, L. Turner, S. Sow, J. M. Dangou, T. Theander and P. Deloron (2006). "Dynamics of anti-VAR2CSA immunoglobulin G response in a cohort of senegalese pregnant women." J Infect Dis **193**(5): 713-20.

Turner, G. D., H. Morrison, M. Jones, T. M. Davis, S. Looareesuwan, I. D. Buley, K. C. Gatter, C. I. Newbold, S. Pukritayakamee, B. Nagachinta and et al. (1994). "An immunohistochemical study of the pathology of fatal malaria. Evidence for widespread endothelial activation and a potential role for intercellular adhesion molecule-1 in cerebral sequestration." Am J Pathol **145**(5): 1057-69.

Udomsangpetch, R., P. H. Reinhardt, T. Schollaardt, J. F. Elliott, P. Kubes and M. Ho (1997). "Promiscuity of clinical Plasmodium falciparum isolates for multiple adhesion molecules under flow conditions." J Immunol **158**(9): 4358-64.

Udomsanpetch, R., K. Thanikkul, S. Pukrittayakamee and N. J. White (1995). "Rosette formation by Plasmodium vivax." Trans R Soc Trop Med Hyg **89**(6): 635-7.

Urban, B. C., D. J. Ferguson, A. Pain, N. Willcox, M. Plebanski, J. M. Austyn and D. J. Roberts (1999). "Plasmodium falciparum-infected erythrocytes modulate the maturation of dendritic cells." Nature **400**(6739): 73-7.

Urban, B. C., N. Willcox and D. J. Roberts (2001). "A role for CD36 in the regulation of dendritic cell function." Proc Natl Acad Sci U S A **98**(15): 8750-5.

Valiyaveettil, M., R. N. Achur, A. Muthusamy and D. C. Gowda (2004). "Chondroitin sulfate proteoglycans of the endothelia of human umbilical vein and arteries and assessment for the adherence of Plasmodium falciparum-infected erythrocytes." Mol Biochem Parasitol **134**(1): 115-26.

van Schravendijk, M. R., S. M. Handunnetti, J. W. Barnwell and R. J. Howard (1992). "Normal human erythrocytes express CD36, an adhesion molecule of monocytes, platelets, and endothelial cells." Blood **80**(8): 2105-14.

Vazquez-Macias, A., P. Martinez-Cruz, M. C. Castaneda-Patlan, C. Scheidig, J. Gysin, A. Scherf and R. Hernandez-Rivas (2002). "A distinct 5' flanking var gene region regulates Plasmodium falciparum variant erythrocyte surface antigen expression in placental malaria." Mol Microbiol **45**(1): 155-67.

Viebig, N. K., B. Gamain, C. Scheidig, C. Lepolard, J. Przyborski, M. Lanzer, J. Gysin and A. Scherf (2005). "A single member of the Plasmodium falciparum var multigene family determines cytoadhesion to the placental receptor chondroitin sulphate A." EMBO Rep **6**(8): 775-81.

Viebig, N. K., E. Levin, S. Dechavanne, S. J. Rogerson, J. Gysin, J. D. Smith, A. Scherf and B. Gamain (2007). "Disruption of var2csa gene impairs placental malaria associated adhesion phenotype." PLoS ONE **2**(9): e910.

Vogt, A. M., A. Barragan, Q. Chen, F. Kironde, D. Spillmann and M. Wahlgren (2003). "Heparan sulfate on endothelial cells mediates the binding of Plasmodium falciparum-infected erythrocytes via the DBL1alpha domain of PfEMP1." Blood **101**(6): 2405-11.

Vogt, A. M., F. Pettersson, K. Moll, C. Jonsson, J. Normark, U. Ribacke, T. G. Egwang, H. P. Ekre, D. Spillmann, Q. Chen and M. Wahlgren (2006). "Release of sequestered malaria parasites upon injection of a glycosaminoglycan." PLoS Pathog **2**(9): e100.

Vogt, A. M., G. Winter, M. Wahlgren and D. Spillmann (2004). "Heparan sulphate identified on human erythrocytes: a Plasmodium falciparum receptor." Biochem J **381**(Pt 3): 593-7.

Voss, T. S., J. K. Thompson, J. Waterkeyn, I. Felger, N. Weiss, A. F. Cowman and H. P. Beck (2000). "Genomic distribution and functional characterisation of two distinct and conserved Plasmodium falciparum var gene 5' flanking sequences." Mol Biochem Parasitol **107**(1): 103-15.

Wahlgren, M., J. Carlson, W. Ruangjirachuporn, D. Conway, H. Helmby, A. Martinez, M. E. Patarroyo and E. Riley (1990). "Geographical distribution of Plasmodium falciparum erythrocyte rosetting and frequency of rosetting antibodies in human sera." Am J Trop Med Hyg **43**(4): 333-8.

Ward, C. P., G. T. Clottey, M. Dorris, D. D. Ji and D. E. Arnot (1999). "Analysis of Plasmodium falciparum PfEMP-1/var genes suggests that recombination rearranges constrained sequences." Mol Biochem Parasitol **102**(1): 167-77.

White, N. J. (1987). "Clinical and pathological aspects of severe malaria." Acta Leiden **56**: 27-46.

WHO (2000). "Severe falciparum malaria. World Health Organization, Communicable Diseases Cluster." Trans R Soc Trop Med Hyg **94 Suppl 1**: S1-90.

Winter, G., Q. Chen, K. Flick, P. Kremsner, V. Fernandez and M. Wahlgren (2003). "The 3D7var5.2 (var COMMON) type var gene family is commonly expressed in non-placental Plasmodium falciparum malaria." Mol Biochem Parasitol **127**(2): 179-91.

Xiao, L., C. Yang, P. S. Patterson, V. Udhayakumar and A. A. Lal (1996). "Sulfated polyanions inhibit invasion of erythrocytes by plasmodial merozoites and cytoadherence of endothelial cells to parasitized erythrocytes." Infect Immun **64**(4): 1373-8.

Appendix

Appendix 1. Table of Mali childhood malaria field isolate details

Data on the 26 Mali isolates for clinical disease manifestation, age, parasitaemia, rosette frequency, platelet-mediated clumping and multiplicity of infection is given, along with percentage of DBLα transcripts detected that were of the DBLα1-type (discussed in chapter 3), and the estimated number of type 3 transcripts present (discussed in chapter 5).

Appendix 2. Phylogenetic network of DBLα transcripts in Mali childhood field isolates (discussed in chapter 3)

A phylogenetic network was created by Dr Graham Stone (University of Edinburgh) to replace the phenogram of childhood isolate DBLα domain transcripts (chapter 3, Fig. 3.13). The network was produced from an initial Clustal W alignment of the amino acid sequences, converted to a nucleotide alignment. The network and phenogram both show separation of sequences into two clades, signifying DBLα1 versus DBLα0-like sequences. Sequences from the cerebral malaria patients (red in network; appendix 2) are significantly concentrated into a 'cerebral malaria clade' ($P<0.001$, chi-squared test). Sequences from the hyperparasitaemia patients (blue) are significantly concentrated in a 'hyperparasitaemia clade' ($P<0.025$, Chi-squared test). Sequences from the uncomplicated malaria patients (green) showed no bias in distribution between the two main clades of the network.

Appendix 3. Publications arising from this thesis

1: Arising from the work presented in chapter 3

Title: Differential *var* gene transcription in *Plasmodium falciparum* isolates from patients with cerebral malaria compared to hyperparasitaemia.

Authors: **Helen M. Kyriacou**, Graham N. Stone, Richard J. Challis, Ahmed Raza, Kirsten E. Lyke, Mahamadou A. Thera, Abdoulaye K. Koné, Ogobara K. Doumbo, Christopher V. Plowe and J. Alexandra Rowe.

Journal: Molecular and Biochemical Parasitology (2006) 150(2): 211-8

Publisher: Elsevier

2: Arising from the work presented in chapter 4

Title: Transcribed *var* genes associated with placental malaria in Malawian women.

Authors: Michael F. Duffy, Aphrodite Caragounis, Rintis Noviyanti, **Helen M. Kyriacou**, Ee Ken Choong, Katja Boysen, Julie Healer, J. Alexandra Rowe, Malcolm E. Molyneux, Graham V. Brown, and Stephen J. Rogerson.

Journal: Infection and Immunity (2006) 74: 4875-4883

Publisher: American Society for Microbiology

3: Arising from the work presented in chapter 6

Title: *In vitro* inhibition of *Plasmodium falciparum* rosetting formation by curdlan sulphate.

Authors: **Helen M. Kyriacou***, Katie E. Steen*, Ahmed Raza, Monica Arman, Pete C Bull, Ivan Havlik and J. Alexandra Rowe. *Joint first authors.

Journal: Antimicrobial Agents and Chemotherapy (2007) 51:1321-6.

Publisher: American Society for Microbiology

4: Arising from work with Lisa Sharling during the course of my PhD but not discussed in this thesis.

Title: Rapid and specific biotin labelling of the erythrocyte surface antigens of both cultured and *ex-vivo Plasmodium* parasites.

Authors: Lisa Sharling, Kordai M.P. Sowa, Joanne Thompson, **Helen M. Kyriacou** and David E. Arnot.

Journal: Malaria Journal (2007) 6:66-72.

Publisher: BioMed Central

Isolate	Clinical disease	Age (mo)	Pt (%)	RF (%)	PMC (%)	Geno-types	DBLα1 (%)	Type 3 transcripts
CM1	Cerebral	28	6.0	19	0	1	83.3	1
CM2	Cerebral	15	9.2	28	0	3	78.6	1
CM3	Cerebral	27	15.0	20	5	3	92.9	1
CM4	Cerebral	79	13.0	22	0	5	5.9	1
CM5	Cerebral	52	10.0	96	0	1	72.2	1
CM6	Cerebral	15	24.0	64	8	3	100.0	1
CM7	Cerebral	28	7.4	20	0	1	100.0	2
CM8	Cerebral	18	20.0	0	53	1	94.7	1
CM9	Cerebral	55	6.0	41	0	2	100.0	0
HYP1	Hyperp	49	18.5	0	0	4	0.0	4
HYP2	Hyperp	51	12.0	16	0	3	6.7	3
HYP3	Hyperp	15	10.0	4	13	1	27.8	1
HYP4	Hyperp	64	11.4	20	0	2	100.0	2
HYP5	Hyperp	39	15.0	15	0	3	40.0	3
HYP6	Hyperp	52	12.0	20	0	3	25.0	3
HYP7	Hyperp	20	11.4	0	0	3	6.3	3
HYP8	Hyperp	50	5.0	0	ND	2	0.0	2
U1	Uncomp	27	5.4	14	0	4	60.0	4
U2	Uncomp	25	3.8	8	0	3	6.7	3
U3	Uncomp	39	5.6	8	0	3	100.0	3
U4	Uncomp	36	3.0	21	0	3	5.6	3
U5	Uncomp	15	1.2	2	0	3	73.7	3
U6	Uncomp	39	3.2	23	ND	1	100.0	1
U7	Uncomp	49	3.0	0	0	3	6.7	3
U8	Uncomp	102	2.8	0	ND	1	5.3	1
U9	Uncomp	80	1.6	0	0	1	83.3	1

Appendix 1: Table showing isolate name, clinical disease manifestation, age (mo: months), parasitaemia (Pt, %), rosette frequency (RF, %) platelet-mediated clumping (PMC, %), multiplicity of infection (genotypes), percentage of amplified DBLα transcripts that were of the DBLα1-type (DBLα1%), and the estimated number of type 3 transcripts present (type 3 transcripts) for the 26 Mali childhood malaria isolates discussed throughout the thesis.

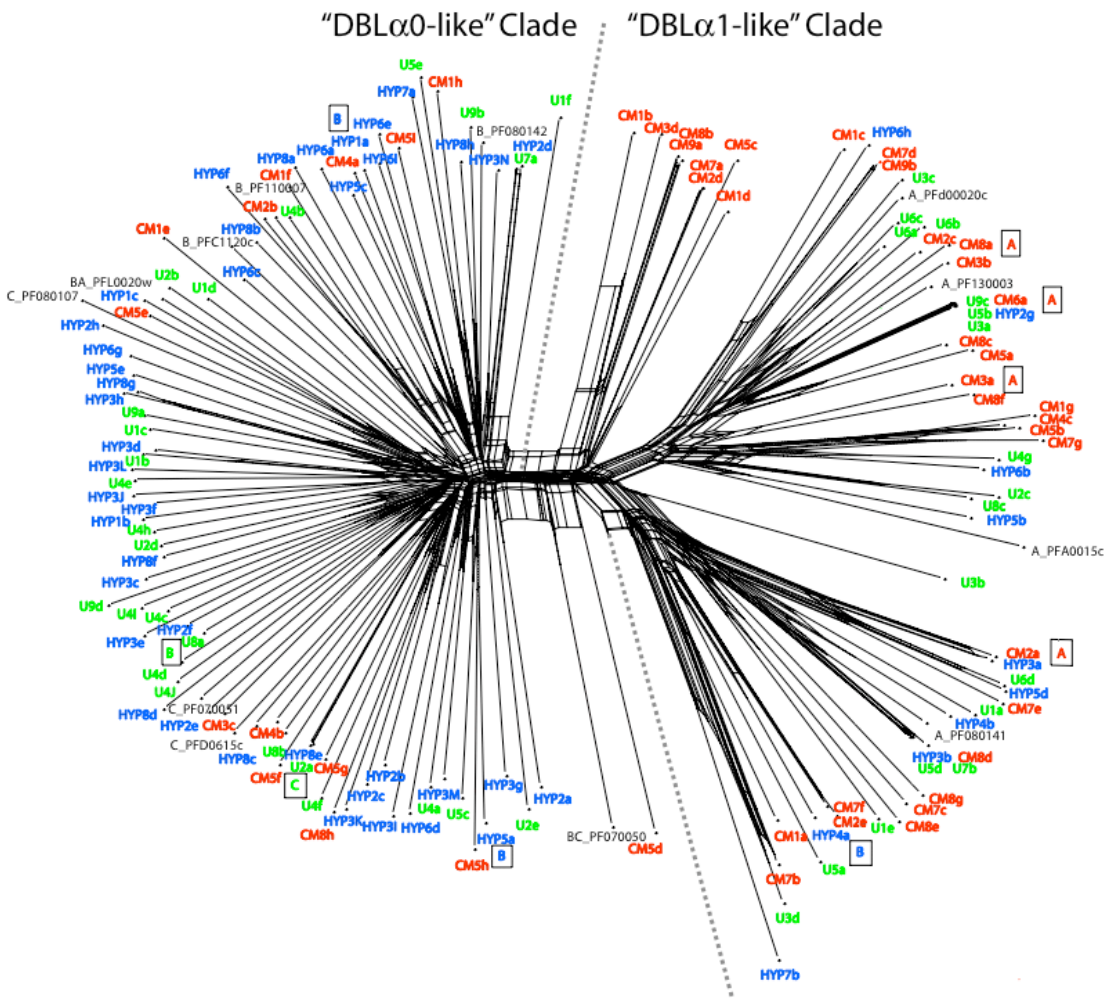

Appendix 2. Phylogenetic network produced by Dr Graham Stone from a Clustal W alignment of Mali isolate DBLα domain transcripts described in chapter 3. Relationships between *var* gene DBLα sequence tags transcribed by *P. falciparum* isolates, generated using Neighbour-Net (Bryant and Moulton 2004). Sequences transcribed by isolates from African children with cerebral malaria (CM, red), hyperparasitaemia (HYP, blue), and uncomplicated malaria (U, green) are compared to a selection of *var* genes from the laboratory clone 3D7. For the 3D7 genes, the gene name is preceded by A, B, C, BA or BC to indicate the group to which the gene belongs. The sequences fall into 2 major clades, with the DBLα0-like sequences to the left of the dotted line and the DBLα1-like sequences to the right. For the predominant gene from 9 of the Malian isolates, the *var* gene upstream region was determined by PCR and is indicated as a boxed letter.